M. Baerns (Ed.)

Basic Principles in Applied Catalysis

Physics and Astronomy | ONLINE LIBRARY

springeronline.com
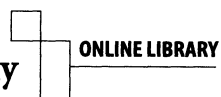
Springer Series in
CHEMICAL PHYSICS

Series Editors: A. W. Castleman, Jr.   F. P. Schäfer   J. P. Toennies   W. Zinth

The purpose of this series is to provide comprehensive up-to-date monographs in both well established disciplines and emerging research areas within the broad fields of chemical physics and physical chemistry. The books deal with both fundamental science and applications, and may have either a theoretical or an experimental emphasis. They are aimed primarily at researchers and graduate students in chemical physics and related fields.

M. Baerns (Ed.)

Basic Principles
in Applied Catalysis

With 170 Figures and 50 Tables

Springer

Professor Dr. Manfred Baerns
Institut für Angewandte Chemie
Berlin-Adlershof e.V.
Richard-Willstätter-Str. 12
12489 Berlin
Germany

Series Editors:

Professor A. W. Castleman, Jr.
Department of Chemistry
The Pennsylvania State University
152 Davey Laboratory
University Park, PA 16802, USA

Professor F.P. Schäfer
Max-Planck-Institut für Biophysikalische Chemie
37077 Göttingen-Nikolausberg, Germany

Professor J.P. Toennies
Max-Planck-Institut für Strömungsforschung
Bunsenstrasse 10
37073 Göttingen, Germany

Professor W. Zinth
Universität München,
Institut für Medizinische Optik
Öttingerstr. 67
80538 München, Germany

Preface

Applied catalysis is based nowadays not only on empirical knowledge but also on the many insights, that have been gained from the fundamental understanding of catalysis. It also comprises knowledge and expertise from catalytic reaction engineering, in particular kinetics of the catalytic reaction and its interplay with heat and mass transfer as well as fluid dynamics and the specific conditions prevailing in the type of reactor used.

Applied catalysis comprises many areas from a reaction point of view, many types of catalytic materials from which catalysts are formed are needed to achieve high selectivities and space-time yields, last but not least catalysts should have a long life time to which its deactivation is detrimental. A catalytic material that fulfils all the demands then often requires special mechanical and thermal treatment to be used in practise.

Various books have been written about specific areas as mentioned above. It is the intention of this contribution to present timely reports by well-recognised experts in the field to outline the state of science and technology in selected but representative areas illustrating the *basic principles of applied catalysis*.

The book is introduced by an overview of the *economic and industrial importance of catalysis*. Thereafter, *selected reactions in heterogeneous catalysis* are presented comprising the partial oxidation of light alkanes, the selective hydrogenation of multiply unsaturated hydrocarbons, catalytic reforming and the application of zeolites in catalysis. Another part of the book covers the *preparation, functionality and characterisation of solid catalytic materials* describing in detail catalyst preparation, tools for high-throughput experimentation in the development of heterogeneous catalysts, the preparation and application of ordered mesoporous materials and the in-situ characterisation of heterogeneous catalysts. *Homogeneous catalysis, polymerisation catalysis and biocatalysis* which nowadays play also an important role in the field of applied catalysis are introduced by three different chapters. Finally, the part *catalytic reaction engineering* deals with kinetics of heterogeneous catalytic reactions, catalyst deactivation, so-called divided catalytic processes as well as structured catalysts and micro-structured reactors.

The book shall guide the experts in practice and science to state-of-the-art knowledge but it also should serve the interested novice to enter the field of applied catalysis on a high level.

The effort in putting together all the chapters was not always easy. I therefore thank all the authors who finally contributed to the completion of the book. In particular, I would like to thank Dr. Angela Köckritz who brought together all these efforts.

Sincere thanks are due to all the reviewers, including many from the Institute for Applied Chemistry Berlin-Adlershof e. V. but also from other institutions who assisted me to bring the many chapters in their final shape.

Finally, I thank Hannelore Gube who did all the fine-tuning and necessary adjustments of the chapters to comply with the requirements of Springer Publisher and its representatives who patiently advised us in many editorial questions.

Berlin, Germany   MANFRED BAERNS
2003

Contents

List of Contributors

Baerns, Manfred
Institute for Applied Chemistry
Berlin-Adlershof,
Richard-Willstätter-Str. 12,
12489 Berlin, Germany

Beller, Matthias
Leibniz-Institut
für Organische Katalyse
an der Universität Rostock e.V.
(IfOK)
Buchbinderstr. 5-6,
18055 Rostock, Germany

Boskovic, Goran
University of Novy Sad,
Faculty of Technology,
Bul. Cara lazara 1,
21000 Novy Sad, Yugoslavia

Cavani, Fabrizio
Dipartimento di Chimica
Industriale
e dei Materiali,
Viale Risorgimento 4,
40136 Bologna, Italy

Claus, Peter
Department of Chemistry,
Ernst-Berl-Institute
of Chemical Engineering
and Macromolecular Chemistry,
Darmstadt University
of Technology,
Petersenstraße 20,
64287 Darmstadt, Germany

Emig, Gerhard
Universität Erlangen-Nürnberg,
Technische Chemie I,
Egerlandstr. 3,
91058 Erlangen, Germany

Gaube, Johann
Department of Chemistry,
Ernst-Berl-Institute
of Chemical Engineering
and Macromolecular Chemistry,
Darmstadt University
of Technology,
Petersenstraße 20,
64287 Darmstadt, Germany

Gjervan, Torbjørn
Department of Chemical
Engineering,
Norwegian University of Science
and Technology NTNU,
7491 Trondheim, Norway

Gläser, Roger
Institute of Chemical Technology,
University of Stuttgart,
70550 Stuttgart, Germany

Holmen, Anders
Department of Chemical
Engineering,
Norwegian University of Science
and Technology (NTNU),
7491 Trondheim, Norway

Hutchings, Graham
Department of Chemistry,
Cardiff University,
P.O. Box 912,
Cardiff, UK, CF10 3TB

Kaminsky, Walter
Institute for Technical
and Macromolecular Chemistry,
University of Hamburg,
Bundesstr. 45,
20146 Hamburg

Kleitz, F.
Max-Planck-Institut
für Kohlenforschung,
Kaiser-Wilhelm-Platz 1,
45470 Mülheim, Germany

Kragl, Udo
Rostock University,
Department of Chemistry,
18051 Rostock, Germany

Prestvik, Rune
SINTEF Applied Chemistry,
7465 Trondheim, Norway

Renken, Albert
Laboratoire de Génie
de la réaction chimique,
Ecole polytechnique
fédérale de Lausanne,
LGRC-EPFL,
1015 Lausanne, Switzerland

Rodemerck, Uwe
Institute for Applied Chemistry,
Berlin-Adlershof,
Richard-Willstätter-Str. 12,
12489 Berlin, Germany

Schimpf, Sabine
Department of Chemistry,
Ernst-Berl-Institute
of Chemical Engineering
and Macromolecular Chemistry,
Darmstadt University
of Technology,
Petersenstraße 20,
64287 Darmstadt, Germany

Schlögl, Robert
Fritz-Haber-Institut der MPG,
Faradayweg 4-6,
14195 Berlin, Germany

Schüth, Ferdi
Max-Planck-Institut
für Kohlenforschung,
Kaiser-Wilhelm-Platz 1,
45470 Mülheim, Germany

Seiler, Harald
DEGUSSA Antwerpen N.V.,
Fumed Silica & Chlorosilanes,
Tijsmanstunnel West,
2040 Antwerpen, Belgium

Trifirò, Ferruccio
Dipartimento di Chimica
Industriale
e dei Materiali,
Viale Risorgimento 4,
40136 Bologna, Italy

Védrine, J.C.
ENSCP,
Laboratoire de Physico-Chimie
des Surfaces,
11 Rue P. & M. Curie,
75005 Paris, France

Weitkamp, Jens
Institute of Chemical Technology,
University of Stuttgart,
70550 Stuttgart, Germany

Wingen, A.
Max-Planck-Institut
für Kohlenforschung,
Kaiser-Wilhelm-Platz 1,
45470 Mülheim, Germany

Wolf, Dorit
DEGUSSA AG, Project House
Catalysis,
Industriepark Hoechst,
65926 Frankfurt, Germany

I   Introduction

The Importance of Catalysis in the Chemical and Non-Chemical Industries

Contents

The Importance of Catalysis in the Chemical and Non-Chemical Industries

Friedrich Schmidt

83024 Rosenheim, Lug ins Land 52, Germany
friedrich.schmidt@sud-chemie.com

Abstract. The chemical industry is an enabling industry. Chemicals are supplied to almost every other industry. The manufacture of goods from oil, coal or gas to everyday consumer products comprises in more or less all cases at least one catalytic step. Through its processes and products industrial catalysis contributes about one quarter to the gross domestic product of the developed countries. At the turn of the century, the value of the catalyst world market, including captive use, was estimated to be about 10 billion US$ with ¼ refining, ¼ polymers, ¼ chemicals and ¼ environment. The goods and services created from petrochemistry, refining and polymerization catalysis on average were estimated to be about 200 to 300 times the value of the catalyst.

Catalysis is truly multidisciplinary with respect to various areas: inorganic chemistry, organic chemistry, bio-chemistry, chemical engineering, bio-engineering, materials science, surface science, kinetics, and theoretical chemistry.

1. Introduction

History reveals, that the chemical industry has almost always reacted to those specific needs that have been identified by society and future economic and ecological; sustainability depends upon corresponding progress in the chemical industry. Because catalytic technologies are used in more than 80 % of the manufacturing processes for chemicals, catalysis is considered to be the fundamental key to progress in the fulfilment of societal needs, which are:
(i)   Health, food and home care:
   -   pharmaceuticals, fats and oils, surfactants, fragrances, super-absorber,
(ii) New materials[1]:
   -   (natural gas-based) monomers for the polymer industry, polymerization technology for high performance polymers

---

[1] The macro-cycles of materials - more or less - have been based on wood and other bio-materials, stone, ceramics, brass, iron, steel, coal , oil and finally gas as raw materials

(iii) Energy, transportation and traffic[2]:
-    in power supply and transportation, catalysis is rigorously involved in the reduction of pollution prior to distribution in the energy channels as well as end-of the pipe control of pollution.
-    For the production of clean motor fuels with high octane or cetane and super ultra low sulfur, progress in catalytic technologies is essential.
-    Almost all conversion processes in a refinery are catalytic ones.
-    Fuel cells for converting hydrogen into power for homes or for the mobile sector require hydrogen production involving many catalytic steps.
(iv) Preservation of environment and resources:
-    Some aspects regarding the preservation of the environment have been discussed above when mentioning the transportation sector.
-    However, stationary sources of pollution are numerous: in chemical plants the concentration of the pollutants in the off-gas and waste water is ultra low but due to the high volumes of throughput there is still room for improvement in reducing the absolute numbers. Reducing the bad odor of the emissions e.g. in the food industry or reducing volatile organic compounds from off-gases in paint producing and paint using industry are other applications where catalysis has a key function.
-    In the near future and particularly in the long term, natural gas will obviously gain increasing importance as raw material for the chemical industry[3]. The conversion of natural gas into chemical intermediates requires numerous catalytic steps. These intermediates may act as building blocks for the polymer industry. High performance (polymer) materials are still one of the major growth areas of the chemical industry. With respect to the fact, that – particularly in view of the globally increasing population - the raw materials for the chemical industry are limited, the utilization of renewable raw material - i.e. bio-material - if possible, will be necessary. Again, catalysis is the key to the efficient conversion of bio-mass into energy or chemicals.

As research in the above areas is very fundamental by nature, it is dominated by long term thinking, rather than by short term product life cycles which, in addition may be influenced by fluctuations of the economy. Progress with effect on sustainability is expected to occur in the areas outlined above.

Catalysis is truly multidisciplinary not only with respect to societal items but also with respect to various disciplines: inorganic chemistry, organic chemistry, bio-chemistry, chemical engineering, bio-engineering, materials science, surface science, kinetics, and theoretical chemistry comprising quantum chemistry and molecular modeling.

Progress in catalysis is society driven. The catalyst industry adds high value to goods produced. The goods and services created from petrochemistry, refining and polymerization catalysis were estimated to be about 200 to 300 times the value of the catalysts [1]. Reducing the cost of production of goods, reducing the consumption of natural resources, reducing emissions routing the direction of

---

[2] The macro-cycles for energy have been more or less based on wood, coal, oil, gas and may be based on hydrogen in the future

[3] Annually, about 110 billion Nm^3 of natural gas are flared (1992 data, 4% of total commercial output are just flared!)

innovation are just aspects of the overall driving force. Through its processes and products industrial catalysis contributes about one quarter to the gross national product of the industrialized countries [2]. Furthermore, the chemical industry employs a large number of workers. US chemical industry employment in 1994 averaged about one million [3], German chemical industry employment roughly half of that value [4].

In 2001 the value of the catalyst world market (including captive use) was estimated at about 12 billion US$. Other sources [5] estimated the 1999 world market for catalysts (including precious metals) to be of the order of 9 billion US$ with 24 % for refining, 23 % polymers, 24 % chemicals and 29 % environment.

The chemical industry has a multiplier function with respect to subsequent industries. Chemicals are supplied to almost every other industry: food, clothing, health care, transportation, to name just a few. Every US automobile for example contains about 2.200 US$ of chemical processing and products [6]. What is more, the fuel for the automobile is coming from a refinery where catalysis plays the dominant role. The role of chemicals in everyday products becomes apparent mostly through polymers (plastics). The manufacture of the plastics from oil, coal or gas comprises in almost all cases at least one catalytic step. But not only cars and trucks rely on polymers, also homes and offices as well as computers. Moreover, an increasing number of industrial plants and trade shops need catalysis to protect the environment from toxic emissions.

Table 1. 2001 Catalyst world market

Area	% of 12 Billion US$	% of 9 Billion US$ [7]
Refining	23	28
Petrochemistry	26	25
Polymerization	16	26
Environment	35	23
thereof 90 % Automotive		

2. Petrochemistry

Petrochemistry, representing about one quarter of the catalyst market, can be broken down as indicated in Table 2. It should be noted, however, that olefins as an important category are not mentioned in the table because presently most of the olefins are produced by steam cracking and some through FCC. "Commodity petrochemicals represent a maturing business, with market growth inevitably tied to GDP growth. Within the developed regions, individual product group growth rates will depend heavily on intermaterial substitution, i.e. the ability of companies and products to penetrate markets held by the competitor" [8]. Reaching and maintaining technology leadership is the common method to generate and sustain the competitive advantage. In the case of commodity chemicals the economics of the process is highly dependent on the cost of raw materials. Technology leadership by decreasing petrochemical manufacturing cost is expected to come through the improvement of catalysts and processes e.g. being able to convert low value alkane feedstock into higher value petrochemicals.

Table 2. 2001 (Petro-) Chemical Catalyst World Market [9]

Area	Billion US$
Ammonia & Methanol	698
Oxidation	537
Hydrogenation	350
Organic Synthesis	292
Aromatics	206
Dehydrogenation	202

2.1   Olefins

Dehydrogenation processes (indicated under dehydrogenation in Table 2) count mainly for iso-butene, to a much smaller extent for propylene and up to now no ethylene has been produced by catalytic dehydrogenation. Because prices for olefins from steam cracking follow the oil price like a shadow [10] independent routes such as the dehydrogenation of low value paraffins are attractive. Table 3 shows the results of a demand study issued by ChemSystems [11] plus some current prices [12].

Table 3. Petrochemicals: estimated demand[9] and current contract prices[10]

Olefin	1998 Demand million tons	2003 Demand, estimated million tons	May 2002 Contract € per ton
Ethylene	80,4	105	510
Propylene	46,0	62	437
Butadiene	7,6	9	410
Benzene	29,0	36	399
p-Xylene	13,3	18	540
Ethylene glycol	10,3	31	-

Ethylene

Uses: more than one half of global ethylene demand is ascribed to polyethylene and other polymers. Other major derivatives are ethylene oxide/glycol, ethylene dichloride/vinylchloride and ethylbenzene/styrene. Smaller use is made of acet-aldehyde, LAO (linear alpha olefins) and vinylacetate.

Propylene

Today, steam crackers and FCC (Fluid Catalytic Cracking) units supply 66 % and 32 % correspondingly of propylene to chemical processes whereas propane dehydrogenation counts for only 2 %. Because FCC units predominantly produce motor gasoline, and steam crackers mostly ethylene, propylene will under these circumstances always remain a by-product. The question remains why traditional alternative commercial routes have not gained a higher market share than 2 %. Obviously the driving power of the state-of the-art dehydrogenation technology is

too weak to benefit from the difference of the cost of the high value propylene as compared to the low value propane. A step-change improvement of the catalyst and the process as well seems to be necessary.

Uses: Polypropylene accounts for about 55 % of propylene output and oxo-alcohols, acrylonitrile and propylene oxide each totals about 9 % while cumene about 7 % of West-European production [13].

Butadiene

Production: Butadiene is a by-product of the FCC process for the production of gasoline, as well as a by-product of the steam-cracking process for the production of olefins. Today about 20 % of the world butadiene demand is produced by dehydrogenation. The best known one-step dehydrogenation process is the Houdry Catadiene process, which has been in operation since 1943.

Uses [14]: Styrene-butadiene rubber (SBR) accounts for 31 % of global butadiene demand, followed by polybutadiene (PBR) at 28 %. Other uses are elastomers such as acrylonitrile-butadiene-styrene (ABS) resins and adipinonitrile with nylon 6,6 being the end-use. Most of the butadiene is extracted from the C4 fraction of the steam cracker (see above). Butadiene prices and margins have been too low to stimulate development of alternative catalytic production routes and even to encourage new projects using existing technology. Rather, conventional catalytic conversion of butadiene together with proven separation technologies have led to a variety of products [15].

2.2   Direct Oxidation of Paraffins

The area can be clustered in three groups: (i) conversion of paraffins to olefins by dehydrogenation, (ii) conversion of paraffins to oxygenates and (iii) conversion of paraffins to nitrogen containing compounds. Due to the importance of innovation in the area of paraffin activation one chapter of the present monograph is exclusively devoted to paraffin conversion: "Partial Oxidation of Light (C_2 to C_4) Hydrocarbons (Fundamentals and Industrial Application)", in addition a few re-marks are added to the oxidative conversion of methane.

2.3   Dehydrogenation

The importance of developing new economical more feasible processes to convert short chain paraffins into high value olefins has been discussed above. The need for a new dehydrogenation technology should not be driven by the demands of today's market. The olefins supply, demand and price issues are effected by several different economic factors and all are of short term nature. For instance, there was a time when the industry was short in propylene and this triggered the development of catalysts containing ZSM-5 and similar additives to boost the propylene yield of the FCC process. However, a short term solution for a particular propylene shortage should not prevent the R&D community from developing a solution for converting low-value paraffin into higher-value olefins, which is a long term issue.

From an industrial point of view the challenges still are: (i) longer cycle time of the catalyst, (ii) higher conversion, (iii) lower steam to paraffin ratio (in cases of steam usage), safe process technology (in case of oxidative dehydrogenation) and better selectivity (in the case of oxidative dehydrogenation). The same criteria are also applicable for alkyl-aromatics such as ethylbenzene. In that case, low steam to oil and better selectivity are today's most important targets for the conversion of ethylbenzene to styrene.

2.4   Methane Conversion

The proven technology of the partial oxidation of methane is the conversion to synthesis gas (see e.g. Baerns and Kondratenko) to produce either chemicals or fuels. The "chemicals" may be hydrogen, ammonia or methanol and the products produced from these chemicals. The fuels may be (i) gasoline via methanol or via Fischer Tropsch or (ii) diesel via waxes from Fischer Tropsch process technology, i.e., the conversion of synthesis gas to hydrocarbons. Because the volumes of gas from the particular sources are huge, large output of products is necessary: "MegaMethanol", fuel, polypropylene, polyethylene…

Methanol can easily be shipped from remote areas where natural gas plants used to be located to the sites of the chemical industry. Enormous quantities of methanol would be used for high value added chemicals such as ethylene or propylene or even higher quantities for fuels.

The real challenge for catalysis and a step change of technology would be the direct conversion of methane to formaldehyde or to acetic acid or, most preferably, to methanol (see e.g. Buyevskaya and Baerns). In the latter case huge volumes are needed for tomorrow's MegaMethanol market.

2.5   Direct Conversion of Paraffins to Nitrogen-containing Compounds

Huge efforts have been devoted to developing new and direct routes to nitriles. But there is still much room for improvement. The recently developed conversion of propane to acrylonitrile is less selective than the proven commercial processes based on propylene feed stock. The lower selectivity causes higher unit consumption of the paraffin relative to the olefin and the plant has to be larger to some extent which results in a higher cost of depreciation. Hence, for the paraffin based processes a step change in performance is necessary to take full benefit of the lower feed stock cost [16].

3.   Refining

Refining, representing another quarter of the world catalyst market, comprises two major processes. As shown in Table 4, a total of 645.000 tons per annum of solid catalyst are produced world-wide, worth 2.2 million US$. The highest catalyst volumes are consumed for catalytic cracking. In Western Europe catalytic reforming is the most important refining process, as can be taken from the figures in Table 5.

Table 4. Refining processes: production and sales

Processes	Thousand tons	%	Billion US$
Cracking	495	77.0	0.7
Hydrotreatments	100	15.5	0.72
Hydrocracking	7	1.1	0.10
Reforming	6	0.9	0.12
Others	~35	5.5	0.56
Total solids	~640-650	100.0	2.2
Alkylation	3100*	-	0.85

« Others »: catalysts for H2 production, polymerization, isomerisation, etherification., Claus, lubes etc...

* approximate values.

Table 5. The gasoline components of different process technologies in the USA and West Europe along with their octane numbers [17]

Source	USA %	W.Eur.%	RON	MON[4]
Distillation	3.8	7.5	65-80	60-75
Reforming	34.0	**40.0**	100	89
FCC	36.0	27.0	93	80
Pyrolyse	~ 0	~ 0	82-96	74-85
Hydrocracking	2	~ 0	85	80
Isomerisation	4.5	10.0	85-88	82-85
Alkylation	13.0	9.0	94	92
Polymerization	~ 0	~ 0	95	82
Butanes	5.0	5.5	95	92
MTBE	1.7	1.0	113-117	95-101

* benzene = low values in the case of low T pyrolysis (VB or Coking) and very high in the case of Steam cracking.

The reformate has very high research octane number (RON)[5] but is also high in aromatics. Today in most cases there is no necessity to completely remove benzene from motor fuel and a significant portion of the benzene and alkyl-benzene fraction is supplied to the aromatics complex. However, the European 2005 Auto Oil Program calls for a significant reduction of aromatics in fuels from the presently 42 vol.-% down to 35 vol.-% in the future. This, obviously, will directly affect naphta reforming, because the production of high RON aromatics is the ultimate goal of the catalytic reforming process. Because of the very high volumes of fuel as compared to chemicals, the excess of aromatics resulting from the reduction of aromatics in fuels (from 43 vol.-% to 34 vol.-%) cannot fully be used by the chemical industry. The entire market for solvents or aromatics being based on the amount of monomers for the polymer industry is too small to cope with the huge volumes which will swap from the refinery to the chemical industry.

---

[4] MON is the motor octane number obtained from a motor test procedure

[5] RON is the research octane number, which basically is calculated from the chemical composition of the gasoline

Table 6. European specification for the year 2005

	Europe 2000	Europe 2005	California (CARB Phase I)[6]
RVP (Summer), bar[7]	6.0	AO-II	5
Sulfur, ppmw	150.0	50	30/80
Benzene, vol.-%	1.0	1.0	0.8/1.2
Olefins, vol.-%	18.0	AO-II	4.0/10.0
Aromatics, vol.-%	42.0	35	22/30
Oxygen, wt.-%	2.7	AO-II	1.8/2.2

Therefore, a considerable amount of the aromatics needs to be converted to components with the highest possible RON. The increase of 1 RON corresponds to about 900.000 US$ per year for a 300.000 tons per annum hydro-isomerisation unit. In Table 5 several major refinery processes to improve RON are shown: these include isomerisation, reformation, addition of FCC-Naphtha, alkylation, addition of oxygenates or polygas or butanes. The effect of these options with respect to the new specifications is different for each particular process. Keeping in mind the Californian ban on MTBE and also the fact that the oxygenate content has to be reduced to half of the present value, one option would be alkylation or/and isomerisation" [18].

Table 7. Specifications of gasoline components [19]

Source	S (ppm)	Arom. vol %	Benz. vol %	Olef. vol %
Distillation	100-200	2-4	1-2	< 1
Reforming	0	60-75	3-5	< 1
FCC	500-2000	25-35	0.7-1.5	40-50
MTBE	0	0	0	-

The naphtha feed stock used for the catalytic reformer comprises a mixture of about 300 different compounds (paraffins, naphthenes and aromatics) in the range of carbon numbers between C5 and C10. The catalytic reactions are dehydrogenation of naphthenes, isomerisation of paraffins and naphthenes, dehydrocyclization of paraffins and hydrocracking. Reforming catalysts generally possess both an acidic and a metallic function. The two functions need to be balanced thoroughly for each reaction condition and feed stock. In principal, it is possible to boost the LPG yield significantly. Special catalysts can increase the C4-yield from about 3-7 wt.-% up to 20-24 wt.-% [20]. For use in the fuels pool, these C4´s need to be converted further to higher molecular weight compounds because of the vapor pressure limitations.

---

[6] CARB is a Californian Clean Air Act
[7] RVP is the vapour pressure measured according to an internationally agreed procedure

4.   The Application of Zeolites in Catalysis

In 1998, the world market for the synthetic zeolites was estimated to be about 1.6 billion US$, of which catalysts represented slightly more than 50 % by value [21] but only about 12 % or 160 thousand tons of zeolites by volume.

The majority of the refining processes indicated in Table 4 are based on zeolites: cracking (FCC), reforming, isomerisation, hydrocracking and to a certain extent, dewaxing, isodewaxing and polymerization. Zeolites of structure type FAU dominate the refining applications both in volume and value. MFI-type and MOR-type zeolite containing catalyst are also widely utilized in the refining processes. Other zeolite structures are applied in niches only.

In the area of petrochemicals, the dominant use of zeolites is in the trans-formation of aromatics (alkylations, isomerisation, disproportionation, trans-alkylation) which, in 1999, correspond to 8.4 % and 6 % of the value and tonnage of petrochemical catalysts, respectively. For the commercial conversion of aromatics, catalysts containing the zeolite structure types MFI, MOR, BEA and MCM-22 as major component are used.

SAPO-34 and MFI based zeolites are used for the conversion of methanol to short chain olefins. Once the demonstration plant scale has turned into commercial success, the demanded zeolite volumes will be of the order of several hundred tonns per plant and per annum.

5.   Homogeneous Catalysis and Polymerization

Polymerization, accounting also for about one quarter of the global catalyst market, is dominated by two major homogeneous processes: ethylene polymerization and propylene polymerization. Two major types of catalyst sys-tems are used. New generations of Ziegler-Natta type and metallocene-type catalysts. Because of the importance of polymerization catalysis, a separate chap-ter of this monograph will deal with that subject.

Other homogeneous catalysed commercial processes for bulk chemicals: are hydroformylation and to a much lesser extent metathesis. Metathesis may achieve greater importance in the future to increase propylene yield from steam-cracking units by reacting butenes and ethylene. In addition, many high-value fine chemicals in the field of health, food and home care are produced via homo-geneous catalysis. This very interesting topic will be discussed in a separate chapter of this monograph.

Hydroformylation: Aldehydes are produced in large quantities by the homo-geneous catalytic reaction of carbon monoxide and hydrogen with an olefin. Most of these so–called oxo-aldehydes are further processed to the corresponding oxo-alcohols. The 1997 consumption figures have been reported to be close to 8 million tons per annum [22]. 66 wt.-% thereof account for n-butyraldehyde for the production of the plasticizer alcohol 2-ethylhexanol (about 33 wt.-%) and n-butanol (about 33 wt.-) for the coatings industry. About 15 wt.-% of the total oxo-alcohol production are C5-C15 plasticizer alcohols and about 9 wt.-% of the total oxo-alcohol comprising iso-butyraldehyde for the polyester and resin industry. The long chain detergent alcohols accounting for about 5 wt.-% of the total oxo-alcohols compete with alcohols from renewable resources.

6.   The Preparation of Catalysts

The preparation of heterogeneous catalysts is still mainly based on the knowledge and experience of man rather than on rational design at molecular and atomistic level. Molecular modeling and molecular design, for the time being, are more often successfully applied to homogeneous catalysts. A somewhat different approach is taken by high-throughput experimentation. Libraries of formulations, physical and chemical properties and catalytic data for various chemical reactions are intentionally created for particular reactions. Over several generations of catalyst preparation, characterization and testing, progress towards the target reaction is achieved. The set of starting data as well as the selection of best candidates (for improvement) between the generations can be done by e.g. genetic algorithm, by chance or semi-empirical, i.e., based on experience, literature data of similar situations and personal knowledge. In spite of the fact, that huge progress has been made in surface and material science and several new physical methods have been introduced to catalysis during the last decades, there is still a long way to go until rational molecular design of catalysts for particular reactions will be common practise.

The reason for this situation may be, that catalysis is a very complex science and technology. Taking zeolites as an example, the design should be precise over many orders of magnitude:

(i)   on the atomistic scale (0,1 nm), the location and particularly the nearest and next nearest neighbours of e.g. the protons need to be designed, then prepared in an experiment, and finally should be preserved under reaction conditions,

(ii)   the residence time of reactants and product molecules close to the active site is determined by zeolite pore (1 nm) and window size, which is known for ideal single crystals, but for agglomerates and polycrystals a variety of different active sites and pores is formed, which either have to be avoided or have to be designed on purpose,

(iii)   moreover, in cases of the successful preparation of single crystals with pre-determined location of the active site and a predetermined pore system, the crystal size (5 – 5000 nm) and morphology should be designed and then realized by experiment because e.g. in catalysis the length of the diffusion path of the products through the crystal influences the probability of consecutive reactions,

(iv)   furthermore, the crystallite size distribution determines the porosity (micro-, meso- and macroporosity, accessibility and residence time) of the shaped catalyst, which in turn influences the crush strength of the particle, which then has to be improved by designing and thereafter using an appropriate type and amount of (inert) binder,

(v)   finally, the shaped particle (1 mm) has to be designed to obtain a maximum of active sites at a minimum of pressure drop in the reactor (1 m).

(vi)   And finally all the specifically designed properties need to be produced and guaranteed throughout a delivery-batch of five up to one hundred tons.

A special chapter of this monograph will deal with the design and preparation of mesoporous materials.

7.   In situ Characterization of Catalysts

In situ characterization of the catalyst in the working stage is a very important tool for getting information on the physical and chemical characteristics of the working catalyst. This monograph will report on current developments in this field. In recent years great progress has been made in developing new methods. In some cases very good correlations have been found between certain physical and chemical properties and the catalyst performance. In several cases these physical and chemical properties could be correlated with particular routes of catalyst production or specific techniques of catalyst activation on an industrial scale. Although these characterization tools help to understand in retrospect why a catalyst or a particular process condition is favorable to the desired product, there are great expectations for the near future that these methods will help to find optimised process conditions or optimised catalyst properties and that these methods will support a rational catalyst and process design in the long term.

8.   Catalytic Reaction Engineering

Catalytic reaction engineering should be an integral part of any rational catalyst and process design. New reactor concepts in combination with new analytical tools to follow in situ the kinetics of a catalytic reaction characterize the progress, that has been made. One of the few unconventional reactor concepts that has already been practice in industry for many years is catalytic distillation. In order to overcome equilibrium constraints this concept is used for a variety of chemical reactions. Miniaturization of catalytic reactor is another new direction of interest. Aiming at the vehicle sector, this technology will become very important in conjunction with the development of small hydrogen processors for fuel cells. Some of the aspects are also dealt within this monograph.

References

1   The Catalyst Group, The Intelligence Report, *"Global Shifts in Catalyst Industry"*, 2000
2   I.E. Maxwell, in *"11th International Congress on Catalysis – 40th Anniversary"*, edited by J.W. Hightower, W.N. Delgass and E. Iglesias, Elsevier, Studies in Surface Science and Catalysis, Vol. 101, p.11986,
3   A.J. Lenz, J. Lafrance, US Department of Commerce, Office of Technology Policy, 1996, "Meeting the Challenghe: US Industry Faces the 21st Century; The Chemical Industry"
4   VCI, "The German Chemical Industry", April 2002, www.vci.de
5   Ch. Marcilly, Studies in Surface Science and Catalysis vol. 135, "Zeolites and Mesoporous Materials at the Dawn of the 21th Century", Eds.: A. Galarneau et al, Proceedings of the 13th International Zeolite Conference, Montpellier, 8-13 July, 2001
6   ibid 3,
7   Chemical Week November 4, 1998 estimate for 2003

8   B.H. Pickover, Chem Systems, Tarrytown, New York, in Hydrocarbon Processing, March 1999, p.30

9   Chemical Week November 4, 1998 estimate for 2003

10   S. Kvisle, H.R. Nilsen, T. Fuglerud, A. Gronvolt, B.V. Vora, P.R. Pujado, P.T. Barger and J.M. Andersen, DGMK-Tagungsbericht 2001-4, page 73, "Proceedings of the DGMK Conference - Creating value from light olefins Production and Conversion", October 10-12, 2001, Hamburg

11   Petroleum Technology Quarterly, PTQ Summer 1999, page 10; cit.: ChemSystems, Petrochemical Capacity and Supply/Demand Database 1999,

12   ECN, 6-12 May 2002

13   ECN Petrochemicals Fact File 2001

14   ibid.,13

15   St. Müller, A. Gammersbach, H.-J. Krämer, F. Kadelat, DGMK-Tagungsbericht 2001-4, page 115, "Proceedings of the DGMK Conference - Creating value from light olefins – Production and Conversion", October 10-12, 2001, Hamburg

16   ibid, 13

17   Ch. Marcilly, Studies in Surface Science and Catalysis vol. 135, "Zeolites and Mesoporous Materials at the Dawn of the 21th Century", Eds.: A. Galarneau et al, Proceedings of the 13th International Zeolite Conference, Montpellier, 8-13 July, 2001

18   F. Schmidt, Proceedings of the IZA Pre-Conference School, Poitier, 2001, to be published

19   ibid. 5

20   A.P. van den Bosch, DGKM Tagungsbericht 9705, Proceedings of the DGMK Conference „C4-chemistry – Manufacture and Use of C4 Hydrocarbons", October 6-8, 1997, Aachen

21   ibid. 19

22   G. Protzmann, K.-D. Wiese, DGMK Tagungsbericht 2000-3, Proceedings of the DGMK Conference „Synthesis Gas Chemistry", September 27-29 2000, Dresden

II Selected Reactions in Heterogeneous Catalysis

Partial Oxidation of C$_2$ to C$_4$ Paraffins

Contents

Partial Oxidation of C_2 to C_4 Paraffins

Fabrizio Cavani and Ferruccio Trifirò

Dipartimento di Chimica Industriale e dei Materiali,
Viale Risorgimento 4, 40136 Bologna, Italy.
cavani@ms.fci.unibo.it

Abstract. This review examines the state–of–the–art in the oxidative transformation of C_2-C_4 alkanes to olefins and to oxygentaed compounds. Chemical, catalytic and technological aspects are discussed, in relation to both current industrial processes and processes under study or development.

1.   Introduction

The interest in the transformation of light alkanes to valuable oxygenated compounds and olefins by means of oxidation has been growing in recent years, due to the possibility of developing new processes of lower environmental impact and of lower cost with respect to current processes for the synthesis of the same chemicals. Many reviews and monographs have been published [1–21], which analyze the fundamental aspects related to the oxidative activation and transformation of light alkanes over heterogeneous catalysts. Table 1 summarizes the possible reactions of C_2 to C_4 alkane selective oxidation which are of industrial interest, and their stage of development.

The possibility of transforming *ethane* to acetic acid in one step is conditioned by the high chemical stability of ethylene, one of the most favoured products in ethane oxidative conversion [22–24]. Ethylene is always obtained together with acetic acid and carbon oxides. For the same reason, one possible commercial exploitation of ethane consists in a reaction where the olefin itself becomes the raw material for the transformation to a valuable chemical, either in the same reactor, or in an *integrated process*, where the ethylene–containing stream exiting from the first reactor is the feedstock (after necessary make–up) for the second reactor. An example might be the two–step ethane oxychlorination to 1,2-dichloroethane, where the ethylene produced by oxidehydrogenation of ethane in the first step may be transformed to the chlorinated desired product in a downstream reactor. An even more advantageous process is the direct transformation of ethane to vinyl chloride; this process was studied in the 1970's, but did not reach commercial application. Interest is now growing again, as documented by recent patents issued by companies which are PVC suppliers [25].

Besides the oxidation of n–butane to maleic anhydride, the second successful heterogeneous gas–phase process involving the oxidation of a paraffin which is soon going to reach the commercialization stage is the ammoxidation of propane to acrylonitrile, developed separately by Standard Oil and by Mitsubishi Chemical, for which fluidized–bed technology is employed [26–32]. Also in this case the stability of the product towards unselective consecutive reactions, has been a key factor for the development of the process till commercialization.

Table 1. Industrial processes and processes under study or development for the **oxidative transformation of light paraffins (C_2–C_4)**

Raw material	Product	Stage of development
Ethane	Vinyl chloride	Pilot plant
Ethane	Acetaldehyde	Research
Ethane	Acetic acid	Demonstrative plant
Ethane	Ethylene	Research
Propane	Acrolein, Acrylic acid	Research
Propane	Propyl alcohol	Research
Propane	Acrylonitrile	Demonstrative plant
Propane	Propylene	Research
n–Butane	Acetic acid	Industrial
n–Butane	Maleic anhydride	Industrial
n–Butane	Butadiene	Industrial, abandoned
Isobutane	Methacrylic acid	Pilot plant
Isobutane	Isobutene	Research
Isobutane	t–Butyl alcohol	Research

Recently, papers have been published which describe attempts to transform isobutane into methacrolein and methacrylic acid in a single step, a process that might replace the aceton–cyanohydrin technology for methyl methacrylate synthesis, and propane to acrylic acid [33–42], which might replace the industrial two–step oxidation of propylene. Interest from industrial companies for these reactions indeed goes back to the 1980's. In these reactions a further problem arises due to the high reactivity of the desired products (methacrylic acid and acrylic acid) which under conditions necessary for alkane activation are not stable and undergo unselective oxidative transformations.

The huge number of papers devoted to the reaction of oxidative dehydrogenations of paraffins is an indication of the scientific and industrial interest for alternatives to catalytic and thermal dehydrogenation/cracking, reactions which suffer from energetic drawbacks and thermodynamic constraints [5, 9, 17–20]. In these cases the advantage gained from the use of a cheaper raw material and of an exothermal process must be weighed against drawbacks such as the loss of valuable hydrogen (coproduced in dehydrogenation and in steam–cracking), the difficulty in separation of CO from the paraffin (in the case of ethane oxi-dehydrogenation, but also of methane oxidative coupling to ethylene), and the formation of traces of corrosive by–products. While in the case of ethane the problem mainly concerns the low reactivity of the molecule (the selectivity to the olefin which is achieved is usually high, due to the low ethylene reactivity and to the nature of the mechanism involved), in the case of oxidehydrogenation of propane and of n–butane to the corresponding olefins the selectivity problem is of

main concern. With the latter molecules, the formation of allylic oxygenated compounds is the reason for the low selectivity achieved, since they are readily transformed to carbon oxides.

Examples of the points which have been considered as key factors in determining the pathway of alkane transformation to the product of selective oxidation are:

1. activation of oxygen and of the alkane, and specifically:
   – role of adsorbed oxygen species [1–3, 6, 7, 11];
   – importance of the mode of alkane adsorption [1–3, 5];
2. reactivity of the reactant and of the product(s):
   – mechanism of activation of the C–H bond (heterolytic vs homolytic activation) [11, 13];
   – role of the stability of the products [9, 10, 12].
3. mechanism of transformation of the reactant:
   –importance of nondesorption of reaction intermediates [9, 10];
   –importance of the relative ratio between intermediate olefin (oxi)dehydrogenation and oxygen insertion in affecting the selectivity to oxygenated products in the oxidation of C$_{>3}$ paraffins [9, 10];
   –role of the nature of the reaction intermediate (hydrocarbon fragment) in determining the direction of oxidative transformation [11];
   –contribution of homogeneous reactions, especially for applications which require temperatures higher than 400–450°C [12];
   –effect of coadsorbates in facilitating the dissociative adsorption of saturated hydrocarbons [12].

The following catalyst features have been considered as fundamental tools to control catalytic performance (most of these aspects may be applied in general to hydrocarbon oxidation, while some of them are specific for alkane transformations):

1. surface of the catalyst, i.e. the nature of the active sites, and how the surface is affected by the bulk features and specifically:
   – density of the active sites [9, 10], which can be explained by the "site isolation" theory [43];
   – role of surface acidity [8, 11];
   – need for intrinsic surface polyfunctionality [9, 10].
2. structure of the catalyst:
   – the redox properties of the metal in transition metal oxide–based catalysts, in terms of reducibility and reoxidizability of the active sites, and the metal–oxygen bond strength [5];
   – the reactivity of specific crystal faces in the different transformations which constitute the reaction network [2, 6];
   – role of structural defects in favouring the mobility of ionic species in the bulk [1, 2];
   – importance of cooperation effects of different phases in obtaining catalysts with improved performances [12, 44];

– importance of the interaction between the support and the active phase in modifying the catalytic properties of the latter [12].

2.   Classes of Catalysts
      for the Selective Oxidation of Alkanes

Catalysts which can activate and oxidize paraffins belong to very different classes, which not only differ in the redox properties and thus in the ability to i) effectively make electrons exchange between the metal cation and the organic substrate, ii) abstract hydrogen from the reactant and iii) possibly insert ionic oxygen into the latter, but also possess very different acid/base properties. It is possible to broadly classify catalysts for alkane oxyfunctionalization into the following classes:

Catalysts based on reducible metal oxides (typically, d-type transition metal oxides), for which a heterogeneous, redox–type mechanism is operating. In general, the mechanism may include the formation of an intermediate alkoxy species (this can also arise from the evolution of an alkyl ion or radical species). This occurs preferentially at lower temperatures (i.e., less than 450–500°C), but the temperature is a function of both i) reaction conditions, such as pressure and reactant concentration, and ii) the alkane reactivity. Either the olefin or other oxygenated products can be the prevailing product, depending on the nature of the alkane and on the redox properties of the active species. The ratio of the rates of evolution of the adsorbed intermediate to yield the desired product and of further reaction to carbon oxides determines the selectivity of the reaction.

It is well known that the oxidation state of transition metal ions which constitute the active component of mixed oxide–based catalysts is a function of the operating conditions of the reaction, since the surface of the catalyst is in dynamic interaction with the gas phase [2, 21]. If operation is carried out under hydrocarbon–rich conditions (thus with molecular oxygen as the limiting reactant), under stationary conditions the active component may possess a lower oxidation state than under hydrocarbon–lean conditions. This also affects the catalytic performance in terms of activity and selectivity. Indeed usually more oxidized surfaces result in more active but less selective catalysts, while the opposite is true for more reduced surfaces. A lower oxidation state for the metal ion corresponds to a surface which is poorer in oxygen ions, and thus exhibits either a lower number of O^{2-}–insertion sites, or possibly an electron–richer surface where the metal–oxygen bond strength is different with respect to the fully oxidized surface, resulting in sites with modified oxidizing properties. All this in practice corresponds to the well–known "site–isolation" theory, developed years ago by Callahan and Grasselli [43], which claims the importance of having a statistically controlled number of surface oxidizing sites in order to favour the selective oxidation reactions against the combustion reactions.

This has been the fundamental driving force for developing processes which operate in the absence (or in the Aresence of very low amounts) of oxygen in the gas phase. Indeed other advantages exist, such as the absence of hazards associated with the possible formation of flammable mixtures, which are instead possible when the hydrocarbon and the oxidant are co–fed. The most important

example is the DuPont process for the oxidation of *n*–butane to maleic anhydride [45–50].

A particular case, which can be considered as intermediate between completely heterogeneous mechanisms and homogeneous reactions, are those reactions which even though they occur on redox–type catalytic systems, include a first step which occurs in the gas phase. An example has been reported by Moro–oka et al. [51, 52] for the oxidation of propane to acrolein over Ag/Bi/V/Mo mixed oxides. In particular, under the conditions employed (temperature around 500°C), the thermal dehydrogenation of propane in the gas phase led to the formation of propene, which was then selectively converted to acrolein on the catalyst surface by O–insertion sites.

Catalysts based on nonreducible metal oxides (or, sometimes, systems which are very difficult to reduce under the reaction conditions), for which the mechanism is initiated on the catalyst and then transferred into the gas phase (or, at least, in the close proximity of the catalyst surface), via radical fragments obtained by homolytic scission of C–H and C–C bonds in the reactant. Electron exchange may occur anyway, but the mechanism of interaction between the catalyst and the reactant is not a classical redox one.

A considerable amount of research work describes the use of these catalyst types. This is the case of methane oxidative coupling, where most active catalysts are those based on alkaline earth oxides, such as MgO and CaO, doped with alkali metal ions, but the same class of catalysts has also been found to be active and selective in the oxidehydrogenation of ethane to ethylene [53–62]. Since these compounds lack bulk–O^{2-}–insertion properties, they are not used when the reaction is aimed at the production of oxygenates.

Systems which are known to operate a nonredox–type activation of molecular oxygen and/or of paraffin are [17]:

1. *Alkaline earth oxides*, doped with various components, the latter being aimed at increasing the contribution of surface defects for hydrocarbon and oxygen activation [55–68]. These are essentially p–type semiconductors, at least at the temperatures used for paraffin activation. Alkali metal–doped and rare earth–doped alkaline earth compounds are amongst the most effective catalysts for ethane oxidehydrogenation. Promotion of chlorine, either directly fed to the reactor with chlorine–containing compounds, or added in the catalyst composition, lowers the reaction temperature considerably, and increases the selectivity to ethylene in methane oxidative coupling and in ethane oxidehydrogenation. The effect of chlorine can be different: i) gas phase reactions involving chlorine radicals can contribute measurably to the activation of the paraffin and to the formation of ethylene from ethane, thus increasing both conversion and selectivity; and ii) chlorine–modified active sites may be involved in the reaction; in particular, chlorine may inhibit the centers responsible for total oxidation.

2. *Rare earth oxides*, which are p–type semiconductors (La_2O_3, Sm_2O_3, Dy_2O_3), even though ionic–type conductivity can contribute in some cases [69–82]. Cerium and praseodymium oxides (which instead are *n*–type semiconductors, and also exhibit remarkable ionic conductivity) are nonselective to C_2 from methane, and in paraffin oxidehydrogenation as well, due to the high activity in

methyl radical attack by active oxygen species, which leaves less time for methyl radical dimerization. Alkaline earth metal–doped or alkali metal–doped rare earth oxides are particularly effective catalysts.

3. *Silica* also exhibits unexpected oxidizing properties [83–86]. It is active in the oxidation of methane to formaldehyde. Silica also is active in the ammoximation of cyclohexanone to cyclohexanone oxime, intermediate in the synthesis of caprolactam. In these cases it has been proposed that surface defects (reduced sites) are the sites for the generation of active oxygen species. The formation of O_2^- species, which are initiators of radical reactions occurring on the solid surface, was detected by means of EPR and measurements of surface potential.

The contribution of homogeneous radical reactions in alkane oxidation can in general be neglected with those catalysts which typically operate at mild temperatures. On the contrary, gas–phase reactions may play a fundamental role when operation is carried out at the higher temperatures, thus typically on nonredox type catalysts [87–92]. Rare earth oxides and alkaline earth oxides, and in general nonreducible metal oxides, activate methane and ethane only at temperatures higher than 500–600°C. Besides the high temperatures used, reactant mixtures often are used with compositions which fall inside the flammability bell, and in the case of more reactive alkanes the temperatures used are close to the autoignition temperatures. In these cases the contribution of homogeneous reactions becomes fundamental, and the mechanism involves the contribution of alkyl radical species, which are generated at the catalyst surface and then may either i) quickly react at the adsorbed state (for instance, be transformed into the corresponding olefin via β–elimination, or undergo nonselective oxidative attack by adsorbed oxygen species), ii) alternatively further react in the close proximity of the catalyst surface (i.e., in the film which develops under laminary flow conditions), or iii) be transferred into the gas phase, where the reaction proceeds.

Catalysts based on noble metals, which are usually considered as nonselective oxidation systems (i.e., they are typically used for combustion), but which under particular reaction conditions may become selective catalysts. Of particular relevance are the results of Schmidt and coworkers, who made an extensive study of paraffin oxidehydrogenation and methane partial oxidation in monolith–type reactors under autothermal conditions [93–99]. Noble metal (Pt, Pd, Rh) coated on ceramic foam monoliths were used. With these systems, control of the oxygen–to–hydrocarbon ratio, coupled with the high surface temperature reached on the very active metal surface, allows the reaction pathway to be addressed towards the formation of olefins. In fact, the key point of this catalyst type is the strong temperature difference between the surface (where temperatures are as high as 1000°C) and the gas phase, due to the limitation of heat exchange through the film. Moreover, in these reactor configurations the residence time with respect to the thin layer of the catalytically active component is a few milliseconds. Very slow deactivation due to coke deposition was observed, and the selectivity to olefins (ethylene from ethane, propylene and ethylene from propane and from *n*-butane, propylene and isobutene from isobutane) was in most cases higher than 60%, at very high paraffin conversions.

3. Technologies aimed at Control of the Oxygen Supply to the Catalyst

In the case of redox type catalysts, the control of the properties of the catalyst is fundamental in order to obtain the best performance. Examples exist in the literature which describe the use of reactor technologies aimed at control of the oxygen supply to the reaction medium for the selective oxidation of paraffins. In particular, there is considerable interest in the use of catalytic membrane reactors, where the oxygen supply is controlled either via selective ionic diffusion (dense membranes), or through control of molecular diffusion (inorganic porous membranes) [100–102].

In porous inorganic membranes, the hydrocarbons and oxygen are fed separately at the core and shell sides of the membrane reactors. One advantage lies in the possibility of supplying oxygen to the reaction zone (where the catalyst is placed) in a distributed fashion over the entire reactor length, instead of feeding it together with the hydrocarbon at the reactor entrance. Therefore, the supply of the oxidant is governed by mass transport laws through the porous membrane. In this way the concentration of oxygen all along the reactor can be kept sufficiently low to kinetically favour the partial oxidation reactions instead of a complete hydrocarbon combustion, and to keep the catalyst at a desired average oxidation level. A further advantage of this configuration is that the reactants are kept separate, so as to avoid any flammability hazard; it is thus possible to feed undiluted fuels.

Most publications which describe the use of membrane reactors deal with methane oxidative coupling [103–106]; a few papers have described the oxidehydrogenation of propane to propylene [107–109]. In the latter case, either a V/Mg/O based catalyst was used, or a V_2O_5/γ–Al_2O_3 based catalyst; in both cases the active component was coated in the form of a thin layer over the ceramic α–alumina membrane. However, no significant membrane effect was found. In the case of the V/Mg/O system, no difference in the performance was observed between the cofeeding mode and the separate feeding mode. On the contrary, an improvement in the selectivity was observed when a hybrid membrane configuration was adopted with separate feeding, where a V/Mg/O catalyst bed was enclosed in a microporous zeolitic membrane reactor. Analogously, no differences between the cofeeding configuration and separate feeding were observed in the case of the V_2O_5/γ–Al_2O_3 based catalyst dispersed on the ceramic membrane [108, 109]. However, an improvement in selectivity to propylene, due to a lower contribution of the consecutive propylene oxidation to carbon oxides, was observed when the performance obtained with the membrane reactor was compared with that of a packed bed reactor. Furthermore, the turnover number was substantially improved. This effect may be attributed to a more efficient transport mechanism (i.e., convection instead of diffusion), as a consequence of the very low residence time of gaseous components with respect to the thin layer of active component (in the order of few milliseconds). A very low residence time of the hydrocarbon in the catalytically active material has also been claimed to be beneficial for selectivity in the formaldehyde dehydrogenation, due to a more narrowly distributed residence time of reactant and product in the pores of the catalytically active layer with respect to the bulk of the same active component [110].

Solid–electrolyte membranes for the ionic diffusion of oxygen are made of ZrO_2, CeO_2, ThO_2, Y_2O_3–ZrO_2, $SrCeO_2$ [111]. Materials exhibiting superior conduction rates are constituted of perovskite solids (La/Sr and Y/Ba/Cu mixed oxides), which can transport oxygen with a rate of $10^{-11} \div 10^{-9}$ mol cm^{-2} s^{-1} through a vacancy diffusion mechanism. The mechanism consists in a dissociative chemisorption of molecular oxygen, with ionization of atoms and transport of the latter through the crystalline lattice up to the opposite surface where they lose the charge and again form oxygen. The driving force for the diffusion of the O^{2-} species can be either a difference of the pressure at the two sides of the membrane, or an electrical potential gradient obtained by electrodes deposited on the sides of the membrane. The possibility of pumping specific ionic oxygen species at a controlled rate directly to the catalytically active surface of the catalyst, may allow very specific oxidation reactions to be carried out, thus with a theoretical very high selectivity to specific products. The limitation of these materials is however the low rate of diffusion, and thus the low productivity which can be achieved. In addition, one technological limit consists in the sealing of these membranes into devices which have to operate at high temperature.

Different applications which make use of oxygen–conducting electrolytes have been claimed, expecially in the oxidative transformations of methane [112, 113]. In this case, a further advantage is the rejection of nitrogen (when air is fed to the shell side of the membrane). In this way it is possible to overcome the problem associated with separation of nitrogen from the products and the unconverted reactant in the methane oxidative coupling. An electrochemical reactor, using yttria–stabilized zirconia (YSZ) as a solid electrolyte, and gold and silver as the anode and the cathode, respectively, has been used for the oxidation of alkanes at temperatures lower than 475°C [114, 115], and for the partial oxidation of methane to syngas [116]. It was reported that ethane, propane, n-butane and isobutane can be oxidized with good specificity to aldehydes and ketones (acetaldehyde from ethane, acetone, propylene oxide and acrylaldehyde from propane, methylvinylketone, methylethylketone and butyraldehyde from n–butane, methacrolein from isobutane), even though at rather low conversion.

Another remarkable example of a reactor technology aimed at the control of oxygen supply is the CFBR (Circulating Fluid Bed Riser) reactor developed by DuPont for the oxidation of n–butane to maleic anhydride (intermediate for tetrahydrofuran synthesis), which is now commercially available [45–50]. Similar technologies for alkane oxidation have been developed (but not made commercial) by ARCO for methane oxidative coupling and for paraffin oxidehydrogenation [117] and also claimed by Monsanto for propane ammoxidation [118]. Indeed, the first example in the field of hydrocarbon selective oxidation was developed for the ammoxidation of m–xylene [119]. All of these processes have a first step which operates under (almost) anaerobic conditions, and a second step where the reduced catalyst undergoes reoxidation by contact with molecular oxygen. It is thus possible to decouple the two steps of the redox reaction in two separate reactors, and make the hydrocarbon (HC) interact with the oxidized catalyst cat_{ox} in the absence of gas–phase oxygen to yield the oxidized product (HCO):

$$HC + cat_{ox} \rightarrow HCO + cat_{red}$$

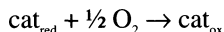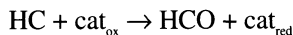$$cat_{red} + \tfrac{1}{2} O_2 \rightarrow cat_{ox}$$

Figure 1 shows the simplified flow–sheet of the DuPont process for tetra-hydrofuran production. Continuous catalyst reactivation by transport from the reaction vessel to the regeneration one is achieved. Very fast, exothermic reactions can be managed better than in fluidized–bed reactors. The operation becomes intrinsically safe, since the hydrocarbon and oxygen are not fed together, but separately in the two vessels. In addition, other advantages with respect to fixed–bed technology or conventional fluidized–beds, are:

1. High flexibility of the plant, since the two sections can be designed and optimized separately by choosing the best conditions for each. Only the oxidation processes involving an oxygen ion transfer from the catalyst surface to the organic substrate occur, while undesired reactions involving molecular oxygen in the gas phase (i.e., homogeneous reactions of combustion) do not occur.
2. Higher throughput, because of the higher gas velocity and the possibility to independently optimize the kinetic conditions for the two stages.
3. Excellent intragrain and interphase heat and mass transfer, because of the fine solid particles used, and of the high gas velocity relative to the solid. Consequently, very high catalyst efficiencies can be achieved, and thermal gradients inside the particle can be considered minimal.
4. Higher product concentration, which means fewer recovery problems.
5. Like in turbulent fluidization, gas–solid contacting is improved with respect to the bubbling/slugging regime.
6. Possibility to achieve better control of temperature in the riser by efficient cooling (quenching) through injection of cold gas along the reaction pathway.

On the other hand, disadvantages are:

1. The need for a catalyst with peculiar properties: high attrition resistance and high availability of active centers even in the absence of one reactant (i.e., ready availability of bulk oxygen).
2. Significant uncertainty in scale–up, due to radial and axial gradients of the solid, and the lack of a model that allows for geometric parameters and discontinuity at the inlet and outlet of the riser to be foreseen.
3. Under anaerobic conditions undesired oxygenated by–products can form, which would be otherwise burnt in the presence of gas–phase oxygen.
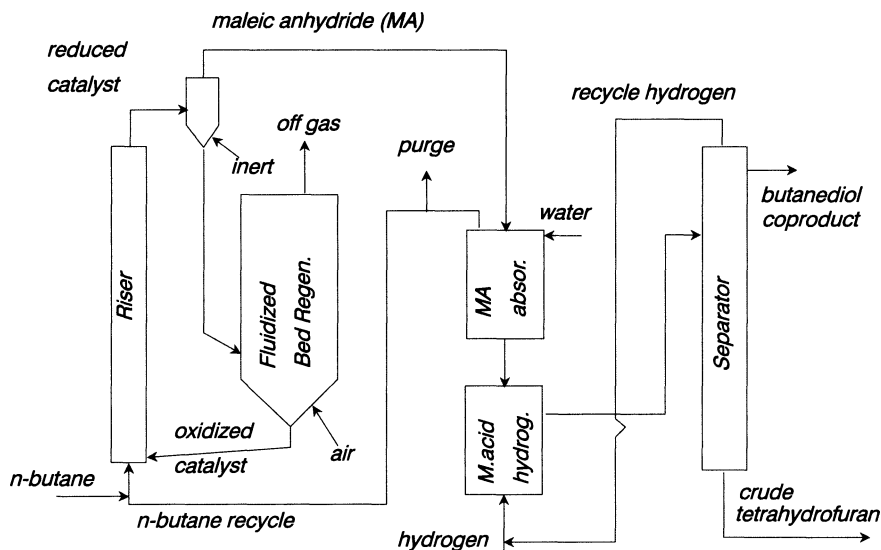
Fig. 1. Simplified flow–sheet of the DuPont process for tetrahydrofuran production.

4.   An Important Property: Catalyst Multifunctionality

From the materials point of view, it appears clear that there are no "simple" catalysts which can be used for the partial oxidation of a paraffin. All of the best systems are either constituted of several different components which cooperate in achieving the final product, or made of multicomponent structures which perform the different functions for a selective transformation. These different functions seem, therefore, to be a necessary feature for the activation of the C–H bond in the saturated substrate, for the multi–electron exchange and for oxygen (or nitrogen, or chlorine) insertion onto the latter [120, 121]. It is more or less clear that the cooperation of acidic and suitable oxidizing properties is a necessary condition. However, this is not sufficient, and best catalytic performances are obtained only when these properties are structured in such a way to allow the final product to be quickly reached, and rapidly desorbed before further oxidative transformations may lower the selectivity. A few examples amongst those described in the following chapters are clear systems having multifunctional properties, which thus couple in the same structure different moieties each one playing a well defined role in the reaction mechanism. This is true for i) vanadyl pyrophosphate, the catalyst for the industrial oxidation of *n*–butane to maleic anhydride, but which is also active for the oxidation of *n*–pentane to maleic and to phthalic anhydrides, ii) polyoxometalates, which are the systems of choice for the selective oxidation of isobutane to methacrylic acid and for propane oxidation to acrylic acid, and iii) mixed oxides which efficiently catalyze the trasformation of propane to acrylonitrile by ammoxidation, and which work well only when two different

functions are present, one aimed at the activation and oxidehydrogenation of propane, and one for the ammoxidation of the olefinic intermediate.

5.   Oxidation of Ethane to Acetic Acid

The oxidation of ethane to acetic acid:

$$C_2H_6 + 1.5 \; O_2 \rightarrow CH_3COOH + H_2O$$
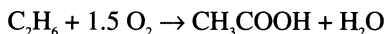
represents a case which is different from the oxifunctionalization of other light paraffins. The absence of intermediate products having allylic methyl groups (the presence of which may direct the reaction pathway towards specific products), as well the propensity of ethane to give radical–like mechanisms, makes the reaction much less sensitive to specific catalyst requirements (i.e, multifunctional sites, aimed at specific transformations and cooperating within the overall mechanism), and much more dependent on reaction conditions.

Catalysts which have been claimed for this reaction can be divided into different classes [122-138]. The first class corresponds to the mixed oxide of Mo/V/Nb (plus other components in minor amounts) first described in the paper by Thorsteinson et al. [122]. This paper can be considered as a milestone in the field of the selective oxidation of paraffins, in view of the number of active compounds which have been developed starting from catalysts therein described, and which exhibit surprising properties in the oxidative transformation of saturated hydrocarbons. Several patents have been issued by Union Carbide [123–127] regarding this catalytic system. The process and the catalyst claimed are aimed at ethane oxidehydrogenation, and acetic acid is only a minor by–product of the reaction. However the use of pressure above atmospheric enhances the formation of acetic acid with respect to that of ethylene. The main peculiarity of the catalyst is its capacity to activate the paraffin at low temperatures (lower than 250°C). Catalysts similar to those claimed by Union Carbide have been studied by Merzouki et al. [128, 129], and by Burch and coworkers [130–132]. In recent patents by Saudi Basic similar compounds (Mo/V/Nb/P/O) have been reported to perform excellently in the oxidation of ethane to acetic acid [133].

A second class of catalysts include V/P mixed oxides, and in particular one with a well–defined crystalline structure, vanadyl pyrophosphate $(VO)_2P_2O_7$, (the catalyst which is used industrially for n–butane oxidation to maleic anhydride), claimed by The Standard Oil Co [134–136]. The same company claims the use of a fluidized–bed reactor for carrying out the reaction, with feeding of fresh ethane and oxygen and recycling most of the reactor effluents after separation of acetic acid. In this way a high concentration of CO_2 is maintained in the reactor in order to better control the temperature rise caused by the exothermic reactions, and also obviate the separation of carbon oxides from ethylene, including the costly cryogenic separation of CO. A flow sheet of the process is illustrated in Figure 2. In this case the catalyst described has the following empirical formula: $Mo_{0.37}Re_{0.25}V_{0.26}Nb_{0.07}Sb_{0.03}Ca_{0.02}O_x$, and is analogous to that described by [140]. A summary of catalyst compositions and performances described in papers and patents is reported in Table 2.

Fig. 2. Simplified flow–sheet of the Standard Oil process for oxidation of ethane to acetic acid.

5.1   Characteristics of Catalysts Based on Mo/V/Nb Mixed Oxides

Catalysts made of Mo/V/Nb mixed oxides possess unique reactivity properties, and are able to activate and oxidize paraffins at low temperature, with performances which are rather unique, starting from substrates having very different reactivity properties, like ethane and propane. Catalysts essentially based on Mo/V/Nb/O (also containing other elements to improve the specific performance in some reactions) have been claimed for the oxidation of ethane and propane, and for ammoxidation of propane. It is thus useful to describe in more detail findings reported in the literature concerning the compounds which constitute the active catalysts.

The catalyst developed by Saudi Basic, based on a Mo/V/Nb mixed oxide (doped with P) gives surprising results in terms of yield of acetic acid [133]. On the contrary of that claimed by other companies, the feed composition is not very rich in ethane, and the limiting reactant therefore is the hydrocarbon. This makes possible the high conversion claimed, and indicates that the major advantage of this kind of catalyst is the possibility to operate under hydrocarbon leaner conditions while keeping high selectivity even at high conversion. It is worth mentioning that also in the case of propane ammoxidation over Mo/V/Nb/Te(Sb)/O–based systems high selectivity to acrylonitrile is obtained at high paraffin conversion.

Table 2. Summary of data characterizing the catalytic performance of several catalysts in ethane oxidation

Catalyst	Ref	Conv. C_2 (%)	Sel. AA (%)	Sel. $C_2^=$ (%)
$Mo_{0.73}V_{0.18}Nb_{0.09}O_x$	128	2.3	100.0	0
$Mo_{0.75}V_{0.22}Nb_{0.03}O_x$	123	7.5	18.4	67.6
$Mo_{2.5}V_{1.0}Nb_{0.32}O_x$	133	65.0	30.5	26.9
$Mo_{2.5}V_{1.0}Nb_{0.32}P_{0.042}O_x$	133	53.3	49.9	10.5
$P_{0.015}Mo_{0.153}V_{0.014}Ti_{1.0}O_x$	139	6.5	38.0	11.0
V/TiO_2	138	0.5	73.0	8.0
$(VO)_2P_2O_7$	135^a	5.7	14.8	48.0
$(VO)_2P_2O_7$	135^b	9.2	7.5	63.4
$V_1P_1Re_{0.016}O_x$	135^a	4.4	27.1	8.2
$Mo_{0.37}Re_{0.25}V_{0.26}Nb_{0.07}Sb_{0.03}Ca_{0.02}O_x$	140	14.0	78.0	12.0

C_2 ethane; $C_2^=$ ethylene; AA acetic acid

Ref 128: T 200°C, P 1 atm;

Ref. 123: 86% C_2, 6% O_2, 8% H_2O, T 323°C, P 8.3 atm;

Ref. 133: 15% C_2, 85% air; T 260°C, P 14 atm;

Ref. 139: 62% C_2, 17% O_2, 10% N_2, 12% H_2O, T 275°C, P 6.3 atm;

Ref. 138: T 225°C, P 1 atm;

Ref. 135: a) 55% C_2, 11% O_2, 34% N_2, T 333°C, P 14 atm; b) 37% C_2, 7% O_2, 56% N_2, T 360°C, P 14 atm;

Ref. 140: T 227°C, P 28 atm.

The selectivity to ethylene decreases with increasing conversion of ethane, while that to acetic acid increases. The compound claimed by Saudi Basic is in large part amorphous, and shows a few diffraction lines relative to a crystalline compound characterized by d values at 4.03 (100% I), 3.57, 2.01 and 1.86 Å. The catalyst is obtained by treatment in air at 350°C of the precipitate from a solution containing the different elements. Doping the compound with phosphorus improves the yield to acetic acid, through a decrease in conversion but an increase in the selectivity to acetic acid (the latter passes through a maximum, while that to ethylene through a minimum, on increasing P content from 0.01 to 1.0 with respect to 1.0 atom of V). The effect of P addition is claimed to be an improvement in acidity, facilitating ethylene adsorption and acetic acid desorption. According to the authors, this increases the consecutive rate of ethylene oxidation to acetic acid.

It is worth mentioning that also the activity of the Mo/V/Nb/O catalysts in ethane oxidation originally claimed by Union Carbide [122, 123], was related to the development of a crystalline phase characterized by a broad X–ray diffraction reflection at d = 4.0 Å. The best composition was found to be $Mo_{0.73}V_{0.18}Nb_{0.09}O_x$, which can reach 10% conversion of ethane at 286°C with almost total selectivity to ethylene. The selectivity decreased with increasing temperature, due to the formation of carbon oxides.

Burch and Swarnakar [130] have compared the reactivity of Mo/V/O and Mo/V/Nb/O systems. The former contains MoO_3, $Mo_6V_9O_{40}$ and $Mo_4V_6O_{25}$ crystalline compounds, while the latter contains also $Mo_3Nb_2O_{11}$, the most intense diffraction line of which occurs at 4.01 Å (samples calcined in air). The addition of Nb increases both activity and selectivity, and the formation of the latter phase

may account for the increase in performance. An ethoxy intermediate was postulated to be the precursor of ethylene formation. The product distribution is independent of the conversion, indicating the absence of consecutive reactions under the conditions used.

Merzouki et al. [128, 129] instead prepared compounds with overall composition $Mo_{0.73}V_{0.18}Nb_{0.09}O_x$ which were characterized by the presence of molybdenum oxides (MoO_3 and $Mo_{18}O_{52}$–like phases), possibly also containing V and Nb in solid solution. Treatment of the catalyst was done in N_2 at 400°C. These compounds are more selective to acetic acid than those described by Burch and Swarnakar. At 25% conversion, a selectivity of 45% to acetic acid and 45% to ethylene is obtained at 200°C, while with increasing temperature the selectivity to acetic acid decreases in favour of ethylene. Other compounds prepared differently however also contain $Nb_{0.09}Mo_{0.91}O_{2.8}$ (a Nb–substituted Mo_5O_{14} phase), and $Mo_{0.67}V_{0.33}O_2$ (a rutile–type V–substituted MoO_2 phase). These catalysts are totally selective to acetic acid at low conversion and temperature; an increase in temperature above 200°C leads to a decrease in selectivity with formation of CO_2 and ethylene.

Ruth et al. [131, 132] prepared catalysts with composition $Mo_{0.73}V_{0.18}Nb_{0.09}O_x$, and depending on the method of preparation obtained either a solid made of a mixture of $Mo_6V_9O_{40}$, $Mo_3Nb_2O_{11}$ and MoO_3 (crystalline at 700°C, largely amorphous at 400°C), by calcination in air, or largely amorphous and containing MoO_2 when calcination was done under nitrogen flow. The former catalyst exhibited good activity and selectivity to acetic acid, and an important role was attributed to the small, high–surface–area grains of amorphous component in the sample calcined at 400°C, having the approximate analytical composition $Mo_{0.84}V_{0.13}Nb_{0.02}O_x$. The authors reported a complete analysis of the mechanism of reaction occurring at the catalyst surface, which takes into account all of the information from the literature. The ethane molecule is first adsorbed in the form of an ethoxide species, which can transform into ethylene via β–elimination. The consecutive reaction of ethylene oxidation to acetaldehyde and acetic acid does not seem to be important on these materials, as well as the hydration of ethylene to ethanol followed by oxidation to acetaldehyde and acetic acid. Rather, since the reactions of ethylene and acetic acid formation occur through parallel routes, α–elimination steps of the ethoxide intermediate is proposed to directly lead to acetaldehyde and acetic acid. [138]. The α–elimination step was found to be favoured at lower temperatures than the β–elimination one, and to possibly occur at different sites [131, 132]. Acetic acid is more stable than ethylene towards consecutive reactions of combustion, and for this reason an increase in the total pressure resulted in an increased formation of acetic acid.

It is clear that the number of compounds or solid solutions which can be formed, even for the same overall catalyst composition, can be very different depending on the preparation conditions of the catalyst, and this causes considerable changes in the catalytic performance.

6. Oxychlorination of Ethane to 1,2–Dichloroethane and to Vinylchloride

Commercial processes for the production of vinyl chloride (VCM) use ethylene as the starting material. The oxychlorination of ethylene to 1,2–dichloroethane (DCE) is the heart of the balanced process to manufacture (VCM). The general scheme of the balanced process is illustrated in Figure 3. Fresh ethylene, together with recycled HCl and either air or oxygen are fed to the oxychlorination reactor, to react over a supported–copper chloride–based catalyst. The DCE produced, after condensation, drying and purification, is cracked (dehydrochlorinated) to VCM, with the coproduction of one mole of HCl which is recycled to the oxychlorination reactor. The additional mole of HCl which is needed for oxychlorination may come from another plant site, i.e. from MDI/TDI, propylene oxide via epichlorhydrine, benzyl chloride or fluorocarbons plants. Alternatively, the oxychlorination is coupled to a direct chlorination reactor, where chlorine and ethylene are fed to make more DCE. When the two reactors produce equimolar amounts of DCE, the HCl produced in the cracking section is enough to supply the oxychlorination reactor.
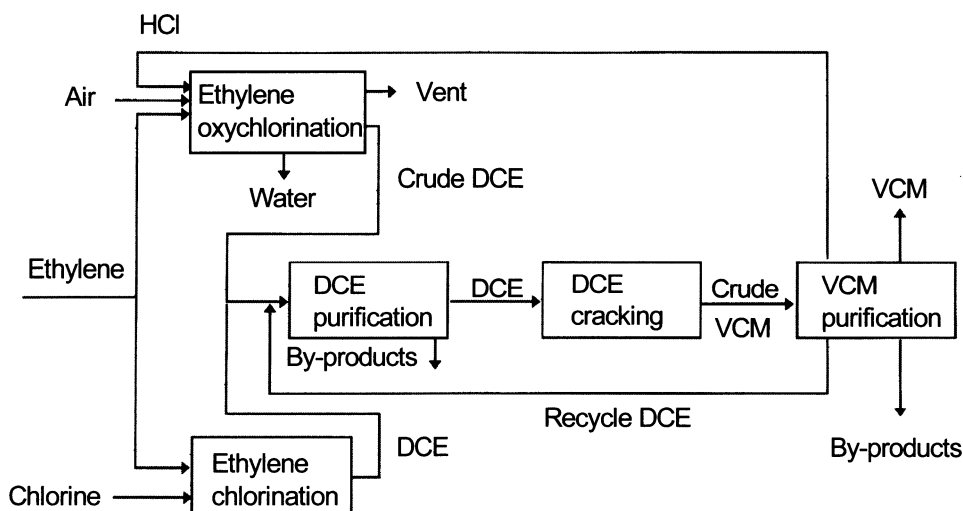

Fig. 3. Scheme of the balanced process of ethylene oxychlorination.

Ethylene represents a significant factor in the cost of VCM production. In general, a reduction in this cost can only be achieved by economies of scale, since industrial processes are technologically well established, and operate close to the maximum efficiency. Therefore, a significant improvement might be represented by the use of ethane as the raw material for VCM production, due to the considerably lower cost of the paraffin with respect to the corresponding olefin.

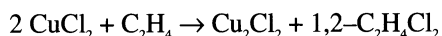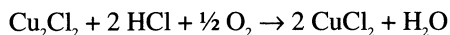$$C_2H_6 + HCl + O_2 \rightarrow CH_2=CH-Cl + 2\ H_2O$$
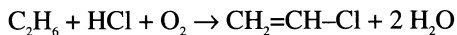
The interest for the ethane oxychlorination goes back to the 1970's. Indeed, several patents claiming heterogeneous catalysts for the direct transformation of ethane were issued in that period [141–146]. In most cases the catalysts claimed include an active phase where copper chloride (or iron chloride) is the main component, together with alkali metal chlorides (K, Cs) and, sometimes, a rare earth chloride. A fluidizable support, usually alumina, is used. In practice, the catalyst formulation is very similar to that industrially used for the oxychlorination of ethylene. Reaction conditions always include temperatures higher than 400°C, and under these conditions a considerable fraction of the paraffin is converted to CO_2 and to chlorinated compounds other than VCM. Notwithstanding the industrial interest, the reaction has never reached industrial application due to the low conversion achieved, the low selectivity to the desired product (due to the hard reaction conditions used), and the problems which arise from the disposal (recycle) of undesired chlorinated compounds.

Recently, European Vinyl Corporation [25, 147–149] has issued some patens claiming a process for the direct transformation of ethane to VCM which overcomes the above mentioned problems, mainly thanks to:

1. The use of reaction conditions which include an excess of HCl with respect to the stoichiometry of the ethane conversion. In the case of ethylene oxychlorination an excess of olefin is used, in order to reach an almost total conversion of HCl, and avoid problems related to the corrosion of downstream apparatus. In the case of ethane oxychlorination, on the contrary, excess of HCl is necessary to maintain the chlorinated form of copper in the active phase, $CuCl_2$, since the oxychloride form, CuClCuO (a mixed Cu^I/Cu^{II} compound) is considered to be the species responsible for total combustion. Therefore this kind of operation makes it possible to reduce the amount of carbon oxides produced. It is claimed that the greater the excess of HCl supplied over its stoichiometric requirement, the greater the beneficial effect on the selectivity. Unconverted HCl is recycled to the reactor, together with unconverted ethane.

2. A catalyst formulation which includes an active phase constituted of copper chloride and potassium chloride, which are present in the atomic ratio of 2:8 (wt. % of 1.3 and 3.4 , respectively), thus with a great excess of the alkali ion. A further component is cerium chloride, which is present at an atomic ratio of 0.5 (0.74 wt.%). Cerium improves the catalytic activity and the formation of chlorinated compounds (especially trichloroethane) at the expense of carbon oxides. This active phase is supported on fluidizable low–surface area alumina (1 m^2/g). The operating temperature of this catalyst is between 450 and 470°C. The composition of this catalyst is very similar to that of the system employed in the Deacon process for the oxidation of HCl to chlorine, based on a mixture of copper chloride and alkali metal chlorides.

At the temperatures which are typical for the oxychlorination of ethylene (220 to 240°C), the mechanism of the reaction is the following:

$$2\ CuCl_2 + C_2H_4 \rightarrow Cu_2Cl_2 + 1,2-C_2H_4Cl_2$$

$$Cu_2Cl_2 + 2\ HCl + \tfrac{1}{2}\ O_2 \rightarrow 2\ CuCl_2 + H_2O$$

where, however, the mechanism of copper reoxidation is indeed constituted of two steps:

$$Cu_2Cl_2 + \tfrac{1}{2}\ O_2 \rightarrow CuOCuCl_2$$

$$CuOCuCl_2 + 2\ HCl \rightarrow 2\ CuCl_2 + H_2O$$
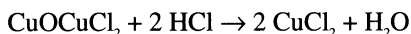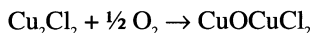
Thus a Cl transfer occurs from the catalyst to the olefin. On the contrary, at the high temperatures needed for the ethane activation and oxidation the mechanism is likely a radicalic one, and involves the generation of Cl_2 (released by the catalyst, which becomes reduced, and is then reoxidized and chlorinated by gaseous HCl and O_2), and the formation of chloroethanes, analogous to what happens in the case of chlorination of methane to $CH_{4-x}Cl_x$. Chloroethanes are then quickly dehydrochlorinated to VCM. Indeed the performance obtained by feeding either HCl or Cl_2 together with ethane and oxygen was almost the same (see Table 3) [25]. Moreover, the MT chlor process developed by Mitsui Toatsu (with catalysts based on supported Cr_2O_3) makes use of temperatures around 400°C for the oxidation of HCl to Cl_2.

One further advantage claimed by EVC is that it is possible to recycle the by-products of the oxychlorination reaction (after applying some treatment), thus considerably reducing the waste of feestock and the effluents to be treated. Part of the by-products are indeed converted to VCM. Chlorinated by-products are i) saturated compounds (ethyl chloride, 1,1-dichloroethane, 1,2-dichloroethane, 1,1,2-trichloroethane), ii) combustion compounds (carbon tetrachloride, chloroform and dichloromethane), and unsaturated compounds (1,1-dichloroethylene, 1,2-dichloroethylene, tri and perchloroethylene). Before recycling, the stream containing saturated and unsaturated chlorinated by-products is fed to a trickle-bed hydrogenation reactor, where they are converted to saturated ones. The latter then undergo transformation to VCM in the oxychlorination reactor.

Table 3 shows the distribution of products for different feed compositions. The maintainance of an excess of HCl in the outlet stream makes it possible to decrease the extent of combustion, from 20% selectivity (with no HCl in the off gas), to 3% (with 10% HCl in the off gas). One of the main reaction products is ethylene, which at these conditions is not chlorinated. Therefore the top of the distillation column for light compounds separation, containing unconverted ethane, ethylene and carbon oxides, is sent to a conventional chlorination reactor, to transform ethylene to 1,2-dichloroethane at mild temperatures; the exit stream is then recycled back to the ethane oxychlorination reactor. The steady state feed to the reactor therefore includes ethane, oxygen (fresh feed), 1,2-dichloroethane, carbon oxides (from the chlorination reactor), ethylchloride, additional 1,2-dichloroethane, 1,1-dichloroethane, 1,1,2-trichloroethane, tetrachloroethane and carbon tetrachloride (from the hydrogenation reactor, which is fed with the base product of the distillation column for pure VCM recovery), and HCl (from the distillation column for anhydrous HCl recovery). Since feeds and purges are adjusted in order to have an exit content of HCl which is the same as that, which enters the ethane oxychlorination reactor, net Cl for the transformation of ethane to chlorinated compounds enters the process as Cl_2 fed to the ethylene chlorination reactor. The simplified flow-sheet of the process is illustrated in Figure 4.

Table 3. Performance of the EVC catalyst for ethane oxychlorination [25].

Catalyst, active components	Cu/K	Cu/K	Cu/K/Ce
Temperature °C,	478.0,	480.7,	466.6,
Pressure bar	0.1	0.1	0.04
$C_2H_6/O_2/HCl/Cl_2/N_2$, mol %	28.7/23/0/16.2/32.2	25.8/28.9/33/0/12.4	21.1/21.1/42.2/0/15.5
Conv. C_2H_6, %	94.8	89.9	94.8
Conv. O_2, %	94.5	93.2	98.1
Yield C_2H_3Cl, VCM, %	32.2	30.0	30.3
Yield C_2H_5Cl, %	13.9	13.8	11.1
Yield C_2H_4, %	16.3	14.8	15.5
Yield $C_2H_2Cl_2$, %	7.9	9.9	11.8
Yield $C_2H_3Cl_3$, %	0.5	0.5	8.7
Yield C_2HCl_3, %	0.6	0.9	1.6
Yield C_2Cl_4, %	5.9	8.4	0.1
Yield $C_2H_4Cl_2$, EDC, %	14.5	12.0	16.9
Yield CO + CO_2, %	5.9	8.4	2.9
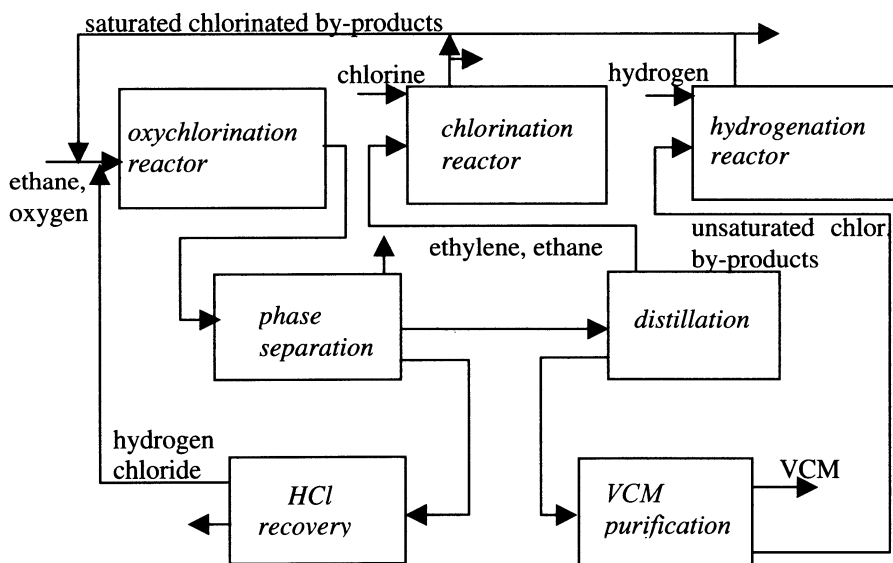
Fig. 4. Simplified flow–sheet of the EVC process for ethane oxychlorination to VCM.

7.   Ammoxidation of Propane to Acrylonitrile

One of the reactions which has been receiving greater attention in recent years is the ammoxidation of propane to acrylonitrile (ACN), as an alternative to the current industrial process of propylene ammoxidation.

$$C_3H_8 + NH_3 + 2\,O_2 \rightarrow CH_2{=}CH{-}CN + 4\,H_2O$$
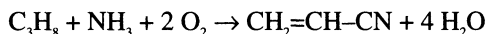
The extensive research has been fully successful in this case, since two different classes of catalysts, i) antimonates having the rutile structure and ii) multimetal molybdates, have been developed up to the stage of commercialization. BP (ex Standard Oil) [150–158], Mitsubishi Chemical [159–161] and Asahi Chem. Industries [162] have each claimed its own process, and have announced the start up of demonstrative plants. Other companies have studied and developed proprietary formulations, but in general catalytic systems belong either to the antimonates family (Standard Oil, Rhodia, BASF, Nitto, Monsanto) [163–169], or to the molybdates family (Mitsubishi, Asahi).

There are a few points which are of relevant interest, related to both scientific and technical aspects of the reaction:

1. The reaction conditions which have been claimed by the various companies are substantially different. As shown in Figure 5, in some cases propane–rich conditions have been claimed, i.e. in earlier patents from Standard Oil. In this case, the conversion of propane is necessarily low, and therefore recycle of unconverted paraffin becomes compulsory. Reaction conditions described include the presence of a ballast (typically, molecular nitrogen and/or steam), and thus simulate the composition of a reactor inlet which includes the recycle stream. Mitsubishi instead first claimed the use of fuel–lean conditions, thus of conditions where very high conversions of propane can be reached. In more recent patents, BP also has claimed the use of analogous conditions, using overstoichiometric oxygen, and propane as the limiting reactant. However, the lower activity of antimonates makes it necessary to use temperatures which are approximately 50 degrees higher than those for the Mitsubishi catalyst.
2. The selectivity to ACN versus propane conversion is plotted in Figure 6 for the best (to our knowledge) performances reported in patents from the different companies; the temperature of reaction is also given in the Figure. In general, best yields obtained with propane–rich conditions lay in the 15–to–20 % yield region. An example is also given for a patent that considers the feeding of halogen promoters, which favour the activation of the paraffin through radicalic mechanisms, thus considerably improving the conversion at propane–lean conditions. Processes which include the additional feed of gas–phase promoters were also claimed by other companies several years ago. However, the most surprising result is that reported by Mitsubishi at hydrocarbon–lean conditions, with a yield to acrylonitrile of 53-55% at 87-89% propane conversion, thus with a selectivity of 60-64% at 410°C.

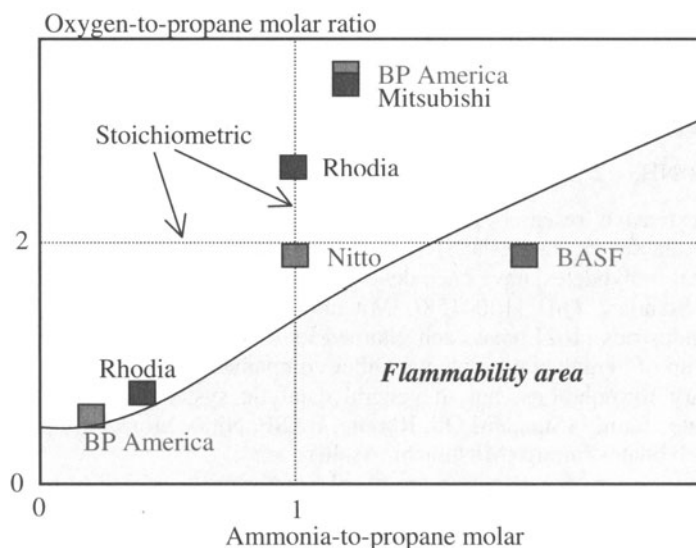Oxygen-to-propane molar ratio

Fig. 5. Feed composition for the process of propane ammoxidation claimed by different companies.

All catalysts claimed are to be considered as "multifunctional" systems. Indeed, the formation of acrylonitrile from propane occurs mainly via an intemediate formation of propylene, transformed to acrylonitrile via an allylic intermediate [121, 168, 170]. Therefore, the catalyst must possess different kinds of active sites: one site (type A) which is able to activate the paraffin and oxidehydrogenate it to the olefin, and one site (type B) which is able to ammoxidize the adsorbed olefinic intermediate. This second step must be very quick to limit as much as possible the desorption of the olefin. In order to obtain effective cooperation, it is necessary to develop a catalyst characterized by the presence of these sites in close proximity one with the other, allowing the quick transformation of each reaction intermediate to the following product up to acrylonitrile. Table 4 summarizes, for each class of catalysts claimed, the type A and type B compounds, responsible for the first and second step, respectively, of the ammoxidation reaction. In all cases the multifunctionality is achieved through the combination of two different compounds: a mixed oxide having the rutile structure (type A compound), and dispersed antimony oxide (type B compound), in BP catalyst. In the Mitsubishi catalyst, the two active species probably correspond to Mo/V/Te(Sb)/O and Mo/Te/O, respectively. Alternatively, in the latter case the system is intrinsically multifunctional, where the different elements which infer the properties to the catalyst are dispersed inside a single mixed oxide.
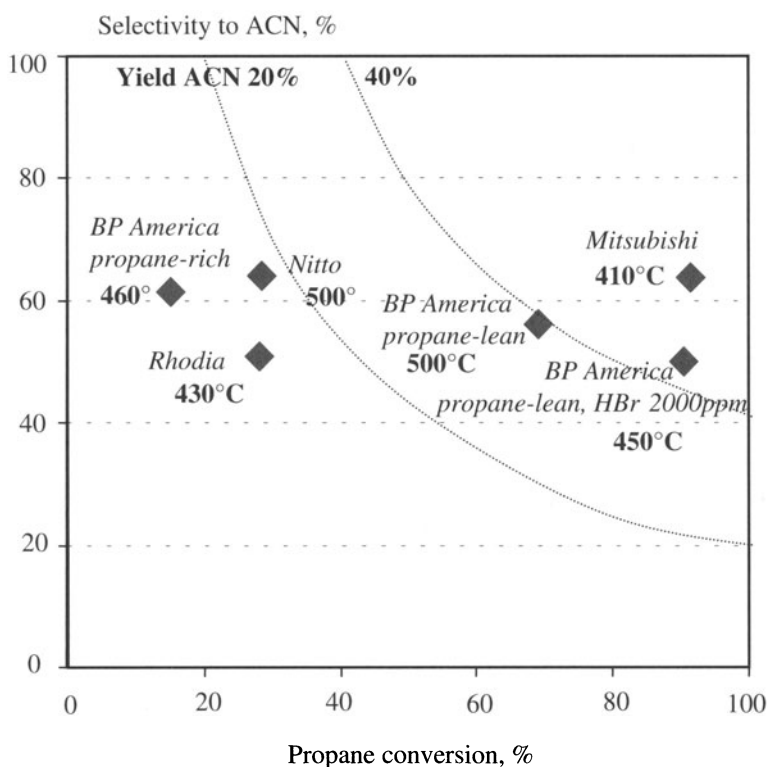
Selectivity to ACN, %

Fig. 6. Best results of selectivity and conversion reported for catalytic systems claimed by different companies.

Table 4. Main catalytic components in systems developed by different companies for propane ammoxidation. See text for explanation.

Catalyst	Type A compound	Type B compound
Mo/V/Te/Nb/(Sb)/O (Mitsubishi, Asahi)	Mo/V/Te(Sb)/O	Mo/Te/O
V/Sb/W/O (BP)	V/Sb/O (rutile)	Sb/O
V/Sb/Sn/O (Rhodia)	Sn/V/Sb/O (rutile)	Sb/O

7.1   Characteristics of Rutile-Type Mixed Antimonates

Several papers have been dedicated to the study of mixed antimonates having the rutile structure. In particular, V/Sb/O and Fe/Sb/O systems have been the object of many investigations, aimed at understanding the nature of these mixed oxides, and finally at the identification of the nature of the active species. Based on the numerous literature data available for these systems, it is possible to draw some conclusions, that can be helpful to understand what are the requirements for developing an active and selective catalyst for propane ammoxidation.

Indeed, the preparation of a truly stoichiometric metal antimonate $MeSbO_4$ is a difficult task. The method of preparation employed affects the nature of the catalysts prepared, but in general non-stoichiometry is a particular feature of these systems, even when conditions are used at best to develop preparations where the solid state reaction between Me and Sb ions is easier, and to obtain ratios between Sb and Me as close as possible to 1.0 [171–174]. The most striking case is the V/Sb/O system, for which the following composition for a V/Sb 1/1 catalyst has been reported, deduced by careful structural studies: $V_{0.92}Sb_{0.92}O_4$ [173]. This cation–deficient structure, having 0.04 cationic positions unoccupied for each O^{2-} anion, contains Sb^{5+} (the only antimony ion which is present), while vanadium is present both as V^{4+} and as V^{3+}. The electroneutrality is guaranteed for the composition $V_{0.28}^{3+}V_{0.64}^{4+}Sb_{0.92}^{5+}O_4$ [175].

However, the ratio between V^{3+} and V^{4+} can vary depending on the method of preparation (of particular importance is obviously the atmosphere and temperature of thermal treatment). This will affect the number of cation vacancies (for V_{tot}/Sb ratio equal to 1.0), within the series theoretically having the two limit compounds $V_1^{3+}V_0^{4+}Sb_1^{5+}O_4$ (the stoichiometric compound, with no cationic vacancies and only V^{3+}) and $V_0^{3+}V_{0.89}^{4+}Sb_{0.89}O_4$ (with the maximum of 0.22 vacant cation positions per formula, and only V^{4+}). This has been referred to as the $V_{1-y}Sb_{1-y}O_4$ series, with y varying between 0 and 0.11 [171, 172, 176], which is preferentially formed by treatment in air. Therefore, the presence of cation vacancies is a consequence of V having an oxidation state higher than 3+. This justifies the tendency of the V/Sb/O system to give such large deviations from the stoichiometry, at least under conditions which are not the most stable from the thermodynamic point of view (for this reason, the temperature of treatment may considerably affect the nature of these non–stoichiometric solids).

Another possibility is to have a ratio between Sb^{5+} and V different from 1.0. It has been reported that the non–stoichiometric series $V_{0.9+x}Sb_{0.9}O_4$ can be obtained, with x ranging from 0 to 0.2, and correspondingly with a degree of vacant cation positions ranging from 0.2 ($V_{0.9}Sb_{0.9}O_4$, with $V_{0.1}^{3+}V_{0.8}^{4+}$, where analogous to the previous case the ratio V_{tot}/Sb is 1.0), to 0 ($V_{1.1}Sb_{0.9}O_4$, with full occupancy of the cation sites, and with vanadium as $V_{0.9}^{3+}V_{0.2}^{4+}$) [177]. In practice, vacant positions in $V_{0.9}Sb_{0.9}O_4$ are progressively occupied by V ions, thus increasing the V/Sb ratio, with also a corresponding increase in the V^{3+}/V^{4+} ratio. The latter is mainly affected by the atmosphere of thermal treatment, and thus finally this parameter affects the V/Sb ratio and the extent of cation site occupancy in the rutile structure.

Berry et al. [171] described a $VSb_{1-y}O_{4-2y}$ series, which does not formally contain cation vacancies, and which is formed when the thermal treatment is carried out in oxygen–impure nitrogen. In this series y = 0 corresponds to the stoichiometric $VSbO_4$ (only containing V^{3+}), while for y at a maximum equal to 0.1 the compound $VSb_{0.9}O_{3.8}$ is obtained, which can also be expressed as $V_{1.05}Sb_{0.95}O_4$, having excess vanadium, and with $V_{0.95}^{3+}V_{0.10}^{4+}$. In practice, it is assumed that the ratio between V^{3+}/Sb^{5+} is always equal to 1.0, and the solid solution is enriched with V^{4+} ions (and obviously with additional O^{2-} ions); this represents a solid solution between $VSbO_4$ and VO_2 (both rutile compounds). Only in the presence of oxygen–free nitrogen it is possible to obtain monophasic compounds of the series $VSb_{1-y}O_{4-1.5y}$. For y = 0.1 the compound $V_{1.039}Sb_{0.935}O_4$ is formed, having a small degree of cation site unoccupancy (0.026 vacancies per unit formula), a ratio V/Sb higher than 1.0, and again the presence of V^{4+}.

In most cases described in the literature, however, the solid solution has been reported to possess either an equal atomic amount of V and Sb, or an excess of V, but never an excess of Sb. Moreover, the latter is also supposed to be present exclusively as Sb^{5+}. Excess Sb, if preparations are carried out with an atomic ratio Sb/V higher than 2, is detected as α–Sb_2O_4 or β–Sb_2O_4 (the latter at calcination temperatures higher than 800°C). Incorporation of small amounts of V in these Sb oxides is also likely, lowering the temperature of the $\alpha \rightarrow \beta$ transformation. Antimony oxide is also present for Sb/V ratios between 1 and 2, in the form of amorphous oxide dispersed over the rutile, as suggested by IR spectroscopy [178, 179].

Different is the case of $FeSbO_4$, for which it is known that the structure can host excess of Sb. Berry and coauthors have demonstrated that on increasing the Sb/Fe ratio an increase in the cell volume of the tetragonal structure occurs [180- 182]. Moreover, instead of a random distribution of iron and antimony in the cation sites, rather cation ordering has been found by means of electron diffraction, with development of a trirutile–like structure. A change from mono to trirutile–like ordering, thus from $Fe^{3+}SbO_4$ up to the limit compound $Fe^{2+}Sb_2O_6$ (with an Sb/Fe ratio equal to 2), as a consequence of the excess of Sb^{5+} in the structure occurs with the progressive reduction of Fe^{3+} to Fe^{2+}. Therefore it is possible that the formation of Sb–rich solid solutions may only occur with metal ions which can exist in the 3+/2+ stable oxidation states. Indeed, the formation of very small amounts of crystalline $(VO)^{2+}Sb_2O_6$ has sometimes been observed [178]. Fe/Sb/O systems have also been studied as catalysts for propane and propene ammoxidation [164, 167, 183–186].

One further aspect concerns the presence of an IR absorption band at around 820–840 cm^{-1}, which is observed in all mixed antimonates, and which is not typical of Me–O stretching vibrations in rutile single oxides, and is not observed in any antimony oxide as well [187]. This band has been attributed to the stretching vibration of Sb^{5+}=O [174, 188], likely present on the surface of the rutile antimonate, and possibly constituting an active site for the propane ammoxidation. Indeed, this vibration could be due to the presence of SbO_x–rich domains in the outer zones of non–stoichiometric rutile crystallites. It is known that in non–stoichiometric $FeSbO_4$ prepared by thermal treatment at 800°C, having excess antimony in the structure, and characterized by a cell volume for the tetragonal cell higher than that of stoichiometric $FeSbO_4$ and by the presence of the IR band at 820 cm^{-1}, a treatment at 1000°C leads to i) a decrease in the cell volume, which becomes similar to that of stoichiometric rutile, and ii) a strong decrease in the intensity of the mentioned IR absorption band [189]. Therefore, it is possible that the development into a well–crystallized, ordered rutile structure occurs as a consequence of a cation redistribution in the lattice at high temperature, with the disappearance of features related to Sb–enrichment.

The best reported performances amongst the variety of compositions which have been claimed for V/Sb/O–based systems are summarized in Table 5 [16, 121].

It is shown that Standard Oil (now BP) has claimed the same catalyst type for both propane–lean conditions [158, 190], with high conversion of the paraffin, and propane–rich conditions [154], with low propane conversion.

Table 5. Performance of V/Sb/O–based catalysts described in the literature.

Catalyst formula	T (°C)	$C_3/NH_3/O_2/H_2O$/inert (mol. %)	C_3H_8 conv. (%)	Sel. AN (%)	Ref
$VSb_5W_{0.5}Te_{0.5}Sn_{0.5}O_x$–$SiO_2$	500	6.5/13/12.9/19.4/48.4	68.8	56.7	190
$VSb_{1.4}Sn_{0.2}Ti_{0.2}O_x$	460	51/10.2/28.6/10.2/0	14.5	61.9	154
$VSb_{1.4}Sn_{0.2}Ti_{0.1}O_x$	480	6.4/7.7/18.6/0/67.3	40.3	47.5	158
$VSb_5Bi_{0.5}Fe_5O_x$–Al_2O_3	440	7.5/15/15/20/42.5	39	77	191
$VSb_5Sn_5O_x$	450	8/8/20/0/64	30	49	169

The main difference between systems claimed by Standard Oil and those claimed by Rhodia [29, 163–165] consists in the nature of the rutile–type oxide which constitutes the carrier of the active phase. In the system developed by Standard Oil, the main component is the $VSbO_4$ compound, which activates the paraffin and transforms it into an olefin–like adsorbed intermediate. The latter may either desorb, or be transformed to acrylonitrile over the SbO_x "overlayers" (often present together with crystalline α–Sb_2O_4), the amount of which is a function of the excess Sb with respect to the rutile formula [192,193]. The latter species acts as a propylene ammoxidation site, and can be indeed present as a mixed compound in multicomponent catalysts: Te/Sb/O, Sn/Sb/O, Fe/Sb/O, Ti/Sb/O. This explains the presence, in many formulations claimed in the patent literature, of additional components, the main role of which is to improve the selectivity in the olefin transformation through the development of mixed compounds. In the system developed by Rhodia, instead, the main component is SnO_2 (cassiterite, having the rutile structure), inactive in the reaction of ammoxidation, which acts as the carrier for the active components: i) V/Sb/O and ii) SbO_x. Tin oxide is also able to disperse these components, through the formation of a solid solution of V and Sb in the tin oxide lattice, thus yielding a multifunctional catalyst where the two active compounds are in intimate contact and can effectively cooperate in the reaction [120, 168, 169].

Other antimonates have been studied as catalysts for this reaction [194–198]. In the case of the Ga/Sb/O system, a decrease in the Ga/Sb ratio (from $Ga_1Sb_1O_4$ to $Ga_1Sb_{49}O_{124}$) leads to a progressive decrease in activity and increase in selectivity to acrylonitrile [194–195]. The best yield has been obtained at 550°C with a catalyst of composition of $Ga_1Sb_{49}O_{124}$, with 28.3% propane conversion and 35.3 % selectivity to acrylonitrile. At lower conversions, a selectivity as high as 68.3 % has been claimed with a $Ga_1Sb_9O_{24}$ catalyst. The performance could be improved by adding Ni, P and W as dopants.

7.2   Characteristics of Multimetal Molybdate–based Catalysts

Catalysts based on molybdates can be classified as follows:
1. Systems based on Bi–molybdates having the scheelite structure; these have been studied mainly by Moro–oka et al. [26]. These systems also contain other components, such as V and Te [52, 199].
2. Systems based on mixed molybdates of V, Nb and Te [200-203]. These are very similar to the catalysts originally developed by Union Carbide for the oxidehydrogenation of ethane to ethylene [122]. Indeed, a very specific composition, namely $Mo_{1.0}V_{0.3}Te_{0.23}Nb_{0.12}O_x$, dispersed in 10–20% silica, seems

to be the best catalyst, coupled to a very delicate preparation procedure, including a thermal treatment in nitrogen flow which has to be carried out at 620°C [161]. The phase composition of the system is not fully understood, since replication of the synthesis of this proprietary catalyst seems to be particularly difficult, possibly leading to different compounds for small variations in the procedure.

The excellent results claimed are due to the very high conversion of propane achieved at mild conditions (reaction temperature 410–440°C) [204–212]. Propane–lean conditions are claimed, and conversions even higher than 90% are reported. The best yield (53.5%), is obtained at a conversion of 89.1% (selectivity is 60.0%), at 420°C and with a catalyst of composition $Mo_1V_{0.3}Nb_{0.15}Te_{0.2}O_x$. Surprisingly, notwithstanding the very high conversion, and the fuel–value of the raw material, which would make burning the unconverted propane to produce high-value steam more economical than recycling it, the process includes recycle of unconverted propane. Indeed, the process makes use of the BOC PSA technology for rejection of N_2 (both present in feed, which contains oxygen-enriched air, and generated in the reactor by ammonia combustion), recovery of the hydrocarbon and recycle of the latter in the reactor [213, 214] (see Fig. 7).
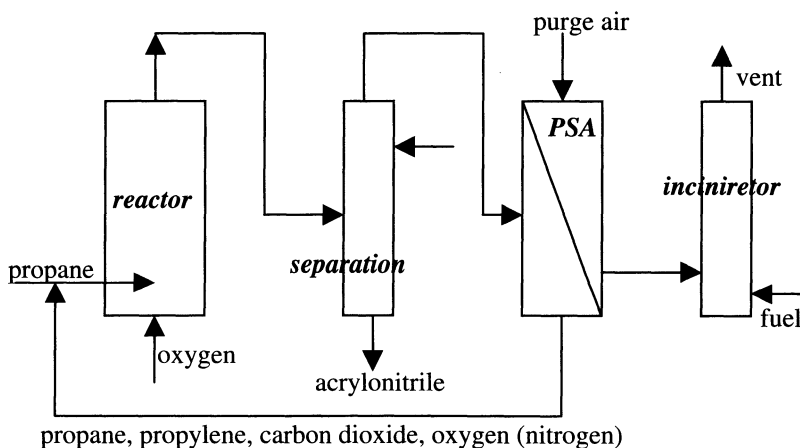

propane, propylene, carbon dioxide, oxygen (nitrogen)

**Fig. 7.** Simplified flow–sheet of the Mitsubishi/BOC process for propane ammoxidation to acrylonitrile

One Mitsubishi patent claims the differentiation of ammonia along the catalytic bed [211]. This might become necessary if the catalyst is particularly active in ammonia combustion to N_2; if all reactants are fed together at the reactor inlet, a rapid decrease in the ammonia concentration after the initial part of the catalytic bed would be obtained. This would also cause, in the second part of the catalytic bed, a transformation of propane to propylene, and not to acrylonitrile, due to the lack of ammonia. Indeed, the Mo/V/Nb/Te/O material is known to be a very active catalyst for light paraffin oxidehydrogenation [122]. Differentiation of ammonia

along the reactor may in part overcome the problem of ammonia combustion, and might also favour the transformation of the olefin formed to acrylonitrile.

Patents from Mitsubishi claim that the active catalyst (obtained by thermal treatment at 620°C in nitrogen flow) exhibits the main X–ray diffraction lines at 2 θ = 22.1, 28.2, 36.2, 45.2, 50.0° [204]. This active phase is referred to as phase M2. Other less intense lines are present, which are attributed to a different phase, M1 (lines at 2θ = 9.0, 22.1, 27.3, 29.2 and 35.4°). The two phases are claimed to cooperate in the ammoxidation of propane, each one having a defined role: in the activation of propane to yield propylene (phase M1), and in the transformation of the latter into acrylonitrile (phase M2) [210]. So it seems that the best performance is obtained in the contemporaneous presence of these two compounds. The catalyst having the pattern corresponding only to phase M1 (obtained by treatment in air at 350°C), is reported to be less active and selective than the catalyst characterized by the presence of both M1 and M2 phases. A number of mixed compounds are known to form amongst the metal ions included in the Mitsubishi catalyst formulation, such as $Mo_6V_9O_{40}$, $Mo_4V_6O_{25}$ (both exhibiting strong reflections at d = 4.06 Å, 2θ = 21.6°), $Mo_3Nb_2O_{11}$ (intense peak at 2θ = 22.2°), $VNbO_4$ [131, 132], $Nb_{0.09}Mo_{0.91}O_{2.8}$, $Mo_{0.67}V_{0.33}O_2$, $V_{0.07}Mo_{0.93}O_{2.8}$ [128, 129] (the latter three compounds all possess the rutile structure), $MoTe_2O_7$ and $Mo_5Te_5O_{16}$ [215] (see also the chapter relative to the oxidation of ethane to acetic acid). Recently, detailed studies led to the proposal of different types of compounds playing the major role in Mo/V/Nb/Te(Sb)/O systems: $Mo_6V_3Te_1O_x$, $Mo_6V_2Sb_1O_x$ [200, 201], $Mo_7VNbTeO_{28}$, which cooperates with $Mo_6VTe_2O_{24}$ and $TeMo_5O_{16}$ to infer optimal catalytic performance to the material [202], and $Mo_{0.61-0.77}V_{0.31-0.19}Nb_{0.08-0.04}O_x$ [203].

8.   Oxidation of Propane to Acrylic Acid

Acrylic acid is presently produced in a two–step oxidation process from pro-pylene, via intermediate acrolein. A one–step process starting from propylene has not yet been commercialized because of inadequate selectivity. Interest exists for the development of a process from propane, due to the lower raw material cost and greater availability [3, 10, 16, 216, 217].

$C_3H_8 + 2\ O_2 \rightarrow CH_2{=}CH{-}COOH + 2\ H_2O$
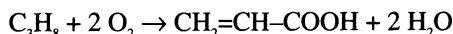
Different processes can be envisaged:
1. A multistep process that integrates conventional dehydrogenation of propane to propylene and oxidation of propylene to acrylic acid;
2. A multistep process that integrates oxidative dehydrogenation and conventional oxidation;
3. The direct oxidation of propane to acrolein or to acrylic acid.

The same process configuration can also be envisaged for the ammoxidation of propane to acrylonitrile; however, in this case the high stability of the product makes it possible to operate at conditions which are close to those required for paraffin activation. Therefore the single–step process is technically more attractive, provided a suitable catalyst can be developed. On the contrary, acrylic acid is not a stable compound, and therefore technical solutions which take into consideration the separation of the two steps are as attractive as the single–step

process. The different schemes proposed for process integration are illustrated in Figure 8.
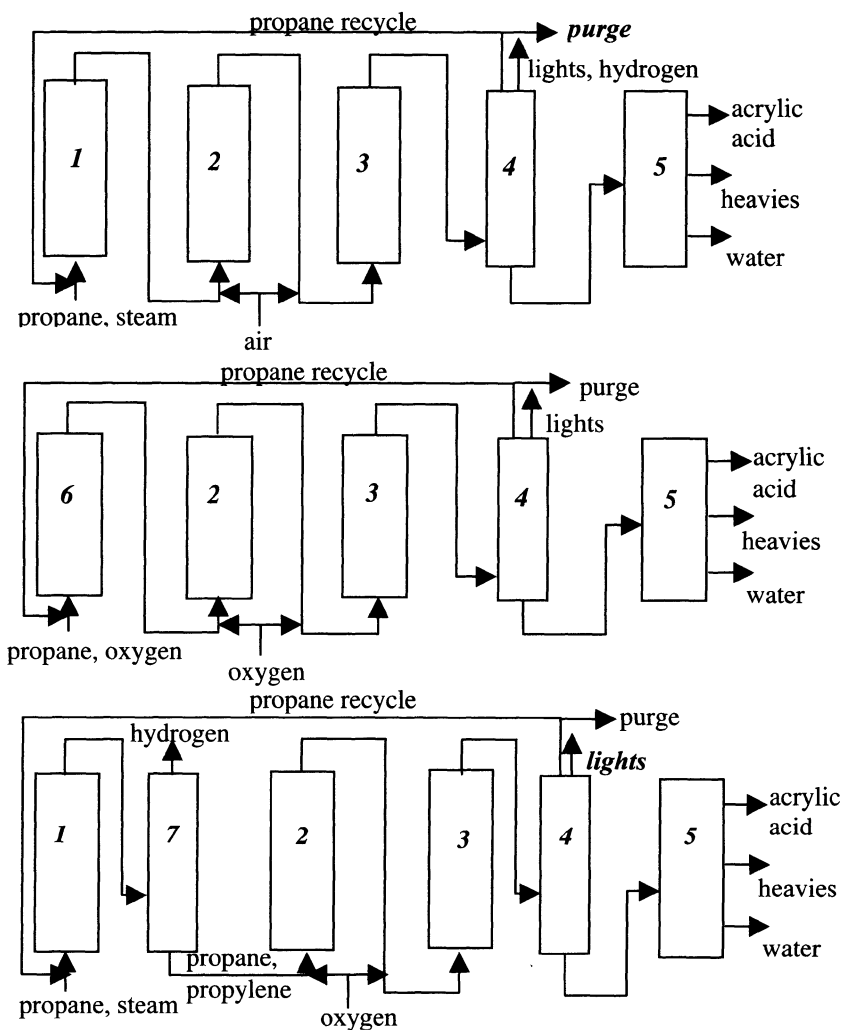

Fig. 8. Simplified schemes for integrated processes proposed by Halcon (top) [218], Union Carbide (middle) [221], and BASF (bottom) [220] for the oxidation of propane to acrylic acid. These schemes have been deduced based on the text of patents, and might not correspond exactly to the actual schemes proposed by these companies. Legend: 1: Reactor for propane dehydrogenation; 2: reactor for propylene oxidation to acrolein; 3: reactor for acrolein oxidation to acrylic acid; 4: quench + absorption towers for recovery of propane; 5: distillation towers for acrylic acid recovery; 6: reactor for propane oxidehydrogenation; 7: absorption tower for hydrogen recovery and separation from propane/propylene.

Integrated processes for paraffin oxidation were first proposed by The Halcon SD Group [218, 219]. In these patents, propane is dehydrogenated, with a catalyst based either on supported Pt or on zinc aluminate. The outlet stream is added with air, without separation of reagents and products, and fed to the first oxidation reactor, filled with a multimetal molybdate–based catalyst for allylic oxidation. Therefore the expensive separation of unconverted propane from propylene is eliminated. However, the presence of molecular hydrogen in the oxidation reactor may possibly give rise to enhanced flammability problems. In the oxidation reactor propylene is oxidized to acrolein (propane is inert), and the outlet stream is fed to the final oxidation reactor filled with a catalyst suitable for the oxidation of acrolein to acrylic acid. The outlet stream is then finally treated to easily recover acrylic acid by water absorption, and then propane and unconverted propylene from other uncondensable gases (H_2, O_2, N_2, light ends) by abatment with an organic solvent. The C_3 fraction is then recovered and recycled. The key features of this process are i) use of an oxidation catalyst which is not active in the oxidation of molecular hydrogen, and ii) oxidized products formed by oxidation of light ends (obtained in the dehydrogenation step) do not contaminate the acrylic acid. The claimed performances for each step are given in Table 6. The overall selectivity to acrylic acid is around 75%.

Table 6. Performances of the two–step Halcon process for propane oxidation to acrylic acid [218].

Reaction step	Conversion (%)	Selectivity (%)
Propane to propylene	29.7	96.5
Propylene to acrolein	91.1	87.4
Acrolein to acrylic acid	92.8	89.1

Integrated processes have also been claimed by other companies. The process claimed by BASF [220] differs from the Halcon process in that hydrogen is separated after the dehydrogenation step, and oxygen is preferably used instead of air in the oxidation reactor. Also in this case having propane as the main inert component in the oxidation reactor makes possible the better control of the reaction temperature, thus minimizing hazards associated with the development of hot spots, that can occur when ballasts having worse thermal conductivity properties than the paraffin are used. Feeds more concentrated in propylene can therefore be handled safely in the oxidation reactor, thus achieving improved productivity to acrylic acid.

In the process claimed by Union Carbide [221], propane is oxidehydrogenated in a first oxidation reactor, using a Mo/V/Nb/O–based catalyst. The outlet stream is then sent to a second oxidation reactor, without any intermediate separation, where propylene is oxidized to acrolein. Finally, the acrolein is oxidized to acrylic acid in a third oxidation reactor. Propane and propylene are recycled to the first reactor, together with oxygen, nitrogen, and carbon oxides. This obviously decreases the propylene requirement for acrolein production with respect to the once–through case.

Different catalytic systems have been claimed in recent years for the direct selective oxidation of propane to acrylic acid [222–234]. In Table 7 the most significant results are reported. In all cases acrylic acid was the main product of selective oxidation, while the formation of acrolein was very low, except for the

Ni/Mo/Te/P/O system, which gave 12.7% selectivity to the aldehyde. Good yields and selectivities have been reported for the following classes of catalysts: i) V/P mixed oxides, ii) P/Mo/V/O polyoxometalates, and iii) Mo/V/Nb/Te mixed oxides. As in the case of propane ammoxidation, the latter catalyst exhibits superior performance in terms of both paraffin conversion and selectivity to acrylic acid, and, also, low formation of other, less desirable, oxygenated compounds. This catalyst has been used by different companies; depending on the method of preparation claimed, the active compound (the M2 phase claimed by Mitsubishi for ammoxidation of propane [204, 210]) can be obtained more or less pure, and, thus, having different catalytic performances.

Table 7. Catalytic performance of different catalysts claimed for propane oxidation to acrylic acid (AA).

Catalyst	Ref.	T (°C)	$C_3/O_2/H_2O/N_2$ (molar %)	C_3H_8 conv. (%)	Sel. AA (%)
$Mo_1Sb_{0.25}V_{0.3}Nb_{0.12}K_{0.013}O_x$	223	420	4.4/7.0/62.3/26.3	48.8	68.5
$BiMo_{12}V_5Nb_{0.5}SbKO_x$	157	400	26.3/10.5/63.2/0	19.0	29.0
$Mo_1V_{0.3}Te_{0.23}Nb_{0.10}O_x$	224	390	3.2/9.6/49/38.2	71.0	59.0
$Mo_1V_{0.3}Te_{0.23}Nb_{0.12}O_x$	205	380	3.3/10/46.7/40	80.1	60.5
$MoSnO_x$	225	360	50/20/0/30	4.0	48.0
$Bi_{0.02}Ni_{0.75}MoO_x$	227	425	60/20/20/0	14.7	30.6
Ni/Mo/Te/P/O	226	460	15/18/6.5/60.5	12.3	23.3
$(VO)_2P_2O_7$	228	355	0.9/31.8/67.4/0	46.0	15.0
$H_3PMo_{12}O_{40}$ (reduced by pyridine)	41	340	20.4/9.9/19.9/49.8	8.7	30.6
$H_2(VO)_{0.5}PMo_{12}O_{40}$–$Cs_3PMo_{12}O_{40}$	233	ng	63/7.5/0/29.5	44.8	22.7
$H_5PV_2Mo_{10}O_{40}$	222	ng	1.7/25/0/73.3	50.0	23.0
$Cs_{2.5}Fe_{0.08}H_{1.26}PVMo_{11}O_{40}$	36	380	30/50/0/20	46.0	27.0

Common features of the above mentioned systems are i) the presence of vanadium inside a definite crystalline framework (vanadyl pyrophosphate for V/P/O mixed oxides, the Keggin $(PMo_{11}V_1O_{40})^+$ anion for polyoxometalates, and the so–called Mitsubishi M2 phase [204] for Mo/V/Nb/Te/O systems), and ii) intrinsic acidity, which is likely to be an important feature to accelerate acrylic acid desorption and avoid consecutive combustion reactions. The surface acidity, however, also affects the nature of by–products, as pointed out by Ai [228–230], who compared the performance of doped V/P/O–based catalysts, and of Keggin– type polyoxometalates. Ai proposed that the mechanism first involves the oxidehydrogenation of the paraffin (the rate–determining step, suppressed by the presence of water in the feed). The olefin is hydrated in part to yield 2–propanol (and thus the acidity of the catalyst is a fundamental property in addressing the reaction pathway and the final selectivity), while a fraction of the olefin is oxidized to acrolein. Water therefore clearly plays an important role in affecting the selectivity. Propanol is the precursor of acetic acid + CO via intermediate acetone, while acrolein is the precursor of acrylic acid. Both products undergo consecutive reactions of combustion. The main by–products, in addition to carbon oxides, are acetic acid and propylene. The ratio between acetic acid and acrylic acid is thus a function of the surface acidity, and for this reason Keggin–type heteropolycompounds, i.e. $H_3PMo_{12}O_{40}$ and $H_3PW_{12}O_{40}$, give a much higher selectivity to acetic acid than V/P/O–based catalysts.

Heteropolyacids have been studied mainly by Ueda [41, 231, 232] and Mizuno [36–39, 234, 235]. The former author claims the importance of having a reduced heteropolycompound to achieve better catalytic performance. On the contrary, Mizuno et al. [36–39] point out that in polyoxometalates having transition metal ions as the cations (Fe^{2+} and Cu^{2+}), the role of the latter is to improve the rate of catalyst reoxidation, especially under oxygen–poor conditions. Another factor claimed to play an important role in affecting the selectivity to acrylic acid is the pore volume and the average pore diameter of the catalyst [233]. A linear relationship was reported to exist between yield to acrylic acid and pore volume, and between selectivity to acrylic acid and average pore diameter. A selectivity as high as 40% could be reached with a V–containing P/Mo/O heteropolyacid, supported over the wide–pore cesium–salt of the $(PMo_{12}O_{40})^{3-}$ Keggin anion, having an average pore diameter of 150 Å and pore volume of 0.10 ml/g.
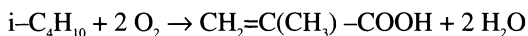
9.   Oxidation of Isobutane to Methacrylic Acid

Methacrylic acid is currently synthesized via the acetone–cyanohydrin route, which consists of an initial reaction between acetone and hydrogen cyanide to give the acetone–cyanohydrin, which is then reacted with an excess of concentrated sulphuric acid to form the methacrylamide acid sulfate. In a successive stage, the methacrylamide is treated with an excess of aqueous methanol; the amide is hydrolyzed and esterified, with formation of a mixture of methyl methacrylate and methacrylic acid. Main drawbacks of this process are the utilization of highly toxic raw materials (HCN) and the coproduction of an equimolar amount of NH_4HSO_4 for each mole of methyl methacrylate, which can not be used for fertilizer production since it is contaminated with organic compounds.
Different alternative routes have been proposed [236]:

1. The BASF process [237], which starts from ethylene, first hydroformylated to give propionaldehyde, then condensed with formaldehyde to produce methacrolein. Methacrolein is then oxidized to methacrylic acid, followed by esterification with methanol.
2. The integrated process developed by Mitsubishi Rayon and Nippon Methacryl Monomer (a joint venture of Sumitomo Chemical and Nippon Shokubai) where isobutene, obtained by conventional technologies of isobutane dehydrogenation and separated from the latter by hydration, is oxidized to methacrolein and then to methacrylic acid. Alternatively, Asahi first carries out the ammoxidation of isobutene to methacrylonitrile, which is then hydrolyzed and esterified.
3. Halcon has developed an integrated process for the selective oxidation of either propane or isobutane [219, 238]. The paraffin is first dehydrogenated; the reactor outlet stream (isobutene, unconverted isobutane and hydrogen) is sent to an oxidation reactor without separation of the components. In this step isobutene is selectively oxidized to methacrolein, while isobutane and hydrogen do not react. Methacrolein is then separated, oxidized, and esterified, while isobutane is recycled to the dehydrogenation reactor after separation of oxygen and of hydrogen. Optionally, hydrogen can be oxidized with a suitable catalyst.

4. Mitsubishi Chemical Industries and Asahi have each developed their own process for the synthesis of methacrylic acid via oxidative dehydrogenation of isobutyric acid. The latter is obtained as a by–product in the oxo–synthesis of n–butyraldehyde from propylene and is therefore available at a reasonable price.

5. Mitsubishi considerably improved the traditional acetone–cyanohydrin process by eliminating process wastes. The acetone–cyanohydrin is first hydrolized to 2–hydroxyisobutylamide (HBD) with a MnO_2 catalyst. HBD then reacts with methylformiate to produce the methyl esther of 2–hydroxyisobutyric acid (HBM), with coproduction of $HCONH_2$ (the reaction is catalyzed by CaO). HBM is finally dehydrated with a zeolite Na–Y to methyl methacrylate. Formamide is converted to HCN, which is used to produce acetone–cyanohydrin by reaction with acetone.

6. Several patents and papers have appeared in the 1980's and 90's claiming the possibility of carrying out the synthesis of methacrylic acid by the one–step oxidation of isobutane in the gas phase, over Keggin–type heteropolycompounds as heterogeneous catalysts [33–42, 239–258].

$$i–C_4H_{10} + 2\ O_2 \rightarrow CH_2{=}C(CH_3)\ –COOH + 2\ H_2O$$

The direct synthesis of methacrylic acid via oxidation of isobutane looks particularly interesting because of i) the low cost of the raw material, ii) the simplicity of the one–step process (above all, if compared to the complexity of the acetone–cyanohydrin route), iii) the very low environmental impact, and iv) the absence of inorganic coproducts. Rohm & Haas Company was the first, in 1981, to claim the one–step oxidation of isobutane to methacrolein and methacrylic acid [42]. Even though no reference to heteropolycompounds is given in the patent, the claimed catalyst compositions are clearly Keggin–type structures. Starting from this patent, a number have followed, mainly from industrial companies from Japan, claiming the use of modified Keggin–type heteropolycompounds as catalysts for the oxidation of isobutane.

A peculiar feature of the claimed processes is that almost all of them use isobutane–rich conditions, with isobutane–to–oxygen molar ratios around 2, and thus with oxygen as the limiting reactant. This, of course, leads to relatively low conversions of the paraffin (almost all patents claim isobutane conversions not higher than 15%), with need for recirculation of the unconverted isobutane. For this reason Sumitomo claims the oxidation of CO to CO_2 (contained in the effluents from the oxidation reactor) in a separate reactor with a supported Pd catalyst, after the condensation of methacrolein and methacrylic acid. CO_2 can then be removed by absorption in a basic solution [243, 244].

In some Mitsubishi patents [245] higher conversions of isobutane are reported, (around 25 %), because an isobutane–to–oxygen ratio of 0.6 is used, closer to the stoichiometric one for the synthesis of methacrylic acid. In all cases steam is present as the main ballast. The role of the steam is to decrease the concentration of isobutane and oxygen in the recycle loop and, thus, keep the reactant mixture outside the flammability region. Water can be easily separated from the other components of the effluent stream, and, moreover, it plays a positive role in the catalytic performance of heteropolycompounds, because it helps in surface reconstruction of the Keggin structure, decomposed during the reaction at high

temperature, and favours desorption of methacrylic acid, saving it from unselective consecutive reactions.

Under the reaction conditions described in patents, methacrolein is a product always present in non–negligible amounts, and therefore a commercial process would require an economical method for recycling not only unconverted iso-butane, but also methacrolein. Patents assigned to Asahi Chem. Ind. [257] claim the use of an organic solvent, a mixture of decane, undecane and dodecane, which can efficiently absorb isobutane and methacrolein from the off–gas, with a 99.5% recovery efficiency. Isobutane and methacrolein are then stripped with air and recycled.

In Asahi patents the use of a catalyst suitable for fluidized–bed operation in CFB reactors is also reported, so as to allow continuous transport of catalyst from the reaction to the regeneration vessel, and vice versa. Also, alternate feeding of isobutane and of oxygen over the catalytic bed allows higher selectivities to be obtained [258]. In this case, the catalyst claimed is an ammonium salt of a P/Mo Keggin–type heteropolycompound. With the CFB reactor 8% isobutane conversion, 54% selectivity to methacylic acid and 17% selectivity to meth-acrolein are obtained. A similar process configuration has also been claimed by Sumitomo [243], which makes use of isobutane and air (in the two separate steps) which are diluted in steam, and a catalyst analogous to that used under usual cofeeding tests. In this case, a conversion of 11.2% is claimed, with a selectivity of 52.9% to methacrylic acid and 12.8% to methacrolein.

There are a few features relative to heteropolycompounds, common to most published papers and patents, which seem to be an important condition to obtain the best performance. In all cases, vanadium is present in the framework of the P/Mo Keggin anion, while the cations include different components, i.e. protons, divalent transition metal ions (preferably Cu^{2+}), and alkali metal ions (preferably Cs^+). The role of Cu ions is to catalyze the reduction of molybdenum, thus increasing the activity of the catalyst [249, 250]. They also affect the surface acidity [33, 249].

According to Asahi patents [240], the heteropolycompound, in order to be active and selective, has to be characterized by the cubic structure, and by a partial degree of reduction (also achieved by *in situ* treatment with isobutene at 450°C). The importance of having molybdenum of the Keggin anion in part reduced has also been claimed by other authors [41, 231, 232, 248, 253]. It is possible that a more reduced catalyst leads to a better selectivity to the product of partial oxidation, and is thus less active in total combustion. This might also explain, why in all cases isobutane–rich conditions are reported, since they are more reducing than those with a low concentration of isobutane (i.e., isobutane–leaner conditions with respect to the flammability zone).

A partially reduced catalyst can be achieved by preparing compounds having organic cations which during thermal treatment are oxidized at the expense of Mo^{6+} [231, 232]. Another possibility is to prepare compounds having cations which can make electrons exchange with Mo^{6+} in the anion, themselves becoming oxidized. It has been found, for instance, that the presence of Sb^{3+} in the compound makes possible the reduction of part of Mo^{6+} at 350–400°C even under oxidizing conditions (i.e., in the presence of air or under hydrocarbon–lean conditions) [254]. The Mo^{5+} species which develop by the redox reaction are stabilized towards reoxidation.

The best results obtained with the various heteropolycompound–based catalysts found in the patent and scientific literature are summarized in Table 8.

Table 8. Summary of results reported in literature for the oxidation of isobutane to methacrolein and methacrylic acid catalyzed by Keggin–type heteropolycompounds

Catalyst	Ref.	T (°C)	τ (s)	$iC_4H_{10}/O_2/H_2O/N_2$ (molar %)	iC_4H_{10} conv. (%)	Selectivity MAC+MAA (%)
$H_xPMo_{12}SbO_y$	42	340	6.1	10/13/30/47	10.0	20+50
$H_xP_{1.1}Mo_{12}V_{1.1}Cu_{0.1}Cs_{1.1}O_y$	240	320	3.6	30/15/20/35	10.3	16.3+55.7
$H_xP_{1.5}Mo_{12}V_1Cu_{0.2}Nd_{0.5}Cs_1O_y$	252	320	3.6	30/15/20/35	12.8	15.9+53.8
$H_xP_{1.5}Mo_{12}VOs_{0.04}Cu_{0.2}Ba_{0.2}K_{0.5}Cs_{0.5}O_y$	245	320	2.4	10/16.8/10/63.2	16.3	10.0+50.1
$H_4PMo_{11}VO_{40}/Ta_2O_5$	255	350	2	4/8/0/88	28.5	41+13.3
$H_xP_{1.5}Mo_{12}V_{0.5}As_{0.4}Cs_{1.8}Cu_{0.3}O_y$	243	320	3.6	26/13/12/49	11.2	11.5+53.6
$H_xP_{1.5}Mo_{12}V_{0.5}As_{0.4}Cs_{1.4}Cu_{0.3}O_y$	256	330	5.4	6.5/15.5/15/63	25.0	42.6+2.5
$H_{3.6}Cu_{2.0}PM_{11}VO_{40}/SiO_2$[a]	241	348	b	15.1/29.6/19.7/35.5	13.0	55.6+11.5
$H_{1.34}Cs_{2.5}Ni_{0.08}PMo_{11}VO_{40}$	239	340	2	17/33/0/50	31.0	29+8
$K_1(NH_4)_xFe_1PMo_{12}O_y$	33	350	3.6	26/13/12/49	10.8	32+8
$(Pyr)_3PMo_{12}O_{40}$	248	300	c	2.2/13.7/33.5/50.6	22.2	51.1+tr
$H_{2.4}Cs_{1.6}P_{1.7}Mo_{11}V_{1.1}O_{40}$	40	349	3.6	26/12/12/50	10.6	37.6+7.9

MAC = methacrolein; MAA = methacrylic acid; [a] 43% of active phase
b W/F 2.1 g h ml^{-1}
c W/F 0.1 g min ml^{-1}

The reaction network consists of parallel reactions of formation of methacrolein, methacrylic acid and carbon oxides, and of consecutive reactions of formation of acetic acid and carbon oxides. Methacrylic acid is also in part formed by consecutive reaction on methacrolein, especially at low temperature [34]. Methacrolein is much less stable than methacrylic acid, and undergoes consecutive reactions of degradation to a much greater extent than the acid [34, 35, 246].

The mechanism of the reaction is illustrated in Figure 9 [34]. The interaction with the catalyst occurs through a classical redox mechanism [246]. The mechanism involves the initial abstraction of a H$^-$ species at the tertiary C atom of the alkane, possibly by an anionic vacancy in the Keggin anion [40]. This is the rate–limiting step of the reaction [246]. An adsorbed alkoxy species is thus formed, which is then converted to an allylic alkoxy species. A dioxyalkylidene species then develops, where the primary carbon atom is connected to the catalyst surface via two C–O–Mo bridges. This intermediate is either transformed to methacrolein (through dissociation of a C–O bond), or to a carboxylate species (via oxidation on a Mo site), which is the precursor for the formation of methacrylic acid [34]. The reduced catalyst is then reoxidized by oxygen.

Catalysts other than polyoxometalates which have been studied for the oxidation of isobutane to methacrylic acid include Pt/SbOx [259], Bi/Mo/Nb mixed oxides [260], and doped V/P mixed oxides [261, 262]. Vanadyl pyrophosphate does not exhibit good performance in the reaction (it is not active, and the only product of partial oxidation is methacrolein). However, when the V/P/O system is doped with other metal ions (preferably Co, Nb, Ni ions), an

unexpected high activity and good selectivities are obtained to methacrylic acid and methacrolein. For instance, with a catalyst having the composition $P_1V_{0.9}Co_{0.09}Nb_{0.3}O_x$, at 280°C a conversion of 23.6% for isobutane was obtained, with a selectivity to methacrylic acid of 21.7% and to methacrolein of 45.2%. The feed composition was isobutane/oxygen/steam/inert 50/25/25/0 molar %.
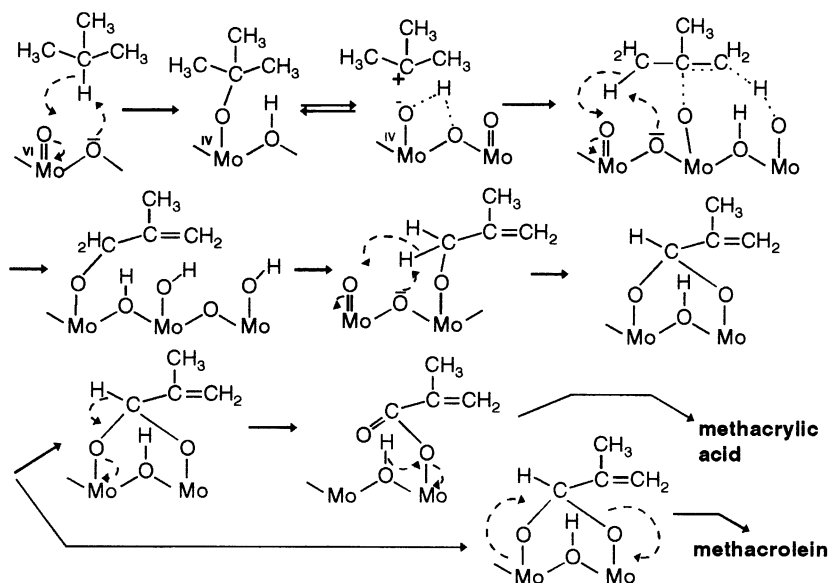

Fig. 9. Proposed mechanism for the oxidation of isobutane to methacrolein and methacrylic acid [34].

10. Oxidation of n–Butane to Maleic Anhydride

Maleic anhydride is one of the intermediate products with the highest forecasted increase in demand in the near future; the expected annual growth is higher than 3 %. Several processes which differ regarding both raw materials (benzene, n–butane, butenes) and technologies employed, have been proposed and commercialized. Since 1974 benzene has been continuously substituted first with a C_4 fraction containing paraffins and olefins and later with n–butane.

$$n-C_4H_{10} + 3.5\ O_2 \rightarrow C_4H_2O_3 + 4\ H_2O$$
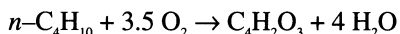
The main reasons for the replacement of benzene with n–butane are the following: i) the higher price of the benzene, ii) environmental problems (benzene is classified as a carcinogen), and iii) quality of the product. Heavy by–products are obtained from benzene (phthalic anhydride, benzoquinone) and lower molecular weight acids from butenes.

10.1 Current Industrial Technologies

The several commercial processes for maleic anhydride production from n-butane differ regarding i) type of reactor (fixed–bed, fluidized–bed, transport–bed), ii) type of recovery of maleic anhydride (aqueous or organic), iii) method of purification of maleic anhydride (azeotropic batch or continuous distillation, thin–layer evaporator), iv) gas phase composition (concentration of *n*–butane: in general not higher than 1.8% in air in fixed–bed reactors, 3.6–5 % in air in fluidized–bed reactors, and higher than 4 % in inerts in the riser reactor for the CFB process), v) procedures of preparation, activation and regeneration of the catalyst, vi) nature and amounts of chemical and physical promoters for the active phase $(VO)_2P_2O_7$, which is common to all the processes, and vii) purity of maleic anhydride and type of downstream processes.

Table 9 reports the main features of the different industrial processes.

Table 9. Main features of the different industrial processes

Process, licensor	Type of reactor	Maleic anh. recovery	Ref.
DuPont	Transport–bed	Aqueous	45–50, 263, 264
ALMA (Alusuisse, Lummus)	Fluidized–bed	Anhydrous	265–267
Alusuisse Italia	Fixed–bed	Anhydrous or aqueous	
Amoco	Fixed–bed		268–271
BP (Sohio)–UCB	Fluidized–bed	Aqueous	272, 273
Denka–Scientific Design	Fixed–bed	Aqueous	274
Mitsubishi Kasei	Fluidized–bed	Aqueous	275, 276
Mitsui Toatsu	Fluidized–bed		277, 278
Monsanto	Fixed–bed	Anhydrous	279–282

A further aspect to take into consideration is the reaction pattern, which affects the value of conversion at which the highest yield of maleic anhydride is obtained. In fact both parallel and consecutive reactions of total combustion are important, and the conversion must be lower than 80 % in order to avoid overoxidation of maleic anhydride. The main by–products are CO and CO_2, while minor amounts of acetic acid, acrylic acid and phthalic anhydride (with overall selectivity lower than 5%) are formed.

The catalyst is for all processes made substantially of a mixed oxide of vanadium and phosphorus characterized by a well–defined crystalline structure, vanadylpyrophosphate $(VO)_2P_2O_7$, prepared by thermal treatment of a crystalline precursor, $(VO)HPO_4 \cdot 0.5H_2O$. Older catalyst formulations were prepared in an aqueous solvent, while in the most recent patents for almost all industrial preparations, organic solvents are preferred.

The several different preparations described in the patents issued by the various companies have been compared and discussed [283]. An empirical formula which can represent all the catalyst formulations is the following: $VP_aMe_bO_x/inert_y$. Wide variations in the value of a (0.8 to 1.5) and a wide spectrum of promoters have been claimed in the patents: Li, B, Zn, Mg, Co, Fe, Ni, Cr, Ti, Mo, W, Bi, Zr, rare earths. However, in the most preferred catalyst composition the value of a ranges from 1.03 to 1.2, the value of b is from 0 to 0.1, Me is one or more chosen among Zn, Li, Mo, Zr, and Fe, the inert is colloidal silica and the value of y ranges from 0 to 10% by weight with respect to the active component.

For fixed–bed applications, the catalyst is pressed into cylindrical pellets. For fluidized–bed reactors, different preparation techniques can be used to increase the attrition resistance of the catalysts:

1. Impregnation of active components onto a support with optimal fluidization properties;
2. Embedding of the active component in an inert material with high attrition resistance;
3. Addition of small amounts of additives to the precursor;
4. Encapsulation of the active component in a thin shell of silica.

The main features of three different processes (which can be taken as representative of the three technologies in fixed–bed, fluidized–bed and transport–bed) are examined below.

The ALMA process is a technology jointly developed by Lummus Crest (expertise in fluidized–bed and catalyst technology) and Alusuisse Italia (expertise in maleic anhydride production from benzene and *n*–butane) [265–267]. A fluidized–bed reactor, and an organic (non–aromatic) solvent recovery system for maleic anhydride are employed. The catalyst is made of unsupported active phase, prepared by spray drying the ball–milled precursor with a small amount of additives. A molar yield of maleic anhydride of 50 % at 80–85 % conversion is claimed, with 4 % *n*–butane in the feed.

A flow diagram of the process is reported in Figure 10. The reactor effluents, after separation of the catalyst in cyclones, are cooled down to 200°C, filtered to remove the fines and delivered to the maleic anhydride recovery system. The fines are in part recycled and in part collected in a catalyst handling system. After separation of the fines, the reactor effluents are scrubbed with cycloaliphatic esters to remove the maleic anhydride without condensation of water. The off–gas is converted in a thermal incinerator, where all organic compounds are burnt to carbon oxides. The maleic anhydride is separated by the solvent, most of which is recycled to the scrubber, while a small part is sent to a solvent purification section. The crude maleic anhydride is then purified from the light ends, which are sent to the incinerator, and from the solvent, which is recycled to the previous separation column.

DuPont de Nemours has developed an integrated process for the production of tetrahydrofuran from *n*–butane [263, 264]. Important key aspects of the process have been the development of a new hardening procedure to prepare catalysts with high attrition resistance, and the development of the CFB reactor (transport–bed) concept for the oxidation of *n*–butane.

A flow diagram of the process is reported in Figure 1. Fresh *n*–butane together with the recycle gas and the reoxidized catalyst enter from the bottom of the riser. After separation of reduced catalyst from the gas stream, the catalyst is introduced into the fluidized–bed where it is oxidized with air before being recycled into the riser. Maleic anhydride is recovered from the off–gas by scrubbing with water and the aqueous maleic acid is reduced to tetrahydrofuran in the hydrogenation reactor.
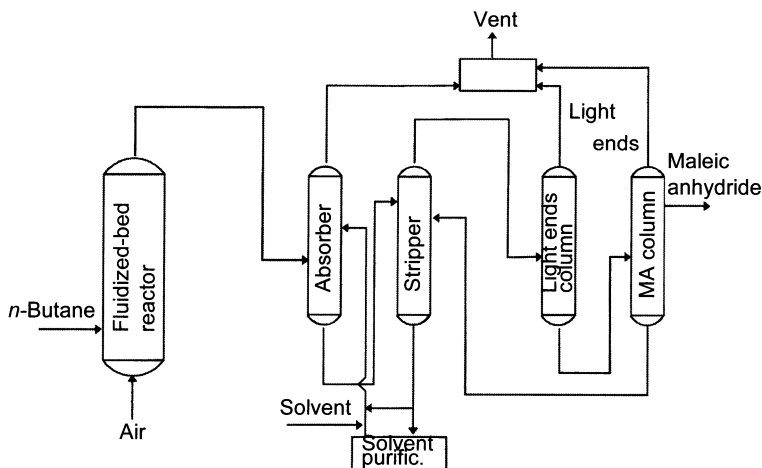
Fig. 10. Simplified flow–sheet of the ALMA process

A catalyst with high attrition resistance is prepared by coating the active component with silica. The catalyst is prepared by grinding the precursor into 2μm particles and forming a slurry with freshly prepared silicic acid to produce a sample containing 10 % silica by weight. When the slurry dries, silicic acid migrates to the surface of the particles and ultimately polymerizes on the surface of the particles. The silica coats the active components and forms a very strong porous shell which gives high mechanical resistance and does not cause loss in selectivity.

In a pilot CFB reactor, a selectivity of 75% to maleic anhydride is obtained up to 50% n–butane conversion, for concentrations of hydrocarbon ranging from 1 to 50%. At higher conversions the selectivity decreases, reaching the value of 60% at 90% conversion. The rate of circulation of the catalyst is affected by the amount of active oxygen available on the catalyst surface. It has also been calculated that the available oxygen is that formed by oxidation of the first monolayer on the surface of $(VO)_2P_2O_7$. The estimated catalyst circulation rate in the plant is 0.5 ton/s for a 100 million lb/yr maleic anhydride plant, which is within the range of commercial FCC reactors.

Monsanto uses a fixed–bed reactor, cooled by molten salts, and organic solvent recovery for maleic anhydride. Several patents have been issued by the scientists of Monsanto directed towards improving their technology by modifying the catalyst composition, the activation procedure, the shape of the catalyst and the reactor technology [279–282]. Catalyst calcined with a multi–step procedure and in the presence of controlled atmospheres (also including steam) [280] needs shorter activation periods, and gives 59% yield to maleic anhydride. In order to decrease the hot–spot temperature, responsible for the catalyst decay, dilution of the catalyst with inert material such as silica or alumina has been proposed. In one patent it was suggested that the catalyst bed should be divided into three portions [279]. In the first part the catalyst is diluted with 30 wt.% inert, in the middle part with 20% inert, and in the final reactor section (where n–butane is more diluted)

the catalyst is not diluted. Particularly shaped structures of V/P/O particles have also been patented [281].

The possibility of using n–butane concentrations in air higher than the lower flammability limit in fixed–bed reactors has also been investigated [282]. This leads to an increase in productivity of maleic anhydride. It is likely that currently a n–butane concentration of approximately 2.4 % is used.

10.2   The Main Features of the Active Catalyst

A great number of scientific papers has been published beginning in the 1970's, dealing with the study of the V/P/O–based catalytic system. These papers have been analyzed in several reviews and monographs, which summarize the most important aspects concerning the reaction and the catalytic system [9, 16, 283–289]. The structure of the vanadyl pyrophosphate is illustrated in Figure 11, where the vanadyl dimers are evident, connected along the a axis through V=O—V bonds, and separated in the bc plane by pyrophosphate groups.

The role of different vanadium phosphate phases, and the role of the valence state of vanadium in the selective oxidation of n–butane to maleic anhydride has been widely studied [290–300]. In general, the fundamental role of the vanadyl pyrophosphate, $(VO)_2P_2O_7$, as the active phase is recognized, but it is also believed that oxidized V^{5+} sites, present as dispersed $VOPO_4$ phases at the surface of the vanadyl pyrophosphate, or in the form of domains at the basal {100} face of $(VO)_2P_2O_7$, are directly involved in the formation of maleic anhydride. The contemporaneous presence of V^{4+} and V^{5+} seems to guarantee the best catalytic performance, even though this has been confuted by some authors [291], who proposed that the best catalytic system is the one which only contains vanadyl pyrophosphate with well–ordered stacking of the (200) planes.

The oxygen species which are involved in the multi–electron transformation of n–butane are both bulk oxygen ions (even though probably limited to a few surface atomic layers), and chemisorbed species [298, 299, 301, 302]. Even though the vanadyl pyrophosphate is very–well crystallized, and formally contains no V^{5+} species, in the reaction environment "patches" of V^{5+} species or dispersed oxidized ions develop, either by chemical adsorption of oxygen, or by oxidation of vanadyl pyrophosphate layers. These species give a fundamental contribution to the mechanism of formation of maleic anhydride. In some cases, $VOPO_4$ phases are already present in the catalyst, expecially when the compound has been calcined in air before reaction [290]. In addition, the formation of oxidized $VOPO_4$ phases in the reactor will be affected by i) the reaction conditions, i.e. temperature and gas phase composition, and ii) the bulk features of the vanadyl pyrophosphate, such as the crystallinity and the P/V ratio [9]. The latter parameter is also affected by the presence of water vapour in the reaction environment [303-305]. Water leads to a surface enrichment of phosphate anions through migration of P.

It is worth mentioning that spent equilibrated catalysts may exhibit a vanadium valence state which varies from 4.00 [290, 291, 306], to 4.02 [299], or even higher [297, 307]. It has been proposed that a limited amount of surface V^{5+} is necessary to obtain the highest selectivity to maleic anhydride, but that excessive vanadium oxidation leads to an enhancement of the consecutive combustion of maleic anhydride [308, 309].
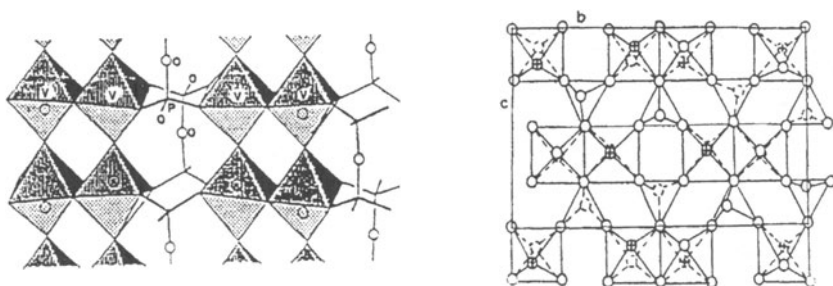
Fig. 11. The vanadyl pyrophosphate, $(VO)_2P_2O_7$, active phase in *n*–butane oxidation

The complex transformation of *n*–butane to maleic anhydride requires several different types of oxidizing attacks on the molecule [262]. The transformation of *n*–butane to maleic anhydride may involve the following steps at the adsorbed state [285]:

1. *n*–butane + ½ O_2 → butenes + H_2O (oxidative dehydrogenation)
2. butenes + ½ O_2 → butadiene + H_2O (allylic H–abstraction)
3. butadiene + ½ O_2 → 2,5–dihydrofuran   (1,4 oxygen insertion)
4. 2,5–dihydrofuran + 2 O_2 → maleic anhydride + 2 H_2O (allylic O–insertion, possibly via γ–but–2–enoic lactone)

or:

4. 2,5–dihydrofuran + ½ O_2 → furan + H_2O (allylic H–abstraction)
5. furan +1.5 O_2 → maleic anhydride + H_2O (electrophilic O-insertion)

Other proposed mechanisms involve either a direct attack of O^{2-} species at the 1,4 C atoms of *n*–butane [310], or an allylic oxidation of an olefinic–like C_4 intermediate to crotonaldehyde, followed by internal cyclization and oxidation [311]. A dienic intermediate has also been proposed by Grasselli et al. [301]. In any case, the reaction patterns proposed evidence the need for different kinds of active sites on the surface of the vanadyl pyrophosphate, able to perform each step in the reaction pathway with high selectivity.

The polyfunctional nature of the vanadyl pyrophosphate is clearly evidenced by the different reactions which can be catalyzed by this material, as summarized in Table 10. Vanadyl pyrophosphate can catalyze most of these transformations with good selectivity. This also indicates that the several steps proposed for the mechanism of *n*–butane oxidation to maleic anhydride can effectively occur on this compound. Moreover, $(VO)_2P_2O_7$ possesses surface acid centres. Acidity is recognized to play important roles in the activation of the paraffin, in the desorption of the acid products, and in accelerating specific transformations over reactive intermediates. The vanadyl pyrophosphate also may favour bimolecular condensation reactions which are not acid–catalyzed, but which are accelerated by the proper geometry of sites at which the molecules are adsorbed. This property likely plays an important role in the mechanism of phthalic anhydride formation from *n*–pentane [312].

Table 10. Classes of reaction catalyzed by the vanadyl pyrophosphate

Reactant	Product	Reaction type
isobutyric acid	methacrylic acid	oxidehydrogenation
cyclohexane	benzene	oxidehydrogenation
hexahydrophthalic anhydride	phthalic anhydride	oxidehydrogenation
paraffin	olefin	oxidehydrogenation
olefin	diolefin	allylic oxidation (H–abstraction)
2,5–dihydrofuran	furan	allylic oxidation (H–abstraction)
tetrahydrophthalic anhydride	phthalic anhydride	allylic oxidation (H–abstraction)
toluene	benzonitrile	benzyl (amm)oxidation
benzene	maleic anhydride	electrophilic oxygen–insertion
butadiene	furan	electrophilic oxygen–insertion
naphthalene	naphthoquinone	electrophilic oxygen–insertion
furan	maleic anhydride	electrophilic oxygen–insertion

One main characteristic of n–butane oxidation is the substantial absence of by–products of partial oxidation other than maleic anhydride. This means that once the alkane has been adsorbed and transformed into the first intermediate species, the latter has to be quickly further converted to the final stable product. If this requirement is not met, the adsorbed olefinic–like intermediate may desorb. This leads to a lower selectivity to the final desired product, because the olefin may be readsorbed on non–specific oxidizing sites yielding other undesired products (aldehydes or acids), which can also be precursors for the formation of carbon oxides. In order to guarantee this selective pathway, the catalyst surface must provide the required arrangement of specific oxidizing sites: the different functional properties must be arranged so as to provide an ensemble of sites (or, alternatively, sites with multifunctional properties) able to allow the reaction pathway from alkane adsorption and activation up to its transformation to the final product to be completed.

An important aspect associated with the reactivity of the V/P/O system concerns catalyst aging, and modifications which occur in the catalyst under reaction conditions. This is an important aspect from an industrial point of view, since the stable (and also the best) performance is usually reached when the catalyst i) is well crystallized, and ii) has reached an "equilibrated" state. Under these conditions the distribution of V species having different valence states is that which is in redox equilibrium with the gas phase. The latter can be more or less reducing, depending on the hydrocarbon–to–oxygen ratio and on the reaction temperature.

The time–on–stream which is necessary to reach this "equilibrated" state, and, thus, to reach a stable catalytic performance, is essentially a function of the characteristics of the fresh catalyst. The greater are the differences with respect to the characteristics of the equilibrated catalyst, the longer the time that is needed (sometimes hundreds of hours) to reach the steady state [300]. Recent works by Bordes et al. [315–318] demonstrate that the transformation of the catalyst precursor, $VOHPO_4 \cdot 0.5H_2O$ into the final catalyst occurs with development of mosaic–like particles of slightly misoriented small crystallites of vanadyl pyrophosphate [314]. Therefore the morphology of the final catalyst may be profoundly affected by the procedure adopted for the thermal treatment, and in turn the morphological features may greatly influence the chemical-physical

properties of $(VO)_2P_2O_7$, and thus its catalytic performance. For this reason, a thermal treatment (activation) which is able to transform the precursor to a catalyst with characteristics very close to those of the equilibrated one may represent a substantial advantage from the industrial point of view. When the thermal treatment of the precursor is carried out in the presence of steam, a well crystallized vanadyl pyrophosphate develops [313], which exhibits a stable catalytic behavior from the very beginning.

An important point is represented by the role of V^{3+} species, present as defects in the vanadyl pyrophosphate structure. It has been reported that defectivity can enhance the activity of V^{4+} ions, thus leading to more active catalysts [300, 319, 320]. Reduced V species develop during the thermal treatment of the precursor when the latter contains organic compounds retained in the interlayer spacing of its layered structure. When the thermal treatment is carried out in nitrogen atmosphere, the organic compounds are released from the solid, and while forming carbon oxides pick up ionic oxygen from the structure, at the same time reducing the V ions [321, 322]. The final extent of reduction of the vanadyl pyrophosphate is approximately proportional to the amount of organic compounds originally retained in the precursor. More reduced catalysts are more active; this is shown in Figure 12, which plots the conversion of *n*–butane and the selectivity to maleic anhydride as functions of temperature for three catalysts having increasing extents of V reduction. Results refer to almost equilibrated catalysts, which had been running under reaction conditions for more than 100 h.

11. Oxidehydrogenation of Paraffins to Olefins

Light olefins (along with methane and aromatics) are obtained from steam cracking of natural gas and of naphtha and from FCC. These established processes are extremely capital–intensive. The products have to be separated and purified for use in downstream plants that require fairly pure feedstocks, and the supply and demand for each coproduct are rarely in balance. Consequently, the increase in demand for olefins in the future might be satisfied by a direct production of individual or specific cuts of olefins in selective processes. In addition, an integration of these plants with downstream plants for olefins transformation into valuable chemicals can be advantageous in many cases.

Commercial processes for the synthesis of light olefins through paraffin dehydrogenation are available, even though their main application is the isobutene synthesis [323]. In the case of propane, a couple of plants are in service, while in the case of ethane thermodynamic constraints would force operation at impracticable temperatures. The commercial catalytic dehydrogenation processes suffer from several constraints, in particular: i) thermodynamic limitations on paraffin conversion; ii) side reactions such as thermal cracking; iii) strongly endothermic reactions to which large amounts of heat must be supplied at temperatures above the reaction temperature; and iv) formation of coke on the catalyst which requires frequent regeneration. With the goal of overcoming these limitations, some alternatives are currently studied, of which the following are the most likely to be implemented: i) optimization of the current dehydrogenation technologies, to *obtain more selective, stable* and environmentally safe catalysts and lower the investments and the utility costs; ii) dehydrogenation coupled with hydrogen

oxidation, in order to supply the heat of reaction inside the catalytic bed while avoiding overheating and to shift the equilibrium toward the desired products; iii) oxidative dehydrogenation, to overcome thermodynamic limitations, to operate an exothermic reaction at low temperatures, and to avoid frequent catalyst regeneration; and iv) membrane–assisted dehydrogenation, to obtain high conversions at low temperatures and to conduct the reactions and separations in the same equipment.
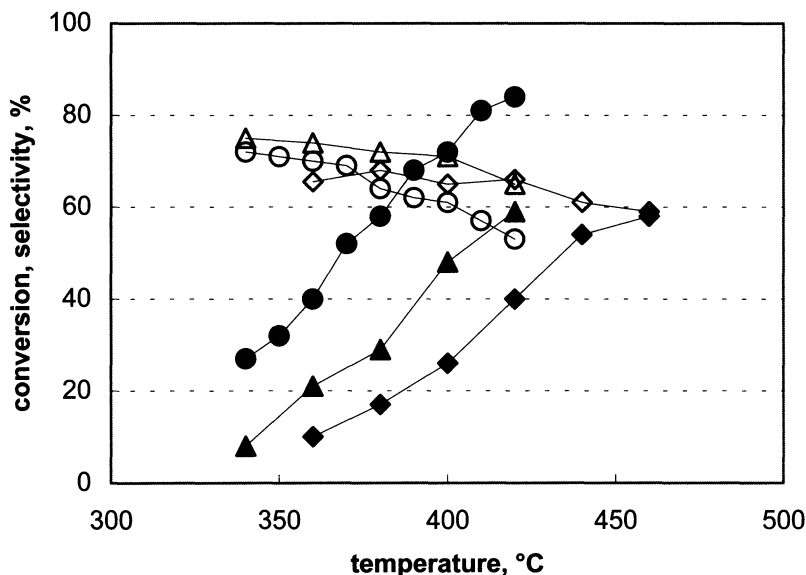

Fig. 12. Conversion of n-butane (full symbols) and selectivity to maleic anhydride (open symbols) as a function of temperature for almost-equilibrated catalysts having different average valence state of V: ◆ ($V^{3.99+}$), ▲ ($V^{4.02+}$) and ● ($V^{3.92+}$) (as determined by chemical analysis of spent catalysts).

The introduction of a hydrogen acceptor like oxygen into the dehydrogenation reaction medium allows a number of technical problems that are met with pure dehydrogenation to be overcome, i.e. the thermodynamical limitations (the reaction becoming practically irreversible), the endothermicity and the deposition of coke on the catalyst.

On the other hand, a number of other technical problems arise:

1. Removal of the heat of reaction from the reaction medium. The oxidative dehydrogenation is exothermic, and is accompanied by even more exothermic combustion reactions. This influences the selection of the proper type of reactor, in order to minimize local hot–spots and to achieve as much as possible isothermal profiles along the catalytic bed.
2. Control of the selectivity; besides carbon oxides, oxygenated products such as acids are highly undesired. Even the formation of traces of these compounds

can give rise to corrosion problems, affect the purity of the final product, and lower the yield.

3. Flammability of the reaction mixtures; the problem becomes determining when feeding hydrocarbon and pure oxygen. Attention must also be given to the composition of the outlet stream, both before and after removal of condensable products (such as water), and when recycling recompressed streams.

The catalysts described in the literature for oxidative dehydrogenation are not simply modifications of dehydrogenation catalysts, achieved by addition of oxidant components, and neither is the polyfunctional nature of dehydrogenation catalysts exploited by carrying out the reaction in the presence of oxygen. On the contrary, brand new classes of catalysts have been developed for the dehydrogenation of paraffins in the presence of oxygen [9, 10, 17, 20, 121, 131, 216]. The different classes of catalysts have some common features, such as the same rate–determining step (formation of an alkyl radical), but considerable differences, as well. For instance, the catalysts belonging to the class of alkali–doped alkaline earth oxides are selective only in ethane oxidative dehydrogenation. Among the catalysts constituted of transition metal oxides, instead, some are active and selective in ethane conversion and unselective for the other paraffins, while other systems show good performance only in the conversion of propane and n–butane, but not in the conversion of ethane.

Particular technical solutions are those where the hydrocarbon is put in contact with the reducible catalyst (based on a transition metal oxide) in the reactor, and the reduced catalyst is reoxidized in a separate fluidized or mobile–bed. This circulating–bed configuration has been proposed by ARCO and by Phillips Petroleum Co for ethane oxidehydrogenation with different catalytic systems [117, 324].

Other technologies utilize the reaction heat for carrying out endothermic reactions, i.e. the pyrolysis of ethane to ethylene (thermal cracking) [325]. Thus, it has been proposed to combine the oxidative coupling of methane with the pyrolysis of ethane recycled in the oxygen–free zone at the top of the reactor (Oxco process [326]).

11.1 The Oxidehydrogenation of Ethane

Among the dehydrogenation reactions, the least feasible one is the dehydrogenation of ethane, which suffers from the most severe thermodynamic constraints. The oxidative dehydrogenation of ethane therefore constitutes a valid alternative to pure dehydrogenation.

$$C_2H_6 + \tfrac{1}{2}\, O_2 \rightarrow C_2H_4 + H_2O$$
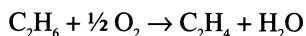
In any case, it is likely that the oxidative dehydrogenation of ethane will become economically competitive with the steam cracking of either naphtha or LPG only when the high selectivity to ethylene makes useless the separation of hydrocarbons from carbon oxides (in particular, the formation of CO is highly undesired) for downstream applications of the olefin. Another major problem can come from the formation of low amounts of condensable, oxygenated products, such as acetic acid.

Generally, the catalysts which have been described to be active and selective in the oxidehydrogenation of ethane can be classified into different groups:

Catalysts based on oxides of Group IA and IIA metals, which are also active for methane coupling [57, 58, 59, 60, 62–65]. These activate ethane at temperatures usually higher than 600°C to form ethyl radicals, which then further react in the gas phase. The most successful of these catalysts is the Li^+/MgO one. The mechanism does not involve a classical redox–type cycle; thus, the catalyst is only involved in C–H scission with radical formation, analogous to what occurs with methane. The role of Li is the generation of Li^+–O^- centers capable of abstracting a H radical and forming the ethyl radical. Such catalysts could be employed after a methane coupling reactor, in order to increase the yield to ethylene through oxidehydrogenation of the ethane formed.

High selectivities and yields to ethylene can be achieved with these catalytic systems, especially when chlorine–containing compounds are also fed to the reactor, or when the catalyst is doped with halides [64, 65]. The promoter effect is maintained by continuous feeding of the chlorine, which modifies the catalyst surface [327]. Chlorine radicals are thought to favour the homogeneous decomposition of ethyl radicals to ethylene. Ethylene yields as high as 34% can be achieved; however, the use of chlorine gives problems related to equipment corrosion.

The selectivity to ethylene increases with increasing temperature up to 700°C. This is due to the fact that the ethyl radical formed at high temperature (600–700°C; for temperatures above 700 °C homogeneous overoxidation of ethylene decreases the selectivity) desorbs and forms ethylene in the gas phase via reaction with oxygen. The high stability of ethylene and the contribution of the heterogeneously–initiated homogeneous reactions lead to the observed high selectivity. At lower temperatures the formation of a surface ethoxy species, precursor of CO_x, occurs preferentially.

Figure 13 summarizes the mechanisms proposed in the literature for the two classes of catalysts, operating at low and high temperature.

A further aspect of these systems is the formation of H_2 under oxidative conditions. H_2 can be formed either via thermal or catalyzed dehydrogenation. Also, a contribution has been proposed due to water–gas–shift equilibrium (over rare earth oxides) or to decomposition of an ethoxy intermediate (formed by interaction between ethyl radical and bulk oxygen) to CO, C and H_2. It was found that catalysts like Ca/Ni/K/O and Li/Mg/O are active in the water–gas–shift at the temperatures at which ethane oxidehydrogenation occurs [328].

Other systems that are active at temperatures higher than 600°C are Li_2O/TiO_2, LiCl/NiO, LiCl/MnO_2 and LiCl/Sm_2O_3. Dopants other than Li^+ have been reported: SnO_2, Na_2O and lanthanides (mainly CeO_2) [329].
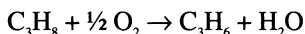
Catalysts based on transition metal oxides: f-elements. Rare earth oxides are remarkably active, and yield ethylene with high productivity and good selectivity [74, 75]. In addition, they are very stable even at high temperature. Doping Sm_2O_3 with alkali metals gives the best performances. These systems are characterized by a mechanism similar to that of Li/Mg/O catalysts, thus with activation of the alkane by adsorbed oxygen rather than by bulk oxygen ion. A detailed study of the reactivity of rare earth oxides has been made by Baerns et al. [216, 330]. It was found that the reaction mixture is ignited at the catalyst surface due to the high activity of the catalyst, and that the heat generated is sufficient for the gas–phase endothermic thermal pyrolysis of the alkane to the olefin. The presence of alkali

metal ions as dopants results in catalysts showing ignition temperatures as low as 440–490°C (the bed temperature rises to 750–850°C). The reaction is completely autothermal, and there is no need for additional external heat input. Rare earth oxides are catalysts which exhibit, together with alkali metal oxides, the highest yields to ethylene, even greater than 50% [331]. This is likely due to the coupling of heterogeneous and homogeneous mechanisms.

Surface mechanism   **Gas-phase mechanism**

$C_2H_6 + O_s^-$

$C_2H_5* + OH_s^-$

O_s^{2-}

$C_2H_5O_s^-$ C_2H_5*

O_s C_2H_4, C_2H_6

O_2

$CO_2, H_2O \blacktriangleleft \cdots\cdots \overset{O_s}{\cdots\cdots} C_2H_5O_2*$ O_2

C_2H_4, OH^- C_2H_4, O_2H*

O_2 O_2

CO, H_2O

$\cdots\cdots\blacktriangleright$ *reactions favoured at low temperature*
$\longrightarrow$ *reactions favoured at high temperature*

Fig. 13. Summary of homogeneous and heterogeneous mechanisms proposed for ethane oxidehydrogenation.

Catalysts based on transition metal oxides: d-elements. In vanadium oxide–based systems the catalyst is reduced by an interaction with the hydrocarbon, through a classical redox cycle [130, 332–334]. These systems can activate ethane at temperatures as low as 400°C, and the entire reaction is heterogeneous, hence controlled by the catalyst. Homogeneous reactions contribute significanty to the total conversion only at high temperatures (i.e., above 550°C).

Mixed oxides of Mo/V/Nb are active in ethane oxidation at temperatures as low as 250°C, with selectivity to ethylene higher than 80% [122, 123]. With these catalysts it is also possible to reach yields of ethylene higher than 30%. However, in this case, the ethylene productivity appears to be too low to have practical application. Mo/V/Nb/O also forms considerable amounts of acetic acid.

Catalysts based on noble metals. Catalysts based on noble metals have been extensively studied by Schmidt et al. [96, 342, 344], where the active component is either spread over ceramic monoliths or supported over fluidizable low–surface area alumina. Pt– and Rh–coated ceramic foam monoliths in autothermal reactors operate at residence times of the order of milliseconds, and very high yields can be obtained at temperatures between 900 and 1000°C. The authors claim that under these conditions the prevailing mechanism is heterogeneous, but the high selectivity achieved and the reaction conditions would rather suggest an heterogeneously–initiated homogeneous mechanism. Slightly lower temperatures

(around 850°C) were achieved with fluidized reactors, and in this case operation was almost isothermal.

Table 11 and Figure 14 summarize the best results reported in the literature.

11.2   The Oxidehydrogenation of Propane

The oxidehydrogenation of propane may represent a valid alternative to industrial dehydrogenation processes.

$$C_3H_8 + \tfrac{1}{2} O_2 \rightarrow C_3H_6 + H_2O$$

Most catalysts described in the literature are based on vanadium oxides as the main component [345-358]; particular attention has been given to the magnesium vanadates. A general feature of most catalytic systems is that the selectivity to propylene decreases as the propane conversion increases [18]. This is due to the presence of allylic hydrogen atoms in the propylene formed which act as centers for consecutive oxidative attacks. This conversion/selectivity trade–off is one of the main differences between ethane and propane. Moreover, the contributions of homogeneous reactions, or of surface–initiated gas–phase reactions, have to be taken into account when the reaction is carried out at temperatures higher than 450–500 °C.

Table 11. Catalyst types and reaction conditions for the oxidehydrogenation of ethane

N.	Catalyst	Ref.	Feed C_2/O_2, (%mol.)	T (°C)
1	$Mo_{0.73}V_{0.18}Nb_{0.09}O_x$	122	9/6	350
2	$Mo_{0.61}V_{0.26}Nb_{0.07}Sb_{0.04}Ca_{0.02}O_x$	124	8/6.5	330
3	$Mo_{0.73}V_{0.18}Nb_{0.09}O_x$	128	9/6	350
4	$Mo_{0.6}V_{0.3}Nb_{0.1}O_x$	130	50/5	460
5	$Mo_{0.56}Re_{0.06}V_{0.26}Nb_{0.07}Sb_{0.03}Ca_{0.02}O_x$	24	21/3.8	325
6	$Ni_1V_{0.3}Sb_{0.6}O_x$	364	41.6/16.8	500
7	3% V_2O_5/SiO_2	332	13/28	600
8	5% V_2O_5/Al_2O_3	338	33/10	500
9	30% B_2O_3/Al_2O_3	328	10/10	550
10	30% B_2O_3/Al_2O_3	335	20/20	550
11	30% B_2O_3/P_2O_5	210	15/15	530
12	$K_2P_{1.2}Mo_{10}W_1Sb_1Fe_1Cr_{0.5}Ce_{0.75}O_x$	380	35/16	470
13	$(VO)_2P_2O_7$	343	2/21	345
14	Sm_2O_3	74	13/3.3	700
15	2%Na_2O/CeO_2	75	11/3	750
16	$SrCe_{0.8}Yb_{0.2}O_{2.9}$	336	21/16.3	600
17	$Cr^{3+}/Zr(HPO_4)_2$	337	6/3	550
18	Li_2O/MgO	64	6.5/8.5	700
19	$Li_2O/MnO_x/Cl^-$	64	6.5/8.5	700
20	Li_2O/MgO	59	12.5/6	700
21	Li_2O/MgO	58	12/6	581
22	$Li_2O/MgO/Cl^-$	65	38/38	650
23	$SnO_2/Li_2O/MgO/Cl^-$	329	38/38	620
24	$Li_2O/CaO/La_2O_3$	340	15/8.5	620

25	SrO/La_2O_3	341	46.7/6.7	850
26	La_2O_3	331	77/23 (pulse)	800
27	$Na-P/Sm_2O_3$	216	45.5/18.2	867
28	$Co_{0.67}P_{0.05}Nb_{0.15}Na_{0.1}K_{0.04}O_x$	324	25/16	675
29	$Pt/\alpha-Al_2O_3$	342	56/29	855

The following is a summary of the catalytic performances of the most important systems described in the literature (the same systems have also been claimed for the oxidehydrogenation of n–butane):
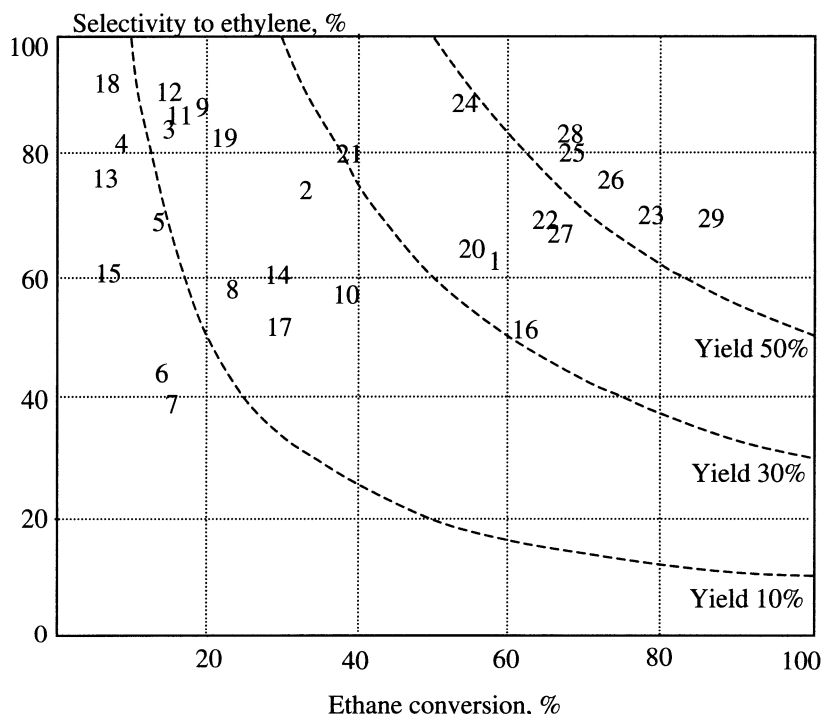
Fig. 14. Best values of selectivity to ethylene and of conversion of ethane for catalysts reported in the literature. Numbers refer to first column in Table 11.

1. V_2O_5 is not a good catalyst for the oxidehydrogenation of paraffins, but the spreading of the oxide onto a support with basic features (such as sepiolite) or over alumina, with the formation of centers with particular chemical–physical features and reactivity, leads to selective catalysts [346]. These catalysts are active at relatively low temperatures (in the 350–450°C range). A selectivity not higher than 40% is obtained, and only at low levels of conversion (not higher than 15%). The combination of V_2O_5 with Nb_2O_5 improves the catalytic properties [350, 351]. Niobium oxide itself, though characterized by low activity, is selective in the formation of propylene. The active phase in V/Nb/O systems was proposed to be the compound $V_2Nb_{23}O_{62}$. With a V/Nb/O catalyst having 3.5% V_2O_5, 7% conversion of propane was reached at 390°C, with a selectivity of 70% to propylene. Recent results [358] point out the importance

of having highly dispersed, tetrahedrally coordinated V^{4+} sites in order to have high selectivity to propylene with V/O-based catalysts.

2. Mg/V/O catalysts have been the object of several investigations in recent years. This system is active in the 550–600°C temperature range, and with respect to V_2O_5 is characterized by improved basicity and surface area [352–354, 356, 357]. This catalyst also leads to the formation of oxygenated by–products. Selectivity to propylene as high as 60% can be reached, with yields of 20–25% and a fairly high productivity. The selectivity generally decreases as conversion increases. Both $Mg_3(VO_4)_2$ (Mg orthovanadate) spread over MgO, and $Mg_2V_2O_7$ (Mg pyrovanadate) are considered to be the most active and selective compounds in C_3–C_4 alkane oxidehydrogenation. Important factors which determine the catalytic performance are the presence of isolated VO_4 units and the reducibility of V^{5+} in the structure. Mg/V/Sb/O systems have been described by Grasselli et al. [365]; the propylene selectivity at low conversion is high (close to 80%), but rapidly declines as the propane conversion increases.

3. Metal–zeolites [347, 359]; the isolation of oxidizing sites is realized by the dispersion of vanadium ions inside catalytically inert matrixes, such as zeolites or zeolitic–like compounds. V–silicalite exhibits relatively high yields, but low productivity. In VAPO–5 isolated VO_4 tetrahedra have been proposed to be the active and selective sites in the alkane oxidehydrogenation.

4. Metal molybdates. Bismuth molybdates and vanadomolybdates are active in the oxidation and ammoxidation of propylene to acrolein, acrylic acid and acrylonitrile. Nickel and cobalt molybdates instead exhibit very high activity in propane oxidehydrogenation; 63.1% selectivity to propylene at 20.9% propane conversion is obtained with β–$NiMoO_4$ [360]. Magnesium molybdates have been claimed by Dow Chem Co for n–butane oxidehydrogenation in two steps, with 80% overall yield to butadiene plus butenes [361]. An extensive study on the reactivity of molybdates has been done by Grasselli et al. [365-367]. The only primary product of oxidation over a silica–supported $Ni_{0.5}Co_{0.5}MoO_4$ catalyst is propylene, while, at propane conversion of 20%, a selectivity around 67% is reached. The mechanism is a redox–type one, involving homolytic C–H bond breaking at the secondary C atom as the rate–limiting step. Maximum yield to propylene is 16% at 34% propane conversion. It was proposed that this system might be efficiently combined with a propylene (amm)oxidation catalyst in an integrated process of transformation of propane to acrylic acid or acrylonitrile.

5. Phosphates of various transition metals have been tested as catalysts for the oxidehydrogenation of propane [362]. These systems are active at temperatures lower than 400°C. As in the case of ethylbenzene oxidehydrogenation, the role of coke (and specifically of oxidized sites in coke which has built–up over metal phosphates) in catalyzing the reaction should be taken into consideration.

6. Other oxides. Rare earth oxides [216] give yields to propylene around 30% (La_2O_3/SrO) at 650–700°C, with a reaction which is ignited at the catalyst surface and then proceeds into the gas phase (thermal pyrolysis). Manganese oxide–based systems have been claimed by Nippon Catalytic Chem Ind [363]:

$Mn_1P_{0.2}O_x$, $Mn_1Sb_{0.25}O_x$, $Mn_1Sb_{0.15}W_{0.05}S_{0.15}Cr_{0.1}O_x$, with a maximum yield to propylene of 15.5% at 530°C.

7. Noble metals. As in the case of ethane oxidehydrogenation, supported noble metals have been checked as catalysts for propylene synthesis both in fluidized beds and in monolithic–type reactors [97, 342], at low residence times. Selectivity to propylene as high as 65% at almost total propane conversion could be achieved under autothermal conditions, with Pt–based catalysts and at high fuel–to–oxygen ratios. No coke deposition and catalyst deactivation was observed during several days of operation. A completely heterogeneous mechanism was proposed, with development of an adsorbed alkyl species via H abstraction by an oxygen species. The adsorbed species is then transformed into the olefin.

The problem of propylene stability towards consecutive unselective oxidative attacks makes finding a suitable catalyst for propane oxidehydrogenation a difficult task. Several systems that can activate the paraffin have been found, but none of them is able to prevent consecutive reactions of the olefin formed. It is likely that the best conditions might come from the coupling of i) an heterogeneous system able to activate propane at (relatively) high temperature, and ii) an homogeneous decomposition of desorbed radical species to propylene. In fact, low temperatures favour the surface–catalyzed consecutive oxidation of propylene to carbon oxides. This happens because the activation energy for the gas–phase dehydrogenation is higher than that for the heterogeneous combustion.

Another possibility to overcome the decrease in selectivity lies in the design of suitable reactor configurations, which may lead to a substantial decrease in the contribution of the consecutive reactions. For instance, it has been recently found that the use of a monolithic–type reactor configuration, where the catalyst (alumina–supported vanadium oxide) is dispersed in the form of a thin layer over a cylindrically shaped ceramic monolith, allows the selectivity to propylene to be maintained at increasing propane conversion. In contrast, in the case of packed-bed reactors with catalyst shaped in particles the propylene selectivity decreases when the conversion increases [109].

A peculiar reactor configuration has been described by Santamaria and Lopez Nieto [368,369]. In a bench–scale fluidized–bed reactor it was possible to perform in separate zones the two reactions of i) paraffin interaction with the catalyst (leading to the olefin and to the reduced catalyst) and ii) reoxidation of the reduced catalyst with molecular oxygen. The two reactions occur in two defined zones (which have separate feed of reactants) of the catalytic bed, thus in practice realizing an *in–situ* decoupling of the redox reaction. The scheme of the reactor is shown in Figure 15. This configuration makes it possible to increase the selectivity to the olefin with respect to the case of cofeed experiments. In practice, the back–mixing of the gas in the reactor is negligible (thus simulating plug–flow). The two reactions are realized separately in the same vessel, while the recirculation of the solid allows cycles of catalyst reduction and reoxidation to be performed efficiently.

Another technical solution aimed at overcoming problems associated with the consecutive reaction of olefin combustion was proposed many years ago, where the endothermal dehydrogenation of propane is coupled to the selective oxidation of molecular hydrogen (produced by dehydrogenation) to water. In this way, it is

theoretically possible to avoid problems associated with the dehydrogenation reaction (i.e., the hydrogen combustion makes it possible to shift the equilibrium towards the formation of propylene, and to avoid the supply of heat from outside the reactor, at high temperature) and those relative to the oxidehydrogenation (low selectivity to propylene due to the combustion reaction). However, a catalyst must be developed which is selective in the combustion of hydrogen but is not active in the combustion of propane and of propylene.
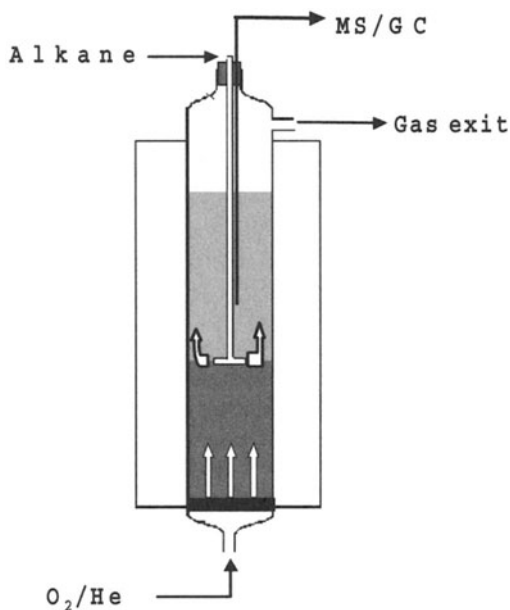
Fig. 15. Scheme of the redox reactor proposed by Lopez Nieto and Santamaria [368,369].

This kind of process configuration was formerly claimed by UOP for the reaction of ethylbenzene dehydrogenation [370, 371], with either a dual catalyst bed (one for ethylbenzene dehydrogenation and one for hydrogen combustion), or with a single multifunctional catalyst having both dehydrogenation and oxidation properties. The same configuration has also been claimed for the dehydrogenation of paraffins [372–374], with a multifunctional catalyst based on Sn/alkali metal–doped Pt, supported either over a spinel oxide, or over alumina, or with a dual catalyst bed, the first one consisting of supported Pt, and the second one for hydrogen combustion made of Cs/Sn–doped or Bi/Sn–doped supported Pt. A selectivity in hydrogen combustion higher than 95% (with thus minimal combustion of the hydrocarbons) is reported.

The reactor configurations claimed refer to the SMART process (Styrene Monomer Advanced Reheat Technology, also developed by UOP together with Lummus), which consists of three in–series reactors. A dehydrogenation occurs in the first reactor, while in the second and third reactors the gas flows radially outward from the center through two catalyst beds separated by screens. Of course, the optimal configuration guarantees an almost isothermal operation, due

to a balance between the heat generated by combustion and the heat required for endothermic dehydrogenation.

More recently, Grasselli et al. have claimed specific catalysts able to selectively oxidize hydrogen with a high conversion of the latter, and with a minimal or nil oxidation of propane and propylene [375–377]. The best catalysts selective in hydrogen combustion are silica–dispersed Bi$_2$O$_3$ (selectivity higher than 99%, with less than 1% combustion of hydrocarbons), Bi$_2$Mo$_3$O$_{12}$ and In$_2$Mo$_3$O$_{12}$. In the presence of molecular hydrogen and in the absence of molecular oxygen the most selective catalysts exhibited the loss of almost all the theoretically removable lattice oxygen, calculated on the basis of the total reduction of Bi cations. Therefore these systems can be efficiently coupled with a catalyst for propane oxidehydrogenation, in a dual–bed reactor configuration.

Choudary et al. [378, 379] have investigated the possibility of coupling the endothermal thermal (noncatalyzed) cracking of light alkanes to olefins with the exothermal (either noncatalyzed or catalyzed) oxidative conversion. Reaction conditions include temperatures higher than 700°C and limited oxygen concentration. This process configuration is highly efficient from the energetic point of view. Moreover, the formation of coke deposits is considerably limited.

11.3   The Oxidehydrogenation of Isobutane

A few papers have appeared in the literature dealing with the oxidative dehydrogenation of isobutane to isobutene [381–387, 390].

$$i\text{–}C_4H_{10} + \tfrac{1}{2}\,O_2 \rightarrow i\text{–}C_4H_8 + H_2O$$
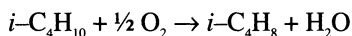
Good results have been obtained with P/W/O Dawson–type heteropolycompounds, which exhibited a fairly constant selectivity to isobutene with increasing isobutane conversion [384–386]. With these catalysts, the contribution of homogeneous radical processes has been postulated to play a fundamental role. In particular, it was found that the conversion of isobutane increases with increasing isobutane concentration in the feed, thus corresponding to a formal order of reaction for isobutane disappearance higher than 1 (Figure 16). Since the selectivity does not decrease when the isobutane partial pressure increases, this leads to a considerable increase in the overall yield to the olefin. The same phenomenon was observed for propane oxidehydrogenation over boria–alumina catalysts, and for propane oxidation over boron phosphate catalysts [388, 389]. In the latter cases it has been proposed that the mechanism begins on the catalyst surface, with generation of alkyl radicals, and that the reaction is then transferred into the gas phase. The order of reaction higher than 1 has been attributed to the presence of homogeneous bimolecular reactions between the paraffin and RO$_2$•, leading to the regeneration of the chain carrier R• and of RO$_2$H, which is then decomposed to the olefin and to oxygenated compounds (propionaldehyde, acetone and acrolein from propane).

Another catalytic system of particular interest for isobutane and propane oxidehydrogenation is made of alumina–supported chromium oxide, which is also active in the corresponding dehydrogenation reactions. It has been found that this catalyst is active at temperatures which are considerably lower than those required when other catalysts are used [390]. At 340°C it converts isobutane to isobutene with 65% selectivity and conversion around 15%.
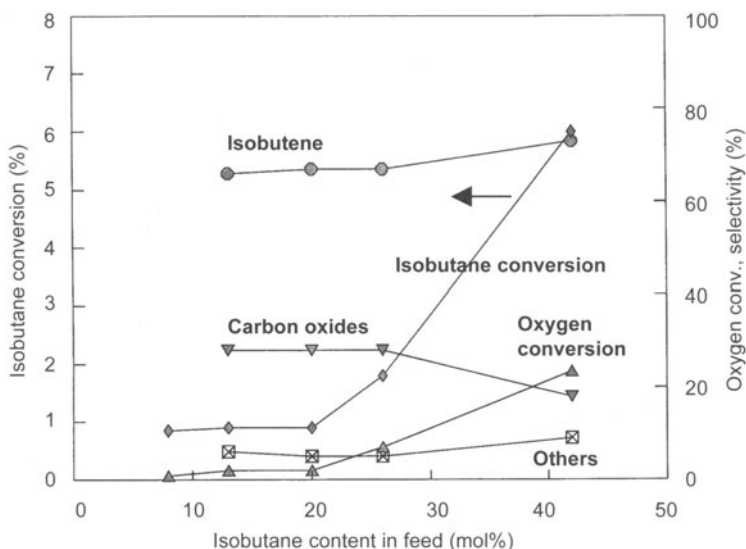
Fig. 16. Effect of the isobutane–to–oxygen ratio on the isobutane conversion and on selectivity to the various products in isobutane oxidehydrogenation catalyzed by P/W Dawson-type heteropolycompounds [384].

12. References

1   A. Bielanski and J. Haber, Oxygen in Catalysis, Marcel Dekker, Inc., New York, 1991.
2   J. Haber, in Heterogeneous Hydrocarbon Oxidation, B.K. Warren and S.T. Oyama, (Eds.), ACS Symp. Series 638, 1996, p. 20.
3   P. Arpentinier, F. Cavani and F. Trifirò The Technology of Catalytic Oxidations, Editions Technip, Paris, 2001, ISBN 2-7108-0777-7.
4   F. Cavani and F. Trifirò, Catal. Today, 51 (1999) 561.
5   H.H. Kung, Adv. Catal., 40 (1994) 1.
6   J.C. Vedrine, G. Coudurier and J.–M. Millet, Catal. Today, 33 (1997) 3.
7   J.C. Vedrine, J.–M. Millet and J.–C. Volta, Catal. Today, 32 (1996) 115.
8   G. Busca, E. Finocchio, G. Ramis and G. Ricchiardi, Catal. Today, 32 (1996) 133.
9   F. Cavani and F. Trifirò, in Catalysis Vol. 11, Royal Society of Chemistry, (1994), p. 246.
10   S. Albonetti, F. Cavani and F. Trifirò, Catal. Rev.–Sci. Eng., 38 (1996) 413.
11   V.D. Sokolovskii, Catal. Rev.–Sci. Eng., 32 (1990) 1.
12   B. Delmon, P. Ruiz, S.R.G. Carrazán, S. Korili, M.A. Vicente Rodriguez and Z. Sobalik, Stud. Surf. Sci. Catal., 100 (1996) 1.
13   R. Burch and M.J. Hayes, J. Molec. Catal., A. Chemical 100 (1995) 13.
14   L.D. Schmidt, M. Huff and S.S. Bharadwaj, Chem. Eng. Sci., 49 (24A) (1994) 3981.

15   G. Centi, F. Cavani and F. Trifirò, Selective Oxidation by Heterogeneous Catalysis, Kluwer Academic/Plenum Publishers, New York, 2001, ISBN 0-306-46265-6.

16   F. Trifirò and F. Cavani, Selective Partial Oxidation of Hydrocarbons and Related Oxidations, Catalytica Studies Division, Mountain View, CA, No. 4193 SO, 1994.

17   F. Trifirò and F. Cavani, Oxidative dehydrogenation and alternative dehydrogenation processes, Catalytica Studies Division, Mountain View, CA, No. 4192 OD, 1993.

18   F. Cavani and F. Trifirò, Catal. Today, 24 (1995) 307.

19   F. Cavani and F. Trifirò, Appl. Catal., A: General, 88 (1992) 115

20   E.A. Mamedov and V. Cortes Corberan, Appl. Catal., A: General, 127 (1995) 1.

21   E.A. Mamedov, Appl. Catal., A: General, 116 (1994) 49.

22   M. Roy, M. Gubelmann–Bonneau, H. Ponceblanc and J.–C. Volta, Catal. Lett., 42 (1996) 93.

23   P. Barthe and G. Blanchard, France Pat. 90 12,519 (1990), assigned to Rhodia.

24   M. Kitson, US Patent 5,260,250 (1993), assigned to BP Chemicals.

25   I.M. Clegg, R. Hardman, Eur. Patent 667,844 (1998), assigned to EVC Technology AG.

26   Y. Moro–oka and W. Ueda, in Catalysis Vol. 11, Royal Society of Chemistry, 1994, p. 223.

27   L.C. Glaeser, J.F. Brazdil, D.D. Suresh, D.A. Orndoff and R.K. Grasselli, US 4,788,173 (1988), assigned to Standard Oil Co.

28   A.T. Guttmann, R.K. Grasselli and J.F. Brazdil, US 4,746,641 (1988), assigned to Standard Oil Co.

29   S. Albonetti, G. Blanchard, P. Burattin, F. Cavani and F. Trifirò, EP 691,306 A1 (1995); assigned to Rhodia.

30   R. Catani, G. Centi, F. Trifirò and R.K. Grasselli, Ind. Eng. Chem., Res., 31 (1992) 107.

31   A. Andersson, S.L.T. Andersson, G. Centi, R.K. Grasselli, M. Sanati and F. Trifirò, Stud. Surf. Sci. Catal., 75 (1993) 691.

32   J. Nilsson, A. Landa–Canovas, S. Hansen and A. Andersson, catal. Today, 33 (1997) 97.

33   F. Cavani, E. Etienne, M. Favaro, A. Galli, F. Trifirò and G. Hecquet, Catal. Lett., 32 (1995) 215.

34   G. Busca, F. Cavani, E. Etienne, E. Finocchio, A. Galli, G. Selleri and F. Trifirò, J. Molec. Catal., 114 (1996) 343.

35   F. Cavani, E. Etienne, G. Hecquet, G. Selleri and F. Trifirò, in Catalysis of Organic Reactions, R.E. Malz (Ed.), Marcel Dekker, (1996), p. 107.

36   N. Mizuno, M. Tateishi and M. Iwamoto, Appl. Catal., A: General, 128 (1995) L165.

37   N. Mizuno, W. Han, T. Kudo and M. Iwamoto, Stud. Surf. Sci. Catal., 101 (1996) 1001.

38   N. Mizuno, M, Tateishi and M. Iwamoto, J. Catal., 163 (1996) 87.

39   N. Mizuno, D.–J. Suh, W. Han and T. Kudo, J. Molec. Catal., A: Chemical, 114 (1996) 309.

40   L. Jalowiecki–Duhamel, A. Monnier, Y. Barbaux and G. Hecquet, Catal. Today, 32 (1996) 237.

41   W. Ueda, Y. Suzuki, W. Lee and S. Imaoka, Stud. Surf. Sci. Catal., 101 (1996) 1065.

42   H. Krieger and L.S. Kirch, US Patent 4,260,822 (1981), assigned to Rohm and Haas Co.

43   J.L. Callahan and R.K. Grasselli, AIChE, 9 (1963) 755.

44   L.–T. Weng and B. Delmon, Appl. Catal., A: General, 81 (1992) 141.

45   E. Bordes and R.M. Contractor, Topics in Catal., 3 (1996) 365.

46   R.M. Contractor, in Circulating Fluidized Bed Technology II, P. Basu and J.F. Large (Eds.), Pergamon Press, Toronto, 1988, p. 467.

47   R.M. Contractor and A.W. Sleight, Catal. Today, 1 (1987) 587.

48   R.M. Contractor, H.E. Bergna, U. Chowdhry and A.W. Sleight, in Fluidization VI, J.R. Grace, L.W. Shemilt and M.A. Bergognou (Eds.), Engineering Foudation, New York (1989), p. 589.

49   R.M. Contractor, D.I. Garnett, H.S. Horowitz, H.E. Bergna, G.S. Patience, J.T. Schwartz and G.M. Sisler, Stud. Surf. Sci. Catal., 82 (1994) 233.

50   E. Kesteman, M. Merzouki, B. Taouk, E. Bordes and R. Contractor, Stud. Surf. Sci. Catal., 91 (1995) 707.

51   Y.–C. Kim, W. Ueda and Y. Moro–oka, Appl. Catal., 70 (1991) 175.

52   Y.–C. Kim, W. Ueda and Y. Moro–oka, Catal. Today, 13 (1992) 673.

53   E.N. Voskresenskaya, V.G. Roguleva and A.G. Anshits, Catal. Rev.–Sci. Eng., 37 (1995) 101.

54   Y. Amenomiya, V.I. Birss, M. Goledzinowski, J. Galuszka and A.R. Sanger, Catal. Rev.–Sci. Eng., 32 (1990) 163.

55   T. Ito, J.–X. Wang, C.–H. Lin and J.H. Lunsford, J. Amer. Chem. Soc., 107 (1985) 5062.

56   D.J. Driscoll and J.H. Lunsford, J. Phys. Chem., 89 (1985) 4415.

57   J.H. Kolts and J.P. Guillory, Eur. Patent 205,765 (1986), assigned to Phillips Petroleum Co.

58   H.M. Swaan, A. Toebes, K. Seshan, J.G. van Ommen and J.R.H. Ross, Catal. Today, 13 (1992) 201 and 629.

59   E. Morales and J.H. Lunsford, J. Catal., 118 (1989) 255.

60   J.A. Roos, S.J. Korf, R.H.J. Veehof, J.G. van Ommen and J.R.H. Ross, Catal. Today, 4 (1989) 441.

61   R. Burch, G.D. Squire and S.C. Tsang, Appl. Catal., 46 (1989) 69; Catal. Today, 6 (1990) 503.

62   J.W.M.H. Geerts, J.M.N. van Kasteren and K. van der Wiele, Catal. Today, 4 (1989) 453.

63   G.A. Martin, A. Bates, V. Ducarme and C. Mirodatos, Appl. Catal., 47 (1989) 287.

64   R. Burch and S.C. Tsang, Appl. Catal., 65 (1990) 259.

65   S.J. Conway and J.H. Lunsford, J. Catal., 131 (1991) 513.

66   K. Otsuka, M. Hatano and T. Komatsu, Catal. Today, 4 (1989) 409.

67   J.M. Thomas, W. Ueda, J. Williams and K.D.M. Harris, J. Chem. Soc., Faraday Trans. I, 87 (1989) 33.

68   W. Ueda, F. Sakyu, T. Isozaki, Y. Morikawa and J.M. Thomas, Catal. Lett., 10 (1991) 83.

69   J.S. Lee and S.T. Oyama, Catal. Rev. –Sci. Eng., 30 (1988) 249.

70   J.M. Deboy and R.F. Hicks, J. Catal., 113 (1988) 517.

71   K. Otsuka, K. Jinno and A. Morikawa, J. Catal., 100 (1986) 353.

72   C.-H. Lin, K.D. Campbell, J.-X. Wang and J.H. Lunsford, J. Phys. Chem., 90 (1986) 534.

73   K.D. Campbell, H. Zhang and J.H. Lunsford, J. Phys. Chem., 92 (1988) 750.

74   E.M. Kennedy and N.W. Cant, Appl. Catal., 75 (1991) 321.

75   E.M. Kennedy and N.W. Cant, Appl. Catal., A: General, 87 (1992) 171.

76   J. Castiglioni, R. Kieffer and P. Poix, in Proceedings of the 16th Iberoamerican Symposium on Catalysis, Santiago, 1994, p. 801.

77   S. Bernal, G.A. Martin, P. Moral and V. Perrichon, Catal. Lett., 6 (1990) 231.

78   G.A. Martin, S. Bernal, V. Perrichon and C. Mirodatos, Catal. Today, 13 (1992) 487.

79 C. de Leitenburg, A. Trovarelli, J. Llorca, F. Cavani and G. Bini, Appl. Catal. A: General, 139 (1996) 161.

80 A. Trovarelli, Catal. Rev.-Sci. Eng., 38 (1996) 439.

81 S.J. Korf, J.A. Roos, L.J. Veltman, J.G. van Ommen and J.H.R. Ross, Appl. Catal., 56 (1989) 119.

82 V.R. Choudhary, S.T. Chaudhari, A.M. Rajput and V.H. Rane, Catal. Lett., 3 (1989) 101.

83 A. Parmaliana, V. Sokolovskii, D. Miceli, F. Arena and N. Giordano, J. Catal., 148 (1994) 514.

84 J.N. Armor and P.M. Zambri, J. Catal., 73 (1982) 57.

85 Y. Barbaux, D. Bouqueniaux, G. Fornasari and F. Trifirò, Appl. Catal., A: General, 125 (1995) 303.

86 A. Bendandi, G. Fornasari, M. Guidoreni, L. Kubelkova, M. Lucarini and F. Trifirò, Topics Catal., 3 (1996) 337.

87 R. Burch and E.M. Crabb, Appl. Catal., 100 (1993) 111.

88 M.Yu. Sinev, L.Ya. Margolis and V.N. Korchak, Russ. Chem. Rev., 64(4) (1995) 349.

89 M.Yu. Sinev, Catal. Today, 24 (1995) 389.

90 D.J. Driscoll, K.D. Campbell and J.H. Lunsford, Adv. Catal., 35 (1987) 139.

91 J.H. Lunsford, Langmuir, 5 (1989) 12.

92 O.V. Krylov, Catal. Today, 18 (1993) 209.

93 D.A. Goetsch, P.M. Witt and L.D. Schmidt, in Heterogeneous Hydrocarbon Oxidation, B.K. Warren and S.T. Oyama, Eds., ACS Symp. Series 638, 1996, p. 124

94 D.A. Hickman and L.D. Schmidt, J. Catal., 138 (1992) 267.

95 D.A. Hickman, E.A. Haupfear and L.D. Schmidt, Catal. Lett., 17 (1993) 223.

96 M. Huff and L.D. Schmidt, J. Phys. Chem., 97 (1993) 11815.

97 M. Huff and L.D. Schmidt, J. Catal., 149 (1994) 127.

98 P.M. Torniainen, X. Chu and L.D. Schmidt, J. Catal., 146 (1994) 1.

99 M. Huff and L.D. Schmidt, J. Catal., 155 (1995) 82.

100 H.P. Hsieh, Catal. Rev.-Sci. Eng., 33 (1991) 1.

101 J.N. Armor, Chemtech, 22 (1992) 557.

102 G. Saracco and V. Specchia, Catal. Rev.-Sci. Eng., 36(2) (1994) 305.

103 J.W. Veldsink, R.M.J. van Damme, G.F. Versteeg and W.P.M. van Swaaij, Chem. Eng. Sci., 47 (1992) 2939.

104 D. Lafarga, J. Santamaria and M. Menendez, Chem. Eng. Sci., 49 (1994) 2005.

105 H. Borges, A. Giroir-Fendler, C. Mirodatos, P. Chanaud and A. Julbe, Catal. Today, 25 (1995) 377.

106 J. Herguido, D. Lafarga, M. Menendez, J. Santamaria and G. Guimon, Catal. Today, 25 (1995) 263.

107 A. Pantazidis, J.A. Dalmon and C. Mirodatos, Catal. Today, 25 (1995) 403.

108 G. Capannelli, E. Carosini, F. Cavani, O. Monticelli and F. Trifirò, Chem. Eng. Sci., 51(10) (1996) 1817.

109 G. Capannelli, E. Carosini, F. Cavani, O. Monticelli and F. Trifirò, Catal. Lett., 39 (1996) 241.

110 V.T. Zaspalis, W. van Praag, K. Keizer, J.G. van Ommen, J.H.R. Ross and A.J. Burggraaf, Appl. Catal., 74 (1991) 205.

111 D. Eng and M. Stoukides, Catal. Rev.-Sci. Eng., 33(3-4) (1991) 375.

112 K. Fujimoto, K. Asami, K. Omata and S. Hashimoto, Stud. Surf. Sci. Catal., 61 (1991) 525.

113   J.E. ten Elshof, B.A. van Hassel and H.J.M. Bouwmeester, Catal. Today, 25 (1995) 397.

114   T. Hayakawa, K. Sato, T. Tsunoda, K. Suzuki, M. Shimizu and K. Takehira, J. Chem. Soc., Chem. Comm., (1994) 1743.

115   A.P.E. York, S. Hamakawa, T. Hayakawa, K. Sato, T. Tsunoda and K. Takehira, J. Chem. Soc., Faraday Trans., 92 (1996) 3579.

116   K. Takehira, T. Hayakawa, S. Hamakawa, T. Tsunoda, K. Sato, J. Nakamura and T. Uchijima, Catal. Today, 29 (1996) 397.

117   R.G. Gastinger, A.C. Jones and J.A. Sofranko, Eur. Patent 253,552, 1987, assigned to Atlantic Richfield Co.

118   R.H. Kahney and T.D. McMinn, US Patent 4,000,178 (1976), assigned to Monsanto Co.

119   M.C. Sze and A.P. Gelbein, Hydroc. Process., 55(2) (1976) 104.

120   F. Cavani and F. Trifirò, Stud. Surf. Sci. Catal., 110 (1997) 19.

121   R.K. Grasselli, Catal. Today, 49 (1999) 141.

122   E.M. Thorsteinson, T.P. Wilson, F.G. Young and P.H. Kasai, J. Catal., 52 (1978) 116.

123   F.G. Young and E.M. Thorsteinson, US Patent 4,250,346 (1981), assigned to Union Carbide Co.

124   J.H. McCain and W.V. Charleston, US Patent 4,524,236 (1985), assigned to Union Carbide Co.

125   J.H. McCain, US Patent 4,568,790 (1986), assigned to Union Carbide Co.

126   R.M. Manyik, J.L. Brockwell and J.E. Kendall, US Patent 4,899,003 (1990), assigned to Union Carbide Chemical and Plastics Co.

127   R.M. Manyik and J.H. McCain, US Patent 4,596,787 (1986), assigned to Union Carbide Co.

128   M. Merzouki, B. Taouk, L. Monceaux, E. Bordes and P. Courtine, Stud. Surf. Sci. Catal., 72 (1992) 165.

129   M. Merzouki, B. Taouk, L. Tessier, E. Bordes and P. Courtine, Stud. Surf. Sci. Catal., 75 (1993) 753.

130   R. Burch and R. Swarnakar, Appl. Catal., 70 (1991) 129.

131   K. Ruth, R. Kieffer and R. Burch, J. Catal., 175 (1998) 16.

132   K. Ruth, R. Burch and R. Kieffer, J. Catal., 175 (1998) 27.

133   K. Karim, M.H. Al-Hazmi and E. Mamedov, US Patent 6,013,597 (2000), assigned to Saudi Basic Ind. Co.; Eur. Patent 938,378 (1999).

134   P.R. Blum and M.A. Pepera, Eur Patent 518,548 (1992), assigned to The Standard Oil Co.

135   P.R. Blum and M.A. Pepera, US Patent 5,300,682 (1994).

136   N.C. Benkalowycz, D.R. Wagner and P.R. Blum, EP 546,677 (1993).

137   F. Blaise, E. Bordes, M. Gubelmann and L. Tessier, EP 627,401 (1994), assigned to Rhone-Poulenc .

138   L. Tessier, E. Bordes and M. Gubelmann, Catal. Today, 24 (1995) 335.

139   A. Aubry, M. Gubelmann and A.M. Le Govic, US Patent 5,750,777, assigned to Rhone-Poulenc .

140   C. Hallett, Eur. Patent 480,594 (1991), assigned to BP Chemicals.

141   W.J. Kroenke and P.P. Nicholas, US Patent 4,461,919 (1984), assigned to The B.F. Goodrich Co.

142   A.J. Magistro, US Patent 4,102,936 (1978), assigned to The B.F. Goodrich Co.

143   H. Riegel, US Patent 3,557,229 (1971), assigned to The Lummus Co.

144   T.P. Li, US Patent 4,300,005 (1977), assigned to Monsanto Co.

145 D.R. Pyke and R. Reid, UK Patent 2,095,242 (1982), assigned to Imperial Chemical Industries.

146 M.A. Kuck, US Patent 3,987,118 (1976), assigned to Stauffer Chem. Co.

147 R. Hardman and I.M. Clegg, Eur. Patent 667,845 (1998), assigned to EVC Technology AG.

148 I.M. Clegg and R. Hardman, Eur. Patent 667,846 (1998), assigned to EVC Technology AG.

149 I.M. Clegg and R. Hardman, Eur. Patent 667,847 (1998), assigned to EVC Technology AG.

150 M.A. Toft, J.F. Brazdil and L.C. Glaeser, US Patent 4,784,979 (1988), assigned to The Standard Oil Co.

151 J.P. Bartek and A.T. Guttmann, US Patent 4,797,381 (1989), assigned to The Standard Oil. Co.

152 L.C. Glaeser, J.F. Brazdil and M.A. Toft, US Patent 4,837,191 (1989), assigned to The Standard Oil Co.

153 M.J. Seely, M.S. Friedrich and D.D. Suresh, US Patent 4,978,764 (1990), assigned to The Standard Oil Co.

154 C.S. Lynch, L.C. Glaeser, J.F. Bradzil and M.A. Toft, US Patent 5,094,989 (1992), assigned to The Standard Oil Co.

155 D.D. Suresh, M.J. Seeley, J.R. Nappier and M.S. Friedrich, US Patent 5,171,876 (1992), assigned to The Standard Oil Co.

156 J.F. Brazdil, L.C. Glaeser and M.A. Toft, US Patent 5,079,207 (1992), assigned to The Standard Oil Co.

157 J.P. Bartek, A.M. Ebner and J.R. Brazdil, US Patent 5,198,580 (1993), assigned to The Standard Oil Co.

158 J.F. Brazdil and F.A.P. Cavalcanti, US Patent 5,576,469 (1996), assigned to The Standard Oil Co.; US Patent 5,498,588 (1996).

159 M. Hatano and A. Kayo, Eur. Patent 318,295 (1988), assigned to Mitsubishi Kasei Co.

160 T. Ushikubo, K. Oshima, T. Umezawa and K. Kiyono, Eur. Patent 512,846 (1992), assigned to Mitsubishi Kasei Co.

161 T. Ushikubo, K. Oshima, A. Kayo, T. Umezawa, K. Kiyono and I. Sawaki, Eur. Patent 529,853 (1992), assigned to Mitsubishi Chemical Co.

162 K. Hamada and S. Komada, US Patent 5,907,052 (1999), assigned to Asahi Kasei Kogyo Kabushiki Kaisha.

163 S. Albonetti, G. Blanchard, P. Burattin, F. Cavani and F. Trifirò, Eur. Patent 723,934 (1996), assigned to Rhodia.

164 S. Albonetti, G. Blanchard, P. Burattin, F. Cavani and F. Trifirò, Eur. Patent 932,662 (1997), assigned to Rhodia.

165 G. Blanchard, P. Burattin, F. Cavani, S. Masetti and F. Trifirò, WO Patent 97/23,287 A1 (1997), assigned to Rhodia.

166 Y. Mimura, K. Ohyachi and I. Matsuura, in Science and Technology in Catalysis 1998, Kodansha, Tokyo, 1999, p. 69.

167 M. Bowker, P. Kerwin and H.-D. Eichhorn, UK Patent 2,302,291 (1997), assigned to BASF.

168 S. Albonetti, G. Blanchard, P. Burattin, T.J. Cassidy, S. Masetti and F. Trifirò, Catal. Lett., 45 (1997) 119.

169 S. Albonetti, G. Blanchard, P. Burattin, F. Cavani, S. Masetti and F. Trifirò, Catal. Today, 42 (1998) 283.

170 G. Centi and S. Perathoner, Catal. Rev-Sci. Eng., 40 (1998) 175.

171 F.J. Berry, M.E. Brett and W.R. Patterson, J. Chem. Soc. Dalton, (1983) 9 and 13.

172 R.G. Teller, M.R. Antonio, J.F. Brazdil and R.K. Grasselli, J. Solid State Chem., 64 (1986) 249.

173 T. Birchall and A.E. Sleight, Inorg. Chem., 15 (1976) 868.

174 G. Centi and F. Trifirò, Catal. Rev.-Sci. Eng., 28 (1986) 165.

175 S. Hansen, K. Ståhl, R. Nilsson and A. Andersson, J. Solid State Chem., 102 (1993) 340.

176 F.J. Berry, M.E. Brett and W.R. Patterson, J. Chem. Soc. Chem. Comm., (1982) 695.

177 A. Landa-Canovas, J. Nilsson, S. Hansen, K. Ståhl, A. Andersson, J. Solid State Chem., 116 (1995) 369.

178 G. Centi and S. Perathoner, Stud.. Surf. Sci. Catal., 91 (1995) 59.

179 G. Centi and P. Mazzoli, Catal. Today, 28 (1996) 351.

180 F.J. Berry, M.E. Brett, R.A. Marbrow and W.R. Patterson, J. Chem. Soc. Dalton Trans., (1984) 985.

181 F.J. Berry, J.G. Holden and M.H. Loretto, J. Chem. Soc., Farady Trans. I, 83 (1987) 615.

182 F.J. Berry, J.G. Holden and M.H. Loretto, Solid State Comm., 59 (1986) 397

183 M.D. Allen and M. Bowker, Catal. Lett., 33 (1995) 269.

184 Z. Magagula and E. van Steen, Catal. Today, 49 (1999) 155.

185 M. Bowker, C.R. Bricknell and P. Kerwin, Appl. Catal., A: General, 136 (1996) 205.

186 S. Poulston, N.J. Price, C. Weeks, M.A. Allen, P. Parlett, M. Steinberg and M. Bowker, J. Catal., 178 (1998) 658.

187 C.A. Cody, L. DiCarlo and R.K. Darlington, Inorg. Chem., 18(6) (1979) 1572.

188 F. Sala and F. Trifirò, J. Catal., 34 (1974) 68.

189 M. Carbucicchio, G. Centi and F. Trifirò, J. Catal., 91 (1985) 85.

190 A.T. Guttmann, R.K. Grasselli and J.F. Brazdil, US Patent 4,788,317 (1988), assigned to The Standard Oil Co.

191 G. Blanchard and G. Ferre, US Patent 5,336,804 (1994), assigned to Rhodia.

192 R. Nilsson, T. Linblad and A. Andersson, J. Catal., 148 (1994) 501.

193 G. Centi, S. Perathoner and F. Trifirò, Appl. Catal., A: General, 157 (1997) 143.

194 V.D. Sokolovskii, A.A. Davydov and O.Yu. Ovsitser, Catal. Rev.-Sci. Eng., 37(3) (1995) 425.

195 Z.G. Osipova and V.D. Sokolovskii, Kinet. Katal., 20 (1979) 910.

196 Y. Sasaki, H. utsumi, K. Miyaki, US Patent 5,139,988 (1992), assigned to Nitto Chem. Ind. Co.

197 R.H. Kahney, T.D. McMinn, US Patent 4,000,178 (1975), assigned to Monsanto Co.

198 S. Albonetti, G. Blanchard, P. Burattin, S. Masetti, F. Trifirò, Stud. Surf. Sci. Catal., 110 (1997) 403.

199 199J.S. Kim and S.I. Woo, Appl. Catal., A: General, 110 (1994) 207.

200 K. Oshihara, T. Hisano and W. Ueda, Topics Catal., 15(2) (2001) 153.

201 W. Ueda and K. Oshihara, Appl. Catal. A: General, 200 (2000) 135.

202 R.K. Grasselli, J.D. Burrington, D.J. Buttrey, P. DeSanto, C.G. Lugmair and A.F. Volpe, Symposium on Multifunctionality of Active Centers in Oxidation Catalysts and their Detection, Irsee, Germany, june 2002.

203 S.A. Holmes, J. Al-Saeedi, V.V. Guliants, P. Boolchand, D. Georgiev, U. Hackler and E. Sobkow, Catal. Today, 67 (2001) 403.

204 T. Ushikubo, K. Oshima, A. Kayo, T. Umezawa, K. Kiyono, I. Sawaki and H. Nakamura, US Patent 5,472,925 (1995) assigned to Mitsubishi Chemical Co.

205 M. Vaarkamp and T. Ushikubo, Appl. Catal., A: General, 174 (1998) 99.

206 T. Ushikubo, K. Oshima, A. Kayou, M. Vaarkamp and M. Hatano, J. Catal., 169 (1997) 394.

207 T. Ushikubo, K. Oshima, T. Numazawa, M. Vaarkamp and I. Sawaki, Stud. Surf. Sci. Catal., 121 (1998) 339.

208 T. Ihara, A. Kayou, H. Kameo, H. Nakamura and C.J. Guo, Stud. Surf. Sci. Catal., 121 (1998) 347.

209 T. Ushikubo, H. Nakamura, Y. Koyasu and S. Wajiki, Eur. Patent 608,838 (1994).

210 T. Ushikubo, K. Oshima, A. Kayou and M. Hatano, Stud. Surf. Sci. Catal, 112 (1997) 473.

211 T. Ushikubo, K. Oshima, T. Ihara and H. Amatsu, US Patent 5,534,650 (1996), assigned to Mitsubishi chemical Co.

212 T. Ushikubo, Y. Koyasu and H. Nakamura, Eur. Patent 767,164 (1996).

213 R. Ramachandran, D.L. Maclean and D.P. Satchell, US Patent 4,849,538 (1989), assigned to The BOC Group.

214 R. Ramachandran and L. Dao, Eur. Patent 646,558 (1994), assigned to The BOC Group.

215 J.C. Bart and N. Giordano, J. Catal., 64 (1980) 356.

216 M. Baerns, O. Buyevskaya, Catal. Today, 45 (1998) 13.

217 M. Baerns, O. Buyevskaya, Erdoel Erdgas Kohle, 116 (2000) 25.

218 S. Khoobiar and R.V. Porcelli, Eur. Patent 117,146 (1984), assigned to The Halcon SD Group.

219 S. Khoobiar, US Patent 4,535,188 (1985), assigned to Halcon SD Gr.

220 W. Hefner, O. Machhammer, H.P. Neumann, A. Tenten and W. Ruppel, H. Vogel, US Patent 5,705,684 (1998), assigned to BASF Aktiengesellschaft.

221 J.L. Brockwell, B.K. Warren, M.A. Young, W.G. Etzkorn and J.M. Maher, WO Patent 9736489 (1997), assigned to Union Carbide Chem Plastic.

222 G. Centi and F. Trifirò, in Catalytic Science and Technology, Vol. 1, Kodansha, Tokyo, (1991) 225.

223 M. Takahashi, X. Tu, T. Hirose and M. Ishii, US Patent 5,994,580 (1999), assigned to Toagosei Co.

224 M. Lin and M.W. Linsen, Eur. Patent 962,253 (1999), assigned to Rohm and Haas Co.

225 G. Blanchard and G. Ferre, Eur. Patent 609,122 (1994), assigned to Rhodia.

226 A. Kaddouri and C. Mazzocchia and E. Tempesti, Appl. Catal., A:General, 180 (1999) 271.

227 J. Barrault, C. Batiot, L. Magaud and M. Ganne, Stud. Surf. Sci. Catal., 110 (1997) 375.

228 M. Ai, Catal. Today, 42 (1998) 297.

229 M. Ai, J. Molec. Catal., A: Chemical, 114 (1996) 3.

230 M. Ai. Catal. Today, 13 (1992) 679.

231 W. Li and W. Ueda, Stud. Surf. Sci. Catal., 110 (1997) 433.

232 W. Li, K. Oshihara and W. Ueda, Appl. Catal., A: General, 182 (1999) 357.

233 J.E. Lyons, A.E. Volpe, P.E. Ellis and S. Karmakar, US Patent 5,990,348 (1999), assigned to Sunoco, Rohm and Haas Co.

234 M. Misono, N. Mizuno, K. Inumaru, G. Koyano and X.H. Lu, Stud. Surf. Sci. Catal., 110 (1997) 35.

235 N. Mizuno, W. Han and T. Kudo, J. Catal., 178 (1998) 391.

236 R.V. Porcelli and B. Juran, Hydroc. Process., march 1986, p. 37.

237 W. Jentzsch, Angew. Chem. Int. Ed. Eng., 29 (1990) 1228.

238 S. Khoobiar, US Patent 4,532,365 (1985), assigned to Halcon SD Gr.

239 N. Mizuno, M. Tateishi and M. Iwamoto, Appl. Catal., A: General, 118 (1994) L1.

240 S. Yamamatsu and T. Yamaguchi, Eur. Patent 425,666 (1989), assigned to Asahi Chem. Co.; Jap Patent 02,042,032 (1990).

241 B. Ernst, T. Haeberle, H.J. Siegert and W. Gruber, DE Patent 42 40 085 A1 (1994), assigned to Röhm GmbH Chemische Fabrik. US Patent 5,380,932 (1995).

242 I. Matsuura and Y. Aoki, Jap. Patent 05,331,085 (1996), assigned to Nippon Catalytic Chem. Ind., CA 121:107989 (1996).

243 K. Nagai, Y. Nagaoka, H. Sato and M. Ohsu, Eur. Patent 418,657 (1990), assigned to Sumitomo Chem. Co.

244 K. Nagai, Y. Nagaoka and N. Ishii, EP 495,504 A2 (1992), assigned to Sumitomo Chem. Co.

245 T. Kuroda and M. Okita, Jap. Patent 04-128,247 (1991), assigned to Mitsubishi Rayon Co.

246 S. Paul, V. Le Courtois and D. Vanhove, Ind. Eng. Chem., Research, 36 (1997) 3391.

247 F. Cavani, A. Lucchi, A. Tanguy and F. Trifirò, DGMK-Conference C4 Chemistry-Manufacture and Use of C4 Hydrocarbons, W. Keim, B. Lücke, J. Weitkamp (Eds.), Tagungsbericht 9705 Hamburg 1997, p. 173.

248 W. Li, W. Ueda, Catal. Lett., 46 (1997) 261.

249 M. Langpape, J.M.M. Millet, U.S. Ozkan and M. Boudeulle, J. Catal., 181 (1999) 80.

250 M. Langpape, J.M.M. Millet, U.S. Ozkan and P. Delichère, J. Catal., 182 (1999) 148.

251 J.B. Moffat, Appl. Catal., A: General, 146 (1996) 65.

252 S. Yamamatsu and T. Yamaguchi, US Patent 5,191,116 (1993) assigned to Asahi Kasei Kogyo Kabushiki Kaisha.

253 F. Cavani, 4ème Conférence sur la Catalyse "Paul Sabbatier", Twelfth European Conference on Catalysis, 5-9 luglio 1999, Strasbourg, Francia, Abstracts p. 22.

254 F. Cavani, A. Tanguy, F. Trifirò and M. Koutyrev, J. Catal., 174 (1998) 231.

255 T. Ushikubo, Jap. Patent 06,172,250 (1992), assigned to Mitsubishi Chem. Ind.

256 Jap. Patent 09,020,700 (1995), assigned to Sumitomo Chem.

257 K. Kawakami, S. Yamamastu and T. Yamaguchi, Jap. Patent 03,176,438 (1991) , assigned to Asahi Chem. Ind. Co.

258 H. Imai, M. Nakatsuka and A. Aoshima, Jap. Patent 62,132,832 (1987), assigned to Asahi Chem. Ind. Co.

259 Y. Iwasawa, K. Asakura and T. Inoue, US Patent 5,864,051 (1999), assigned to UOP.

260 I. Matsuura, H. Oda and K. Oshida, Catal. Today, 16 (1993) 547.

261 I. Matsuura and Y. Aoki, US Patent 5,329,043 (1994), assigned to Nippon Shokubai Co.

262 F. Cavani and F. Trifirò, Appl. Catal. A: General, 157 (1997) 195.

263 R.M. Contractor, US Patent 4,668,802 (1987), assigned to DuPont.

264 R.M. Contractor, in Circulating Fluidized bed Technology III, (P. Basu, M. Horio and M. Hasatani, Eds.), Pergamon, Toronto (1990), p. 39.

265 S.C. Arnold, G.D. Suciu, L. Verde and A. Neri, Hydroc. Process., 64 (9) (1985) 123

266 G.D. Suciu, G. Stefani and C. Fumagalli, US Patent 4,511,670 (1985), assigned to Lummus Crest Inc. and Alusuisse Italia SpA.

267 G.D. Suciu, G. Stefani and C. Fumagalli, US Patent 4,594,433 (1986), assigned to Lummus Crest Inc. and Alusuisse Italia SpA.

268 H. Taheri, US Patent 5,117,007 (1992), assigned to Amoco Co.

269 M.S. Haddad, B.L. Meyers and W.S. Eryman, US Patent 4,996,179 (1991), assigned to Amoco Co.

270 M.S. Haddad and W.S. Eryman, US Patent 5,134,106 (1992), assigned to Amoco Co.

271 H. Taheri, US Patent 5,011,945 (1991), assigned to Amoco Co.

272 Chem. Eng. News, november 4th (1991) 34

273 N.J. Bremer, D.E. Dria and A.M. Weber, US Patent 4,448,893 (1984), assigned to Standard Oil Co.

274 B.J. Barone, US Patent 5,158,923 (1992), assigned to Scientific Design Co. Inc.

275 S. Ushio, Chem. Eng., 20 (1971) 107.

276 M. Hatano, M. Masayoshi, K. Shima and M. Ito, US Patent 5,128,299 (1992), assigned to Mitsubishi Kasei Co.

277 T. Kiyoura, J. Takashi, Y. Kogure and K. Kanaya, Eur. Patent 384,749 (1990), assigned to Mitsui Toatsu Chem. Inc.

278 J. Takashi, T. Kiyoura, Y. Kogure and K. Kanaya, US Patent 5,155,235 (1992), assigned to Mitsui Toatsu Chem. Inc.

279 M.J. Mummey, Eur. Patent 326,536 81989), assigned to Monsanto Co.

280 J.R. Ebner and W.J. Andrews, US Patent 5,137,860 (1992), assigned to Monsanto Co.

281 J.R. Ebner and R.A. Keppel, US Patent 5,168,090 (1992), assigned to Monsanto Co.

282 G.K. Kwentus and M. Suda, US Patent 4,501,907 (1985), assigned to Monsanto Co.

283 F. Cavani and F. Trifirò, Stud. Surf. Sci. Catal., 91 (1995) 1.

284 F. Cavani and F. Trifirò, Chemtech, 24 (1994) 18.

285 G. Centi, F. Trifirò, J.R. Ebner and V. Franchetti, Chem. Rev., 88 (1988) 55.

286 G. Hutchings, Appl. Catal., 72 (1991) 1.

287 Catal. Today, Special Issue on Vanadyl Pyrophosphate, G. Centi (Ed.), 16 (1993).

288 M. Abon and J.-C. Volta, Appl. Catal., 157 (1997) 173.

289 G.J. Hutchings, C.J. Kiely, M.T. Sananes-Schulz, A. Burrows, J.C. Volta, Catal. Today, 40 (1998) 273.

290 S. Albonetti, F. Cavani, F. Trifirò, P. Venturoli, G. Calestani, M. Lopez Granados and J.L.G. Fierro, J. Catal., 160 (1996) 52.

291 V.V. Guliants, J.B. Benziger, S. Sundaresan, I.E. Wachs, J.-M. Jehng and J.E. Roberts, Catal. Today, 28 (1996) 275.

292 V.V. Guliants, J.B. Benziger, S. Sundaresan, N. Yao and I.E. Wachs, Catal. Lett., 32 (1995) 379.

293 J.-C. Volta, Catal. Today, 32 (1996) 29.

294 M. Abon, K.E. Bere, A. Tuel and P. Delichere, J. Catal., 156 (1995) 28.

295 Y. Zhang, R.P.A. Sneeden and J.C. Volta, Catal. Today, 16 (1993) 39.

296 M.T. Sananes-Schulz, F. Ben Abdelouahab, G.J. Hutchings and J.C. Volta, J. Catal., 163 (1996) 346.

297 C.J. Kiely, A. Burrows, S. Sajip, G.J. Hutchings, M.T. Sananes, A. Tuel and J.-C. Volta, J. Catal., 162 (1996) 31.

298 Y. Schuurman, J.T. Gleaves, J.R. Ebner and M.J. Mummey, Stud. Surf. Sci. Catal.,, 82 (1994) 203.

299 Y. Schuurman and J.T. Gleaves, Catal. Today, 33 (1997) 25.

300 C. Cabello, F. Cavani, S. Ligi and F. Trifirò, Stud. Surf. Sci. Catal., 119 (1998) 925.

301 P.A. Agaskar, L. DeCaul and R.K. Grasselli, Catal. Lett., 23 (1994) 339.

302 V.V. Guliants, J.B. Benziger and S. Sundaresan, Stud. Surf. Sci. Catal., 101 (1996) 991.

303 B. Kubias, F. Richter, H. Papp, A. Krepel and A. Kretschmer, Stud. Surf. Sci. Catal., 110 (1997) 461.

304 Z.Y. Xue and G.L. Schrader, J. Phys. Chem., B, 103 (1999) 9459.

305 E.W. Arnold III and S. Sundaresan, Appl. Catal., 41 (1988) 225.

306 G. Calestani, F. Cavani, A. Duran, G. Mazzoni, G. Stefani, F. Trifirò and P. Venturoli, Stud. Surf. Sci. Catal., 92 (1995) 179.

307 J.R. Ebner and M.R. Thompson, Catal. Today, 16 (1993) 51.

308 F. Cavani, G. Centi, A. Riva and F. Trifirò, Catal. Today, 1 (1987) 17.

309 F. Cavani, G. Centi, F. Trifirò and R.K. Grasselli, Catal. Today, 3 (1988) 185.

310 J. Haber, R. Tokarz and M. Witko, in Heterogeneous Hydrocarbon Oxidation, B.K. Warren and S.T. Oyama (Eds.), ACS Symp. Series 638, Washington, 1996, p. 249.

311 B. Kubias, U. Rodemerck, H.-W. Zanthoff and M. Meisel, Catal. Today, 32 (1996) 243.

312 F. Cavani, A. Colombo, F. Giuntoli, E. Gobbi, F. Trifirò and P. Vazquez, Catal. Today, 32 (1996) 125.

313 G. Mazzoni, G. Stefani and F. Cavani, Eur. Patent 804,963 A1 (1997), assigned to Lonza SpA.

314 N. Duvauchelle, E. Kesteman, F. Oudet and E. Bordes, J. Solid State Chem., 137 (1998) 311.

315 N. Duvauchelle and E. Bordes, Catal. Lett., 57 (1999) 81.

316 K. Aït-Lachgar, M. Abon and J.C. Volta, J. Catal., 171 (1997) 383.

317 K. Aït-Lachgar, A. Tuel, J.M. Herrmann, J.M. Krafft, J.R. Martin, J.C. Volta and M. Abon, J. Catal., 177 (1998) 224.

318 P.T. Nguyen, A.W. Sleight, N. Roberts, W.W. Warren, J. Solid state Chem., 122 (1996) 259.

319 P.L. Gai and K. Kourtakis, Science, 267 (1995) 661.

320 F. Cavani, S. Ligi, T. Monti, F. Pierelli, F. Trifirò, S. Albonetti and G. Mazzoni, Catal. Today, 61 (2000) 203.

321 S. Ligi, F. Cavani, S. Albonetti, G. Mazzoni, WO 0072963 (2000), assigned to Lonza SpA.

322 S. Albonetti, F. Cavani, S. Ligi, F. Pierelli, F. Trifirò, F. Ghelfi and G. Mazzoni, Stud. Surf. Sci. Catal., 143 (2002) 963.

323 D.E. Resasco and G.L. Haller, in Catalysis Vol. 11, Royal Society of Chemitry, Cambridge, (1994), p. 379.

324 A.D. Eastman, J.P. Guillory, C.F. Cook and J.B. Kimble, US Patent 4,835,127 (1989), assigned to Phillips Petroleum Co.

325 H. Mimoun, A. Robine, S. Bonnault and C.S. Cameron, Appl. Catal., 58 (1990) 269.

326 J.H. Edwards, K.T. Do and R.J. Tyler, Stud. Surf. Sci. Catal., 61 (1991) 489.

327 R. Burch, S. Chalker and S.J. Hibble, Appl. Catal. A: General, 96 (1993) 289.

328   R.L. Keiski, O. Desponds, Y.F. Chang and G.A. Somorjai, Appl. Catal A: General, 101 (1993) 317.

329 S.J. Conway, D.J. Wang and J.H. Lunsford, Appl. Catal. A: General, 79 (1991) L1.

330 O.V. Buyevskaya and M.Baerns, Catal. Today, 42 (1998) 315.

331 V.R. Choudary and V.H. Rane, J. Catal., 135 (1992) 310.

332 S.T. Oyama and G.A. Somorjai, J. Phys. Chem., 94 (1990) 5022.

333 J. Le Bars, A. Auroux, J.C. Vedrine and M. Baerns, Stud. Surf. Sci. Catal., 72 (1992) 181.

334 S. Bordoni, F. Castellani, F. Cavani, F. Trifirò and M.P. Kulkarni, Stud. Surf. Sci. Catal., 82 (1994) 93.

335 Y. Murakami, K. Otsuka, Y. Wada and A. Morikawa, Bull. Chem. Soc. Japan, 63 (1990) 340.

336 O.J. Velle, A. Anderson and K.J. Jens, Catal. Today, 6 (1990) 567.

337 M. Loukah, G. Coudurier and J. Vedrine, Stud. Surf. Sci. Catal., 72 (1992) 191.

338 J. Le Bars, A. Auroux, S. Trautmann, M. Baerns, in Proceedings DGMK Conference on Selective Oxidation in Petrochemistry, DGMK, Hamburg, 1992, p. 59.

339 G. Colorio, J.C. Vedrine, A. Auroux and B. Bonnetot, Appl. Catal., A: General, 137 (1996) 55.

340   L. Ji and J. Liu, Chem. Comm., (1996) 1203.

341   V.R. Choudhary, B.S. Uphade and S.A.R. Mulla, Angew. Chem. Int. Ed. Eng., 34 (1996) 665.

342   S.S. Bharadwaj and L.D. Schmidt, J. Catal., 155 (1995) 403.

343   P.M. Michalakos, M.C. Kung, I. Jahan and H.H. Kung, J. Catal., 140 (1993) 226.

344   S.S. Bharadwaj, C. Yokoyama and L.D. Schmidt, Appl. Catal., A: General, 140 (1996) 73.

345   A. Corma, J. Lopez Nieto, N. Paredes, M. Perez, Y. Shen, H. Cao and S.L. Suib, Stud. Surf. Sci. Catal., 72 (1992) 213.

346   A. Corma, J.M. Lopez Nieto, N. Paredes, A. Dejoz and I. Vazquez, Stud. Surf. Sci. Catal., 82 (1994) 113.

347   P. Conception, J.M. Lopez Nieto and J. Perez Pariente, Catal. Lett., 19 (1993) 333

348   J.G. Eon, R. Olier and J.C. Volta, J. Catal., 145 (1994) 318.

349   R.H.H. Smits, K. Seshan, H. Leemreize and J.R.H. Ross, Catal. Today, 16 (1993) 513.

350   R.H.H. Smits, K. Seshan and J.R.H. Ross, in Catalytic Selective Oxidation, S.T. Oyama and J.W. Hightower (Eds.), ACS Symp. Series 523 (1993).

351   R.H.H. Smits, K. Seshan and J.R.H. Ross, J. Chem. Soc., Chem. Comm., (1991) 558.

352   O.S. Owen and H.H. Kung, J. Molec. Catal., 79 (1993) 265.

353   M.C. Kung and H.H. Kung, J. Catal., 134 (1992) 668.

354   M.D. Chaar, D. Patel, M.C. Kung and H.H. Kung, J. Catal., 105 (1987) 483.

355   K.T. Nguyen and H.H. Kung, J. Catal., 122 (1990) 415.

356   D.S.H. Sam, V. Soenen and J.C. Volta, J. Catal., 123 (1990) 417.

357   X. Gao, P. Ruiz, Q. Xin, X. Guo and B. Delmon, Catal. Lett., 23 (1994) 321.

358   A. Brückner, P. Rybarczyk, H. Kosslick, G.-U. Wolf and M. Baerns, Stud. Surf. Sci. Catal., 142 (2002) 1141.

359   359G. Centi, S. Perathoner, F. Trifirò, A. Aboukais, F.C. Aissi and M. Guelton, J. Phys. Chem., 96 (1992) 2617.

360   C. Mazzocchia, C. Aboumrad, C. Daigne, E. Tempesti, J.M. Herrmann and G. Thomas, Catal. Lett., 10 (1991) 181.

361   B. Khazai, G.E. Vrieland and C.B. Murchison, Eur. Patent 409,355 A1 (1991), assigned to Dow Chem. Co.

362   Y. Takita, K. Yamashita and K. Moritaka, Chem. Lett., (1989) 1903.

363   E. Matsunami and N. Kishimoto, Eur. Patent 963,788 (1999), assigned to Nippon Catalytic Chem. Ind.

364   R.X. Valenzuela, J.L.G. Fierro, V. Cortés Corberan and E.A. Mamedov, Catal. Lett., 40 (1996) 223.

365   J.N. Michaels, D.L. Stern and R.K. Grasselli, Catal. Lett., 42 (1996) 135 and 139.

366   D.L. Stern, J.N. Michaels, L. DeCaul and R.K. Grasselli, Appl. Catal., A: General, 153 (1997) 21.

367   D.L. Stern and R.K. Grasselli, Stud. Surf. Sci. Catal., 110 (1997) 357.

368   J. Soler, J.M.Lopez Nieto, J. Herguido, M. Menendez and J. Santamaria, Ind. Eng. Chem., Research 38 (1999) 90.

369   J.M. Lopez Nieto, J. Soler, J. Herguido, M. Menendez and J. Santamaria, J. Catal., 185 (1999) 324.

370   T. Imai, US Patent 4,435,607 (1984), assigned to UOP.

371   T. Imai and R.J. Schmidt, US Patent 4,886,928 (1989), assigned to UOP.

372   R.R. Herber and G.J. Thompson, US Patent 4,806,624 (1989), assigned to UOP.

373   L.E. Drehman and D.W. Walker, US Patent 3,670,044 81972), assigned to Phillips Petroleum Co.

374   T. Imai and D.Y. Jan, US Patent 4,788,371 (1988), assigned to UOP.
375   J.G. Tsikoyiannis, D.L. Stern and R.K. Grasselli, J. Catal., 184 (1999) 77.
376   P.A. Agaskar, R.K. Grasselli, J.N. Michaels, P.T. Reischman, D.L. Stern and J.G. Tsikoyiannis, US Patent 5,530,171 (1996), assigned to Mobil Oil Co.
377   P.A. Agaskar, J.G. Tsikoyiannis, D.L. Stern, R.K. Grasselli, J.N. Michaels and P.T. Reischman, and , US Patent 5,563,314 (1996), assigned to Mobil Oil Co.
378   V.R. Choudary, V.H. Rane and A.M. Rajput, AIChE J., 44 (1998) 2293.
379   V.R. Choudary and S.A.R. Mulla, Ind. Eng. Chem., Research, 36 (1997) 3520.
380 F. Cavani, M. Koutyrev and F. Trifirò Catal. Today, 28 (1996) 319.
381   Y. Takita, K. Kurosaki, Y. Mizuhara, and T. Ishihara, Chem Lett. (1993), 335.
382   M.A. Uddin, T. Komatsu and T. Yashima, J. Catal., 150 (1994) 441.
383   W. Zhang, D.L. Tang, X.P. Zhou, H.L. Wan and K.R. Tsai, J. Chem. Soc. Chem. Commun. (1994) 771.
384   F. Cavani, C. Comuzzi, G. Dolcetti, R.G. Finke, A. Lucchi, F. Trifirò and A. Trovarelli, in Heterogeneous Hydrocarbon Oxidation, B.K. Warren and S.T. Oyama (Eds.), ACS Symp. Series 638, Washington, 1996, p. 140.
385   C. Comuzzi, A. Primavera, A. Trovarelli, G. Bini and F. Cavani, Topics in Catal., 9 (1999) 251.
386   C. Comuzzi, G. Dolcetti, A. Trovarelli, F. Cavani, J. Llorca and R.G. Finke, Catal. Lett., 36 (1996) 75.
387   F. Cavani, C. Comuzzi, G. Dolcetti, E. Etienne, R.G. Finke, G. Selleri, F. Trifirò and A. Trovarelli, J. Catal., 160 (1996) 317.
388   O.V. Buyevskaya, M. Kubik and M. Baerns, in Heterogeneous Hydrocarbon Oxidation, B.K. Warren and S.T. Oyama (Eds.), ACS Symp. Series 638, Washington (1996), p. 155.
389   K. Otsuka, Y. Uragami, T. Komatsu and M. Hatano, Stud. Surf. Sci. Catal., 61 (1991) 15.
390   R. Grabowski, B. Grzybowska, J. Sloczynski and K. Wcislo, Appl. Catal., A: General, 144 (1996) 33

Recent references

1   J.M. Thomas, Topics Catal., 15 (2001) 85
2   R.K. Grasselli, Topics Catal., 15 (2001) 93
3   G. Emig and M.A. Liauw, Topics Catal., 21 (2002) 11
4   R. K. Grasselli, Topics Catal., 21 (2002) 79
5   M. Misono, Topics Catal., 21 (2002) 89
6   J.C. Vedrine, Topics Catal., 21 (2002) 97
7   L.M. Madeira, M.F. Portela, Catal. Rev.- Sci. Eng., 44 (2002) 247
8   J.M.M. Millet, H. Roussel, A. Pigamo, J.L. Dubois, J.C. Dumas, Appl. Catal., A: General, in press 2003.
9   M. Banares, Catal. Today, 51 (1999) 319

Selective Hydrogenation
of Multiple Unsaturated Compounds

Contents

Selective Hydrogenation
of Multiple Unsaturated Compounds

Sabine Schimpf, Johann Gaube, Peter Claus

Dep. Chemistry, Ernst-Berl-Institute of Chemical Engineering and
Macromolecular Chemistry, Darmstadt University of Technology,
Petersenstraße 20, 64287 Darmstadt, Germany

Abstract. Selective hydrogenation reactions are wildly spread in chemical industry, such as the selective hydrogenation of alkadienes in petrochemical industry and the selective hydrogenation of α,β-unsaturated aldehydes in the production of Fine Chemicals. Considering the selective hydrogenation of alkadienes, tools for tailoring catalyst design are the modeling of the interrelation between chemical reaction and mass transfer based on fundamental studies of the kinetics and the reaction mechanism, where the focus is laid on the hydrogenation of 1,3-butadiene, 1,3-cyclooctadiene and benzene. Factors controlling the intramolecular selectivity of the hydrogenation of α,β-unsaturated aldehydes, such as acrolein, crotonaldehyde, citral and cinnamaldehyde, to unsaturated alcohols are the metal particle size and morphology of the supported metals, metal-support interactions and the influence of the nature of active sites in bimetallic catalysts. Surprisingly monometallic silver and gold catalysts are also convenient to produce unsaturated alcohols. Industrial applications of selective hydrogenations are given.

1.   Introduction

The purpose of this chapter is to review the present status of selective hydrogenation of multiple unsaturated compounds, a field which is of importance for both the scientific impact for our knowledge in heterogeneous catalysis as well as its industrial application. The review is focussed on the selective hydrogenation of alkadienes and α,β-unsaturated aldehydes. Because the former represent organic compounds with two identical conjugated functional groups the catalyst has to hydrogenate one of these identical functional groups with high selectivity, and than the hydrogenation is called to be regioselective. In cases where an organic molecule consists of different (conjugated) functional groups the ability of a hydrogenation catalyst to discriminate among these groups is often referred to as chemoselectivity. However, concerning the addition of hydrogen at a given position of a functional group stresses again the problem of regioselectivity. In both cases the problem of selectivity became one of the important problems in heterogeneous catalysis.

   The first part of this review is focussed on the selective hydrogenation of alkadienes where the first section reports on type of catalysts, the kinetics of 1,3-

butadiene and of 1,3-cyclooctadiene hydrogenation as these are the most important and best studied examples of selective alkadiene hydrogenations. The next section is devoted to the chemical engineering aspects of selective hydrogenation. Modeling of the interrelation between chemical reaction and mass transfer provides a tool for tailoring catalyst design. In the following section the mechanism of alkadiene hydrogenation is discussed. The final section deals with the partial hydrogenation of benzene to cyclohexene, introduced as an industrial process in 1990.

The second part describes the factors, controlling the intramolecular selectivity of the hydrogenation of α,β-unsaturated aldehydes, with special emphasis on the metal particle size and morphology of the supported metals, metal-support interactions and the influence of the nature of active sites in bimetallic catalysts. The next section deals with the reactions mechanism of the hydrogenation of α,β-unsaturated aldehydes exemplified for the hydrogenation of crotonaldehyde. In the last section the potential of silver and gold as catalysts for the hydrogenation of α,β-unsaturated aldehydes is shown. Finally the last part of this chapter gives an overview of industrial applications of selective hydrogenation of multiply unsaturated organic compounds.

2.   Selective Hydrogenation of Alkadienes towards Alkenes

The pyrolysis of naphtha for the production of ethene, propene, butenes, 1,3-butadiene and aromatics is the key process in the modern petrochemical industry. Selective hydrogenations play an important role for the nearly complete removal of alkynic compounds from the C_2, C_3 and C_4 cuts. For instance, for polymer grade ethene the ethyne content must be reduced from 1-2 % ethyne in the C_2 cut to a value of less than 1 ppm. More than 50 % of the ethyne is converted to ethene despite the very high ethene to ethyne ratio of $> 10^6$ at the reactor outlet. Supported palladium catalysts are extremely effective for this reaction [1,2]. Another important application of hydrogenation is the removal of traces of 1,3-butadiene from the C_4 fraction by Pd/Al_2O_3 catalysts following its extractive separation. 1,3-Butadiene has now become a surplus product, and its selective hydrogenation, mainly to 1-butene, is carried out on an industrial scale. Furthermore, the selective hydrogenation of 1,5-cyclooctadiene, obtained by cyclic dimerization of 1,3-butadiene, to cyclooctene on Pd/Al_2O_3 and of benzene to cyclohexene on ruthenium catalysts are of increasing importance.

2.1   Catalysts for Selective Hydrogenation

Of the Group VIII noble metals, palladium shows by far the highest selectivity with respect to alkenes in alkyne and (cyclo-)alkadiene hydrogenation. Because of the relatively high reaction rate and thus the strong influence of mass transfer processes on the selectivity catalysts of the egg-shell type with a very thin active layer of palladium on alumina are generally used. Additives are applied in order to suppress or reduce undesired side reactions such as the green oil formation in the selective hydrogenation of acetylene [3]. A detailed study on the morphology of Pd deposits on alumina has been carried out by Freund and co-workers [4]. Fig. 1

shows a STM image of Pd grown on Al$_2$O$_3$/NiAl (110) at 300 K. The particles adopt the form of small crystals limited by planes with a (111) orientation which is apparent from electron scattering diagrams.
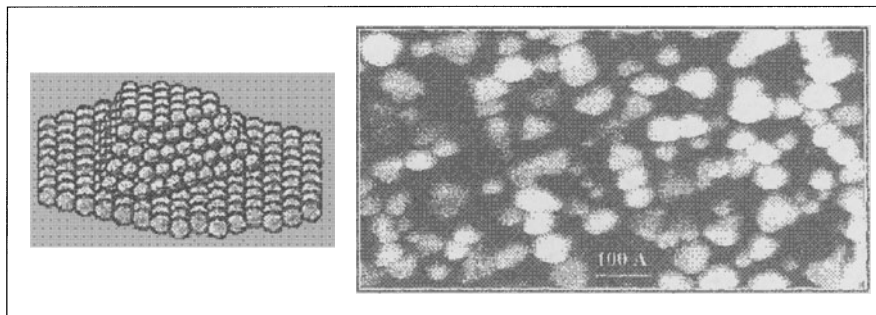
Fig 1. STM image of Pd grown on Al$_2$O$_3$/NiAl (110) at 300 K [4].

1,3-Butadiene is hydrogenated on supported Pd catalysts with a selectivity of 100 %, whereas on supported Pt the hydrogenation under comparable conditions leads to a marked fraction of butane [5,6]. Therefore it is of interest to compare these catalysts in order to find the factors which are responsible for the exceptionally high selectivity obtained when Pd catalysts are employed. The preference for π-coordination of the intermediate alkene on Pd may favor its desorption, while the more strongly di-σ-adsorption opens the chance of subsequent hydrogenation. The isomerisation in the course of 1-butene hydrogenation shows a much higher rate on Pd than on Pt catalysts [7,8]. Boitiaux et al., Augustine et al. [9] and Gault et al. [10] interpreted this phenomenon by the predominance of π-allyl species on Pd.

The selectivity of alkadiene hydrogenation to alkenes is determined by the ratio of the rates of alkene desorption and the consecutive hydrogenation. We may assume that the differences in selectivity on Pd and on Pt depend on different rates of desorption due to specific modes of adsorption. The hypothesis that the rate of alkene desorption determines the selectivity finds support by the strong increase of alkene selectivity as the temperature is raised [11] for the hydrogenation of 1,3-butadiene on Pt, as shown in Fig. 2. The same dependence was found for the hydrogenation of ethyne [12].

However, it should also be considered that the rate of hydrogenation depends on the mode of adsorption and on the availability of activated hydrogen, as discussed by Bates et al. [13]. It is well known that Pd and Pt show marked differences in the adsorption and particularly in absorption of hydrogen. Finally, it should be noted that the formation of carbonaceous species on the metal surface strongly impedes the clear interpretation of experimental results. The conclusion drawn from this comparison is that there may be some starting points to find an explanation for the outstanding properties of palladium. However, the development of a sound theory of selective hydrogenation still remains a difficult task.
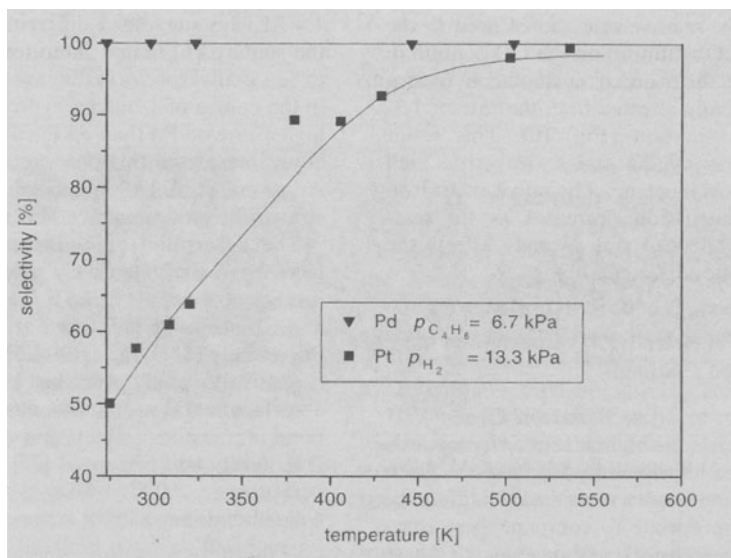
Fig. 2. Temperature dependence of selectivity in 1,3-butadiene hydrogenation over palladium and platinum (adapted from Ref. [11]).

2.2   Kinetics of 1,3-Butadiene and 1,3-Cyclooctadiene Hydrogenation

The selectivity patterns for the hydrogenation of 1,3-butadiene over supported group VIII noble metals [13] demonstrate that Pd plays an outstanding role by providing 100% selectivity to butenes. Also the hydrogenation of 1,3-cyclooctadiene (COD) on palladium exhibits a 100 % selectivity to cyclooctene (COE). Figure 3 shows the development of concentrations in a batch experiment applying
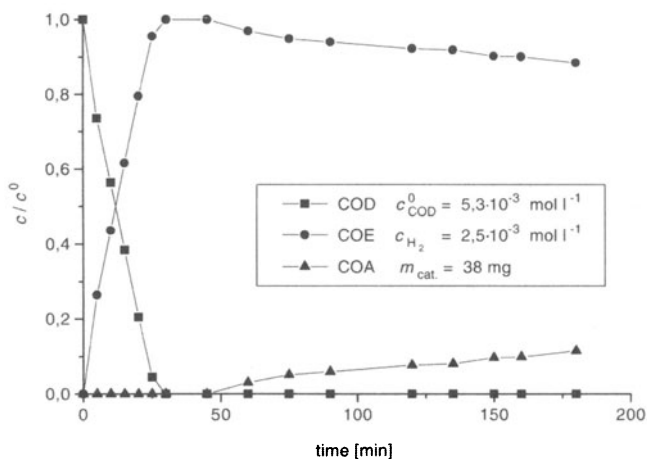
Fig. 3. Concentrations as a function of reaction time in the liquid phase hydrogenation of COD [14]; reaction volume 100 ml.

palladium black suspended in a solution of the C_8 compound in an inert alkane [14]. The consecutive hydrogenation to cyclooctane (COA) does not start until the diene has been hydrogenated down to trace quantities. The determination of the lowest concentration of alkadiene that still inhibits alkene hydrogenation is, however, a very difficult task because the ratio of hydrogen and diene has to be controlled with extremely high precision in order to prevent mass transfer effects which inevitably would lead to a reduction of selectivity.

$$C_4H_{6ad} \xrightarrow[+2H]{k_1} C_4H_{8ad} \begin{array}{c} \xrightarrow{k_{des}} C_4H_8 \\ \searrow[k_2] \\ {+2H} \quad C_4H_{10} \end{array}$$
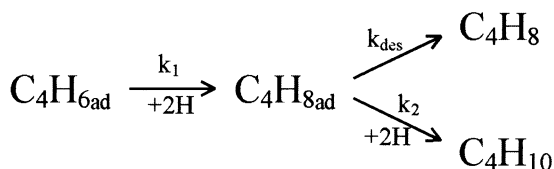
Scheme 1

Alkenes formed by hydrogenation may either undergo desorption or subsequent hydrogenation (Scheme 1). Since in 1,3-butadiene and 1,3-cyclooctadiene hydrogenation 100 % selectivity with respect to the (cyclo)-alkene is achieved, the ratio of k_{des}/k_2 is very high. 1,3-Butadiene and 1,3-cyclooctadiene are much more strongly adsorbed than the (cyclo)alkenes. The stronger adsorption of the alkadiene relative to the alkene suggests that both double bonds interact with the surface. Marked differences in the free energies of adsorption of alkadienes or alkynes and alkenes will result in a very high surface coverage of the more strongly adsorbed hydrocarbon, so that the intermediate alkene is hindered from readsorption by the more strongly bound alkadiene. In the absence of alkadiene, however, the alkenes are hydrogenated over Pd with similar reaction rates [11].

The kinetics of hydrogenation of both 1,3-butadiene and 1,3-cyclooccatdiene show reaction orders higher than unity in hydrogen and slightly negative orders with respect to the (cyclo)alkadiene. Bond et al. [6] presented the following rate law for the hydrogenation of 1,3-butadiene on Pd/Al$_2$O$_3$:

$$r_1 = k_1 \times p_{H_2}^{1.7} \times p_{C_4H_6}^{-0.7} \tag{1}$$

A reaction order of > 1 in hydrogen, and an order < 1 in butadiene are demonstrated in Fig. 4 and Fig. 5 by plots of reaction rates versus partial pressures hydrogen and butadiene respectively. Fig. 5 shows that with increasing butadiene pressure, the reaction order of the diene approaches zero. A literature survey makes it obvious that the combination of reaction orders in hydrogen $n_{H_2} > 1$ and the alkadiene $n_{alkadiene} < 0$ have been found frequently. This is the case for the hydrogenation of butadiene over Pt and Pd [11], ethyne over Pt [11,15] and even ethene over Pt [16]. However, reaction orders of unity in hydrogen and of zero with respect to the alkadiene are observed frequently [17].
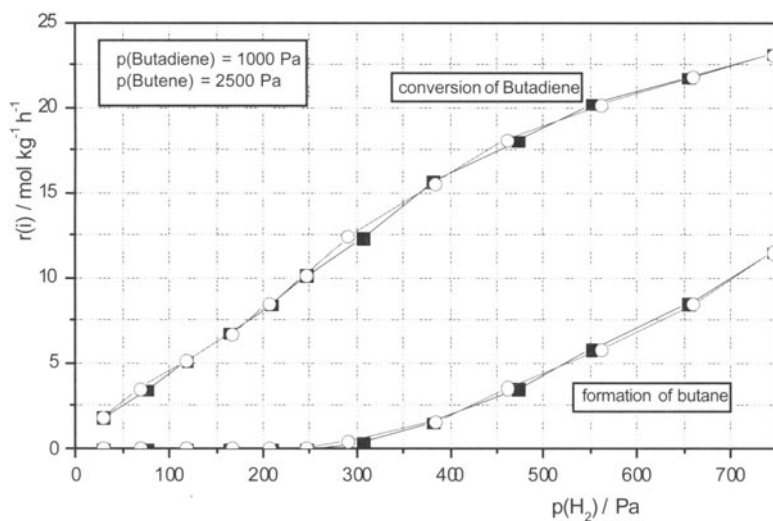
Fig. 4. Reaction rate of butadiene conversion and formation of butane versus partial pressure of hydrogen.

A detailed kinetic study [18] on the hydrogenation of 1,3-cyclooctadiene (COD) had led to a relatively simple interpretation of reaction orders in alkadiene hydrogenation. With increasing 1,3-cyclooctadiene partial pressure the reaction order in hydrogen approaches unity and that in 1,3-cyclooctadiene (COD) zero;
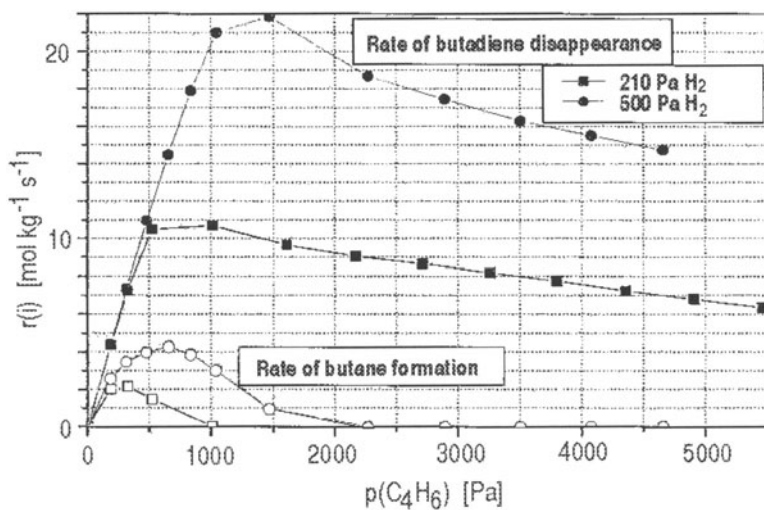
Fig. 5. Reaction rate of butadiene conversion and formation of butane versus partial pressure of butadiene.

values which have been frequently reported. The first term of the following kinetic equation represents this limiting case:

$$r_1 = k_1 p_{H_2}^1 p_{COD}^0 + r_1 k' \frac{p_{H_2}}{K''+p_{COD}} \tag{2}$$

It is assumed that chemisorption of hydrogen or its dissociation are the rate determining steps. Strong support for this assumption is that in the reaction of 1,3-butadiene with mixtures of hydrogen and deuterium the hydrogen exchange $H_2 + D_2 \underset{\leftarrow}{\overset{\rightarrow}{}} 2HD$ is virtually inhibited by the presence of 1,3-butadiene [13], and hence the surface coverage of hydrogen atoms must be very low. This means that activated hydrogen is immediately consumed by hydrogenation. As could be shown by sorption studies there is a full surface coverage with 1,3-butadiene. However, the gaps between chemisorbed cycloalkadiene molecules may be large enough for hydrogen to be adsorbed. This view suggests that there is no direct competition between the cycloalkadiene and hydrogen for chemisorption, as already assumed by Phillipson et al. [19].
The second term of eq. 2 accounts for additional activation of hydrogen in the course of reaction events. In the time interval between cycloalkene desorption and (cyclo)alkadiene chemisorption hydrogen gains an additional chance of access to the surface. This can be understood as a perforation of the adsorption layer caused by the reaction itself and thus counteracting the hindrance of hydrogen access. This term is consequently assumed to be proportional to the reaction rate. The ratio p_{H_2} / p_{diene} expresses the competition between H_2 and COD for chemisorption in the interval between COE desorption and COD chemisorption. Equation 2 solved for r_1,

$$r_1 = \frac{k_1 \times p_{H_2}}{1 - k' \dfrac{p_{H_2}}{k''+p_{diene}}} \tag{3}$$

represents the dependence of the reaction rate of diene hydrogenation of both the partial pressures of hydrogen and diene in agreement with experimental data. The dependence of the rate of diene conversion on both p_{H_2} and p_{diene} is shown in Fig. 6. At high diene concentration and low hydrogen concentration the limiting cases, reaction order zero in diene and first order in hydrogen are demonstrated. The combination of non-competitive and partly competitive adsorption of hydrogen and the unsaturated hydrocarbon is also discussed by Dumesic et al. for the hydrogenation of ethylene on Pt [20].
Another explanation of a reaction order > 1 in hydrogen has been given by Vannice [21] with the assumption that the surface may be partly blocked by dehydrogenated species. This blocking effect decreases as the hydrogen pressure is raised. The increasing number of sites capable for hydrogen activation and a first order in hydrogen of this activation results in a formal order > 1. The negative reaction order in alkadiene may be generally interpreted by a slight increase of the density of alkadiene coverage as the partial pressure is raised.
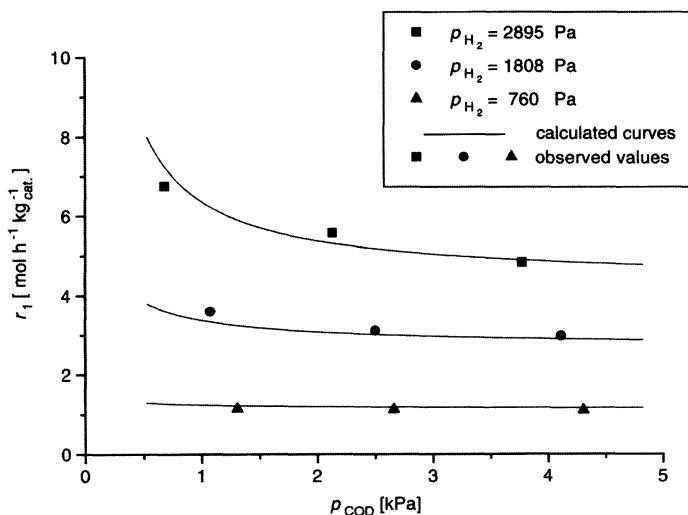
Fig. 6. Dependence of COD hydrogenation rates on COD partial pressure at different hydrogen pressures [18].

In the presence of 1.3-butadiene and also 1.3-cyclooctadiene the hydrogenation of primarily formed butenes and cyclooctene, respectively, is completely suppressed. Even though this observation is due to a much stronger adsorption of the dienes when compared to that of the (cyclo)alkenes, the so-called thermodynamic factor, this effect cannot be explained by a simple displacement of the (cyclo)-alkene in the course of an equilibration. Sorption studies for 1,3-butadiene and 1-butene on highly dispersed Pd black have revealed that 1.3-butadiene reaches saturation at an adsorption stoichiometry of one butadiene molecule to four Pd surface atoms, while the saturation with respect to 1-butene is reached already at a ratio of one butene molecule to five Pd surface atoms. If Pd with maximum butadiene coverage is exposed to 1-butene, no exchange of butadiene by butene is observed as expected. The opposite experiment, i.e. exposing a butene-saturated Pd surface to butadiene, leads to the displacement of butene. However, it takes 5-6 h to complete this exchange. Whereas the selective butadiene hydrogenation, including desorption of 1-butene, shows a turn over frequency (TOF) of about 1 s^{-1}, the TOF of butene displacement is smaller than 10^{-2} s^{-1}. This slow exchange shows that desorption of butene formed during hydrogenation cannot be understood by simple displacement. This discrepancy is not surprising if the energetic aspect of the reaction is considered. The reaction enthalpy of selective butadiene hydrogenation is $\Delta H = -124$kJ mol^{-1}. At the moment of the reaction this enthalpy is concentrated on the butene molecule just formed. The corresponding adiabatic temperature increase is roughly 900K!. Dissipation of this energy can occur by collision with neighboring molecules and also via the chemisorption bonds to the Pd lattice. Then, vibrations perpendicular to the surface are activated so that the desorption of butene molecules just formed is favored. An analogy is the chemical activation of s-butyl radicals which are formed during gas phase

hydrogenation of cis-2-butene. In addition to the energy loss by collision, chemical activation can even cause the rupture of a C-C bond [22]. Further support of the hypothesis of desorption by chemical activation is the desorption of adsorbed molecules caused by exposition to the radiation of UV or IR lasers [23,24].

2.3   Role of Mass Transfer in Selective Hydrogenation

In his famous article "Relation between Catalytic Activity and size of Particle" Thiele [25] noted that in the case of consecutive reactions the selectivity towards the intermediate may strongly decrease with an increasing dimensionless number, later known as the Thiele modulus. Twenty years later, Wheeler [26] derived equations which describe the selectivity of the intermediate B in the consecutive reaction A →B→C as a function of reactivity, diffusivity and of pellet size.

2.3.1   Gas Phase Hydrogenation

Even if catalysts of the egg-shell type with a very thin (< 20 μm) active layer of palladium on alumina are used for selective hydrogenations, mass transfer in the pores of this layer can strongly influence the selectivity because of the high reaction rate observed in hydrogenation. A comprehensive study on the role of mass transfer in selective hydrogenation has been carried out for the gas phase hydrogenation of cyclooctadiene [27-29]:

$$1\text{,}3\text{-cyclooctadiene} \xrightarrow{\ r_1\ } \text{cyclooctene} \xrightarrow{\ r_2\ } \text{cyclooctane} \qquad (4)$$
$$\text{COD} \qquad\qquad\quad \text{COE} \qquad\qquad \text{COA}$$
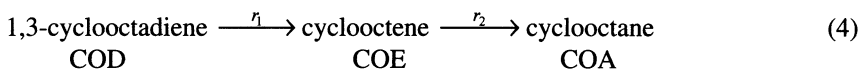
The intrinsic reaction rate r_1 is approximately first order with respect to hydrogen and independent of the partial pressures of COD and COE:

$$r_1 = k_1 \times C_{H_2}^1 \cdot C_{COD}^\circ \qquad (5)$$

The intrinsic reaction rate r_2 is represented by a Langmuir-Hinshelwood rate expression:

$$r_2 = \frac{k_2 \times K_{COE} \times p_{COE}}{1 + K_{COE} \times p_{COE} + K_{COD} \times p_{COD}} \times C_{H_2} \qquad (6)$$

These reaction rates are related to the volume of the palladium-containing layer. The ratio of the adsorption constants is $K_{COD}/K_{COE} > 10^3$ so that in the presence of COD the reaction rate r_2 is almost zero. The concentrations of the components in the pores of the active layer are calculated from the mass balance. Since the diffusion coefficient of hydrogen is about ten times larger than that of the C_8 components, a nearly constant concentration of hydrogen in the active layer is assumed. Thus for the calculations the hydrogen concentration of the gas phase is substituted. With these simplifications the system is described only by the mass

balance equation of COD and the corresponding boundary conditions where the coordinate along the active pores is x, with x = 0 at the outer rim and x = L at the inner rim:

$$\frac{d^2\left(C_{COD}/C_{COD.s}\right)}{d\left(x/L\right)^2} = \varphi^2 \tag{7}$$

with the Thiele modulus

$$\varphi = L \times \sqrt{\frac{k_1}{D_{eff}} \times \frac{c_{H_2}}{c_{COD.s}}} \tag{8}$$

The boundary conditions are:

(i) $\left(\dfrac{c_{COD}}{c_{COD.s}}\right)_{x/L=0} = 1$ \hfill (9)

(ii)   The gradient of c_{COD} at x = 0 is obtained from the steady state condition that the flow of COD into the active layer is equal to the amount of converted COD:

$$D_{eff} \cdot \left(\frac{dC_{COD}}{dx}\right)_{x=0} = x' \cdot k_1 \cdot C_{H_2}, \tag{10}$$

corresponding to

$$\left(\frac{d\left(c_{COD}/c_{COD.s}\right)}{d\left(x/L\right)}\right)_{x/L=0} = -\frac{x'}{L} \times \varphi^2 \tag{11}$$

where x'/L is the position in the active layer where $c_{COD} = 0$. Therefore, the active layer is covered by COD in the range $0 \leq x/L \leq x'/L$. Integration leads to

$$\frac{c_{COD}}{c_{COD.s}} = 1 - \frac{x'}{L}\frac{x}{L}\varphi^2 + \frac{1}{2}\varphi^2\left(\frac{x}{L}\right)^2 \tag{12}$$

and hence

$$\frac{x'}{L} = \frac{\sqrt{2}}{\varphi} \tag{13}$$

In Fig. 7 calculated concentration profiles along the active pores are shown. The apparent reaction rates which are related to the mass of the catalyst are given by

$$COD \rightarrow COE : r_1^* = \frac{x'}{L} \frac{V_{Pd}}{V_P} \frac{1}{\rho_P} k_1 \frac{p_{H_2}}{RT} \tag{14}$$

$$COE \rightarrow COA : r_2^* = \left(1 - \frac{x'}{L}\right) \frac{V_{Pd}}{V_P} \frac{1}{\rho_P} \times k_2 \frac{K_{COE} P_{COE}}{RT + K_{COE} P_{COE}} \frac{p_{H_2}}{RT} \tag{15}$$

V_{Pd}/V_P is the volume of the Pd-containing layer related to the volume of the pellet. (ρ_p is the density of the pellet).
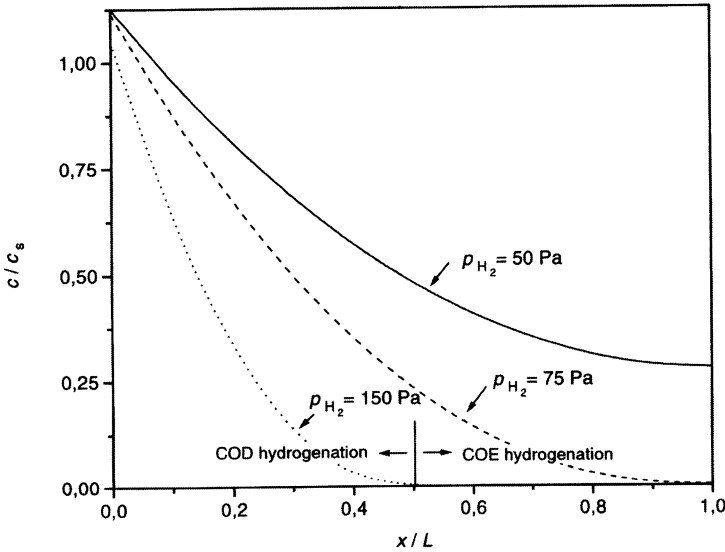
Fig. 7. Dimensionless concentration profiles across the active shell for different hydrogen pressure [18].

Hydrogenation of COE is only possible by readsorption of COE on that fraction of the active layer which is not covered by COD, i.e. the fraction $(1 - x'/L)$, thus COD and COE hydrogenation takes place in different zones of the active layer. These are indicated in Fig. 7.

Two cases can be distinguished as shown in Fig. 7.

(i) $\dfrac{c_{COD}}{c_{COD.s}} \geq 0$ at $\dfrac{x}{L} = 1, \; \varphi^2 \leq 2$ \tag{16}

The palladium-containing layer is completely covered by COD (x'/L=1). Therefore the apparent reaction rates are

$$r_1^* = \frac{V_{Pd}}{V_P}\frac{1}{\rho_P}k_1\frac{p_{H_2}}{RT}$$

$$r_2^* = 0$$

(17)

corresponding to 100 % selectivity with respect to COE.

(ii) $\dfrac{c_{COD}}{c_{COD.s}} = 0$ at $0 < \dfrac{x'}{L} < 1$, $\varphi^2 > 2$

(18)

The active layer is only covered by COD in the range 0 < x/L < x'/L. The apparent reaction rates are

$$r_1^* = \frac{1}{L}\sqrt{2D_{eff}k_1}\,\frac{V_{Pd}}{V_P}\frac{1}{\rho_P}\frac{1}{RT}\sqrt{p_{COD.s}\,p_{H_2}}$$

$$r_2^* = \frac{V_{Pd}}{V_P}\frac{1}{\rho_P}\left(1 - \frac{x'}{L}\right)k_2\,\frac{K_{COE}\cdot p_{COE}}{RT + K_{COE}\cdot P_{COE}}\cdot\frac{p_{H_2}}{RT}$$

(19)

with $x'/L = \sqrt{2}/\varphi$.

The calculated apparent reaction rates are shown in Fig. 8 as a function of the hydrogen pressure. The onset point of consecutive COE hydrogenation corresponds to the condition $\varphi^2 = 2$ ($c_{COD} = 0$ at x = L) and divides the diagram into two parts. The left part is characterized by $\varphi^2 \le 2$ and 100 % COE selectivity and the right by $\varphi^2 > 2$ and reduced COE selectivity. This model was validated by experiments in which all parameters were varied, namely L, k_1 (via Pd loading), D_{eff} (via the dependence on the total pressure) and finally $p_{COD.s}$ and p_{H2} [30].
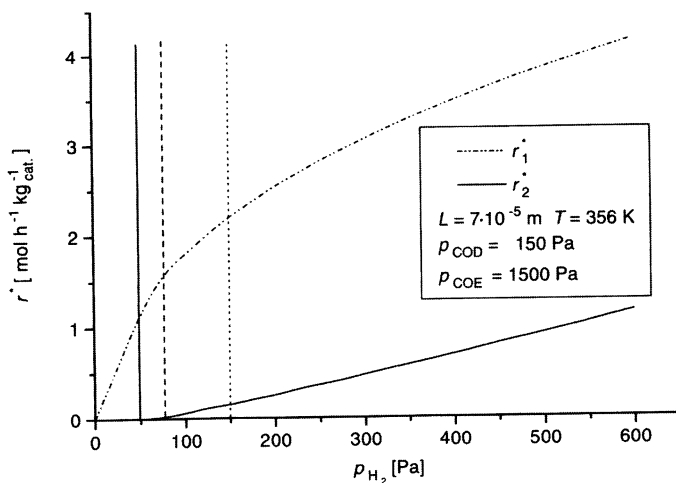
Fig. 8. Dependence of the apparent reaction rates for COD and COE hydrogenation on partial pressure [18].

The condition $\varphi^2 = (1/L^2)(D_{eff}/k_1)(p_{H_2}/p_{COD,s}) \leq 2$ for 100 % selectivity is the key for the successful design of an egg-shell catalyst. For complete COD conversion the ratio $p_{H_2}/p_{COD,s}$ must be chosen such that a minimal excess of hydrogen is guaranteed. All other parameters can be adjusted by appropriate preparation of the catalyst. For example, k_1 is approximately proportional to the Pd content of the active layer. Even D_{eff} can be adjusted to a certain extent by the total pressure and the pore diameter, so that mass transfer is less determined by Knudsen diffusion. The limiting case is very sensitive to the thickness of the active layer L. Therefore, a highly selective catalyst must have a uniform thickness of the Pd covered layer. If Pd is deposited in deeper regions of the pellet, for example in narrow fissures, then mass transfer limitation resulting in cycloalkene hydrogenation occurs for a small fraction of Pd at much lower $p_{H_2} : p_{COD,s}$ ratio than for the main part of the catalyst. It is a difficult task to avoid such uneven patches in the active layer. The development of catalysts providing a very high selectivity depends strongly on improved preparative methods for such ideal egg-shell catalysts [31-34].

If the thickness of the active layer L is obtained by microscopy the experiment $r_1^* = f(p_{H_2})$ at constant $p_{COD,s} \approx p_{COD}$ can serve as appropriate method for the determination of D_{eff} on the basis of the condition for the onset point of consecutive COE hydrogenation.

$$\varphi_{COD}^2 = 2 \qquad \longrightarrow \qquad D_{eff} = \frac{L^2}{2} \cdot k_1 \cdot \frac{p_{H_2}^*}{p_{COD}} \qquad (20)$$

$p_{H_2}^*$ is the hydrogen pressure at the onset point and k_l is obtained from the plot $r_1^* = f(p_{H_2})$ in the range $\varphi^2 < 2$.

2.3.2   Liquid Phase Hydrogenation

This section follows a study of Wuchter [35] on the liquid phase hydrogenation of COD. The liquid phase hydrogenation differs from the gas phase hydrogenation first of all by a lower effective diffusivity in the liquid filled pores of the catalyst. With regard to the hydrocarbon the low diffusivity is usually compensated by a much higher concentration and consequently higher gradients of concentration. However, the Thiele modulus with regard to hydrogen is much higher in the case of liquid phase hydrogenation because of the low diffusivity in the liquid filled pores. The drastic fall of the hydrogen concentration towards the pellet center in this case favors the selectivity towards the intermediate products. Usually the concentration of hydrogen in the liquid phase is of the same order of magnitude as in the case of gas phase hydrogenation. Such concentrations correspond to a hydrogen pressure $p_{H_2} < 5$ bar. For the intrinsic reaction rate r_1 we can use the same expression as for the hydrogen gas phase is assumed approximately first order with respect to hydrogen and independent of the partial pressures of cyclooctadiene and cyclooctene.

$$r_1 = k \cdot C_{H_2} \tag{21}$$

In contrast to the gas phase hydrogenation also the mass balance equation of hydrogen must be taken into account, so that the liquid phase hydrogenation is represented by the following set of mass balance equations and the corresponding boundary conditions.

$$\frac{d^2 C_{H_2}}{dx^2} = \frac{k_1}{D_{H_2,eff}} \cdot C_{COD}^\circ \cdot C_{H_2}^1 \; ; \text{mass balance } H_2 \tag{22}$$

$$\frac{d^2 C_{COD}}{dx^2} = \frac{k_1}{D_{COD,eff}} \cdot C_{COD}^\circ \cdot C_{H_2}^1 \; ; \text{mass balance COD} \tag{23}$$

with the boundary conditions

$$C_{H_2}(x = 0) = C_{H_2,s} \; ; \qquad \left(\frac{dC_{H_2}}{dx} \right)_{x=x'} = 0 \tag{24}$$

$$C_{COD}(x = 0) = C_{COD,s} \; ; \qquad \left(\frac{dC_{COD}}{dx} \right)_{x=x'} = 0 \tag{25}$$

The boundary condition for hydrogen at x= x' is based on the simplification that the consumption of hydrogen by hydrogenation of cyclooctene in the back part of the active layer x'< x < L is negligible. Otherwise the evaluation of x' where $C_{COD}(x') = 0$ needs a rather complicated iteration. Since the rate of cyclooctene hydrogenation is markedly lower than the rate of diene hydrogenation and reaction states of a relatively high rate of cyclooctene formation are not of interest this simplification is justified particularly because it renders possible an algebraic solution.

The solutions are:

$$C_{H_2}(x) = C_{H_{2,s}} \frac{\cosh\left(\sqrt{\frac{k_1}{D_{H_{2,eff}}}} \cdot (x'-x)\right)}{\cosh\left(\sqrt{\frac{k_1}{D_{H_{2,eff}}}} \cdot x'\right)} \tag{26}$$

$$C_{COD}(x) = C_{H_{2,s}} \cdot \frac{D_{H_{2,eff}}}{D_{COD,eff}} \cdot \frac{\cosh\left(\sqrt{\frac{k_1}{D_{H_{2,eff}}}} \cdot x'\right)}{\cosh\left(\sqrt{\frac{k_1}{D_{H_{2,eff}}}} \cdot x'\right)} \tag{27}$$

with $C_{COD}(x') = 0$ follows

$$x' = \sqrt{\frac{D_{H_{2,eff}}}{k_1}} \, arc \cos h \left(\frac{1}{1 - \frac{C_{COD,s}}{C_{H_{2,s}}} \cdot \frac{D_{COD,eff}}{D_{H_{2,eff}}}}\right) \tag{28}$$

The calculation of the effective reaction rate, taking into account the influence of mass transfer liquid phase → outer surface of the catalyst pellet, and finally the numerical integration of the material balance of a batch experiment

$$\int_{C^\circ_{COD}}^{C_{COD}} \frac{dC'_{COD}}{r_{A,COD}} = t \tag{29}$$

gives the concentration of COD, and approximately also that of COE as a function of time. The parameter of the model k_1 and $D_{H_{2,eff}}$ are obtained by fitting the model to experimental data. Fig. 9a shows the concentration curves of COD

and COE for a batch experiment at constant hydrogen pressure. Fig. 9b gives the interesting detail of the calculated curve.
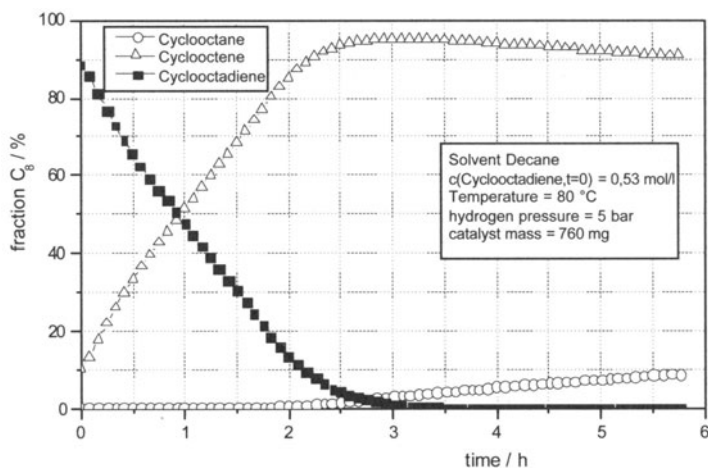
Fig. 9a. Formation of cyclooctene and cyclooctane or conversion of cyclooctadiene versus reaction time at constant partial pressure of hydrogen (5 bar).
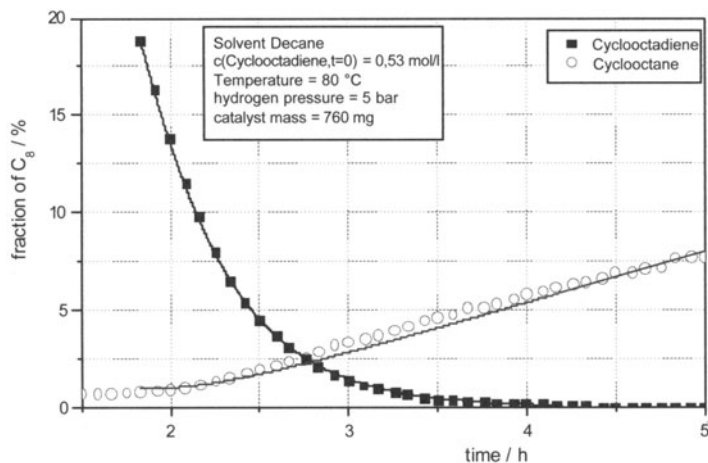
Fig. 9b. Formation of cyclooctene and cyclooctane or conversion of cyclooctadiene versus reaction time at constant partial pressure of hydrogen (5 bar): experimental data (symbols) and calculated (line).

The estimated reaction rate constant $k_{1,li} \approx 90$ s^{-1} is of the same order of magnitude as the rate constant $k_{1,g} \approx 200$ s^{-1} determined for the gas phase hydrogenation. Therefore the conclusion is drawn, that in both cases, liquid phase and gas phase hydrogenation, the access of hydrogen through the dense adsorption layer to the catalyst surface and the subsequent dissociation can be regarded as the rate determining step of the reaction.

2.4   Mechanisms of Alkadiene Hydrogenation

Complex mechanistic schemes have been derived from studies of the hydrogenation and experiments in the presence of deuterium of several alkadienes like propadiene (diene with cumulated double bonds), 1,2-butadiene, 1,3-butadiene and some higher adjacent and conjugated dienes. Alkadiene hydrogenation mechanism and, thus, selectivity mainly depends on the nature of the individual metal. Exemplifying by 1,3-butadiene hydrogenation, all three isomeric n-butenes are observed as initial reaction products, and, in general, 1-butene is the major product. However, 1-butene/2-butene ratio and the relative yields of trans- and cis-2-butene vary widely with the kind of metal and the extent of hydrogenation. On palladium the *trans : cis* ratio of the 2-butenes is larger than 10 [6,36,37]. A high *trans : cis* ratio is also obtained for Pd catalysts in industrial processes [31,32]. 1-Butene is formed via 1,2-addition, and 2-butenes are formed via 1,4-addition of hydrogen to adsorbed 1,3-butadiene. Meyer and Burwell [36] proposed a mechanism in which semihydrogenated 1,3-butadiene can be adsorbed as *syn-* 1 or *anti-π*-allyl 2 species.
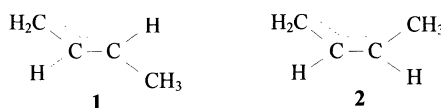
The ratio of the two conformations of adsorbed 1,3-butadiene should be similar to the proportion of *syn-* and *anti-*1,3-butadiene in the gas phase, which is about 1: 10 [6,19,38]. It is supposed that in the case of butadiene hydrogenation on Pd the semihydrogenated intermediates of 1,3-butadiene do not readily interconvert so that a high proportion of *trans-*2-butene results. This hypothesis of π-allylic intermediates in 1,3-diene hydrogenation has been recently confirmed by G. C. Bond [39] who interpreted by the same token consistently the selectivity pattern of isopren hydrogenation. However at reduced butadiene pressure the ratio of obtained *trans-* and *cis-*2-butene approaches the thermodynamic equilibrium of *trans/cis*-ratio of 2.4, even though the consecutive hydrogenation to butane and isomerisation of 1-butene is suppressed. Obviously the anti π-allyl 2 species is stabilized when the surface is densely covered with butadiene at relatively elevated partial pressure of butadiene. This stabilized anti π-allyl species is hydrogenated towards trans-2-butene but not isomerized via the *syn-*species and hydrogenated to *cis-*2-butene. In the case of butene isomerisation the density of the adsorption layer of butene is lower than in the case of butadiene so that the mutual transformation of *anti-* and *syn-π*-allyl species is possible.

These experimental results and discussion of 1,3-butadiene hydrogenation suggest also the isomerisation of butenes via π-allylic intermediates. Support for

this mechanism comes from the analysis of the position of deuterium in deuterated butenes by combined mass spectrometry and microwave spectroscopy [40].

Cofeeding of carbon monoxide causes a drastic decrease of both the rate of hydrogenation and of isomerisation. Carbon monoxide competes with hydrogen for sites on the surface of the catalyst so that the activation of hydrogen is hindered. Therefore, in the case of CO addition a given rate of hydrogenation is reached at a much higher hydrogen pressure than in the reference experiment without CO addition. At the same rate of hydrogenation also the same rate of isomerisation is observed as shown in Fig. 10a and Fig. 10b. Obviously both hydrogenation and dehydrogenation steps depend well defined on the coverage with hydrogen so that isomerisation and hydrogenation are strictly interrelated [38].
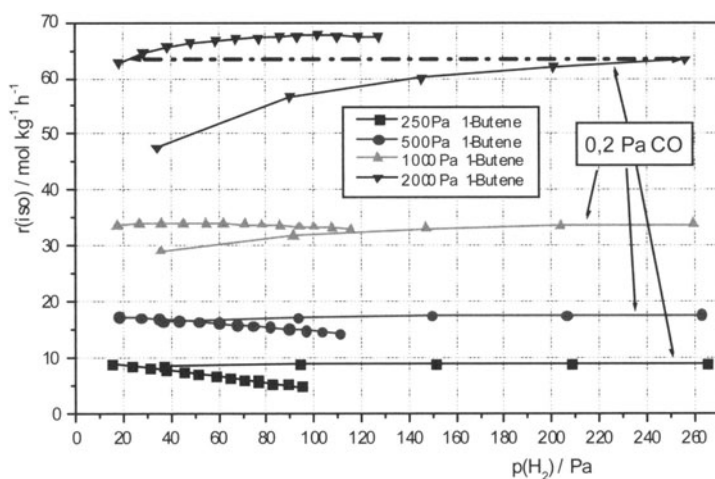
Fig. 10a. Comparison of the rates of isomerisation versus partial pressure of hydrogen at constant partial pressures of 1-butene at 250, 500, 1000 and 2000 Pa with and without 0,2 Pa carbon monoxide [38].
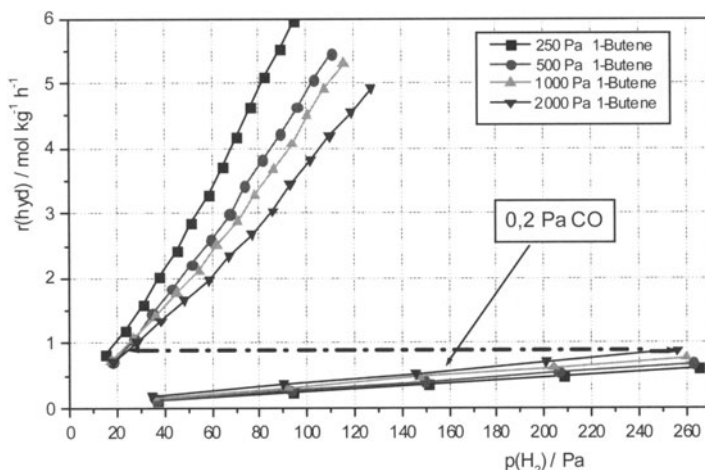
Fig. 10b. Comparison of the rates of hydrogenation versus partial pressure of hydrogen at constant partial pressures of 1-butene at 250, 500, 1000 and 2000 Pa with and without 0,2 Pa carbon monoxide.

Note, that in the field of surface science recent studies with simple alkenes show how the reaction conditions (high pressures up to a few hundred mbar) and/or high-temperatures can influence the internal and surface structure of the metal (called adsorbate-induced restructuring) and how the adsorbate structure and adsorption site distribution of CO and hydrocarbons on metal aggregates depends on pressure. For example, Somorjai and co-worker have applied the infrared-visible sum frequency generation (SFG) to ethylene hydrogenation on Pt (111) in order to monitor the surface vibrational spectrum in-situ under usual reaction conditions of 1 bar and 295 K [41]. With this new method they could correlate kinetic measurements with surface adsorbate concentrations. All surface species discussed in alkene hydrogenation studies [42] as π-bonded ethylene, di-σ-bonded ethylene, ethyl and also ethylidyne were observed. In accordance with the former study of Beebe et al. [43,44] it could be shown that the spectator species ethylidyne is completely uncorrelated with the rate of hydrogenation. Also the di-σ-bonded ethylene is uncorrelated with the hydrogenation. Therefore the conclusion has been drawn that π-bonded ethylene is directly hydrogenated to ethane.

However, nowadays, in-situ studies using SFG, high-pressure scanning electron microscopes, environmental high-resolution transmission electron microscopy are among the most promising tools to bridge the gap between fundamental surface science studies and real world catalysis.

In this context, theoretical studies of van Santen and co-workers [45] on the hydrogenation of ethylene on Pd (111) have revealed using first-principle density functional calculations (DFT) that under high ethylene coverage the hydrogenation occurs via π-bonded ethylene. From this fundamental study the general conclusion can be withdrawn that weakening the metal-adsorbate bond strength will lower the intrinsic activation energy for hydrogenation reactions and surface

coverage effects are important in reaction path analysis. Caution must be exercised in determining catalytic reaction pathways based on information collected for the most stable adsorption species alone so that the less stable surface species may in fact be the kinetically significant reaction intermediate.

2.5   Partial Hydrogenation of Benzene to Cyclohexene

Benzene is hydrogenated to cyclohexane on an industrial scale. In most processes, platinum catalysts are employed. Minor amounts of cyclohexene are obtained, if the degree of benzene conversion is kept below 1 %. In 1963, Hartog and Zwietering [46] investigated the liquid phase hydrogenation of benzene and found that ruthenium is the only catalyst of Group VIII metals on which at least a small yield of cyclohexene of about 0.1% at 20 % benzene conversion was obtained. The cyclohexene selectivity could be markedly increased when an alcohol, such as methanol or butanol, was added to the liquid benzene [47,48]. However, the most important step to an improved selectivity was to carry out the hydrogenation in an agitated two-liquid-phase system. The two phases are benzene/cyclohexene and water, to which salts of transition metals are added [49]. On this basis several companies developed processes for the production of cyclohexene from benzene [50-59]. At present, the best result is a cyclohexene selectivity of 70 % at a degree of benzene conversion of 85 % [60].

A tremendous number of catalysts were tested. It turned out that supported ruthenium catalysts are best suited. These catalysts are usually prepared by impregnation of the carrier by an aqueous ruthenium chloride solution. Oxides of lanthanides such as La_2O_3 were found to be particularly suited [53,59]. A special type of supported ruthenium catalyst is prepared by mixing a dissolved ruthenium chloride-alcohol complex and tetrahydroxysilane or aluminium tri-*s*-butoxide (sol-gel process). Very small ruthenium crystallites with a diameter below 2nm are obtained. The exceptional feature of this catalyst is that addition of salts to the aqueous phase is not necessary [61-63]. The other supported catalysts are promoted by salts of transition metals such as Ni, Fe, Co and Zn which are directly added by impregnation or coprecipitation or added to the aqueous phase [49,53,55,57,58,64].

In order to reach reasonable selectivities to cyclohexene, the catalyst particles must be suspended in the aqueous phase [65,66]. Hydrogen and benzene are dispersed as bubbles and droplets. The solubility of benzene in water is about eight times higher than that of cyclohexene. Therefore, it is assumed that water enhances the removal of cyclohexene from the catalyst surface [63,67]. Furthermore, the access of hydrogen to the catalyst particles is moderated because of the low solubility of hydrogen in water. The diffusion of hydrogen through the adherent water layer of the particles is regarded as the rate determining step [66]. Access of benzene and a fast removal of cyclohexene from the catalyst surface are determined by the specific structure of the hydrogen bond network in the adherent layer. It is assumed that this structure depends on the cations which are adsorbed on the surface and, hence, make the ruthenium particles more hydrophilic [64,66,12]. A particular effect was found by Nagahara and Konishi [54], who performed the hydrogenation in a system containing supported ruthenium particles suspended in an aqueous salt solution to which fine particles of oxides, such as

oxides of Zr, Ti, Nb and Ta, were added. Cyclohexene yields of about 60 % were achieved at benzene conversions of 80-90% [54,68].

To date, kinetic studies are scarce because of the complexity of the multiphase reaction. In the work by Struijk et al. [66], a reaction order of unity with respect to hydrogen has been determined. This result is in accordance with the assumption that the diffusion of hydrogen through the adherent water layer of particles is the rate determining step.

The question as to whether benzene is converted following a stepwise Horiuti-Polanyi mechanism [69] or whether there exists also a direct route from benzene to cyclohexane [65,70] is controversially discussed. Recently, it was shown for the system Ru/La_2O_3 suspended in an aqueous $ZnCl_2$ solution that the selectivity to cyclohexene approaches unity with decreasing degree of benzene conversion, so that a direct route from benzene to cyclohexane can be excluded [71].

The first and until now the only plant for partial hydrogenation of benzene to cyclohexene (60 000 t a^{-1}) was constructed by Asahi Chemical Industry Co., Japan, in 1990. In this process, benzene is converted into cyclohexene using a ruthenium-zinc catalyst. The aqueous phase contains salts and oxides as additives. The partial hydrogenation of benzene is carried out at 420-450 K and 5-7MPa in an agitated reactor or in a series of agitated reactors [72]. The reactor contains a thoroughly dispersed organic/aqueous/catalyst mixture through which hydrogen is blown. In order to separate the multiphase reactor liquid into an organic phase and a water phase a stationary zone inside the reactor is provided, or the separation occurs in a decanter.

Some research work has been undertaken in order to substitute the four phase procedure (gas, aqueous liquid, non aqueous liquid, solid catalyst) by a more simple one. For example, Döbert [71] and Gescheidle [73] could show that the presence of a non aqueous phase is not crucial to reach a high selectivity. Gaseous benzene is blown through an aqueous suspension of the catalyst, e.g. ruthenium supported on La_2O_3. The gaseous product flow leaving the reactor contains cyclo-hexene, cyclohexane and non converted benzene. It is not necessary to separate the catalyst unless the deactivated catalyst has to be removed and replaced by fresh one. A series of tank reactors can be easily arranged in order to realize a high degree of benzene conversion and to approach the performance of a tubular reactor that is characterized by the highest selectivity with respect to the desired intermediate product cyclohexene.

The most simple procedure would be the selective gas phase hydrogenation of benzene. Unfortunately selectivities obtained with this procedure are very low. On coated Ru with methanol as modifier selectivities up to 45 % at conversion degrees of 5 %, i.e. a yield of 2.3 %, and on a Ru/SiO_2 sol-gel catalyst with water as modifier selectivities up to 10 % at a conversion degree of 30 %, i.e. a yield of 3% are observed [74]. Obviously an adsorption layer of the modifier is not sufficient to effect a high selectivity of cyclohexene.

3.   Selective Hydrogenation of α,β-unsaturated Aldehydes

The selective hydrogenation of organic substrates containing various unsaturated functional groups is an important step in the industrial preparation of fine chemicals and has been attracting much interest for fundamental research in

catalysis. For example, allylic alcohols obtained by preferred hydrogenation of the C=O group of α,β-unsaturated aldehydes are valuable intermediates for the production of perfumes, flavoring and pharmaceuticals [75]. The general scheme of the reaction network for this reaction is shown in Fig. 11.
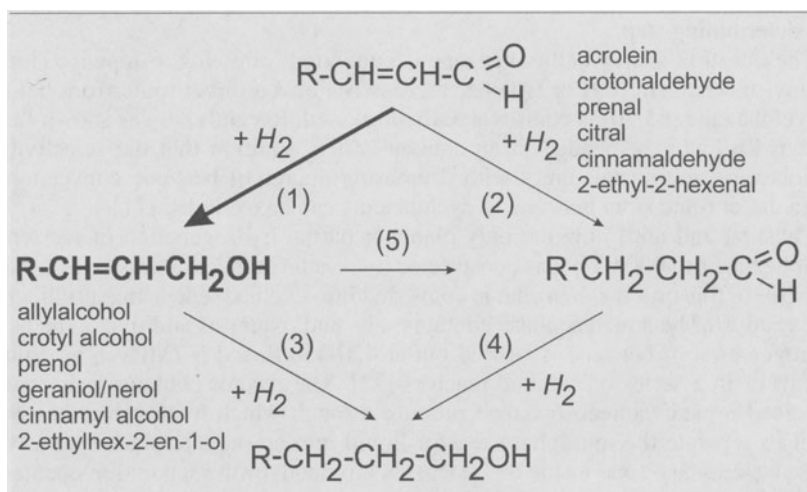
Fig. 11. Scheme of the reaction network of the hydrogenation of α,β-unsaturated aldehydes [76].

In the presence of most of the conventional group VIII metal hydrogenation catalysts, α,β-unsaturated aldehydes are hydrogenated predominantly to saturated aldehydes by reduction of the C=C group or to saturated alcohols as this reaction is thermodynamically preferred. Therefore, it is necessary to find catalysts which will preferentially activate and thus control the intramolecular selectivity by hydrogenating the C=O group while keeping the olefinic double bond intact (Fig. 11, reaction 1 vs. 2). Besides the preferentially hydrogenation of the C=O group, the catalyst has to suppress additionally consecutive reactions. The consecutive hydrogenations in this case, are the hydrogenations to the saturated alcohol (reactions 3 and 4) and the isomerisation of the allylic alcohol (reaction 5). Note, that all pathways of Fig. 11 are thermodynamically possible, however, the hydrogenation of the C=C group in α,β-unsaturated aldehydes is more favorable than the hydrogenation of their C=O group [77]. Thus, selectivity to unsaturated alcohol must be controlled by changes in the rate constants of both competitive reactions and in the adsorption constants of the components.

It must be noted here, that the hydrogenation of α,β-unsaturated aldehydes is strongly influenced by **steric effects of substituents at the conjugated double bond** [78-80]. The selectivity to allylic alcohols can be increased with an increasing substitution (R) of the terminal carbon atom of the C=C group, e.g. in the order acrolein, crotonaldehyde and cinnamaldehyde (R = H, CH_3, C_6H_5 respectively). Fig. 12 gives an comparison between acrolein and crotonaldehyde hydrogenation over Rh-Sn/SiO_2 catalysts [81]. While the turnover frequency for the formation of the saturated aldehyde increased from 0.53 to 0.69 s^{-1} by

substituting the methyl group by a hydrogen atom, a strong decrease of the turnover frequency for the formation of the unsaturated alcohol from 1.47 to 0.29 s^{-1} was found [81].
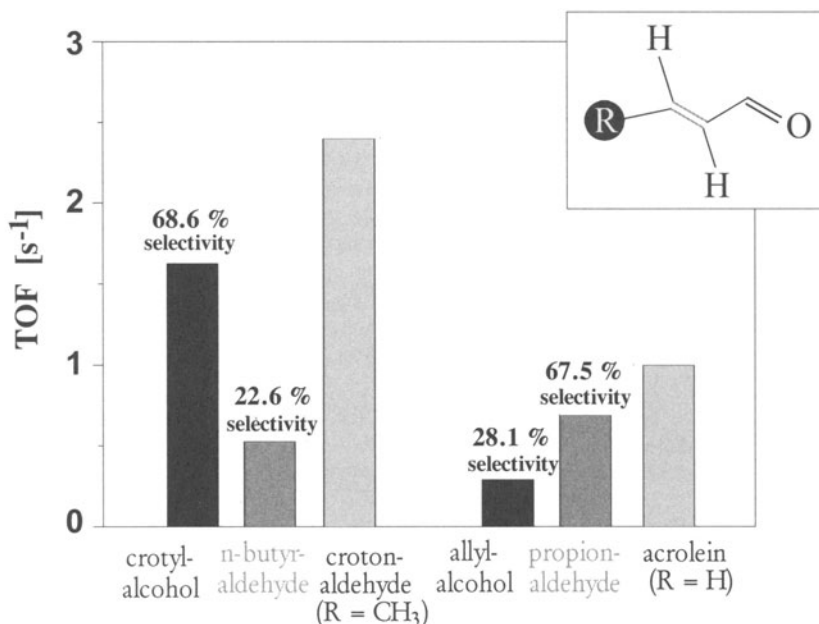
Fig. 12. Turnover frequencies and selectivities to allylic alcohols and saturated aldehydes of the gas phase hydrogenation of crotonaldehyde and acrolein over a bimetallic Rh-Sn/SiO$_2$ catalyst (T = 413 K, p$_{total}$ = 2 MPa, H$_2$/CA = 20, W/F$_{CA}^0$ = 9.87 g h mol^{-1}).

Several attempts have been made to develop suitable catalytic systems for the selective hydrogenation of α,β-unsaturated aldehydes to unsaturated (allylic) alcohols. Because of the strong influence of a substituent at the C=C group on the intramolecular selectivity, lower α,β-unsaturated aldehydes as acrolein and crotonaldehyde are much more difficult to hydrogenate selectively to the corresponding unsaturated alcohols than citral and cinnamaldehyde. Therefore, after compiling the factors that influence the C=O vs. C=C group hydrogenation (Fig. 13), the next chapter will be mainly focussed on the most important approaches to increase the selectivity of the C3 and C4 allylic alcohols.

Factors controlling the intramolecular selectivity of the hydrogenation of α,β-unsaturated aldehydes	References
⇀ Nature of the individual metal	75,76,82,83
⇀ Electronic and steric influence of the support	90
⇀ Metal-support interactions	77,80,102,105,108
⇀ Metal particle size and morphology	78,79,120-122
⇀ Selective poisoning	76
⇀ Influence of a second metal	112-115,117,124,138
⇀ Pressure effect	76,124
⇀ Steric effects of substituents at the conjugated double bond	79-81

Fig. 13. Overview of the factors controlling the intramolecular selectivity of the hydrogenation of α,β-unsaturated aldehydes.

3.1   Metal Particle Size and Morphology

The influence of steric constraints on the metal surface, i.e. of particle-size effects on selectivity has been paid less attention and gave, in the case of aliphatic α,β-unsaturated aldehydes, controversial results. Nitta et al. reported that Co/SiO$_2$ prepared by a precipitation method from cobalt chloride exhibit high selectivity to unsaturated alcohols which increases with increasing mean size of cobalt crystallites [84-86]. The residual chloride in the catalyst precursor was concluded to be responsible for the homogeneous crystallite distribution during reduction in hydrogen. Studies on competitive adsorption between the products of the first hydrogenation step showed a lower adsorption constant on larger cobalt particles for the unsaturated alcohol than for the saturated aldehyde [85]. In liquid phase hydrogenations of higher α,β-unsaturated aldehydes over Pt, Rh and Ru catalysts, selectivity to the unsaturated alcohol is generally increased with increasing metal particle size [87-89]. On large metal particles, Gallezot et al. claimed that the adsorption of the C=C group of cinnamaldehyde is hindered by a steric repulsion between the metal surface and the aromatic ring thus favoring hydrogenation of the C=O group [87,89,90]. In contrast, the hydrogenation of citral into unsaturated alcohols (E- and Z-isomers geraniol and nerol, respectively) over ruthenium catalysts was independent on the Ru particle size [91,92].

However, data for particle-size effects in gas phase hydrogenations of lower α,β-unsaturated aldehydes such as acrolein and crotonaldehyde are scarce. Coq et al. reported that the selectivity towards allyl alcohol in acrolein hydrogenation over Ru catalysts (at conversions < 1 %) is not structure-sensitive [93]. On the other hand, a marked increase of selectivity towards the unsaturated alcohol with increasing platinum particle size has been observed by Lercher et al. studying the hydrogenation of crotonaldehyde over Pt/SiO$_2$ catalysts [94]. The high fraction of

Pt(111) surfaces was concluded to favor the adsorption of the α,β-unsaturated aldehyde via the C=O group. By using a partially reducible support like TiO_2 instead of silica and combining cycles of high-temperature reduction (at 777 K), oxidation (at 673 K) and a second reduction step (at 473 K) higher selectivities up to 64 % were observed (see also Chapter 3.2.) [94]. Recently, it has been shown by extended Hückel calculations [95] and experimental studies on hydrogenation of 3-methylcrotonaldehyde (prenal) at 353 K over well-defined surfaces, Pt (111) and Pt(110), that the adsorption mode of α,β-unsaturated aldehydes depends strongly on the exposed crystal face (Fig. 14) [96-98].
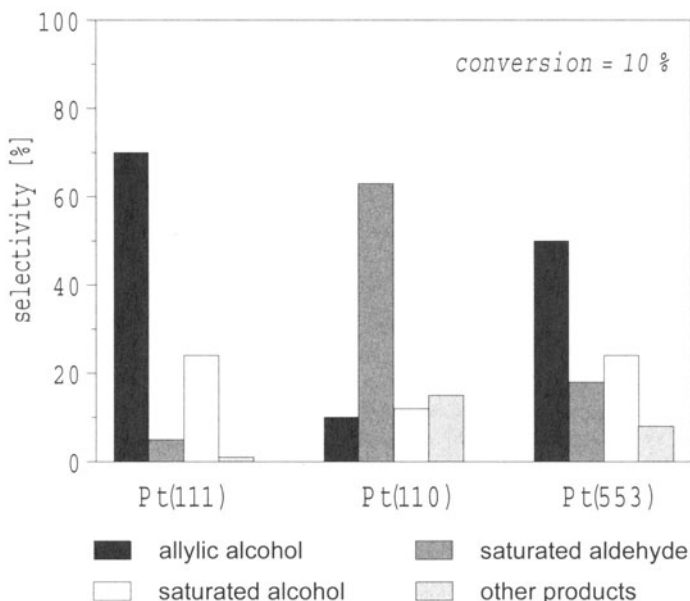
Fig. 14. Selectivity to allylic alcohol, saturated alcohol, saturated aldehyde and other products on different Pt single crystal surfaces in the hydrogenation of 3-methylcrotonaldehyde at conversions of 10 % (T = 353 K, p_{H2} = 200 torr, p_{prenal} = 7 · 10^{-3} torr, [96]).

While on Pt (111) the unsaturated alcohol was formed with a selectivity of 65 % at 10 % conversion [97], the main products on Pt(110) were the saturated aldehyde (63 %) and alcohol (12 %) [98]. On a catalytic surface that is closer to real catalyst surfaces than low-index planes, namely Pt(553) which is made up of a regular arrangement of (111) terraces and (111) mono-atomic steps, evidence for the structure sensitivity was obtained leading to a lower selectivity of unsaturated alcohol (50 % at 10 % conversion) than on the Pt(111) surface [99]. Moreover, the stepped platinum surface gave a higher selectivity towards saturated aldehyde than the flat plane (18 % instead of 5 %) [96].

Recent work of Guerreo-Ruiz et al. [100] conducting crotonaldehyde hydrogenation over carbon-supported molybdenum nitrides showed that a higher crotyl alcohol selectivity is associated with the (200) planes of the γ-Mo_2N crystallites and, thus, the structure-sensitivity of this reaction.

3.2   Metal-Support Interactions

Oxidized metal species at the interface between small metal particles and the support material which are usually known as strong **metal-support interactions** (SMSI) [101] considered to be responsible for the increase of the selectivity towards the unsaturated alcohol. Hydrogenation and deuteration experiments with acrolein over Pt/Nb_2O_5 and Ir/Nb_2O_5 and the use of deuterated acrolein by Iwasawa et al. [102,103] were strongly indicative for activation of the carbonyl bond by SMSI. From these studies it was concluded that hydrogen, dissociatively adsorbed on pure metal sites, migrates across the surface to the interfacial region and hydrogenates the CIO group of the α,β-unsaturated aldehyde which adsorbs on the metal-NbO_x interface in a η^4-(C,C,C,O) adsorption mode. The adsorption of both functional groups was also proposed by Beranek et al. [104] because similar adsorption constants for crotonaldehyde in the Langmuir-Hinshelwood rate expressions for the formation of crotyl alcohol and butyraldehyde were obtained.

Vannice et al. [77] observed a marked shift in activity for the hydrogenation of the C=O group of crotonaldehyde when high-temperature reduced (HTR) titania supported Pt catalysts were used (T_{red} = 773 K). Turnover frequencies were one order of magnitude higher than those of Pt/TiO_2 reduced at 473 K, Pt/SiO_2 or Pt/Al_2O_3 catalysts. The explanation for the control of selectivity is the generation of new active sites (Ti^{3+}, O vacancies), which are able to chemisorb and thus activate especially the carbonyl group. This is schematically illustrated in Fig. 15.
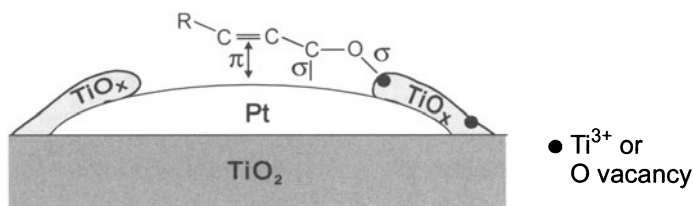
Fig. 15. Adsorption configuration of α,β-unsaturated aldehydes on SMSI catalysts, [77].

Results with other titania supported Group VIII metal catalysts showed again the influence of the metal deposited on TiO_2 where Rh [105], Ni [106] and Ru [107] gave a considerably lower selectivity to crotyl alcohol. Ir/TiO_2-HTR and Os/TiO_2-HTR produced crotyl alcohol with selectivities up to 48 % during transient reaction conditions [107]. The phase composition of titania used as support for HTR platinum catalysts has a strong influence on the activity in crotonaldehyde hydrogenation which decreased with increasing anatase content [108]. While selectivity to crotyl alcohol ranged from 30 to 40 % at low crotonaldehyde conversions independent of the catalyst support used, a Pt/TiO_2-HTR catalyst with an anatase content of 65 % produced 53 % crotyl alcohol at 80 % conversion.

In recent studies with Pt/CeO_2 prepared from a non-chlorine containing Pt precursor it was demonstrated that with increasing the reduction temperature up to 973 K the crotyl alcohol selectivity reached more than 80 % until crotonaldehyde conversion of ca. 40 % [109]. The performance of this SMSI type catalyst was

attributed to the formation of CePt$_5$ alloy lowering the activity of C=C group hydrogenation. The level of selectivity obtained with ceria based platinum catalysts [109,110] is comparable with that of Pt/ZnO [111] and superior to the above mentioned Pt/TiO$_2$ catalysts. Studying the latter, selectivities up to 64 % in the case of Pt particles of 12 nm in size were obtained by Lercher et al. [94] (see also Chapter 3.1). Here, effects of particle size (see below) and promotion by TiO$_x$ were discussed to be additive. However, it has to be noted that this is not case for Pt/CeO$_2$ catalysts where rather alloy formation than Pt particle size governs the selectivity to the unsaturated alcohol [109].

3.3   Influence of a Second Metal

Improving the selectivity by simply adding salts of electropositive d electron elements (e.g. Fe and Co) or p electron elements (e.g. Sn, Ge) to a catalyst-containing reaction mixture in the case of liquid phase hydrogenations of α,β-unsaturated aldehydes [112-115] is one of the oldest approaches [116] done in laboratories of organic chemists. Characterization of catalyst particles after reaction by Gallezot and co-workers using scanning transmission electron microscopy (STEM) and energy-dispersive X-ray spectrometry (EDX) showed the presence of in-situ formed true bimetallic Pt-Fe particles [117]. The observed increase of allylic alcohol selectivity was explained by an electron transfer from the much more electropositive iron atoms to platinum. The second metal was considered as acting as Lewis adsorption sites for the oxygen atom of the C=O bond, where the polarized functional group is easily hydrogenated by addition of hydrogen chemisorbed on the nearby platinum atoms [117]. Indeed, XANES measurements indicate electron transfer from Fe to Pt atoms in reduced Pt-Fe/C prepared ex-situ by co-impregnation [118]. Many groups examined these type of catalysts, using different preparation methods, varying the noble metal to second metal ratio [75,76,115,118,119] and trying to characterize the active site in order to understand the control of the intramolecular selectivity.

Monometallic Rh, Pt or Ru catalysts were also modified by applying ex-situ techniques (incipient wetness, co-impregnation) followed by calcining and subsequently reducing the precursor material in flowing hydrogen. In the case of a controlled surface reaction (CSR) of organometallic compounds (e.g. (n-C$_4$H$_9$)$_4$Sn)) with supported highly-dispersed metals (Rh, Pt, Ru) well-defined bimetallic catalysts can be obtained that exhibit either alloy particles or a metallic surface modified by grafted butyltin fragments [120-122].

For example, Basset et al. (e.g. [120-122]) prepared Rh[M-(n-C$_4$H$_9$)$_x$]$_y$/SiO$_2$ catalysts (M = Ge, Sn, Pb) by partial hydrogenolysis, at 373 K, of (n-C$_4$H$_9$)$_4$M on the surface of silica supported rhodium. In the presence of a grafted butyltin fragment (x = 2, y = 1), the hydrogenation of citral in the liquid phase at 7.6 MPa and 340 K produced a selectivity of 96 % geraniol/nerol at 100 % conversion. The high selectivity was attributed to electronic and steric effects, the latter may favor the adsorption of the less hindered functional group of citral, e.g. the C=O group. By treating the organo-bimetallic catalyst (Sn/Rh = 1) at 630 K under hydrogen, removal of the remaining butyl groups occured [120] and a strong decrease of the selectivity of geraniol/nerol to 6 % [120] was observed, whereas in contrast a value of around 80 % can be taken from [122] for Rh[Sn-(n-C$_4$H$_9$)$_x$]$_y$/SiO$_2$ with x = 0 and y = 1.

Also a highly-temperature (773 K) reduced Pt-Sn/MgO catalyst (Sn/Pt = 0.5) prepared via the CSR method and applied by Recchia et al. [123] for the hydrogenation of citral at 373 K and 2 MPa in a trickle-bed reactor gave a selectivity to geraniol and nerol of 97 % at 100 % conversion at a contact time of 79.5 s. It is noteworthy that no deactivation was observed.

By the method of controlled surface reaction Claus et al. [75,124] achieved a high selectivity to crotyl alcohol (S_{max} = 75 % at 15 % conversion) over Rh-Sn/SiO$_2$ in the gas phase hydrogenation of crotonaldehyde if the bimetallic catalysts were finally reduced in hydrogen at 623 K. The morphology of the true bimetallic particles, as shown by STEM/EDX analysis, was identical to the monometallic catalyst, and the particle size distribution again had a average size of 2 nm [125]. This suggests that no sintering occurs during the hydrogenolytic decomposition of the partially alkylated metal-tin precursor. Therefore, the catalytic properties during hydrogenation are related to the effect of tin. An electron transfer to rhodium atoms is suggested in the case of such nanosized Rh-Sn alloy particles which provide an additional evidence for the results of XANES and EXAFS measurements on bimetallic catalysts [120,126]. Therefore, bimetallic catalysts which exhibit surface polarity due to negatively charged Rh (or Pt, Ru) and positively charged Sn are selective for C=O group hydrogenation.

It was shown that the turnover frequencies for the formation of crotyl alcohol and n-butyraldehyde, and thus, the intramolecular selectivity of the gas phase hydrogenation of crotonaldehyde strongly depends on the Sn/Rh ratio of the alloy catalyst [75].

However, the nature of the active sites in metal-tin phases and the kind of modification of the matrix metal (e.g. Rh) by Sn via electronic (ligand) effects and /or dilution with metallic tin are still the subject of discussion [123,127-134].

3.4   Reaction Mechanism

Taking into account theoretical approaches and the experimental behavior of metal catalysts towards the hydrogenation of α,β-unsaturated aldehydes as discussed before a reaction mechanism of the hydrogenation of α,β-unsaturated aldehydes can be proposed [76] which is shown for crotonaldehyde hydrogenation in a simplified scheme (Fig. 16).
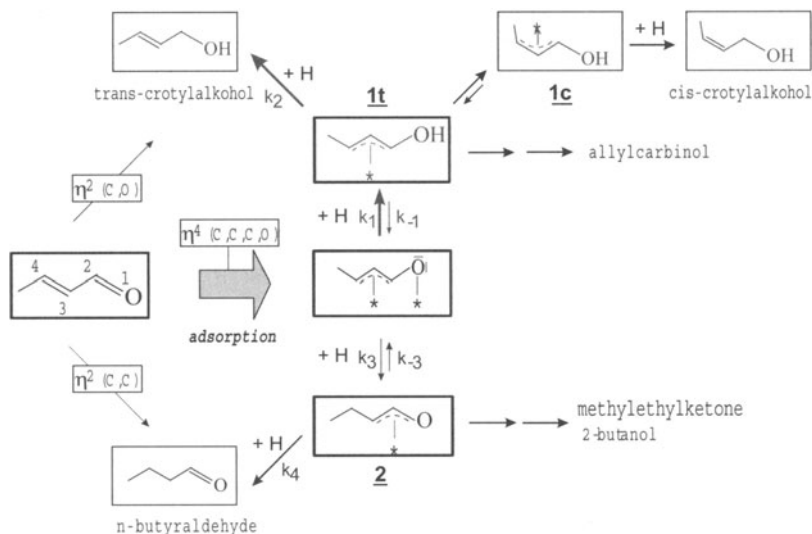
Fig. 16. Reaction mechanism of the hydrogenation of crotonaldehyde (**1t**: trans-π-allylic surface species; **1c**: cis-π-allylic surface species; **2**: oxo-π-allylic surface species).

Depending on (i) the nature of the individual metal (Os, Ir and Ru favor C=O hydrogenation while Pd remains completely unselective), (ii) steric constraints in the metal environment, (iii) modification of the metal surface by a second metal, (iv) steric and electronic effects of supports and ligands and (v) substitutents on the C=C group, the pathways of allylic alcohol and saturated aldehyde formation can be totally different following the classical Horiuti-Polyani mechanism via η^2-(C,O) and η^2-(C,C) adsorption modes, respectively, or involving π-allylic and oxo-π-allylic surface species. For the formation of the latter species an adsorption configuration of an α,β-unsaturated aldehyde is necessary that takes into account both functional groups like η^2-(C,C) + η^1-(O) or η^2-(C,C) + η^2-(C,O) or η^4-(C,C,C,O). Such an adsorption mode on a well-characterized (see Chapt. 3.3.) bimetallic surface is shown in Fig. 17.
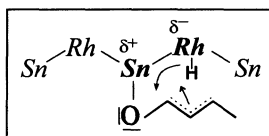
Fig. 17. Adsorption mode of crotonaldehyde on a bimetallic Rh-Sn ensemble.

From this mode allylic surface species can proceed by adding the first hydrogen atom either to the carbonyl oxygen atom (formation of **1t**), or to the terminal carbon atom of the C=C group (formation of **2**). Concerning the adsorption mode, note the analogy between bimetallic surfaces and oxidized metal species at the interface between small metal particles and the support material (see Fig. 15).

Involvement of both functional groups during the adsorption step is not only shown by XANES [135], HREELS [136] and theoretical calculations [137]. Also the formation of cis-crotyl alcohol, whose selectivity increased with increasing atomic ratio Sn/Rh and the formation of 2-butanol and ethyl methyl ketone in crotonaldehyde hydrogenation or of 2-propanol and acetone in acrolein hydrogenation, respectively [75,81,93,138] are experimental indications for a mechanism based on π-allylic and oxo-π-allylic intermediates as half-hydrogenated species. Ketone formation by opening of an oxirane ring as was reported by Coq et al. [93] could be due to electron-deficient metallic sites at the metal-support interface or to the electronic state of a second metal (e.g. $Sn^{\delta+}$) as described for bimetallic catalysts.

3.5   Selective Hydrogenation with Silver and Gold Catalysts

Silver catalysts are well known for the oxidation of ethylene to ethylene oxide and for the production of formaldehyde from methanol. Surprisingly, *monometallic* silver catalysts were also able to hydrogenate selectively the C=O group of α,β-unsaturated aldehydes in the gas phase [81]. In the hydrogenation of crotonaldehyde for five Ag/SiO_2 catalysts, prepared by different preparation techniques, the selectivity to the unsaturated alcohol was found to be (59 ± 3) %, independent on the particle size in the range of 3.7 nm $\leq \bar{d}_{Ag} \leq$ 6.3 nm. Moreover, the specific activities were similar in magnitude and exhibit no clear trend with particle size. Consequently, the hydrogenation of crotonaldehyde over these Ag/SiO_2 catalysts appears to be structure-insensitive. Titania supported silver catalysts reduced in hydrogen at low temperature (473 K, LTR) or high temperature (773 K, HTR), showed a quite different behavior. These silver particles exhibit rather narrow size distributions and very low mean particle sizes ($\bar{d}_{Ag}$ = 2.8 $\pm$ 1.9 nm for Ag/TiO_2-LTR, $\bar{d}_{Ag}$ = 1.4 $\pm$ 0.5 nm for Ag/TiO_2-HTR), i.e. an exceedingly high dispersion (D_{Ag} = 0.46 and 0.69, respectively). The LTR catalyst gave a higher selectivity to crotyl alcohol (53 %) than the ultradispersed HTR catalyst (28 %). This pronounced change in selectivity suggests the hydrogenation of crotonaldehyde over these Ag catalysts to be qualified as structure-sensitive with the rate determining step depending critically on the silver particle size and thus on the silver surface structure, investigated with conventional (CTEM) and high-resolution transmission electron microscopy (HRTEM). If hydrogenation of the C=O group of the α,β-unsaturated aldehyde is favored by face atoms, most likely the increased fraction of Ag (111) planes of the larger silver particles will give higher formation rates of the desired unsaturated alcohol. The nanostructural features of the catalysts, as their silver particle size distribution, mean particle size and dispersion was found to be dependent markedly on the preparation method. The application of sol-gel technique and impregnation as preparation methods followed by appropriate methods of pretreatment gave well dispersed silver catalysts [144].

Even more impressing than the successful use of monometallic Ag catalysts is the fact that monometallic Au catalysts are also able to produce the allylic alcohols. The use of gold in catalysis is a relatively new field and has attracted much interest in recent time. For long time gold has been considered as poorly active, because of its d^{10} configuration and the fact, that pure gold surfaces do not adsorb oxygen, hydrogen or carbon monoxid. This had to be revised when Haruta et al. found that gold is nevertheless able to activate these substrates if it is well

dispersed in ultrafine nanoparticles on appropriate supports [145]. Small supported gold particles were successfully used as oxidation catalysts, especially for the low temperature oxidation of carbon monoxide [146-148], but they are also useful in hydrogenation reactions. Using titania or zirconia supported Au catalysts, with gold particles in the range of 1-5 nm prepared by various preparation techniques in the hydrogenation of acrolein these catalysts show considerable selectivities to the allylic alcohol up to 43 % (conversions < 10%). As before for the Ag catalysts, it was concluded, that the adsorption of the CO group is favored by face atoms, so that the increased fraction of dense (111) planes of the larger gold particles will give higher formation rates of allylic alcohol. For extremely small gold particles paramagnetic F-centers (trapped electrons in oxygen vacancies) of the support were observed. Structural analysis point that the influence of small gold particles on the intramolecular selectivity of the hydrogenation of conjugated functional groups originates from active sites comprising paramagnetic F-centers of strong one-electron donating character and electron-rich particles. The origin of the antiphatetic structure sensitivity of the hydrogenation of the C=O vs C=C group may be attributed to quantum size effects which alter the electronic properties of sufficiently small gold particles [149]. In contrast, no crotyl alcohol was detected by Hutchings et al. [150] during crotonaldehyde hydrogenation over Au/SiO_2 at 523 K where the saturated aldehyde was the main product (selectivity > 97 %) and the conversion increased from 11 % to 22 % during time on stream of 180 min. Improved crotyl alcohol selectivities were achieved with Au/ZnO (52 % at 9 % conversion) and Au/ZrO_2 (38 % at 12 % conversion) at 527 K (Au loading: 5 %). By comparison with Au/ZnO and Au/ZrO_2, these authors concluded, that interfacial sites, responsible for C=O group adsorption, were absent in the case of SiO_2 and the adjacent large gold particles. Furthermore, they reported that the crotyl alcohol selectivity further increased by addition of a sulfur-containing compound.

4. Industrial Applications of Selective Hydrogenation of Multiply Unsaturated Organic Compounds

Selective hydrogenation processes of unsaturated hydrocarbons are widely used in the Downstream Treatment of Naphta Cracking. Many alternative processes have been developed depending on the specific fractionation concepts of the reaction product of naphtha cracking. A comprehensive review on hydrotreatment has been presented by Derrien [1]. Contributions published by experts of IFP [151], BASF [31], Hüls [32], CDTECH [152] and KataLeuna Catalysts [2] give excellent information about new processes and trends and selected processes are given which are mainly focussed on C_2H_2 hydrogenation [12].

The selective hydrogenation of the C_3 fraction with the aim to remove propyne and propadiene can be performed as a gas or liquid phase process. The latter is preferred because of the dissolution of oligomers formed during the hydrogenation. The average alkyne and diene content of a typical C_3 fraction is roughly 4 vol%. Therefore, the two-phase hydrogenation is preferably carried out in a tubular reactor under approximately isothermal conditions. Cooling is performed with boiling ammonia or propene. A well known process of this type is the Bayer cold-hydrogenation process [34]. Similar processes have been developed by IFP and BASF. The diene and alkyne content is reduced to below 10 ppm with a se-

lectivity towards propene of about 80 % [1,27]. At an effluent specification of 10 ppm diene and alkyne, employment of a metal-promoted Pd catalyst gives a 1 % higher propene yield than that obtained with an unpromoted Pd catalyst [151,153]. For achieving high alkene selectivities it is important to ensure a homogeneous wetting of the catalyst pellets. Insufficient wetting causes a partial interruption of mass transfer which favors overhydrogenation. An efficient design to assure a uniform gas-liquid distribution is crucial for both types of two-phase reactors, the isothermal tubular reactor and the adiabatic reactor.

The raffinate of the butadiene extraction process still contains up to 1 % of residual butadiene. Several processes are available to reduce this content to below 10 ppm by selective hydrogenation. For example, the SHP process developed by Hüls AG [32] consists of one adiabatic reactor operated at about 303 K. Since the required hydrogen is completely dissolved, it is an exclusively liquid phase reactor avoiding the problems concerning liquid-gas distribution and wetting of the catalyst pellets as discussed above. In order to suppress readsorption of butenes, which would lead to consecutive hydrogenation and isomerisation of 1-butene, a few ppm of carbon monoxide are added to the feed gas.

The selective hydrogenation of the crude C_4 cut, containing up to 65 % butadiene [31], is performed in a series of adiabatic trickle-bed reactors. For the removal of the large reaction heat the bulk of the product leaving the first stage is pumped through a heat exchanger and recycled to the reactor inlet. The temperature increase between reactor inlet and outlet is determined by the recycle ratio and the reaction rate which is controlled by the hydrogen pressure. The adiabatic temperature increase of a butadiene-butene mixture corresponding to 1 % butadiene conversion is approximately 10 K, so that for conversion of butadiene from 65% to 5% and a recycle ratio of 10, a temperature increase of 60 K results. The number of reactors in series, the value of the recycle ratio, the space velocity and the hydrogen pressure depend on the butadiene content of the feedstock and the product specifications required. Another possibility is the reduction of the butadiene content in one or two stages to about 1% followed by the liquid phase process with dissolved hydrogen as mentioned above [32] for a final reduction down to 10 ppm.

Although the selective hydrogenation of α,β-unsaturated aldehydes to unsaturated allylic alcohols is of great synthetic and industrial interest, at this moment an industrial application for a direct (one-step) heterogeneously catalyzed process does not exist. Acrolein which is produced during the propylene oxide process of ARCO Chemical Technology is hydrogenated to allyl alcohol over copper-cadmium catalysts with selectivities around 70 % [154]. To substitute cadmium based catalysts, the authors group developed bimetallic silver-indium catalysts for the selective hydrogenation of acrolein in the gas phase and the liquid phase which produced allyl alcohol with selectivities up to 74 % at nearly complete acrolein conversion [155,156].

However, applying the concept of biphasic catalysis on hydrogenation of α,β-unsaturated aldehydes to allylic alcohols, industrial important yields up to 99 % can be obtained, as shown for the hydrogenation of prenal (3-methyl-2-butenal) to prenol (3-methyl-2-buten-1-ol) [157,158]. Joo et al. [159] demonstrated the effects of pH on the molecular distribution of water soluble ruthenium (II) hydrides and its consequences on the intramolecular selectivity.

Heterogeneously catalyzed hydrogenations are also widely used for the preparation of many synthetically useful organic compounds. Although not the aim of this review, it should be however mentioned here that one of the main goals of

research on this field is the development of enantioselective heterogeneous catalysts. Platinum catalysts which have been modified with chinchonia alkaloid are very effective to hydrogenate a-ketoesters with high enantiomeric excess (95 %) [160,161].

References

1.   M.L. Derrien: Stud Surf. Sci Catal. **27**, 613 (1986)
2.   H.D. Neubauer, A. Heilmann, J. Kötter, R. Schubert, Selective Hydrogenations and Dehydrogenations (Eds: M. Baerns and J. Weitkamp), Kassel, Germany, 1993, p. 67-74.
3.   Süd-Chemie: private communication
4.   H.-J. Freund: Angew. Chem. Int. Ed. Engl. 36, 452 (1997)
5.   G. Webb: Ph.D. Thesis, University of Hull, England (1963)
6.   G.C. Bond, G. Webb, P.B. Wells, J.M. Winterbottom: J. Chem. Soc. 3218 (1965)
7.   J.P. Boitiaux, J. Cosyns, E. Robert: Appl. Catal. 32, 145 (1987)
8.   J.P. Boitiaux, J. Cosyns, E. Robert: Appl. Catal. 35, 193 (1987)
9.   R.L. Augustine, F. Yaghmaie, J.F. Van Peppen: J. Org. Chem. 49, 1865 (1984)
10. F.G. Gault, J. J. Rooney, C. Kernball: J. Catal. 1, 255 (1962)
11. G.C. Bond, P.B. Wells: Adv. Catal. 15, 91 (1964)
12. H. Arnold, F. Döbert, J. Gaube: in Handbook of Heterogeneous Catalysis, G. Ertl, H. Knözinger, J. Weitkamp (Eds.) (Wiley-VCH, Weinheim, Germany), Vol. 5, 1997, pp. 2165-2186
13. A.J. Bates, Z.K. Leszcynski, J.J. Phillipson, P.B. Wells, G.R. Wilson: J. Chem. Soc. A (London) 2435 (1970)
14. Ch. Elsner, B.M. Stein, unpublished results
15. G.C. Bond, J. Sheridan: Trans. Faraday Soc. 48, 651 (1952)
16. G.C. Bond: Trans. Faraday Soc. 52, 1235 (1956)
17. B. Tardy, C. Noupa, C. Leclercq, J.C. Bertolini, A. Hoareau, M. Treilleux, J.P. Faure, G. Nihoul: J. Catal. 129, 1 (1991)
18. C. Weimer, D. Reinig, S. Göbel, H. Arnold, J. Gaube: in Selective Hydrogenations and Dehydrogenations, M. Baerns, J. Weitkamp (Eds.), Kassel, Germany, 1993, pp. 131-138.
19. J.J. Phillipson, P.B. Wells, G.R. Wilson: J. Chem. Soc. A (London) 1351 (1969)
20. J.A. Dumesic, D.F. Rudd, L.M. Aparicio, J.E. Rekoske, A.A. Trevino: The Microkinetics of Heterogeneous Catalysis, (ACS Professional Reference Book, American Chemical Society, Washington, DC 1993), Chapt. 5, p. 113
21. S.D. Lin, M.A. Vannice: J. Catal. 143, 563 (1993)
22. G.H. Kohlmaier, B.S. Rabinovitch: J. Chem. Phys. 38, 1692 (1963)
23. Th. Mull, B. Baumeister, M. Menges, et al.: J. Chem. Phys. 96, 7108 (1992)
24. J. Heidberg, U. Noseck, M. Suhren, H. Weiss: Discuss. Meeting of the Deutsche Bunsengesellschaft, Lahnstein, Germany, 1992
25. E.W. Thiele: Ind. Eng. Chem. 31, 916 (1939)
26. A. Wheeler: Adv. Catal. 3, 249 (1951)
27. T. Haas, C. Otto, J. Gaube, Dechema Monographie Katalyse, Frankfurt, Germany, 1989, 118, pp. 205-220
28. T. Haas, J. Gaube: Chem. Eng. Technol. 12, 45 (1989)
29. D. Reinig, D. Hönicke, J. Gaube: Chem.-Ing.-Tech. 63, 839 (1991)

30. D. Reinig: Ph.D. Thesis, TH Darmstadt, Germany (1992)
31. H.M. Allmann, Ch. Herlon, P. Polanek in Selective Hydrogenations and Dehydrogenations, M. Baerns, J. Weitkamp (Eds.), Kassel, Germany, 1993, pp. 1-17.
32. K.H. Walter, W. Droste, D. Maschmeyer, F. Nierlich in Selective Hydrogenations and Dehydrogenations (Eds: M. Baerns, J. Weitkamp), Kassel, Germany, 1993, pp. 31-48.
33. C. Otto, J. Gaube: Chem. Ing. Tech. 61, 644 (1989)
34. H. Lauer: Erdöl, Kohle-Erdgas-Petrochem. 6, 249 (1983)
35. N. Wuchter: Ph.D. Thesis, TU Darmstadt, Germany (2000)
36. E.F. Meyer, R.L. Burwell: J. Am. Chem. Soc. 85, 2881 (1963)
37. J.P. Boitiaux, J. Cosyns, S. Vasudevan: Appl. Catal. 6, 41 (1983)
38. J.M. Winterbottom: in Catal. and Chem. Proc., R. Pearce, W. R. Patterson (Eds.), (Wiley, New York, 1981) p. 304
39. G.C. Bond: J. Mol. Catal. A. 118, 333 (1997)
40. M.J. Ledoux, F.G. Gault: J. Chem. Soc. Farad. Trans. I 74, 2652 (1978)
41. P.S. Cremer, X. Su, Y.R. Shen, G.A. Somorjai: J. Am. Chem. Soc. 118, 2942 (1996)
42. G.A. Somorjai, G. Rupprechter: J. Phys. Chem. B 103, 1623 (1999)
43. T.P. Beebe, J.T. Yates: J. Am. Chem. Soc. 108, 663 (1986)
44. T.P. Beebe, M.R. Albert, J.T. Yates: J. Catal. 96, 1 (1985)
45. M. Neurock, V. Pallassana, R.A. van Santen: J. Am. Chem. Soc. 122, 1150 (2000)
46. F. Hartog, P. Zwietering, J. Catal. 2, 79 (1963)
47. F. Hartog, J.H. Tebben, C.A.M. Weterings: Proceedings of the 3rd International Congress on Catalysis, W.M.H. Sachtler, G.C.A. Schuit, P. Zwietering (Eds.), Amsterdam, 1964, Vol. II, pp. 1210-1224.
48. F. Hartog: US Patent 3391206 (1968)
49. W. C. Drinkard: Ger. Patent 2221137 (1972)
50. M.M. Johnson, G.P. Nowack: US Patent 3793383 (1974)
51. S. Niwa, J. Imamura, F. Mizukami, K. Shimizu, Y. Orito: US Patent 4495373 (1985)
52. H. Ichihashi, H. Yoshioka: Eur. Patent 214530 (1987)
53. O. Mitsui, Y. Fukuoka: US Patent 6678861 (1987)
54. H. Nagahara, M. Konishi: Eur. Patent 220525 (1987)
55. F. Matsunaga, F. Fukuhara, Y. Mitsuki: Eur. Patent 316142 (1987)
56. F. Fukuhara, F. Matsunaga, Y. Nakashima: Eur. Patent 323192 (1989)
57. R. Fischer, R. Dostalek, L. Marosi: Eur. Patent 554765 (1993)
58. K. Yamashita, H. Obana, I. Katsuta: Eur. Patent 552809 (1993)
59. M.A. Richard, C.J. de Deken, D.K. Yee: PCT WO 931 16971 (1993)
60. Y. Fukuoka, H. Nagahara, M. Konishi: Shokubai 35, 34 (1993)
61. S. Niwa, F. Mizukami, S. Isoyama, T. Tsuchiya, K. Shimizu, S. Imai, J. Imamura: J. Chem. Tech. Biotechnol. 36, 236 (1986)
62. F. Mizukami, S. Niwa, M. Toba, T. Tsuchiya, K. Shimizu, J. Imamura: Stud. Surf. Sci. Catal. 31, 45 (1987)
63. F. Mizukami, S. Niwa, S. Ohkawa, A. Katayama: Stud. Surf. Sci. Catal. 78, 337 (1993)
64. J. Struijk, R. Moene, T. van der Kamp, J.J.F. Scholten: Appl. Catal. A 89, 77 (1992)
65. C.U.I. Odenbrand, S.T. Lundin: J. Chem. Tech. Biotechnol. 30, 677 (1980)
66. J. Struijk, M. d'Angremond, W.J.M. Lucas-de Regt, J.J.F. Scholten: Appl. Catal. 83, 263 (1992)
67. S. Niwa, F. Mizukami, J. Imamura, K. Itabashi: Sekiyu Gakkaishi 32, 299 (1989)
68. H. Nagahara: Hyomen 30, 951 (1992)
69. J. Horiuti, M. Polanyi: Trans. Faraday Soc. 30, 1164 (1934)

70. Y. Fukuoka, M. Kono, H. Nagahara, M. Ono: J. Chem. Soc. Jpn. 11, 1223 (1990)
71. F. Döbert, J. Gaube: Catal. Lett. 31, 437 (1995)
72. K. Yamashita, H. Obana, I. Katsuta: Eur. Patent 552809 (1993)
73. T. Gescheitle: Ph.D. Thesis, TU Darmstadt, Germany (1998)
74. J. Petzloff, J. Gaube: Chem.-Ing.-Technol. 8, 21, 651 (1998)
75. P. Gallezot, D. Richard: Catal. Rev.-Sci. Eng. 40, 81 (1998)
76. P. Claus: in Topics in Catalysis, G.A. Somorjai, J.M. Thomas, (Eds.) Special Issue Fine Chemicals Catalysis, Part II; D. Blackmond, W. Leitner, (Eds.) (Baltzer Science Publishers: Bussum, The Netherlands, 1998) 5, p. 51
77. M.A. Vannice, B. Sen: J. Catal. 115, 65 (1989)
78. P. Gallezot, A. Giroir-Fendler, D. Richard: Catal. Lett. 5, 169 (1990)
79. P. Gallezot, B. Blanc, D. Barthomeuf, M.I. Pais da Silva: in Stud. Surf. Sci. Catal., Vol. 84, Zeolithes and Related Microporous Materials: State of the Art 1994, J. Weitkamp, H.G. Karge, H. Pfeifer, W. Hölderich (Eds.) (Elsevier, Amsterdam, 1994) p. 1433
80. H. Yoshitake, Y. Iwasawa: J. Catal. 125, 227 (1990)
81. P. Claus: in Catalysis of Organic Reactions. Chemical Industries Series, Vol. 68, R.E. Malz (Ed.) (Marcel Dekker, New York, 1996) p. 419.
82. C. Ando, H. Kurokawa, H. Miura: Appl. Catal. A 185, L181 (1999)
83. U. K. Singh, M. A. Vannice, J. Catal. 199, 73 (2001)
84. Y. Nitta, Y. Hiramatsu, T. Imanaka: Chem. Express 4, 281 (1989)
85. Y. Nitta, K. Ueno, T. Imanaka: Appl. Catal. 56, 9 (1989)
86. Y. Nitta, Y. Hiramatsu, T. Imanaka: J. Catal. 126, 235 (1990)
87. A. Giroir-Fendler, P. Gallezot, D. Richard: Catal. Lett. 5, 175 (1990)
88. S. Galvagno, G. Capannelli, G. Neri, A. Donato, R. Pietropaolo: J. Mol. Catal. 64, 237 (1991)
89. C. Minot, P. Gallezot: J. Catal. 123, 341 (1990)
90. D. Richard, P. Fouilloux, P. Gallezot: in Proc. 9th Int. Congr. Catal., Vol. 3, Characterization and Metal Catalysts, M.J. Phillips, M. Ternan (Eds.), Calgary, 1988, p. 1074
91. S. Galvagno, C. Milone, A. Donato, G. Neri, R. Pietropaolo: Catal. Lett. 18, 349 (1993)
92. S. Galvagno, C. Milone, G. Neri, A. Donato, R. Pietropaolo: in Heterogeneous Catalysis and Fine Chemicals, M. Guisnet, J. Barbier, J. Baurrault, C. Bouchoule, D. Duprez, G. Pérot, C. Montassier (Eds.), Elsevier, Amsterdam, 1993; Vol. 78, p. 163
93. B. Coq, F. Figueras, P. Geneste, C. Moreau, P. Moreau, M. Warawdekar: J. Mol. Catal. 78, 211 (1993)
94. M. Englisch, A. Jentys, J.A. Lercher: J. Catal. 166, 25 (1997)
95. F. Delbecq, P. Sautet: J. Catal. 152, 217 (1995)
96. Y. Berthier, C.M. Pradier: Bull. Soc. Chim. Fr. 134, 773 (1997)
97. T. Birchem, C.M. Pradier, Y. Berthier, G. Cordier: J. Catal. 146, 503 (1994)
98. C.M. Pradier, T. Birchem, Y. Berthier, G. Cordier: Catal. Lett. 29, 371 (1994)
99. T. Birchem, C.M. Pradier, Y. Berthier, G. Cordier: J. Catal. 161, 68 (1996)
100. A. Guerreo-Ruiz, Y. Zhang, B. Bachiller-Baeza, I. Rodriguez-Ramos: Catal. Lett. 55, 165 (1998)
101. S.J. Tauster, S.C. Fung, R.L. Garten: J. Am. Chem. Soc. 100, 170 (1978)
102. H. Yoshitake, K. Asahma, Y. Iwasawa: J. Chem. Soc. Farad. Trans. 85, 2021 (1989)
103. H. Yoshitake, Y. Iwasawa: J. Catal. 125, 227 (1990)
104. J. Simoník, L. Beránek: Coll. Czechoslov. Chem. Commun. 37, 353 (1972)
105. P. Claus, D. Selent: Chem.-Ing.-Techn. 67, 586 (1995)

106. C.G. Raab, J.A. Lercher: Catal. Lett. 18, 99 (1993)

107. J. Kaspar, M. Graziani, G.P. Escobar, A. Trovarelli: J. Mol. Catal. 72, 243 (1992)

108. P. Claus, S. Schimpf, R. Schödel, P. Kraak, W. Mörke, D. Hönicke: Appl. Catal. 165, 429 (1997)

109. M. Abid, R. Touroude: Catal. Lett. 69, 139 (2000)

110. A. Sepulvedo-Escribano, F. Coloma, F. Rodriguez-Reinoso, J. Catal. 178, 649 (1998)

111. M. Consonni, D. Jokic, D. Yu Murzin, R. Touroude: J. Catal. 188, 165 (1999)

112. S. Galvagno, A. Donato, G. Neri, R. Pietropaolo, D. Pietropaolo: J. Mol. Catal. 49, 223 (1989)

113. S. Galvagno, A. Donato, G. Neri, R. Pietropaolo: Catal. Lett. 8, 9 (1991)

114. Z. Poltarzewski, S. Galvagno, R. Pietropaolo, P. Staiti: J. Catal. 102, 190 (1986)

115. E. Tronconi, C. Crisafulli, S. Galvagno, A. Donato, G. Neri, R. Pietropaolo: Ind. Eng. Chem. Res. 29, 1766 (1990)

116. W.F. Tuley, R. Adams: J. Am. Chem. Soc. 47, 3061 (1925)

117. D. Richard, J. Ockelford, A. Girior-Fendler, P. Gallezot: Catal. Lett. 3, 53 (1989)

118. B. Moraweck, P. Bondot, D. Goupil, P. Fouilloux, A.J. Renouprez: J. de Phys., C8, 48, 297 (1987)

119. P. Claus: Chem.-Ing.-Techn. 67, 1340 (1995)

120. B. Didillon, A. El Mansour, J.P. Candy, J.P. Bournonville, J.M. Basett: in Stud. Surf. Sci. Catal., Vol. 59: Heterogeneous Catalysis and Fine Chemicals II, M. Guisnet, J. Barrault, C. Bouchoule, D. Duprez, G. Pérot, R. Maurel, C. Montassier (Eds.) (Elsevier, Amsterdam, 1991) p. 137

121. B. Didillon, J.P. Candy, F. Le Peletier, O.A. Ferretti, J.M. Basett: in Stud. Surf. Sci. Catal., Vol. 78: Heterogeneous Catalysis and Fine Chemicals III, M. Guisnet, J. Barbier, J. Barrault, C. Bouchoule, D. Duprez, G. Pérot, C. Montassier (Eds.) (Elsevier, Amsterdam, 1993) p. 147

122. J.P. Candy, B. Didillon, E.L. Smith, T.B. Shay, J.-M. Basset: J. Mol. Catal. 86, 179 (1994)

123. S. Recchia, C. Dossi, N. Picoli, A. Fusi, L. Sordelli, R. Psaro: J. Catal. 184, 1 (1999)

124. P. Claus, D. Hönicke: in Catalysis of Organic Reactions, Chemical Industries Series, Vol. 62, M. G. Scaros, M. L. Prunier (Eds.) (Marcel Dekker, New York, 1995) p. 431

125. P.A. Crozier, P. Claus, in: Proc. Microscopy, Microanalysis, eds G.W. Bailey, J.M. Corbett, R.V.M. Dimlich, J.R. Michael, N.J. Zaluzec (Microscopy Society of America, San Francisco Press, 1996) p. 224

126. A. Jentys, B.J. McHugh, G.L. Haller, J.A. Lercher: J. Phys. Chem. 96, 1324 (1992)

127. G. F. Santori, M. L. Casella, G. J. Siri, H. R. Aduriz, O. F. Ferretti: Appl. Catal. A 197, 141 (2000)

128. J. L. Margitfalvi, Gy. Vanko, I. Borbath, A. Tompos, A. Vertes: J. Catal. 190, 474 (2000)

129. J. L. Margitfalvi, I. Borbath, E. Tfirst, A. Tompos: Catal. Today 43, 29 (1998)

130. J. L. Margitfalvi, I. Borbath, M. Hegedüs, S. Göbölös, F. Lonyi: React. Kinet. Catal. Lett. 68, 133 (1999)

131. H. Berndt, H. Mehner, P. Claus: Chem.-Ing.-Techn. 67, 1332 (1995)

132. F. Coloma, J. Llorca, N. Homs, P. Ramirez de la Piscina, F. Rodriguez-Reinoso, A. Sepulveda-Escribano: Phys. Chem. Chem. Phys. 2, 3063 (2000)

133. S. Nishiyama, T. Hara, S. Tsuruya, M. Mitsai, J. Phys. Chem. B: 103, 4431 (1999)

134. F. Humblot, D. Didillon, F. Lepeltier, J. P. Candy, J. Corker, O. Clause, F. Bayard, J. M. Basset: J. Amer. Chem. Soc. 120, 137 (1998)

135. A. Jentys, M. Englisch, G.L. Haller, J.A. Lercher: Catal. Lett. 21, 303 (1993)

136. N. F. Brown, M. A. Barteau: J. Am. Chem. Soc. 114, 4258 (1992)

137. F. Delbecq, P. Sautet: J. Catal. 152, 217 (1995)
138. P. Claus, P. Kraak, R. Schödel: in Studies in Surface Science and Catalysis, Vol. 108, Heterogeneous Catalysis and Fine Chemicals IV, H.U. Blaser, A. Baiker, R. Prins (Eds.) (Elsevier, Amsterdam, 1997) p. 281
139. A. Jentys, M. Englisch, G.L. Haller, J.A. Lercher: Catal. Lett. 21, 303 (1993)
140. N. F. Brown, M. A. Barteau: J. Am. Chem. Soc. 114, 4258 (1992)
141. F. Delbecq, P. Sautet: J. Catal. 152, 217 (1995)
142. R. Touroude: J. Catal. 65, 110 (1980)
143. M.A. Vannice: Catal. Today 12, 255 (1992)
144. P. Claus, H. Hofmeister: J. Phys. Chem. B. 103, 2766 (1999)
145. M. Haruta, N. Yamada, T. Kobayashi, S. Iijima: J. Catal. 115, 301 (1989)
146. M. Haruta: Catal. Today 36, 153 (1997)
147. J.D. Grunwaldt, M. Maciejewski. O.S. Becker, P. Fabriziolo, A. Baiker: J. Catal. 186, 458 (1999)
148. L. Guczi, D. Horváth, Z. Pászti, L. Tóth, T.E. Horváth, A. Karacs, G. Peto: J. Phys. Chem. B 104, 3183 (2000)
149. P. Claus, A. Brückner, C. Mohr, H. Hofmeister: J. Am. Chem. Soc. 122, 11430 (2000)
150. J. E. Bailie, G. J. Hutchings: Chem. Commun. 2151 (1999)
151. J.P. Boitiaux, C.J. Cameron, J. Cosyns, F. Eschard, P. Sarrazin: in Selective Hydrogenations and Dehydrogenations, M. Baerns, J. Weitkamp (Eds.), Kassel, Germany, 1993, p. 49-57
152. G. Gildert, R. Barchas: in Selective Hydrogenations and Dehydrogenations, M. Baems, J. Weitkamp (Eds.), Kassel, Germany, 1993, p. 59-66
153. J.P. Boitiaux, J. Cosyns, M. Derrein, G. Leger: Hydrocarbon Processing, 64, 51 (1985)
154. R. A. Grey: US Patent 5892066 (1997)
155. P. Birke, P. Claus, R. Geyer, P. Kraak, M. Lucas, R. Schödel: Patent DE 198 19 396 A1 (1998)
156. P. Claus, M. Lucas: 5th European Congress on Catalysis, Symposium 19 "Catalysis by silver and gold", Limerick, 02-07 Sept. 2001, subm.
157. J. M. Grosselin, C. Mercier, G. Allmang, F. Grass, Organometallics, 10, 2126 (1991)
158. Applied Homogeneous Catalysis by Organometallic Complexes. (Eds. B. Cornils, W. A. Herrmann) (VCH Weinheim 1996)
159. F. Joo, J. Kovacs, A. Cs. Benyei, A. Katho: Catal. Today 42, 441 (1998)
160. H. U. Blaser: Catal. Today 37, 437 (1997)
161. T. Mallat, A. Baiker: Appl. Catal. A 3, 200 (2000)

Catalytic Reforming

Contents

Catalytic Reforming

Torbjørn Gjervan[1], Rune Prestvik[2], and Anders Holmen[1]

[1] Department of Chemical Engineering, Norwegian University of Science and Technology (NTNU), N-7491 Trondheim, Norway
Holmen@chembio.ntnu.no
[2] SINTEF Applied Chemistry, N-7465 Trondheim, Norway

Abstract. Catalytic reforming is an important refinery process for the production of high-octane gasoline, hydrogen, and aromatics from naphtha. The most important reactions occurring are dehydrogenation of naphthenes, dehydrocyclisation of paraffins, isomerisation, and dehydroisomerisation. In addition, the process suffers from catalyst deactivation by coking. The catalyst employed in reforming is bifunctional in nature consisting of a noble metal supported on alumina. Hydrogenation/Dehydrogenation reactions are catalysed by the noble metal, e.g. platinum. Isomerisation reactions are catalysed by the support, which is acidic in nature. The alumina supported platinum catalyst has been used for decades but has been improved by the addition of a second element such as rhenium, tin or iridium. The chemical state of the second element and the exact role of the element in bringing about higher stability in catalytic reforming have been intensively studied for many years. Due to environmental concerns the aromatic content of gasoline will have to be reduced. In addition, the possible introduction of hydrogen as an alternative motor vehicle fuel may seriously threaten the role of catalytic reforming in the future.

1   Introduction

Catalytic reforming is an important process in today's refineries and is one of the largest users of catalysts in the chemical industry. According to the International Petroleum Encyclopedia (1999) [1] there are 755 catalytic reforming plants world-wide with a total capacity of more than 11 million barrels per calendar day. The reforming process involves the reconstruction of low-octane hydrocarbons boiling in the gasoline range into more valuable high-octane gasoline components, such as aromatics and highly branched paraffins, without significantly changing their carbon numbers. Catalytic reforming is a major refining process due to the large and still increasing demand for motor fuel, and for high-value aromatic hydro-carbons such as benzene, toluene and xylenes (BTX) being important building blocks of the petrochemical industry.

Figure 1.1 illustrates how the catalytic reforming unit is integrated in a typical motor fuels refinery. Feedstocks are hydrodesulphurised straight-run heavy naphthas and cracker naphthas. The liquid C_{5+} product (reformate) from the reformer typically account for 30-50% by volume of the total gasoline pool [2]. The reformate is blended with other available refinery streams such as isomerate (branched paraffins), naphtha from catalytic cracking, coking, and visbreaking (rich in olefins and aromatics), alkylate (highly branched paraffins), and straight run naphtha in order to obtain the desired gasoline properties. Tetraethyl lead are

still being added as an octane booster to the gasoline in some countries, but are most likely to be phased out globally due to strong environmental concerns and the introduction of car exhaust catalysts that are poisoned by lead. It is expected that 84% of all gasoline sold in the world will be unleaded in 2005 [3]. MTBE has been used in gasoline to replace lead and aromatics as octane-boosting components and to increase the content of oxygen in reformulated gasoline, but due to concerns about MTBE contamination in groundwater the use of this additive has become very controversial. Small amounts (ca 1%) of other additives are put in to protect against engine corrosion, condensation (water) and deposition of coke.
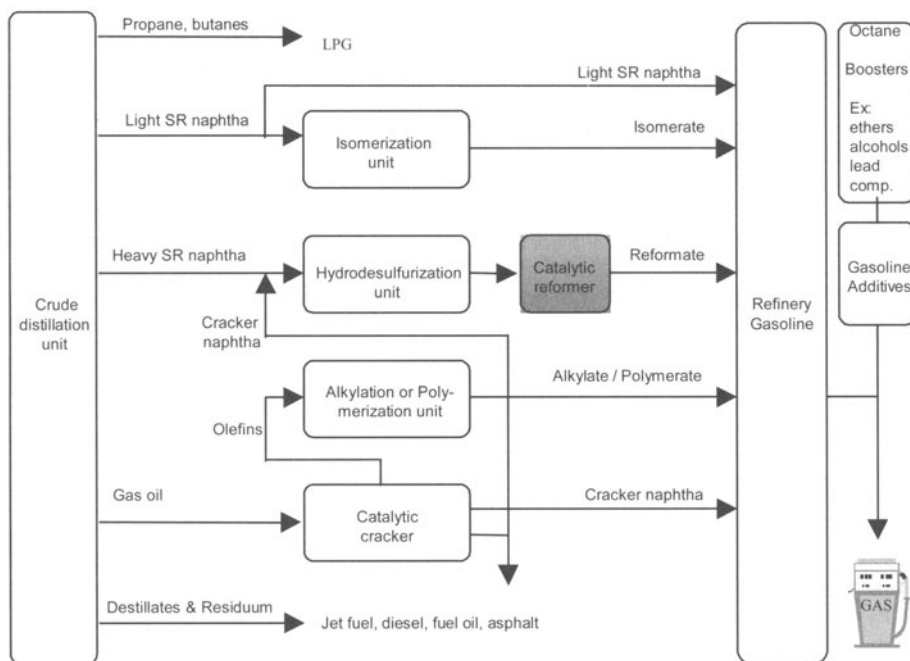
Fig. 1.1. Example of a processing scheme for refinery gasoline production with catalytic reforming. SR = Straight-Run

Hydrogen is an important product from the reforming process and it is usually the main hydrogen source for hydroprocessing, such as hydrodesulphurization and hydrodenitrification, demetallation and aromatic saturation. The hydrogen yield is typically in the range of 1-5 wt%. The unwanted light paraffins that are also formed in the reaction (5-20 wt% yield) are normally used as fuel gas (C_1-C_2) and liquefied petroleum gas (C_3-C_4). The butanes may also be mixed into the gasoline pool to increase volatility.

1.2   Fundamentals

1.2.1   Feedstocks / Octane Ratings

The feedstocks for reforming are characterized by their distillation range, their hydrocarbon composition and a number of overall properties (density, molecular weight, octane number), as well as the concentrations of sulphur and nitrogen. The reformer feed properties vary depending on the type of crude, the initial and end point distillation cuts and the amount of the feedstock originating from heavier parts of the crude. A normal feedstock contains 40-70% paraffins, 20-50% naphthenes, 5-20% aromatics and 0-2% olefins and the density is in the range of 0.68-0.76 g/ml. The amount of sulphur and nitrogen has been reduced to ppm levels by hydrotreating in order not to poison the reforming catalyst (and the car exhaust catalyst). Olefins, most of that are present in the cracker naphtha, will be hydrogenated as well. The distillation range is usually cut between C_6 and C_7 in the light end because the C_6 fraction partly will crack to gases and partly form unwanted benzene (in a fuels refinery). In addition the C_6 naphthenes have a higher octane number than their dehydrogenated products as shown in Table 1.1. The light fraction of the naphtha is instead usually upgraded by isomerisation. As the reforming catalyst is more subjected to coke formation using heavier hydrocarbons, the end boiling point is also limited normally up to 150-180°C. For a refinery in BTX operation the preferred naphtha feedstock is narrowed to a pure C_6-C_8 cut.

The purpose of catalytic reforming is to increase the octane number of the feedstock up to a level that makes it suitable as an automotive fuel. Taking the gasoline specifications and the available blending stocks into account an octane number for reformate of 95-102 is usually needed. The octane number represents the ability of a gasoline to resist detonation or knocking during combustion of the compressed air/gasoline mixture in the engine cylinder. The higher the octane number, the less is the tendency for knocking - which strongly limits the efficiency of the automobile engine. In practice two ratings are usually measured and are designated Research Octane Number (RON) and Motor Octane Number (MON) and differ only in the type of engine and test procedure used. RON represents the engine performance at low speed while MON is representative for high speed driving. The octane number displayed on the pumps at service stations is usually either the RON value or an average octane value ½ (RON + MON). In the literature usually RON is used if nothing else is stated. By definition the octane number of n-heptane is zero and the octane number of iso-octane (2,2,4-trimethylpentane) is 100. The octane number for a gasoline is defined as the volume percent of iso-octane in blending with n-heptane that equals the knocking performance of the gasoline being tested. Some gasoline components have octane numbers exceeding 100 and have to be characterized by use of mixtures. A usual mixture contains 20% of the actual compound and 80% of an n-heptane/iso-octane (40:60) mixture. A hypothetical "blending octane number" is then obtained by extrapolating from 20 to 100 % concentration. The blending octane number is specific for the mixture and usually different from the octane number of the pure component as seen for a range of different hydrocarbons with octane numbers < 100 in Table 1.1.

Table 1.1 Research octane numbers for a range of pure hydrocarbons and in blending [4].

Hydrocarbon	Research Octane Number Pure	Research Octane Number Blending
Paraffins		
n-Butane	94	113
Isobutane	>100	122
n-Pentane	62	62
2-Methylbutane	92	100
n-Hexane	25	19
2-Methylpentane	73	82
n-Heptane	0	0
3-Methylhexane	52	56
n-Octane	<0	-18
n-Nonane	<0	-18
Naphtenes		
Methylcyclopentane	91	107
Ethylcyclopentane	67	74
Cyclohexane	83	110
Aromatics		
Benzene	-	98
Toluene	>100	124
1,2-Dimethylbenzene	-	120
1,3-Dimethylbenzene	>100	145
1,4-Dimethylbenzene	>100	146

Table 1.1 shows that aromatics generally have much higher octane numbers than naphthenes, olefins, and paraffins and are therefore the most desired products. The octane number of the aromatics (except for benzene) is always above 100. Straight chain paraffins have very low octane numbers (RON < 0 for n-octane and n-nonane), but the octane number increases markedly with the degree of branching (RON > 100 for 2,2,3-trimethylbutane). The octane number of the paraffins declines as the number of carbon atoms increases and is very low for paraffins with more than seven carbon atoms. Unsaturation (paraffins to olefins) also result in an octane enhancement. Branching does not positively influence naphthenic hydrocarbons and their octane values are in average not very high. The above comparison show that the desired products for obtaining high octane numbers are aromatics and highly branched paraffins or olefins, although the latter group is not formed in the reformer due to thermodynamic limitations. An increase in the octane number can therefore best be obtained by transformation of naphthenes into aromatics and of linear paraffins into branched paraffins - or even better into aromatics.

1.2.2   Reactions

The major reactions contributing to the improvement of the octane number are (a) dehydrogenation of cyclohexanes to aromatics, (b) dehydroisomerization of alkyl-cyclopentanes to aromatics, (c) isomerization of straight-chain paraffins to branched paraffins and (d) dehydrocyclization of paraffins into aromatics. Other important reactions are (e) hydrocracking and hydrogenolysis (carbon-carbon bond scissions), which result in low molecular weight paraffins, and (f) coke formation. Like most other hydrocarbon reactions at elevated temperatures, reforming reactions are accompanied by formation of carbonaceous residue (coke) which may poison the active sites of the catalyst. The relative importance of the

reforming reactions depends on the nature of the catalyst, the composition of the feedstock and the conditions of operation.

(a) Dehydrogenation of naphthenes

(b) Dehydroisomerization of naphthenes

(c) Isomerization of paraffins

(d) Dehydrocyclization of paraffins

(e) Hydrocracking and hydrogenolysis

(f) Coke formation
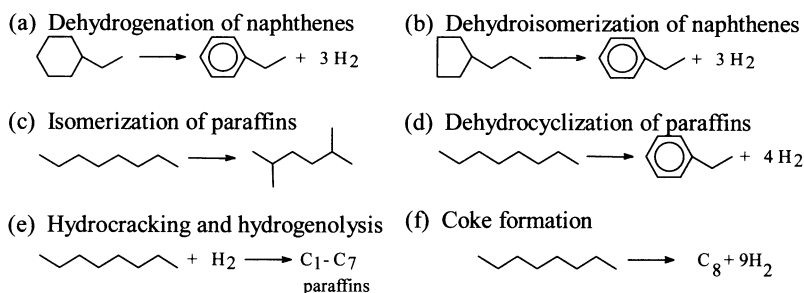
Fig. 1.2. Major catalytic reforming reactions exemplified with some C_8 hydrocarbons

Fig. 1.2 gives examples of these major reactions in the reforming of C_8 hydrocarbons. The reforming catalyst is a bifunctional catalyst with a metal function for hydrogenation and dehydrogenation reactions and an acid function for hydrocarbon rearrangements. Both the metal and acid sites on the Pt/Al_2O_3 catalyst are dispersed on the surface of the carrier material. The two catalyst functions interact through the olefins, which are key intermediates in the reaction network. The bifunctional reaction network shown in Fig. 1.3. was originally proposed by Mills and co-workers [5] but has later been modified [6]. The vertical paths in the figure take place on the metal and the horizontal paths proceed on the acid sites. The conversion of n-hexane into iso-hexanes first involves dehydrogenation on the metal to yield n-hexene. The hexene migrates to a neighboring acid site where it is isomerized (carbonium ion mechanism). Finally the iso-paraffin is formed by hydrogenation of the iso-olefin at a metal site. It has been shown that mechanical mixtures of particles containing each of the two functions are active for isomerization at rates comparable to the rates for the dual function catalyst [7]. Therefore, the two types of sites in the dual function catalyst can operate individually and the olefin intermediates can migrate between the sites by gas phase diffusion.
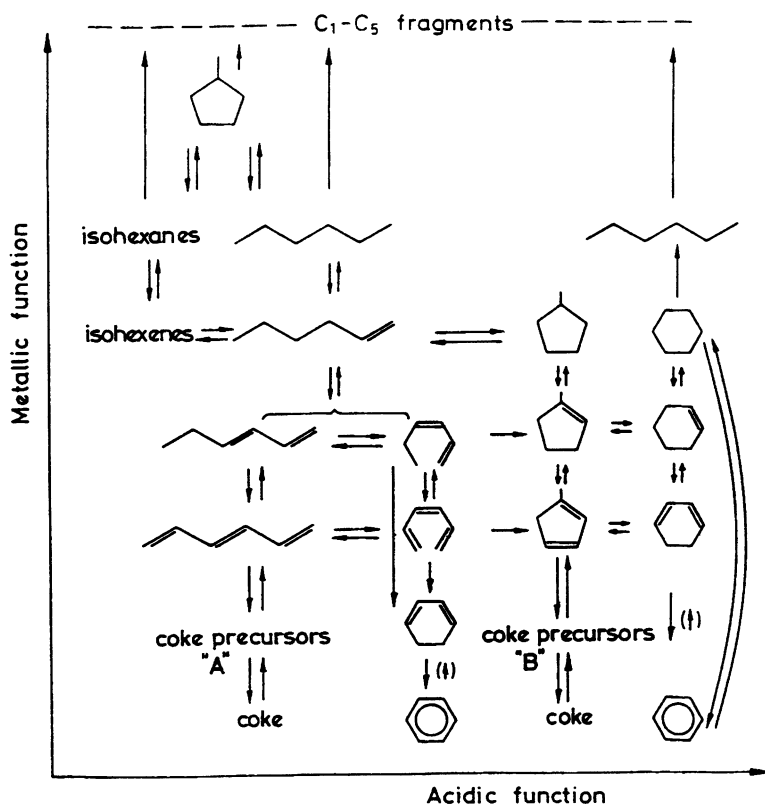
Fig. 1.3. Reaction network for the reforming of C_6 hydrocarbons [6].

1.2.3 Thermodynamics

Table 1.2 shows equilibrium constants and heats of reaction for some reactions of C_6 and C_7 hydrocarbons occurring at 500°C, reflecting the overall thermo-dynamics of catalytic reforming. Generally, the heats of reaction depend only slightly on the number of carbon atoms in the molecule. The formation of aromatics from cyclohexanes produces a significant RON increase, and from Table 1.2 it can be observed that the dehydrogenation of cyclohexanes to yield aromatics is strongly endothermic and the conversion is favoured by high temperature and low pressure. The equilibrium constants show that the reactions are almost completely displaced to the aromatics at 500°C. An increase in hydrogen partial pressure or total pressure will, however, shift the equilibrium toward the naphthenes. The effects of temperature and pressure on the concentration of toluene in equilibrium with C_7 naphthenes are shown in Fig. 1.4.

Table 1.2. Thermodynamic data, at 500°C, of some typical reforming reactions with C_6 and C_7 hydrocarbons.

Reaction type	Reaction	K_p (p in atm)	ΔH_R (kJ/mol)
Dehydrogenation	Cyclohexane $\Leftrightarrow$ Benzene + 3 H_2	6×10^5	221
	Methylcyclohexane $\Leftrightarrow$ Toluene + 3 H_2	2×10^6	216
	n-Hexane $\Leftrightarrow$ 1-Hexene + H_2	0.04	130
Dehydroisomerization	Methylcyclopentane $\Leftrightarrow$ Benzene + 3 H_2	5.2×10^4	75
Isomerisation	n-Hexane $\Leftrightarrow$ 2-Methylpentane	1.14	-5
	n-Heptane $\Leftrightarrow$ 2-Methylhexane	41.69	-6
	Methylcyclopentane $\Leftrightarrow$ Cyclohexane	0.09	-16
Dehydrocyclisation	n-Hexane $\Leftrightarrow$ Benzene + 4 H_2	7.8×10^4	266
	n-Heptane $\Leftrightarrow$ Toluene + 4 H_2	2.1×10^6	252
Hydrocracking	n-Heptane + H_2 $\Leftrightarrow$ Propane + n-butane	3.1×10^3	-52
Hydrogenolysis	n-Heptane + H_2 $\Leftrightarrow$ Methane + n-Hexane	1.2×10^4	-62

Source: Calculated from API Research Project [8].
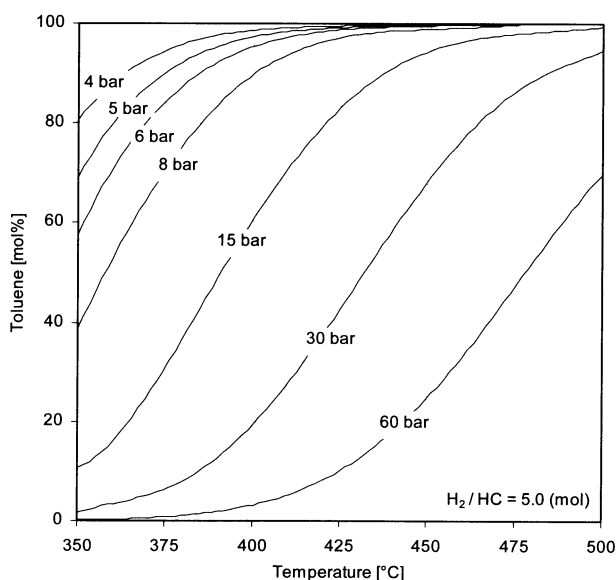
Fig. 1.4. The effect of temperature and pressure on the concentration of toluene in thermodynamic equilibrium with H_2 and C_7 naphthenes.

The thermodynamics of the dehydroisomerisation of cyclopentanes is similar to that of the dehydrogenation reactions, but the reaction is slightly less endo-thermic and the equilibrium constant is lower. Since the reaction involves an isomerisation step, the rate is lower than for pure dehydrogenation reactions, but high enough for the equilibrium to be approached under normal reforming conditions.

Paraffin dehydrocyclisation is a key reaction in catalytic reforming. It results in the highest RON improvement of all the reactions occurring in the process. Conversion of n-heptane into toluene equals a difference of over 100 RON units. The thermodynamics is similar to that of dehydrogenation of naphthenes. However, the rate of the reaction is slow, thermodynamic equilibrium is not reached and the reaction is kinetically controlled.

The isomerisation of paraffins is rapid and the conversion to isoparaffins is limited by the thermodynamic equilibrium. The heat of reaction is low (mildly exothermic) and temperature has only a moderate effect on the conversion within the temperature window typically applied in catalytic reforming (450-520°C). A low reaction temperature is the most favourable thermodynamically. Since the number of reactant and product molecules in the reaction are equal, neither the total nor the hydrogen pressure influences the equilibrium notably. Most fortunately, the equilibrium favours the more desirable (higher-octane) branched isomers. Isomerisation therefore makes a significant contribution to the octane improvement.

Paraffin dehydrogenation is strongly endothermic. At equilibrium, only very small concentrations of olefins can exist at the hydrogen partial pressures normally employed in reforming as reflected by the small K_p in Table 1.2. Thus the contribution of olefins to the octane number of reformate remains very low. Nevertheless, the olefins are important reaction intermediates in some of the reforming reactions. The thermodynamics sets an upper limit on the attainable concentration of olefins in the system and may therefore limit the overall rate for these reactions. In addition, the olefins may be further dehydrogenated and polymerised, particularly at low hydrogen pressure, and form carbonaceous residue (coke) covering the active surface.

The naphthenes isomerisation reactions are mildly exothermic. The equilibrium between methylcyclopentane and cyclohexane clearly favours the former at typical reforming conditions. The reaction is, however, relatively rapid and equilibrium is established under reforming conditions.

Hydrocracking is promoted under hydrogen pressure. It involves rupture of carbon-carbon bonds producing light paraffins as products. The reaction results in a loss of reformate yield, valuable hydrogen is consumed and is therefore in general unwanted. However, a limited degree of hydrocracking - transforming the heaviest paraffins into lighter ones having higher octane ratings as well as concentrating the aromatics - will increase the octane number of the reformate and is often needed to reach a specified RON level. The cracking reaction involves a classical carboniumion mechanism that favours the formation of propane and butanes.

Hydrogenolysis is a carbon-carbon bond scission reaction that is, as for hydrocracking, very feasible thermodynamically. Both hydrocracking and hydrogenolysis are very exothermic and highly favoured by low temperature from a thermodynamic point of view. However, the reaction rates are relatively slow and the reaction is solely kinetically controlled. Unlike hydrocracking, hydrogenolysis produces large amounts of methane and ethane.

1.2.4 Kinetics

Dehydrogenation reactions occur readily on commercial reforming catalysts at the temperatures employed during catalytic reforming, and equilibrium is reached

relative fast. Isomerisation of paraffins is also a fairly rapid reaction, and equilibrium is usually approached. However, the equilibrium concentration of some of the products is not fully attained. Dehydrocyclisation, hydrocracking, and coking are reactions that are kinetically controlled, and the product composition will depend on the relative rates of the various reactions, controlled by factors such as temperature, pressure and catalyst composition.

The temperature has an obvious impact on the kinetics of the reforming reactions. Fig. 1.5 a) clearly demonstrates that the research octane number (RON) of the liquid product increases as the temperature is increased during reforming of straight-run naphtha from North Sea crude [9]. Even though it is favourable from a thermodynamic point of view with high temperature conditions, the selectivity to unwanted cracking products will increase more than the desired products. This is due to a higher activation energy of the cracking reaction compared to reactions such as dehydrocyclisation. It is evident from Fig. 1.5 b) that the reformate yield decreases with increasing temperature due to increased selectivity to unwanted reactions such as hydrocracking.
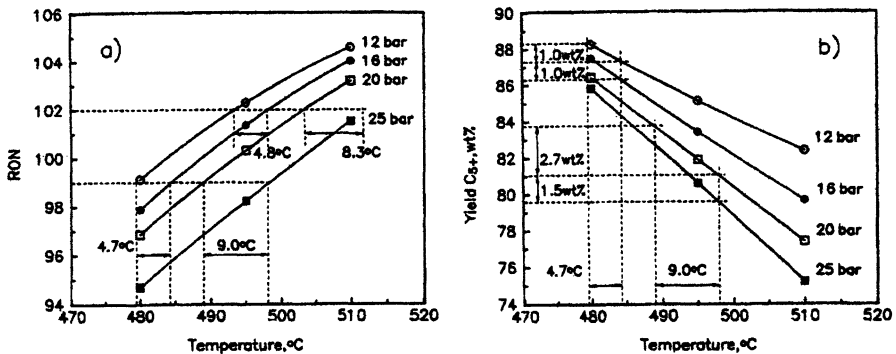
Fig. 1.5. RON (a) and reformate yield (b) as a function of the reaction temperature at different reaction pressures [9].
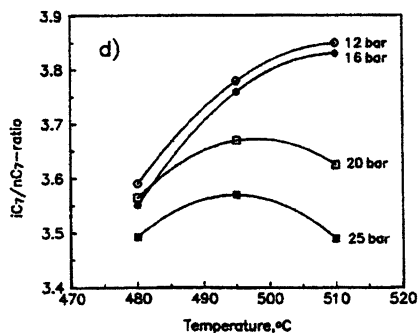
Fig. 1.6. iC_7/nC_7 ratio as a function of the reaction pressure at 12,16,20, and 25 bar [9].

Higher selectivity to cracking as a function of temperature can also be observed from Fig. 1.6, which shows the i/n-ratio of C_7 paraffin isomers at different reaction temperatures and reaction pressures. Multi-branched isomers are secondary products formed via single-branched isomers [10], and equilibrium is largely attained between normal paraffins and their single-branched isomers [11]. However, i-C_7 cracks more easily than n-C_7 and the i/n-ratio is therefore not thermodynamically controlled. At low reaction pressures this trend is not evident and the selectivity to i-C_7 increases with increasing temperature until thermodynamic equilibrium is attained at 510°C at 12 and 16 bar. At higher reaction pressure there is a net consumption of i-heptanes due to hydrocracking and there is a large drop in the i/n-ratio.
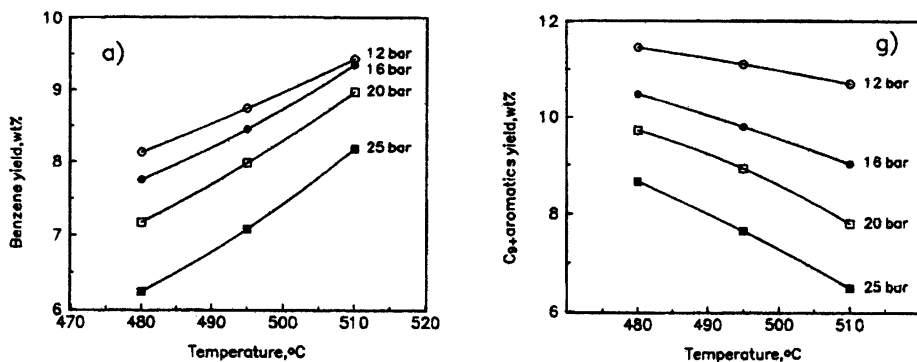
Fig. 1.7. Yield of benzene and C_{9+} aromatics as a function of reaction temperature and pressure [9].

As dehydrogenation and dehydrocyclisation are favoured at high temperature the yield of benzene increases with increasing temperature as shown in Fig. 1.7.

Furthermore, benzene production is favoured at low reaction pressures. On the contrary the yield of C_{9+} aromatics (for example) decreases with increasing temperature and increasing pressure as a consequence of side chain hydrode-alkylation.

Figs. 1.5, 1.6, and 1.7 all demonstrate the beneficial effect of low reaction pressure operation in order to obtain high yields of reformate and high-octane products. From Fig. 1.5 a) it can be observed that for a given severity in the range 99-102 RON, the temperature can be lowered by 8-9°C when going from 25 bar to 20 bar. At the same time the formation of carbonaceous deposits is favoured and it is therefore important to keep a certain pressure in order to suppress catalyst deactivation caused by coke formation. In order to be able to run at low-pressure conditions emphasis must be put on catalyst optimisation to make the catalyst more stable and active at less severe process conditions.

Measurements of individual reaction rates during reforming are made difficult by the complexity of the overall reaction and due to catalyst deactivation during operation. There exist several kinetic simulation models that describe the reaction kinetics during catalytic reforming. In such models certain simplifications are made in order to reduce the number of reaction species and reaction pathways involved.

1.2.5   Catalyst

The catalyst used in commercial reforming processes is a bifunctional catalyst involving an acidic function and a dehydrogenation-hydrogenation function. The latter is provided by a noble metal such as platinum. Most modern reforming catalysts consist of platinum promoted with elements such as Re, Sn, and Ir in order to enhance the stability and selectivity of the catalyst. The metals are usually deposited on a chlorinated porous high surface area alumina which act as the acidic function of the catalyst.

The Catalyst Support

The acidic function of the catalyst promotes skeletal rearrangement and the support usually consists of one of the two alumina crystallite forms η-Al_2O_3 or γ-Al_2O_3 [12]. In order to selectively crack low octane n-paraffins acidic zeolites having shape-selective cracking properties have also been employed together with conventional reforming catalyst [13-15].

The aluminas are made from aluminium hydrates, η-Al_2O_3 from gibbsite or bayerite and γ-Al_2O_3 from bohemite, by calcination in air or vacuum. Both forms are highly stable aluminas with a spinel structure (cubic close packing) charac-terised by high surface area. Both Brønstedt and Lewis acidity may exist on the alumina surface and the fraction of each depend on the degree of hydration [16]. Based on techniques such as ammonia adsorption and IR measurements Peri [16-18] proposed an idealised model for the surface alumina and suggested that the catalytic activity of these supports were closely related to certain acid sites (aluminium ions that act as Lewis acids) created by the desorption of hydroxyl groups on the surface. On the other hand, Knözinger and Ratnasamy [19] have shown that the catalytic activity is primarily not due to such Lewis acid sites.

These authors attributed the catalytic activity to OH groups with neighbouring defects sites created in the partially dehydroxylated surface.
The acidity

of the support is enhanced by treating the alumina with halogens, preferable chloride in the form of HCl or carbon chlorides. Gates et al [20] proposed a model illustrated in Fig. 1.8 where the acidity of the OH groups are strengthened by the inductive effect exerted by an adjacent Cl⁻ ion.

$$
\begin{array}{ccccccc}
H & H & H & \delta^+ & \delta^+\,H & H & H \\
| & | & | & & | & | & | \\
O & O & O \;{\dashrightarrow}\; Cl \;{\dashleftarrow}\; O & & O & O \\
& & Al & & Al & &
\end{array}
$$
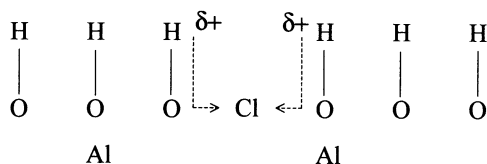
Fig. 1.8. Enhancement of the Brønstedt acidity by adjacent Cl⁻ ions [20]

Increasing the acidity of the support with a high chlorine content will lead to excessive unwanted hydrocracking while a low content results in low activity for isomerization and dehydrocyclization. Chlorine is removed from the support by water present in the feedstock and during operation the chlorine content must be maintained by continuously adding chlorine to the feedstock at a fixed Cl/H_2O ratio.

The Pt/Al₂O₃ Catalyst

Platinum is the preferred metal in reforming catalyst both due to its high activity and to its good selectivity characteristics. Table 1.3 shows the results obtained by Ciapetta et al. [21] when comparing the activities for dehydrogenation of cyclohexane on various metal-oxide catalysts and other supported metals. It is clearly illustrated that platinum is by far the most active metal for dehydrogenation even when compared to palladium, iridium and rhodium.

Table 1.3. Cyclohexane dehydrogenation activities of supported metal and metal oxide catalysts [21].

Catalyst, wt%	Dehydrogenation acivity (μmoles benzene/g catalyst/s)
34% Cr_2O_3 cogelled with Al_2O_3	0.5
10% MoO_3 coprecipitated with Al_2O_3	3
5% Ni on Al_2O_3 or SiO_2-Al_2O_3	13
5% Co on Al_2O_3	13
0.5% Ir on Al_2O_3	190
1% Pd on Al_2O_3	200
5% Ni on SiO_2	320
1% Rh on Al_2O_3	890
0.5% Pt on Al_2O_3 or SiO_2-Al_2O_3	1400-4000

Differential flow reactor at 427°C, 6.8 atm, H_2/HC = 6 (mole ratio), activity determined after 30 min on stream, pre-treated with H_2 at reaction conditions, LHSV varied to give differential operation

Except for naphthene dehydrogenation, which is structure insensitive and is depending on the number of exposed platinum atoms only, the other reforming reactions are favoured kinetically by small crystallite sizes [22]. The smaller the platinum ensembles are, the more stable and resistant to coke formation is the catalyst [23]. Considering also the high cost of the platinum metal, it is desirable to deposit it onto the porous alumina support in a highly dispersed form possibly atomically dispersed. Sufficient activity and high dispersion require only small amounts of platinum and the current commercial catalysts typically contain in the order of 0.2-0.4 wt% of platinum. Depending on the preparation technique the metal particle size can vary in the range 0.8 to 1000 nm [20]. Fig. 1.9. shows an annular dark field image of a Pt-Re/Al_2O_3 catalyst (single piece of alumina) and a corresponding X-ray spectrum of one metal particle obtained using combined scanning transmission electron microscopy and electron-dispersive X-ray analysis [24]. The metal particles detected, observed as small white dots, varies from 1 nm to 0.5 nm in size. Particles below this size were not measurable due to resolution limitations of the microscope applied [25].
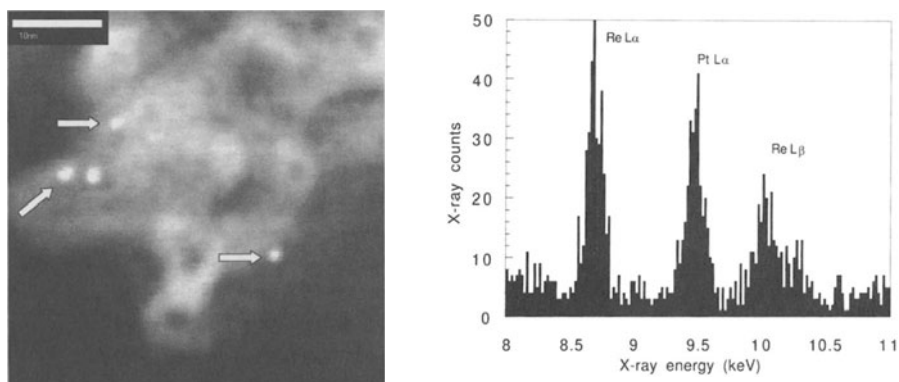
Fig. 1.9. Annular dark field image of a single piece of a PtRe/Al₂O₃ catalyst and an EDX-spectrum of collected X-rays emitted from a single metal particle [24]. The Pt and Re signals detected clearly shows that the metal particle is bimetallic. Information about the composition of the particles can be obtained by collecting EDX-spectra from a large number of particles.

The dispersion of the platinum on the support can be measured be a number of techniques such as electron microscopy, X-ray line broadening, small-angle x-ray scattering, and gas chemisorption [26]. Metal dispersion measurement by selective H_2 chemisorption and H_2-O_2 titration is a frequently applied method for characterisation of reforming catalysts. In order to calculate the dispersion from H_2 chemisorption the H/Pt stoichiometry has to be defined, and in most studies a H/Pt stoichiometry of unity has been applied [27]. Volumetric chemisorption of hydrogen of the standard 0.3 wt% Pt/Al₂O₃ Akzo CK 303 catalyst, typically yields a dispersion of 90-95% [28].

The PtRe/Al₂O₃ Catalyst

One of the first bimetallic catalysts was introduced by Chevron in 1969 [29] and was based on platinum and rhenium. Today, catalysts based on these elements are among the most important in industrial catalytic reforming. Other common additives ranged in commercial availability are tin [30], iridium [31] and germanium [32]. In the patent literature a number of other additives have also been reported. The most frequently studied and utilised catalyst will be described in the following chapters.

The presence of rhenium markedly decreases the rate of deactivation by coke formation allowing long runs at relatively low pressures. Due to the high hydrogenolysis activity of rhenium sulphur is added to deactivate the rhenium sites. The rhenium content in an industrial catalyst is similar to the amount of platinum. However, the tendency points toward higher rhenium to platinum ratios

(for example 0.2 wt% Pt-0.4 wt% Re) which presumably will increase the dilution of platinum with rhenium.

The higher stability of the Pt-Re(S) catalyst compared to the monometallic Pt/Al$_2$O$_3$ catalyst has been claimed to be due to a different location of the coke [33] and to a different nature of the coke [34] rather than due to a lower amount of coke deposited. Pt-Re catalysts may operate satisfactorily with coke levels approaching 25 wt% [35]. In Table 1.4. the change in the nature and amount of the coke with the addition of Re and S is shown. After having added sulphur to the catalyst, the carbon deposition is reduced from 200 to 116 μmol/g cat, and the carbon species are much richer in hydrogen [36].

Table 1.4. Carbon and hydrogen retained on the catalyst [36]

Catalyst	Carbon retained (μmol/g cat)	Hydrogen retained (μmol/g cat)	H/C
Pt/Al$_2$O$_3$-Cl	342	126	0.37
PtRe/Al$_2$O$_3$-Cl	200	101	0.51
PtRe(S)/Al$_2$O$_3$-Cl	116	185	1.58

Different theories have been proposed to explain the beneficial role of Re in modifying the catalytic performance of the Pt-Re system. It has been claimed that Re prevents sintering of Pt [29,37] or that Re acts independently as an active ingredient in the modification of the carbonaceous deposits [38]. The most common explanation of the effect of Re on the catalytic properties of the Pt-Re catalyst is that Re is associated with Pt in bimetallic particles and the interaction of such bimetallic particles with sulphur [39-43]. Sulphur adsorbs primarily on rhenium atoms and suppresses the unwanted high hydrogenolysis activity known for Pt-Re alloys. Biloen et al [43] proposed a model, shown schematically in Fig. 1.10 where the rhenium atoms which adsorb sulphur divide the metal crystallite surface effectively into smaller platinum entities and become obstacles against the transformation of soft coke into deleterious graphitic coke, a reaction demanding larger ensembles of metal surface atoms.
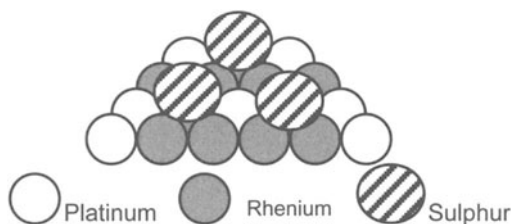
Fig. 1.10. A model for the active surface sites of Pt-Re/Al$_2$O$_3$ [43]

Since sulphur mainly adsorbs on rhenium, the number of surface platinum atoms is not significantly reduced upon sulphurisation. It has been demonstrated that sulphur is preferentially bound to the Re atom. Michel et al [44] have observed that after sulphiding and hydrogen stripping only 10% of the Pt and all

of the Re was covered with irreversibly adsorbed S. This has been attributed to the much lower electron affinity of Re [45], and the increases in the electron affinity of Pt by the Re-S bond.

Direct evidence for bimetallic particle formation has been difficult to obtain because of the extremely small size of the metal crystallites (<10 Å) and the subject has been a matter of controversy for over two centuries. However, modern characterisation techniques have clearly proven the existence of bimetallic Pt-Re particles as demonstrated in Fig. 1.11. The individual particle size was found from studying STEM images, whereas the composition is obtained from EDX analysis of each metal particle (A STEM image of a Pt-Re/Al$_2$O$_3$ catalyst is shown in Fig. 1.9) [24].
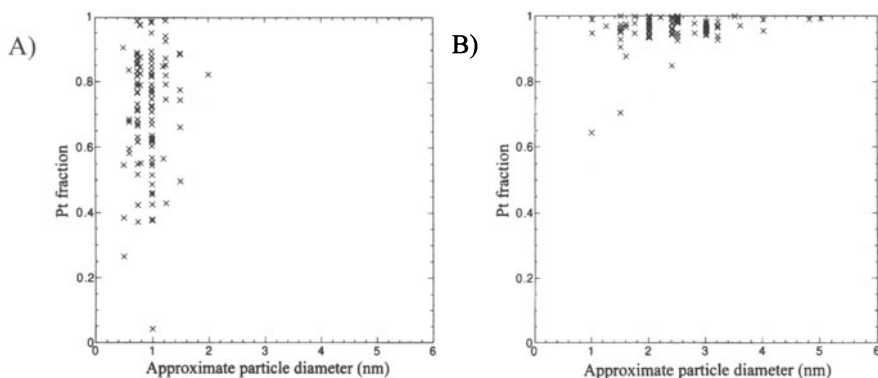
Fig. 1.11. Pt content vs crystallite size measured by ultra high-resolution combined STEM/EDX analysis of individual (x) Pt-Re crystallites on the EUROPT-4 catalyst (0.3-0.3 wt% Pt-Re/Al$_2$O$_3$) [24]. (A) High (B) Low 'alloying' degree.

The PtSn/Al$_2$O$_3$ Catalyst

The catalyst stability of Pt-Sn/Al$_2$O$_3$ catalysts is close to that of Pt-Re/Al$_2$O$_3$, but the selectivity is better at low pressures and the resistance to platinum sintering is high. Tin does not possess any hydrogenolysis activity and therefore the catalyst does not have to be treated with sulphur prior to use. These features make this catalyst preferable in low-pressure reforming units with frequent regeneration.

To explain the advantageous effect of Sn in the Pt-Sn system two different mechanisms have been proposed. Either is Pt modified by an "ensemble effect" where Sn decreases the number of contiguous Pt atoms, or Sn changes the electronic environment of the Pt atoms. The exact role of Sn in the Pt-Sn system is closely related to the chemical state of Sn in the system. Diverging results from the literature may be due to different catalyst preparation, pre-treatment and experimental techniques applied.

Dautzenberg et al [46] have argued for the formation of an alloy and that the beneficial effect of Sn is due to the "ensemble" effect. Bacaud et al [47] suggest that alloying accounts for the decrease in catalytic activity related to Pt. In addition it was also suggested that if part of the Pt was unalloyed, its activity is

also inhibited due to an electronic effect of Sn ions. Coq and Figueras [48] studied the conversion of methyl cyclopentane on the Pt-Sn system. It was observed that the addition of Sn had a stabilisation effect on the catalytic activity and resulted in a decrease of the hydrogenolysis. Thus, it was concluded that the main role of Sn is to dilute the Pt surface. Li et al [49] concluded that the presence of Sn oxides improves the stability of the catalyst by blocking Pt particle sintering, and that the presence of Pt-Sn bimetallic particles significantly depresses hydrogenolysis. Paál et al [50] rationalised the changes in activity and selectivity brought about by Sn in terms of geometric effects, with Sn as a solid solution in Pt or as an alloy diluting multiatomic Pt sites.

Burch [47] suggested that the special properties of Pt-Sn catalysts cannot be due to a geometrical effect in which Sn divides the surface up in small clusters of Pt atoms as not sufficient metallic Sn was found. The beneficial effect of Sn was attributed to the change in the electronic properties of small Pt crystallites and to the modification of the acidic properties of the support [51]. As a result self-poisoning is reduced and the selectivity to nondestructive reactions is increased. Sexton et al [52] supported the conclusions made by Burch suggesting that Sn(II) is a surface modifier of γ-Al$_2$O$_3$ and that the reactivity changes are most likely due to the changes in the electronic interaction between Pt and Sn(II)-γ-Al$_2$O$_3$. Parera et al [53] stated that the alloying of Pt with Sn could result in an electron transfer from Pt to Sn, creating electron deficient Pt atoms, which influence markedly the adsorption-desorption steps of the catalytic reaction. It was also suggested that both electronic and geometric effects act together to yield the great decrease in hydrogenolysis.

Catalyst Preparation and Pretreatment

The procedures for catalyst preparation and pretreatment are very important for the properties of the final catalyst. Platinum metal and the second metal is usually incorporated onto the alumina support by one or two successive impregnations of solutions containing HCl and metal precursors such as H$_2$PtCl$_6$, HReO$_4$ and SnCl$_4$. The catalysts are then dried, treated in oxygen containing atmosphere (400-600°C), and finally reduced (500-550°C) in hydrogen to convert the platinum oxide species into active zero valent metal. While platinum is usually fully reduced at these temperatures, the reduction degree of rhenium and tin has been a matter of discussion [39,46,47,54-58]. The Pt-Sn catalyst is fully activated after reduction, but the Pt-Re catalyst needs first to be sulphurised. Sulphur is added in the form of H$_2$S or some carbon sulphide diluted in hydrogen until Re saturation as recognised by sulphur breakthrough at the rector exit. Weakly adsorbed sulphur on platinum is flushed off by H$_2$ prior to naphtha introduction.

The pretreatment conditions and drying temperature has a significant influence on the final state of the metal particles of the Pt-Re/Al$_2$O$_3$ and Pt-Sn/Al$_2$O$_3$. In order to obtain bimetallic particles, intimate contact between Pt and the second metal has to be ensured. In the case of the Pt-Re catalyst contact can be obtained during reduction as the Re oxide species can migrate on the surface. The mobility is controlled by the degree of surface hydration and the drying temperature prior to reduction is very important. Figure 1.12 shows the characteristic TPR profiles of two catalyst samples dried at 240°C and 520°C, respectively [57].
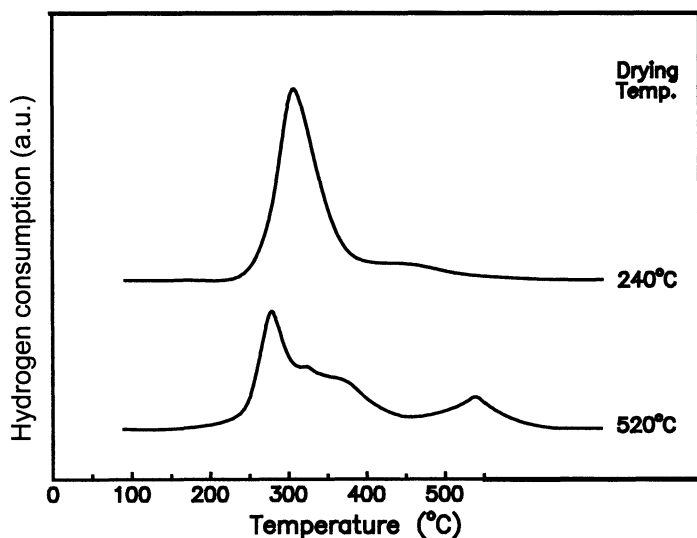
Fig. 1.12. TPR profiles of the PtRe/Al$_2$O$_3$ catalyst dried at 240°C and 520°C [57].

The TPR profile of the catalyst dried at 240°C show only one peak at 300°C and the hydrogen consumption corresponds to almost complete reduction [57]. This profile is characteristic of simultaneous reduction of Pt and Re and hence the formation of bimetallic particles. Mobile Re oxide species are catalytically reduced by Pt metal atoms on the surface when they get in contact. The catalyst dried at 520°C display a more complex TPR curve which can be attributed to the fact that some of the Re is reduced at higher temperatures forming monometallic particles. The reduction mechanism of the Re oxide species is schematically presented in Fig. 1.13. Hydroxyl groups on the support enables Re oxide species to migrate when the catalyst is dried at 240°C (Fig. 1.13 a). When the catalyst is dried at 520°C the surface is more dehydrated resulting in less Re oxide mobility (Fig 1.13.b).
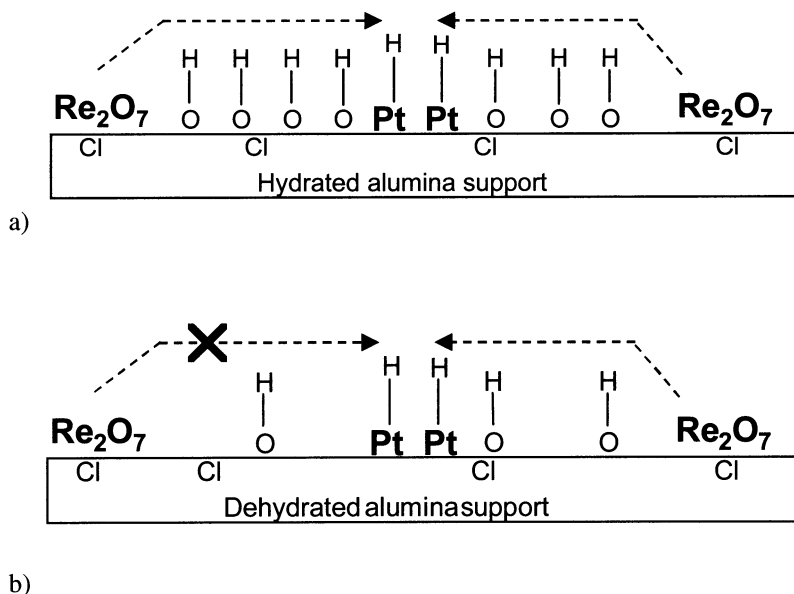
Fig. 1.13. Proposed reduction mechanism for the platinum catalysed reduction of rhenium for catalyst dried at 240°C a) and 520 °C b) [28].

Even if the valence state of Sn is debated in the Pt-Sn system it seems to be a general agreement that Pt may catalyse the reduction of Sn oxides [29,59]. Sn oxides are less able to migrate than Re oxides due to the very strong interaction with the alumina support. Lieske and Völter [59] reported that high temperature calcination (500°C) results in more alloyed particles as Pt (IV) and/or Sn (IV) oxide species are mobile at these conditions. According to the same authors an increasing Sn content gives an increasing amount of alloyed particles. In order to obtain bimetallic PtSn particles, contact between Pt and Sn can be obtained during the preparation step by employing a PtSn complex precursor such as $[Pt(NH_3)_4][SnCl_6]$ [50,60-62] and $[PtCl(SnCl_3)(PPh_3)_2]$ [63]. Investigation of both the Pt-Sn/Al$_2$O$_3$ [52,64] and the Pt-Sn/SiO$_2$ system [65] has shown that the impregnation procedure is very important and that co-impregnation leads to more bimetallic formation than a sequential impregnation procedure.

1.2.6 Catalyst Deactivation and Regeneration

Catalyst Deactivation by Coke Formation

During reforming operation the catalyst may be subjected to deactivation by poisoning, sintering, and by the formation of coke. Coke formation is the main cause for deactivation determining the cycle length of the catalyst. Coke formation is favoured at high temperatures and low hydrogen pressures, which are also conditions favourable for the formation of aromatic compounds. Reactions leading to coke formation on the support are acid catalysed polymerisation and cyclisation

of olefins to give higher molecular weight compound that undergoes further dehydrogenation, cyclisation, and further polymerisation. Poisoning begins on the metal sites with the formation of olefins and aromatics. These species can slowly be transformed to coke on the metals or migrate to the acid support by gas phase transport or surface diffusion. Coke formed on the acid sites is more resistant, and this poisoning is probably the origin of long term deactivation in reforming. In order to keep constant conversion when the coke builds up on the catalyst, the temperature is increased. This usually results in a liquid yield reduction unless the deactivation of acid sites balances the activity increase caused by the higher temperature.

Strong dehydrogenation reactions involved in coking are suppressed by the presence of hydrogen. During the reaction part of the carbonaceous material which is continuously formed will be removed by hydrogen – cleaning the catalyst surface. A small amount of coke is deposited on the metal sites on bifunctional catalysts, whereas the majority of the coke is accumulated on the support. The mechanism of coke removal involves hydrogen spillover from the metal to the alumina support. Iridium and rhenium are known to promote the methanation of coke. The degree of platinum dispersion affects the ease of coke removal, as coke formed on large platinum ensembles is more dehydrogenated than the coke formed on well-dispersed catalysts and will be less reactive with hydrogen.
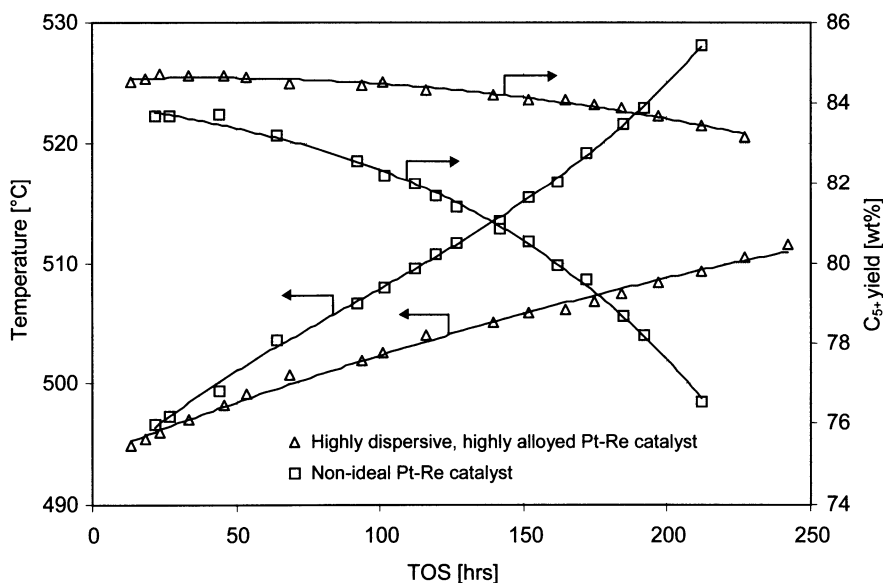
Fig. 1.14. Reaction temperature and reformate yield as a function of time on stream during accelerated deactivation of commercial Pt-Re catalyst (Unpublished results).

Fig. 1.14 shows the activity decline and the change in reformate yield due to coke formation of a commercial reforming catalyst as a function of time on stream. The beneficial effect of having the metal particles present in a highly alloyed form is also demonstrated. By adjusting the pre-treatment conditions as

discussed previously it is possible to control the degree of alloy formation and thus obtaining better performance of the catalyst. The addition of rhenium and sulphur to the Pt/Al$_2$O$_3$ catalyst greatly enhances the stability of this catalyst system. This has been claimed to be due to changes in the location [33] and nature [34] of the coke rather than only due to the amount produced. The quantity of the coke can be characterised by techniques such as temperature programmed oxidation (TPO) whereas the composition of the coke can be analysed by investigating the coke combustion products or by IR studies of the hydrocarbon deposits [66]. Fig. 1.15 shows examples of TPO profiles of the Pt/Al$_2$O$_3$, Re/Al$_2$O$_3$, and Pt-Re/Al$_2$O$_3$ catalyst (coke formed during nC$_6$ reaction) obtained when monitoring the CO$_2$ evolution during temperature programmed oxidation [36]. The peaks identified can be assigned to carbon formed on either Pt (low temperature peaks) or the support. The two first peaks of the Pt-Re/Al$_2$O$_3$ catalyst have been attributed to oxidation of carbon formed on Pt and the peak in the middle to the oxidation of carbon located on Re. It is assumed that coke formed on the Pt sites is either catalytically oxidised or that the nature of coke surrounding the metal sites is different resulting in an oxidation at lower temperatures. The two last peaks are therefore attributed to the oxidation of carbon located on the support.
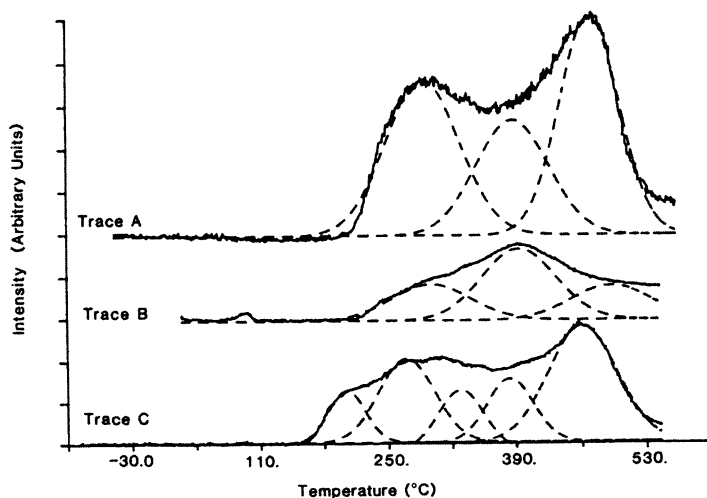
Fig. 1.15. TPO profiles obtained when measuring the CO$_2$ evolution during temperature programmed oxidation [36]

Coke formation is favoured at high temperatures and low hydrogen pressures, which are also conditions favourable for the formation of aromatic compounds. It is therefore a question of process costs and frequency of regeneration when optimising the operation conditions. In addition to temperature and pressure, the rate of coke formation is obviously also dependent of the feedstock composition. The deactivation rate is faster if the feed contains aromatics, naphthenes, and paraffins in the C$_8$-C$_{10}$ hydrocarbon range than if it contains lower molecular

weight hydrocarbons. Fig.1.16 clearly demonstrates the effect of the final boiling point (FBP) of naphtha on catalyst deactivation [67].
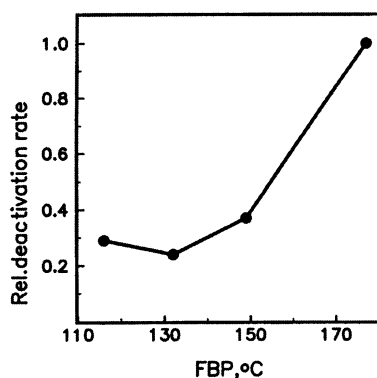
Fig. 1.16. The deactivation rate relative to the one for the base naphtha, as a function of naphtha FBP. The deactivation rate was measured as the temperature rise needed to maintain 102.4 RON [67].

Catalyst Deactivation by Poisoning

Poisoning refers to the strong adsorption of impurities in the feedstock, resulting in temporary or permanent inhibition of active sites. Typical impurities associated with the naphtha feed are sulphur in form of organic sulphides, nitrogen compounds, metals, and halides. In addition products formed during reaction may cause poisoning.

Table 1.5 shows the initial toxicity of the various impurities on the Pt/Al_2O_3 catalyst as measured by Barbier et al [68]. The initial toxicity is defined as number of platinum atoms poisoned by one molecule/atom of poison. It can be seen that Hg^{2+} is extremely toxic to the catalyst inhibiting as many as 15 Pt atoms by adsorption. Generally, metal impurities show strong affinity for platinum and form stable chemical compounds. Metal poisons are rarely eliminated by catalyst regeneration and will cause permanent damage.

Table 1.5. Initial toxicity of some compounds on Pt/Al$_2$O$_3$ [68].

Poison	Initial toxicity	Relative metal activity at poison saturation
SO$_2$	1.0	0
Thiophene	5.0	0
Dibenzothiophene	4.5	0
NH$_3$	0.1	0.67
Pyridine	0.12	0.042
CO	1.18	0
H$_2$O	0.00018	0.5
As(C$_6$H$_5$)$_3$	1.9	0
Na^{2+}	0	0
Fe^{2+}	1.1	0
Cu^{2+}	2.0	0
Hg^{2+}	15	0
Pb^{2+}	5.2	0

Sulphur is considered as the major poison of reforming catalysts and is present in the feed as organic sulphur compounds at concentrations up to 1500 ppm [69]. Although the adsorption of small amounts of sulphur is beneficial to the Pt and Pt-Re catalyst, excessive sulphurisation will affect the metal activity strongly. The toxicity of sulphur is a result of both the blocking of active sites and the modification of the electronic properties of these sites. It is important to use proper pretreatment conditions of the naphtha feed in order to avoid severe poisoning of the catalyst. In case of the Pt-Re/Al$_2$O$_3$ catalyst a maximum sulphur level of 0.5 ppm is recommended [29].

Nitrogen compounds in form of organic compounds decomposing into ammonia will inhibit the acid function of the catalyst. In the presence of water ammonia results in the leaching of chlorine by the formation of ammonium chloride [70]. Water and oxygenates will also cause leaching of chloride resulting in decreased acidity of the alumina, whereas halides present in the feed will have the opposite effect.

Catalyst Deactivation by Sintering

Sintering is the loss of active surface area of the catalyst due to high temperatures and most of the sintering in reforming catalysts occurs during regeneration by coke burning.

Metal sintering is the agglomeration and growth of metal crystallites. The extent and rate of this process is very much influenced by factors such as the temperature, atmosphere, and chloride content. Changes in Pt dispersion during treatment in oxygen atmosphere has been reviewed by Wanke et al [71]. The authors proposed a model where the sintering of Pt particles is governed by the formation of Pt^{4+} species. The stability and mobility of these surface species determines the degree of sintering of the catalyst, and at high temperatures sintering occurs rapidly.

In order to decrease the extent of sintering the catalyst must contain a sufficient amount of chlorine, as it is known to slow down sintering. The addition of a second metal to the Pt catalyst has also been claimed to induce an beneficial effect on the sintering characteristics of Pt. Kluksdahl [29] attributed the higher stability

of the Pt-Re catalyst to the increased resistance to sintering due to the formation of Pt-Re alloys.

In addition to sintering of the metal particles sintering of the alumina support occurs. This is the change in pore structure causing loss of surface area and acidity. In opposition to metal particle sintering this is an irreversible process and determines therefore the total lifetime of the catalyst.

Catalyst Regeneration

When the reactor temperatures during operation no longer can be increased to compensate for activity loss (burner limitations) or the reformate selectivity of the reforming catalyst is too low for economical use, the catalyst has to be regenerated by oxidative removal of the coke. Coke combustion with oxygen starts at the coke deposited on the metal particles due to the catalytic action of platinum and the higher hydrogen content of deposits. This has been demonstrated by TPO experiments as shown in Fig. 1.15. By the action of oxygen spillover the coke burning will spread to the support. Because of the exothermic nature of oxidation, the procedure usually starts at a fairly low temperature (200-300°C) and with a low oxygen concentration (1-2%) in order to avoid temperature runaway and hot spots in the catalyst bed. The temperature and oxygen concentration is gradually increased up to 500°C and 21% (air). After coke combustion the chlorine content is low and the metal is partly sintered. The catalyst has to be "rejuvenated" in order to get it back to its initial state.

Restoration of acidity and metal dispersion is obtained by oxychlorination. Fig. 1.17 shows the schematic presentation of the mechanism of redispersion by oxychlorinaton [70]. Here, the catalyst is exposed to chlorine (HCl, Cl_2 or carbon chlorides) together with oxygen at approximately 500°C, leading to a displacement of OH groups with Cl and a complete metal redispersion probably involving oxychlorinated platinum intermediates [72]. Often, chlorine addition starts already in the coke combustion step (combined coke burning/oxychlorination) in order to minimise chlorine loss and damage to the metal function. In the case of bimetallic catalysts the amount of chlorine prior to reduction may influence on the degree of alloyed metal particles [73]. After reduction the catalyst is sulphided in order to deactivate the superactive sites responsible of unwanted hydrogenolysis and hydrocracking reactions.

PLATINUM REDISPERSION BY OXYCHLORINATION
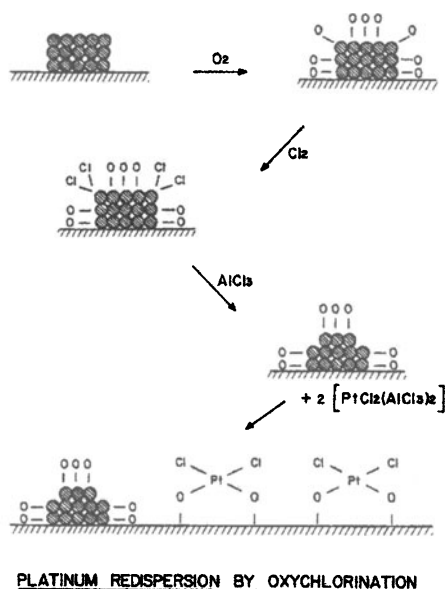
Fig. 1.17. Schematical presentation of the mechanism of redispersion by oxychlorination of Pt/Al$_2$O$_3$ catalysts [70].

1.3   Industrial Application

1.3.1   History

The first catalytic reformer started its operation in 1940. This was the fixed-bed Hydroforming process, using a molybdenum alumina catalyst. The catalyst lost activity as a result of coke deposition, but most of the original activity was regained on regeneration in air. However, the major breakthrough came with the introduction of alumina-supported platinum catalysts and the commercialisation by UOP of the Platforming process in 1949. The catalyst was more active by an order of magnitude or more than the first generation of molybdenum-based catalysts. The operating conditions (450-510°C, 35-50 bars) were selected to minimise coke laydown and the catalyst was not regenerated. In the 1950's more than 10 new commercial processes based on the platinum catalysts were developed. Most of these included facilities for catalyst regeneration, allowing operation at higher temperatures and lower pressures.

During the 1960's, higher-octane gasolines were necessitated by improvements in automobile engines, and in the 1970's and 1980's, environmental concerns, especially the phasing out of lead were the main driving forces. A significant catalyst improvement occurred in the late 1960's with the introduction of the Pt-Re alumina catalyst by Chevron in 1968 [29] and the new Rheniforming process

two years later. The catalyst was more stable and could be operated at lower pressures and higher temperatures favouring the thermodynamics of aromatic formation. Subsequently, other bimetallic or multimetallic catalysts incorporating metals such as Ir, Sn and Ge came into the market. The higher stability and selectivity produced by the new catalysts does, however, require extensive feed purification because they are more vulnerable to sulfur poisoning. The new generation of bimetallic catalysts lead to the introduction of new processes, especially designed for low-pressure operation. The most significant innovation was the introduction of continuous catalyst regeneration (CCR) by UOP. This allows steady-state reforming operation with fresh catalyst performance at optimum process conditions. Most new units are of this type.

The platinum based bimetallic catalysts Pt-Re and Pt-Sn are dominating the present market. Because of the high stability, Pt-Re is usually the catalyst choice for units with periodical regeneration while Pt-Sn catalysts are used in CCR units because of better reformate selectivity at low pressures. The patent literature describes a number of new catalyst materials for reforming (such as metals on zeolites) and the combined use of different catalysts in the reactors. However, their catalytic performance has to be improved in order to replace the current Pt/alumina based systems. In fact, the catalysts in present use are still being improved as is seen by a continuous increase in commercial cycle lengths (run time in between regeneration). Modern semi-regenerable units may in fact operate for two to three years between regenerations at relatively severe operating conditions.

1.3.2   Reactor Design and Operation Conditions

The overall reforming process is endothermic and the most endothermic reactions occur very rapidly. It follows that a large amount of heat must be added to the reactants in order to maintain a desired temperature level throughout the catalyst bed. Addition of heat to packed beds is associated with technical difficulties. Considering the heat duties, a fluidized bed reactor would be preferable, but the high cost of the reforming catalyst makes it uneconomical. The solution is to divide the catalyst charge among several reactors (usually 3 to 4) which are run adiabatically and with interstage heating in between.

When the feedstock enters the first reactor, the temperature falls rapidly as the cyclohexanes are dehydrogenated and almost quench the reactions. As a result, the residence time is short and the size of the first reactor is small compared to the other reactors. The effluent is reheated and enters the second reactor where it undergoes further dehydrogenation, dehydroisomerization and isomerization. The temperature drop of the second reactor is lower than in the first one. In the last reactor, which often contains about half of the total catalyst charge, the slower reactions, namely dehydrocyclization, hydrocracking and hydrogenolysis dominate. The exothermic cracking reactions in the last reactor causes a lower delta T (higher exit temperature) in the last reactor and shifts the naphthene-aromatic equilibria in favour of further dehydrogenation as well.

The reforming processes are classified according to the frequency and mode of regeneration. Semiregenerative processes are characterised by operation over long periods until complete plant shutdown during regeneration. This is suited for operating conditions where the catalyst deactivation is slow. The majority of reformers are of this type.

Cyclic processes have an additional 'swing' reactor that replaces one of the others when its catalyst charge needs to be regenerated. This type of process is not the most common because it requires that the reactors are of equal size and because of the technical complexity. Most new reforming units are based on continuous catalyst regeneration (CCR). In this design the reactors are usually stacked on top of one another. The catalyst is continuously withdrawn from the bottom of the reactor section, transported to a regeneration unit, regenerated and returned to the top of the reactor train.

High-pressure processes (20-50 bar) are operated at temperatures in the range of 470-520°C, high hydrogen to hydrocarbon mol ratios (4-10) and liquid hourly space velocities ranging from 1 to 6. Medium pressure (10-20 bar) and low-pressure (3-10) processes operate at slightly higher temperatures to optimise conversion into aromatics. The choice of conditions will depend on the feedstock quality, the product octane required, the catalyst stability and the regeneration capacity available. High-pressure operation causes higher rate of hydrocracking and therefore a lower reformate yield. On the other hand the rate of deactivation is reduced. The recent development of much more stable catalysts has increased the interest in low-pressure reforming. Since reformers are operated adiabatically and because the catalyst charge is unevenly divided among the reactors space velocity and temperatures are not constant. The space velocity in the first reactor may be more than twice of that for the last reactor. To evaluate catalyst activity, a weighted average bed temperature (WABT) is often calculated. WABT is the sum of the average of the inlet and outlet temperatures of each reactor multiplied with the weight fraction of catalyst in each reactor. The operating conditions of a modern medium-pressure unit are given in Table 1.6.

Table 1.6. Operating conditions for a semi-regenerative medium pressure unit.

H_2/HC inlet	Reactor			
	1	2	3	Total
Inlet temperature [°C]	485	485	485	
Exit temperatur [°C]e	395	440	460	
Average pressure [barg]	12	11	9	
WHSV per reactor [h^{-1}]	8	5	1.1	0.8
Percent of total catalyst charge	10	16	74	100

Reformers are operated to give a constant product octane number. As the catalyst is deactivated, the reactor temperature is gradually increased. The temperature increase during a cycle may be in the range of 20-40 degrees and the coke content of the catalyst may reach levels of 10-40 wt%. The decline in reformate yield in the cycle, if any, depends heavily on the catalyst stability (coke amount and coke tolerance).

1.4 Outlook

1.4.1 Reforming and the Environment

In the recent decades it has become clear that the rapid utilisation of hydrocarbons as fuels are associated with strong environmental concerns. The inevitable

formation of CO_2 upon combustion is recognised as a global problem and is a driving force for the development of more efficient engines and alternatives to hydrocarbons as fuels. The combustion of gasoline results in a number of additional emissions such as CO, NO_x, SO_x and unburned hydrocarbons. Unsaturated gasoline components (aromatics and olefins) increase the formation of exhaust particles (smog). The air pollution related to traffic cause severe health problems in highly populated areas. The exposure to gasoline vapours during handling and the possibilities of leakage during storage and transportation are other problems of consideration. The hazards of benzene exposure (carcinogenic) are known.

To meet these problems, governments have progressively implemented stronger regulations on the specifications of gasoline and other fuels. Exhaust catalysts have been introduced to reduce emissions of CO and NO_x. Tetraethyl lead is being phased out as an octane booster as it is both an unwanted contaminant and because it poisons the exhaust catalysts. Both volatility and end boiling points in gasoline are being reduced and maximum levels of benzene, sulfur, total olefins and total aromatics are set. In the US, the Clean Air Act Amendments forced refiners to add minimum levels of oxygen (as oxygenates) to the fuel in order to reduce emissions of unburned hydrocarbons. The most common oxygenate was methyl tert butyl ether (MTBE) which has a high octane number (RON 120). Ethanol (RON 99) is used to a lesser extent. Table 1.7 outlines the gasoline specifications in the US, the European Union and in Japan for year 2000 and 2005.

Table 1.7. Gasoline specifications for the US, the European Union and Japan [74-76].

Specifications	USA	EU		Japan
Max. values	2000	2000	2005	2000
RVP [kPa]		60		78
S [wppm]	50	150	50	100
O [wppm]	2.2	2.7		
Benz. [vol%]	1.0	1		1
Arom. [vol%]	35	45	35	
Olef. [vol%]	15	18		
Lead (max.) [g/l]	-	0.005	-	

The new regulations will have great impact on reformers operating conditions and refineries configuration. Reid vapour pressure constraints will result in eliminating butanes from gasoline. Reduction of the benzene content can be achieved by processing the C_6 fraction by isomerization, by choosing reaction conditions disfavouring aromatics dealkylation (cracking) or by fractionation of the reformate. With aromatics being the main product from catalytic reforming and contributing most to the octane enhancement, aromatics reduction requires high amounts of other high-octane gasoline blending stocks. The alkylation and oligomerisation processes will likely become more important in the future, as the product is purely paraffinic, sulphur free and with high octane ratings. Olefins reduction sets an upper level of the amount of cracker naphtha as blending stock. Cracker naphtha is also practically the only source of sulphur in gasoline and the new specifications will require increased CCR hydroprocessing capacity. The use of MTBE, especially in the US, as an oxygen source and octane booster has been necessary in order to fulfil the specifications for unleaded gasoline. However, the high stability and high solubility of MTBE in water was not anticipated by the

industry and USA is faced with groundwater contamination due to unavoidable leakage. Odour and taste problems and questions regarding the toxicity of MTBE are about to ruin a number of large drinking water reserves. The use of MTBE is likely discontinued within two or three years. As a new main source of oxygen, other compounds such as methyl carbonate and ethanol (used in parts of the world already), will have to be considered.

1.4.2 Reforming Outlook

The demand for aromatics for the petrochemical industry (BTX) and for high-octane gasoline will increase, especially in the developing countries of the world. Because of gasoline regulations, the importance of the reforming process as a gasoline supplier will be reduced. However, refineries are dependent on the valuable hydrogen produced by reforming for hydroprocessing purposes. In the future, gasoline-range components in the crude oil (naphtha) will likely be fractionated and the different components converted by various processes according to their potentials. For instance, the isomerization reaction equilibria favoured by low reaction temperatures have suffered in the reforming process. Although the reforming process and the reforming catalysts are considered mature, the research for more stable and more selective catalysts will continue. Advanced research instrumentation gives a better understanding of the chemistry involved. New speciality materials with strong shape selective properties (such as zeolites) may have potentials as future catalysts.

The main purpose of catalytic reforming is to produce high-octane gasoline components. Due to environmental concern of the ever-increasing number of cars, focus is recently been put on fuel cell cars using H_2 as the fuel. H_2 is a clean and very efficient energy carrier and is by many believed to be the fuel of the future. H_2 can be produced from a number of sources including water, but it is most likely that oil and gas will be the main source of H_2. H_2 can be produced in large units, filled and stored onboard the vehicle or it can be produced onboard by reforming of liquid fuels such as methanol or straight run gasoline. In any case such a development will have a great impact on the refinery configuration and in particular on catalytic reforming.

Acknowledgements

References

1   International Petroleum Encyclopedia, vol 32. (Penn Well Publishing Co, Tulsa, OK 1999)

2   J.H. Gary and G.E. Handwerk : *Petroleum Refining Technology and Economics*, 3 edn. (Marcel Dekker, Inc., New York 1994)

3   M. Walsh : *The Global Phaseout of Leaded Gasoline: A Successful Initiative* (1999) http://earthsummitwatch.org/gasoline.html. (Earth Summit Watch Program)

4   American Petroleum Institute Research Project 45 (1954) Sixteenth Annual Report

5   G.A. Mills, H. Heinemann, T.H. Milliken and A.G. Oblad, Ind.Eng.Chem **45**, 134 (1953)

6   Z. Paal, J. Catal. **105**, 540 (1987)

7   P.B. Weisz and E.W. Swegler, Science **126**, 31 (1957)

8   F.D. Rossini, K.S. Pitzer, R.L. Arnett, R.M. Braum and G.C. Pimentel : *API Research Project 44: Selected Values of Physical and Thermodynamic Properties of Hydrocarbons and Related Compounds.* (Carnegie Press, Pittsburgh 1953)

9   K. Moljord, H.G. Hellenes, A. Hoff, I. Tanem, K. Grande and A. Holmen, Ind. Eng. Chem.Res., **35**, 99-105 (1996)

10   P.A.Van Trimpont, G.B. Marin, G.F. Froment, Ind. Eng. Chem.Res, **27**, 51 (1988)

11   W.S. Kmak, A.N. Stuckey: Powerforming Process Studies with a Kinetic Simulation Model (Paper N0. 56a), AIChE National Meeting, New Orleans, March 1973.

12   J.P. Boitiaux, J.M. Devés, B. Didillon and C.R. Marcilly : Catalyst Preparation, in *Catalytic Reforming of Naphtha*, G.J. Antos, A.M. Aitani, and J.M. Parera (Eds.) (Marcel Dekker, Inc., New York 1995)

13   N.Y. Chen and W.E. Garwood, J. Catal. **52**, 453 (1978)

14   C.J. Plank, E.J. Rossininski and E.N. Givens (1973): US Patent US 4,141,859.

15   N.Y. Chen (1973): US Patent 3,729,409.

16   J.B. Peri, The Journal of Physical Chemistry **69**, 211 (1965)

17   J.B. Peri, The Journal of Physical Chemistry **69**, 220 (1965)

18   J.B. Peri, The Journal of Physical Chemistry **69**, 231 (1965)

19   H. Knözinger and P. Ratnasamy, Catal.Rev.-Sci.Eng. **17**, 31 (1978)

20   B.C. Gates, J.R. Katzer and G.C.A. Schuit : *Chemistry of Catalytic Processes.* (McGraw-Hill inc., New York 1979)

21   P.H. Emmet : *Catalysis. Alkylation, Isomerization, Polymerization, Cracking and Hydroreforming*, vol VI. (Reinhold Publishing Corporation, New York 1958)

22   G.A. Somorjai and J. Carrazza, Ind. Eng. Chem. Fundam. **25**, 23 (1986)

23   J. Barbier, G. Corro, Y. Zhang, J.P. Bournonville and J.P. Franck, Appl. Catal. **13**, 245 (1985)

24   R. Prestvik, B. Tøtdal, C.E. Lyman and A. Holmen, J. Catal. **176**, 246 (1998)

25   C.E. Lyman, J.I. Goldstein, D.B. Williams, D.W. Ackland, S. von Harrach, A.W. Nicholls and P.J. Statham, Journal of Microscopy **176**, 85 (1994)

26   C.R. Adams, H.A. Benesi, R.M. Curtis and R.G. Meisenheimer, J. Catal. **1**, 336, (1962)

27   J.E. Benson and M. Boudart, J. Catal. **4**, 704, (1965)

28   R. Prestvik : Characterization of the metal function of a Pt-Re/Al2O3 reforming catalyst, Doctor of Engineering Dissertation, The Norwegian Institute of Technology (1995)

29   H.E. Kluksdahl: U.S. Patent 3415737 (1968).

30   R.E. Rausch: U.S Patent 694872 (1977)

31   J.H. Sinfelt: U.S. Patent 3953368 (1976)

32   G.J. Antos: U.S. 803693 (1978)

33   J. Beltramini and D.L. Trimm, Appl. Catal. **32**, 71 (1987)

34   W.M.H. Sachtler, J.Mol.Catal. **25**, 1 (1984)

35   A.S. AlKabbani, Hydrocarbon Processing, July 1999, 61 (1999)

36   S.M. Augustine, G.N. Alameddin and W.H.M. Sachtler, J. Catal. **115**, 217, (1989)

37   Y.I. Yermakov and B.N. Kuznetsov, J.Mol.Catal. **9**, 13 (1980)

38   R.J. Bertolacini and R.J. Pellet : The function of Rhenium in Bimetallic Reforming Catalysts, in *Catalyst Deactivation* (Elsevier Scientific Publishing Company, Amsterdam 1980) pp. 73-77

39   D.R. Short, S.M. Khalid and J.R. Katzer, J. Catal. **72**, 288 (1981)

40   F.H. Ribeiro, A.L. Bonivardi and G.A. Somorjai, Catal. Lett. **27**, 1 (1994)

41   V.K. Shum, J.B. Butt and W.H. Sachtler, J. Catal. **96**, 371 (1985)

42   A. Bensaddik, A. Caballero, D. Bazin, H. Dexpert, B. Didillon and J. Lynch, Appl. Catal. **162**, 171 (1997)

43   P. Biloen, J.N. Helle, H. Verbeek, F.M. Dautzenberg and W.M.H. Sachtler, J. Catal. **63**, 112 (1980)

44   C.G. Michel, W.E. Bambrick and R.H. Ebel, Fuel Processing Technology **35**, 159 (1993)

45   J. Biswas, G.M. Bickle, P.G. Gray, D.D. Do and J. Barbier, Catal.Rev.-Sci.Eng. **30**, 161 (1988)

46   F.M. Dautzenberg, J.N. Helle, P. Biloen and W.M.H. Sachtler, J. Catal. **63**, 119 (1979)

47   R. Burch, J. Catal. **71**, 348 (1981)

48   B. Coq and F. Figureras, J. Catal. **85**, 197 (1984)

49   Y.-X. Li and K.J. Klaubunde, J. Catal. **126**, 173 (1990)

50   Z. Paál, A. Gyóry, I. Uszkurat, S. Olivier, M. Gurin and C. Kappenstein, J. Catal. **168**, 164, (1997)

51   R. Burch and L.C. Garla, J. Catal. **71**, 360 (1981)

52   B.A. Sexton, A.E. Hughes and K. Foger, J. Catal. **88**, 466 (1984)

53   J.M. Parera, J.N. Beltramini, C.A. Querini, E.E. Martinelli, E.J. Churin, P.E. Aloe and N.S. Figoli, J. Catal. **99**, 39 (1986)

54   B.H. Isaacs and E.E. Petersen, J. Catal. **77**, 43 (1982)

55   F. Hilbrig, C. Michel and G.L. Haller, The Journal of Physical Chemistry **96**, 9893 (1992)

56   C. Bolivar, H. Charcosset, R. Frety, M. Primet, L. Tournayan, C. Betizeau, G. Leclercq and R. Maurel, J. Catal. **39**, 249 (1975)

57   R. Prestvik, K. Moljord, K. Grande and A. Holmen, J. Catal. **174**, 119 (1998)

58   C. Meitzner, G.H. Via, F.W. Lytle, S.C. Fung and J.H. Sinfelt, The Journal of Physical Chemistry **92**, 2925 (1988)

59   H. Lieske and J. Volter, J. Catal. **90**, 96 (1984)

60   A. El Abed, S.E. El Qebbaj, M. Guérin, C. Kappenstein, H. Dexpert and F. Villain, J. Chim. Phys. **94**, 54 (1997)

61   C. Kappenstein, M. Guerin, K. Lazar, K. Matusek and Z. Paak, J.Chem.Soc.Faraday.Trans. **94**, 2463 (1998)

62   C. Kappenstein, M. Saouabe, M. Guérin and P. Marecot, Catal. Lett. **31**, 9 (1995)

63   J. Llorca, P. Ramírez de la Piscina, J.L.G. Fierro, J. Sales and N. Homs, J.Mol.Catal. **118**, 101 (1997)

64   G.T. Baronetti, S.R. Miguel, O.A. Scelza and A.A. Castro, Appl. Catal. **24**, 109 (1986)

65   S.M. Stagg, C.A. Querini, W.E. Alvarez and D.E. Resasco, J. Catal. **168**, 75 (1997)

66   P. Marecot and J. Barbier : Deactivation by coking, in *Catalytic Naphtha Reforming*, G.J.Antos, A.M. Aitani, and J.M. Parera (Eds.)   (Marcel Dekker, Inc., New York 1995)

67   K. Moljord, K. Grande, I. Tanem, and A. Holmen, in *Deactivation and testing of hydrocarbon-processing catalysts*, P. O'Connor, T. Takatsuka, G.L. Woolery (Eds.), ACS Symposium Series No. 634 (ACS 1995) pp. 268-282

68   J. Barbier: *Deactivation and Poisoning in Catalysis*. (Marcel Dekker, New York 1985), p.121

69   J.N. Beltramini: Deactivation by Poisoning and Sintering , in *Catalytic Naphtha Reforming*, G.J. Antos, A.M. Aitani, and J.M. Parera (Eds.)   (Marcel Dekker, Inc., New York 1995)

70   P. Franck and G. Martino: *Progress in Catalyst Deactivation*. (Martinus Nijhoff, The Hague 1982)

71   S.E. Wanke, J.A. Szymura and T.T. Yu : *Catalyst Deactivation*   (Marcel Dekker, New York 1986)

72   H. Lieske, G. Lietz, H. Spindler and J. Völter, J. Catal. **81**, 8 (1983)

73   T. Gjervan, M. Rønning, R. Prestvik, B. Tøtdal, C.E. Lyman, and A. Holmen, in *Studies in Surface Science and Catalysis*, A. Corma, F.V. Melo, S. Mendioroz, J.L.G. Fierro (Eds.), Proceedings of the 12th ICC, Granada, Spain, July 9-14 2000, Vol 130A (Elsevier, Amsterdam 2000), pp. 3189-3194

74   G. Martino: Catalysis for oil refining and pertochemistry, recent developments and future trends, in *Studies in Surface Science and Catalysis*, A. Corma, F.V. Melo, S. Mendioroz, J.L.G. Fierro (Eds.), Proceedings of the 12th ICC, Granada, Spain, July 9-14 2000, Vol 130A (Elsevier, Amsterdam 2000), pp. 83-103

75   E.L. Hartman, D.W. Hanson, B. Weber, Hydrocarbon Processing, 77 (1998)

76   Petroleum Association of Japan: Annual Review 1999 (http://www.paj.gr.jp/html/english/index.html)

The Application of Zeolites in Catalysis

Contents

The Application of Zeolites in Catalysis

Roger Gläser and Jens Weitkamp

Institute of Chemical Technology
University of Stuttgart, 70550 Stuttgart, Germany
jens.weitkamp@po.uni-stuttgart.de

Abstract. In this chapter, the most important applications of zeolite catalysts in the refining and petrochemical industries are highlighted. In an introductory section, the key features of zeolites and the methods for tailoring their properties related to their application as catalysts are briefly discussed. A short overview of the preparation of synthetic zeolites is also included. One major section deals with zeolite applications in petroleum refining. Processes such as catalytic cracking, isomerisation of light gasoline and light alkenes, isobutane alkylation and conversion of methanol to gasoline or olefins are addressed. The versatility of zeolite catalysts is reflected in the section on applications in petrochemistry. Here, the manufacture of alkylaromatics as well as oxidation, ammoxidation and amination reactions are treated.

1. Introduction

Since the early 1960s the application of zeolites in heterogeneous catalysis has been continuously expanding. Nowadays, a plethora of chemical reactions has been found to benefit from zeolite catalysis. It was the availability of phase-pure, synthetic zeolites through the pioneering work of *Barrer* and *Milton* that enabled researchers to systematically investigate zeolites as solid catalysts in a variety of chemical conversions. Above all, the introduction of the synthetic zeolites X and Y in the fluid catalytic cracking (FCC) process in 1962 marked the beginning of industrial zeolite catalysis which has nowadays found numerous applications, mainly in petroleum refining and petrochemistry. Beside those traditional areas, new applications of zeolite catalysts, *e.g.*, in the manufacture of organic intermediates and fine chemicals, are steadily emerging. Although zeolites as multifunctional materials are increasingly utilized in other areas, such as sensor or membrane technology, their main application – especially in terms of financial market size - still lies in heterogeneous catalysis.

This review covers the basic principles of zeolite catalysis including a short outline on zeolite synthesis and the methods of post-synthesis modification. Due to the intense research efforts in the past decades some areas of catalysis by zeolites have reached a certain level of maturity, and a wealth of scientific studies and numerous reviews and textbooks are devoted to zeolite catalysis [1-4]. An exhaustive and comprehensive treatment of zeolite-catalyzed reactions on the limited number of pages allotted to this contribution is therefore impossible, nor is it intended. Instead, the most prominent and important examples for zeolite applications in industrial catalysis have been selected and serve to demonstrate the

versatility of zeolites as solid catalysts. For more details, the reader will be referred to original works or review articles in the corresponding sections.

2.   Nomenclature (what is a Zeolite?)

According to a widely accepted definition given by *Barrer* [5] and *Breck* [6], zeolites are crystalline aluminosilicates with a negatively charged macromolecular inorganic framework. This framework is comprised of intracrystalline channels and voids with characteristic geometry and architecture which contain freely mobile and exchangeable cations for charge compensation and reversibly adsorbed water. The general formula

$$Me_{x/z}[(AlO_2)_x(SiO_2)_y] \cdot n\, H_2O$$
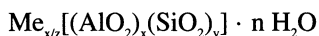
reflects the chemical composition of zeolites, where Me stands for a metal cation with the positive charge z. The three-dimensional network consists of neutral $SiO_{4/2}^-$ and negatively charged $[AlO_{4/2}]^-$-tetrahedra (generally $TO_{4/2}$) that share common oxygen atoms. The density of negative charges on the framework is consequently determined by its aluminum content $(x/(x+y))$ or the framework n_{Si}/n_{Al}-ratio. Due to charge density restrictions, two $[AlO_{4/2}]^-$ tetrahedra cannot be directly adjacent, and the n_{Si}/n_{Al}-ratio is, hence, always ≥ 1 (*Löwenstein*'s rule [7]).

The structure of zeolites can be thought of to be generated by connecting the $TO_{4/2}$-tetrahedra as the primary building units via oxygen bridges to so-called secondary building units (SBU) which typically represent cages within the zeolite structure. Some of these SBUs, such as the sodalite or the pentasil units, are displayed in Figure 1 in a way that the vertices represent the T-atoms of the primary $TO_{4/2}$-units and two adjacent $TO_{4/2}$-units are linked via their common O-atom along the connecting line. Further linking of the SBUs leads to tertiary building units, *e.g.*, layers, which are eventually connected to generate the zeolite structure with its characteristic pore system. For example, the 14 $TO_{4/2}$-tetrahedra of the pentasil unit are first connected to chains, then, by mirror imaging of those chains, to planes which are finally stacked together to form the framework structure of zeolite ZSM-5 and its all-silica ($n_{Si}/n_{Al} = \infty$) analogue silicalite-1. Two systems of intersecting pores, one being straight the other sinusoidal, make up the three-dimensional channel structure of this zeolite. The cross section of the pores of zeolite ZSM-5 is confined by a ring of 10 $TO_{4/2}$-tetrahedra, ZSM-5 is therefore referred to as a 10-membered-ring zeolite. Other zeolite structures have unidimensional systems of parallel pores such as zeolites ZSM-22 or ZSM-12 (Figure 1). A broad structural diversity of geometries and dimensions of pores, channels or cages in zeolite structures exists which is addressed in the following section (*vide infra*).

According to the classification of *Liebau et al.* [8,9], zeolites, which are members of the family of tectosilicates, represent one of two sub-classes of the porolites (or porosiles for the purely siliceous analogues) beside the clathralites the windows of which are formed by six $TO_{4/2}$-tetrahedra.
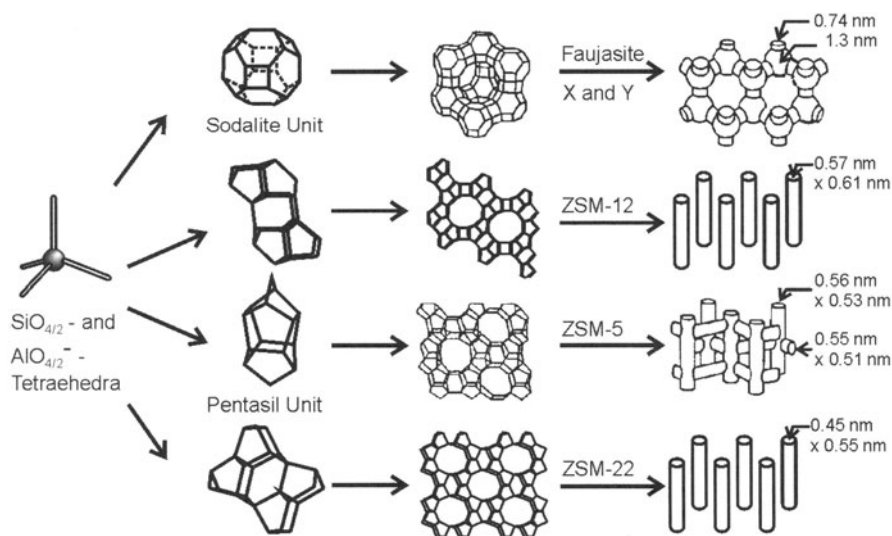
Fig. 1. Structures of four selected zeolites (from top to bottom: faujasite or zeolites X,Y; zeolite ZSM-12; zeolite ZSM-5 or silicalite-1; zeolite Theta-1 or ZSM-22) and their micropore architecture and dimensions.

Among the unique features of zeolites compared to more conventional catalysts or catalyst supports are (i) their strictly uniform pore diameter and (ii) their pore width in the range of molecular dimensions. This uniform pore diameter of zeolites in the micropore range ($d_p \leq 2.0$ nm) is depicted for selected zeolites in Figure 2 as opposed to the broad pore size distribution of two typical macroporous solids ($d_p > 50$ nm), *i.e.*, silica gel and activated charcoal. Also shown is the pore width of the recently discovered M41S family of materials [10], the most prominent example being MCM-41 with a hexagonal array of parallel channels, the diameter of which lies in the mesoporous range (2.0 nm $\leq d_p < 50$ nm). While the pore size distribution of each individual member of the M41S-type materials is comparably narrow as that of zeolites, the pore diameter can be adjusted over the indicated range via proper choice of the synthesis conditions. The term "mesoporous zeolites" that has been used for this class of solids is, however, imprecise in that, despite the regularly ordered pore system, the pore walls are amorphous in contrast to those of the crystalline zeolites.

As a major consequence of their pore width in the order of molecular dimensions, zeolites can act as "molecular sieves", a notion introduced by *McBain* in 1932 [11] and meant to describe that only molecules up to a given size can enter the voids inside a given zeolite. At the same time, these spatial constraints inside the zeolite pores enable shape-selective catalysis, a principle on which numerous industrial processes are based (*cf.* section 4).

Almost 250 years after the term "zeolite" has been coined by *Cronsted* [12], it is nowadays used in a much broader sense. Beyond the definition given above, it
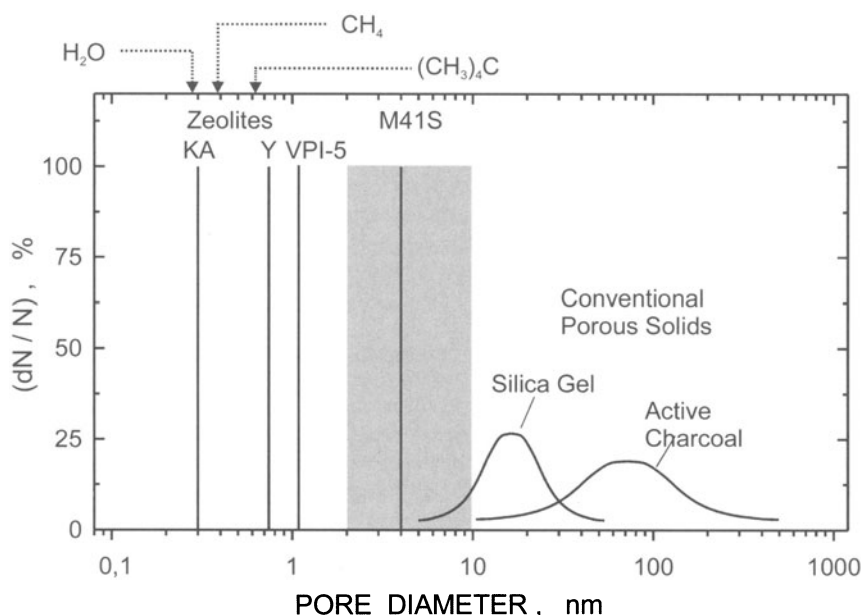
Fig. 2. Typical pore diameter distributions of porous solids (K-A is the K^+ form of zeolite A, VPI-5 is a microporous aluminophosphate with 18-membered-ring pores; for the description of M41S materials see text). For comparison, the kinetic diameters of water, methane and neopentane are also indicated.

encompasses the aluminum-free pure silica analogues of the zeolites as well as alumino- or gallophosphates with zeolite-like framework structures. Also included are crystalline porous silicates in which the T-atoms of a zeolite network are isomorphously substituted by other elements than Al, such as B, Ga, Ge, P, Ti, Fe, V or Co. All these zeolite-related materials containing elements other than silicon and aluminum are sometimes referred to as "zeotypes" after *Dyer* [13]. The regular array of micropores with well defined dimensions is the unifying principle which renders this wealth of materials attractive for catalysis (and other applications).

3.   Broad Variety of Zeolite Structures Available Today

A broad variety of zeolite structures is known today including, beside those of merely synthetic materials, also those of the naturally occurring zeolite minerals. The number of reported zeolite structures is steadily growing as new synthetic strategies are being developed and computer-assisted techniques allow the analysis of increasingly complex structures and suggest hypothetical, but yet unknown topological frameworks [14]. 98 structures are included in the 1996 issue of the *Atlas of Zeolite Structure Types* [15], and an additional 35 structures

have up to date (January 2001) been approved by the Structure Commission of the International Zeolite Association (IZA). This commission maintains a database of zeolite structures providing detailed crystallographic information on the internet [16]. In the course of their discovery, synthetic zeolites have been labelled in different ways, *e.g.*, after isostructural minerals (faujasite, mordenite, ferrierite), alphabetically (zeolites A, X, Y or Alpha, Beta, Omega) or by acronyms of the academic or industrial laboratory where they have first been synthesized (ZSM (Mobil), EU (Edinburgh University, ICI), SSZ (Chevron)) followed by a running number. Zeolites with different names may therefore have the same structure. For unification the Structure Commission of the IZA has assigned each of the approved structures a mnemonic three-letter code such as MFI for zeolite ZSM-5 and silicalite-1 or FAU for zeolites X and Y (isostructural to the mineral faujasite).

Rather than the exact crystallographic topology, it is the architecture and the spaciousness of the pore system of a zeolite that is of prime importance for its catalytic performance. First of all, the pore width decides which molecules will be able to enter the intrazeolitic voids. Figure 3 shows the range of the crystallographic pore width in dependence of the number of tetrahedra that form the ring circumscribing the pore. In cases of structures with different pore systems or deviations of the cross section from circular, the largest pore diameter is indicated. The total number of zeolite structures with the respective number of ring atoms is also given in the Figure. The vast majority of zeolites has pores confined by 8-, 10- or 12-membered rings, referred to as narrow, medium or large pores, applications, because virtually all species involved in chemical reactions do not fit through the narrow pore apertures. Super-large pores with more than 12-membered rings have so far not been observed with aluminosilicate zeolites, but
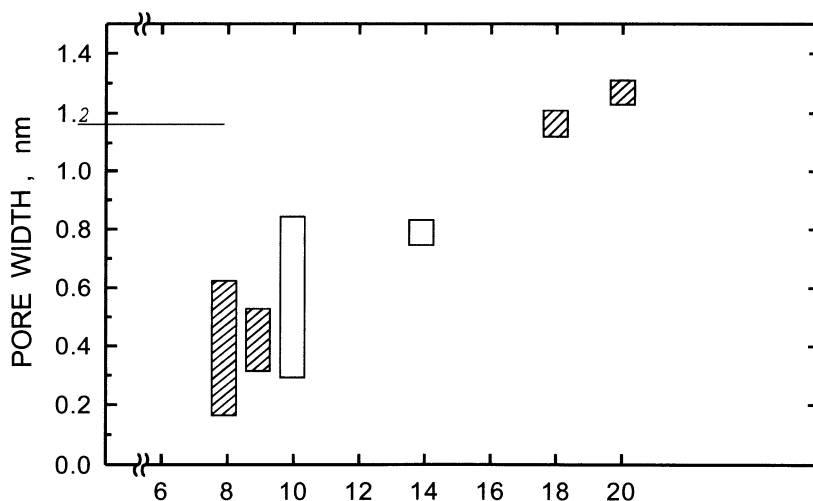
Fig. 3. Range of crystallographic pore diameters of zeolites approved by the Structure Commission of the International Zeolite Association (IZA) [16].

only with alumino- or gallophosphates such as $AlPO_4$-8 (14-membered rings), VPI-5 (18-membered rings) or cloverite (20-membered rings). Generally, it should be noted that under conditions of catalytic conversions the zeolite lattice is often very flexible and dynamic so that the effective pore width may considerably exceed the crystallographic one. Beside the pore diameter also the dimensionality as well as the spaciousness or particular local constraints within the pore system exhibit an important influence on catalytic processes. Especially the catalytic potential of zeolites with intersecting channels or cavities of different diameters like NU-87, EU-1 or SSZ-24 have yet been explored only scarcely [17].

4. Properties of Zeolites that Render them Attractive as Catalysts

One of the main properties that make zeolites attractive catalysts for a broad spectrum of chemical conversions is their high thermal stability. While most zeolites remain intact at temperatures up to *ca.* 650 °C, structural collapse of some high-silica zeolites only occurs at temperatures above 1000 °C [18]. In the following, three further key properties of zeolite catalysts, namely acidity, shape selectivity and the concentration effect, will be briefly addressed.

4.1   Acidity

The increased acidity of zeolites compared to amorphous silica-alumina catalysts has been an important factor for their successful use in industrial catalytic applications. For an unambiguous description of the solid-state acidity of zeolites a clear distinction of the following parameters is required:

- the *nature* (or type) of the acid sites, *i.e.*, Brønsted *versus* Lewis acidity,
- the *density* (or concentration or, less precisely, the number) of the acid sites,
- the *strength* (or, more precisely, the strength distribution) of the acid sites,
- the *location* of the acid sites within the zeolite framework (accessibility for reactants) and at the external *versus* internal surface and
- the geometric *distribution* of the acid sites over the zeolite crystal.

Both Brønsted and Lewis acid sites occur in zeolites. As clearly shown by *Jacobs* [19] and *Karge* [20] using IR spectroscopy, it is now established that the strong Brønsted acid sites are bridging OH-groups consisting of hydroxyl protons associated with framework oxygen ions bonded to negatively charged tetrahedrally coordinated framework aluminum (SiOHAl). The maximum density of those acid sites is therefore directly related to the charge density of the polyanionic zeolite framework, *i.e.*, to the n_{Si}/n_{Al}-ratio. As the density of aluminum atoms in the zeolite framework increases (*i.e.*, the framework n_{Si}/n_{Al}-ratio decreases), the strength of the Brønsted acid sites decreases. Quantum chemical calculations indicate that this effect has its origin in the lower electronegativity of aluminum *versus* silicon atoms in the vicinity of a given Al-OH group (concept of the next nearest neighbors, NNN [21]). Thus, an isolated Al-OH surrounded by

silicon atoms only is predicted to have the highest acid strength. Consequently, the variation of the density of aluminum atoms in the zeolite framework represents an important tool to adjust the strength and density of acid sites in zeolite catalysts. Similarly, the acid strength may be tuned (in most cases lowered) by incorporating other trivalent elements such as B, Ga or Fe in the zeolite framework or by exchanging cations on extra-framework positions at constant n_{Si}/n_{Al}-ratio. It is also obvious, that the bond angles of the Si-O-Al bonds, *i.e.*, the zeolite structure and the crystallographic position of the atom bearing the OH-group, exhibit an influence on the acid strength, although this is less pronounced than that of the n_{Si}/n_{Al}-ratio [22].

The most important ways to generate Brønsted acid sites in zeolites are through ion exchange (see sub-section 6.1). The cations present in a zeolite can be directly exchanged by protons only, if the zeolite is sufficiently resistant to aqueous mineral acids. In many instances, however, mineral acid treatment causes framework dealumination or even structural collapse. Preferably, an ion exchange with aqueous ammonium salt solutions is applied followed by a thermal decomposition of the ammonium ions in order to yield the proton form of the zeolites according to

$$NH_4^+ + Na^+Z^- \quad \underset{-Na^+}{\rightarrow} \quad NH_4^+Z^- \quad \underset{-NH_3}{\overset{\approx 300-400°C}{\rightarrow}} \quad H^+Z^- . \tag{1}$$
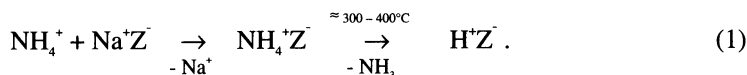
Brønsted acid sites are also obtained by ion exchange of a multivalent cation like, *e.g.*, La^{3+}, Mg^{2+}, Ca^{2+}, with subsequent partial dehydration of the coordination sphere of the metal cation at elevated temperature. Under the influence of the strong electrostatic fields of the dehydrated cation, the last water molecules remaining coordinated dissociate into a proton bonded to the zeolite framework and a hydroxide ion still bonded to the metal. This pathway of acid site formation is known as the Hirschler-Plank mechanism [23,24].

$$[La(H_2O)_n]^{3+} + 3 Na^+Z^- \quad \underset{-3 Na^+}{\rightarrow} \quad [La(H_2O)_n]^{3+} (Z^-)_3 \quad \underset{-(n-2) H_2O}{\overset{\approx 300°C}{\rightarrow}}$$

$$[(LaOH)(H_2O)]^{2+} H^+ (Z^-)_3 \quad \rightarrow \quad [La(OH)_2]^+ (H^+)_2 (Z^-)_3. \tag{2}$$
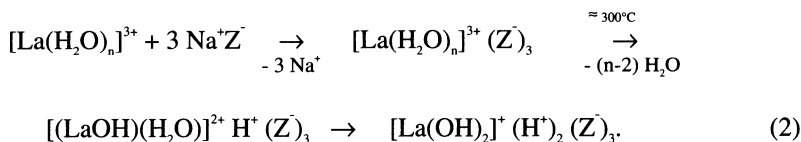
When a noble metal cation is reduced by hydrogen, *e.g.*, during the preparation of a bifunctional zeolite catalyst, Brønsted acid sites are formed inevitably (eq. (3)).

$$[Pt(NH_3)_4]^{2+} + 2 Na^+Z^- \quad \underset{-2 Na^+}{\rightarrow} \quad [Pt(NH_3)_4]^{2+} (Z^-)_2 \quad \underset{-4 NH_3}{\overset{\approx 300°C}{\rightarrow}}$$

$$Pt^{2+} (Z^-)_2 \quad \overset{+H_2}{\rightarrow} \quad Pt^0 2 H^+ Z^- . \tag{3}$$
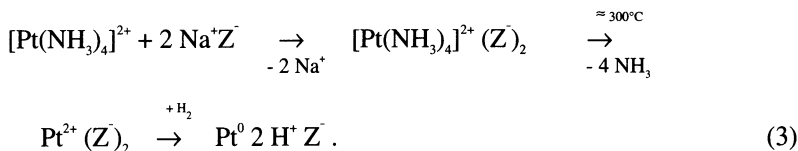
Lewis acid sites in zeolites are usually formed upon heating the proton forms to temperatures above *ca.* 500 °C where the cleavage of water from the zeolite surface occurs ("dehydroxylation"). As proposed by *Kühl* [25] and later confirmed by IR spectroscopic measurements [26] the true Lewis acid sites are represented by $[AlO]^+$ units which are removed from the zeolite lattice upon heating.

Zeolites with basic sites are also available today, and an increasing amount of investigations are concerned with this topic [27,28]. Basic sites can, for instance, be generated by oxide clusters of alkali metals that are introduced into the zeolites by ion exchange of alkali metal ions or by impregnation of the zeolite with alkali metal salts followed by thermal treatment.

A multitude of techniques for the characterization of zeolite acidity have been applied. Among these are titration techniques, temperature-programmed desorption of preadsorbed bases and microcalorimetry [29]. Spectroscopic methods like IR- and MAS NMR- spectroscopy also provide most valuable information on the acidity of zeolite catalysts which is covered in an excellent recent review [30]. Continuous progress is also being made in the modeling and description of acid sites in zeolites by quantum chemical methods [31,32]. Since the catalytic activity of zeolites in hydrocarbon conversions is directly correlated to their acidity (density and strength of Brønsted acid sites) the catalytic activity of a zeolite in a test reaction can be exploited as a measure for its acidity. As test reactions, the disproportionation of ethylbenzene [33,34] and cracking of hydrocarbons, *e.g.*, n-hexane (Alpha-test) [35,36], have been recommended depending, *inter alia*, on the pore width of the zeolites to be evaluated.

Due to their crystallographically defined positions the acid sites are often uniformly distributed over the zeolite crystallites. It may, occasionally, occur that the framework aluminum atoms and, hence, the acid sites, are concentrated in regions close to the external surface or, conversely, at the center of the zeolite crystals ("zoning").

4.2   Shape Selectivity

The fact that the dimensions of the species involved in chemical reactions are of the same order of magnitude as those of the pores and cavities of zeolites often imposes a strong influence on the selectivity of zeolite-catalyzed reactions. A catalytic reaction proceeds in a shape-selective manner, if its selectivity depends unambiguously on the pore width or pore architecture of the solid catalyst [37]. Shape selectivity is a unique feature of heterogeneous catalysis by zeolites. Several reviews and monographs on shape-selective catalysis are available, *e.g.* refs. [4,37,38].

Whether or not shape selectivity occurs in a particular case, does not only depend on the pore system of the zeolite catalyst, but also on the dimensions of the species involved, *i.e.*, the reactant molecules, the products molecules, the reaction intermediates and the transition states. After the classical concept of *Weisz* [39] and *Csicsery* [40] shape selectivity effects are usually classified into the three different types exemplified in Figure 4.

Reactant Shape Selectivity

This case of shape selectivity is encountered, if only those reactant(s) can be converted that are of proper size to enter the intrazeolitic pores. Consequently, the reaction is selective towards the conversion of slim and slender reactant molecules, whereas bulkier molecules that cannot diffuse into the zeolite pores are excluded from being converted.

Product Shape Selectivity

When a chemical reaction inside a zeolite leads to products of different molecular size, the diffusion of the smaller product molecules out of the zeolite pores will be preferred, and only this product may be detected in the reactor effluent. The other product which is too bulky to leave the zeolite pores may undergo consecutive reactions to either smaller molecules or to higher molecular species that remain adsorbed in the zeolite, eventually leading to catalyst deactivation by pore blockage. Product shape selectivity may be viewed as the reverse of reactant shape selectivity.

Restricted Transition State Shape Selectivity

Under the local constraints inside a zeolite pore one reaction may be favored over other parallel or consecutive reactions, if the corresponding transition state (or intermediate) is less bulky. For instance, the pores of a zeolite may provide sufficient space for the transition state of the intramolecular isomerisation of meta-xylene, while the transition state of the bimolecular transalkylation reaction is too bulky to be accommodated inside the pores and, hence, no disproportionation products can be formed (Figure 4).

   From the above definitions it is obvious that both reactant and product shape selectivity are based on mass transfer effects, *i.e.*, the diffusion into or out of the zeolitic pore system. Restricted transition state shape selectivity, by contrast, results from intrinsic chemical effects due to the steric demand of the transition state (or intermediate) in the confined environment of the intrazeolitic voids. In contrast to the latter the extent of reactant and product shape selectivity depends on the diffusion path length, *i.e.*, the size of the zeolite crystallites.

   The progress in catalysis by zeolites and related microporous materials has also brought about many new examples for shape selectivity effects. Thus, the utilization of shape selectivity is no longer restricted to acid-catalyzed hydrocarbon conversions, but applications in redox reactions [42] and photochemistry [43] have been reported as well. Similarly, the sophistication of the utilization of shape selectivity effects in catalysis by zeolites has been considerably increased, on the one hand, by the availability of an increasing number of zeolites with different pore geometries and structures and, on the other hand, by the improvement of post-synthetic modification techniques which allow the tailoring of pore sizes (pore size engineering), such as ion exchange or chemical vapor deposition (*cf.* section 6).

   The effective pore width of zeolite catalysts under operating conditions can be probed by exploiting the effects of shape selectivity. Several hydrocarbon conversions have been thoroughly investigated for this purpose and may be recommended as test reactions depending, for instance, on the range of the pore diameter and on the nature of the catalyst (mono- or bifunctional) to be evaluated [41].

REACTANT SHAPE SELECTIVITY

PRODUCT SHAPE SELECTIVITY

RESTRICTED TRANSITION STATE SHAPE SELECTIVITY
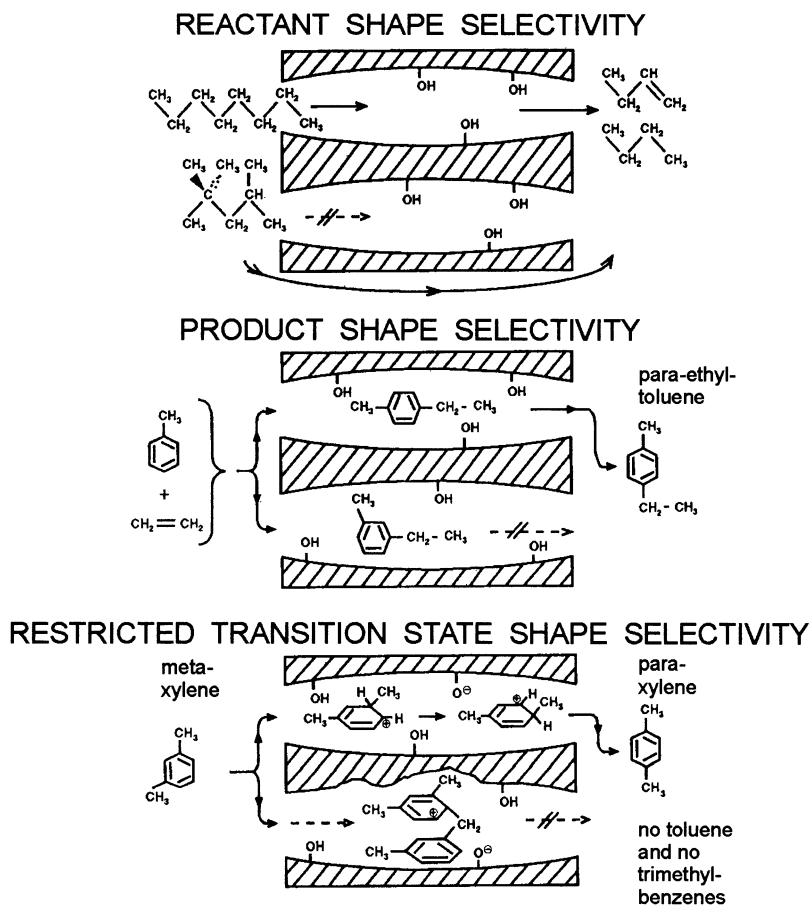
Fig. 4. Classification of shape selectivity effects in zeolite catalysis after *Weisz* and *Csicsery*, adapted from ref. [41].

In extension of the classical idea of shape selectivity according to *Weisz* and *Csicsery*, some new concepts have evolved to explain more recent research results of zeolite catalysis. These include the cage or window effect, inverse or secondary shape selectivity, molecular traffic control and keylock or pore mouth catalysis. A critical discussion of these concepts may be found in ref. [37].

4.3   The Concentration Effect

At variance to catalytic conversions in homogeneous phases the concentration of reactants at or near the catalytically active sites on solid catalysts is dependent on adsorption equilibria. Adsorption capacity and affinity on zeolites is widely determined by their specific pore volume and by the hydrophilic/hydrophobic properties of the internal surfaces. At the maximum loading, which is reached with zeolites already at comparably low relative pressures of the adsorptives, the adsorbate is often present in a "concentrated", liquid-like state filling the accessible pore volume of the zeolite. A reactant adsorbed inside a zeolite catalyst may therefore experience - in addition to the electrostatic fields of the inorganic zeolite framework - a reaction environment resembling that of a liquid phase at high pressure. This effect has been convincingly demonstrated by the rate enhancement of Diels-Alder reactions if conducted in zeolite catalysts, *e.g.*, the cyclodimerization of butadiene [44]. Other effects of the surface concentration of reactants or products on zeolite surfaces may also be used to direct the selectivity of a catalytic conversion. For instance, alcohols have been added as co-adsorbents to the cyclohexanone oxime feed in the zeolite-catalyzed Beckmann rearrangement in order to facilitate desorption of the product ε-caprolactam by competitive adsorption [45].

5.   Hydrothermal Synthesis of Zeolites

The increasing demand of zeolitic materials for industrial applications had an important impact on the development of procedures and strategies for the production of synthetic zeolites. Naturally occurring zeolites, although available in considerable amounts, almost always suffer from shortcomings preventing their application as catalysts, such as the association with other, partly amorphous, phases, the contamination with unwanted impurities or poor (hydro)thermal stability. Moreover, the limited number of naturally available zeolite types and the narrow range of their framework compositions, crystallite sizes and morphologies call for synthetic materials with constant product quality and properties sensibly tailored towards the particular catalytic application. This section gives a short overview of hydrothermal zeolite synthesis and exemplifies the industrial production of faujasite and zeolite ZSM-5 which are by far the most important zeolites from the viewpoint of catalysis.

5.1   General Aspects

Hydrothermal synthesis is by far the most important route to zeolitic materials, both on the laboratory and on the industrial scale. The general conditions closely resemble those of the formation of natural zeolite minerals. However, synthesis conditions are adapted to accomplish significantly faster zeolite formation, *e.g.*, by higher temperature or higher alkalinity of the synthesis mixture. For more recent approaches to zeolite synthesis including the fluoride route (fluoride ions as mineralizing agents), the crystallisation from non-aqueous solvents, the dry-gel synthesis route or the application of microwave heating, the reader is recommended to consult refs. [46-49].

Starting Compounds for Zeolite Syntheses

Since zeolite synthesis commonly involves condensation of smaller species and structural (re)orientation of loosely bonded amorphous networks, the starting compounds need to be sufficiently reactive. Typical sources of aluminum include sodium aluminate ($NaAlO_2$), aluminum salts $Al(NO_3)_3 \cdot 9\ H_2O$, $Al_2(SO_4)_3 \cdot 18\ H_2O$) or (freshly precipitated) aluminum hydroxide, and sources for silicon are sodium silicate, $e.g.$, waterglass, silicic acid, silica gel, silica sol and silicon alkoxides. In special cases, clays or other solid aluminosilicates serve as precursors for zeolitic materials. Alkali metal hydroxides or other strong bases such as ammonia are added to obtain a high pH of the synthesis mixture in the range of 10 to 14, and complex or organic cations play a vital role as structure-directing agents ($vide$ $infra$).

Typical Synthesis Procedure

The typical steps that are part of a zeolite synthesis are schematically illustrated in Figure 5. First, two or more separate reactant solutions or suspensions are prepared and slowly mixed in a defined order at low temperature. Commonly under vigorous stirring and occasionally after adjustment of the pH, a gelation process is initiated leading to an amorphous gel phase consisting either of homogeneously dispersed species (cross-linked sol particles) or of a separate solid phase (dense aggregates of sol particles). Initiated by the mineralizing agent OH^-, mono- and small oligomeric silicate units, $e.g.$, $SiO(OH)_3^-$, $SiO_2(OH)_2^{2-}$, $Si_4O_8(OH)_6^{2-}$, are liberated from the gel into the solution. Their nature and distribution depend on the pH and the total silicate concentration of the mixture. This solubilization is accompanied by a condensation of silicate species with for-mation of structurally diverse oligomers or clusters ("precursors" in Figure 5) under the influence of a structure-directing agent, if present. Such oligomers, as characterized in synthesis gels and silicate solutions by ^{29}Si NMR studies [50], are depicted in Figure 6. These oligomers are obviously precursors for the secondary building units of the zeolite frameworks ($cf.$ section 2). After homogenizing the synthesis gel as a vital step for successful zeolite preparation, the synthesis gel may be aged for a time between some hours and several days to allow for both further cross-linking and partial dissolution of the amorphous silicate framework.

For crystallisation of the solid zeolite the synthesis gel is placed in a sealed, temperature-resistant vessel. High-silica zeolites are crystallized in steel auto-claves at temperatures typically ranging from 100 to 250 °C and accordingly elevated pressure [51], whereas crystallisation of low-silica zeolites is usually carried out at lower temperatures of 70 to 100 °C [6,52] where polypropylene bottles can be used. During heating-up of the synthesis mixture an increasing amount of the gel and other oligomers formed initially at low temperature is dissolved leading to an increasing amount of silicate and aluminate anions as mono- and dimers, until eventually a high level of supersaturation is reached and crystallisation nuclei are formed by association of the silicate mono- and dimers. This nucleation process is responsible for an induction period frequently observed in zeolite formation and is decisive for the structure type of the zeolite phase that will crystallize. It is dependent, among other parameters, on the heating rate and the nature and concentration of structure directing-agents present in the solution. In some cases, for instance, when nucleation is kinetically limited or when nuclei
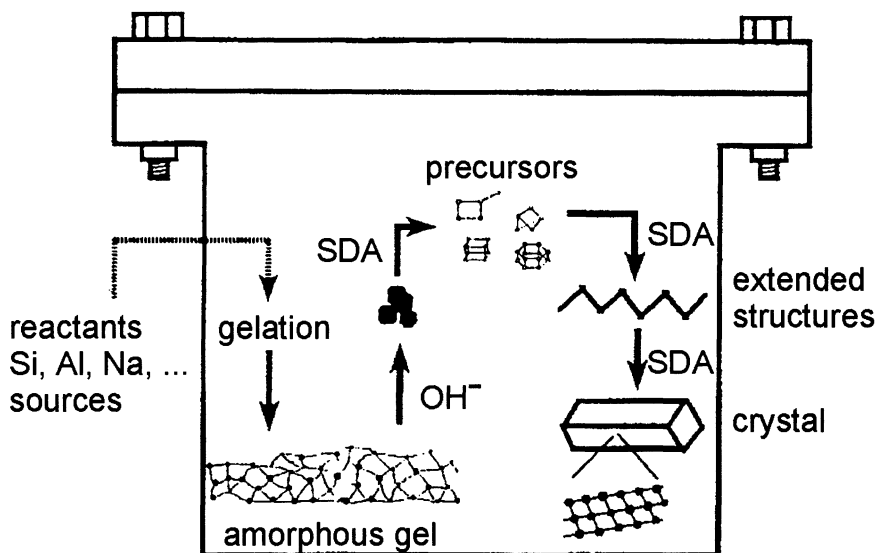
Fig. 5. Schematic representation of the steps leading to zeolite formation by hydrothermal synthesis, adapted from ref. [46].
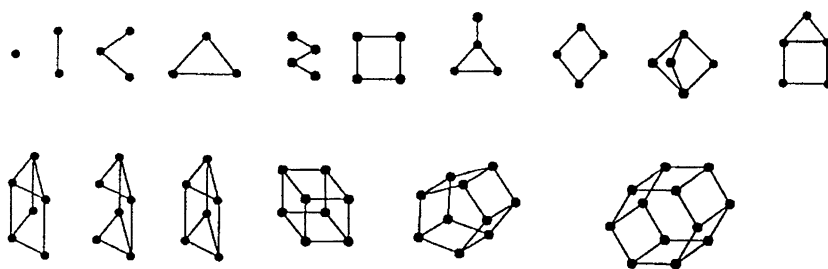
Fig. 6. Silicate oligomers characterized in solution at low temperature by ^{29}Si NMR spectroscopy [50].

leading to two or more different zeolite phases can form simultaneously, crystallisation seeds or nucleation gels are added to the synthesis gel before raising the temperature, in order to direct the crystallisation towards the desired zeolite product. After nucleation has started, extended structures are built and crystal growth occurs. Since the rate of mass transfer of primary building units to the nuclei or the expanding particles exerts an important influence on the rate of crystal growth relative to that of nucleation, crystallisation is carried out either under static or under dynamic conditions (stirring or shaking), depending on the

zeolite to be synthesized. Typical durations for the crystallisation of zeolites are in the range of one to several days.

Since zeolites are, by nature, thermodynamically metastable phases, a rapid quenching of the synthesis mixture after completion of the crystallisation period is necessary to avoid that the zeolite undergoes unwanted phase transformations. Finally, the solid product is separated from the mother liquor by filtration or centrifugation, thoroughly washed and dried. Organic molecules occluded in the zeolite during synthesis and occupying space inside the pores that needs to be available for the reactant and product molecules of a catalytic reaction are usually removed by a thermal and/or oxidative destruction (calcination). Defined conditions for this treatment are necessary in order to avoid structural collapse of the zeolite framework.

Factors Affecting Zeolite Synthesis

The *chemical composition of the synthesis gel* can be regarded to have the most important influence on the processes occurring during zeolite formation. Thus, the nucleation and crystallisation kinetics are affected by the nature and concentration of the species present in the synthesis mixture. Above all, the pH, *i.e.*, the alkalinity of the synthesis mixture is of crucial importance, since it affects dissolution and condensation rates of the intermediate species. The synthesis gel composition also exerts a strong influence on the type of zeolite being formed as well as on its properties, such as its framework n_{Si}/n_{Al}-ratio, the aluminum distribution and the crystallite size and morphology.

The composition of a synthesis gel is commonly characterized by the relative molar ratios of the components in their oxide form, although the oxides may not have been actually added to the synthesis mixture.

$$a\ Al_2O_3 \cdot b\ SiO_2 \cdot c\ M_2O \cdot d\ H_2O \cdot e\ R_2O$$

Here, M and R stand for an inorganic and an organic cation, respectively, and a, b, c, etc. represent the molar ratios with a mostly taken as unity for a reference point. It is also common to calculate particular molar ratios with a known influence on the product, for instance $n_{Al_2O_3}/n_{SiO_2}$ or n_{OH^-}/n_{SiO_2}, to characterize gel compositions. In a system with the same starting materials and under a constant set of conditions, the molar ratios of the components determine what type of zeolite can be obtained. The compositional range in which a certain zeolite type forms is called the crystallisation field of the zeolite. Frequently, such crystallisation fields are represented within triangular diagrams, as shown in Figure 7 [53]. The figure shows that the crystallisation fields for different zeolites are of different dimension and shape indicating that the composition of a gel from which a certain zeolite crystallizes can be rather narrow or broad. Note that, according to the *Löwenstein rule* (*cf.* section 2), zeolites with $n_{SiO_2}/n_{Al_2O_3} < 2$, *i.e.*, $n_{Si}/n_{Al} < 1$, do not exist and, hence, the right half of the triangular diagram displayed in Figure 7 in all instances remains empty.

The *conditions during crystallisation* mainly affect the nature of the solid product obtained and the time required for its formation. The transformation of the
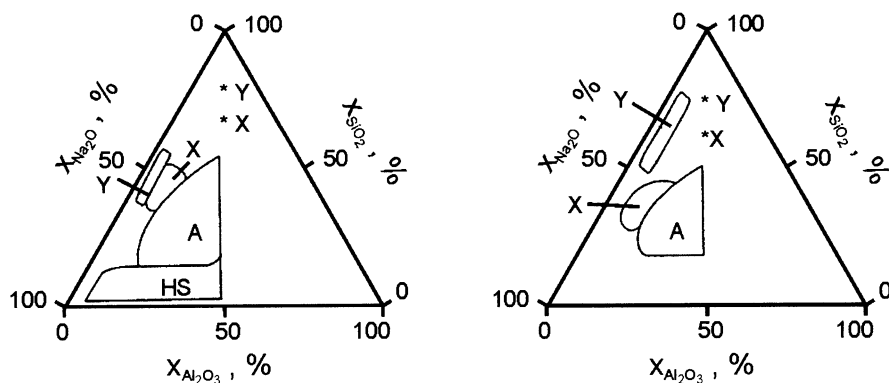
Fig. 7. Crystallisation fields for zeolites X, Y and A from the system Na_2O-Al_2O_3-SiO_2-H_2O at 100 °C and a water content of 90 to 98 mol-%, after ref. [53] (HS: hydroxysodalite; left: sodium silicate, right: colloidal silica as silica source). The asterisks represent typical zeolite product compositions.

amorphous gel into the crystalline zeolite is typically expressed in terms of an increasing relative crystallinity taking the final zeolite product as a reference. The crystallisation time must be carefully optimized for each zeolite synthesis. A prolongation of the crystallisation time often leads to unwanted phase transformations. According to *Ostwald's rule* of successive phase transformation the thermodynamically least favorable phase crystallizes first and is transformed into the more stable, and, in most cases, denser phase like zeolite ZSM-5 via mordenite to quartz [54]. Similarly, denser zeolite phases may form when crystallisation is conducted at higher temperatures. Nevertheless, an increase of the reaction temperature within a limited range usually brings about faster crystallisation. Under the hydrothermal synthesis conditions, the amount of water in the liquid phase, which is necessary to stabilize the pores of the forming solid, decreases with temperature. Thus, an upper temperature limit exists for the formation of each specific zeolite and of zeolites in general [46].

Both *ageing* and *seeding* generally have an accelerating effect on the crystallisation kinetics. While ageing shortens the induction period of zeolite formation due to facilitated build-up of nuclei, seeding allows crystal growth to start immediately without preceding nucleation.

The role of *templates or structure-directing agents (SDAs)* in a synthesis gel is to direct the crystallisation towards the desired zeolite type. The influence of templates is not restricted to a single step, but may affect several processes during zeolite preparation. The chemical nature of templating agents is diverse and includes cationic species, both inorganic, *e.g.*, Na^+, K^+, Ca^{2+}, Sr^{2+}, and organic, *e.g.*, quaternary (tetraethyl-, TEA^+, tetrapropylammonium, TPA^+) or diquaternary ammonium cations, *e.g.*, 1,6-hexanediammonium (diquat-6), neutral molecules, *e.g.*, ethers, alcohols and amines, or ion pairs. While some zeolite structure types only crystallize in the presence of one particular organic template, a given organic template may support the formation of several zeolite types. Thus, zeolites ZSM-4, ZSM-5, ZSM-23, and others, may be obtained in the presence of pyrrolidine.

However, the reverse case is also known, *i.e.*, the synthesis of a given zeolite type with a variety of templates, such as ZSM-5 with amines, alcohols, quaternary ammonium cations [46,48,49].

The exact role of the templates in zeolite synthesis is not well understood, but approaches to a rational understanding are being developed and continuously refined on the basis of spectroscopic and computational methods, see, *e.g.*, refs. [55-57]. One type of template effect is the stabilization of a certain zeolite structure by specific interactions with the framework like hydrogen bonds or charge matching. During synthesis, the template molecule is included in a preferred orientation and location inside the pores, channels or cages of the zeolite structure and fills a space corresponding to its size and shape (Figure 8). A true templating effect may especially work with cationic species in that they arrange silicate monomers in their immediate vicinity in a way that their condensation leads to cage-like structural units with the template molecule embedded in their center. According to *Vaughan* [58] primary and secondary cations can be distinguished. While the former promote the formation of extended structures like faujasite sheets, the latter control the pattern of connecting those extended structures to the final zeolite framework as illustrated in Figure 9 for faujasite and zeolite EMT. Still another template effect operates in the formation of the mesoporous materials of the M41S family [10]. Surfactant molecules arranged to micellar structures by self-assembly interact with the silicate species in solution and are occluded as shaped pore fillers during the silicate condensation (liquid crystal templating, LCT). This may be viewed as an additive effect on the precipitation of an amorphous silicate [59].
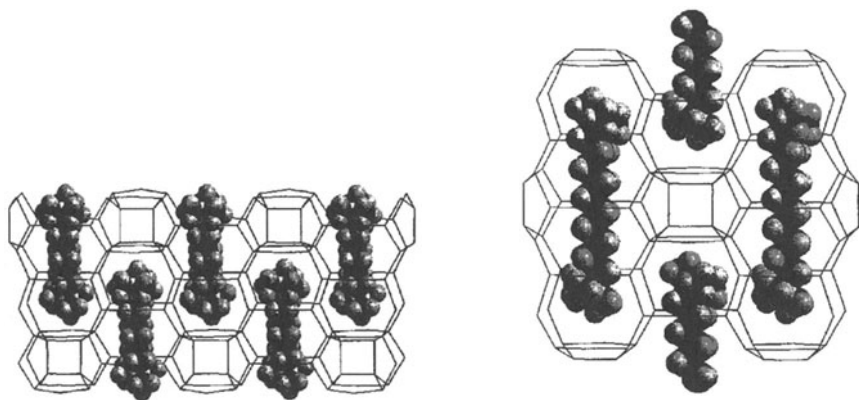
Fig. 8. Location of template molecules in zeolite structures: $[(CH_3)_3N(CH_2)_6N(CH_3)_3]^{2+}$ in zeolite ZSM-50 (left) and $[(CH_3)_3N(CH_2)_{10}N(CH_3)_3]^{2+}$ in zeolite NU-87, adapted from ref. [55].
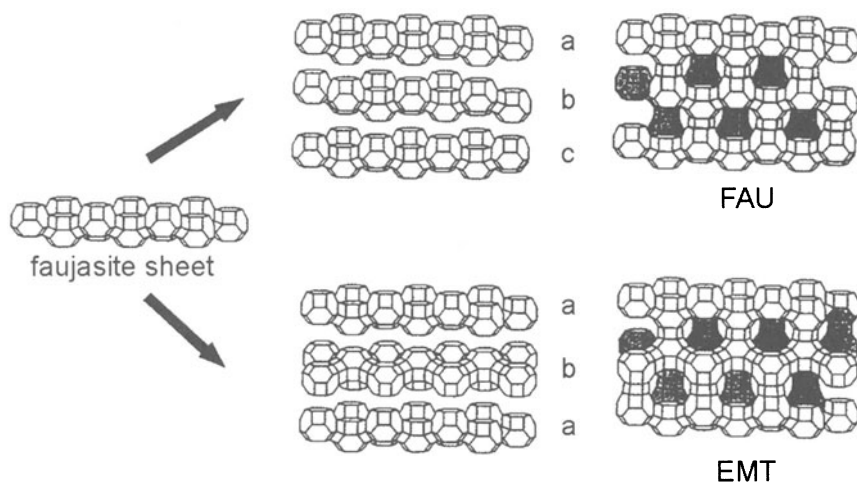
Fig. 9. Extended structures to explain the template effect in the formation of zeolites faujasite and EMT, adapted from ref. [56].

5.2   Faujasites

The structurally identical large-pore zeolites X and Y are of major importance as adsorbents and catalysts. In particular, the high demand of zeolite Y as active catalyst for the FCC process has to be met by the synthesis of highly phase-pure and crystalline material on an industrial scale (*cf.* section 7.1). As indicated by their crystallisation fields (*cf.* Figure 7), zeolites X and Y can be synthesized from the same chemical sources and at similar conditions, but at a higher silica content than zeolite A which is mainly used as water softener in laundry detergents. In general, zeolite production is carried out batchwise, but continuous processes have also been developed [60]. The industrial synthesis of zeolite Y is achieved in the absence of organic templates and with typical gel compositions of $Al_2O_3 \cdot$ (8.0-10.0) $SiO_2 \cdot$ (2.3-3.5) $Na_2O \cdot$ (120-180) H_2O. Figure 10 shows a schematic representation of industrial zeolite production starting from a silicate and an aluminate solution that are blended together to form the hydrogel. The time-consuming ageing step of one ore more days in earlier zeolite production is nowadays avoided by addition of seeding mixtures, often in colloidal form. The gel is subsequently transferred to open tank reactors with sizes of several cubic meters, sometimes above one hundred, where crystallisation occurs within 24 to 72 h at 85 to 100 °C. Beside the nature and the purity of the raw materials it is, above all, the temperature, the crystallisation time and the reactant concentration that influence the quality of the final product. If the crystallisation time is too long, the denser phases zeolite P or cancrinite may form.
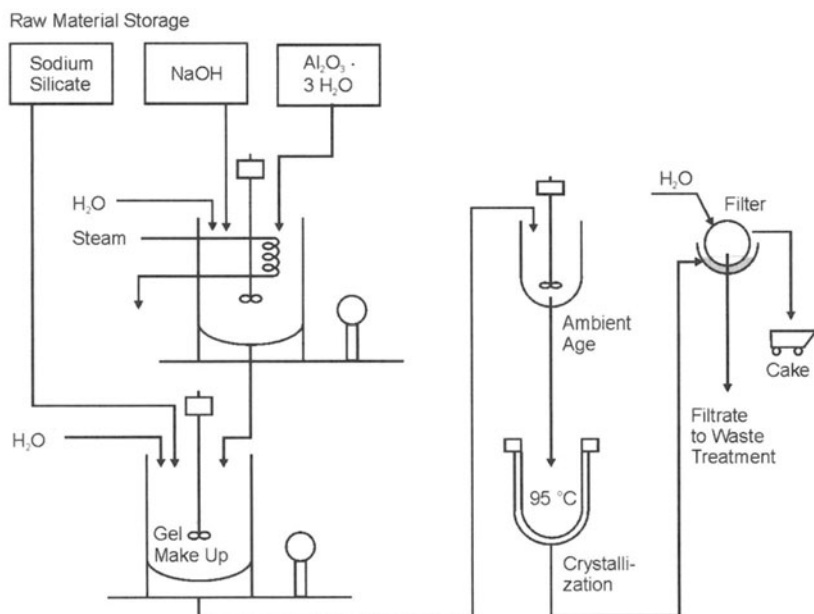
Fig. 10. Schematic representation of industrial zeolite production by the hydrogel process, after ref. [18].

Hydroxysodalite is the main product, if the water content of the hydrogel is reduced from 90-98 mol-% to 60-85 mol-% at otherwise constant reactant ratios [46].

Although zeolite Y as the major component of FCC catalysts is required with a high n_{Si}/n_{Al}-ratio for reasons of acid strength and hydrothermal stability, it is commercially synthesized with $n_{Si}/n_{Al} = 2.5$ to 2.8 and subjected to post-synthesis modification to increase the silica content. This detour is more economic than the direct synthesis of the zeolite with higher silica content, since the reduction of n_{Na_2O}/n_{SiO_2} and n_{Na_2O}/n_{H_2O} in the gel would require significantly longer crystallisation.

Another industrial route to zeolite Y is the "kaolin conversion process" which is applied in numerous variations for the production of FCC catalysts, *e.g.*, by Engelhard [61]. The advantage of this process is that the clay mineral serving as the starting material can be shaped to the desired catalyst particles before conversion to the zeolite phase. To induce zeolite formation a silicon source has to be added. For FCC catalyst production the conversion of clay to zeolite is intentionally incomplete, and the product is a matrix-embedded zeolite Y, thus avoiding separate steps of synthesis of the active zeolite phase and successive catalyst formulation. For instance, a suspension of both tempered and hydrated kaolin with zeolite seed crystals and sodium silicate is spray-dried to obtain microgranules, which are subsequently treated with sodium silicate and sodium hydroxide at 98 °C to obtain a catalyst containing > 40 wt.-% zeolite NaY [61]. This material is subjected to dealumination and ion exchange to obtain the active catalyst phase.

5.3   ZSM-5

Zeolite ZSM-5 is of utmost importance for a vast number of applications that encounter shape selectivity effects as discussed later in this article. According to the original patent of *Argauer* and *Landolt* [62] the gels for synthesis of zeolite ZSM-5 have typical compositions in the range $Al_2O_3 \cdot 29\,SiO_2 \cdot Na_2O \cdot (9\text{-}17)\,(TPA)_2O \cdot (450\text{-}480)\,H_2O$. These gels contain the quaternary tetrapropyl-ammonium cation TPA^+ as a template, but, as mentioned earlier, zeolite ZSM-5 can be synthesized in the presence of many other structure-directing agents or even in the absence of any organics as well. Depending on the organic molecules present, different silicon and aluminum sources are preferred. Generally, the crystallisation temperatures are higher than for zeolite Y, *i.e.*, 150 - 180 °C or even above 200 °C in case of organic-free synthesis gels. As a major advantage over synthetic faujasites, zeolite ZSM-5 can be obtained by direct synthesis in a broader range of n_{Si}/n_{Al}-ratios, typically 13 to 50 in the absence and 15 to infinity in the presence of organic templates. Analcime or zeolite mordenite have been observed as by-products upon increasing $n_{Al_2O_3}/n_{SiO_2}$ and n_{Na_2O}/n_{SiO_2} [46,48,63].

Moreover, the choice of synthesis gel compositions and crystallisation conditions allows zeolite ZSM-5 to be prepared with very different crystal dimensions and morphologies as well as distributions of aluminum over the zeolite crystal. ZSM-5 synthesized in the presence of organic cations is enriched in aluminum at the outer crystallite shell, whereas the aluminum content at the outer crystallite sphere is lower than the bulk when the synthesis gel is purely inorganic [46]. The control over these parameters by zeolite synthesis can be successfully utilized for tuning the catalytic properties of zeolite ZSM-5.

6.   Methods for Tailoring the Catalytic Properties of Zeolites

Several methods for "post-synthesis modification" can be applied in order to tune the catalytic properties of the zeolites. The most important methods for post-synthesis modification of zeolites will be briefly addressed in the following. A recent review by *Kühl* [64] provides more detailed and extensive information. Formulation and shaping of catalyst particles [65] can also be viewed as a post-synthesis modification step, but will not be treated here.

6.1   Ion Exchange in Aqueous Suspension

The polyanionic nature of the aluminosilicate framework is the basis for the ion exchange properties of zeolites. The charge-compensating cations can migrate out of the zeolite pores and be replaced by others, if selectivity is favorable. Ion exchange can be achieved by simple procedures and is commonly carried out by suspending the zeolite in an aqueous solution of a salt containing the cation to be introduced at room temperature or slightly above (up to *ca.* 85 °C) to facilitate the mass transfer of the in- and out-going species. This is usually done batchwise, often in several steps to obtain high exchange rates, but continuous processes are also applied in industrial practice [66]. Control of the pH is often necessary to avoid either structural damage of the zeolite at low pH or precipitation of

hydroxides onto the zeolite surface in the case of exchange with multivalent transition metal ions like Zn^{2+} or Co^{2+} at high pH.

Formally, the exchange of the cations A and B can be represented by the equilibrium

$$z_A B^{z_B+}(z) + z_B A^{z_A+}(s) \leftrightarrows z_A B^{z_B+}(s) + z_B A^{z_A+}(z) \quad (4)$$
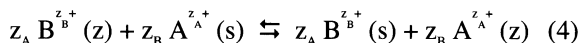
where z_A, z_B are the cation charges, (z), (s) refers to the zeolite or the solution. The position of this equilibrium is reflected by ion exchange isotherms in which the equivalent fractions of cation A or B in the zeolite are plotted in dependence of the equivalent fraction of the same cation in solution. Examples for ion exchange isotherms for univalent metal cations with zeolites Na-X and Na-Y are shown in Figure 11. While the theoretical maximum exchange capacity is determined by the framework n_{Si}/n_{Al}-ratio, only partial exchange may be possible, for instance, if the cation is too bulky to fit into the small cages inside the zeolite structure.

The exclusion of a cation from voids inside a zeolite is known as the "ion sieve effect". Partial exchange is observed, e.g., for Rb^+ and Cs^+ which cannot penetrate the 6-membered-ring windows of the sodalite cages of zeolite Na-Y and, thus, can only occupy cation positions inside the spacious supercages. The sodium cations are left in or even forced into the small cages and remain unexchangeable [67]. Similar limitations apply for cations with a high ion potential and, thus, a strongly bonded hydration shell like Li^+, Mg^{2+} or La^{3+} [68], although slow ion exchange may occur in case of, at least partial, dehydration of the coordination sphere of the cation.
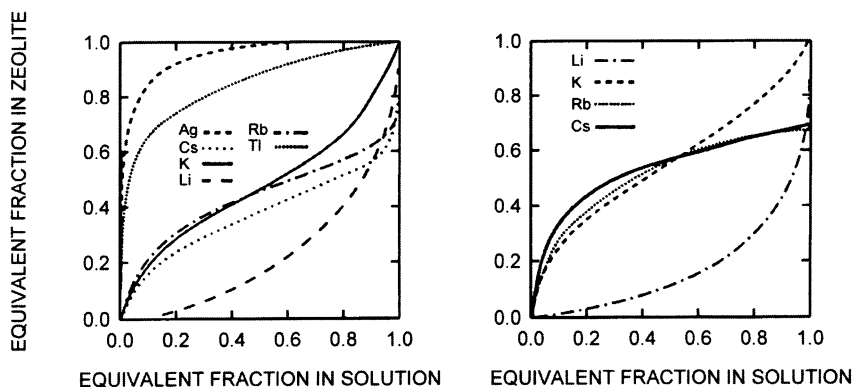
Fig. 11. Ion exchange isotherms of univalent cations in 0.1 N aqueous solution at 25 °C with zeolite Na-X (n_{Si}/n_{Al} = 1.23, left part) and with zeolite Na-Y (n_{Si}/n_{Al} = 2.82, right part), after ref. [67].

6.2   Solid-State Ion Exchange

Cation exchange in zeolites can also be achieved by a solid-state reaction. The microporous solid in its ammonium or hydrogen form is intimately admixed with a salt of the metal to be introduced (mostly halides or oxides) and heated in a stream of inert gas to temperatures of up to 800 °C. The high temperature and the evolving hydrogen halide or water vapor during the ion exchange may cause partial damage to the zeolite framework.

Solid-state ion exchange offers an interesting alternative to conventional ion exchange in aqueous suspension when (i) the cation with its hydration shell or coordination sphere is too bulky to enter the zeolite pores or (ii) the solid containing the in-going cation in the desired valence state is insoluble or unstable in water. For instance, Cu(I) can best be incorporated into zeolite Y by solid-state ion exchange with CuCl [69], and Hg_2Cl_2 or AgCl can be used as water insoluble starting compounds for solid-state ion exchange in zeolites [70]. An example for case (i) has been described in ref. [71]: The noble metals Pt, Pd and Rh were introduced via solid-state ion exchange into the small-pore zeolites ZSM-58, ZK-5 and SAPO-42. The successful introduction of the noble metals into the zeolite pores was proven by shape-selective hydrogenation of 1-hexene from a gaseous mixture with 2,4,4-trimethylpent-1-ene. Conventional aqueous ion exchange fails for these small-pore zeolites due to exclusion of the bulky complex metal cations from the pores.

In an excellent recent review, *Karge* and *Beyer* [72] discuss in much detail the techniques and opportunities of solid-state ion exchange in zeolites, including other variants of the method, such as contact-induced, vapor phase-mediated and reductive solid-state ion exchange, the potential of which for the preparation of zeolite catalysts still await complete evaluation.

6.3   Framework Dealumination

The term dealumination generally refers to the removal of aluminum from the zeolite framework, even though the overall aluminum content of the zeolite may not drastically change. Aluminum may still reside in the pores either on cation positions or as deposits of other compounds like amorphous silica-alumina or aluminum salts which is all referred to as "extra-framework aluminum". Many procedures for framework dealumination are known which may be subdivided into thermal treatments, hydrothermal treatments, extraction of framework aluminum with acid and replacement of framework aluminum with silicon from silicon halides or hexafluorosilicate [64]. Due to the sometimes harsh conditions applied, creation of secondary pores (mesopores) and production of crystal defects with partial, but considerable loss of crystallinity can occur during dealumination.

Dealumination may be brought about by heating the ammonium form of a zeolite to temperatures above 500 °C in the presence of steam. Based on early work of *McDaniel* and *Maher* [73] this method leads to the production of the industrially important ultrastable Y zeolites (USY zeolites) which maintain their structure up to 1000 °C. It has been found that the vacancies that are inevitably formed by removal of aluminum from the framework are replaced by silicon causing lattice stabilization [74]. The origin of the silicon is still a matter of some debate, sources which have been envisaged include amorphous parts from

structural damage of the zeolite or adjacent silicon atoms with a concomitant migration of the vacancies [75]. After steaming, the extra-framework aluminum species and amorphous particles are removed from the zeolite by washing with dilute acid or alkali.

Dealumination by treatment with silicon halides or hexafluorosilicates offers the advantage of immediate annealing of the lattice vacancies due to aluminum removal by incorporation of silicon. Reacting zeolites with $SiCl_4$ vapor at temperatures of 250 to 500 °C in an inert atmosphere and subsequent washing of the solid product with dilute mineral acid directly leads to high-silica zeolites with $n_{Si}/n_{Al} > 100$. The zeolites obtained are hydrophobic and mainly used as adsorbents for exhaust gas cleaning. A broad range of dealumination degrees can be obtained for many zeolite types by this method depending on the temperature and duration of the treatment [64,75]. Dealumination with $(NH_4)_2SiF_6$ occurs in aqueous solution at ca. 90 °C and can be applied to zeolites Beta and Y, although somewhat lower dealumination degrees are attained as compared to the treatment with $SiCl_4$. The dealumination of zeolite Y with $(NH_4)_2SiF_6$ is applied on an industrial scale in the manufacture of FCC catalysts. Similar to solid-state ion exchange, dealumination of the zeolites L, ZSM-5, mordenite and Y can be achieved by heating a solid mixture of the zeolite with $(NH_4)_2SiF_6$ [76]. Other agents such as F_2, $CrCl_3$, H_4EDTA, are also effective for framework dealumination of zeolites [64,77], but they are not used in industrial practice.

6.4   Miscellaneous Modification Techniques

As the reverse of dealumination, aluminum atoms may be inserted into the zeolite framework by reaction with $AlCl_3$ vapors or in aqueous solution with $(NH_4)_3AlF_6$. Such methods that allow to change the chemical composition of zeolites by isomorphic incorporation of heteroelements into framework positions are referred to as "secondary synthesis". They can now be applied to several zeolites, e.g., zeolites Y, mordenite and Beta, and to a variety of metals, viz. B, Ga, Fe, Ti, V and others [64].

The immobilization of transition metal complexes and chelates inside zeolite cavities is another method to modifiy the catalytic activity for redox reactions. Typical examples are phthalocyanines, salen, ethylenediamine complexes or metallocenes of Co, Cu, Fe or Ni [78]. These are introduced into the zeolite either by the flexible ligand method, i.e., by complexation of the transition metal with the preformed ligand inside the zeolite cavity, by ship-in-the-bottle synthesis, i.e., building-up the ligand for the complex from smaller units inside the zeolite cavities, or by occlusion of the preformed complex during zeolite synthesis.

Methods for post-synthesis tailoring of the effective pore width of zeolites are summarized under the term "pore size engineering" [79]. These techniques include ion exchange (vide supra), chemical vapor deposition of metal chlorides (CVD), but also reactions of surface hydroxyl groups of the zeolite with alkoxides of Si, Ge, P, other metal-organic or macro-molecular compounds, with the aim of either filling spaces within the pores and channels for pore-size reduction or of selectively reducing the width of the pore entrances to obtain catalysts with tuned shape selectivity.

7.   Zeolites as Catalysts in Petroleum Refining

Zeolites are utilized as catalysts in a number of central processes in petroleum refining. In many of these processes they have replaced amorphous silica-alumina catalysts which are less strongly acidic and lack the opportunity of shape-selective conversion. In a recent review *Naber* et al. state: "If zeolites were not available today, the cost of refining worldwide would increase by at least 10 billion US $ per annum" [80]. Instead of a description of the processes themselves the emphasis of this section will be on the specific role and contribution of the zeolite catalysts, including feed options and product spectra. Table 1 gives an overview of the most important zeolites applied as catalysts in petroleum refining. It is apparent from this table that, in view of the large structural variety of zeolites nowadays available (*cf.* section 3), only a small number of these have actually found their way to industrial application.

7.1   Fluid Catalytic Cracking (FCC)

Fluid catalytic cracking (FCC) is applied to convert vacuum gas oil and, much less frequently, residues to more valuable C_3- and C_4-hydrocarbons, gasoline, light cycle oil (LCO), an aromatics-rich fraction in the boiling range of middle distillates, and heavy cycle oil (HCO) [81]. Of these, gasoline is by far the most abundant product. FCC represents the single most important application of zeolite catalysts consuming 40 % of the overall catalyst cost in the refining industry [82]. FCC is even the most widespread conversion process with a worldwide capacity of *ca.* 600 Mt/a and a zeolite catalyst demand of 300,000 t/a [80]. The higher activity of zeolites as compared to the previously used amorphous silica-alumina catalysts allowed to switch from fluidized-bed crackers to riser reactors with contact times of only a few seconds. Furthermore, increased gasoline yields at

Table 1. Zeolite catalysts in petroleum refining processes.

Zeolite	Cation/Form	Application
Faujasite (Y)	RE [1], H Pd/H, Pt/H, Ni-Mo/H, Ni-W/H	Fluid catalytic cracking Hydrocracking
Mordenite	Pt/H	Isomerisation of light gasoline
L	Pt/K, Pt/Ba,K	Aromatization, Reforming of gasoline
ZSM-5	H H Ga/H	M-Forming, Dewaxing, Fluid catalytic cracking (additive), Methanol to gasoline, Aromatization of LPG [2]
Erionite	Ni/H	Selectoforming
Ferrierite	H	Isomerisation of light alkenes
SAPO-11	H	Isodewaxing

[1] RE :   Rare earth
[2] LPG :   Liquefied petroleum gas

lower rates of coke and gas formation (Figure 12, left-hand part) and higher stability are among the advantages of zeolite catalysts.

Modern FCC catalysts typically contain 20 to 30 wt.-% zeolite Y. Initially, zeolites exchanged with rare-earth cations (RE-Y) and a high density of acid sites were used. These catalysts were highly active for gasoline production, but the quality of the gasoline reflected by the research octane number (RON) and the motor octane number (MON) was relatively poor. This can be explained by a favored bimolecular hydrogen transfer from naphthenes to olefins, *i.e.*, the initial cracking products, forming paraffins and aromatics (Figure 12, right-hand part). Nowadays, dealuminated zeolite Y is used as FCC catalyst obtained by post-synthesis treatments (*cf.* section 6.3). Dealumination also occurs to some extent under process conditions [3,81]. This dealuminated catalyst offers the advantages of (i) increased (hydro)thermal stability of the zeolite, also supported by rare-earth ion exchange, and (ii) a lower hydrogen transfer activity (which is often ascribed to the reduced density of acid sites [3,81]) and, thus, lower yields of aromatics and coke, but also a somewhat reduced overall gasoline yield. Above all, however, the increased cracking *versus* hydrogen transfer rate leads to an accelerated olefin formation and a correspondingly higher gasoline quality needed to meet the increasing demands towards high-octane fuels. The increased acid strength in the dealuminated zeolite causes some overcracking of the reactive alkenes to yield LPG that can be used for alkylate production (*cf.* section 7.6). As a rough measure for the balance between cracking and hydrogen transfer activity of commercial FCC catalysts, and, hence, between gasoline quality and yield, the unit cell size (UCS) of the zeolite is frequently used, since it directly reflects the aluminum content of the zeolite framework [83,84].
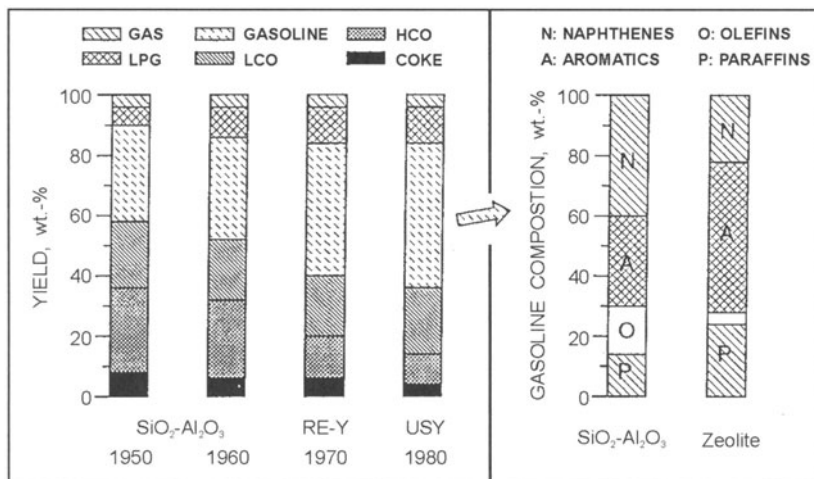
Fig. 12. Typical gasoline yield and composition in FCC over amorphous silica-alumina and over zeolite catalysts (LPG: liquefied petroleum gas; LCO: light cycle oil; HCO: heavy cycle oil).

Coke deposits are burnt off from the catalyst with air in a separate fluidized-bed regenerator at temperatures above 700 °C. These harsh regeneration conditions require a high (hydro)thermal stability of the zeolite to minimize dealumination and structural damage during operation. Other reasons for catalyst loss during FCC processing include mechanical abrasion in the riser reactor and the regenerator, ion exchange by salts or deposition of metals, above all vanadium and nickel, which are impurities of the feed, especially in distillation residues.

Zeolite ZSM-5 is used as a catalyst additive, typically 0.5 to 3 wt.-%, to "boost" the octane number of FCC gasoline. This medium-pore zeolite preferentially cracks n-paraffins with the lowest octane number, mainly due to reactant shape selectivity, but also due to restricted transition state shape selectivity [86]. With zeolite ZSM-5 as an additive, slightly less gasoline is produced with a concomitant increase in the yield of LPG, especially of propene and butenes (Table 2). To supply even more of these lower alkenes, especially of propene, the use of zeolite H-ZSM-5 in higher ratios in FCC catalysts (5 to 20 wt.-%) is another option [80]. Depending on its state of activity ZSM-5 also catalyzes skeletal isomerisation or cracking of the alkenes [87]. Beside zeolite Y, other large-pore zeolites, including Beta and ZSM-20 [86,88], have been extensively tested as FCC catalysts, yet, zeolite Y modified by rare-earth ion exchange and dealumination continues to be the best choice in terms of cost and performance [81].

For more detailed information on the complex chemistry governing FCC and the issues of catalyst technology, octane enhancement and catalytic cracking of residues, the reader's attention is drawn to a number of review articles and books [81,88-92].

Table 2. Effect of the addition of zeolite ZSM-5 (5.9 wt.-%) to an industrial FCC catalyst, after ref. [85].

	without H-ZSM-5	with H-ZSM-5	
Product	Yield / wt.-%	Yield / wt.-%	Difference / wt.-%
H_2S	0.5	0.5	0.0
C_2^-	4.0	3.6	- 0.4
propane	1.5	1.5	0.0
propene	5.1	6.2	+ 1.1
n-butane	1.1	1.1	0.0
isobutane	4.6	4.4	- 0.2
butenes	6.6	7.6	+ 1.0
gasoline (to 215 °C)	50.4	48.9	- 1.5
LCO (to 350 °C)	13.9	14.9	+ 1.0
HCO	7.2	7.1	- 0.1
coke	5.1	4.2	- 0.9
total	100.0	100.0	0.0
RON of gasoline	91.3	92.3	
MON of gasoline	80.5	80.7	

7.2   Hydrocracking

As a competitive process to FCC, hydrocracking is applied to convert heavy gas oils into valuable transportation fuels. Hydrocracking is carried out at milder temperatures (300 to 450 °C) than FCC (*ca.* 500 °C) and under hydrogen pressure of 80 to 250 bar over bifunctional catalysts containing both a hydrogenation/dehydrogenation and an acid component. An example is Pd (*ca.* 0.5 wt.-%) on ultrastable zeolite Y (USY). The lower temperatures and the suppression of coke formation due to the continuous product hydrogenation allow catalyst lifetimes of up to several years.

The activity balance of the two catalytic functions is of prime importance for conversion and product selectivity. Also, the mass transfer between the hydrogenation/dehydrogenation and the acid sites within the zeolite catalyst may become the rate determining step, if the two sites are too far apart (intimacy criterion after *Weisz* [93]). If the de-/hydrogenation function is predominant ("ideal hydrocracking" [94,95]) primary isomerisation and hydrocracking can be achieved, whereas with a stronger acid function, consecutive (secondary) isomerisation and hydrocracking reactions inevitably occur. The catalyst (and the process conditions) can, therefore, be designed to maximize either the yields of middle distillates, *i.e.*, diesel and jet fuel of high quality, or branched alkanes in the boiling range of gasoline.

Further advantages of hydrocracking include the possibility of processing lower-grade, higher-boiling feedstocks, a very clean operation without emissions of SO_x and NO_x and products which are virtually sulfur-free. On the other hand, disadvantages of catalytic hydrocracking are high capital and operating costs associated with the hydrogen consumption, pressure generation and equipment safety and a lower gasoline quality in terms of octane numbers.

As in FCC the higher acid strength of zeolites relative to amorphous silica-alumina catalysts gives higher conversions in hydrocracking, but also higher stability, nitrogen resistance and naphtha selectivity [96]. The bifunctional zeolites are in most cases based on zeolite USY (*vide supra*). The hydrogenation/dehydrogenation function is either provided by a noble metal like Pd (0.1 to 1 wt.-%) or by sulfided oxides of Ni or Co in combination with Mo or W [96]. While the degree of dealumination does not strongly influence the overall conversion, the selectivity for middle distillate is improved upon removal of framework aluminum [97]. Furthermore, dealumination of the zeolitic hydrocracking catalyst supports the formation of mesopores that facilitate the transport of the larger feed molecules to the catalytically active sites. Exclusion of the interior pore system leading to a less efficient conversion of heavy oil fractions and diffusional limitations of the primarily formed alkenes resulting in increased secondary cracking are reasons why zeolites with narrower pores than zeolite Y have not been used in hydrocracking. This has been shown for the conversion of n-alkanes over different zeolite catalysts, where a decrease in the relative rates of isomerisation and cracking with decreasing pore diameter of the zeolite catalyst was observed [98]. More recent studies were consequently directed towards larger-pore materials such as VPI-5, cloverite [99] or MCM-41 [100], yet none of these more recent materials succeeded in replacing zeolite Y in commercial hydrocracking catalysts.

A completely different application of hydrocracking on zeolite catalysts has recently been developed for the utilization of aromatics which will have to be

reduced in automotive gasoline in the near future as a consequence of restrictive legislation, *e.g.*, the Auto-Oil Programme of the European Union [101]. Hydrocracking of aromatics or cycloalkanes (accessible from aromatics through conventional ring hydrogenation) can be conveniently accomplished over bifunctional or acid zeolites, such as Pd/H-ZSM-5 or H-ZSM-5, respectively, to yield a product composed predominantly of ethane, propane and n-butane [102,103]. These lower alkanes may, in turn, serve as a high-quality, synthetic steamcracker feed, thus contributing to the increasing demand for ethylene and propylene. Still another application are zeolite-supported noble metal catalysts with high sulfur and nitrogen tolerance. Such catalysts are being industrially applied, *e.g.*, in the Shell Middle Distillate Hydrogenation Process (SMDH) since 1992 to deeply hydrogenate and hydrodecyclize aromatics in light cycle oils for fuel production [104].

7.3   Dewaxing

The aim of dewaxing is a selective removal of waxy normal or slightly branched paraffins in order to improve the cold flow properties of gas oils and lubricating base oils. This is achieved by shape-selective (hydro)cracking of the above-mentioned alkanes at 300 to 400 °C and hydrogen pressures of 20 to 50 bar over catalysts based on the 10-membered-ring zeolite H-ZSM-5 [4,105] in Mobil processes (Mobil Distillate Dewaxing, MDDW; Mobil Lube Dewaxing, MLDW). Products are light hydrocarbons in the boiling range of gasoline and LPG as shown in Figure 13 along with a schematic flow-sheet of the process. A higher selectivity has been reported to be obtainable over zeolite H-ZSM-23 with a one-dimensional pore system [105]. A higher extent of secondary cracking observed with smaller crystallites of zeolite ZSM-5 is indicative of a diffusion-limited reaction. The application of MFI-type catalysts with B, Fe or Ga isomorphously substituted in the zeolite framework was reported to give somewhat higher selectivities due to the reduced acid strength, however, at the expense of activity [106].

   In order to avoid the yield loss associated with cracking of the n-paraffins, which is particularly unfavorable in case of the higher-value lubricating base oils, an isomerisation into branched isomers which possess significantly lower meltingpoints is favorable ("isodewaxing"). For this purpose, zeolite catalysts with a strong preference for isomerisation over hydrocracking are needed. Zeolites with low activity, *i.e.*, high n_{Si}/n_{Al}-ratio, and structures with pore systems other than ZSM-5 such as MCM-22 and Beta [107], seem to allow the bulkier isomerisation products to diffuse out of the pore system readily and to avoid overcracking of the larger reactants as a result of increased residence time inside the zeolite pores. Recently, a process for isodewaxing has been commercialized by Chevron on the basis of SAPO-11 doped with 1 wt.-% platinum [108]. This catalyst is particularly suited due to its mild acid strength and since its constrained one-dimensional pore system (pore width: 0.39 x 0.63 nm) gives rise to transition state shape selectivity prohibiting isomerisation to more highly branched products which would undergo rapid consecutive cracking.

   Similar to dewaxing, reactant shape selectivity is involved in processes for cracking linear alkanes (C_7 to C_{10}) to improve the octane number of gasoline from

catalytic reformers, *i.e.*, the Selectoforming and the M-Forming processes, with concomitantly reduced
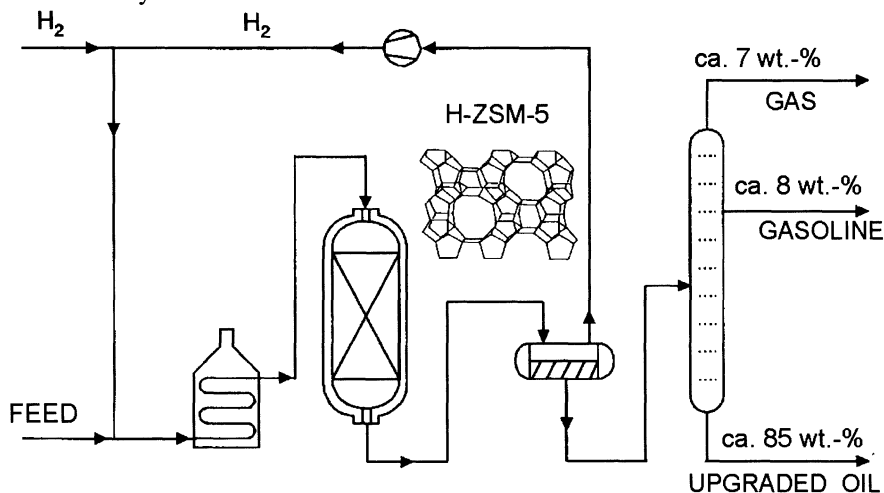
Fig. 13. Schematic flow-sheet of catalytic dewaxing of heavy gas oil.

gasoline yield. While the narrow-pore zeolite Ni/H-erionite has been applied in the former process, zeolite H-ZSM-5 serves as a catalyst in the latter. In M-Forming, cracking of both n-alkanes and mildly branched iso-alkanes occurs, and the alkenes produced as primary cracking products may undergo consecutive reactions, *e.g.*, alkylation of aromatics present in large amounts in the gasoline from reformers [3,109,110].

7.4   Isomerisation of Light Gasoline

Skeletal isomerisation of the C_5/C_6-hydrocarbons in light gasoline fractions is carried out to convert linear to branched paraffins in an equilibrium-limited reaction with the aim to increase the octane number of gasoline. With a bifunctional zeolite catalyst, viz. Pt/H-mordenite, the process is operated at temperatures around 250 °C and hydrogen pressures of *ca.* 30 bar (Shell Hysomer process). In the total isomerisation process (TIP) the Hysomer process is combined with a zeolite-based n-/iso-paraffin separation by adsorption, *e.g.*, by the Isosiv process, and the n-paraffins are recycled to the isomerisation reactor [111].

   Zeolites offer a chlorine-free alternative to the more active chlorided Pt/alumina catalysts. With the zeolite catalyst, however, higher process temperatures are needed at which the equilibrium is less favorable for the desired highly branched isomers. Other zeolites have been tested in the laboratory as catalysts for paraffin isomerisation, viz. Omega and Beta. For a review covering the mechanism of paraffin isomerisation and the processes applied see ref. [112].

7.5   Isomerisation of Light Alkenes

The skeletal isomerisation of light alkenes, though not yet practiced on a commercial scale, is of interest for the production of branched isomers, above all isobutene and isopentene. These can, in turn, be converted with light alcohols on acid catalysts, typically organic ion exchange resins, to ethers used as oxygen-containing anti-knock additives to gasoline. The most prominent ether used for this purpose is methyl-*tert.*-butyl ether (MTBE). After years of a steady increase of the worldwide MTBE consumption, its future has recently become a matter of serious environmental debates, especially in California: MTBE, which has a characteristic odor and is readily soluble in water, has occasionally been detected on the groundwater after leakages of gasoline tanks. In California, this led to a ban on MTBE as a gasoline additive from 2002 onwards [113].

The formation of iso-alkenes from n-alkenes, though seemingly a simple and straightforward reaction, suffers from various drawbacks which all contribute to a severe limitation of the product yields. Among these drawbacks are an unfavorable position of the equilibrium and undesired side reactions, such as the formation of oligomers of the alkenes and the build-up of coke associated with a rapid catalyst deactivation.

Several medium-pore zeolites such as H-ZSM-22 [114], H-ZSM-23 [115] or SAPO-11 [116] have been proposed as catalysts for the isomerisation of n-butenes. Another medium-pore zeolite, however, has found the most widespread attention, viz. H-ferrierite [117] which possesses a system of intersecting 8- and 10-membered-ring pores. H-ferrierite exhibits unusually high activity, stability and selectivity for isobutene (*ca.* 90 % at more than 40 % conversion of n-butenes). The precise reasons for the unusually high performance of this particular zeolite catalyst are a matter of ongoing debate, and at least three different mechanisms have been advocated: (i) A monomolecular mechanism which would involve a primary carbenium ion and is perhaps operative inside the 8-membered-ring pores [118,119]; (ii) a bimolecular mechanism initiated by dimerization of n-butenes and followed by skeletal rearrangements and cleavage of the resulting iso-octenes [117,120]; (iii) pore mouth catalysis, *i.e.*, conversion at or near the entrance of the zeolite pores, with the high selectivity towards isobutene either due to an isomerisation reaction catalyzed by carbonaceous deposits entrapped inside the zeolite pores [121,122] or due to preferred desorption of isobutene over addition of n-butene which would lead to formation of by-products [123].

7.6   Alkylation of Isobutane with Light Alkenes

The acid-catalyzed conversion of isobutane from C_4-cuts of catalytic cracking with light alkenes, typically butenes, yields highly branched iso-alkanes as high-octane gasoline components like 2,4,4-trimethylpentane (iso-octane), the reference substance for octane quality with RON = 100. Due to environmental and safety concerns about the use of HF and H_2SO_4 as catalysts in the conventional liquid-phase alkylation processes, strong endeavors have been devoted to the development of solid acids as catalysts for the alkylation of isobutane with butenes.

The alkylate produced over large-pore acidic zeolite catalysts, such as rare-earth exchanged zeolite Y or zeolite H-Beta is, in principle, of comparably high

quality as that obtained with HF or H_2SO_4. In fixed-bed operation, however, zeolite catalysts are deactivated after a relatively short time-on-stream with respect to alkylation activity, and oligomerization of the olefin component occurs instead (Figure 14) [124]. The origin of this "deselectivation" must be related to a decline and, eventually, the complete loss of the hydride transfer activity of the catalyst brought about by carbonaceous deposits [125]. In addition to the most extensively studied faujasite-type catalysts, a number of further, structurally different zeolites like MCM-22, MCM-36, ZSM-3 or ZSM-18 have been explored as potential catalysts in isobutane/butene alkylation with, so far, limited success [126]. More promising results were recently achieved by using acid zeolite catalysts in continuously stirred tank reactors where the concentration of the olefin, which is likely to be the source of catalyst deactivation, is extremely low at any location inside the reactor [127].
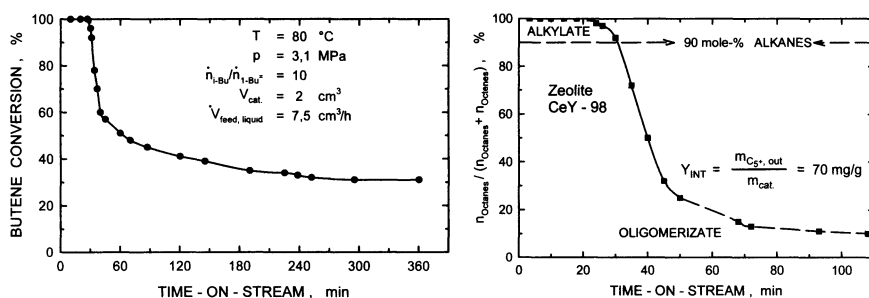
Fig. 14. Conversion of 1-butene with isobutane (left) and composition of the C_8 fraction (right) over zeolite Ce-Y-98 at 80 °C, after ref. [124]. The dashed line at 90 mol.-% alkanes in the C_8 product fraction marks the (arbitrarily chosen) limit between alkylation and oligomerization.

7.7   Aromatics from Light Paraffins (Cyclar Process)

As a cheap feedstock LPG, comprised mainly of C_3- and C_4-alkanes, from refineries can be converted over zeolitic catalysts into aromatics in the BTX-range (benzene, toluene, xylenes) that are used for gasoline blending and as raw materials for petrochemical applications. The Cyclar process jointly developed by BP and UOP uses zeolite Ga/H-ZSM-5 as a bifunctional catalyst at temperatures of 450 to 500 °C [128]. Gallium acting as a de-/hydrogenation component, may be introduced into the zeolite with a loading of typically 1 to 5 wt.-% by ion exchange, impregnation or isomorphous substitution. In the former two cases, a high dispersion of gallium is reached by applying several oxidation/reduction cycles [129].

The net reaction to the aromatics represents a dehydrocyclodimerization (DHCD), *e.g.*, of propane to benzene, involving dehydrogenation, dimerization, cyclization and hydrogen transfer steps. The balance between the de-/hydrogenation and the acid function of the zeolite catalyst is, therefore, of crucial importance for appreciable aromatics selectivity. While gallium seems to

play a key role in dehydrogenating the alkanes and the intermediate alkenes and cyclic oligomers to aromatics, the acid sites are important for oligomerization of the alkenes and cracking to build-up a pool of alkenes serving as intermediates on the way to the aromatic products [129]. Unbalanced acid or de-/hydrogenation activity of the catalyst may favor cracking or hydrogenolysis, both leading to a loss of carbon by formation of methane and ethane or ethene. With zeolite H-ZSM-5 the requirements for acidity are best met with an n_{Si}/n_{Al}-ratio of 15 to 30. Furthermore, the formation of polynuclear aromatics and coke are kept at a low level with the ZSM-5-type catalyst. Under the spatial constraints inside the pores of zeolite ZSM-5 the formation of coke is significantly retarded. This lower tendency of medium-pore zeolites in general, and ZSM-5 in particular, towards coke build-up as compared to large-pore zeolites or macroporous catalysts may be viewed as a shape selectivity effect and is a often a decisive criterion for the selection of zeolite catalysts [130,131].

Another option for aromatics production is the Aromax process of Chevron which converts C_6- to C_8-alkanes as a feed. A disadvantage of the zeolite catalyst used in this process, i.e., Pt/Ba,K-L, is the extremely high sensitivity to sulfur poisons [132,133] requiring deeply hydrotreated, essentially sulfur-free feed-stocks.

The importance of aromatics-producing processes is, as a whole, expected to decrease as a response to legislative limitations of the aromatics content in transportation fuels that will have to be met in the coming years [134].

7.8   Methanol to Gasoline (MTG) and Methanol to Olefins (MTO)

Most processes for the production of fully synthetic gasoline are based on synthesis gas $(CO + H_2)$ which can be obtained from a wide variety of sources including natural gas, petroleum distillation residues or coal. However, the current oil prices make synthesis gas-based processes economically viable only under very specific circumstances [3]. In the MTG process methanol as a product from synthesis gas is catalytically converted over zeolite H-ZSM-5 into a high-quality gasoline. One commercial MTG plant, based on natural gas as a raw material, has been in operation in New Zealand for years. From a technical point of view, this plant was very successful, yet limited information is available on the economics of this process route.

The conversion of methanol can also be carried out to yield lower alkenes (methanol to olefins, MTO process) which, in turn, might be used as feed for gasoline production. Alternatively, the olefins produced via MTO may be converted catalytically into higher boiling fuels, such as jet fuel or diesel fuel, or directly serve as petrochemical raw materials.

The MTG reaction comprises a complex series of acid-catalyzed steps. Formation of the various products proceeds through consecutive steps as is evident from the product distribution shown in Figure 15 as a function of space time [135,136]. Obviously, the product formed most rapidly from methanol is dimethyl ether. It appears as a typical intermediate, and at more severe conditions, a pool of C_2- to C_5-alkenes is formed. These, in turn, undergo consecutive reactions at still higher space times: The products appearing under these conditions are higher alkenes, alkanes and aromatics. A reasonable pathway for their formation from C_2- to C_5-alkenes includes oligomerization of the latter into higher alkenes with six or more

carbon atoms followed by cyclization and hydrogen transfer, so that alkanes and aromatics result. In the past, there has been considerable debate in the literature as to how the first carbon-carbon bond is formed during the MTG or MTO reactions, and a variety of principally different mechanisms have been advanced for this seemingly crucial step [135,137,138]. Among these are, beside concerted reactions, mechanisms via carbocations, carbenes, oxonium ylides and free radicals. From today's point of view, these intricate mechanistic debates were essentially resolved by *Haag* [139]: He proposed that the essential carbon-carbon bond forming mechanism consists of the acid-catalyzed alkylation of alkenes by methanol or dimethyl ether. In the steady state, there is a *pool of olefins* with different structures and carbon numbers inside the zeolite pores, and the rate of carbon-carbon bond formation (through the above-mentioned alkylation) and carbon-carbon bond cleavage (through cationic β-scission) equal each other. Prime factors which govern the composition of the olefin pool inside the pores are (i) the reaction temperature, (ii) the pressure and (iii) the pore width and architecture of the zeolite catalyst.

The importance of shape selectivity during the MTG reaction in zeolite H-ZSM-5 cannot be overemphasized: Firstly, the formation of coke and the concomitant catalyst deactivation are remarkably slow (*cf.* section 7.7), so that adiabatic fixed-bed reactors can be employed with one surplus swing reactor which is put on-stream when, after typical on-stream times of several weeks, one
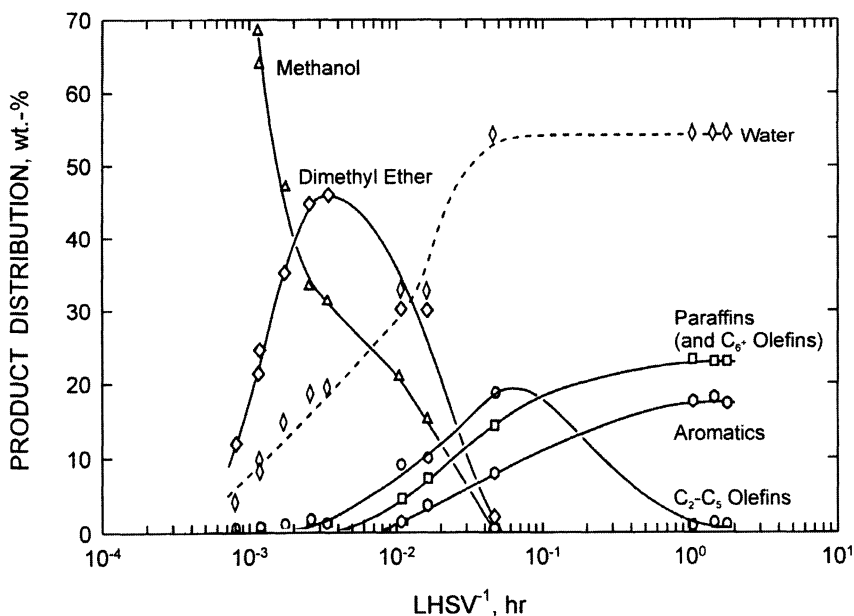
Fig. 15. Product distribution for methanol conversion at 370 °C and atmospheric pressure over H-ZSM-5 in dependence of space time, after ref. [138].
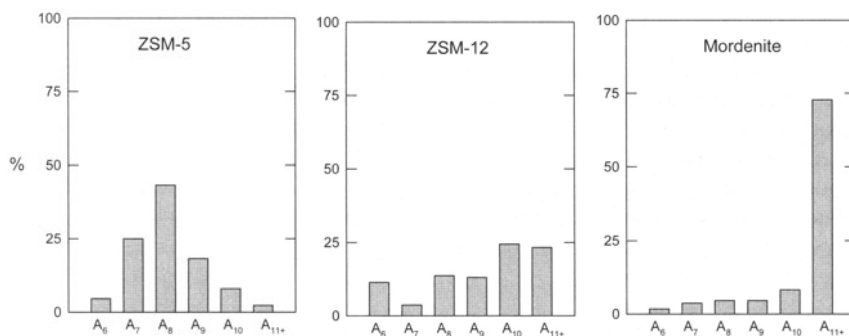
Fig. 16. Aromatics distribution for methanol conversion over different zeolite catalysts (pore diameter: ZSM-5: 0.56 nm, ZSM-12: 0.60 nm, mordenite: 0.70 nm), adapted from ref. [138].

catalyst bed has to be regenerated. Secondly, virtually no heavy hydrocarbons with more than 10 carbon atoms are formed in the MTG process (see data for ZSM-5 in Figure 16). Thirdly, clear shape selectivity effects appear in the distribution of individual product isomers: while (under typical process conditions, *i.e.*, *ca.* 400 °C and 20 bar) the three xylene isomers are essentially at equilibrium, the slender isomers 1,2,4-trimethylbenzene and 1,2,4,5-tetramethylbenzene (durene) are strongly preferred in the fractions of the C_9- and C_{10}-aromatics, respectively. The relatively high durene concentration is an undesirable feature of gasoline from the MTG process since, due to its high melting point of *ca.* 80 °C, durene may precipitate from the gasoline. The problem may be overcome by catalytic ring hydrogenation of durene in a hydrofinishing reactor downstream of the MTG reactors [138].

Instead of producing high-octane gasoline as the main product of methanol conversion, the reaction can be directed towards lower alkenes (MTO) as well, *i.e.*, mainly ethene and propene. Measures which favor MTO over MTG are higher reaction temperatures and a lower acid strength of the zeolite catalyst [135,140]. Earlier MTO catalysts were based on zeolite ZSM-5 as well, but no commercial unit was erected, since the competitiveness against the conventional manufacture of low olefins by steamcracking was not reached. Recently, a novel MTO process was developed by Norsk Hydro/UOP which seems to be based on the 8-membered-ring silicoaluminophosphate H-SAPO-34 [135]. With this narrow-pore catalyst, the yield of ethene plus propene seems to be significantly enhanced, and it could well be that this new MTO technology reaches profitability under certain circumstances.

In a rigorous sense, MTO is a petrochemical rather than a refinery process. A number of other petrochemical processes take advantage of zeolite catalysts. These processes are discussed in the subsequent sections.

8.   Zeolites as Catalysts in Petrochemistry

In many petrochemical applications, zeolite catalysts replaced more conventional liquid acids, such as H_2SO_4, HF, $AlCl_3$ or BF_3 which are less benign from an environmental or safety point of view. It is another salient feature of petrochemical processes, as opposed to refinery operations, that a single compound or a few single compounds are usually aimed at. The realm of zeolite catalysis in petrochemistry is the manufacture of specific aromatics, and both acid catalysis and shape selectivity are of utmost importance.

8.1   Ethylbenzene Manufacture (Mobil-Badger Process)

Ethylbenzene is an important intermediate on the way to styrene and polystyrene. It is readily produced by alkylation of benzene with ethylene in the Mobil-Badger process [3,141] which relies on acid forms of medium-pore zeolites such as H-ZSM-5 or, perhaps, H-MCM-22. Since the first commercial application of this process in 1980 by American Hoechst in Bayport, Texas, more than 25 plants have been put on-stream worldwide, and the current capacity amounts to more than 7 Mt/a [142]. Figure 17 shows a schematic representation of the process which is operated in the gas phase typically at 15 to 30 bar and 380 to 450 °C [143]. Two fixed-bed reactors are applied for continuous operation, one for conversion and the other for regeneration of the deactivated catalyst by coke burning. Ethylbenzene yields above 98 % can be achieved (based on ethene conversion) with diethylbenzenes as the main by-products. These and unconverted benzene are separated and recycled for transalkylation to ethylbenzene.

The reaction over acid zeolites follows classical Friedel-Crafts pathways via carbenium ion intermediates. To suppress the undesired oligomerization of ethene and re-cracking leading to alkenes in the C_3- to C_6-range, benzene is present in a 3- to 10-fold excess in the feed. Like in previously described processes, e.g., the Cylcar process, coke formation over zeolite H-ZSM-5 is slow and allows catalyst cycles on the order of several weeks or months [3,141,142]. In contrast, large-pore zeolites such as H-Y or H-mordenite would deactivate very rapidly and are, hence, unsuitable for ethylbenzene production [142]. Apart from diethylbenzenes, only minor amounts of more highly alkylated benzenes are formed owing to the shape-selective properties of the zeolite catalysts employed. Due to the reversibility of the alkylation more highly alkylated products, once built-up inside the zeolite pores, can ultimately undergo dealkylation and transalkylation reactions, and the products do have egress from the zeolite pores. The confined space inside the zeolite pores, an excess of the benzene over ethylene in the feed and a relatively low reaction temperature around 400 °C are means to favor mono- over polyalkylation. Recently, processes for zeolite-catalyzed ethylbenzene manufacture with aqueous ethanol as the alkylating agent over zeolite ZSM-5 in the liquid phase and by catalytic distillation have been envisaged [142].

ETHYLENE   BENZENE   ETHYLBENZENE

DIETHYL-
BENZENES

BENZENE

HEAVY
ENDS
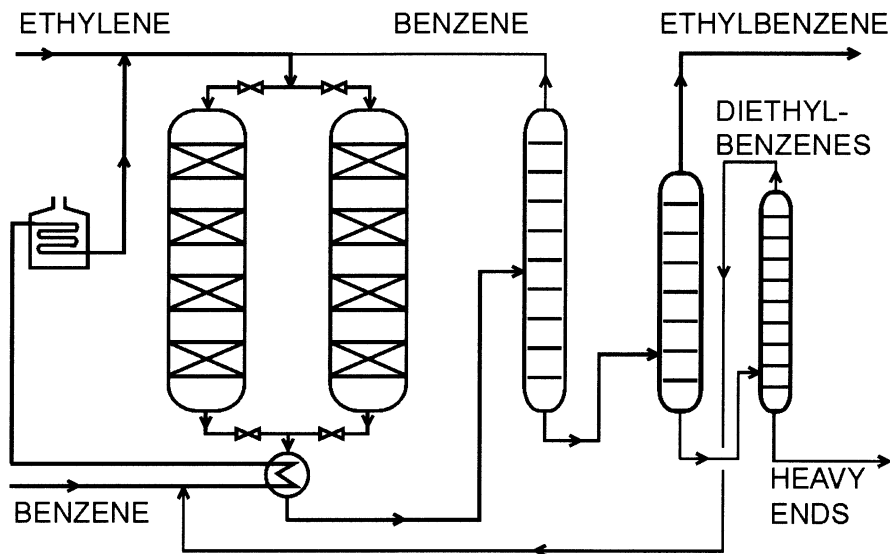
Fig. 17. Schematic process flow-sheet of the Mobil-Badger process for the production of ethylbenzene from ethene and benzene over zeolite H-ZSM-5, after ref. [143].

8.2   Isopropylbenzene Manufacture

Similar to the Mobil-Badger process, benzene can be alkylated with propene to isopropylbenzene (cumene). Since this product and the intermediates involved in bimolecular alkyl group transfer are bulkier than those in ethylbenzene production, large-pore zeolites seem to be more appropriate catalysts for cumene manufacture. Undesired shape selectivity effects which could occur in too narrow pores include a hindered diffusion of cumene and a substantial formation of n-propylbenzene which is very difficult to separate from the desired cumene [142]. Thus, a dealuminated H-mordenite with $n_{Si}/n_{Al} > 100$, labelled "3DDM" (three-dimensional dealuminated mordenite), is used in the Dow process [144-146]. Complete propene conversion is already reached at 130 °C. This low operation temperature and the larger pore diameter of the zeolite catalyst cause the formation of a larger fraction of dialkylated products, so that an additional reactor for their transalkylation with benzene is required. In another cumene process developed by Enichem, zeolite H-Beta is being used as catalyst [147,148]. Interestingly, zeolite H-MCM-22, which possesses relatively narrow 10-membered-ring pores but very spacious cages, has also been reported to be employed for the manufacture of cumene in a variant of the Mobil-Badger process [147].

Shape-selective catalysis over large-pore zeolites has also been successfully applied in the alkylation of benzene with long-chain n-alkenes, *e.g.*, n-decene, as intermediates to linear alkylbenzene sulfonate surfactants [149] and for iso-

propylation of binuclear aromatics, *e.g.*, naphthalene and biphenyl, to obtain intermediates to liquid crystal polymers [150].

8.3   Isomerisation of Xylenes

The C_8-fractions from catalytic naphtha reforming and pyrolysis gasoline consist mainly of xylenes and ethylbenzene. Among the xylenes the meta-isomer is predominating for thermodynamic reasons (*vide infra*), whereas the ortho- and the para-isomers are the desired ones, since they are needed as starting materials for the production of phthalic and terephthalic acid, respectively. In particular, para-xylene is consumed in large amounts for the production of polyesters like polyethylene terephthalate (PET). The main objective of xylene isomerisation is, therefore, to convert meta-xylene (after a separation from the isomers through adsorption, *e.g.*, in the UOP Parex process [151] which is working on zeolitic adsorbents) into its isomers and to approach as closely as possible the isomer equilibrium (*e.g.*, at 400 °C 24.1 mol-% ortho-, 52.4 mol-% meta-, and 23.5 mol-% para-xylene). At the same time, all side reactions, in particular the competing disproportionation of xylenes into toluene and trimethylbenzenes, must be suppressed to the maximal possible extent.

The shape-selective influence of zeolite catalysts on xylene isomerisation becomes apparent from Figure 18 where the relative rates of isomerisation and disproportionation are plotted *versus* the pore diameter. Disproportionation is inhibited most efficiently due to spatial constraints on the transition states of the bimolecular transalkylation inside the pores of zeolite H-ZSM-5. Intramolecular methyl group shifts leading to the desired isomerisation are, thus, favored [152].

Four process options for xylene isomerisation using catalysts based on zeolite H-ZSM-5 have been developed by Mobil, *i.e.*, *Mobil Low Pressure Isomerisation* (MLPI), *Mobil Vapor Phase Isomerisation* (MVPI), *Mobil High-Temperature Isomerisation* (MHTI) and *Mobil High Activity Isomerisation* (MHAI). The specific features of these process variants have been discussed in the literature [3,153-155]. Apart from differences in process configuration, reaction conditions and feed options, these processes use different ways to handle the ethylbenzene which is usually present in the feed, which is hard to separate from the desired para-xylene, and which could accumulate in the recycle loop of the process and lead to xylene losses due to transalkylation reactions. While ethylbenzene is diproportionated to benzene and diethylbenzenes in the MVPI process, it is hydrodealkylated to benzene and ethane over a catalyst containing a small amount of platinum in MHTI. The corresponding changes in the fractions of lighter products (fuel gas) and higher aromatics are shown in Table 3.

If bifunctional catalysts are applied for xylene isomerisation as, *e.g.*, in the older Octafining process, which worked on a platinum catalyst supported on amorphous silica-alumina, ethylbenzene can be isomerized to xylenes. Xylene hydrogenolysis to light gases limits the achievable product yields, as also shown in Table 3. More recently, bifunctional zeolite-based catalysts, such as Pt/mordenite or Pt/ZSM-23, have been investigated for xylene isomerisation [3].
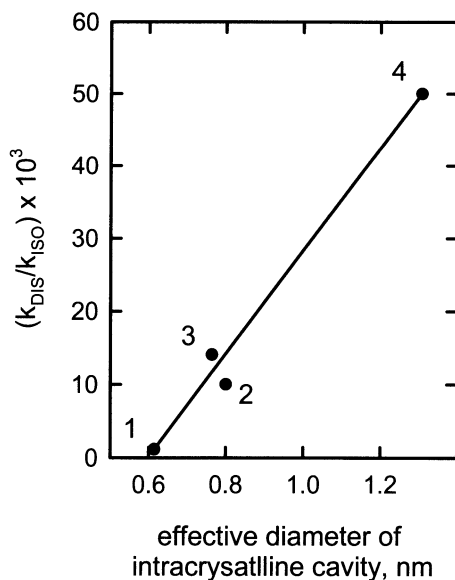
Fig. 18. Relative rate constants of disproportionation and isomerisation of xylenes as a function of the pore diameter of zeolite catalysts (1: H-ZSM-5, 2: H-ZSM-4 (H-omega), 3: H-mordenite, 4: H-Y), after ref. [152].

Table 3. Feed and product composition (wt.-%) obtained in xylene isomerisation in the Mobil Vapor Phase Isomerisation (MVPI), Mobil High-Temperature Isomerisation (MHTI) and in Octafining [154].

	MVPI	MHTI	Octafining
Feed			
Xylenes and ethylbenzene	100.0	100.0	100.0
Hydrogen	0.1	0.2	1.3
Total	*100.1*	*100.2*	*101.3*
Product			
Fuel gas	0.8	4.7	8.5
C_{5+}-non-aromatics	-	-	7.2
Benzene	7.7	11.2	4.3
Toluene	1.2	1.8	4.1
Para-xylene	77.9	80.1	68.9
C_{9+}-aromatics	12.5	2.4	8.3
Total	*100.1*	*100.2*	*101.3*

8.4   Disproportionation of Toluene

Zeolite-catalyzed toluene disproportionation is another means of producing xylenes, in this case with the co-production of benzene, sometimes in high purity

Table 4. Product composition (wt.-%) obtained in the Mobil Toluene Disproportionation Process (MTDP) with unmodified zeolite ZSM-5 and in the Mobil Selective Toluene Disproportionation Process (MSTDP) with pre-coked zeolite ZSM-5 [3,142,152].

Products	MTDP	MSTDP
C_{5-}	1.5	1.8
Benzene	17.9	13.9
Toluene	57.4	70.0
Ethylbenzene	0.2	0.6
Para-xylene	4.7	11.4
Meta-xylene	11.5	1.4
Ortho-xylene	5.2	0.3
C_{9+} aromatics	1.8	0.6
Total	*100.2*	*100.0*

[142]. Since the disproportionation rate in zeolite ZSM-5 is 5000 times lower than that of isomerisation, the processes are carried out at higher temperatures, *e.g.*, 450 to 470 °C in the Mobil Toluene Disproportionation Process (MTDP) [3,152,154,155]. Due to the larger effective pore width of the zeolite at this high temperature, the conversion is not shape-selective, and the xylene isomer distribution is close to equilibrium. Selective production of para-xylene can, however, be achieved, if the effective pore width of the zeolite is reduced by a well defined coke deposition procedure as applied in the Mobil Selective Toluene Disproportionation Process (MSTDP), thus slowing down the diffusion rates of the bulkier ortho- and meta-isomers relative to para-xylene. Table 4 compares typical product distributions of MTDP and MSTDP. Increased selectivity for para-xylene is also achieved over zeolite ZSM-5 modified with phosphorus, magnesium or silica representing a typical example of pore-size engineering (*cf.* section 6.4). Similar catalyst technology finds use in the selective para-xylene manufacture via alkylation of toluene with methanol [3].

8.5   Oxidation and Ammoximation

The introduction of redox-active elements into zeolites and related microporous materials opens up interesting options for heterogeneously catalyzed selective oxidations. The search for so-called "redox molecular sieves" as catalysts in combination with environmentally friendly oxidants, above all oxygen (or air) or hydrogen peroxide, is a highly dynamic research area that has recently been reviewed by *Bellussi* and *Rigutto* [156] and by *Arends* et al. [42]. This section focuses on commercial applications and highlights some recent examples.

The most intensely studied representative of redox zeolites is the medium-pore material titanium silicalite-1 (TS-1), *i.e.*, silica with the framework structure of ZSM-5 and framework silicon atoms substituted by titanium at typical ratios of $n_{Si}/n_{Ti} = 40$ to 90 [157]. This material catalyzes the selective oxidation of numerous organic substrates with aqueous H_2O_2 at mild conditions (20 to 150 °C) as shown in Figure 19 [158]. Of these, the hydroxylation of phenol to hydroquinone and catechol and the ammoximation of cyclohexanone to cyclohexanone oxime are carried out on an industrial scale. In a process of Enichem with a capacity of

100,000 t/a phenol is hydroxylated in aqueous solution at a conversion level of 25 to 30 % and high diphenol selectivities, *i.e.*, 84 % based on conversion of H_2O_2 and 90 to 94 % based on phenol conversion [159]. The shape selectivity over the TS-1 catalyst is reflected by the preferred formation of the para-isomer and a considerable suppression of side reactions leading to polynuclear aromatics and tar as compared to homogeneously catalyzed processes [160].

The suitability of TS-1 as a catalyst for the liquid-phase ammoximation of cyclohexanone with H_2O_2 and ammonia without the co-production of ammonium sulfate or nitrogen oxides as encountered in conventional processes has been demonstrated in a pilot plant by Enichem. At 80 to 95 °C, yields of cyclohexanone oxime, an important intermediate in the manufacture of thermoplastic polyamides, as high as 99 % based on cyclohexanone and 90 % based on H_2O_2 can be achieved [161]. The limited long-term stability of the catalyst due to removal of titanium and dissolution of the bulk zeolite in the alkaline reaction medium as well as pore blockage by heavier by-products is a problem that still deserves further attention [161].

Other redox metals beside titanium, which have been incorporated into the framework of microporous catalysts, include V, Sn, Cr, Cu, Co and Fe, to enumerate just a few [42]. Examples for selective catalysts with molecular oxygen as the oxidizing agent are CoAPO-5 for the selective oxidation of cyclohexane [162], CrAPO-5 for the oxidation of alkyl aromatics and secondary alcohols [163,164] and, more recently, the 8-membered-ring materials CoAPO-18 or MnAPO-18 setting a new landmark in the direct oxidation of both terminal methyl groups in linear alkanes, *e.g.*, of n-hexane to adipic acid [165]. Zeolite Fe-ZSM-5 has also been used for the direct hydroxylation of benzene to phenol in the gas phase with nitrous oxide as the oxidant [166], and the same reaction seems to be catalyzed by iron-free H-ZSM-5 [167,168].
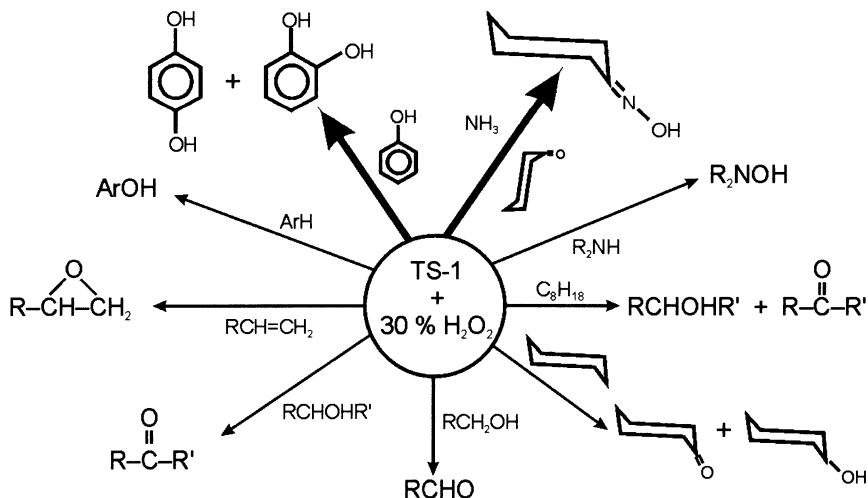
Fig. 19. Selective oxidation of organic substrates with aqueous hydrogen peroxide catalyzed by TS-1, after ref. [158].

Transition metal chelates immobilized as guest compounds in zeolite cavities also find increasing attention as selective oxidation catalysts [42,78,169,170]. The encapsulated complexes which often display higher stability than in homogeneous solution exhibit well defined active sites making the catalysts interesting for enzyme mimicking ("zeozymes"). The formation of adipic acid from cyclohexane with iron phthalocyanine [171] or from cyclohexene with the bipyridine complex $[Mn(bpy)_2]^{2+}$ [172] and the conversion of n-hexane with molecular oxygen to 1-hexanol and 1-hexanal over copper phthalocyanine [173], all encapsulated in the supercages of zeolite Y, may serve as examples.

To overcome limitations on the molecular size of reactants that can be converted, transition metal containing zeolites with larger pores have been developed including, for instance, V-NCL-1 [174] or Ti-UTD-1 (unidimensional 14-membered-ring channels) [175,176]. Particularly bulky reactants can be oxidized over mesoporous redox molecular sieves, e.g., norbornene or 2,6-di-*tert.*-butyl phenol over Ti-MCM-41 [177]. The use of mesoporous materials as oxidation catalysts, either with redox-active metals like Fe, Cr, V and Mn incorporated into the pore walls or as supports for transition metal complexes or enzymes, has recently been reviewed by *Corma* [178] and *Corma* and *Kumar* [179], respectively.

8.6   Amination

Nucleophilic substitution of methanol by ammonia can be catalyzed by acidic zeolites for the manufacture of methylamines which are important intermediates for fine chemicals production [180]. The conversion of methanol with ammonia has been intensively studied over various zeolitic catalysts [158,181-183]. Zeolites are utilized in this conversion with the aim to reduce the fraction of the thermodynamically preferred formation of trimethylamine (TMA) in favor of the desired dimethylamine (DMA) and monomethylamine (MMA) by shape selectivity effects. The influence of the pore dimensions of zeolite catalysts on the selectivity for the methylamines is compared to the thermodynamic equilibrium distribution and the worldwide consumption in Table 5 showing the preferred formation of mono- and dimethylamine, especially over the small-pore zeolites H-Rho, H-ZK-5 and H-chabazite. A process by Nitto Chemicals using a catalyst based on a modified steamed and alkali ion-exchanged mordenite catalyst with a capacity of 50,000 t/a has been reported to be on-stream in Japan since 1985 [184]. At 320 °C in the gas phase and at methanol conversions above 95 %, selectivities of *ca.* 50 % for DMA and of < 5 % for TMA have been claimed [185,186].

Also possible are aminations of alcohols with two to four carbon atoms over cobalt- or nickel-exchanged Y-type zeolites, of phenol to aniline over H-ZSM-5 and of multifunctional substances such as ethanolamine to ethylene diamine over H-mordenite [183].

Table 5. Distribution of mono-, di- and trimethylamine (mol-%) obtained in the conversion of methanol with ammonia over various zeolite catalysts at 325 °C and methanol conversions above 90 %, thermodynamic equilibrium values after ref. [181]; worldwide consumption, as of 1987, after ref. [180].

Catalyst	Pore diameter / nm	MMA	DMA	TMA
H-Y	0.74	15	12	73
H-mordenite	0.70	18	13	69
H-ferrierite	0.54	33	29	38
H-Rho	0.51	34	53	13
H-ZK-5	0.39	26	63	11
H-chabazite	0.37	43	46	11
Thermodynamic equilibrium		17	21	62
Consumption (worldwide)		33	53	14

The acid-catalyzed addition of ammonia to alkenes is another route to primary alkylamines. A variety of acidic zeolites with different structures have been tested for the amination of C_2- to C_4-alkenes [183]. With zeolite H-ZSM-5, for instance, and at typical reaction conditions of 300 to 400 °C, high pressures of up to 300 bar and with an excess of ammonia, selectivities for the amines between 95 to 98 % at olefin conversions of *ca.* 10 % are achieved [187,188]. A disadvantage of this route is the tendency towards deactivation which is pronounced with zeolites X and Y, but less so after rare-earth ion exchange or with Al-, Fe- or B- containing MFI-type zeolites [183]. Although low temperatures favor selective amination, a minimum temperature is needed for activation of the alkenes. Thus, amination yields decrease in the order isobutene > propene > ethene making isobutene amination the only technically attractive reaction which reaches an equilibrium conversion of 9 % at 300 °C. BASF uses this process in a multi-purpose unit with a capacity of 8,000 t/a to produce *tert.*-butylamine, presumably over modified zeolite ZSM-5 as a catalyst [189]. Recently, zeolites SSZ-26, SSZ-33, SSZ-37 and CIT-5 have been claimed as catalysts for the amination of bulky alkenes [190,191].

Zeolite catalysts can also be applied for the amination of various compound types, such as ethers, epoxides, halogenated hydrocarbons or carbon monoxide [183,192], yet these amination reactions are beyond the scope of the present review.

9.   Where does Catalysis on Zeolites Stand?

Fourty years after their introduction into industrial practice, zeolite catalysts have conquered an impressive number of large-scale processes. The most important of these and the advantages offered by zeolites over more conventional catalysts have been discussed in the present contribution. So far, the domain of zeolite catalysis continues to be in petroleum refining and basic petrochemistry. There is little doubt, however, that, in the decades ahead, zeolite catalysts will find more and more applications in the manufacture of higher-value products, *i.e.*, of organic intermediates carrying functional groups or even of certain fine chemicals. It has

sometimes been argued that zeolite catalysis is, by now, a mature field of science and technology. The extent to which such and similar statements reflect the real situation depends on how exactly they are meant: While it is certainly true that a huge amount of information has been accumulated on the synthesis, structure, post-synthesis modification, physico-chemical characterization and catalytic application of zeolites, this does by no means rule out that there is further and ample room for significant improvements, innovations or even breakthrough discoveries in catalysis by zeolites.

It is perhaps justified to look at zeolites as one of the big and industrially very successful classes of solid catalysts. Other members of this family of materials include metals, transition metal oxides and sulfides. From the fact that zeolites represent by far the youngest member of this family, some people were tempted from time to time to expect too much from zeolites or to promise too much about their capabilities. This (and the latter in particular) is regrettable, yet from the facts that some arduous expectations were not met and some promises were not fulfilled, one should by no means conclude that zeolite catalysis has come to its end.

Here are a few research directions in zeolite catalysis along which we expect significant progress in the future:

(i)   There are by now (*cf.* Figure 3) 133 crystallographically distinct zeolite structures of which, however, less than 10 (*cf.* Table 1) have found applications as catalysts on an industrial scale. Many of the remaining structures are candidates for catalysis, yet their performance is largely unexplored.

(ii)   In the vast majority of cases, zeolite catalysts have been employed in an acid (or bifunctional) form. The acid strength of zeolites turned out to be higher than that of many other solid acids, *e.g.*, of amorphous SiO_2-Al_2O_3, hence the relatively high activity of zeolite catalysts. Techniques are available to lower the acid strength of zeolites, if this is beneficial for catalysis. Conversely, some applications call for superacid sites in zeolites with a much enhanced strength of the acid sites. The generation of such sites without sacrificing the traditional advantages of zeolites (thermal stability, lack of toxicity and corrosiveness, environmentally benign operation) continues to be a challenge.

(iii) Zeolites are ideal hosts for a large variety of catalytically active guests. The exploration of zeolite-hosted guests as catalysts touches many fields of heterogeneous catalysis, including base catalysis, enantioselective and diastereoselective catalysis, highly selective catalysis on transition metal complexes or even catalysis by enzymes. It is obvious that catalysis by zeolite-hosted guests has strong links to the heterogenization of homogeneous catalysis.

(iv)   With the advent of highly sensitive spectrometers and sophisticated computers for data handling, the direct (in-situ) observation of working zeolite (or other solid) catalysts and of the adsorbates on their surfaces becomes more and more feasible [193]. From such in-situ spectroscopic techniques, we expect much new insight into the complex series of steps

involved in zeolite catalysis and this, in turn, might contribute to a rational design of improved catalytic materials.

(v)   Completely novel materials are steadily emerging from modern solid-state chemistry and materials science. Many of these materials are porous, and again a considerable portion of these possess regularly formed micro- or mesopores (excellent descriptions of such materials can be found in refs. [194,195]). The potential of these materials in catalysis is largely unexplored – obviously the communities of solid-state chemists and experts in heterogeneous catalysis have to be brought together.

Indeed, catalysis on zeolites has matured in that zeolites have found their firm place in the family of catalytically most important materials. Other members of this family will continue to provide better solutions to many open problems in catalysis. On the other hand, nobody who deals with heterogeneous catalysis can afford to ignore zeolites and their potential in the solution of numerous open catalytic problems.

References

1   J. Weitkamp and L. Puppe (Eds.): *Catalysis and Zeolites – Fundamentals and Applications* (Springer, Berlin, Heidelberg 1999) 564 pp.
2   J. Weitkamp, Solid State Ionics **131**, 175-188 (2000)
3   P.M.M. Blauwhoff, J.W. Gosselink, E.P. Kieffer, S.T. Sie and W.H.J. Stork, in *Catalysis and Zeolites – Fundamentals and Applications*, J. Weitkamp and L. Puppe (Eds.) (Springer Verlag, Berlin, Heidelberg, New York 1999) pp. 437-538
4   N.Y. Chen, W.E. Garwood and F.G. Dwyer: *Shape Selective Catalysis in Industrial Applications*, Chem. Ind. **65** (Marcel Dekker, New York 1996) 282 pp.
5   R.M. Barrer, Pure Appl. Chem. **51**, 1091-1100 (1979)
6   D.W. Breck: *Zeolite Molecular Sieves* (Wiley, New York 1974) 771 pp.
7   W. Löwenstein, Am. Mineralogist **39**, 92-96 (1954)
8   F. Liebau: *Structural Chemistry of Silicates – Structure, Bonding and Classification* (Springer, Berlin, Heidelberg, New York, Tokyo 1985) 347 pp.
9   F. Liebau, H. Gies, R.P. Gunawardane and B. Marler, Zeolites **6**, 373-377 (1986)
10   J.S. Beck, J.C. Vartuli, W.J. Roth, M.E. Leonowicz, C.T. Kresge, K.D. Schmitt, C.T.-W. Chu, D.H. Olson, E.W. Sheppard, S.B. McCullen, J.B. Higgins and J.L. Schlenker, J. Am. Chem. Soc. **114**, 10834-10843 (1992)
11   J.W. McBain: *The Sorption of Gases and Vapours by Solids* (Rutledge and Sons, London 1932) p. 169
12   A.F. Cronsted, Svenska Vetenskaps Akademiens Handlingar Stockholm **17**, 120-123 (1756)
13   A. Dyer: *An Introduction to Zeolite Molecular Sieves* (John Wiley and Sons, Chichester 1988) 149 pp.
14   M.M.J. Treacy, K.H. Randall and S. Rao, in *Proceedings of the 12th International Zeolite Conference*, Baltimore, Maryland, USA, June 1998, Vol. I, M.M.J. Treacy, B.K. Marcus, M.E. Bisher, J.B. Higgins (Eds.) (Materials Research Society, Warrendale, Pennsylvania 1998) pp. 517-532

15   W.M. Meier, D.H. Olson and C. Baerlocher: *Atlas of Zeolite Structure Types* (Elsevier, London 1996) 229 pp.

16   http://www.iza-structure.org/databases

17   S. Ernst, in *Molecular Sieves, Science and Technology*, H.G. Karge and J. Weitkamp (Eds.), Vol. 1 – Synthesis (Springer, Berlin, Heidelberg, New York 1998) pp. 65-96

18   E. Roland and P. Kleinschmit, in *Ullmann's Encyclopedia of Industrial Chemistry*, B. Elvers and S. Hawkins (Eds.), Vol. A 28 (Verlag Chemie, Weinheim 1996) pp. 475-504

19   P.A. Jacobs, in *Carboniogenic Activity of Zeolites* (Elsevier, Amsterdam 1977) pp. 38-84

20   H.G. Karge, in *Catalysis and Adsorption by Zeolites*, G. Öhlmann, H. Pfeifer, R. Fricke (Eds.), Stud. Surf. Sci. Catal. **65** (Elsevier, Amsterdam 1991) pp. 133-156

21   J. Dwyer, in *Innovation in Zeolite Materials Science*, P.J. Grobet, W.J. Mortier, E.F. Vansant and G. Schulz-Ekloff (Eds.) Stud. Surf. Sci. Catal. **37** (Elsevier, Amsterdam 1988) pp. 333-354

22   J.A. Rabo and G.J. Gajda, Catal. Rev. - Sci. Eng. **31**, 385-439 (1990)

23   A.E. Hirschler, J. Catal. **2**, 428-439 (1963)

24   C.J. Plank, in *Proceedings of the 3ʳᵈ International Congress on Catalysis*, W.M.H. Sachtler, G.C.A. Schuit and P. Zwietering (Eds.), Vol. 1 (North-Holland Publishing Company, Amsterdam 1965) p. 727

25   G.H. Kühl, in *Molecular Sieves*, J.B. Uytterhoeven (Ed.), Proc. 3rd International Conference on Molecular Sieves (Leuven University Press, Leuven (Belgium) 1973) pp. 227-229

26   P.A. Jacobs and H.K. Beyer, J. Phys. Chem. **83**, 1174-1177 (1979)

27   H. Hattori, Chem. Rev. **95**, 537-558 (1995)

28   J. Weitkamp, M. Hunger and U. Rymsa, Microporous Mesoporous Mater. (2001), in press

29   P.A. Jacobs, in *Characterization of Heterogeneous Catalysts*, F. Delannay (Ed.), Chem. Ind. **15** (Marcel Dekker, New York, Basel 1984) pp. 367-404

30   H.G. Karge, M. Hunger and H.K. Beyer, in *Catalysis and Zeolites – Fundamentals and Applications*, J. Weitkamp and L. Puppe (Eds.) (Springer Verlag, Berlin, Heidelberg 1999) pp. 198-326

31   R.A. van Santen and G.J. Kramer, Chem. Rev. **95**, 637-660 (1995)

32   J. Sauer, in *Zeolites and Related Microporous Materials: State of the Art 1994*, J. Weitkamp, H.G. Karge, H. Pfeifer and W. Hölderich (Eds.) Stud. Surf. Sci. Catal. **84**, Part C (Elsevier, Amsterdam 1994) pp. 2039-2057

33   H.G. Karge, J. Ladebeck, Z. Sarbak and K. Hatada, Zeolites **2**, 91-102 (1982)

34   H.G. Karge, K. Hatada, Y. Zhang and R. Fiedorow, Zeolites **3**, 13-21 (1983)

35   P.B. Weisz and J.N. Miale, J. Catal. **4**, 527-529 (1965)

36   W.O. Haag, R.M. Lago and P.B. Weisz, Nature. **309**, 589-591 (1984)

37   J. Weitkamp, S. Ernst and L. Puppe, in *Catalysis and Zeolites – Fundamentals and Applications* J. Weitkamp and L. Puppe (Eds.) (Springer Verlag, Berlin, Heidelberg 1999) pp. 327-376

38   C. Song, J.M. Garcés and Y. Sugi (Eds.): *Shape-Selective Catalysis*, ACS Symp. Ser. **738** (American Chemical Society, Washington, D.C. 2000) 389 pp.

39   P.B. Weisz, Pure Appl. Chem. **52**, 2091-2103 (1980)

40   S.M. Csicsery, Pure Appl. Chem. **58**, 841-858 (1986)

41   J. Weitkamp and S. Ernst, Catal. Today **19**, 107-149 (1994)

42   I.W.C.E. Arends, R.A. Sheldon, M. Wallau and U. Schuchardt, Angew. Chem. Int. Ed. **36**, 1144-1163 (1997)

43   V. Ramamurthy, in *Photochemistry in Organized and Constrained Media*, V. Ramamurthy (Ed.) (VCH Publishers, New York, Weinheim 1991) pp. 429-493

44   R.M. Dessau, J. Chem. Soc., Chem. Commun., 1167-1168 (1986)

45   T. Komatsu, T. Maeda and T. Yashima, Microporous Mesoporous Mater. **35-36**, 173-180 (2000)

46   E.J.P. Feijen, J.A. Martens and P.A. Jacobs, in *Preparation of Solid Catalysts*, G. Ertl, H. Knözinger and J. Weitkamp (Eds.) (Wiley-VCH, Weinheim 1999) pp. 262-284

47   R.W. Thompson, in *Molecular Sieves, Science and Technology*, H.G. Karge and J. Weitkamp (Eds.), Vol. 1 – Synthesis (Springer, Berlin, Heidelberg, New York 1998) pp. 1-33

48   R. Szostak: *Molecular Sieves – Principles of Synthesis and Identification* (Van Nostrand Reinhold, New York 1989) 524 pp.

49   M.L. Occelli and H. Kessler (Eds.): *Synthesis of Porous Materials*, Chem. Ind. **69** (Marcel Dekker, New York 1997) 718 pp.

50   A.V. McCormick and A.T. Bell, Catal. Rev. – Sci. Eng. **31**, 97-127 (1989)

51   P.A. Jacobs and J.A. Martens (Eds.): *Synthesis of High-Silica Aluminosilicate Zeolites*, Stud. Surf. Sci. Catal. **33** (Elsevier, Amsterdam 1987) 390 pp.

52   R.M. Barrer: *Hydrothermal Chemistry of Zeolites* (Academic Press, London 1982) 360 pp.

53   D.W. Breck and E.M. Flanigen, in: *Molecular Sieves* (Society of Chemical Industry, London 1968) pp. 47-61

54   F.-Y. Dai, M. Suzuki, H. Takakashi and Y. Saito, in *New Developments in Zeolite Science and Technology*, Y. Murakami, A. Iijima and J.W. Ward (Eds.), Stud. Surf. Sci. Catal. **28** (Kodansha, Tokyo and Elsevier, Amsterdam 1986) pp. 223-230

55   A. Moini, K.D. Schmitt, E.W. Valyocsik and R.F. Polomski, Zeolites **14**, 504-511 (1994)

56   E.J.P. Feijen, J.A. Martens and P.A. Jacobs, in *Zeolites and Related Microporous Materials. State of the Art 1994*, J. Weitkamp, H.G. Karge, H. Pfeifer and W. Hölderich (Eds.), Stud. Surf. Sci. Catal. **84**, Part A (Elsevier, Amsterdam 1994) pp. 3-21

57   J.-P. Gilson, in *Zeolite Microporous Solids: Synthesis, Structure, and Reactivity*, E.G. Derouane, F. Lemos, C. Naccache and F.R. Ribeiro (Eds.), NATO ASI Series C, Mathematical and Physical Sciences **352** (Kluwer Academic Publishers, Dordrecht 1992) pp. 21-48

58   D.E.W. Vaughan, in *Catalysis and Adsorption by Zeolites*, G. Öhlmann, H. Pfeifer, R. Fricke (Eds.), Stud. Surf. Sci. Catal. **65** (Elsevier, Amsterdam 1991) pp. 275-286.

59   F. Schüth and K. Unger, in *Preparation of Solid Catalysts*, G. Ertl, H. Knözinger and J. Weitkamp (Eds.) (Wiley-VCH, Weinheim 1999) pp. 60-84

60   E. Roland, in *Zeolites as Catalysts, Sorbents and Detergent Builders*, H.G. Karge and J. Weitkamp (Eds.), Stud. Surf. Sci. Catal. **46** (Elsevier, Amsterdam 1989) pp. 645-659

61   US Patent 4 493 902, Jan. 15, 1985, assigned to Engelhard Corp. (Inv.: S.M. Brown, V.A. Durante, W.J. Reagan and B.K. Speronello)

62   US Patent 3 702 886, Nov. 14, 1972, assigned to Mobil Oil Corp. (Inv.: R.J. Argauer and R. Landolt)

63   B. Burger, K. Haas-Santo, M. Hunger and J. Weitkamp, Chem. Eng. Technol. **23**, 322-324 (2000)

64   G.H. Kühl, in *Catalysis and Zeolites – Fundamentals and Applications*, J. Weitkamp and L. Puppe (Eds.) (Springer Verlag, Berlin, Heidelberg, New York 1999) pp. 81-197

65   J.F. Le Page, in *Preparation of Solid Catalysts*, G. Ertl, H. Knözinger and J. Weitkamp (Eds.) (Wiley-VCH, Weinheim 1999) pp. 579-589

66   H. Sherry, Zeolites **13**, 377-383 (1993)

67   H.S. Sherry, J. Phys. Chem. **70**, 1158-1168 (1966)

68   L.V.C. Rees and T. Zuyi, Zeolites **6**, 201-205 (1986)

69   M. Hartmann and B. Boddenberg, in *Zeolites and Related Microporous Materials: State of the Art 1994*, J. Weitkamp, H.G. Karge, H. Pfeifer and W. Hölderich (Eds.), Stud. Surf. Sci. Catal. **84**, Part A (Elsevier, Amsterdam 1994) pp. 509-517

70   H.G. Karge, V. Mavrodinova, Z. Zheng and H.K. Beyer, in *Guidelines for Mastering the Properties of Molecular Sieves*, D. Barthomeuf, E.G. Derouane and W. Hölderich (Eds.), NATO ASI Series B, Physics **221** (Plenum Press, New York 1990) pp. 157-168

71   J. Weitkamp, S. Ernst, T. Bock, A. Kiss and P. Kleinschmit, in *Catalysis by Microporous Materials*, H.K. Beyer, H.G. Karge, I. Kiricsi and J.B. Nagy (Eds.), Stud. Surf. Sci. Catal. **94** (Elsevier, Amsterdam 1995) pp. 278-285

72   H.G. Karge and H.K. Beyer, in *Molecular Sieves – Science and Technology*, H.G. Karge and J. Weitkamp (Eds.), Vol. 3 - Modification (Springer, Berlin, Heidelberg 2001), in press

73   C.V. McDaniel and P.K. Maher, in *Molecular Sieves* (Society of Chemical Industry, London 1968) pp. 186-195

74   J. Klinowski, J.M. Thomas, C.A. Fyfe and G.C. Gobbi, Nature **296**, 533-536 (1982)

75   R. Szostak, in *Introduction to Zeolite Science and Practice*, H. van Bekkum, E.M. Flanigen and J.C. Jansen (Eds.), Stud. Surf. Sci. Catal. **58** (Elsevier, Amsterdam 1991) pp. 153-199

76   H.K. Beyer, G. Borbély-Pálne and J. Wu, in *Zeolites and Related Microporous Materials: State of the Art 1994*, J. Weitkamp, H.G. Karge, H. Pfeifer and W. Hölderich (Eds.), Stud. Surf. Sci. Catal. **84**, Part B (Elsevier, Amsterdam 1994) pp. 933-940

77   J. Scherzer, in *Catalytic Materials*, T.E. White, Jr., R.A. Dalla Betta, E.G. Derouane and R.T.K. Baker (Eds.), ACS Symp. Ser. **248** (American Chemical Society, Washington, D.C. 1984) pp. 157-200

78   G. Schulz-Ekloff and S. Ernst, in *Preparation of Solid Catalysts*, G. Ertl, H. Knözinger and J. Weitkamp (Eds.) (Wiley-VCH, Weinheim 1999) pp. 405-477

79   E.F. Vansant: *Pore Size Engineering in Zeolites* (J. Wiley and Sons, Chichester and Salle und Sauerländer, Aarau 1990) 145 pp.

80   J.E. Naber, K.P. De Jong, W.H.J. Stork, H.P.C.E. Kuipers and M.F.M. Post, in *Zeolites and Related Microporous Materials: State of the Art 1994*, J. Weitkamp, H.G. Karge, H. Pfeifer and W. Hölderich (Eds.), Stud. Surf. Sci. Catal. **84**, Part C (Elsevier, Amsterdam 1994) pp. 2197-2219

81   R. von Ballmoos, D.H. Harris ans J.S. Magee, in *Handbook of Heterogeneous Catalysis*, G. Ertl, H. Knözinger and J. Weitkamp (Eds.), Vol. 4 (Wiley-VCH, Weinheim 1997) pp. 1955-1986

82   G. Martino, P. Courty and C. Marcilly, in *Handbook of Heterogeneous Catalysis*, G. Ertl, H. Knözinger and J. Weitkamp (Eds.), Vol. 4 (Wiley-VCH, Weinheim 1997) pp. 1801-1818

83   H. Fichtner-Schmittler, U. Lohse, G. Engelhardt and V. Patzelová, Crystal Research and Technology 19, K1-K3 (1984)

84   J.R. Sohn, S.J. DeCanio, J.H. Lunsford and D.J. O'Donnell, Zeolites **6**, 225-227 (1986)

85   U. Graeser, W. Keim, W.J. Petzny and J. Weitkamp, Erdöl, Erdgas, Kohle **111**, 208-218 (1995)

86   A. Corma, Chem. Rev. **95**, 559-614 (1995)

87   F.G. Dwyer, F. Degnan, in *Fluid Catalytic Cracking: Science and Technology*, J.S. Magee and M.M. Mitchell, Jr. (Eds.), Stud. Surf. Sci. Catal. **76** (Elsevier, Amsterdam 1993) pp. 499-530

88   J. Scherzer, Catal. Rev. - Sci. Eng. **31**, 215-354 (1989)

89   J. Biswas and I.E. Maxwell, Appl. Catal. **63**, 197-258 (1990)

90   M.L. Occelli (Ed.): *Fluid Catalytic Cracking*, ACS Symp. Ser. **375** (American Chemical Society, Washington, D.C. 1988) 353 pp.

91   M.L. Occelli (Ed.): *Fluid Catalytic Cracking II*, ACS Symp. Ser. **452** (American Chemical Society, Washington, D.C. 1991) 374 pp.

92   M.L. Occelli and P O'Connor (Eds.): *Fluid Catalytic Cracking III*, ACS Symp. Ser. **571** (American Chemical Society, Washington, D.C. 1994) 386 pp.

93   P. B. Weisz, Adv. Catal. **13**, 137-190 (1962)

94   H. Schulz and J. Weitkamp, Ind. Eng. Chem., Prod. Res. Dev. **11**, 46-53 (1972)

95   H. Pichler, H. Schulz, H.O. Reitemeyer and J. Weitkamp, Erdöl, Kohle-Erdgas-Petrochem. **25**, 494-505 (1972)

96   J.W. Ward, Fuel Process. Technol. **35**, 55-85 (1993)

97   A. Hock, T. Huizinga, A.A. Esener, I.E. Maxwell, W.H.J. Stork, F.J. van de Meerakker and O. Sy, Oil Gas J. **89**, April 22, 77-82 (1991)

98   J.A. Martens, P.A. Jacobs and J. Weitkamp, Appl. Catal. **20**, 239-281 (1986)

99   J.A. Martens and P.A. Jacobs, in *Catalysis and Zeolites – Fundamentals and Applications*, J. Weitkamp and L. Puppe (Eds.) (Springer Verlag, Berlin, Heidelberg 1999) pp. 53-80

100   A. Corma, Q. Kan, M.T. Navarro, J. Perez-Pariente and F. Rey, Chem. Mater. **9**, 2123-2126 (1997)

101   Directive 98/70/EC, Official Journal of the European Communities L 350, 58-68 (1998)

102   J. Weitkamp A. Raichle, Y. Traa, M. Rupp and F. Fuder, Chem Comm., 403-404 (2000)

103   J. Weitkamp A. Raichle, Y. Traa, M. Rupp and F. Fuder, Chem Comm., 1133-1134 (2000)

104   J.P. van den Berg, J.P. Lucien, G. Germaine and G.L.B. Thielemans, Fuel Process. Technol. **35**, 119-136 (1993).

105   J.G. Bendoraitis, A.W. Chester, F.G. Dwyer and W.E. Garwood, , in *New Developments in Zeolite Science and Technology*, Y. Murakami, A. Iijima and J.W. Ward (Eds.), Stud. Surf. Sci. Catal. **28** (Kodansha, Tokyo and Elsevier, Amsterdam 1986) pp. 669-675

106   I.E. Maxwell, J.K. Minderhoud, W.H.J. Stork and J.A.R. van Veen, in *Handbook of Heterogeneous Catalysis*, G. Ertl, H. Knözinger and J. Weitkamp (Eds.), Vol. 4 (Wiley-VCH, Weinheim 1997) pp. 2017-2038

107   US Patent 4 419 220, Dec. 06, 1983, assigned to Mobil Oil Corp. (Inv.: R.B. La Pierre, R.D. Partridge, N.Y. Chen and S.S. Wang)

108   S.J. Miller, Microporous Mater. **2**, 439-449 (1994)

109   S.D. Burd and J. Maziuk, Oil Gas J. **70**, July, 03, 52-60 (1972)

110   N.Y. Chen, W.E. Garwood and R.H. Heck, Ind. Eng. Chem. Res. **26**, 706-711 (1987)

111   I.E. Maxwell and W.H.J. Stork, in *Introduction to Zeolite Science and Practice*, H. van Bekkum, E.M. Flanigen and J.C. Jansen (Eds.), Stud. Surf. Sci. Catal. **58** (Elsevier, Amsterdam 1991) pp. 571-630

112   S.T. Sie, in *Handbook of Heterogeneous Catalysis*, G. Ertl, H. Knözinger and J. Weitkamp (Eds.), Vol. 4 (Wiley-VCH, Weinheim 1997) pp. 1998-2017

113   K.D. Miller, Oil Gas J. **98**, July 10, 52-55 (2000)

114   US Patent 5 157 194, Oct. 20, 1992, assigned to Mobil Oil Corp. (Inv.: I. Rahmim, A. Huss, Jr., D.N. Lissy, D.J. Klocke and I.D. Johnson)

115   W.-Q. Xu, Y.-G. Yiu, S.L. Suib and C.-L. O'Young, J. Catal. **150**, 34-45 (1994)

116   S.M. Yang, D.H. Guo, J.S. Lin and G.T. Wang, in *Zeolites and Related Microporous Materials: State of the Art 1994*, J. Weitkamp, H.G. Karge, H. Pfeifer and W. Hölderich (Eds.), Stud. Surf. Sci. Catal. **84**, Part C (Elsevier, Amsterdam 1994) pp. 1677-1684

117   H. Mooiweer, K.P de Jong, B. Kraushaar-Czarnetzki, W.H.J. Stork and B.C.H. Krutzen, in *Zeolites and Related Microporous Materials: State of the Art 1994*, J. Weitkamp, H.G. Karge, H. Pfeifer and W. Hölderich (Eds.), Stud. Surf. Sci. Catal. **84**, Part C (Elsevier, Amsterdam 1994) pp. 2327-2334

118   P. Meriaudeau, R. Bacaud, L.N. Hung and A.T. Vu, J. Mol. Catal. A **110**, L177-L-179 (1996)

119   D. Rutenbeck, H. Papp, H. Ernst and W. Schwieger, Appl. Catal. A: General **208**, 153-161 (2001)

120   H. Liu, G.D. Lei and W.M.H. Sachtler, Appl. Catal. A: General **146**, 165-180 (1996)

121   M. Guisnet, P. Andy, Y. Boucheffa, N.S. Gnep, C. Travera and E. Benazzi, Catal. Lett. **50**, 159-164 (1998)

122   P. Andy, N.S. Gnep, M. Guisnet, E. Benazzi and C. Travera, J. Catal. **173**, 322-332 (1998)

123   L. Domokos, M.C. Paganini, F. Meunier, K. Seshan and J.A. Lercher, in *12th International Congress on Catalysis*, A. Corma, F.V. Melo, S. Mendioroz and J.F.G. Fierro (Eds.), Stud. Surf. Sci. Catal. **130**, Part A (Elsevier, Amsterdam 2000) pp. 323-328

124   J. Weitkamp and S. Ernst, in *Proceedings of the 13th World Petroleum Congress*, Vol. 3 (Wiley, Chichester 1993) pp. 315-318

125   J. Weitkamp and Y. Traa, Catal. Today **49**, 193-199 (1999)

126   J. Weitkamp and Y. Traa, in *Handbook of Heterogeneous Catalysis*, G. Ertl, H. Knözinger and J. Weitkamp (Eds.), Vol. 4 (Wiley-VCH, Weinheim 1997) pp. 2039-2069

127   G.S. Nivarthy, A. Feller, K. Seshan and J.A. Lercher, in *12th International Congress on Catalysis*, A. Corma, F.V. Melo, S. Mendioroz and J.F.G. Fierro (Eds.), Stud. Surf. Sci. Catal. **130**, Part C (Elsevier, Amsterdam 2000) pp. 2561-2566

128   D. Seddon, Catal. Today **6**, 351-372 (1990)

129   S.B. Abdul Hamid and E.G. Derouane, in *Zeolites and Related Microporous Materials. State of the Art 1994*, J. Weitkamp, H.G. Karge, H. Pfeifer and W.

Hölderich (Eds.), Stud. Surf. Sci. Catal. **84**, Part C (Elsevier, Amsterdam 1994) pp. 2335-2344

130   D.E. Walsh and L.D. Rollmann, J. Catal. **49**, 369-375 (1977)

131   D.E. Walsh and L.D. Rollmann, J. Catal. **56**, 195-197 (1979)

132   P.W. Tamm. D.H. Mohr and C.R. Wilson, in *Catalysis 1987*, J.W. Ward (Ed.), Stud. Surf. Sci. Catal. **38** (Elsevier, Amsterdam 1988) pp. 335-353

133   G.B. McVicker, J.L. Kao, J.J. Ziemiah, W.E. Gates, J.L. Robbins, M.M.J. Treacy, S.B. Rice, T.H. Vanderspurt, V.R. Cross and A.K. Gosh, J. Catal. **139**, 48-61 (1993)

134   A. Raichle, Y. Traa and J. Weitkamp, Chem. Ing. Tech., accepted for publication

135   M. Stöcker, Microporous Mesoporous Mater. **29**, 3-48 (1999)

136   C.D. Chang and A.J. Silvestri, Chemtech **17**, 624-631 (1987)

137   G.J. Hutchings and R. Hunter, Catal. Today **6**, 279-306 (1990)

138   C.D. Chang, in *Handbook of Heterogeneous Catalysis*, G. Ertl, H. Knözinger and J. Weitkamp (Eds.), Vol. 4 (Wiley-VCH, Weinheim 1997) pp. 1894-1908

139   W.O. Haag, in *Proceedings of the 6th International Zeolite Conference*, D. Olson and A Bisio (Eds.) (Butterworths, Guildford 1984) pp. 466-478

140   C.D. Chang, Catal. Rev. – Sci. Eng. **26**, 323-345 (1984)

141   F.G. Dwyer, in *Catalysis of Organic Reactions*, W.R. Moser (Ed.) (Marcel Dekker, New York 1981) pp. 39-50

142   J.S. Beck and W.O. Haag, in *Handbook of Heterogeneous Catalysis*, G. Ertl, H. Knözinger and J. Weitkamp (Eds.), Vol. 5 (Wiley-VCH, Weinheim 1997) pp. 2123-2136

143   F.G. Dwyer, P.J. Lewis and F.M. Schneider, Chem. Eng. **83**, No. (1), 90-91 (1976)

144   US Patent 4 891 448, Jan. 02, 1990, assigned to Dow Chemical Co. (Inv.: J. Garcés, J.J. Maj, G.J. Lee and S.C. Rocke)

145   US Patent 5 015 797, May 14, 1991, assigned to Dow Chemical Co. (Inv.: G.J. Lee, J. Garcés and J.J. Maj)

146   G.R. Meima, M.J.M. van der Aalst, M.S.U. Samson, J.M. Garces and J.G. Lee, in *Proceedings from the 9th International Zeolite Conference*, R. von Ballmoos, J.B. Higgins and M.M.J. Treacy (Eds.), Vol. II (Butterworth-Heinemann, Boston 1993), pp. 327-334

147   G.R. Meima, M.J.M. van der Aalst, M.S.U. Samson, J.M. Garces and J.G. Lee, in *Proceedings of the DGMK-Conference "Catalysis on Solid Acids and Bases"*, Berlin, March 14-15, 1996, Tagungsbericht 9601, (Eds.) (German Society for Petroleum and Coal Science (DGMK), Hamburg 1996) pp. 125-138

148   C. Perego, S. Amarilli, G. Bellussi, O. Cappellazzo and G. Girotti, in *Proceedings of the 12th International Zeolite Conference*, Baltimore, Maryland, USA, June 1998, Vol. II, M.M.J. Treacy, B.K. Marcus, M.E. Bisher, J.B. Higgins (Eds.) (Materials Research Society, Warrendale, Pennsylvania 1998) pp. 575-582

149   US Patent 4 301 317, Nov. 17, 1981, assigned to Mobil Oil Corp. (Inv.: L.B. Young)

150   Y. Sugi and M. Toba, Catal. Today **19**, 187-211 (1994)

151   J.A. Johnson and A.R. Oroskar, in *Zeolites as Catalysts, Sorbents and Detergent Builders*, H.G. Karge and J. Weitkamp (Eds.), Stud. Surf. Sci. Catal. **46** (Elsevier, Amsterdam 1989) pp. 451-467

152   D.H. Olson and W.O. Haag, in *Catalytic Materials*, T.E. White, Jr., R.A. Dalla Betta, E.G. Derouane and R.T.K. Baker (Eds.), ACS Symp. Ser. **248** (American Chemical Society, Washington, D.C. 1984) pp. 275-307

153   H. Heinemann, Catal. Rev. – Sci. Eng. **15**, 315-328 (1977)

154	W.W. Keading, G.C. Barile and M.M. Wu, Catal. Rev. – Sci. Eng. **26**, 597-612 (1984)
155	N.Y. Chen and W.E. Garwood, Catal. Rev. – Sci. Eng. **28**, 185-267 (1986)
156	G. Bellussi and M.S. Rigutto, in *Advanced Zeolite Science and Applications*, J.C. Jansen, M. Stöcker, H.G. Karge and J. Weitkamp (Eds.) Stud. Surf. Sci. Catal. **85** (Elsevier, Amsterdam 1994) pp. 177-213
157	B. Notari, in *Chemistry of Microporous Crystals*, T. Inui, S. Namba and T. Tatsumi (Eds.) Stud. Surf. Sci. Catal. **60** (Elsevier, Amsterdam 1991) pp. 343-352
158	P.B. Venuto, Microporous Mater. **2**, 297-411 (1994)
159	US Patent 4 396 783, Aug. 02., 1983, assigned to Anic S.p.A. (Inv.: A. Esposito, M Taramasso and C. Neri)
160	B. Notari, in *Innovation in Zeolites Materials Science*, P.J. Grobet, W.J. Mortier, E.F. Vansant and G. Schulz-Ekloff (Eds.) Stud. Surf. Sci. Catal. **37** (Elsevier, Amsterdam 1988) pp. 413-425
161	R.K. Grasselli, in *Handbook of Heterogeneous Catalysis*, G. Ertl, H. Knözinger and J. Weitkamp (Eds.), Vol. 5 (Wiley-VCH, Weinheim 1997) pp. 2326-2329
162	B. Kraushaar-Czarnetzki, W.G.M. Hoogervorst and W.J.H. Stork, in *Zeolites and Related Microporous Materials: State of the Art 1994*, J. Weitkamp, H.G. Karge, H. Pfeifer and W. Hölderich (Eds.), Stud. Surf. Sci. Catal. **84**, Part C (Elsevier, Amsterdam 1994) pp. 1869-1876
163	R.A. Sheldon, J.D. Chen, J. Dakka and E. Neeleman, in *New Developments in Selective Oxidations II*, V.C. Corberán and S.V. Bellón (Eds.), Stud. Surf. Sci. Catal. **82** (Elsevier, Amsterdam 1994) pp. 515-526
164	J.D. Chen and R.A. Sheldon, J. Catal. **153**, 1-8 (1995)
165	J.M. Thomas, R. Raja, G. Sankar and R.G. Bell, Nature **398**, 227-230 (1999)
166	V.I. Sobolev, A.S. Kharitonov, Ye.A. Paukshtis and G.I. Panov, J. Mol. Catal. **84**, 117-124 (1993)
167	R. Burch and C. Howitt, Appl. Catal. A: General **103**, 135-162 (1993)
168	E. Klemm, Habilitation Thesis, University of Erlangen-Nuremberg (2001)
169	J. Weitkamp, U. Weiß and S. Ernst, in *Catalysis by Microporous Materials*, H.K. Beyer, H.G. Karge, I. Kiricsi and J.B. Nagy (Eds.), Stud. Surf. Sci. Catal. **94** (Elsevier, Amsterdam 1995) pp. 363-380
170	R.F. Parton, D. De Vos and P.A. Jacobs, in *Zeolite Microporous Solids: Synthesis, Structure, and Reactivity*, E.G. Derouane, F. Lemos, C. Naccache and F.R. Ribeiro (Eds.), NATO ASI Series C, Mathematical and Physical Sciences **352** (Kluwer Academic Publishers, Dordrecht, Boston, London 1992) pp. 555-578
171	F. Thibault-Starzyk, R.F. Parton and P.A. Jacobs, in *Zeolites and Related Microporous Materials: State of the Art 1994*, J. Weitkamp, H.G. Karge, H. Pfeifer and W. Hölderich (Eds.), Stud. Surf. Sci. Catal. **84**, Part B (Elsevier, Amsterdam 1994) pp. 1419-1424
172	P.P. Knops-Gerrits, F. Thibault-Starzyk and P.A. Jacobs, in *Zeolites and Related Microporous Materials: State of the Art 1994*, J. Weitkamp, H.G. Karge, H. Pfeifer and W. Hölderich (Eds.), Stud. Surf. Sci. Catal. **84**, Part B (Elsevier, Amsterdam 1994) pp. 1411-1418
173	R. Raja and P. Ratnasamy, in *11ᵗʰ International Congress on Catalysis – 40ᵗʰ Anniversary*, J.W. Hightower, W.N. Delgass. E. Iglesia and A.T. Bell (Eds.), Stud. Surf. Sci. Catal. **101** (Elsevier, Amsterdam 1996) pp. 181-190
174	K.R. Reddy, A.V. Ramaswamy and P. Ratnasamy, J. Catal. **143**, 275-285 (1993)
175	K.J. Balkus, Jr., A. Khanmamedova, A.G. Gabrielov and S.I. Zones, in *11ᵗʰ International Congress on Catalysis – 40ᵗʰ Anniversary*, J.W. Hightower, W.N.

Delgass. E. Iglesia and A.T. Bell (Eds.), Stud. Surf. Sci. Catal. **101** (Elsevier, Amsterdam 1996) pp. 1341-1348

176   K.J. Balkus, Jr., A.K. Khanmamedova, A. Scott and J. Hoefelmeyer, in *Proceedings of the 12th International Zeolite Conference*, Baltimore, Maryland, USA, June 1998, Vol. II, M.M.J. Treacy, B.K. Marcus, M.E. Bisher, J.B. Higgins (Eds.) (Materials Research Society, Warrendale, Pennsylvania 1998) pp. 1403-1408

177   P.T. Tanev, M. Chibwe and T.J. Pinnavaia, Nature **368**, 321-323 (1994)

178   A. Corma, Chem. Rev. **97**, 2373-2419 (1997)

179   A. Corma and D. Kumar, in *Mesoporous Molecular Sieves 1998*, L. Bonneviot, F. Béland, C. Danumah, S. Giasson and S. Kaliaguine (Eds.), Stud. Surf. Sci. Catal. **117** (Elsevier, Amsterdam 1998) pp. 201-222

180   F. Fetting and U. Dingerdissen, Chem. Eng. Technol. **15**, 202-212 (1992)

181   M. Kaene, Jr., G.C. Sonnichsen, L. Abrams, D.R. Corbin, T.E. Gier and R.D. Shannon, Appl. Catal. **32**, 361-366 (1987)

182   F.J. Weigert, J. Catal. **103**, 20-29 (1987)

183   W.F. Hölderich and H. van Bekkum, in *Introduction to Zeolite Science and Practice*, H. van Bekkum, E.M. Flanigen and J.C. Jansen (Eds.), Stud. Surf. Sci. Catal. **58** (Elsevier, Amsterdam 1991) pp. 631-726

184   M. Misono and N. Nojiri, Appl. Catal. **64**, 1-30 (1990)

185   US Patent 4 578 516, Mar. 25, 1986, assigned to Nitto Kogaku Kogyu Kabushiki Kaisha (Inv.: Y. Ashina, T. Fujita, M. Fukatsu and J. Yagi)

186   US Patent 4 582 936, Apr. 15, 1986, assigned to Nitto Kogaku Kogyu Kabushiki Kaisha (Inv.: Y. Ashina, T. Fujita, M. Fukatsu and J. Yagi)

187   DEA 3 326 579, July 23, 1989, assigned to BASF AG (Inv.: V. Taglieber, W. Hölderich, W.D. Mross and G. Saladin)

188   DEA 3 327 000, July 27, 1983, assigned to BASF AG (Inv.: V. Taglieber, W. Hölderich, W.D. Mross and G. Saladin)

189   A. Chauvel, B. Delmon and W.F. Hölderich, Appl. Catal. A: General **115** (1994) 173-217

190   PCT Patent WO 97/21661, June 19, 1997, assigned to BASF AG (Inv.: K. Eller, R. Kummer and P. Stops)

191   EPA 0 778 259, June 11, 1997, assigned to BASF AG (Inv.: K. Eller, R. Kummer and P. Stops)

192   T. Mallat and A. Baiker, in *Handbook of Heterogeneous Catalysis*, G. Ertl, H. Knözinger and J. Weitkamp (Eds.), Vol. 5 (Wiley-VCH, Weinheim 1997) pp. 2334-2348

193   M. Hunger and J. Weitkamp, Angew. Chem. (2001), in press

194   A.K. Cheetham, G. Ferey and T. Loiseau, Angew. Chem. **111**, 3466-3492 (1999)

195   S.A. Schunk and F. Schüth, in *Molecular Sieves, Science and Technology*, H.G. Karge and J. Weitkamp (Eds.), Vol. 1 – Synthesis (Springer, Berlin, Heidelberg 1998) pp. 229-263

Recently published reviews

196   Industrial Applications of Zeolites, G.F. Froment and P.A. Jacobs (Eds.), series of 5 reviews related to the topic of this chapter, Top. Catal. **13**, 349-394 (2000)

197   C. Marcilly, in *Zeolites and Mesoporous Materials at the Dawn of the 21ˢᵗ Century*, A. Galarneau, F. Di Renzo, F. Fajula, J. Vedrine (Eds.), Stud. Surf. Sci. Catal. **135** (Elsevier, Amsterdam 2001) pp. 37-60

198   J.A. Lercher and A. Jentys, in *Handbook of Porous Solids*, F. Schüth, K.S.W. Sing and J. Weitkamp (Eds.), Vol. 2 (Wiley-VCH, Weinheim 2002) pp. 1097-1156

199   A. Corma and A. Martínez, in *Handbook of Porous Solids*, F. Schüth, K.S.W. Sing and J. Weitkamp (Eds.), Vol. 5 (Wiley-VCH, Weinheim 2002) pp. 2825-2922

200   *Zeolites for Cleaner Technologies*, M. Guisnet and J.-P. Gilson (Eds.), Catalytic Science Series, Vol. 3 (Imperial College Press, London 2002) 378 pp.

III   Preparation, Functionality and Characterization of Heterogeneous Catalysts

Heterogeneous Catalyst Preparation

Contents

Heterogeneous Catalyst Preparation

Graham J. Hutchings[a] and Jacques C. Védrine[b]

[a] Department of Chemistry, Cardiff University,
   P.O. Box 912, Cardiff, UK, CF10 3TB
[b] Professeur J.C. Védrine, ENSCP, Laboratoire de Physico-Chimie des
   Surfaces, 11 Rue P. & M. Curie, 75005, Paris, France
   jacques-vedrine@enscp.jussieu.fr

Abstract. In this chapter, the different preparation processes for the synthesis of heterogeneous catalysis are described, including co-precipitation, sol-gel technique and hydrothermal method. The extension to the different steps of industrial scale preparation is also considered. The preparation of supported catalysts by different techniques, including incipient wetness method, classical impregnation at a given pH, is also described.

   These methods are applied for the preparation of single or mixed metal oxides, heteropolyoxometallates, clays and metals either as bulk or as supported materials. In addition, some emphasis is placed on the preparation of acid and base catalysts and some specific examples are described.

1   General Introduction

Contemporary solid catalysts are rather refined and sophisticated materials derived from commercially available chemicals. The variety of such chemicals for the preparation is quite wide, indeed some catalysts can be prepared by many different routes but, in general, some general elementary steps or operations have to be followed. These steps or operations are based on two approaches, (a) detailed knowledge of the scientific laws which govern chemical and physical trans-formations based on the fundamentals of inorganic or solid state chemistries, or (b) empirical observations related to carefully guarded know-how. For many years, this carefully guarded knowledge led to heterogeneous catalyst preparation being considered a "black art" rather than a scientific endeavour. Recent studies have, in part, changed this perception, but much remains to be done and, at present, too few detailed preparation studies have been undertaken. One reason for this paucity of definitive study is that many industries are highly secretive concerning preparation methodology, this real know-how represents the true intellectual property of catalyst preparation. Although general methods are disclosed in the patent literature, often these prove difficult to replicate, sometimes due to inappropriate experience and, sometimes, due to different purity of reagents and other ill-defined factors. To some extent, this was encapsulated by Syd Andrews' reference to a "general muck theory of catalysis" since it is often the parts of the catalyst that are not analysed for, what Andrews referred to as "little bits of muck between well defined crystallites", that play a role in catalyst preparation and performance. The advent of new analytical and microscopic techniques has started, finally, to shed light in this area.

In general, catalysts used in industrial reactors must have the correct *texture*, *attrition resistance*, and *shape* for the application. Texture is a collective term for surface area, pore structure and bulk density. This is one of the most important factors to be addressed at the outset of catalyst preparation. For example, partial oxidation catalysts typically have low surface area and mesopores together with macropores. Higher surface area materials would, generally, lead to non-selective oxidation due to sequential oxidation of the desired product. In contrast, catalysts for hydrocarbon formation often require high surface areas (e.g. methanol conversion to gasoline). Hence, at the outset of a catalyst preparation, it is important to consider the desired texture required for the material and this must be based on a knowledge of the chemistry of the target catalysed reaction. The attrition resistance and shape of catalyst particles are factors dealt with in subsequent stages of catalyst preparation but, again, need to be considered at the outset of the process. For example, it is important to recognise whether the catalyst must withstand thermal shock, e.g. in car exhaust catalysts, or abrasion, e.g. in entrained bed reactors. The primary variables are solute concentration in solution, temperature, pressure, pH, time (ageing, ripening, ...). Three types of catalyst can be distinguished :

1.   Bulk catalysts and supports
2.   Impregnated catalysts starting from preformed supports
3.   Mixed-agglomerated catalysts

A typical industrial operation for manufacturing catalysts can comprise :
1.   Precipitation or other synthesis process (e.g. sol-gel, solid-solid, flame hydrolysis, vapour deposition)
2.   Hydrothermal transformation
3.   Decantation, filtration, centrifugation
4.   Washing
5.   Crushing and grinding
6.   Forming and/or shaping operations
7.   Calcination
8.   Impregnation
9.   Mixing
10. Activation, reduction

In general, catalyst preparation can be schematically represented as :

Chemicals ⟶ Catalyst Precursor ⟶ Form ⟶ Final Catalyst
(control impurities)   (texture)   (texture, shape   (texture,
                                      attrition resistance)   attrition resistance)
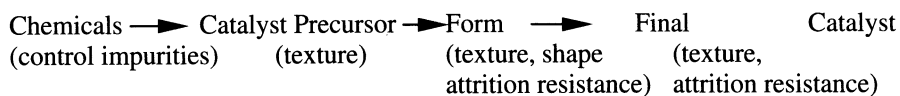
Bulk catalysts comprise mainly active substances but some inert binder is often added to aid the forming and/or shaping operation. This is the case, for instance, for silica-alumina for cat-cracking, copper and chromium oxide for the water gas shift reaction, iron molybdate for the oxidation of methanol to formaldehyde, vanadyl pyrophosphate for butane oxidation to maleic anhydride, etc. However, in some cases, bulk catalysts are used as prepared, without the need for addition of the binder. Typically, this involves catalysts prepared by high temperature fusion,

e.g. the iron-based ammonia synthesis catalyst. The need for the addition of binder, or the requirement for pelleting, solely depends on the strength required for the catalyst under the reaction conditions and the reactor type it is used in. This requires consideration of attrition resistance, and catalysts required for use in entrained-bed reactors will need different strength characteristics than those used in fixed-bed reactors.

Supported catalysts are prepared for a large variety of reasons such as obtaining bifunctional catalysts, high dispersion of the active phase, better diffusion of gases through the bed, better mechanical resistance to attrition (moving or fluidised beds reactors), better thermal conductivity, improved catalytic properties induced by active phase-support interaction, to name but a few of the many potential applications/requirements of heterogeneous catalysts.

In this Chapter, we will discuss initially some general principles concerning the methods for the preparation of heterogeneous catalysts (sections 2 and 3). Following these general comments, examples for the preparation of oxide (section 4), metal (section 5) and acid-base catalysts (section 6) will be given to exemplify more specifically the detail.

2   Preparation of Bulk Catalysts

2.1   Precipitation Method

This is the most widely used method, because it is usually facile and economic. However, the method is rather demanding since it necessitates product separation after precipitation and large volumes of salt-containing solutions. Some industrial catalysts obtained by precipitation and co-precipitation are given in Table 1. One proceeds usually by *precipitation* from a solution by adding a selected solution to reach the necessary pH. It gives either lyophobic crystallised precipitates or lyophilic precipitates in the form of gels, amorphous or poorly crystallised. Nucleation, which corresponds to the appearance of solid seed crystals in the mother liquor, can be homogeneous or heterogeneous. For the *homogeneous nucleation*, the seeds are formed from a pure solution through an interaction between ions or molecules that starts an irreversible crystallisation by forming agglomerates under conditions of supersaturation. This continues up to simple saturation in the solution. *Heterogeneous nucleation*, which is more common, has the seeds formed through contact with any solid that can lower the energy barrier enough for their formation. The solid can be impurity, walls of the apparatus, or an intentionally added seed. The growth of the nuclei is an heterogeneous process occurring at the solid-solution interface at a rate depending on the supersaturation extent. The dimension of the crystals produced depends on the ratio of the rate of nucleation to that of the crystal growth. The greater this ratio is, the smaller will be the crystallites and vice versa.

Table 1. Some industrial catalysts prepared by precipitation or coprecipitation [taken from ref 1]

Catalysts	Important applications
SiO_2-Al_2O_3	acid catalysed reaction e.g. FCC isomerisation,
Fe_2O_3	Fisher Tropsch reaction, ethyl benzene to styrene
TiO_2	major component of DeNOx catalysts
ZrO_2-SO_4^{2-}	strong acid reactions
Cu-ZnO/Al_2O_3	methanol synthesis
$(VO)_2P_2O_7$	selective oxidation of butane to maleic anhydride
	oxidation of pentane to phtalic anhydride + maleic
	anhydride
Cu-Cr oxides	hydrogenations, combustion reactions
$AlPO_4$	acid-catalysed reactions, polymerisation
Sn-Sb oxides	oxidation, as propene to acrolein or isobutene to
	methacrolein
Bi molybdates	propene selective oxidation/ammoxidation to
	acrolein/acrylonitrile
V-Mo oxide	selective oxidation of acrolein to acrylic acid

In the case of *co-precipitation* for mixed oxides, the crystals will appear as soon as the solubility limit is reached. The right choice of salt precipitating in similar conditions is thus crucial. Also the pH should be carefully adjusted and preferably kept constant during precipitation. It is, therefore, considered preferable to add continuously the salts to be precipitated to the precipitating agent solution rather than the reverse. Two methods can be identified, (a) constant pH method and (b) variable pH method in which the pH continuously changes during precipitation until a desired end-point is reached. Continued stirring of the precipitate in the precipitating solution (often called mother liquor) can change the properties of the precipitate markedly. This process is referred to as ageing.

The main factors influencing the properties of the final product are summarised in Figure 1.
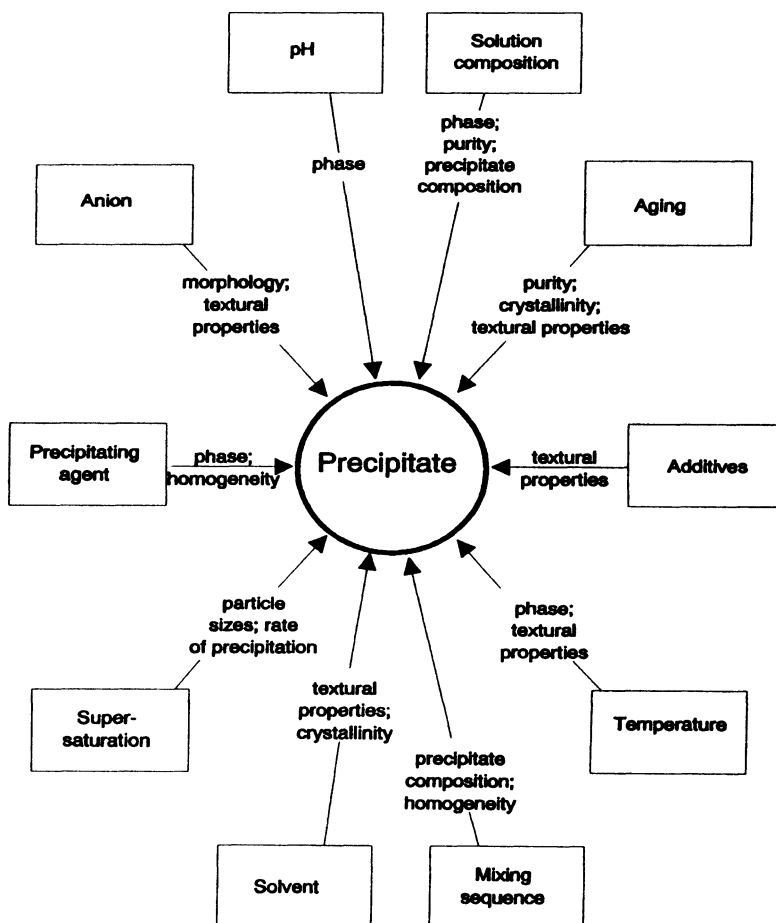
Fig. 1. Parameters affecting the properties of final precipitate (reproduced from ref. 1 p. 77)

2.2   Sol-Gel Method

A second well used method is based on the *sol-gel process* which allows the preparation of *aerogels* or *xerogels*. A *sol* is a suspension of solid particles in a liquid as colloidal particles in the nm to µm size range. A *gel* is a coagulated form of sols (solid encapsulating a liquid). The sol-gel synthesis is an established and widely spread preparation technique employing monometallic alkoxides $M(OR)_n$ which are hydrolysed to create polymeric oxide gels [2-11]. The first step corresponds to a partial hydrolysis with *monomer* formation:

$$M(OR)_n + x\ H_2O \rightarrow M(OH)_x(OR)_{n-x} + x\ ROH$$

The second step involves a condensation, which creates M-O-M bonds and forms a *sol* by dehydration or dealcoholation according to:

$$M\text{-}OH + M\text{-}H_2O \rightarrow M\text{-}OH\text{-}M + H_2O \text{ (olation)}$$

$$\text{-}M\text{-}OH + HO\text{-}M\text{-} \rightarrow \text{-}M\text{-}O\text{-}M\text{-} + H_2O \text{ (oxolation)}$$

or

$$\text{-}M\text{-}OH + RO\text{-}M\text{-} \rightarrow \text{-}M\text{-}O\text{-}M\text{-} + ROH$$
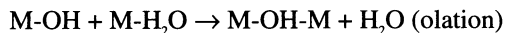
Note that olation process is much faster than oxolation.

The third step is the formation of a gel in which a cross-linked gel forms during drying or ageing of the gel. For example:

$$(n+1) (C_2H_5O)_3SiOH \rightarrow (C_2H_5O)_3Si[OSi(OC_2H_5)_2]_nOH + n\ C_2H_5OH$$
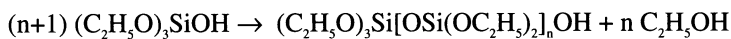
and then by cross-linking

$$\overset{+\ n\ H_2O}{(C_2H_5O)_3Si[OSi(OC_2H_5)_2]_nOH \rightarrow (C_2H_5O)_3Si[OSi(OC_2H_5)OH]_nOH + n\ C_2H_5OH}$$

$$(C_2H_5O)_3Si[OSi(OC_2H_5)OH]_nOH \overset{\Delta,\ -H_2O,\ -\ C_2H_5OH}{\longrightarrow} SiO_2 \text{ gel}$$
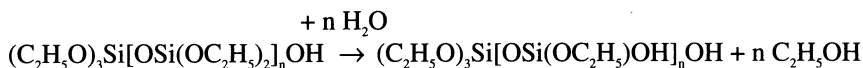
As polymerisation and cross-linking progress, the viscosity of the sol gradually increases until the sol-gel transition point is reached. At this point the viscosity abruptly increases and gel formation occurs. Further increases in cross-linking are promoted by drying or other dehydration methods. Maximum density can be achieved in a process called "densification" in which the isolated gel is heated above its glass transition temperature. The densification rate and transition (sintering) temperature are influenced primarily by the morphology and composition of the gel.

The water to alkoxide ratio, the nature and number of the alkyl group (length, steric hindrance, molecular weight), the size and oxidation state of the cation, i.e. its ability to change its coordination state, the pH, the time in solution (ageing) and the temperature are important parameters. Gels prepared at low pH and R value normally possess a lower cross-linked content. *Alcogels* are formed in alcohols and *hydrogels* in water. If the liquid (solvent) is removed by evaporation one obtains solid *xerogels*, if it is removed by supercritical drying one gets *aerogels* [6].

From a fundamental viewpoint, it can be considered that *sol gel* chemistry is that of nucleophilic reactions in which the important parameters are the steric hindrance of the alkoxy groups, the electronegativity of the central metal atom and the ability of the central positively charged metal to increase in coordination number. The reactivity of the alkoxide increases as the electronegativity decreases and size of the central atom increases. Inorganic acids may act as catalysts by reversibly protonating negatively charged alkoxide ligands, thus increasing the rate by providing a better leaving group. Basic catalysts provide improved nucleophilic attack and result in deprotonation and, therefore, enhance condensation. In the case of transition metals oxides reactivity is very high and the coordination number is more important that the existing oxidation state. In general, the ease of hydrolysis of metal alkoxides decreases as the chain length of

the alkyl groups is increased. Also, the more water repellent the alcohol, the less readily the alkoxide hydrolyses.

To prevent agglomeration, chelating agents are used, e.g. acetyl acetone, acetyl acetoacetate, glycol.... The glycol controls the crystallite size in a manner depending on upon the carbon number of the glycol such as C_2 , $C_3 < C_6 \ll C_4$.

If hydrolysis and condensation rates are slow, *sols* are obtained, if hydrolysis rate is slow and condensation rate is fast, *precipitates* form, if hydrolysis rate is fast and condensation rate is slow, *polymeric gels* are synthesised and, if hydrolysis and condensation rates are fast, *colloidal gels or gelatinous precipitates* are formed [3].

Hydrogels and flocculates result from a sol formed of micelles which remain separated due to electrical charges on the surface and in the surrounding solution. These charges stop coagulation of the micelles into multi-micelles particles. The *hydrogel* results from a three-dimensional reticulation of these micelles in a web-like framework that encapsulates water molecules. This reticulation follows a polycondensation process similar to that producing the micelles. It takes place sufficiently slowly to be followed experimentally. The time required depends on the chemical nature of the original salts, on the concentration of micelles, the temperature, the ionic nature of the solution and especially the pH. The density of the gel increases with the concentration of the initial salts in the solution and with the speed of the gel formation. Flocculates are usually denser than hydrogels, but in both cases the elementary solid particle has the dimension of the original micelle. The difference between precipitates, flocculates and hydrogels is not always clear. For instance zeolites and molecular sieves are usually prepared from the starting point of an amorphous gel of silica and alumina, or other oxide, to form a very porous crystalline material. At variance in the case of alumina, amorphous or, more or less crystallised products are obtained depending on the starting salts and the pH, as illustrated in Figure 2.
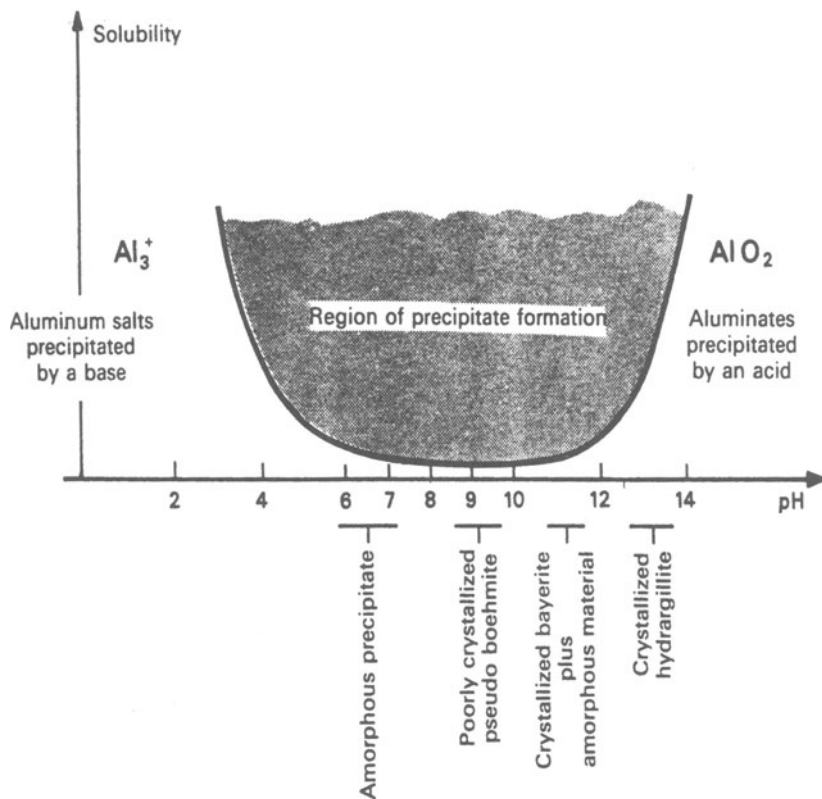
Fig. 2.   Precipitation regions of alumina as a function of the pH (reproduced from ref. 12 p. 84)

Binary and ternary oxides have been prepared by sol-gel process. For preparing mixed oxides or hydroxides, several possibilities exist

- co-precipitation by changing the pH of an aqueous solution
- mixing sols of different hydroxides or oxides
- mixing of sol and solution followed by gelation
- preparing double alkoxides or alkoxy salts
- slow hydrolysis of two precursors

The great difficulty that resides in the simultaneous hydrolysis of both the alkoxides is that the rates of hydrolysis are frequently different. If no care is taken one generates one oxide coating the other one. The homogeneity of the mixed oxide gels depends on the relative reactivities of the two alkoxides.

For the preparation of double salts and alkoxides, the most popular method involves dissolving the two alkoxides in a mutual solvent, mixing the solutions, and refluxing at elevated temperatures, e.g. refluxing an aluminium *sec*-butoxide

and magnesium methoxide in alcohol at 327 °C. One can also prepare a double alkoxide by refluxing the oxide of the first element with the alkoxide of the second element in alcohol. Bradley [13] provided an excellent summary of available double alkoxides and techniques used in their synthesis.

Another way around the problem of heterogeneity is to pre-hydrolyse the more reactive alkoxide in moist air to passivate the hydrolysis process, or to hydrolyse first the less reactive alkoxide separately into long chain polymers on which some hydroxyl groups would remain and to which the second alkoxide could be anchored.

Some examples of the use of sol gel technique for the synthesis of catalysts are given in Table 2.

One of the most important factors that determines *gel structure* is the hydrogen bonding, due to hydroxyl groups remaining in the gel even after drying. The sol-gel evolution can be distinguished by three phases: (i) ageing, polymerisation taking place in the liquid phase, (ii) in the formation step a macroscopic lattice appears leading to an amorphous network, and (iii) in the stabilisation step the gel volume decreases as the solvent evaporates leading to a rigid structure.

Polymerisation induced colloid aggregation (PICA) method has been proposed for the controlled aggregation of zirconia colloids into aggregated particles within a narrow size distribution [14].

Table 2. Some proposed materials prepared by sol-gel technique for given reactions [taken from ref. 1]

Catalysts	Reaction
V_2O_5, V_2O_5/TiO_2, V_2O_5-WO_3/TiO_2	selective catalytic reduction of NOx
Nb_2O_5/SiO_2	isomerisation of n-butene
Cr_2O_3	fluorination of $C_2Cl_3F_3$ with HF
Pt-Sn/Al_2O_3	n-heptane dehydrocyclisation, propane dehydrogenation
transition metal /Al_2O_3	polymerisation/co-polymerisation of alkenes
Ni-Mo/TiO_2-ZrO_2	hydrodesulfurisation of gas-oil
PbO-ZrO_2, PbO-Al_2O_3	nitroxidation of alkenes
Li^+/MgO promoted by Cl^-	oxidative dehydrogenation of ethane
Pt/TiO_2	oxidation of CO
Pd/SiO2	hydrogenation of phenylacetylene

A polymer formed in the colloidal sol from urea and formaldehyde assists the aggregation of zirconia particles. Further calcination allows to get rid of the polymer and to sinter zirconia particles into desired beads (ø ~ 100 nm) up to 900 °C, which increased mechanical strength and maintained their porous characteristics.

2.3   Other Methods

2.3.1   Hydrothermal Synthesis

Some other methods, in particular for the preparation of mixed oxides, zeolites and other molecular sieves consist in solid-solid reaction at high temperature in dry or in hydrothermal conditions. The synthesis of molecular sieve materials is

well documented and, generally, this involves a classical precipitation method at a given pH under atmospheric pressure such as for zeolites (silica-alumina as A-, X or Y-types), but also more typically by adding relatively bulky alkyl carbonium cations to the solution, e.g. tetra-alkyl ammonium cations that have been used as templating agent since the pioneering work by Barrer in the early 1960s [15]. The synthesis is then hydrothermal under autogeneous water pressure at the chosen temperature (usually 150-200 °C). The most typical syntheses were those of (i) MFI (ZSM-5) using tetrapropyl ammonium hydroxide as templating agent, (ii) $AlPO_4$, MeAPO molecular sieves initiated by the work of Flanigen from Union Carbide in the 1980s [16, 17] to try to reproduce silica-alumina zeolite structures or expand to new structures, and (iii) mesoporous materials of controlled pore size and narrow size distribution in the 2-10 nm range, such as MCM 41, HMS, initiated by the work of Mobil's researchers in the early 1990s [18,19]. This huge effort in molecular sieve materials, resulting in several hundreds of new structures with large variety of monodisperse pore size, mono or tri dimensional network, acidic or redox properties has opened a tremendous hope for new catalysts. Entrapping organic complexes within the zeolite porous system, initiated in the 1970s at IRC, CNRS, Villeurbanne [20,21], and further designated as "ship in the bottle" has also opened new fields for the heterogenisation of homogeneous catalysts and enzymatic catalysis. For mesoporous materials the wall thickness appeared also as determining the thermal stability [22] and the location (accessibility) of the active sites [23]. It is not our objective to describe in this chapter this huge field of catalyst preparation (it is presented in another chapter) but to mention this field of intense research activities, including a few examples of zeolites used industrially as for faujasite (X or Y-type), mordenite (MOR), beta (BEA), ZSM-5 (MFI) or SAPO-34.

2.3.2   Flame Hydrolysis

In this technique a precursor (usually a volatile metal chloride or carbonyl), hydrogen and air or oxygen are brought into contact in the flame of a torch. The precursor is hydrolysed by water formed by hydrogen combustion. Close but different to this method is the *flame oxidation* in which the volatile precursor compound is oxidised and not hydrolysed, hydrogen being not added in the torch feed, for instance to produce coarser pigment grade TiO_2 by oxidising $TiCl_4$. The reaction is then weakly exothermic and necessitates the feed to be preheated up to 1000 °C.

A related process is *spray pyrolysis* which is a droplet to particle process against a gas to particle process in the former two cases. These three processes are commonly called *aerosol processes*.

The flame hydrolysis process is used to produce high surface area oxides [24-26] such as $AlCl_3$ [24], TiO_2, Fe_2O_3 [25], and many others on a large industrial scale. The most well known example is fumed silica [26]. The process is suitable for all volatile compounds able to give an inorganic oxide by oxidation, hydrolysis or decomposition (e.g. alcoholate decomposition). Some examples are given in Table 3.

Table 3. Major oxides produced by flame hydrolysis [taken from ref. 1]

Product	Precursor
Al_2O_3	$AlCl_3$
$AlPO_4$	$AlCl_3$-PCl_3
$AlBO_3$	$AlCl_3$-BCl_3
Al_2O_3-SiO_2	$AlCl_3$-$SiCl_4$
Bi_2O_3	$BiCl_3$
Cr_2O_3	CrO_2Cl_2
Fe_2O_3	$Fe(CO)_5$, $FeCl_3$
GeO_2	$GeCl_4$
NiO	$Ni(CO)_4$
MoO_3	$MoCl_5$, MoO_2Cl_2
SiO_2	$SiCl_4$
SnO_2	$SnCl_4$, $Sn(CH_3)_4$
TiO_2	$TiCl_4$
V_2O_5	$VOCl_3$
WO_3	WCl_6, $WOCl_4$
ZrO_2	$ZrCl_4$

2.3.3   Other Methods

Some other preparation methods can also be used such as *molten salts*, *vapour deposition (CVD)*, *surface organo metallic chemistry* grafting,.... but these are considered more exotic and are restricted, at present, to the laboratory scale and, consequently, will not be developed further in this Chapter.

2.4   Forming Operations

When a precipitate is formed and dried, typically a fine powder is obtained. The next step for industrial catalysts is either calcination and then forming or vice versa. This depends mainly if calcination causes large structural changes, which may then destroy an earlier forming operation. Two extremes cases can be distinguished depending if micro granules or granules in the millimetre range are required.
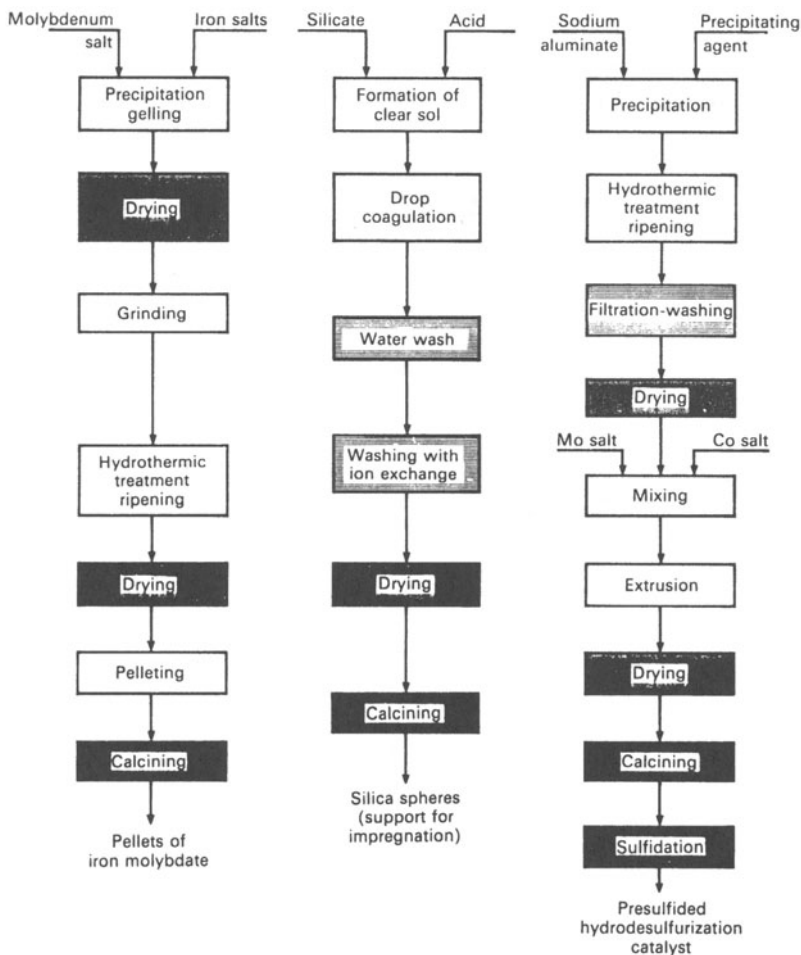
Fig. 3. Typical arrangements of unit operations for manufacturing catalyst (reproduced from ref. 12 p.105)

For *micro granules*, two main processes exist:

(i)   *Spray-drying* accomplishes drying and forming simultaneously. It consists in spraying microdroplets of the product to be dried into a flow of hot gas. Beads of 7-700 μm can be formed. This is used for fluidised bed catalytic cracking microbeads formed from silica-alumina/clay doped with rare earth exchanged Y-type zeolite.

(ii)   Drop coagulation can be performed from metastable sols suspended in a different liquid phase and correspond to simultaneous gelling, ripening and forming. The aqueous sol is distributed in the form of droplets by a vibrating sparger whose noses are sized to the desired diameter of the beads. Brace GmbH (Alzenau, Germany) has commercialised such an

equipment. The bead size distribution is quite narrow and the bead size ranges from 100 μm to 1 mm.

For *granules*, the raw material in the form of powder or paste can be transformed by pelletising, extrusion or pan granulation (agglomeration of the powder into beads by moistening it as it rolls in a rotating pan).

For industrial catalyst preparation operations the typical steps necessary are shown schematically in Figure 3.

3   Preparation of Supported Catalysts

3.1   Simple Impregnation

A way of improving the dispersion of an active phase is to spread it on a support. The preferred preparation starts from a preformed support which already possesses its desired porous texture and mechanical toughness. The active species is introduced by impregnation with a solution containing a precursor, the choice of which is crucial for the final dispersion. Another important factor is the sequence of the different steps of the impregnation. There are a number of possibilities, (i) the incipient wetness impregnation followed by drying (no equilibrium could be reached), (ii) equilibrated deposition followed by filtration and then drying of the precipitate and, (iii) the equilibrated precipitation followed by drying by evaporation of the solvent without filtration. One can also distinguish impregnation with *no interaction* when no specific interaction occurs and *impregnation with interaction* when a specific interaction is foreseen. In the former case, the dispersion depends on the precursor solubility, i.e. on the nature of the starting salts, the velocity of precipitation of the precursor during drying and on the porous structure of the support. The support acts as a spacer, i.e. it maintains the separation of the small crystals formed and slows down the crystal growth process. The interaction of the active phase and the support is physical in nature, but there is always some chemical interaction, giving rise sometimes at the extreme to a sort of chemical compound at the interface. For example some aluminate can be formed when alumina, a very common support, is used. The scientific aspects of this interaction will be developed subsequently. In the latter case (i.e. with interaction) the impregnation takes advantage of the interaction of the impregnating solution with the support so as to obtain high dispersion of the precursor, up to 1 (atomic dispersion). The problem is to maintain a high dispersion in the subsequent steps of drying, calcination and, eventually, reduction. In order to perform an impregnation with an effective interaction it is necessary to consider that true ion exchange reactions occur during the impregnation between ions of the precursor in solution and that of the support surface. These reactions are characterised by rate constants and equilibrium constants. The kinetics of exchange is usually very fast for reactions highly favoured by thermodynamics and will lead to a non-uniform distribution of the precursor inside the particle, since diffusion of the precursor within the pores is a slow process. In order to improve the dispersion, the exchange process can be retarded by competitive adsorption/exchange of other ions. This is well known when preparing supported Pt^0 particles, for which Cl^- or NH_4^+ ions are added to a

solution of hexacholoroplatinic acid or platinum tetramine chloride, respectively, to improve the metallic particle dispersion [28,29].

It must also be considered that the surface of a support changes its polarisation according to the value of the pH of the solution with respect to the isoelectric point of the solid (IEPS)[29], sometimes designated the zero charge point (ZCP) or the pristine point of zero charge (PPZC). Schematically the equation involved in the surface polarisation is written:

in an acid medium:$\qquad$ $S\text{-}OH + H^+A^- \leftrightarrow S\text{-}OH_2^+ A^-$

in a basic medium:$\qquad$ $S\text{-}OH + B^+OH^- \leftrightarrow S\text{-}O^-B^+ + H_2O$
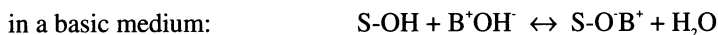
where S designates the surface. This is depicted in Figure 4 [27]. At pH below the IEPS point the surface is positively charged and attracts anions for simple electrostatic reasons, while above the IEPS point cations will be attracted by the negatively charged surface. The capacity of ion adsorption as a function of pH can be done either by measuring the electrophoresis velocity or by neutralisation experiments at constant pH. Some IEPS values for commonly used supports are given in Table 4.
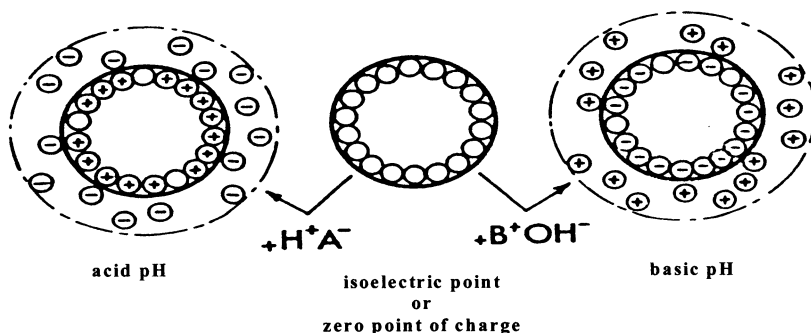
Fig. 4.   Schematic representation of a surface polarisation of an oxide particle as a function of the pH of the solution (reproduced from ref 27)

Table 4. Isoelectric points of various oxides [28]

Oxide	IEPS	Adsorption
Sb_2O_5	< 0.4	
WO_3 hydrous	< 0.5	Cations
SiO_2	1.0 - 2.0	
MnO_2	3.9 - 4.5	
SnO_2	~ 5.5	
TiO_2 (anatase, rutile)	~ 6	Cations
$\gamma\bullet$- Fe_2O_3	6.5 - 6.9	or
ZrO_2 hydrous	~ 6.7	Anions
CeO_2 hydrous	~ 6.75	
Cr_2O_3 hydrous	6.5 - 7.5	
$\alpha\bullet, \gamma$ - Al_2O_3	7.0 - 9.0	
α - Fe_2O_3	~ 8.9	Anions
ZnO	8.4 - 9.0	
La_2O_3 hydrous	8.7 - 9.7	
MgO	~ 10.4	
	12.1 - 12.7	

A deposition-precipitation method to get an uniform distribution of small metal particles has been proposed by Geus et al [ref.1, p. 247]. In this method urea is added to the metal solution which is mixed with the support at room temperature. Then the temperature is raised to 70-90 °C, where hydrolysis takes place according to:

$$CO(NH_2)_2 + H_2O \leftrightarrow 2\ NH_4^+ + CO_2 + 2\ OH^-$$
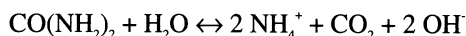
The hydroxyl groups produced are homogeneously distributed in the solution, resulting in homogeneous local pH within the solution. As precipitation occurs at lower concentration on the surface than in the bulk of the solution, due to support-precursor interaction, precipitation is achieved on the support surface exclusively.

Another point, which is obvious but has only recently been considered scientifically by Che and co-workers [30-32], who proposed the concept of *interfacial coordination chemistry*, is the partial dissolution of the support surface by the impregnation solution at the pH chosen and the formation of an adsorption layer. They consider that the active phase-support physical or chemical interaction described above for alumina support is not really relevant. They prefer to consider *selective and non-selective* or *reversible and non reversible interaction* at a molecular level. In this approach the authors consider the solid oxide support (in general, its surface hydroxyl groups) and the transition metal complex (TMC) solution interaction and the "ad surface layer" between the solution and the positively or negatively charged surface of the support shown schematically below:

$$\left|\ e\tau\ + [M(H_2O)_6]^{2+} \qquad \leftrightarrow \qquad \right|\ e\tau\ .....[M(H_2O)_6]^{2+'}$$
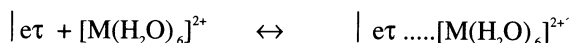
The molecular species between the surface and the metal complex from the solution may be formed without giving rise to a separate solid phase and is then difficult to identify. However such species could be identified such as the formation of Ni phyllosilicates such as Ni antigorite in the preparation of Ni/SiO$_2$ catalyst [33]. A specific example is the study of the impregnation of alumina with an heptamolybdate solution [32]. It involves reaction in the aqueous phase of $[Mo_7O_{24}]^{6-}$ with $[Al(H_2O)_6]^{3+}$ cations formed by slight surface dissolution of the alumina support. If the heptamolybdate solution is maintained over the alumina for several hours, some heteropolyanions $[Mo_6Al(OH)_6O_{18}]^{3-}$ are formed while stopping rapidly the reaction by freeze-drying keeps the original $[Mo_7O_{24}]^{6-}$ anion. After calcination at 400 °C the former sample gives large MoO$_3$ crystals while in the latter case the MoO$_x$ species formed are well dispersed. This example shows that the knowledge of the kinetics of the interfacial reaction is important for the formation of well dispersed oxide phase on an oxidic support. Geochemists have known about the phenomenon for some time since it explains many slow geochemical processes observed in the nature.

Another example is worthy of mention. When preparing a molybdenum oxide phase dispersed on silica, it was observed [34] that the dispersed MoO$_x$ species were different and presented different catalytic properties as a function of molybdenum loading at the same neutral pH of the solution at the start of the precipitation (IEPS for silica equals about 2). At low loading, acidic properties were observed and these were shown to arise from silico molybdic acid, known to be a strong acid, formed at the interface. At a higher loading, a bidimensional MoO$_x$ layer was formed which exhibited low acidity but catalysed the reaction of propene to allylic alcohol via nucleophilic attack. For MoO$_3$ crystallites formed at high molybdenum loading (above monolayer coverage) the oxidation of propene gave acrolein via an allylic attack, following a redox Mars and van Krevelen mechanism.

3.2   Co-Impregnation

The principles governing a simple precursor remain valid when the operation concerns two precursor agents. It obviously implies that exchangeable ions have the same polarity and are compatible in solution at the chosen pH. Selectivity coefficients should thus be close. Otherwise two successive impregnations should be carried out.

4   Oxide Catalyst Preparation

Oxides are used extensively in catalysed processes either as catalysts, supports, or precursors to active catalysts. For example, mixed oxides are readily transformed to supported high area metal catalysts on reduction *in situ* in the reactor, or can be transformed to sulfide by reaction with hydrogen sulfide or dimethyldisulfide *in situ* in the reactor. Hence, oxide preparation is a general starting point underpinning the origin of many commercial catalysts. In view of this diversity, this section will deal with only selected examples that are designed to emphasise key features.

4.1   Single Oxides

Single oxides are not often used as catalysts, but they are often used as catalyst supports and, consequently, their preparation can be of crucial importance. However, some single oxides, e.g. MgO and γ-Al_2O_3, have been used as catalysts as well as supports. It should be recognised that oxides can be prepared by a variety of methods, e.g. oxidation of the metal or thermal decomposition of nitrates, carbonates, basic carbonates, hydroxides, and some of these precursors are prepared through precipitation techniques. Hence, it is important to consider single oxides as a starting point for oxide preparation. MgO preparation serves as an example of the importance of controlling the morphology of crystallites. MgO was shown by Lunsford to be an effective catalyst for methane coupling [35]. However, evaluation of the subsequent catalyst literature [36] showed that MgO could exhibit distinctly different catalytic performance, even though all the samples were described as pure MgO. MgO is cubic and all exposed faces can be indexed as (100), (010) or (001) and, by powder X-ray diffraction, all these MgO catalysts were identical. A detailed study of MgO showed that the preparation method can influence the morphology of the crystallites [37]. Three methods of preparation were investigated (i) thermal decomposition of the hydroxide, (ii) burning Mg in air (ribbon residue) and (iii) thermal decomposition of the basic carbonate (3 $MgCO_3$.$Mg(OH)_2$.$3H_2O$) and all materials were calcined at 800°C. When tested for methane coupling (Table 5), the MgO (ribbon residue) and MgO ex hydroxide gave similar C_2 selectivities but the ex hydroxide sample has a higher surface area and, consequently, was more active. The MgO ex basic carbonate was much more selective to C_2 hydrocarbons. Calcination of the samples at 1100°C showed that the ex basic carbonate sample now gave the same C_2 selectivity as the MgO (ribbon residue). Detailed transmission electron microscopy [37] showed that MgO samples displayed different morphologies and the catalytic performance could be linked to these differences in morphology. The MgO (ribbon residue) showed cubic morphology (100 planes) with a broad size distribution of crystallites (100 - 200 nm). The MgO ex hydroxide showed cubic morphology with 100 planes, together with much smaller particles (20 - 40 nm). The MgO ex basic carbonate (800°C) was much less regular in shape and the surface of the crystallites appeared to be highly faceted (often referred to as higher index mean planes, pseudo (111)) with small particles (20 - 40 nm) which, on calcination to 1100°C, became similar in morphology to those of Mg (ribbon residue).

Table 5. Methane coupling over MgO[a]

Catalyst[b]	MgO ribbon residue (800)	MgO hydroxide (800)	MgO basic carbonate (800)	MgO ribbon residue (1100)	MgO ribbon residue (1100)
Surface area $(m^2\,g^{-1})$	5	21	32	3	5
GHSV (h^{-1})c	714	7059	2000	714	1429
O_2 conversion[d] (%)	97.0	97.8	98.1	89	86
Selectivity (%)					
ethane	19	32	17	19	21
ethene	10	31	12	12	8
CO	18	15	28	27	21
CO_2	53	22	43	42	49

[a]   Reaction conditons : 10^5 Pa (1 bar), $CH_4/O_2 = 6{:}1$, He as diluent, 700°C
[b]   Figures in parenthesis give calcination temperature.
[c]   GHSV varied to control O_2 conversion.
[d]   Oxygen is limiting reagent.

Hence, MgO provides a relatively simple demonstration of how catalyst morphology and, consequently, catalytic performance, can be controlled by the preparation route. These results help to explain how different samples of "pure" MgO could give different catalytic performances.

4.2   Mixed Oxides

Mixed oxides are the usual precursors to active catalysts commonly encountered in commercial operations. There are four general methodologies used for the synthesis of mixed oxides :

(a)   co-precipitation
(b)   precipitation *via* chemical reaction between reactive precursors
(c)   impregnation or adsorption onto a support
(d)   fusion (high temperature treatment).

These will each be discussed in turn by reference to specific examples, since it is not the intention of this overview to describe a great number of preparations.

4.2.1   Co-Precipitation

A number of catalysts and catalyst precursors are prepared as precipitates from basic medium. There are two general methods (a) constant pH and (b) increasing/decreasing pH to desired end point. The former provides the most control over the precipitation procedure.

(a) constant pH method

In this method, a basic solution and a solution of the metal cations is typically co-fed to a thermostatted vessel which is stirred and the mixed solution is maintained at a constant pH. This method has been extensively studied, e.g. $CuO/ZnO/Al_2O_3$, the precursor for the Cu methanol synthesis catalysts [38]; NiO/Al_2O_3, the precursor for the Ni steam refining catalyst [39]; $CuMn_2O_4$, synthetic hopcalite for low temperature CO oxidation [40]; Au/ZnO, catalysts for low temperature oxidation [41,42] and $CoMn_2O_4$, the precursor for high selectivity Fischer-Tropsch catalysts [43], and considerable details concerning the method are given in these studies. A number of factors are crucial in such preparations.

(i)   *choice of base*   It is important to consider the solution chemistry of the cations under consideration. For example, aqueous ammonia is often the base of choice for precipitations since, on subsequent drying and calcination, the NH_4^+ cation is decomposed to give NH_3 and a surface hydroxyl group. However, for Cu^{2+} soluble complexes form with NH_4^+ and so aqueous ammonia is an unsuitable precipitating agent. For Cu^{2+}, Na_2CO_3 is typically used and extensive washing of the precipitate is required to remove residual adsorbed Na^+ from the surface of the catalyst precursor [44].

(ii)   *choice of metal salt*   The anions present in the metal salt solution can act as catalyst poisons (e.g. chlorine acts as a reversible poison for Cu catalysts [44]) and, consequently, the metal salts used in catalyst preparation must be selected with care. Typically, nitrates are favoured since any nitrate anion adsorbed on the surface of the precipitate can readily be decomposed in the calcination step of the preparation. In this way, nitrate leaves no residue on the catalyst. Use of chlorides or sulfates can lead to the retention of either chlorine or sulfur on the catalyst surface, and hence these salts are usually avoided.

(iii)   *choice of pH*   Different cations form precipitates at different pHs (Figure 5). It is important to select a pH at which both cations are precipitated by the selected base. For example, Co and Mn both exhibit the onset of precipitation at pH <5 as hydroxides and so pH 6.0 would be suitable. For the $CuO/ZnO/Al_2O_3$ catalyst for methanol synthesis prepared by co-precipitation, the optimum pH is determined to be at *ca.* pH 7 (Figure 6).

(iv)   *variation of cation ratio*   This can be closely controlled through variation of the ratio of the metal cations in the starting solution. However, it should be recognised that the ratio of metal cations in the precipitate often does not reflect that of the starting reagents. This is because cations can exhibit different rates of reactions with the base and often an equilibrium is established with cations remaining in solution and cations contained in the precipitate (i.e. dissolution and re-precipitation). A number of additional factors affect this process, including : *rate of stirring, rate of reagent additives* and *temperature*.
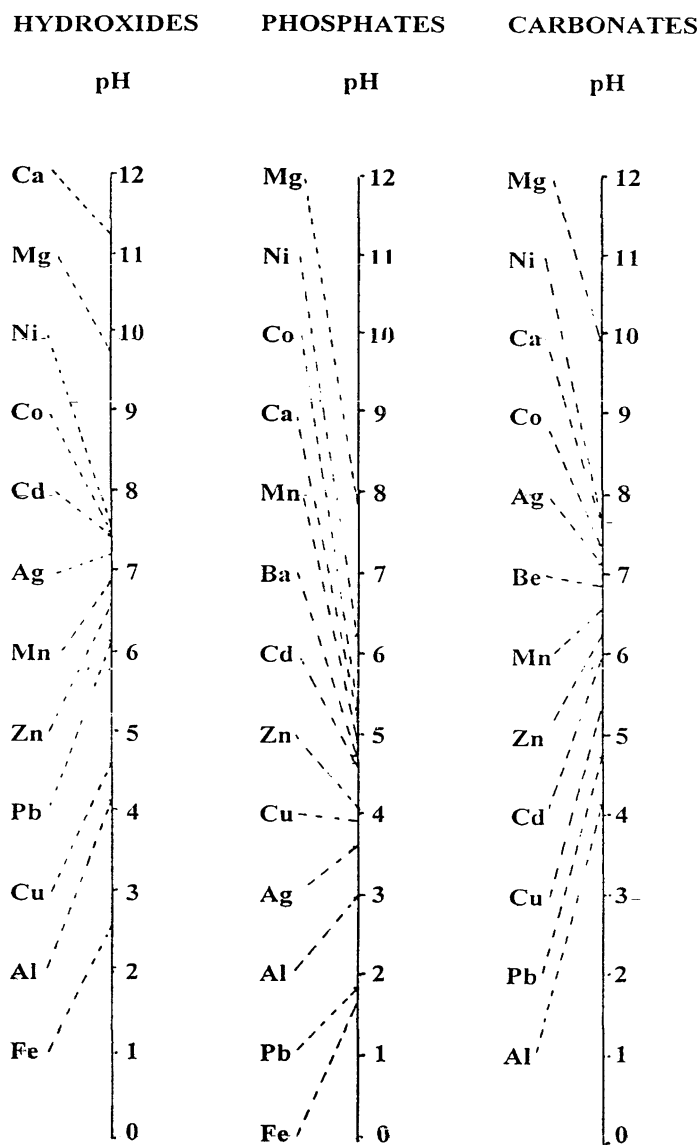
Fig. 5. Approximate pH values (at 26°C) at which precipitation of various metal salts commences.

(v)   ageing The dissolution and re-precipitation of cations can lead to an important aspect of catalyst preparation, namely, ageing. This is when the precipitate is purposely left in contact with the precipitating solution for a period of time. This has been shown to be particularly important for CuO/ZnO catalysts [44], Au/ZnO catalysts [42] and $CuMn_2O_4$ catalysts [40]. For example, ageing of the $CuMn_2O_4$ catalyst significantly affects the crystallinity of the precipitate and leads to marked changes in catalytic performance (Figure 7). During ageing, agglomeration of precipitate particles occurs to form larger particles, changing the morphology of the precipitate and, also, the nature of the precipitate may change, for example in the CuO/ZnO system, a range of structures can form (e.g. gerhardite, a basic nitrate of Zn and Ca $((Cu, Zn)_2(OH)_3NO_3)$; aurichalcite, a basic carbonate of Cu and Zn $((Zn, Cu)_5(OH)_6(CO_3)_2)$; malachite, a basic carbonate of Cu and Zn $((Cu, Zn)_2(OH)_2CO_3))$ and the ageing process can influence the relative proportions of these phases.
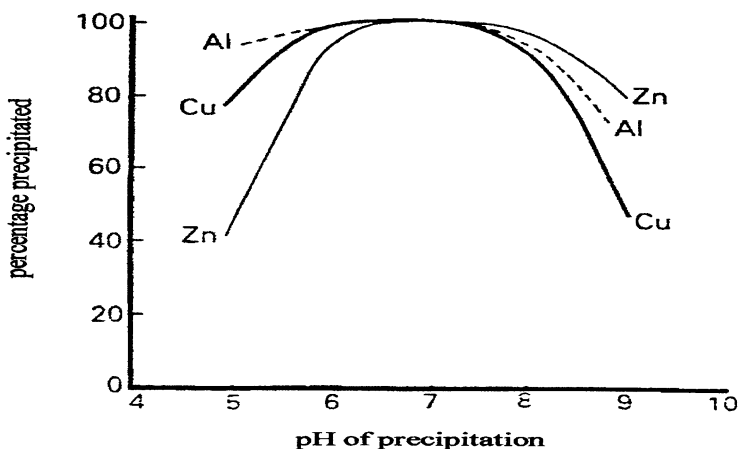
Fig. 6.   Variation with pH on the properties of copper/zinc oxide catalysts prepared by precipitation (reproduced from ref. 44).
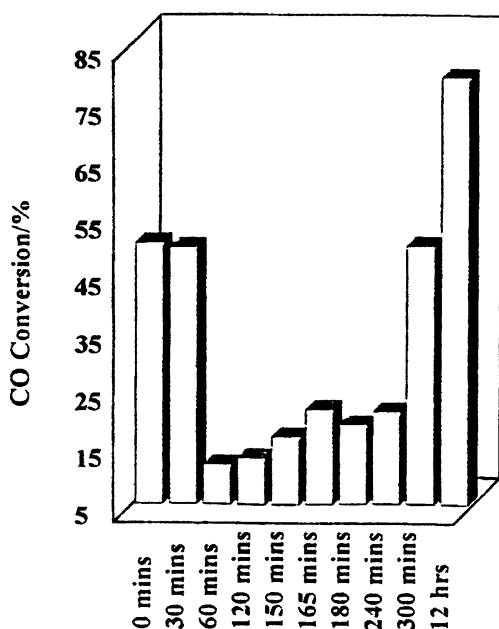
Fig. 7.   Effect of ageing CuMnO$_x$ precipitates on their catalytic performance for CO oxidation at 25°C (reproduced from ref. 40)

(b) variable pH method

This method is rarely used [44]. A solution of metal cations in the required ratio is added in a controlled way to a solution of a base, or vice versa. The pH of the precipitating solution, therefore, varies and the process is stopped when a pre-designated pH is reached. The factors identified above as important for the constant pH-method remain important for this method. It is a method that is often used for the preparation of iron containing catalysts, since Fe^{3+} precipitates at pH < 3 for hydroxides and phosphates (Figure 5). Hence, if mixed oxides containing iron are required, the constant pH method often produces inhomogeneous precipitates, since Fe^{3+} will rapidly precipitate at high pH, whereas the other cation precipitation may be slower. For this reason, the variable pH method is often preferred in combination with post-precipitation calcination.

4.2.2   Precipitation via Extended Chemical Reaction

This can, perhaps, be considered as a subset of the previously described co-precipitation methodology; however, in this case a number of solution or surface processes occur prior to the formation of the final catalyst. In addition, co-precipitation involves the reaction between an acid and a base but, in many cases,

a catalyst precursor can be formed in the absence of a base. This is particularly the case for the formation of phosphates, e.g. $AlPO_4$, BPO_4 and VPO catalysts. Typically, a metal salt is reacted with a phosphorus compound, typically phosphoric acid under controlled conditions. Choice of the metal salt can influence the catalyst precursor structure. For example, with $AlPO_4$, a catalyst for the formation of isoprene from the dehydration of 2-methylbutanal, using the reaction of aluminium chloride with phosphoric acid gives a mixture of cristobalite and tridymite phases of $AlPO_4$, whereas use of aluminium sulfate gives pure tridymite [45]. The trydimite phase is inactive as a catalyst and, hence, the choice of reagent can be crucial in obtaining the desired catalytic performance.

The most studied phosphate catalysts are *VPO catalysts* which are used for the oxidation of alkanes [46-48]. For these catalysts, $VOHPO_4.0.5H_2O$ is formed as the low temperature precursor phase and this is transferred *in situ* in the reactor in the presence of the alkane/air mixture to form the active catalyst that comprises mainly $(VO)_2P_2O_7$, together with some $VOPO_4$ phases. However, some catalyst manufacturers partly deliver fully *ex situ* pretreated catalysts to ensure that the pretreatment is fully controlled.

A number of preparative routes for $VOHPO_4.0.5H_2O$ have been published. The main aim of these preparations is first the control of the purity of the precursor and, secondly, the control of the morphology of the precursor. The second point is of crucial importance since the transformation to the final catalyst involves two topotactic transformations [49] (a) direct ($VOHPO_4.0.5H_2O$ to $(VO)_2P_2O_7$) at the edge of the precursor crystallites, and (b) indirect ($VOHPO_4.0.5H_2O$ to $\delta VOPO_4$ to $(VO)_2P_2O_7$) at the centre of the precursor crystallites. In addition, control of the morphology also controls the surface area, and commercial catalysts typically have surface areas of *ca* 30 $m^2 g^{-1}$. To date, virtually all preparations have the same specific activity, regardless of the preparation route and, consequently, control of surface area dictates the activity of the fabricated catalyst [50].

Early research recognised that $VO(H_2PO_4)_2$ then present in catalysts can lead to lower surface area [50]. $VO(H_2PO_4)_2$ transforms to $VO(PO_3)_2$ at a much lower temperature than the transformation of $VOHPO_4.0.5H_2O$ to $(VO)_2P_2O_7$. It is thought that the presence of $VO(PO_3)_2$ arrests the development of the surface area of the final catalysts. However, it was also recognised that $VO(H_2PO_4)_2$ is highly soluble in water, whereas the desired precursor phase is insoluble. Most preparations now use a simple hot water extraction step to remove the undesired $VO(H_2PO_4)_2$ from the precursor prior to the fabrication and activation step.

Early preparation methods used the reaction of V_2O_5 with HCl as a reducing agent either with water or an alcohol as a solvent. Following reduction of the V(V) to V(IV), the solution was reacted with H_3PO_4 (either 85% or 100%) and the precursor was formed by a prolonged reflux step. This method typically led to the formation of significant quantities of $VO(H_2PO_4)_2$ being formed and, in the absence of a hot water extraction step, gave variable catalytic performance.

Most preparations now do not use HCl, and only the alcohol is used as a reducing agent. Johnson *et al.* [51] showed that V_2O_5 and H_3PO_4 could be reacted with isobutanol under reflux for 16 h to form very pure $VOHPO_4.0.5H_2O$. A number of subsequent studies have shown that a range of alcohols can be used. Johnson *et al.* [51] also showed that the preparation could be carried out in two steps :

$$V_2O_5 + H_3PO_4 \xrightarrow{H_2O} VOPO_4.2H_2O$$

$$VOPO_4.2H_2O + alcohol \longrightarrow VOHPO_4.0.5H_2O + aldehyde/ketone$$
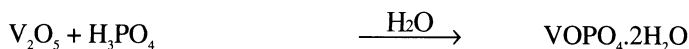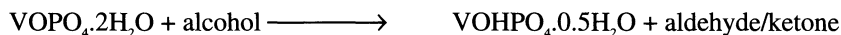
It was subsequently shown that the choice of the alcohol for the dihydrate based route can readily control the morphology of the catalyst precursor [52]. Typically, primary alcohols give very thin platelet morphology, arranged in rosettes (Figure 8), which are retained on activation, whereas secondary alcohols have much thicker platelets and lower surface area. More recently, Livage and co-workers [53] have shown that active catalysts for methanol oxidation can be prepared from the hydrogen of $VO(OR)_3$ which involve $VOPO_4.2H_2O$ as an intermediate in the preparation. They also report that the morphology can be controlled by the solvent and, in their reactions, THF is shown to give the best performance.
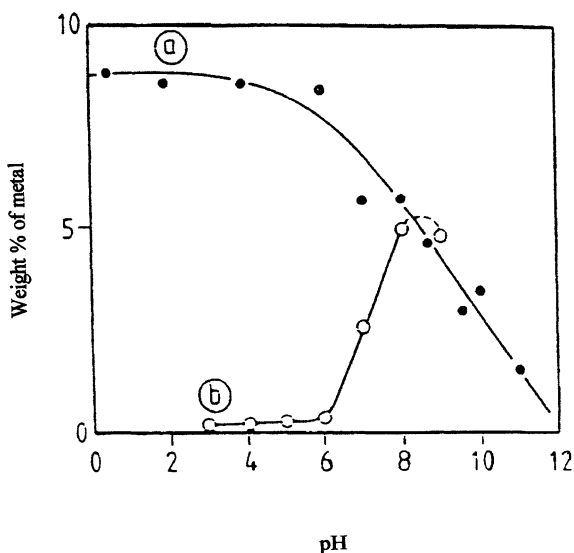
Fig. 8.   Metal uptake as a function of pH for 300 μm Al_2O_3 particles : (a) tungsten, (b) cobalt (reproduced from ref. 54)

Comparative studies of the aqueous HCl route (designated VPA), the isobutanol route (designated VPO) and the dihydrate route (designated VPD) are shown in Table 6. The catalysts have very different surface areas but the overall activity is proportional to the surface area. This is a further clear example of the catalyst preparation method controlling the catalyst morphology and activity of the final catalysts.

Table 6. Comparison of the catalytic performance of final catalysts derived from VOHPO$_4$.0.5H$_2$O prepared via different routes.

Catalyst	S_{BET}/m^2 g^{-1}		n-butane[a] conv./%	Product selectivity/%		
	Precursor	Final catalyst		MA	CO	CO$_2$
VPA[b]	3	4	11	51	41	7
VPO[c]	11	14	27	52	34	14
VPD[d]	32	43	62	64	21	14

[a]   Reaction conditons : 72 h activation, 385°C, 1.5% n-butane in air; GHSV = 1000 h^{-1}
[b]   VPA = catalyst precursor prepared by reduction of V$_2$O$_5$ with aqueous HCl
[c]   VPO = catalyst precursor prepared by reduction of V$_2$O$_5$ with isobutanol
[d]   VPD = catalyst precursor prepared by refluxing VOPO$_4$.2H$_2$O with isobutanol.

4.2.3   Impregnation / Adsorption Methods

Impregnation and adsorption methods are commonly used to add catalyst components to pre-formed support materials. They are also more specially used to add promoters to catalysts prepared by other methods, since they represent the simplest procedure by which this can be achieved. For example, catalysts used for the hydrotreatment of hydrocarbons for the removal of S, N and O containing molecules are typically sulfided molybdenum or tungstate catalysts supported on γ-alumina and promoted by cobalt or nickel. The catalysts are prepared by impregnation [54]. The processes involved in these impregnation methods are complex, and in general, there are two methods of impregnation/adsorption, (a) incipient wetness and (b) controlled adsorption from solution.

The **incipient wetness** involves a pore filling technique and is suitable for low loadings of additives. In addition, it is a very facile method and requires very little time; however, it can be difficult to control and can give non-uniform deposition of the impregnated material on the support. In particular, on drying, the material can migrate to the pore mouth and this accentuates the non-uniformity of the final product. Notwithstanding this severe disadvantage, the method is widely used.

The method can briefly be described as follows :

(i)   determine the porosity of the support to the solvent (typically water) so that the pores are just filled, i.e. the support appears to be just moistened by the solvent.

(ii)   prepare a solution of a suitable soluble salt in water (e.g. ammonium metatungstate) so that the concentration of the salt gives the desired loading of the additive when the pores are totally filled. The salt is selected

so that it can be thermally decomposed in the calcination step to give an oxide.

(iii)   the prepared solution is contacted with the support so that the pores are totally filled. Care should be taken at this stage since the adsorption process can be highly exothermic.

(iv)   dry the material (120 °C, 16 h).

(v)   calcine the material (550 °C, 16 h). In this step, the salt decomposes to form an oxide.

Uniform filling of the pores can be achieved using the incipient wetness technique, using concentrated solutions at pH values that minimise adsorption. The pH is adjusted to take account of the isoelectric point of the support (Table 4). To overcome the problem of aggregation during the drying step and non-uniformity of the adsorption using the incipient wetness technique, greater quantities of liquid can be used and, in the extreme, this involves the use of a large excess of dilute solution, which has been used by Wang and Hall [55] to prepare monolayer molybdenum/alumina catalysts.

Controlled adsorption from solution uses highly diluted solutions of the additive and the pH is adjusted to control the rate of adsorption. The method has been optimised for $MoO_3/\gamma\text{-}Al_2O_3$ and $WO_3/\gamma\text{-}Al_2O_3$ catalysts [54]. The pH is used to control two factors, (a) the surface charge of the support (Table 4) and (b) the size of oxyanions of molybdenum and tungsten. An example of the control of surface charge affecting adsorption is shown in Figure 8 for the adsorption of cobalt and tungsten species onto $\gamma\text{-}Al_2O_3$. The isoelectric point of alumina is *ca.* pH 8-9 and the lack of adsorption of cobalt at pH < 6 is due to the inability of the positively charged cobalt cations to adsorb in the positively charged alumina surfaces. Additionally, at pH > 8, cobalt precipitates from the solution as hydroxides or basic carbonates. Hence, for alumina, there is a very narrow pH window which can be used for the controlled adsorption of positively charged cations [56,57]. The reverse situation is observed for the tungsten, and also molybdenum, species due to the negative charge of the tungstate and polytungstate anions which are readily adsorbed onto the positively charged alumina surface below pH = 8.

The solution chemistry of the oxyanion of tungsten and molybdenum is complex. For tungsten, a variety of species containing one, six and twelve tungsten atoms can be present in aqueous solution which, at present, can be controlled to some extent by the selection of the solution pH [54].

$$12\ WO_4^{2-} \underset{minutes}{\overset{pH \sim 6}{\rightleftharpoons}} 2\ W_6O_{21}(OH)^{5-} \underset{weeks}{\overset{pH \sim 4}{\rightleftharpoons}} W_{12}O_{39}^{6-}$$

$$days \updownarrow$$

$$W_{12}O_{41}^{10-}$$
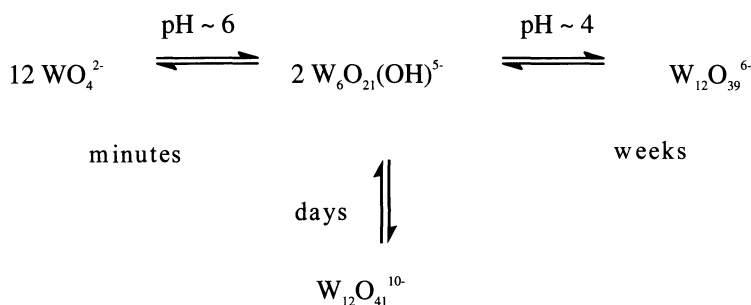
Hence, for freshly prepared solutions at pH > 6, the relatively small WO_4^{2-} anion will be dominant and, for solutions at pH < 6, much larger anions will be present. Maitra *et al.* [54] demonstrated that this can affect the uniformity of coverage of tungsten (Figure 9) and that uniform coverage of tungsten species can be achieved using dilute solutions at pH 9.5, since the pH minimises both the rate of adsorption and the size of the anion.

4.2.4   Fused Catalysts

The manufacture of catalysts by the fusion of oxides is not commonly used [44]. In this process, oxides are mixed together and heated above their melting points in a high temperature arc-furnace. The technique can give very uniform materials as long as phase separation does not occur during the melting or the subsequent cooling. The product from the fusion method has negligible surface area, but can be used to provide a mixed oxide that, on reduction, leads to the formation of a higher area supported metal catalyst. The most important catalyst made by this method is the promoted iron ammonia synthesis catalyst precursor [44]. Magnetite (Fe_3O_4) is heated in an arc-furnace at 1600°C, together with promoters calcium, potassium and alumina. The product is very strong and does not require further fabrication, as is the case with all the methods previously cited.
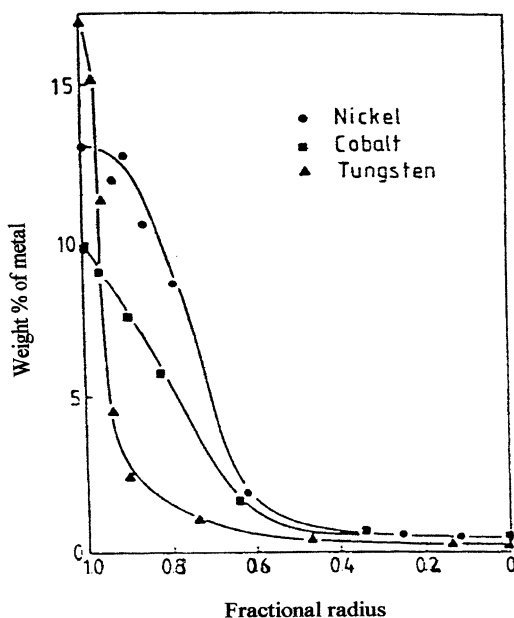
Fig. 9. Tungsten content as a function of fractional radius following impregnation of 1.6 mm diameter pellets for 0.7 h under various conditions: • pH = 9.5, 8000 ppm W; • pH = 5.7, 5000 ppm W; • pH = 3.0, 8000 ppm W (reproduced from ref. 54).

5   Metal Catalyst Preparation

Metal catalysts form the basis of a wide range of important industrial processes for the oxidation, hydrogenation and transformation of hydrocarbons. As with oxide catalysts, metal catalysts can be prepared by a range of methods and the key features of these will be described in this section.

5.1   Reduction of Oxides

This is a very commonly used procedure, i.e. first form an air stable oxide precursor and prepare the final active catalyst through *in situ* reduction in the reactor [44]. For example, the $CuO/ZnO/\gamma\text{-}Al_2O_3$ precursor prepared from co-precipitation is reduced to produce highly dispersed copper metal particles supported on $ZnO/\gamma\text{-}Al_2O_3$ which is used as a methanol synthesis catalyst. In addition, the Fe_3O_4 precursor prepared from fusion is reduced to produce a high area iron catalyst for the synthesis of ammonia. In the reduction process, it is essential that the concentration of water vapour, formed by the reduction of the oxide by hydrogen, is minimised. This is because metal particles sinter at elevated temperature and this process is accelerated by the presence of water vapour. In addition, the reduction process is highly exothermic and, consequently, the reduction must be carried out very slowly to avoid excessive heating of the reduced catalysts, since this will also lead to sintering. For these reasons, dilute H_2 in an inert carrier (typically N_2) is used and the catalyst reduction of a commercial catalyst charge can take several days [44].

5.2   Unsupported Metal Catalysts

For most catalytic processes, it is essential that the surface area of the metal catalyst particles is as high as practically possible. This can only usually be achieved by placing the metal particles onto a refracting support, or a support that plays an additional role in the process, e.g. adsorption of reactive species (e.g. the interface between Au particles and the supporting oxide is considered to be the active site for CO oxidation at ambient temperature [41,42]). Some metal catalysts are, however, used in unsupported forms. For example, the promoted iron ammonia synthesis catalyst prepared by the reduction of the fused magnetite precursor is an example of an unsupported metal catalyst.

One of the most widely used unsupported metal catalysts is the precious metal gauze catalyst. This is used in applications where very high gas velocities are required to achieve the desired selectivity. For example, platinum rhodium alloy metal gauzes are used for the oxidation of ammonia to nitric oxide for the synthesis of nitric acid and nitrates, and silver metal gauzes are used for the oxidation of methanol to formaldehyde. Such gauze catalysts are woven from fine wires and several layers of these gauzes are used in the commercial plant. However, for both these applications, supported metal catalysts can also be used. A central feature of platinum rhodium alloy gauze catalysts is the restructuring that occurs during the initial reaction period on exposure to ammonia/oxygen mixtures [58]. The restructuring gives rise to a much higher surface area and the

catalyst activity increases, in this sense the unreacted metal gauze catalyst is a low temperature precursor to the active metal catalyst surface.

Raney metal catalysts which are used extensively for low temperature hydrogenation reactions, can be regarded as unsupported metal catalysts but, in this case, the high metal surface area (typically 100 $m^2 g^{-1}$) is probably stabilised by traces of residual alumina which may act as a support. Raney metal catalysts (Ni, Ca, Co) are prepared as metal-aluminium alloys using conventional techniques. The aluminium is removed by digestion with aqueous sodium hydroxide to leave a porous metal catalyst, together with some alumina formed by oxidation of the aluminium.

A further example of an unsupported metal catalyst are CuNi alloys, useful for hydrogenation reactions. These can be prepared by reduction of a mixed oxide formed by co-precipitation from a solution of the mixed nitrates. This is shown schematically below.

$Cu(NO_3)$ (aq) CO_3^{2-} $CuNi(OH)_2CO_3$ suspend in oil $[Cu_2O.NiO]$
$Ni(NO_3)_3$(aq) $\longrightarrow$ basic carbonate $\longrightarrow$ solid solution
                                        precipitate H_2
                                                            180-190 °C
                                                                              $\downarrow$ unstable

CuNi alloy   340 °C   Cu+Ni (not detected   280 °C   Cu+Ni   240 °C   Cu+NiO
$\longleftarrow$ $\longleftarrow$ $\longleftarrow$
active catalyst   by XRD) H_2/oil H_2/oil
                    inactive for hydrogenation
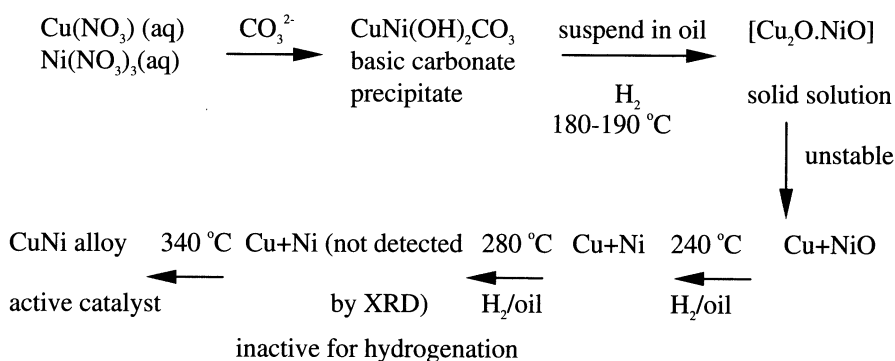
In this preparation, the Cu_2O is reduced initially and then the Cu that is formed catalyses the reduction of the NiO. The final stage of the preparation involves a high temperature annealing stage that is essential for the formation of an alloy. Supported alloy catalysts of this type can be prepared if alumina is co-precipitated initially.

5.3   Supported Metal Catalysts

Although many supported metal catalysts are prepared by reduction of oxide precursors, some, notably precursor metal catalysts, are prepared by impregnation of a support with a solution of a metal salt, dried and then heat treated to thermally decompose the metal salt. For example, chloroplatinic acid is thermally unstable and decomposes to Pt at elevated temperatures. The factors controlling dispersion and coverage for the impregnation method have been covered in an earlier section (see Section 3.1) [28,29].

6   Acid-base catalysts

Acid-base catalysts constitute one of the major family of industrial catalysts. In a recent review paper Tanabe and Hölderich [59] gave a list of the acid-base catalysts that are frequently used industrially. From a general survey of the patent literature, they found over 127 industrial processes that use solid acid or base catalysts, (81 % use solid acids, 11 % use solid acid-base and 8 % use solid bases). Within these solid catalysts, 41 % are zeolites, 31 % oxides and complex oxides, 11 % phosphates, 9 % ion exchange resins , 4 % clays and 4 % other materials.

6.1   Acid Catalysts

As indicated above, they constitute the largest part of the acid-base catalyst family. They include phosphoric acid supported on silica, resins such as Nafion® or Amberlyst®, silica-alumina, sulfated oxides (particularly sulfated zirconia), aluminium phosphates, molecular sieves (in particular zeolites such as faujasite-type (Y or X) as component of FCC catalyst, ZSM-5 (MFI), mordenite (MOR), beta (BEA)) pillared clays, chlorinated alumina, heteropolyoxometallates and their alkaline salts, in particular of Keggin structure, as bulk catalysts or supported. The methods of preparation of these materials can be different as we have described earlier in Sections 2.1 and 2.2 of this Chapter, including classical precipitation or co-precipitation at a given pH as for oxides, or mixed oxides, in which case the sol-gel technique can also be used depending on the properties required. For zeolites and, in a more general terms for molecular sieves, hydrothermal treatment is used when necessary. For sulfated zirconia special care of the choice of the precursor and of the sulfating agent is necessary. It is known that best catalysts are obtained when starting from zirconium hydroxyl [60] rather than from the calcined zirconia itself. The sulfating agent could be ammonium sulfate, easily handled at industrial scale although sulfuric acid is preferable and a monolayer coverage corresponds to the optimum loading of the zirconia.

6.1.1   Heteropolyoxometallates:

These compounds [61,62] have been known since Berzelius in 1826 but appear in Catalysis in the 1970s in partial oxidation and acid-type reactions (see Table 7) because of their redox and acid properties. They are molecular moieties of general formula: $X_x M_y O_z^{q-}$, where X is an heteroatom such as P or Si and M a transition metal such as W. Mo, V.... The Keggin anion such as $PW_{12}O_{40}^{3-}$ is the most common heteropolyanion with a central tetrahedral moiety $(XO_4)^{n-}$ surrounded by 12 octahedra MO_6 distributed in four groups of trimers M_3O_{13}. The typical method for the preparation of heteropolyacids is the acidification of aqueous solutions of oxoanions of addenda atoms and heteroatoms, according to the reaction:

$$12 \, WO_4^{2-} + HPO_4^{2-} + 23 \, H^+ \rightarrow [PW_{12}O_{40}]^{3-} + 12 \, H_2O$$
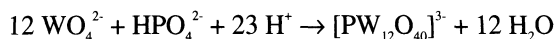
Table 7. Some heterogeneous acid and selective oxidation catalysed reactions of HPAs [taken from ref.1]

Catalyst	Reaction	Specific features
$H_3PW_{12}O_{40}$	$CH_3COOH + C_2H_5OH \bullet\bullet\bullet$ $CH_3COOC_2H_5 + H_2O$	T = 150 °C, selectivity 91% at 90% conversion
$H_3PW_{12}O_{40}$	alkylation of aromatics	T = 30 - 100 °C
$Cs_{2.5}H_{0.5}PW_{12}O_{40}$	alkylation of isobutane by butene	T = 20-40 °C
$Pd_{1.5}PW_{12}O_{40}$	isomerisation of alkanes	T = 210 °C
$H_3PW_{12}O_{40}$	$CH_3OH(CH_3OCH_3) \bullet C_1$-$C_6$ hydrocarbons	T = 300 °C
$Cs_{2.5}H_{0.5}PW_{12}O_{40}$	isobutene+ methanol $\bullet$ methyl isobutyl ether	T = 290 °C, selectivity $(C_2$-C_4 alkenes) 74%
$H_6P_2W_{18}O_{62}$	benzene + $HNO_3 \bullet$ nitrobenzene	T = 50 °C
$CsH_3PMo_{11}V_1O_{40}$	methacrolein to methacrylic acid	---
$H_3PMo_{12}O_{40}$	isobutane to methacrylic acid	T = 280 °C, 80-85 %
$H_5PMo_{10}V_2O_{40}$	isobutyric acid to methacrylic acid	selectivity
$H_5PMo_{10}V_2O_{40}$	pentane to phthalic + maleic anhydrides	T = 350 °C, 45% selectivity T = 300 °C, 72% select., 52% conv. T = 310 °C, 55% selectivity in MA

Acidification is generally achieved by addition of a mineral acid. The formation rate is usually high and crystallisation can be performed at room temperature. The hydrolysis and condensation are also fast and depend on the pH and on the solvent. For instance, the $PW_{12}O_{40}^{3-}$ anion decomposes above pH 2 and coexists with lacunary anions $PW_{11}O_{39}^{7-}$ and $PW_9O_{34}^{9-}$. In this respect, pure $H_3PW_{12}O_{40}$ acid is usually extracted by ether from an acid solution, the so-called etherate method. The bottom layer is the heteropoly-etherate which is drawn-off and then decomposed by addition of water and the ether is removed. The remaining aqueous solution is allowed to evaporate until crystallisation occurs.

Acid alkaline salts of the heteropolyacids (HPAs) such as $H_3PW_{12}O_{40}$ are prepared from the aqueous solution of the acid and adding dropwise an aqueous solution of the alkaline salt which could be acetate, carbonate, chloride, oxalate, or other anion, at room temperature and at a given controlled rate (e.g. 1 cm³ min⁻¹). The white colloidal solution can either be evaporated to give a solid at 50 °C or filtered, washed and then dried. The alkaline composition and nature and catalytic properties of the material will obviously depend on the method chosen. In most of the cases one considers that the alkaline salts, which have high surface area with respect to the starting acid, are in fact composed of the totally exchanged and non acidic salts such as $A_3PW_{12}O_{40}$ with the heteropolyacid deposited on it. This explains why such catalysts are so active.

The acid forms and their salts with cations of small size, e.g. Li^+, Na^+, Cu^{2+}, Ni^{2+} (group A salts) are soluble in both water and polar solvents and can exhibit "*pseudo-liquid behaviour*", while their salts with cations of larger diameter are insoluble such as for K^+, Rb^+, Cs^+, NH_4^+, Tl^+ (group B salts). The group B salts are

usually porous and develop surface areas up to 200 m^2 g^{-1} compared with a few m^2 g^{-1} for group A salts, and are much more thermally stable. For instance the K and Cs salts of $H_3PMo_{12}O_{40}$ have been reported to be stable up to 640 and 690 °C, respectively. The intergranular porosity can vary from ultramicropores (ø < 0.6 nm) to mesopores (ø > 1.8 nm) depending on the synthesis parameters. The acidity has been shown to be essentially of Brønsted-type with high acid strength [63]. This arises from the delocalisation of the negative charge on the large Keggin anions, resulting in a weak lattice oxygen anion - proton interaction.

Mixed-coordinated heteropoly compounds such as $H_{3+x}PMo_{12-x}V_xO_{40}$ (x = 1-3) can also be prepared. One can acidify an aqueous solution of sodium phosphate and sodium metavanadate with concentrated sulfuric acid and add to it an aqueous solution of Na_2MoO_4 - $2H_2O$. *Mixed Mo and W heteropolyacids* can be prepared from $Na_2HPO_4 \cdot 12H2O$, Na_2WO_4 and Na_2MoO_4 - $2H_2O$ mixed solutions. After one hour mixing at 80 °C, hydrochloric acid is added at room temperature and the heteropolyacid extracted with diethyl ether (vide supra), and crystallised at room temperature. The acids can also be used as starting compounds and held in the mixture for 6 h at 80 °C. The mixed compound is then extracted with ether and recrystallised. Reproducible syntheses necessitate a strict and accurate control of the pH.

Heteropoly compounds can be used either as bulk catalysts or deposited on inorganic or polymeric supports, usually using either the incipient wetness impregnation method or intercalation between clay layers, such as layered silicates (e.g. smectite) or layered double hydroxides (e.g. $[Zn_2Al(OH)_6]NO_3$ - $2H_2O$) to create new class of microporous catalysts. Supports such as porous silicas (including MCM-41[64] or HMS [65]), alumina, titania, zirconia [66], active carbons [67], ions exchange resins and high surface area HPAs salts [68] have been used. Note that basic supports such as MgO and Al_2O_3 cannot be used since they may decompose the HPAs.

Heteropolyacids have been proposed as catalysts for many acid-type reactions such as alcohol dehydration, esterification, alkylation (isobutane by butenes, in particular) or alkane isomerisation [69-71] as presented in table 7.

6.1.2   Clays

Clays are quite versatile materials [72,73] used by man since primitive times. One distinguishes two groups. The *cationic clays* are commonly encountered as natural materials and the *anionic clays* which are more scarce. Cationic clays are usually prepared starting from natural minerals, whereas the anionic clays that are used industrially are synthetic. The *cationic clays* have negatively charged layers such as for silico-aluminate and cations provide the compensating charges in the interlayer space, these can be protons which consequently induce acidic properties. The *anionic clays* have positively charged metal hydroxide layers with charge balancing anions and consequently exhibit basic character, in addition, water molecules are located interstitially.

The majority of clay minerals are composed of hydrous layered silicates, in which the basic building blocks are $Si(O,OH)$ tetrahedra and $M(O,OH)_6$ octahedra with M = Al^{3+}, Mg^{2+}, Fe^{3+} or Fe^{2+}. Combination of a layer of tetrahedra and a layer of octahedra gives rise to the layer ca. 0.7 nm thick in a 1:1 mineral such as kaolinite or serpentine for M = Al^{3+} or Mg^{2+}, respectively, while combination of one sheet of octahedra sandwiched between two sheets of tetrahedra gives the 2:1

mineral, ca. 1 nm thick. Depending on the cation Al^{3+} or Mg^{2+}, one may have dioctahedral or trioctahedral minerals, based on the number of octahedral sites occupied per unit cell.

Acid treatment of the clay, in particular montmorillonite, is performed either by simple washing with a mineral acid solution, which results in an exchange of the cations by protons or by heating the clay suspended in a mineral acid solution at refluxing temperature (e.g. 95 °C). For instance, the commercial modified montmorillonite designated K10 from Süd Chemie or Fluka is used industrially for hydrocarbon cracking. Clays or acid treated clays can also be used as supports for many inorganic salts catalysts, including Lewis acids as $ZnCl_2$ and ferric or copper nitrates.

Anionic clays are natural or synthetic lamellar hydroxides of a structure similar to that of brucite $Mg(OH)_2$, designated as hydrotalcite-type (HT) or layered double hydroxide (LDH). the former name derives from the extensive studies of hydrotalcite, a Mg/Al hydroxycarbonate. The general formula is:

$$[M_{1-x}^{z+}M_x^{3+}(OH)_2]^{b+}[A_{b/n}^{n-}], mH_2O$$
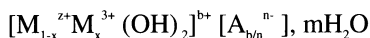
where M is a metal, A the interlayer anion, and b = x or 2x-1 for z = 2 or 1, respectively.

6.1.3   Pillared Clays

The main objective of introducing pillars between the sheets of a clay is to prepare porous materials in which the interlayer space can be both controlled and larger than 0.7 nm in size. Many different pillaring species have been described in the literature: organic compounds (alkyl ammonium and bicyclic cations), metal tris chelates, organo metallic complexes, metal oxide sols and polyoxocations. Usually it is performed using a clay with a relative low negative charge density (to avoid too large stuffing which may result in loss of interlayer space access). Many polyoxocations, such as those based oxy-hydoxycations of Zr, Ni, Fe, Cr, Mg, Si, Bi, Be, Nb, Ta, Mo, Ti, Ga, Cu, have been reported. The better defined pillars are $[Al_{13}O_4(OH)_{24}(H_2O)_{12}]^{7+}$ of Keggin structure which is most commonly used and, to a lesser extent, the tetramer $[\{Zr(OH)_2 . 4H_2O\}_4]^{8+}$ or the octamer $[(TiO)_8(OH)_{12}]^{4+}$.

The preparation of cationic pillared clays consists of a controlled hydrolysis carried out in the solution or in the interlayer space. If C represents the clay, A^+ the exchangeable cation and P_n^{x+} the cationic polymer, the following exchange occurs in the gallery:

$$CA_x + P_n^{x+} \rightarrow CP_n + xA^+$$
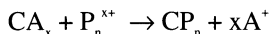
The cationic polymer is formed by condensation according to the reaction:

$$nP^{z+} \Leftrightarrow P_n^{x+} + (nZ - x)H^+ + yH_2O$$
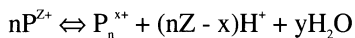
For the Al_{13} oxomacrocation, the hydrolysis is achieved in solution by the addition of carbonates (e.g. Na, Mg, Zn) to a solution of $AlCl_3$ or by the addition of alkali hydroxides (this is widely used) or by dissolving metallic aluminium in HCl or $AlCl_3$. The ageing of the polymer solution obviously plays an important, but not easily reproducible, role.

Pillared clays have an interesting architecture since the interlayer distance can be tuned from 0.6 to 1.2 nm and their chemical functions such as Brønsted or

Lewis acidity, can be varied upon preparation and activation. They are poorly crystalline and their stability is limited, particularly above 600 °C. Some applications have been described in separation technology and fine chemical catalysis, such as the synthesis of chiral sulfoxides on Ti-pillared montmorillonite, or the transformation of syngas to light alkenes on mixed Fe-Al-pillared montmorillonite and many others [72]. An example of pillaring montmorillonite with Zr and Al hydroxy macocations and of their acid and catalytic properties for isobutane alkylation with butene described by Marme et al. [74].

Anionic clays can also be pillared by highly charged anions since, as described above, they are natural or synthetic lamellar mixed hydroxides with interlayer spaces containing exchangeable anions. As shown in Table 8, one can distinguish the isopolyanions (or heteropolyoxometallates) and the heteropolyanions (or isopolyoxometallates) with a Keggin structure and the ferro- or ferricyanides.

Pillared anionic clays (PILACs) materials may be prepared by different methods:

- Exchange of inorganic anions
- Exchange of organic anions
- Structure reconstruction in presence of a swelling agent (e.g. meixnerite, a Al/Mg clay, + glycerol + long chain organic compounds such as adipate or toluene sulfonate)
- Direct coprecipitation

The PILACs materials are not easy to prepare for the following reasons:

1. Exchange is more difficult than in cationic clays because of the high charge density (higher or equal to 4 e^- nm^{-2} rather than 1 e^- nm^{-2}), which creates strong electrostatic forces between the brucite sheets and the anions, with subsequent blocking of the interlayer space by the anions themselves.
2. Hydrolysis of the pillaring anions can be caused by the anionic clays, depending on the nature of the cations.
3. Anionic clays may decompose in the synthesis conditions, chosen on the basis of the stability of the pillaring agent.
4. Carbonates compete with the pillaring anions, readily giving rise to mixed phases, due to their high affinity with the positively charged sheets.
5. The anionic clay structure is only stable at relatively low temperatures.

Table 8. Values of d_{001} spacing and surface area for some pillared anionic clays [73]

Anionic clay	Pillaring agent	d_{001} spacing / nm	surface area / $m^2\,g^{-1}$
Zn/Al	$V_{10}O_{28}^{6-}$	1.19-1.23	169
Li/AlMg/Al	$V_4O_{12}^{4-}$	0.95	-
Zn/Al	$Mo_7O_{26}^{6-}$	1.22	71
Zn/Al	α - $H_2W_{12}O_{40}^{6-}$	1.46	63
Mg/Al	α - $SiV_3W_9O_{40}^{7-}$	1.46	155
Mg/Al	$PV_3W_9O_{40}^{9-}$	1.20	136
Mg/Al	$Fe(CN)_6^{4-}$	1.10	246
	$Fe(CN)_6^{3-}$	1.10	235

The PILACs materials are prepared with the objective to create new useful porous networks for shape selective adsorption or for heterogeneous or photo catalysts. In catalysis, one of the objectives was the immobilisation of homogeneous or biomimetic catalysts in order to increase their service time and facilitate their recovery and recycling. An interesting application is waste water purification treatment at room temperature using phthalocyanins intercalated in anionic clays [75,76]. The catalyst can be recovered by filtration. The PILACs are also quite interesting in the sense that they can entrap more active phase than more conventional supports. Note that up to now they are mainly used at low reaction temperatures in catalytic processes.

6.1.4   Other Types of Acid Catalysts

Acid-type reaction such as alkane isomerisation can also be catalysed by oxycarbides. Carbides such as molybdenum or tungsten carbides are known to exhibit pseudo-metallic features since the pioneering work of Gault [77] and Boudart and co-workers in the early 1970s [78-80]. It was thought that they could replace expensive noble metals. More recently it was observed that slight oxidation of some carbides give oxycarbides (e.g. $MoO_{2.42}C_{0.23}H_{0.78}$) with quite interesting isomerisation properties [80,81], in particular for long chain linear alkanes to form branched isomers [81]. This proceeds with formation of a metallocyclobutane intermediate rather than via the usual carbocation intermediate. A low cracking reaction rate was observed that was at variance with classical acid-type catalysts. The preparation method of the sample was particularly crucial to get the required oxycarbide structure [81].

6.2   Basic Catalysts

As mentioned above only a few industrial processes use heterogeneous basic catalysts, although important reactions such as isomerisations, additions, alkylations and cyclisations are carried out industrially using liquid bases. Some reviews papers have dealt with this field [82-85]. There are some advantages and disadvantages. As *advantages* one has high activity and selectivity, novel transformations and no corrosion or effluent issues. As *disadvantages* one has high activation temperature (in excess of 400 °C due often to decomposition of

carbonates formed by CO_2 from ambient air during catalyst storage), deactivation by water and acids, rapid coke formation. The main catalytic systems are:

- Alkali ion exchanged zeolites,
- Modified alkali ion exchange zeolites (modification by metallic alkali such as Na formed by decomposing sodium azide or by depositing an alkali ion oxide such as Cs oxide),
- alkaline earth oxides such as CaO, BaO and MgO and mixed metal oxides such as Al_2O_3-MgO,
- Alkali metals such as Cs, K, Na deposited on a range of supports such as carbon, Al_2O_3, SiO_2, ZrO_2 or TiO_2,
- Alkali metal amide on alumina such as $(M)NH_3$ / Al_2O_3 with M = Na, K, Eu, Yb,... or KNH_2 / Al_2O_3,
- Supported alkali metal - metal oxide such as Na-Na_2O/ Al_2O_3,
- KF / Al_2O_3 [84,88]
- K_2FeO_4/ Al_2O_3, pyridinium chlorochromate/ Al_2O_3 [86,87]
- Clays such as hydrotalcites,
- Oxynitrides such as silicon oxynitride, aluminophosphate alumino oxynitrides (ALPONs) [89,90]

A *super base* is defined by its Hammett's parameter $H_- > 30$ such as for Na - NaOH/Al_2O_3, a *strong base* by $H_- > 20$ such as for KOH/Al_2O_3, a *medium base* by $H_- > 10$ such as NaOH or hydrotalcites and a *weak base* by $H_- < 10$ such as for R-NH_2 or alkali exchanged zeolites.

The main reactions catalysed by solid bases are hydrogenations, aldol condensations, isomerisations, alkylations, partial oxidations, epoxidations, and others. The activation of the reagents usually proceeds by proton abstraction resulting in the formation of a carbanion. In oxidation reactions it could also be proton abstraction from the oxidant, which then becomes nucleophilic and its reactivity changes.

In partial oxidation reactions, for instance using pyridinium chlorochromate on basic alumina, the substrate is activated by the base and one has oxidation of secondary alcohols to ketones and of primary allylic alcohols to α,β-unsaturated aldehydes resulting in yields higher than 95%. At variance, for K_2FeO_4 on basic alumina, primary aliphatic alcohols are oxidised with very low yields while secondary are oxidised with high yields. This permits preferential oxidation of a secondary alcohol group for molecules containing several alcohol groups, such as for 1,3-butanediol oxidised to 4-hydroxy-2-butanone on K_2FeO_4/Al_2O_3, as shown below:

$$CH_3\text{-}CH(OH)\text{-}CH_2\text{-}CH_2(OH) \rightarrow CH_3\text{-}C(O)\text{-}CH_2\text{-}CH_2\text{-}OH$$
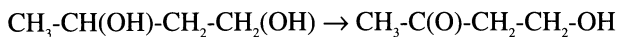
The oxidant can also be activated by the base and becomes nucleophilic. For instance a substrate with two electron-withdrawing groups Z_1-CH_2-Z_2 can be oxidised on KF/Al_2O_3 with S-methyl methane sulfothioate ($CH_3SSO_2CH_3$) as oxidant to thioketals {$Z_1(Z_2)C(SCH_3)_2$} with Z_1 = -COOEt and Z_2 = -COOEt, -COCH_3, -Ph [86]. KF/Al_2O_3 catalyst can also be used in presence of iodine for the oxidative coupling of the same type of substrate, Z_1-CH_2-Z_2, leading to the corresponding alkanes or alkenes with Z_1 = -COOEt, -CN and Z_2 = -COOEt, -CN,

-Ph, -SPh. It was proposed [87] that the carbanion gives one electron to the iodine, leading to a free radical and an iodide ion. The coupling between the free radicals gives the alkane or alkene in absence or presence of another iodine molecule, respectively. KF/Al_2O_3 gives rise to oxidation of weakly acidic compounds to ketones with molecular oxygen [88]. The yield strongly depends on the pKa values. For instance, if the reaction is performed at room temperature in acetonitrile, for fluorene (pK_a = 23) the yield is 92% against 15% for diphenylmethane a less acidic substrate (pK_a = 34). The reaction can also be performed without solvent but the pKa value dictates the reaction temperature. For instance, a temperature of 150 °C is required for fluorene (pK_a = 23, 100% yield), 200 °C for xanthene (pK_a = 30, 95% yield) and 200 °C for diphenylmethane (pK_a = 34, 92% yield). The mechanism proposed assumes that the carbanion attacks molecular oxygen to give an alkylperoxide anion, which subsequently loses a hydroxide anion to give the corresponding ketone.

The most important oxidation reaction with nucleophilic oxidants is the epoxidation of electron-deficient alkenes, via conjugate addition of the oxidant and subsequent intramolecular substitution. For instance KF/Al_2O_3 as a base and ter-butyl hydroperoxide as oxidant is able to epoxidise α,β-unsaturated ketones, acyclic ketones containing aromatic substituents such as chalcone, cyclic ketones, etc. KF/Al_2O_3 represents a particular case of basic catalyst since it has been developed by organic chemists and it is at present a commercially available common reagent [84] and it is frequently used for fine chemical syntheses. There are some more examples to be considered. KF/Al_2O_3 is a catalyst used for demethylation of p-methoxyacetophenone to p-hydroxyacetophenone by reflux in ethylene glycol (selectivity of 30% for 96% conversion, dioxalane is also formed as a by-product). It is shown that the basicity of KF is increased by alumina which increases demethylation (OH^- and AlO_2^- species). Side chain monoalkylation of para-xylene by butadiene is realised on a Na/K_2CO_3 catalyst (Amoco process), cyclisation of $(CH_3)_2C=N-CH_3$ with SO_2 occurs at 427 °C to give the 4-methylthiazole ($C_3H_2SN-CH_3$), which is a systematic fungicide, is performed on Cs/ZSM-5 (Merck process), dehydration of ethanocyclohexane to ethylene cyclohexane is carried out on $NaOH/ZrO_2$ (Sumitomo Chemical process), alkyne to alkadiene isomerisation on KNH_2/Al_2O_3. To prepare these supported catalysts, an aqueous solution of either hydroxide, carbonate, nitrate or aceetate is impregnated onto the desired support, the material is calcined to decompose the salt, e.g. at 400 °C. Supporting alkali metals are usually prepared by deposition of the metal vapour, resulting in strongly basic catalysts. These materials have been reported to be quite interesting for a large variety of isomerisation reactions.

Potassium amide KNH_2/Al_2O_3 is a further interesting example. It is prepared as follows [84]: alumina and a small amount of Fe_2O_3 (catalyst for converting K metal to its amide in liquid ammonia) are heated in a reactor under vacuum at 500 °C for 3h. A piece of K metal is added to the reactor under nitrogen. After the reactor is set under vacuum, liquid ammonia is introduced. The blue colour due to solvated electrons disappears after 10 min. indicating that KNH_2 is formed. After 1h, the reactor is warmed up to room temperature for removing the remaining ammonia and then heated up to 300 °C. Such catalyst is quite active for a variety of reactions such as isomerisation, dimerisation,... Some catalytic data are given in Tables 9 and 10 for dimethyl but-1-ene isomerisation (Table 9) and phenylacetylene dimerisation into two enantiomers Z (cis) and E (trans) 1,4-diphenylbut-1-ene-3-yne (Table 10).

Table 9. Influence of the support on the catalytic activity of KNH_2/support at - 62 °C for the isomerisation of 2,3-dimethyl but-1-ene [84] with 63g catalyst and 24 mmol reagent in a batch reactor

Support	Reaction time / min	Conversion / %
Al_2O_3	10	70
Al_2O_3-MgO (Mg/Al = 2)	30	19
CaO	30	19
SiO_2	30	0
TiO_2	30	0
CaO^a	10	63

a   Without KNH_2

Table 10. Catalytic activities of various solid bases for the dimerisation of phenylacetylene at 90 °C after 5h with 27 mmol reagent and 0.5g [84]

Catalysts	yield / %	Z : E [a]
KNH_2/Al_2O_3	53	96 : 4
CaO	21	57 : 43
$Eu(NH_3)$/Al_2O_3	16	70 : 30
$Yb(NH_3)$/Al_2O_3	7	62 : 38
MgO	4	62 : 38
Al_2O_3	2	55 : 45

a   Z and E represent the two enantiomers of the dimers 1,4 diphenyl but-1-ene-3-yne cis and trans, respectively.

Hydrotalcites (HT) and hydrotalcite-like materials (HTlc), i.e. layered double-metal hydroxides (LDH) are active, when heated at about 400 °C to obtain the dehydrated, non carbonated and dehydroxylated mixed oxides, especially the Mg-Al combinations. They are used as catalysts for many reactions such as polymerisation of β-propiolactone and propylene oxide, aldol condensation of acetone and formaldehyde to methyl vinyl ketone, Knoevenagel condensation of benzaldehyde with activated methylenic compounds, Claisen-Schmit condensation, isomerisation of olefines, etc.. Magnesium and aluminium ions are often partly replaced by transition metals able to catalyse patial oxidation reactions. For instance Kaneda et al [91] used, for the Baeyer-Villiger oxidation of cyclopentanone, a combination of molecular oxygen and benzaldehyde on HT with different Mg/Al ratios (from 1 to 6) and different anions (CO_3^{2-}, Cl^- and p-toluene sulfonate).They postulated that the reaction proceeds in two steps. Firstly, the benzaldehyde is auto-oxidised by oxygen to perbenzoic acid, which subsequently transfers an oxygen atom to the ketone. If transition metals are introduced in the HT structure (e.g., $Mg_3AlM_{0.3}CO_3$ with M = Cu or Fe) the catalysts are even better for the Baeyer-Villiger oxidation of ketones [92].

   The strategy to immobilise an active metal complex, in particular Ru, in the HT or HTlc structures and to introduce in addition transition metals, such as Co, Mn,

Fe or Zn, has also been studied by Kaneda et al. [93,94] to promote the oxidation of allylic and benzylic alcohols as well as aromatic compounds with benzylic positions with molecular oxygen. Layered double hydroxides, including HTs and HTlcs, have also been intercalated [84] with oxometallates, in particular vanadates, molybdates, sulfates,... and polyoxometallates, in particular of Keggin structure with Si and P as central atom and transition metals such as Mn^{2+}, Fe^{2+}, Co^{2+} and Cu^{2+} in the structure, and anionic complexes, such as tetracationic and tetraionic Mn-porphyrins, Zn-phthalocyanine, Co(II)-tetrasulfophthalocyanines, Co(II)-phthalocyanine tetracarboxylic and tetrasulfonic acids, etc. Catalytic properties are usually not as good as in the liquid homogeneous phase but the stereo selectivities were different but they represent interesting new effort for replacing homogeneous catalysts by more friendly heterogeneous systems.

7. General Conclusions

In this chapter we have shown how the preparation of heterogeneous solid catalysts necessitates extensive care in the experimental conditions: pH, temperature, concentration, ageing, ripening, forming, etc and how it could be the determining factor for catalytic properties. It is, most the time, a confidential, jealously guarded, know-how of industry, since in many cases some specific preparation details are crucial for catalytic properties. A typical example can be found for VPO catalysts which, for the same compound (vanadyl pyrophosphate), preparation and reactor modifications in the last 20 years have allowed the yield in maleic anhydride from butane oxidation to be improved from 30 to more than 60%. An important aspect is to understand the exact reasons of such improvements, in particular the role of all promoters/additives found in the patent literature. They certainly correspond to chemical modifications, crystallite growth changes (e.g. size, shape, defects, shear planes in the crystalline structure). By chance, basic research has been widely expanded in the last 20 years in both the industrial and academic communities and more knowledge has been gained on the subject. Nevertheless it remains a domain that is poorly understood and which appears to some researchers as not sufficiently intellectually rewarding; because of this, basic research in this area remains a major issue for the future. Any research which tackles the topic of catalyst preparation in a definitive manner will be able to make a major contribution to heterogeneous catalysis.

References

1   G. Ertl, H. Knözinger and J. Weitkamp (ed.), "Handbook of Heterogeneous Catalysis", Wiley VCH, Weinheim, 1997
2   B.J.J. Zelinski and D.R. Uhlmann. J. Phys. Chem. Solids 45, 1069 (1984)
3   J. Livage, M. Henry and C. Sanchez, Prog. in Solid State Chem. 18, 259 (1988)
4   R.J. Ayen and P.A. Iacobucci, Rev. Chem. Eng. 5, 157 (1988)
5   C.J. Brinker and G.W. Scherrer, "Sol-Gel Science: The Physics and Chemistry of Sol-Gel Process, Academic Press, New York (1990)
6   M.A. Vicarini, G.A. Nicolaon and S.J. Teichner, Bull. Soc. Chim. Fr. 2, 431 (1970)

7   S.J. Teichner, G.A. Nicolaon, M.A. Vicarini and G.E.E. Gardes, Adv. Colloid Interface Sci. 5, 245 (1976)
8   H.D. Gesser and P.C. Goswami, Chem. Rev. 89, 765 (1989)
9   G.M. Pajonk, Appl. Catal. 72, 217 (1991)
10   J. Livage, Catal. Today 41, 3 (1998)
11   J.P. Jolivet, "De la solution à l'oxyde", CNRS Editions, Paris (1994)
12   J.-F. Le Page, "Applied Heterogeneous Catalysis, Design-manufacture-use of solid catalysts", Technip, Paris (1987)
13   D.C. Bradley, R.C. Mehrotra and D.P. Guar, in "Metal Oxides", Academic Press, London (1978)
14   A.N. Sathyagal, P.W. Carr and A.V. McCormick, J. Colloid and Interf. Sci. 219, 20 (1999)
15   R.M. Barrer and P.J. Denny, J. Chem. Soc. 971 (1961)
16   S.T. Wilson, B.M. Lok, C.A. Messina, T.R. Sannan and E.M. Flanigen, J. Am. Chem. Soc. 104, 1146 (1982)
17   E.M. Flanigen, B.M. Lok, R.L. Patton and S.T. Wilson, Pure Appl. Chem. 58, 1351 (1986)
18   C.T. Kresge, M.E. Leonowicz, W.J. Roth, J.C. Vartuli and J.S. Beck, Nature 359, 710 (1992)
19   J.S. Beck, J.C. Vartali, W.J. Roth, M.E. Leonowicz, C.T. Kresge, K.D. Schmidt, C.T.W. Chu, D.H. Olson, E.W. Sheppard, S.B. McCullen, J.B. Higgins and J.L. Schenker, J. Am. Chem. Soc. 114, 10834 (1992)
20   J.C. Védrine, E.G. Derouane and Y, Ben Tâarit, J. Phys. Chem. 78, 531 (1974)
21   M. Primet, J.C. Védrine and C. Naccache, J. Mol. Catal. 4, 411 (1978)
22   N. Coustel, F. Di Renzo and F. Fajula, J. Chem. Soc., Chem. Commun. 967 (1994)
23   F. Di Renzo, B. Chiche, F. Fajula, S. Viale and E. Garrone, Stud. Surf. Sci. Catal. 101, (1996) 851
24   R. Caillat, J.P. Cuer, J. Elston, F. Juillet, R. Pointud, M. Prettre and S. Teichner, Bull. Soc. Chim. Fr. 152 (1959)
25   P. Vergnon and H.B, Landousi , Ind. Eng. Prod. Res. Dev. 19, 147 (1980)
26   H. Klöfer, German patent assigned to Degussa, 762, 723 (1942)
27   J.-F. Le Page, Applied Heterogeneous Catalysis, Design-manufacture-use of solid catalysts, Technip, Paris, 485 (1987)
28   C. Perego and P. Villa, in: The catalytic process from laboratory to the industrial plant, D. Sanfilippo (ed.) Italian Chemical Society, Maraschi, Melegnano, 25 (1994)
29   J.-P. Brunelle, Pure Appl. Chem. 50, 1211 (1978)
30   M. Che, Proc.10th Intern. Congress on Catal., Akademiai Kiadó, Budapest, 31 (1993)
31   X. Carrier, J.-F. Lambert and M. Che, J. Am. Chem. Soc. 119, 10137 (1997)
32   X. Carrier, J.-F. Lambert amd M. Che, Stud. Surf. Sci. Catal. 121, 311 (1999)
33   G. Dalmai-Imelik, C. Leclercq and A. Maubert-Muguet, J. of Solid State Chem. 16, 129 (1976)
34   T.-C.Liu, M. Forissier, G. Coudurier and J.C. Védrine, J. Chem. Soc., Faraday Trans. 85, 1607 (1989)
35   T. Ito and J.H. Lunsford, Nature 314, 721 (1985)
36   G.J. Hutchings, M.S. Scurrell and J.R. Woodhouse, Chem. Soc. Rev. 18, 251 (1989)
37   J.S.J. Hargreaves, G.J. Hutchings, R.W. Joyner and C.J. Kiely, Catal. Today 13, 401 (1992)
38   J.C.J. Bart and R.P.A. Sneeden, Catal. Today 2, 1 (1987)
39   D.C. Puxley, I.J. Kitchener, C. Komodromos and N.D. Parkyns, Stud. Surf. Sci. Catal. 16, 237 (1983)

40   G.J. Hutchings, A.A. Mirzaei, R.W. Joyner, M.R.H. Siddiqui and S.H. Taylor, Catal Lett. 42, 21 (1996)

41   M. Haruta, N. Yamada, T. Kobayashi and S. Ijima, J. Catal. 115, 301 (1989)

42   G.J. Hutchings, Gold Bull. 29, 123 (1996)

43   G.J. Hutchings, M. van der Riet and R. Hunter, J. Chem. Soc., Faraday Trans. 1 85, 2875 (1989)

44   M.V. Twigg, Catalyst Handbook, Wolfe Publishing, Frome (1989)

45   G.J. Hutchings, I.D. Hudson, D. Bethell and D.G. Timms, J. Catal. 188, 291 (1999)

46   G. Centi (Ed.), Forum on vanadyl pyrophosphate catalysts, Catal. Today. 16 (1) (1994)

47   B.K. Hodnett, Catal. Rev. -Sci. Eng. 27, 373 (1985)

48   G. Centi, F. Trifiro, J.R. Ebner and V.M. Franchelta, Chem. Rev. 88, 55 (1988)

49   C.J. Kiely, A. Burrows, G.J. Hutchings, K.E. Bere, J.C. Volta, A. Tuel and M. Abon, Faraday Discuss. 105, 105 (1996)

50   G.J. Hutchings, Appl. Catal. 72, 1 (1991)

51   J.W. Johnson, D.C. Johnson, A.J. Johnson and J.R. Bradey, J. Am. Chem. Soc. 106, 8123 (1984)

52   M.T. Sananes, I.J. Elllison, S. Sajip, A. Burrows, C.J. Kiely, J.C. Volta and G.J. Hutchings, J. Chem. Soc., Faraday Trans. 1 92, 137 (1996)

53   S.A. Ennaciri, K. Malka, C. Louis, P. Barboux, C. R'Kha and J. Livage, Catal. Lett. 62, 79 (1999)

54   A.M. Maitra, N.W. Cant and D.L. Trimm, Appl. Catal. 27, 9 (1986)

55   L. Wang and W.K. Hall, J. Catal. 77, 252 (1982)

56   M. Komiyama, R.P. Merrill and H.F. Harnberger, J. Catal. 63, 35 (1980)

57   P.H. Tewari and W. Lee, J. Coll. Interface Sci. 52, 77 (1975)

58   L.D. Schmidt and D. Luss, J. Catal. 22, 269 (1971)

59   K. Tanabe and W.F. Hölderich, Appl. Catal. A: General 181, 399 (1999)

60   F.R. Chen, G. Coudurier, J.-F. Joly and J.C. Védrine, J. Catal. 143, 616 (1993)

61   M.T. Pope, Heteropoly and Isopoly Oxometallates, Springler-Verlag, Berlin (1983)

62   I.V. Kozhevnikov, Catal. Rev.-Sci. Eng. 37, 311 (1995)

63   N. Essayem, Y.Y. Tong, H. Jobic and J.C. Védrine, Appl. Catal. A: General 194-195, 109 (2000)

64   I.V. Kozhevnikov, K.R. Kloetstra, A.Sinnema, H.W. Zandbergen and H. van Bekkum, J. Mol. Catal. A: Chemical 114, 287 (1996)

65   F. Marme, G. Coudurier and J.C. Védrine, Microp. and Mesop. Mater. 22, 151 (1998)

66   E. López-Salinas, J.G. Hernández, I. Schifter, E. Torres-García, J. Navarrete, A. Gutiérrez-Carillo, T. López, P.P. Lottici and D. Bersani, Appl. Catal. A: General 193, 215 (2000)

67   P. Dupont, J.C. Védrine, E. Paumard, G. Hecquet and F. Lefebvre, Appl. Catal. A: General 129, 217 (1995

68   P.-Y. Gayraud, N. Essayem and J.C. Védrine, Catal. Lett. 56, 35 (1998)

69   A. Corma and A. Martínez, Catal. Rev.-Sci. Eng. 35, 483 (1993)

70   A. Corma, V. Gomez and A. Martínez, Appl. Catal. A: General 119, 83 (1994)

71   N. Essayem, S. Kieger, G. Coudurier and J.C. Védrine, Stud. Surf. Sci. Catal. 101, 591 (1996)

72   E. Kikuchi and T. Masuda, in Pillared Clays, Catal. Today 2, 297 (1988)

73   A Vaccari, Catal. Today 41, 53 (1998)

74   F. Marme, G. Coudurier and J.C. Védrine, Stud. Surf. Sci. Catal. 121, 171 (1999)

75   M.E. Pérez-Bernal, R. Ruano-Casero and T.J. Pinnavia, Catal. Lett. 11, 55 (1991)

76   M. Chibwe and T.J. Pinnavia, J. Chem. Soc., Chem. Comm. 279 (1993)

77   J.M. Muller and F. Gault, Bull. Soc. Chim. Fr. 2, 416 (1970)

78   M. Boudart and R. Levy, Science, 181 (1973).

79   J.S. Lee, S.T. Oyama and M. Boudart, J. Catal. 106, 125 (1987)

80   F.H. Ribeiro, R.A. Dalla Betta, M. Boudart, J.E. Baumgartner and E. Iglesia, J. Catal. 130, 86 (1991)

81   C. Bouchy, C. Pham-Huu, B. Heinrich, C. Chaumont and M.J. Ledoux, J. Catal. 190, 92 (2000)

82   H. Hattori, Stud. Surf. Sci. Catal. 78, 3 (1993)

83   H. Hattori, Chem. Rev. 95, 527 (1995)

84   Y. Ono and T. Baba, Catal. Today 38, 321 (1997)

85   J.M. Fraile, J.I. Garcia and J.A. Mayoral. Catal. Today 57, 3 (2000)

86   D. Villemin, A. Ben Alloum and F. Thibault-Starzyk, Synth. Commun. 22, 1359 (1992)

87   D. Villemin and A. Ben Alloum, Synth. Commun. 22, 3169 (1992)

88   D. Villemin and M. Ricard, React. Kin. Catal. Lett. 52, 255 (1994)

89   P. Grange, P. Bastians, R. Conanec, R. Marchand and Y. Laurent, Appl. Catal. A: General 114, L191 (1994)

90   A. Massinon, J.A. Odriazola, P. Bastians, R. Cananec, R. Marchand, Y. Laurent and P. Grange, Appl. Catal. A:General 137, 9 (1996)

91   K. Kaneda, S. Ueno and T. Imanaka, J. Chem. Soc., Chem. Commun. 797 (1994)

92   K. Kaneda, S. Ueno and T. Imanaka, J. Mol. Catal. A:Chemical 135, 135 (1995)

93   K. Kaneda, T. Yamashita, T. Matsushita and K. Ebitani, J. Org. Chem. 63, 1750 (1998)

94   T. Matsushita, K. Ebitani and K. Kaneda, Chem. Commun. 265 (1999

High-Throughput Experimentation
in the Development of Heterogeneous Catalysts

**Tools for Synthesis and Testing of Catalytic Materials
and Data Analysis**

Contents

High-Throughput Experimentation
in the Development of Heterogeneous Catalysts
Tools for Synthesis and Testing of Catalytic Materials
and Data Analysis

U. Rodemerck and M. Baerns

Institute for Applied Chemistry Berlin-Adlershof,
Richard-Willstätter-Str. 12, 12489 Berlin. Germany

Abstract. High-throughput synthesis and testing of solid materials has recently gained special attention in heterogeneous catalysis. Various technical solutions have been developed for parallel catalyst preparation, catalyst testing and fast analysis of reaction products. Optimisation algorithms are applied for the effective search for the optimal catalyst in the multi-parameter space defined by varying catalyst compositions, preparation methods and reaction conditions. The present state of the high-throughput technologies is briefly reviewed and illustrated by various case studies.

1. Introduction

High-throughput synthesis and testing of solid materials has gained special attention in the search and optimisation of catalytic materials since about 1997. The basic concept for accelerating the development process comprises parallel synthesis, screening and testing of a large number of materials based on heuristic approaches, which, in turn, include fundamental and empirical knowledge on catalysis and appropriate optimisation procedures when progressing in the development process. In high-throughput experimentation an extensive amount of data is being accumulated. For handling of these data and extraction of knowledge therefrom in the form of relationships between the chemical and physical properties of the materials and their catalytic performance suitable data storage and analysis capabilities are required.

For industry, the driver behind this innovative technique is the expectation of shortening the development time in finding a suitable catalyst and hence, to reduce the time-to-market of a new catalyst or even a new catalytic process. Various estimates have been made by how much the development time can be decreased; reductions to 0.1 to 10 % of conventional times for catalyst search and optimisation have been reported. The present authors tend to a more conservative estimate of 1 to 10 %. For science, high-throughput experimentation may become a means of accumulating large amounts of catalytic data within a short-time

period, which may then be analysed from a fundamental point of view for their generic understanding.

The present state of the high-throughput technologies is briefly reviewed and illustrated by various case studies. Synthesis and testing of materials are key issues, which have many facets. The choice of elements or compounds exhibiting a potential catalytic property and being the basis for synthesizing a first library (generation) of materials needs empirical expertise as well as fundamental knowledge. After testing the materials for their catalytic performance further optimisation is necessary, which requires the use of a suitable algorithm to design, prepare and test subsequent generations of materials. Also fundamental insights may be derived from the various performances of different materials, which serves as feedback to the development process. Finally, after identifying an optimum material for maximum performance a scale-up to real size catalysts from catalyst preparations in the amount of a few mg to at least several 100 g is required. This demands comprehensive structural characterization of the solid material; this area is, however, not dealt with since similar tasks exist also in conventional catalyst development.

2.   Selection of Potential Catalytic Elements for Defining the Multi-Compositional Space

Many parameters influence the catalytic activity, selectivity, and stability of inorganic heterogeneous catalysts. First, the chemical elements and their concentration are the prerequisite to generate a catalyst composition with the desired active sites for a given reaction network. Furthermore, the catalyst structure is mainly determined by the preparation method as well as the calcination and formation procedure. Last, but not least, also the reaction conditions (temperature, pressure, composition of the gas phase) influence the catalyst performance. This means that the real catalyst only exists when the catalytic reaction proceeds.

Consequently, a high number of parameters have to be considered in defining the parameter space in which good catalysts are expected to exist. Recently, Senkan has discussed the number of possible catalyst compositions [1]. Based on 50 chemical elements, which can be used to design a catalyst, 1225 binary, 19600 ternary, and 230000 quaternary combinations are possible. Much higher numbers are, of course, obtained when allowing for different molar fractions of the components and taking into consideration the different modes and parameters of preparation. Due to this so-called combinatorial explosion it is not possible to prepare and test all possible catalysts even when applying highly sophisticated high-throughput set-ups. Therefore, introduction of previous knowledge to restrict the number of parameters is the key basis of an effective experimental design which may be supplemented in a way accounting for serendipity.

For illustration, establishing a pool of elements in searching for new catalysts in the oxidative dehydrogenation of ethane to ethylene, the selection of materials was more recently shown by Grubert et al. [2, 3]. This is based on a similar procedure, which was put forward by Buyevskaya et al. [4] for the oxidative dehydrogenation of propane. Regarding the possible reaction mechanisms metal oxides with the required properties were chosen (Table 1). The oxides were then randomly com-

bined to mixed-metal oxide catalysts to generate a first generation, the catalytic results of which were then used for optimising the composition. This is outlined in section 4.

Table 1. Selection of a pool of elements from fundamental knowledge for designing catalyst compositions for the oxidative dehydrogenation of ethane (after [2])

Assumed mechanism	Required property	Metal oxide
Participation of removable lattice oxygen (Mars-van Krevelen mechanism)	Redox properties: medium Me-O binding energy	Cr_2O_3, CuO, MnO_2, MoO_3, WO_3, Ga_2O_3, CoO, SnO_2
Activation by adsorbed oxygen	Dissociative adsorption of oxygen	CaO, La_2O_3
Activation by lattice oxygen	Non-removable lattice oxygen: high Me-O binding energy	ZrO_2

3. Experimental Strategies for Designing and Testing Large Catalyst Libraries

By applying a real combinatorial design of catalyst libraries (full grid search) the whole parameter space has to be screened defining individual steps for each parameter (e.g. concentration levels for the components). All catalysts from these libraries have to be tested for their catalytic performance, which than results in deriving a dependency of the catalytic results (activity, selectivity, stability) from each individual parameter. Unfortunately, this means that very high numbers of catalytic materials have to be prepared and tested which, of course, increases with the number of elements. To overcome this problem, the number of parameters can be restricted using the chemist's intuition or the available knowledge. On the other hand, so-called stage-one experimental methods are applied, which allows preparing and testing thousands of samples in a short period of time.

Stage-one screening has been used by SYMYX for CO oxidation [5] using Pt-Pd-Rh and Pd-Rh-Cu libraries and for oxidative dehydrogenation of ethane to ethylene [6-9]. The group of Senkan generated a library of ternary composed supported metal catalysts (Pt-Pd-In) for the dehydrogenation of cyclohexane to benzene [10] and searched for new catalysts for the selective reduction of NO by propene applying a combinatorial variation of compositions for quaternary composed Pt-Pd-In-Na catalysts [11]. Richter et al. also screened a quarternary library for the deNO$_x$ reaction [12]. The same concept was also applied for establishing a library of polyoxometalates containing W, V, Mo and P [13].

A method of saving efforts in preparing a large number of different catalytic materials is the split-and-pool approach - already well known in combinatorial chemistry - which was recently adapted to heterogeneous catalysis by Newsam et

al. [14, 15]. For preparing a catalyst library, a large number of beads consisting of a support material were covered by the catalytic active materials in different preparation steps (Fig. 1).
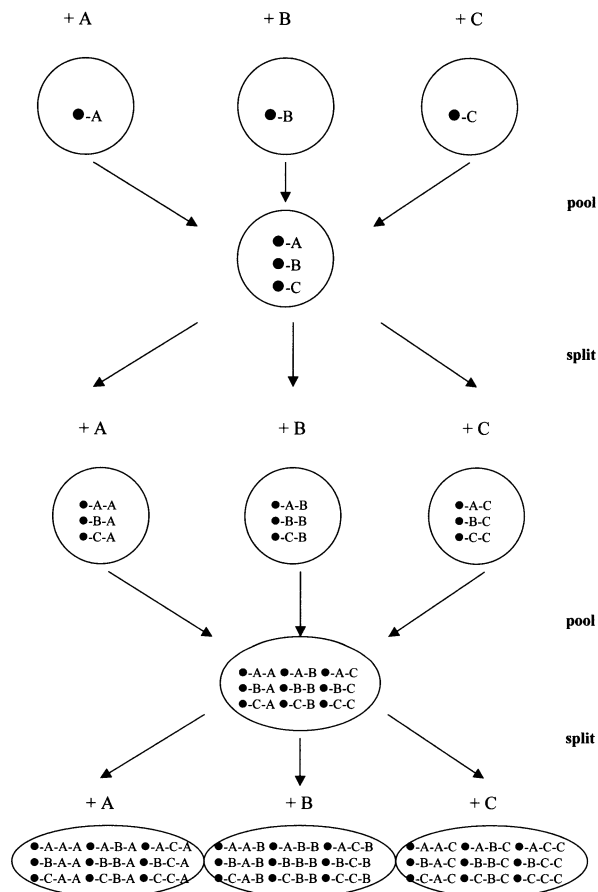
Fig. 1 Principle of the split-and-pool method for preparation of large libraries of mixed-metal oxide catalyst. The black dots represents the beads covered by the components A, B, and C. After three steps 27 combinations of components have been prepared.

First, equal amounts of the beads are charged to different vessels. To each vessel the solution containing one active element is added. After drying, each of the vessels contains a defined number of single beads covered with one element or compound respectively. In the next step, all beads are mixed (or pooled) and then evenly distributed again to the vessels. In this way each vessel contains beads covered by all but only one single catalytic compound per bead. Then, again solutions of catalyst components were given to the beads; after repeating the already described treatment process and redistribution again components are

added. After several steps, all possible qualitative combinations of catalyst components are contained in the library, where each single bead represents a defined catalyst composition (Figure 1). As an example, 3000 Al_2O_3 beads were prepared by combining Mo, Bi, Fe, Co, Ni in some concentration steps. 384 individual beads were tested simultaneously in a multi single-bead reactor; the reaction products of each bead were analyzed by a screening mass spectrometer [16-18]. The catalysts showing the best performance were then analysed by micro X-ray fluorescence to identify their elemental composition.

Recently Sun et al. [19] also described the application of a split-and-pool method in heterogeneous catalysis. The authors prepared a catalyst library composed of supported noble metals (Pt, Au, Rh, Ir). X-ray fluorescence analysis showed that catalysts containing the metals in different concentration steps could be prepared. For identification of the single beads the authors suggested to adsorb different combinations and concentrations of three fluorescent dyes onto the surface of the support beads. In a proof-of-principle experiment it was possible to identify the individual dye-marked beads by their fluorescence intensities.

4. Algorithms for Designing Subsequent Generations of Materials Compositions

4.1   Genetic Algorithms

Genetic algorithms are optimisation tools, which are inspired by the adaptation of living species to natural environment demands in biological systems. Based on modification, selection and survival of the fittest, which is repeated in each generation a better adaptation is achieved when going from one generation to the next. A general description of the mathematical fundamentals of genetic algorithms has been given in [20-23]. The use of genetic algorithms for catalyst optimisation has some advantages with respect to other optimisation methods: (i) Genetic algorithms are global optimisation tools, i.e. the best catalysts in a pre-defined parameter space can be found with high probability. (ii) The optimisation is done in parallel; this fits well with high-throughput experimentation, which uses parallel preparation and testing techniques. In fact, a whole catalyst generation consisting normally between 50 to 150 different compositions, can be prepared and tested in one high-throughput experiment. In contrast to this, other optimisation methods depend on the experimental results before defining the next data point and so, one catalyst after the other has to be prepared and tested. (iii) No pre-derived knowledge or assumptions on the topology of the parameter space is necessary to initialize the algorithm.
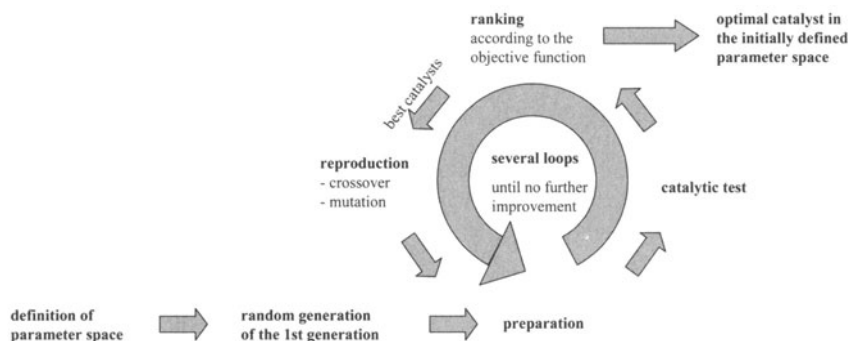
Fig. 2 Optimisation of catalyst composition by genetic algorithms

Wolf et al. [24] firstly applied genetic algorithms to optimise the composition of heterogeneous catalysts. Based on a pool of chemical elements covering the parameter space to be searched for the optimum catalyst composition an initial generation of catalysts is generated stochastically. For the optimisation an objective function has to be defined, which can be the yield, space-time yield or selectivity of the desired product or any other value to be optimised. The catalysts of the first generation are prepared and tested by high-throughput experimentation and are ranked according to the value of the objective function. The best catalysts are used for generating the second catalyst generation. Here, the evolutionary operators are applied: crossover (exchange of components between two catalysts), qualitative mutation (one or more element are taken off from the catalyst or new ones are added) and quantitative mutation (the concentration of a catalyst component is changed). The principle of the optimisation is illustrated in Fig. 2.

The genetic algorithm has been successfully applied to different types of heterogeneously catalyzed reactions: Oxidative dehydrogenation of ethane (Fig. 3) [2, 3, 25] and propane [4, 24, 26, 27], catalytic combustion of hydrocarbons at low temperature [28], partial oxidation of propane to acrolein and acrylic acid [29, 30] and light paraffin isomerisation [31]. For further illustrative information reference is made to the examples below.
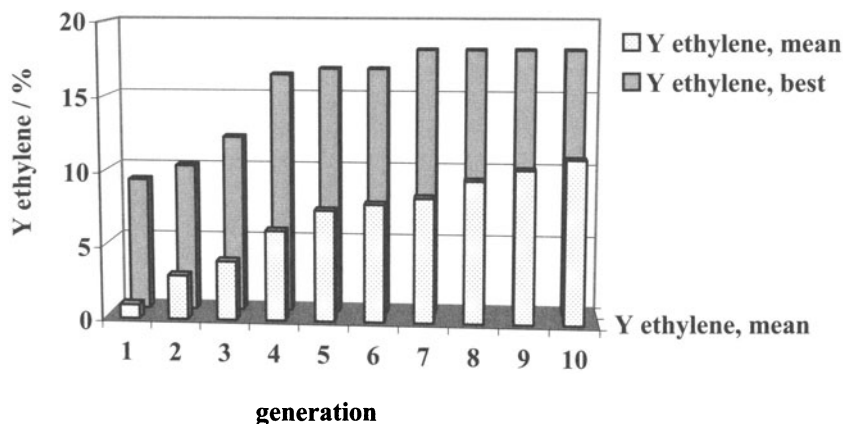
Fig. 3 Example of catalyst optimisation applying a genetic algorithm: Oxidative dehydrogenation of ethane to ethylene (after [32])

In a recent report Wolf [33, 34] could show by mathematical simulation that genetic algorithms, if proper adapted, can be successfully applied to catalytic problems even when good catalysts only exist in very small areas of the parameter space. This was illustrated by the selective oxidation of ethane to acetic acid on Pd- or Rh-doped Mo-V-Nb, Mo-V-W, and V-P mixed oxide catalysts. The optimal catalyst has the composition $Mo_1V_{0.25}Nb_{0.12}Pd_{0.0005}O_x$. The content of Pd as Pd^{2+} is very low and higher amounts of Pd existing as Pd^0 clusters result in CO_x as main reaction product: furthermore, a special preparation mode is necessary to obtain the selective catalyst. Using a standard genetic algorithm Pd is not contained in the optimised catalyst due to its total oxidation activity. However, when using a step-wise strategy for optimisation of the composition, a modified genetic algorithm finds the optimum after ca 30 generations. This example clearly shows that genetic algorithms should be adapted to the catalytic problem to be solved and that pre-knowledge has to be used in encoding the catalyst's components, which reflects its functionality.

4.2   Artificial Neural Networks

Artificial Neural Networks (ANN) have been developed using the analogy to the data processing in biological neural systems, where the correlation between input data and output data is represented by the connections between the individual neurons. The most often used ANN's are multilayer perceptrons, which are constructed of layers of neurons (input layer, one or several hidden layers, output layer) and connections between the neurons (see Fig. 4).

In high-throughput experimentation, ANN's are valuable tools for the correlation of catalytic results (conversion, selectivities, yields, space-time yields)

with the properties of the catalysts (composition, structure, physical and chemical properties) and/or the reaction conditions. Due to the possibility of mathematical modeling of such dependencies, catalytic results for given input parameters can be predicted.
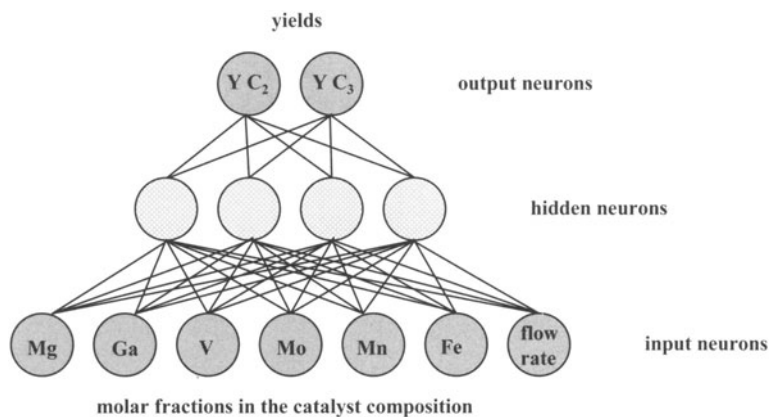
Fig. 4 Example of an ANN with one hidden layer (architecture 7-4-2) for modeling the dependency between catalyst composition (input neurons) and performance (output neurons) for the oxidative dehydrogenation of propane to propene and ethylene (after [42])

The first application of ANN's to catalysis was the estimation of the acid strength of mixed oxides [35]. Applications to heterogeneous catalysis, i.e. modeling relationships between the catalysts and their reactivity have been reported by Hattori, Kito and co-workers [36, 37] for the oxidative dehydrogenation of ethylbenzene and the oxidation of butane, by Sasaki et al. [38] for the decomposition of NO into N_2 and O_2, Hou et al. [39] for the acrylonitrile synthesis from propane, Sharma et al. [40] for the Fisher-Tropsch synthesis, and Huang et al. [41] for the oxidative coupling of methane.

In connection with high-throughput experimentation Holena and Baerns [42] used different architectures of multilayer perceptrons to model the dependency of propene and ethylene yields on the composition of the catalysts in the oxidative dehydrogenation of propane as a model reaction. This was done on the basis of 211 experimental testing results for catalysts each composed of at least three elements from the group of Fe, Ga, Mg, Mn, Mo, and V. The following data were used to train 230 different ANN architectures: elemental composition and gas flow rate of the feed (7 input neurons), yield of propene and ethylene (2 output neurons). Comparing the different nets, the best results were obtained by structures consisting of numbers of input neurons – hidden neurons – output neurons being equal to 7-3-2, 7-4-2, 7-5-2, and 7-6-2. Additionally, rules were extracted from the ANN, which allows identifying areas in the multi-dimensional parameter space where high propene yields are to be expected. Experimental verification of the predicted propene yields for different catalyst compositions, which were not known before, showed that the ANN describes the multi-parameter space very well [43]. A similar approach was recently reported by

Corma et al. [44] who trained different net architectures with data of the oxidative dehydrogenation of ethane to ethylene.

Cundari et al. [45] applied ANN's and genetic algorithms to the design of optimal composed catalysts for the ammoxidation of propane. An ANN was trained with 26 sets of experimental data (molar fractions of the six components the catalysts are composed of as inputs; activity and selectivity as outputs). A genetic algorithm was applied to search for the optimal catalyst composition using the trained ANN to generate virtual experiments. As a result, better catalysts than previously reported, were predicted. However, the best predictions were obtained for catalyst compositions outside the range of the training data and no experimental verification of these results has been reported.

5.   Experimental Tools

Various experimental tools have been developed both for preparation and for catalytic screening of solid materials. These tools depend mainly on the objective whether it is just screening of the materials in a semi-quantitative manner (stage I) for their catalytic performance or whether full quantitative testing (stage II) is applied.

Stage I screening comprises the preparation of very small amounts of materials by techniques like sputtering or ink-jet printing resulting in thin films or spots of the material on support surfaces. The catalytic screening aims at roughly discriminating between the reactivity of different samples. Therefore, analytical techniques like determining reaction heats by IR imaging, semi-quantitative detection of reaction products by mass spectroscopy (MS), IR spectroscopy or chemical reaction with fluorescence or dye indicators are sufficient.

In stage II testing catalytic materials are prepared and tested near to conventional methods and conditions. Amounts of several hundred milligrams to several grams are prepared, mostly by robotic systems, via impregnation or precipitation techniques. For quantitative determination of activity and selectivity of the materials parallel reactors with well-defined operating conditions are used. The results are comparable to such derived from conventional lab-scale micro-reactors and have to be scaled-up in the next step for pilot-plant operation.

5.1   Synthesis of Materials for Heterogeneous Catalysis

A first attempt for preparing hundreds of differently composed inorganic materials by high-throughput methods was reported by Hanak already in 1970 [46]. This early approach, however, was not continued for lack of computer power in the laboratories at that time. In the beginning of the last decade of the 20th century materials such as luminophors, high-temperature super-conductors, and magnetic materials were prepared automatically in parallel in the form of thin films by sputtering using masks and solution based technologies [47-49]. In establishing this new field the foundation of the SYMYX Corp. in Santa Barbara, USA played an important role. In principle, the same methods have been used for preparation of heterogeneous catalyst in the so-called stage I screening [48].

Combinatorial methods using preparation methods close to conventional approaches have been developed by Akporiaye et al. for the synthesis of up to 1000 differently composed zeolites via a hydrothermal method using PTFE block multi-autoclaves with 100 cavities each. Characterization of all samples by X-ray diffraction delivers ternary or quaternary phase diagrams in the searched parameter spaces [50, 51]. High-speed synthesis of aluminium-rich zeolites and silesquioxanes has been described in [52]. The silesquioxanes were used as precursors for Ti catalysts being highly active in the liquid-phase epoxidation of 1-octene.

A hydrothermal method was also applied to prepare mixed oxide catalysts. Small amounts of 37 samples of titanium silicalite were prepared on a silicon wafer and analyzed by X-ray diffraction to be amorphous or crystalline [53].

Hill and Gall [13] prepared an array of differently composed $[PW_xMo_yV_zO_{40}]^{n-}$ polyoxometalates. From stock solutions of Na_2WO_4, Na_2MoO_4, $NaVO_3$ and Na_2HPO_4 37 catalyst samples were prepared and tested for the homogeneously catalyzed selective oxidation of tetrahydrothiophene to the corresponding sulf-oxide.

The influence of synthesis parameters on the preparation of supported Au catalysts was systematically studied by Wolf and Schüth [54]. The catalysts were prepared by deposition-precipitation on various supports applying different pH values, temperatures of calcination, Au contents and washing procedures. By using high-throughput methods for both preparation and catalytic testing in CO oxidation optimal preparation parameters for highly active catalysts were deter-mined.

Nele et al. [55] used a statistical (factorial) experimental design to analyze the deposition-precipitation and aging parameters in the preparation of silica-supported Ni catalysts. In the factorial design nominal Ni content, precipitation temperature, aging temperature, aging time, agitation, and $NiNO_3$ concentration had been included. From the experiments a model was derived which describes the change of catalyst surface area with preparation conditions.

Cassell et al. [56] used different composed materials spotted on a wafer to catalyze the growth of carbon nanotubes.

In general, liquid handling robotic systems already known to be suitable for pharmaceutical combinatorial chemistry are widely applied to prepare catalysts using impregnation, precipitation and slurry preparation techniques [28, 54, 57-60].

5.2   Catalytic Testing of Materials

Stage I screening is represented by methods using a few mg of materials samples deposited at wafer surfaces or in small cavities or miniaturized channels. Wafer based technologies have been used to analyze arrays of differently composed materials for H_2 oxidation by IR thermographic detection of the reaction heats [61], CO oxidation by MS detection of CO_2 [5], NO reduction [5], oxidative dehydrogenation of ethane to ethylene over MoVNbO catalysts analyzing the re-action mixture by a combination of MS and a photothermal deflection (PTD) cell [6, 7]. The early IR thermographic detection of reaction heats [61] has been im-proved by emission correction [62, 63].

A method for discovering highly effective electrocatalysts from a 645-membered electrode array using parallel fluorescence detection of generated protons was described by Reddington et al. [64]. Fluorescence imaging was also used for finding new catalysts for methanol oxidation in a direct methanol fuel cell [65] for electrochemical reduction of benzoquinone [66] and for the electrochemical oxygen reduction and water oxidation [67]. A method allowing a more accurate comparison of electrocatalysts is the multi-electrode array developed by Sullivan et al. [66]. An 8 x 8 electrode array immersed in a single electrochemical cell allows measuring the electrochemical current at each electrode by a computer-automated set-up.

Screening methods between stage I and stage II are the reactor set-up of Senkan combined with the REMPI (resonance enhanced multi photon ionization) method [10, 68] or with a scanning MS [69], the scanning MS screening of powdered materials of Maier´s group [70] and the MS screening of differently composed materials in the channels of a monolithic reactor [71].

Stage II reactor set-ups are represented by fixed-bed reactors operating in parallel. An early development is the six-flow reactor system of Kapteijn and Moulijn the application of which to different reactions has been summarized in [72]. In this set-up each of the 6 reactors is connected to a separate gas supply with mass-flow controllers. Rodemerck at al. used a common gas supply for a 15-reactor set-up [28, 57]. Hahndorf et al. described a 64-channel reactor set-up consisting of a ceramic block with 64 drillings, flow-restrictor devices to feed all reactors with a constant flow of reactants and a very fast analyzing tool consisting of a fast GC and a time-of-flight MS [59]. A parallel reactor set-up containing 16 channels in a block of brass has been developed by the group of Schüth and tested for low-temperature CO oxidation [58]. The same group described a 49-channel reactor made of stainless steel, which can be operated close to conventional conditions at higher temperatures and pressures up to 50 bar [73].

Microreactors should be well suited for parallel testing of catalysts since their dimensions can be designed very exactly which makes it possible to have the same flow regime in each reactor. Miniaturization allows the integration of high numbers of reaction channels in one set-up and lowers the costs for process gases and catalyst samples. Most applications of microreactors are in homogeneous reactions but they have also been applied to test catalysts for gas-phase reactions. Zech described a stack of plates with 35 channels each the surface of which was covered by an alumina-supported active catalytic material [16, 74]. To determine activity and selectivity the product gases were analyzed by a scanning MS, i.e. the MS inlet capillary is moved to the outlets of the distinct plates for analyzing gas samples.

Parallel reactors for three phase reactions have been developed by Lucas et al. who described the parallelization of small batch autoclaves [75]. For 15 selective hydrogenation reactions the hydrogen pressure decrease was monitored on-line. A three phase reactor for simultaneous testing of 25 catalyst samples up to 50 bar has been described by Thomson et al. and also tested for a selective hydrogenation reaction [76].

The group of Maier developed set-ups for the high-throughput preparation and testing of photo catalysts for the oxidative degradation of harmful substances in water [77], which were successfully applied for discovering active and selective catalysts.

Special interest in high-throughput screening has been dedicated to fast analytical tools to determine activity and selectivity of catalysts. In principle, it is possible to operate the reactors in parallel and analyze the effluents sequentially by switching from one reactor outlet to the next one. This approach demands a fast analytic system, and so mass spectrometers have been widely used [5, 16, 28, 57, 69-71, 74]. It is also possible to use fast GC or GC/MS systems [59] in such a way.

IR thermography is a really parallel method, which allows looking at all the catalysts at the same time [61-63, 78]. The quantitative detection of reaction heats emerging from the catalyst beds is a good measure for the activity of catalysts, but no selectivity data can be derived by this method although this is often of high importance. Another IR-based method which allows also the quantitative determination of product selectivities is the so-called FT-IR imaging technology [79-82]. A new reactor set-up allows analyzing the products of 16 reactors simultaneously using an FTIR spectrometer and a focal plane array (FPA) detector [81, 82]. The authors describe the application of the method to CO oxidation and CO adsorption studies. The method can be extended to higher numbers of reactors; theoretically, arrays of up to 250,000 samples can be analyzed by such an FPA.

Also the REMPI (resonance-enhanced multiphoton ionization) technology allows a real parallel quantitative determination of reaction products [10, 68]. A laser beam selectively ionizes one chemical compound the concentration of which is than determined at the outlets of the reactors by a simple electrode array. By variation of the laser frequency different molecules can be ionized. Unfortunately, this method is not suitable for all reaction products of interest and especially difficult to apply if complex mixtures of similar compounds have to be analyzed.

The photo-acoustic detection of reaction products is another method, which can be applied in parallel [83]. A laser beam stimulation of product molecules leads to a pressure increase and the resulting shock wave can be detected by a microphone. The method was used for parallel testing of catalysts in CO oxidation and oxidative dehydrogenation of ethane.

Chemically sensitive sensors have been shown to be valuable tools for determining the concentration of reaction products in gas streams. Yamada et al. [84] developed an array of gas sensors, which can determine the concentrations of reaction products in the CO oxidation and in the selective oxidation of propane to oxygenates. For the determination of hydrogen concentrations a 96-element sensor array has been developed which is based on the chemo-optical properties of WO_3 [85, 86]. The set-up was used for searching a Ti, Pt, Ni, Au, Pd, Al, Ag, Ge library for catalysts showing a high electrochemical H_2 production rate.

6.   Scientific Input in the Final Optimisation Process

When applying optimisation routines in searching for optimal catalyst compositions several loops of preparing and testing have to be passed through. In each of these loops new knowledge about the relationship between catalyst composition and reactivity is generated. This knowledge can be used to accelerate the optimisation process. The optimisation routine itself uses the empirical knowledge generated, as is done by applying the genetic algorithm. At an advanced level, it is

also possible to extract basic knowledge or rules from the previous experiments, which make it sometimes desirable to change the search principles, i.e., the pool of elements determining the parameter space or the frequency and ratio of cross-over and mutation.

One example of using scientific input in the final optimisation strategy has been reported by Baerns et al. [25]. The authors applied an evolutionary strategy to search for new catalysts for the oxidative dehydrogenation of propane to propene using a pool of potentially active and selective redox-type metal oxides. After running four loops of the genetic algorithm the results were evaluated in order to identify the oxides being useful for high propene yields. In a second evolutionary approach the useful components were combined with additional metal oxides of different properties (acidity, basicity, oxygen adsorption) establishing a new pool of elements. After running five further generations a slightly higher propene yield was reached for the optimised catalysts as compared to the first evolutionary optimisation. The best catalysts of both the first and the second optimisation approach applied were well characterized by XRD, EPR, UV/vis, XPS, and transient oxygen adsorption measurements leading to the conclusion that catalysts resulting in high propene yields contain well-dispersed V sites and no adsorbed surface oxygen. Based on this knowledge the authors applied VO_x-on-MCM41/48 catalysts, which are known to contain isolated V sites on the surface [87]. These catalysts resulted in much higher propene yields, i.e., almost twice as much compared to the V-containing mixed-oxides catalysts of the two evolutionary optimisation procedures (Fig. 5).
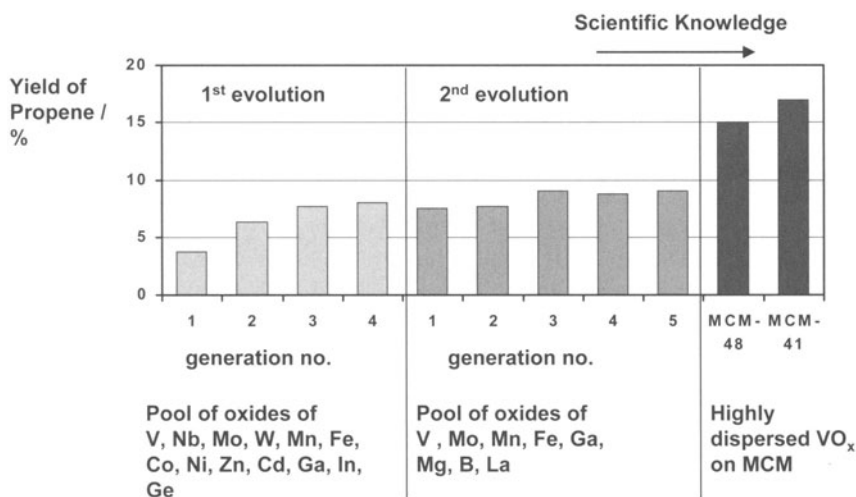
Fig. 5 Incorporation of scientific knowledge into the optimisation routine applying an evolutionary strategy for catalyst optimisation for the oxidative dehydrogenation of propane (after [25])

Up to now, scientific input has been reported not to any broader degree because of the lack of the general availability of fast catalyst characterization methods. Therefore, only small numbers of catalyst samples are usually well characterized

by different methods. However, new characterization tools working in parallel are in the development stage and will be available in the near future. Applying these methods a broad base of scientific knowledge will be generated, which can be used in combination with data-analysis software to establish structure-reactivity relationships for heterogeneous catalysts; in this way also the fundamentals in heterogeneous catalysis will benefit.

7. Success Stories

High-throughput experimentation has now being applied for more than five years. Some service companies, like Symyx, Avantium, and hte, indicate that work is occurring successfully; also numerous academic groups use combinatorial catalysis for faster development of new catalytic materials. Since most of the catalyst developments are made in close cooperation with industry results are often confidential and have not become known. Furthermore, from patent applications it is mostly not obvious if the catalysts have been discovered via combinatorial or conventional methods. Thus, only successful applications of high-throughput experimentation for the development of new catalysts, which has been reported in the open literature, is covered by this review.

Maier and co-worker [77] used their home-made set-ups for the high-throughput preparation and testing of photo catalysts for the oxidative degradation of harmful substances in water. TiO_2 is well known to be an effective photo catalyst. However, the knowledge on the catalytic performance of other oxides and the influence of doping materials is rare. Thus, the authors prepared and tested ca 100 catalytic materials based on TiO_2, SnO_2, and WO_3 each doped by 15 elements of the periodic table. As a result, new dopants for TiO_2 as well as new photo catalysts based on SnO_2 and WO_3 were discovered. The authors stated that probably high numbers of doped oxides showing activity in photo catalysis exist, which can be easily discovered by high-throughput experimentation techniques.

Another example in environmental catalysis is the development of low-temperature total oxidation catalysts for hydrocarbons in air by Rodemerck et al. [28]. The authors applied a genetic algorithm to search for catalytic materials catalyzing the total oxidation of low-concentration propane at temperatures below 100 °C. After preparing and testing three generations of altogether 210 catalyst samples using automated high-throughput set-ups it was found that Ru/TiO_2 catalysts doped by different elements are able to oxidize propane to CO_2 at 50-100 °C. Such catalysts can be applied to remove small amounts of hydrocarbons (some ppm) from air in the air liquefaction for oxygen and nitrogen separation since the dangerous condensation of hydrocarbons into liquid oxygen has to be avoided.

Applying high-throughput technology researchers at Symyx Technol. Inc. found new catalysts for the oxidative dehydrogenation of ethane to ethylene [7-9]. In the first stage catalyst libraries of 144 members each were screened using a wafer technology and mass spectrometry for CO_2 detection and photothermal deflection spectroscopy for ethylene detection. After screening V-Al-Nb, Cr-Al-Nb, and Cr-Al-Ta mixed-metal oxides libraries active and selective catalysts were identified and scaled-up to the 20 g scale [7].

At Symyx specially designed high-throughput set-ups were developed for the direct amination of benzene to aniline [88]. Around 25,000 samples were screened in miniaturized autoclaves in about one year. In a second stage promising catalysts were scaled-up and optimised using conventional autoclaves. An optimised catalyst, Rh/Ni-Mn/K-TiO$_2$ achieved 95% selectivity of aniline at 10% conversion and was shown to be stable.

New effective electrocatalysts have been identified applying high-throughput methods. Chen et al. [67] reported on combinatorial discovery of bifunctional oxygen reduction – water oxidation catalysts. Searching 715 combinations of a five-element array (Pt, Ru, Os, Ir, Rh) Pt$_{4.5}$Ru$_4$Ir$_{0.5}$ was found to show higher activity for both reactions than the previously described catalysts. New active quaternary composed catalysts for the electrochemical methanol oxidation in direct methanol fuel cells (DMFC) were found by Choi et al. [65] whose optimal composition was identified by high-throughput screening via fluorescence imaging.

8.   Outlook

Development of catalytic materials and of other functional materials by high-throughput experimentation will receive even more attention than already prevailing. The main incentive for applying this technique in industrial practice is based on the opportunity to reduce development times and hence, the time-to-market for the materials or in catalysis in addition, the design of a catalytic process. Against these expectations it is not surprising that there are many efforts to further improve all the techniques involved in high-throughput synthesis, screening and testing materials.

The improvement efforts comprise the advancement of existing synthesis robots with the aim of increasing their applicability to different methods such as precipitation, impregnation, hydrothermal and sol-gel-type synthesis; in many circumstances it will be also desirable to control certain variables during the preparation process, i.e., surrounding gas atmosphere, pH value of the liquid in the various vials, temperature etc.

Screening and testing set-ups have to be designed for establishing accurate conditions especially temperature when dealing with highly exothermic reactions. Up to now the quantitative determination of catalytic performance is often a rate-limiting step since mostly no true parallel chemical analysis of the products formed is possible unless rather sophisticated and complex methods are applied.

Intelligent handling of the huge amounts of data being generated in high-throughput experimentation is a still not fully resolved challenge. Data compilation, management and analysis needs special attention to take full advantage of the inherent knowledge created which will certainly contribute to the fundamental understanding of catalysis.

The success stories in applying the novel techniques will without any doubt become more visible and their number will significantly increase in the near future.

References

[1]   S. Senkan, Angew. Chem., 113, 322, (2001)

[2]   G. Grubert, D. Wolf, N. Dropka, S. Kolf and M. Baerns, *4th World Congress on Oxidation Catalysis* (Berlin/Potsdam, Germany), Rapid discovery of new catalytic materials for the oxidative dehydrogenation of ethane to ethylene by an evolutionary approach, pp. 113 (2001)

[3]   G. Grubert, E. Kondratenko, S. Kolf, M. Baerns, P. v. Geem and R. Parton, Catalysis Today, , (submitted)

[4]   O. V. Buyevskaya, A. Brückner, E. V. Kondratenko, D. Wolf and M. Baerns, Catal. Today, 67, 369, (2001)

[5]   P. Cong, R. D. Doolen, Q. Fan, D. M. Giaquinta, S.Guan, E. W. McFarland, D. M. Poojary, K. Self, H. W. Turner and W. H. Weinberg, Angew. Chem., 111, 867, (1999)

[6]   P. Cong, A. Dehestani, R. Doolen, D. M. Giaquinta, S. Guan, V. Markov, D. Poojary, K. Self, H. Turner and W. H. Weinberg, Applied Physical Sciences,Proc. Natl. Sci. USA, 96, 11077, (1999)

[7]   Y. Liu, P. Cong, R. D. Doolen, H. W. Turner and W. H. Turner, Catal. Today, 61, 87, (2000)

[8]   Y. Liu, P. Cong, R. D. Doolen, H. W. Turner and W. H. Weinberg, Studies in Surface Science and Catalysis 130, 1859, (2000)

[9]   A. Hagemeyer, B. Jandeleit, Y. Liu, D. M. Poojary, H. W. Turner, A. F. Volpe and W. H. Weinberg, Appl. Catal. A: Gen., 221, 23, (2001)

[10] S. M. Senkan and S. Ozturk, Angew. Chem., 111, 867, (1999)

[11] K. Krantz, S. Ozkru and S. Senkan, Catal. Today, 62, 281, (2000)

[12] M. Richter, M. Langpape, S. Kolf, G. Grubert, R. Eckelt, J. Radnik, M. Schneider, M.-M. Pohl and R. Fricke, Appl. Catal. B: Environm., 36, 261, (2002)

[13] C. L. Hill and R. D. Gall, Journal of Molecular Catalysis A Chemical, 114, 103, (1996)

[14] J. M. Newsam, S. A. Schunk and J. Klein; DE 100059890 A1; 1 Dec. 2000;

[15] J. M. Newsam, S. A. Schunk and J. Klein; WO 02/43860 A2; 30 Nov. 2001;

[16] T. Zech, , University of Chemnitz, Chemnitz 2002.

[17] T. Zech, J. Klein, D. Demuth and S. A. Schunk, *IMRET 6* (New Orleans), The integrated materials chip for high-throughput experimentation in catalysis research (2002)

[18] D. Demuth, J. Klein, S. A. Schunk, W. Strehlau, A. Sundermann and T. Zech, Chem.-Ing.-Techn., 74, 557, (2002)

[19] Y. Sun, B. C. Chan, R. Ramnarayanan, W. M. Leventry, T. E. Mallouk, S. R. Bare and R. R. Willis, J. Comb. Chem., 4, 569, (2002)

[20] T. Bäck and H.-P. Schwefel, Evolutionary computation, 1, 1, (1993)

[21] D. B. Fogel, , University of California, San Diego 1992.

[22] D. E. Goldberg, *Genetic Algorithms in Search, Optimisation and Machine Learning*, Addison Wesley, Reading, MA 1989

[23] V. Nissen, *Evolutionäre Algorithmen (in German)*, Deutscher Universitätsverlag, Bamberg, Germany 1994

[24] D. Wolf, O. V. Buyevskaya and M. Baerns, Appl. Catal. A: Gen., 200, 63, (2000)

[25] M. Baerns, O. Buyevskaya, G. Grubert and U. Rodemerck, in E.G. Derouane, V. Parmon, F. Lemos, F.R. Ribeiro (Eds.): *Principles and methods for accelerated catalyst design and testing*, Kluwer Academic Publishers 2002, p. 85

[26] O. V. Buyevskaya, D. Wolf and M. Baerns, Catal. Today, 62, 91, (2000)

[27] M. Langpape, G. Grubert, D. Wolf and M. Baerns, DGMK-Tagungsbericht, 4, 227, (2001)

[28] U. Rodemerck, D. Wolf, O. V. Buyevskaya, P. Claus, S. Senkan and M. Baerns, Chem. Eng. J., 82, 3, (2001)

[29] M. Baerns, O. Buyevskaya, P. Claus, U. Rodemerck and D. Wolf; DE 19843242 A1; Sept. 11, 1998; Institut für Angewandte Chemie Berlin-Adlershof e.V.

[30] M. Baerns, O. Buyevskaya, P. Claus, U. Rodemerck and D. Wolf; PCT WO 00/15341; Sept. 10, 1999; Institut für Angewandte Chemie Berlin-Adlershof e.V.

[31] A. Corma, J. M. Serra and A. Chica, in E. G. Derouane, V. Parmon, F. Lemos and F. R. Ribeiro (Eds.): *Principles and methods for accelerated catalyst design and testing*, Kluwer, Dordrecht 2002, p. 153

[32] G. Grubert, E. Kondratenko, S. Kolf, M. Baerns, P. v. Geem and R. Parton, Catal. Today, , (in press)

[33] D. Wolf, in E.G. Derouane, V. Parmon, F. Lemos, F.R. Ribeiro (Eds.): *Principles and methods for accelerated catalyst design and testing*, Kluwer Academic Publishers 2002, p. 125

[34] D. Wolf and M. Baerns, in J. N. Cawse (Ed.): *Experimental design for combinatorial and high throughput materials development*, John Wiley & Sons, Inc. 2003, p. 147

[35] S. Kito and e. al., Industrial and Engineering Chemistry Research, 31, 979, (1992)

[36] T. Hattori and e. al., Catalysis Today, 23, 347, (1995)

[37] S. Kito and e. al., Applied Catalysis A: General, 114, L173, (1994)

[38] M. Sasaki and e. al., Applied Catalysis A: General, 132, 261, (1995)

[39] Z.-Y. Hou and e. al., Applied Catalysis A: General, 161, 183, (1997)

[40] B. K. Sharma and e. al., Fuel, 77, 1763, (1998)

[41] K. Huang and e. al., Applied Catalysis A: General, 219, 61, (2001)

[42] M. Holena and M. Baerns, in J. N. Cawse (Ed.): *Experimental design for combinatorial and high throughput materials development*, Wiley 2003, p. 163

[43] M. Holena and M. Baerns, Catal. Today, , (submitted)

[44] A. Corma, J. M. Serra, E. Argente, V. Botti and S. Valero, CHEMPHYSCHEM, 3, 939, (2002)

[45] T. R. Cundari, J. Deng and Y. Zhao, Ind. Eng. Chem. Res., 40, 5475, (2001)

[46] R. Dagani, Chem. Eng. News, 77, , (1999)

[47] R. F. Service, Science, 277, 474, (1997)

[48] P. G. Schultz and X.-D. Xiang, Current Opinion in Solid State and Material Science, 3, 153, (1998)

[49] B. E. Baker, N. J. Kline, P. J. Treado and M. J. Natan, J. Am. Chem. Soc., 118, 8721, (1996)

[50] D. E. Akporiaye, I. M. Dahl, A. Karlsson and R. Wendelbo, Angew. Chemie, 110, 629, (1998)

[51] D. Akporiaye, I. Dahl, A. Karlsson, M. Plassen, R. Wendelbo, D. S. Bem, R. W. Broach, G. J. Lewis, M. Miller and J. Moscoso, Microporous and Mesoporous Materials, 48, 367, (2001)

[52] P. P. Pescarmona, J. J. T. Rops, J. C. v. d. Waal, J. C. Jansen and T. Maschmeyer, J. Mol. Catal. A: Chem., 182-183, 319, (2002)

[53] J. Klein, C. W. Lehmann, H.-W. Schmidt and W. F. Maier, Angew. Chemie, 110, 3557, (1998)

[54] A. Wolf and F. Schüth, Appl. Catal. A: Gen., 226, 1, (2002)

[55] M. Nele, A. Vidal, D. L. Bhering, J. C. Pinto and V. M. M. Salim, Appl. Catal. A: Gen., 178, 177, (1999)

[56] A. M. Cassell, S. Verma, L. Delzeit, M. Meyyappan and J. Han, Langmuir, 17, 260, (2001)

[57] U. Rodemerck, P. Ignaszewski, M. Lucas and P. Claus, Chem. Eng. Technol., 23, 413, (2000)

[58] C. Hoffmann, A. Wolf and F. Schüth, Angew. Chemie, 111, 2971, (1999)

[59] I. Hahndorf, O. Buyevskaya, M. Langpape, G. Grubert, S. Kolf, E. Guillon and M. Baerns, Chem. Eng. J., 89, 119, (2002)

[60] J. N. Al-Saeedi and V. V. Guliants, Appl. Catal. A: Gen., 237, 111, (2002)

[61] F. C. Moates, M.Somani, J. Annamalai, J. T. Richardson, D. Luss and R. C. Willson, Ind. Eng. Chem. Res., 35, 4801, (1996)

[62] A. Holzwarth, H.-W. Schmidt and W. F. Maier, Angew. Chemie, 110, , (1998)

[63] M. T. Reetz, M. H. Becker, K.M.Kühling and A. Holzwarth, Angew. Chemie, 110, 2792, (1998)

[64] E. Reddington, A. Sapienza, B. Gurau, R. Viswanathan, S. Sarangapani, E. Smotkin and T. Mallouk, Science, 280, 1735, (1998)

[65] W. C. Choi, J. D. Kim and S. I. Woo, Catal. Today, 74, 235, (2002)

[66] M. G. Sullivan, H. Utomo, P. J. Fagan and M. D. Ward, Anal. Chem., 71, 4369, (1999)

[67] G. Chen, D. A. Delafuente, S. Sarangapani and T. E. Mallouk, Catal. Today, 67, 314, (2001)

[68] S. M. Senkan, Nature, 394, 350, (1998)

[69] S. Senkan, K. Krantz, S.Ozturk, V. Zengin and I. Onal, Angew. Chem., 111, 2965, (1999)

[70] M. Orschel, J. Klein, H.-W. Schmidt and W. F. Maier, Angew. Chem., 111, 2961, (1999)

[71] U. Rodemerck, P. Ignaszewski, M. Lucas, P. Claus and M. Baerns, Topics Catal., 13, 249, (2000)

[72] J. Perez-Ramirez, R. J. Berger, G. Mul, F. Kapteijn and J. A. Moulijn, Catal. Today, 60, 93, (2000)

[73] C. Hoffmann, H.-W. Schmidt and F. Schüth, J. Catal., 198, 348, (2001)

[74] P. Claus, D. Hönicke and T. Zech, Catal. Today, 67, 319, (2001)

[75] M. Lucas and P. Claus, Chemie Ingenier Technik, 73, 252, (2001)

[76] S. Thomson, C. Hoffmann, S. Ruthe, H.-W. Schmidt and F. Schüth, Appl. Catal. A: Gen., 220, 253, (2001)

[77] C. Lettmann, H. Hinrichs and W. F. Maier, Angew. Chemie, 113, 3258, (2001)

[78] A. Holzwarth and W. F. Maier, Platinum Metals Rev., 44, 16, (2000)

[79] C. M. Snively, S. Katzenberger, G. Oskarsdottir and J. Lauterbach, Optics Letters, 24, 1841, (2000)

[80] C. M. Snively, G.Oskarsdottir and J.Lauterbach, J. Comb. Chem., 2, 243, (2000)

[81] C. M. Snively, G. Oskardottir and J. Lauterbach, Catal. Today, 67, 357, (2001)

[82] C. M. Snively, G. Oskardottir and J. Lauterbach, Angew. Chemie, 113, 3117, (2001)

[83] T. Johann, A. Brenner, M. Schwickardi, O. Busch, F. Marlow, S. Schunk and F. Schüth, Angew. Chem., 114, 3096, (2002)

[84] Y. Yamada, A. Ueda, Z. Zhao, T. Maekawa, K. Suzuki, T. Takada and T. Kobayashi, Catal. Today, 67, 379, (2001)

[85] T. F. Jaramillo, A. Ivanovskaya and E. W. McFarland, J. Comb. Chem., 4, 17, (2002)

[86] S. H. Baeck, T. F. Jaramillo, C. Brändli and E. W. McFarland, J. Comb. Chem., 4, 563, (2002)
[87] H. Berndt, A. Martin, A. Brückner, E. Schreier, D. Müller, H. Kosslick, G.-U. Wolf and B. Lücke, J. Catal., 191, 384, (2000)
[88] A. Hagemeyer, R. Borade, P. Desrosiers, S. Guan, D. M. Lowe, D. M. Poojary, H. Turner, H. Weinberg, X. Zhou, R. Armbrust, G. Fengler and U. Notheis, Appl. Catal. A: Gen., 227, 43, (2002)

Ordered Mesoporous Materials:
Preparation and Application in Catalysis

Contents

Ordered Mesoporous Materials:
Preparation and Application in Catalysis

A. Wingen, F. Kleitz and F. Schüth

Max-Planck-Institut für Kohlenforschung,
Kaiser-Wilhelm-Platz 1, 45470 Mülheim, Germany

Abstract. Ordered mesoporous materials can be synthesized with various different pore sizes, structures and framework compositions. Many different synthesis procedures have been developed and a high degree of control over the properties of the resulting materials has been achieved. The remarkably high surface areas of such materials and the narrow pore size distribution make these materials highly suitable for applications in catalysis. Without further modification, ordered mesoporous materials can be used as acid catalysts and as supports. In framework modified form, for instance with titanium, applications in redox catalysis have been described. In addition, many different catalytically active species can be supported, such as noble metals, base metal oxides, and molecular species. This chapter will cover the basics of the synthesis and characterization of such materials and review the state of the art with respect to catalytic applications.

1.   Introduction

Porous materials have been intensively studied with regard to technical applications as catalysts, catalyst supports, and adsorption media. According to the IUPAC definition[1], porous materials are divided into three classes: microporous (pore size < 2 nm), mesoporous (2-50 nm) and macroporous (>50 nm) materials. The best known members of the family of microporous materials are zeolites. However, applications of zeolites in catalysis, although important and numerous, are limited by the relatively small pore sizes that are available. Research has, therefore, been focused on enlarging the pore sizes into the mesopore range, allowing larger molecules to enter the pore system. Porous glasses and porous gels, as well as intercalated layered materials are examples for early mesoporous solids, which, however, have disordered pore systems and broad pore-size distributions.

The first synthesis of an ordered mesoporous material was described in a patent filed in 1969[2], however, due to a lack of analysis, the remarkable features of this product could not be recognized[3]. In 1992, the same material was obtained by Mobil Corporation scientists[4]. MCM-41 (Mobil Composition of Matter) shows a highly ordered hexagonal array of uni-dimensional pores with a very narrow pore size distribution. The walls, however, are amorphous. Other related phases, such as MCM-48 and MCM-50 were reported in this early publication as well. At approximately the same time, an alternative approach to mesoporous materials was

described by Yanagisawa et al.[5]. Kanemite, a layered silicate, serves as a silicate source. The obtained material is designated as FSM-n (Folded Sheet Mesoporous Materials-n), where n is the number of carbon atoms in the surfactant chain used to synthesize the material. Meanwhile, a large research effort has been focussed on synthesis and characterization of a variety of different, although related materials. Several reviews have already been published[6,7,8,9,10]. This chapter will address synthetic aspects, but will mainly focus on catalysis.

2.   Techniques for Characterization

The standard procedure for characterizing mesoporous materials usually involves three independent techniques: adsorption analysis gives information about the porosity of the materials, whereas diffraction techniques (XRD) and transmission electron microscopy (TEM) supply insight in the degree of structural order. In the following, these techniques will be introduced with emphasis on their limitations. We will focus on the characterization of the most investigated member of the M41S family, namely MCM-41. In MCM-41, uni-dimensional pores are, as mentioned before, hexagonally organized, resulting in a honeycomb structure. Due to this uni-dimensional channel system MCM-41 is often claimed to be less attractive for catalytic applications, since mass transfer limitations could be expected. However, most synthetic procedures leading to MCM-41 result in the formation of very small primary particles, for which diffusion lengths in the mesopores will be short and mass transfer limitations thus will not be important.

2.1   Sorption Analysis

Sorption analysis is widely used to obtain information about the surface area of mesoporous materials and their pore-size distribution[11,12,13]. For MCM-41, the isotherm is of type IV according to the IUPAC classification[14]. It is characterized by a sharp capillary condensation step at a relative pressure of about 0.4. Uptake at
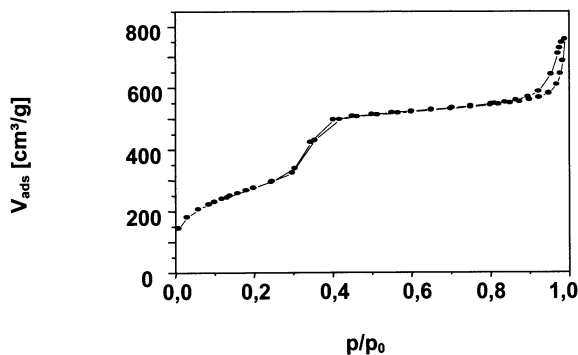
Fig. 1: Typical N_2 sorption isotherm of MCM-41

very low relative pressure is due to monolayer adsorption and no indication for microporosity[15,16]. A typical N_2 isotherm obtained for MCM-41 is shown in Figure 1. The calculation of the surface area according to the Brunauer-Emmett-Teller (BET) method and the calculation of the pore size distribution according to the Barrett-Joyner-Halenda (BJH) method[17,18] are the most commonly used algorithms to extract textural properties from the sorption isotherm data. The BET method is based on several assumptions[14], that are partly not valid for such materials. Consequently, the BET surface areas should be taken as only approximately correct and are most useful to compare similar samples. The BJH method is based on the Kelvin equation, that requires the existence of a meniscus to allow the calculation of the correlation between relative pressure, at which adsorption or desorption occurs, and the pore size. However, if the step for N_2 at 77 K lies below a relative pressure of 0.42, the meniscus of the pore confined liquid is not stable any longer, and therefore application of the BJH algorithm is no longer justified. Nevertheless, calculated pore sizes are probably still in the right range. Other methods based on density functional theory[16,19] (D.F.T.) or Monte Carlo simulation[20] are more accurate, but less disseminated and not available in most standard software packages.

MCM-41-type silicas have been used as adsorbents to test methods of pore size evaluation based on the Kelvin equation, the 4V/S method and the method of Horvath and Kawazoe[18,21]. Pore sizes evaluated from XRD lattice parameters and void fraction have been used as standard values. It was shown that the Kelvin equation for the hemispherical meniscus, corrected for the statistical film thickness, is in quite good agreement with an experimental relation between the pore size and the capillary condensation pressure. Comparison of specific surface areas determined by different methods strongly suggests that when nitrogen adsorption data are used, the BET method overestimates the specific surface area.

Summarizing, mesopore size distribution can be extracted relatively reliably if the nitrogen isotherm is of Type IV[22]. Because of network-percolation effects, analysis of the desorption branch of the hysteresis loop may give a misleading picture of the pore size distribution, and if a steep step in the desorption branch occurs which meets the adsorption branch at a relative pressure of 0.42 for nitrogen, rather the adsorption branch should be used for the calculation.

2.2   X-ray Diffraction (XRD)

The XRD pattern of MCM-41 typically shows low-angle reflections, that are due to the ordered hexagonal array of parallel silica tubes (Fig. 2). These reflections can be indexed as (100), (110), (200), (210) and so on. The lattice parameter a, i.e. the sum of pore diameter and wall thickness, is obtained   via a = 2d(100)/√3. Since the reflections are usually rather broad, the determination of the d-values often just results in an approximate value. Whereas the typical XRD pattern exhibits three or four reflections, it was referred to highly ordered materials with five or even more reflections[23,24,25]. However, a higher number of reflections does not necessarily indicate a higher structural order of the material. The simulation[26] of diffraction patterns for MCM-41 materials with different degrees of defects revealed that a decrease in the domain size results in a loss of reflections, whereas the XRD patterns are just slightly influenced by an even large number of defects in the hexagonal pore structure.
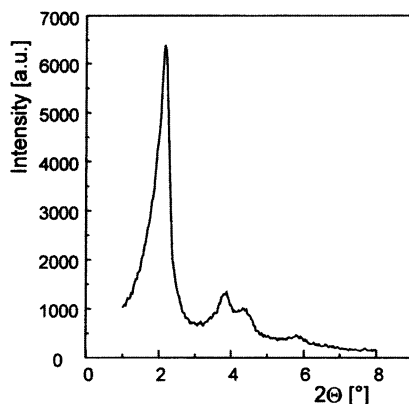
Fig. 2. Typical XRD of MCM-41

MCM-48, the cubic member of the M41S family, exhibits X-ray diffraction patterns showing several reflections, that can be attributed to a cubic phase with the space group Ia3d. The reflections of the lamellar structure MCM-50 can be indexed to $h00$.

A whole new range of mesoporous M41S analogues were developed following the initial reports, including SBA-1 (cubic Pm3n) and SBA-2 (cubic P6$_3$n), SBA-3, APM (acid prepared mesostructure), HMS (hexagonal mesoporous silica) SBA-15 or MSU-V and MSU-X (for references, see Table 1). These materials often exhibit X-ray diffraction patterns with lower content of information (one single reflection) and they can also contain random arrays of pores. However, most of them are characterized by a narrow pore size distribution, a very high surface area, and a high hydrocarbon adsorption ability.

One should note, that the XRD analysis of materials with large characteristic length can be very difficult, since part of the primary beam could be superimposed on reflections at very low angles below 1.5° (2θ) and lower.

2.3   Transmission Electron Microscopy (TEM)

Transmission electron microscopy is a suitable tool for answering the questions that remain after X-ray diffraction measurements have been carried out. However, it is not a substitute for X-ray diffraction, since usually only a rather small part of the sample is analyzed. To get a representative view of the quality of the sample, a great number of TEM images has to be examined. MCM-41 materials often show fingerprint-like structures[27] in addition to the ordered honeycomb type structures which are usually presented in literature. Upon closer examination these fingerprint-like structures reveal two dislocation and two disclination defect structures, that are similar to corresponding structures detected in pure liquid-crystal phases[28]. Other regions exhibit equidistant parallel lines, that are due to pores oriented parallel to the image plane[29]. Other regions may appear disordered, but this can be due to the zone axis not being properly aligned with the electron beam, as tilt

experiments can reveal. Whereas the sum of pore diameter and wall thickness is relatively easy to determine, the demarcation between pore and wall is difficult to detect, since the image is dependent on the focus conditions.[26,30]   A typical TEM micrograph (SBA-15) is shown in Figure 3.
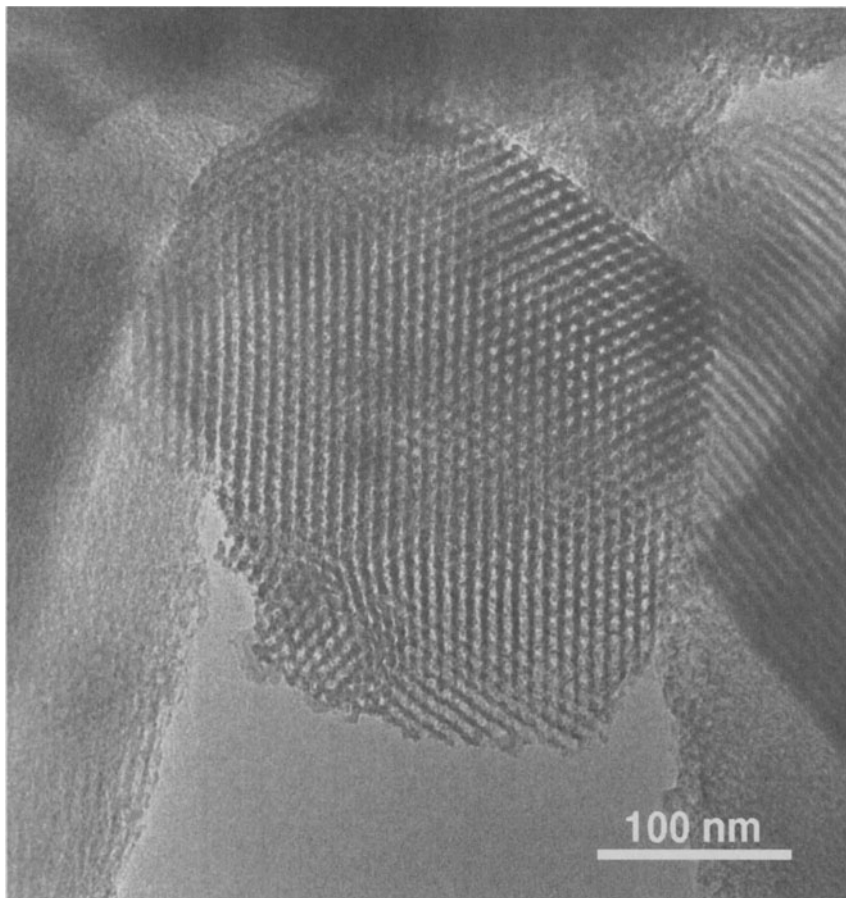
Fig. 3: Typical TEM of an ordered mesoporous silica. Shown is an SBA-15 sample with a pore size of approximately 6.5 nm

3.   Synthesis

3.1   General Remarks

At the time of the discovery of MCM-41, porous glasses and porous gels were already known as mesoporous materials, and mesoporosity was found in precipitates with textural porosity between the primary particles. However, these materials were characterized by broad pore-size distributions. By intercalation of layered materials such as double hydroxides, titanium and zirconium phosphates or clays,

further mesoporous materials were accessible, also exhibiting broad mesopore-size distributions and additional micropores.

The synthesis of an ordered mesoporous material was already described in a patent filed in 1969[2]. However, due to a lack of analysis these early scientists were unable to recognize the remarkable features of their product. Reproducing this synthesis, Di Renzo and coworkers[3] found that the obtained material was identical with mesoporous MCM-41, which was patented by scientists of the Mobil Oil Corporation in 1991. The characteristic approach for the synthesis of ordered mesoporous materials is the use of templates, that enable the specific formation of pores with predetermined size. However, in contrast to zeolite synthesis where single molecules serve as templates, aggregates of molecules are used to obtain mesoporous materials. In case of MCM-41, the formation of the inorganic-organic composites is usually based on electrostatic interactions between charged surfactants and silicate species. Beck et al.[31] early proposed two possible main pathways for liquid crystal templating, the first pathway being silicate-initiated and the second liquid-crystal-initiated. Later it turned out that the reaction can proceed via both of them. In most cases, however, cooperative self assembly between the surfactant and the inorganic species is the major driving force.
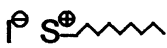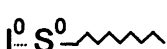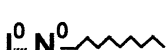
Surfactant properties and concentrations, and additional ions determine which factors govern the synthesis most strongly[32,33]. MCM-41 can, for example, be formed over a wide range of surfactant concentrations[34]. Monnier et al.[35,36] investigated how MCM-41 forms at concentrations where spherical micelles are present, and proposed again a silicate-initiated mechanism. According to this, the oligomeric silicate polyanions first act as multidentate ligands for the cationic surfactant head groups, leading to a surfactant-silica-interface with a topology dependent on the solution conditions. The negative charge at the interface decreases with progressive polymerisation of the silicate. Charge density matching determines the final structure of the solid formed, and intermediate phases, such as a lamellar phase, can be present. Firouzi et al.[37] have worked under conditions where the silicate species do not polymerize in order to decouple self-assembly and polymerisation. They proved, that a micellar cetyltrimethylammonium bromide solution forms a hexagonal phase in the presence of anionic silica species. Another route is assumed to proceed via the formation of cylindrical, silicate coated micelles which then assemble to the hexagonal mesostructure[30].

The prediction of surfactant aggregates and the corresponding mesophases in surfactant-water systems was made possible by Israelachvili et al.[38], who developed a microscopic model according to which the dimensionless packing parameter g plays a key role. g is defined as $g = V/a_0 l_c$, where V is the effective volume of the hydrophobic chain of the surfactant, a_0 is the effective aggregate surface area of the hydrophilic head group, and l_c is the effective hydrophobic chain length. In addition to the molecular geometry of the surfactant molecule, solution conditions such as ionic strength, pH, co-surfactant concentration and temperature affect the packing parameter[39]. An increase in the packing parameter results in phase transitions corresponding to a decrease in the surface curvature. Stucky et al.[40,41] proposed a synthesis-space diagram for a ternary system composed of NaOH, cetyltrimethylammonium bromide and tetraethylorthosilicate, and a detailed investigation of binary and ternary systems was later carried out by Firouzi et al.[37] Vartuli et al.[42] observed that also the surfactant to silica ratio has a substantial impact on the composite structure obtained.

3.2   Synthesis Pathways

Pathways described in chapter 3.2.1-3.2.3 are listed in Table 1. Pure silica mesoporous materials, that are mainly of interest as catalyst supports, are given as examples. The text, however, will mainly summarize approaches that led to non-silicious materials, since materials like that will more likely be interesting as supports exhibiting strong metal support interactions, or even as active components. Monnier et al.[35] were the first to suggest the possibility to substitute silicate by metal oxides for which condensable polyions exist. Subsequently, mesostructured surfactant composites made from a variety of metals have been synthesized[43]. However, only a few mesostructures could be calcined without structural collapse, and therefore, obtained in a porous form. The thermal instability was attributed to the existence of several relatively stable oxidation states of the metal centers and thus oxidation or reduction reactions during calcination[44]. In addition, incomplete condensation of the species inside the pore walls might be responsible[45]. From the catalytic point of view, materials are of minor interest as long as the pores are blocked by template and the internal surface is not accessible. Therefore, syntheses that just lead to mesostructured template-oxide composites will not be mentioned in the text.

Table 1: Synthesis pathways with examples for the synthesis of pure silica mesoporous materials. [1] J.C. Vartuli et al., Chem. Mater. **6**, 2317, 1994 ; [2] J.C. Vartuli et al., in Proceedings of 209th ACS National Meeting, Division of Petroleum Chemistry, Anaheim, 21, 1995; [3] Q. Huo et al., Nature **368**, 317, 1994 ; [4] Q. Huo et al., Chem. Mater. **6**, 1176, 1994; [5] Q. Huo et al., Chem. Mater. **8**, 1147, 1996; [6] Q. Huo et al., Science **268,** 1324, 1995; [7] (a) G.S. Attard et al., Nature **378**, 366, 1995, (b) P.T. Tanev, T.J. Pinnavaia, Science **267**, 865, 1995 ; [8] P.T. Tanev et al., J. Am. Chem. Soc. **119**, 8616, 1997; [9] S.A. Bagsahw et al., Science **269**, 1242, 1995; [10] D. Zhao et al., Science **279**, 548, 2000 ; [11] E. Prouzet, T.J. Pinnavaia, Angew. Chem. Int. Ed. Engl. **9**, 500, 1997.

$I^{\ominus}\ S^{\oplus}$ ~~~~	- MCM-41, MCM-48[1], MCM-50[2] (basic conditions)
$I^{\oplus}\ S^{\ominus}$ ~~~~	
$I^{\oplus}X^{\ominus}S^{\oplus}$ ~~~~	- SBA-1[3,4,5], SBA-2[6], SBA-3[6] (APM acid prepared mesostructures) - templating from LC mesophases[7]
$I^{\ominus}X^{\oplus}S^{\ominus}$ ~~~~	
$I^0\ S^0$ ~~~~	- HMS (hexagonal mesoporous silica)[8] - MSU-V (Michigan State University)[8,9]
$I^0\ N^0$ ~~~~	- SBA-15[10] - MSU-X[9,11] - templating from LC mesophases[7]
I–S ~~~~	

3.2.1   Ionic Surfactants

The first mesoporous transition metal oxide reported was TiO_2 with hexagonal structure[46]. The mesostructure is prepared by using an anionic surfactant with phosphate head groups and titaniumalkoxy precursors, which were stabilized with bidentate ligands such as acetylacetone. After calcination the porous TiO_2 exhibits surface areas of about 200 m^2/g. By using zirconium sulfate as a precursor, Ciesla et al.[47,48] succeeded in synthesizing hexagonal mesostructured surfactant composites. In case of a post-synthesis treatment with phosphoric acid or reduction of the amount of sulfate in the composite, the material could be calcined, and zirconium oxo-phosphate and zirconium oxide-sulfate with pores in the range between micropores and mesopores were obtained. Treatment of the zirconium sulfate surfactant mesostructure with chromate solutions results in binary transition metal oxide frameworks, that are also stable upon calcination[49]. Surface areas of up to 370 m^2/g can be reached. A mesoporous aluminophosphate was prepared by dissolving a hydrated aluminophosphate in KF, followed by treatment with a solution of cetyltrimethylammonium bromide in tetramethylammonium hydroxide[50].

Recently, the synthesis of a new family of metal germanium sulfide mesostructured materials has been reported[51]. In the presence of quaternary alkylammonium surfactants, $[Ge_4S_{10}]^{4-}$ anions in formamide solution self-organize with metal cations (Co^{2+}, Ni^{2+}, Cu^+ and Zn^{2+}) to build well ordered hexagonal metal germanium sulfide mesostructures. 40 % of the surfactant could be removed with acetone as a solvent.

McGrath et al.[52] developed a new phase using cetylpyridinium chloride as a surfactant. This phase is similar to an aerogel or xerogel, but exhibits two interpenetrating networks containing water. The pore size can be varied by adjusting the concentration of surfactant, and the porous material is obtained by removing the water at low temperature. Interestingly, this approach allows to produce mesoporous materials in monolithic form.

3.2.2   Nonionic Surfactants

If amine surfactants[53] or polyethylene oxide surfactants[54] are used instead of ionic ones, hydrogen bonding is the driving force for the formation of mesophases. Therefore, the surfactant can be recovered by extraction, which is advantageous both from an economical and an ecological point of view. Using amines as templates, Tanev and Pinnavaia[53] prepared so-called HMS (*hexagonal mesoporous silica*) materials, that are, compared to MCM-41, of minor long range hexagonal order, but exhibit thicker walls[55]. Lamellar silicas can be synthesized with $H_2N(CH_2)_nNH_2$ as a template[56,57]. These materials are denoted as MSU-V (*Michigan State University*) and exhibit high surface areas after calcination. Polyethylene oxide monoethers as well as Pluronic- and Tergitol-type surfactants were used to form materials showing worm-like disordered mesopores with pore sizes ranging from 2.0 nm to 5.8 nm[58]. These materials are called MSU-X. The same approach can lead to mesoporous alumina[59]. Thermally stable, ordered, mesoporous $SiAlO_{3.5}$, $SiTiO_4$, Al_2O_3, Al_2TiO_5 TiO_2, ZrO_2, $ZrTiO_4$, ZrW_2O_8, HfO_2, Nb_2O_5, Ta_2O_5, WO_3, SnO_2, with pore sizes up to 14 nm were synthesized with amphiphilic poly(alkylene oxide) block copolymers and inorganic salt precursors in non-

aqueous solutions[60]. The materials contain nanocrystalline domains within relatively thick amorphous walls.

The accessibility of MCM-41 at non-ionic surfactant concentrations under which liquid crystals are formed, has already been mentioned. Via this pathway, known as "true liquid crystal templating" approach, highly ordered cubic and lamellar mesoporous materials could be obtained[61], as well as mesoporous palladium[62] and platinum[63,64] and mesoporous platinum films[65].

Zinc phosphate phases were synthesized with the chiral molecule d-glucosamine hydrochloride as a template[66]. In addition to a layered phase a mesoporous phase with 3.2 nm pores and crystalline and ordered walls could be obtained. A mesoporous titanium oxo-phosphate, synthesized with an industrial non-ionic polyethylenoxide template, has been reported by Thieme et al.[67]. The material shows a type IV N_2-sorption isotherm, a BET-surface area of 350 m^2/g, pore sizes of approximately 4.5 nm, and thermal stability up to 550 °C.

3.2.3   Ligand Assisted Assembly

In the ligand assisted assembly approach, covalent bonds are formed between the inorganic precursors and the organic surfactant molecule[68]. In addition to hexagonal mesostructured silicas[23], mesoporous hexagonal niobia[68] and tantalum oxide[69] could be successfully prepared via this approach. The synthesis of Nb- and Ta-TMS1 (*t*ransition metal oxide *m*esoporous molecular *s*ieve No.1) involves the hydrolysis of long-chain amine complexes of niobium or tantalum alkoxides. The respective phase is formed by self-assembly of the metal-alkoxide-amine complexes. The template can be removed by extraction, leading to open porous structures with surface areas of up to 500 m^2/g. Further, in case of niobia, a phase with three-dimensional hexagonal symmetry (Nb-TMS2), a cubic phase (Nb-TMS3) and a layered phase (Nb-TMS4) could be obtained[70].

3.2.4   Polymer Templating

Inorganic frameworks composed of oxides of Si, Ti, Zr, Al, W, Fe, Sb, and a Zr/Y mixture were formed from metal alkoxide precursors templated around polystyrene (latex) spheres[71]. Monodispersed latex spheres were ordered into close-packed arrays by centrifugation. The interstices between latex spheres were permeated by the alkoxide, which hydrolyzed and condensed. The synthesis has also been expanded to other compositions including aluminophosphates and hybrid organosilicates, as well as silicates with bimodal distributions of meso- and macropores. Transition metal-containing polymerizable lyotropic liquid crystals were prepared from sodium p-styryloctadecanoate by ion exchange with water-soluble metal chlorides, nitrates and acetates. It was found that cadmium(II), manganese(II) and cobalt(II) p-styryloctadecanoate form an inverted hexagonal lyotropic phase at 22 °C, while the copper(II) salt forms a columnar hexagonal thermotropic phase. The monomers can be cross-linked photolytically in their respective liquid crystal phases with retention of phase architecture to yield polymer networks containing ordered micro-domains of transition metal ions[72]. Yang et al.[73] produced porous silica, niobia and titania over length scales ranging from 10 nanometers to several micrometers by combining micromolding, polystyrene sphere templating

and cooperative assembly of inorganic sol-gel species with amphiphilic triblock copolymers.

3.3   Morphology Control

In order to obtain efficient solid-phase catalysts, control on the macroscopic length scale is crucial with respect to the size of the particles, textural and structural porosity and mechanical strength. Typically, the conventional Si-MCM-41 synthesis leads to a material consisting of loose agglomerates of very small particles. That is actually more suitable to perform catalytic reactions, as long as the powders can be shaped into pellets, extrudates etc., since the diffusion length in the narrow channels is small. However, the formation of mesoporous materials as thin films, fibers, spheres or monoliths is also of great interest with regard to various applications. Many such approaches have been described, mostly relying on the acidic synthesis. The formation of mesoporous materials as thin films[74,75], fibers[76,77,78], tubes[79], spheres[80,81,82,83,84] or monoliths[85,86] has been reported, following various pathways, which include either self-organization, or shaping procedures, such as spray-drying[78], aerosol processing[84], fiber-pulling[77], spin- and dip[87,88]-coating etc. These methods shall, although certainly of interest, not be discussed here in detail, since well established techniques for the shaping of catalysts by conventional means are probably more straightforward and are known in the catalysis community.

3.4   Mesoporous Metallosilicates

Much effort has been focussed on the introduction of heteroatoms, particularly aluminum, in the siliceous framework to modify the composition of the inorganic walls[31,42,89,90]. This seems especially important with respect to catalytic applications, since substitution of silicon allows fine-tuning of the acidity or creation of redox properties, similar as observed in amorphous alumosilicates or zeolites.

Aluminum incorporation seems to be of special interest if, as in zeolites, this results in the formation of ion exchange sites and Brønsted acidity. MCM-41 containing trivalent elements (prepared by impregnation, ion exchange or substitution), have been reported to have interesting catalytic activities (see references listed in 4.1.1). These metallosilicates are usually synthesized by

B[91], Fe[92], Ga[93], Ti[155,156] etc. in the silica framework. Generally, incorporation of aluminum in the framework of MCM-41 increases the acid site concentration, ion exchange capacity, and also the hydrothermal stability of the material[94,95]. It is known that the substitution of tetrahedral aluminum in a silica framework requires the introduction of extra-framework charge compensating cations. Such cations are usually principal interaction sites for guest molecules that adsorb and react in the channels.

Structurally these acidic aluminum containing mesoporous materials are intermediates between amorphous silica-alumina and zeolites. Similar to zeolites, they have a long range order with the well defined pores and like amorphous silica-alumina they do not have short range order. Since the local environment around the acid sites corresponds to amorphous materials, they exhibit a weaker acidity than zeolites, and correspond to silica-alumina in number of acid sites and acid

strength distribution. They contain larger pores than zeolites and, thus, are more suitable for catalytic reactions involving substrates which are too big to enter the pores of zeolites, like cracking or hydrocracking of bulky hydrocarbons, for example[96,97,98].

For acid-base catalysis, the surface properties of materials are of crucial importance, since the strength of acid sites depends on the local environment of the aluminum atoms. The aluminum framework is in tetrahedral coordination and creates one excess charge. This charge is compensated by cations. If these cations are replaced with protons by ion exchange with NH_4^+ followed by calcination, Brønsted acidity is induced[99]. Typical aluminum containing as-made MCM-41 samples show both tetrahedrally and octahedrally coordinated aluminum[100], but a variation in the aluminum source enables the formation of exclusively tetrahedrally coordinated aluminum[101,102]. Different authors have found different aluminum sources most suitable to obtain aluminum in tetrahedral positions, therefore, the synthesis procedure is relevant as well. Controlling the ordering and local aluminum structure remains a challenge, but by now aluminosilicate MCM-41 mesophase solids with a high degree of order and silicon to aluminum molar ratios approaching unity seem to be available[103]. For example, Si:Al ratios as low as 1:1 have been obtained by using aluminosilicate oligomers of the type $Al_xSi_{8-x}(OH)_xO_{20-x}^{8-}$ ($0 \leq x \leq 4$)[104]. The common technique used to distinguish framework and extra-framework aluminum is ^{27}Al MAS NMR[97,102], but the results are sometimes ambiguous and a combination of several techniques is therefore necessary to fully analyze the acidity of such samples[105].

In order to modify the catalytic activity of the MCM-41 materials, especially to create redox properties, several other metal ions were incorporated (Ti, Zr, V, Cr, Mn, Fe, Co, Cu, Ge, La and Ce[106]) into the silica framework. Similar to zeolites, the incorporation of transition metals ions could isolate these active centers and thus make them highly efficient. The catalytic behavior is strongly influenced by the nature, the local environment and the stabilization of the metal introduced, and by the hydrophobic properties of the surface. Especially Ti-MCM-41 – analogous to TS-1 or Ti-β - has been shown to be a promising catalyst for selective oxidation of organic molecules using peroxides (see 4.1.2). Incorporation of Ti in MCM-41 is generally achieved via a direct synthesis procedure which involves addition of a titanium source, such as titanium isopropoxide in ethanol, to the gel for hydrothermal synthesis[107,156]. Post-synthesis addition of Ti is also possible[108]. Traditional methods such as ion exchange and incipient wetness impregnation have their limitations, and new efficient methods are required. More suitable seem to be grafting techniques, for instance using metallocene complexes.

4.   Catalytic Properties

Mesoporous aluminosilicate materials are of great interest in catalysis. They show high surface areas (> 1000 m^2/g), often high thermal stability (1273 K) and they have ion exchange properties. Transition metal ion modified materials are redox active and could be used for different classes of catalytic reactions. The non-siliceous ordered mesoporous solids could be used as catalysts in various reactions as such, or could be interesting supports, such as the titanias and the zirconias. The open mesoporous structure facilitates mass transfer of reactants to catalytic sites,

with the pore diameters allowing the diffusion of even bulky molecules. Finally, the meso-structured pore system enables the fixation of space-active complexes. Furthermore, in support applications for metal particles or metal oxides, the exceedingly high surface areas, especially for non-siliceous materials, can be advantageous compared to conventional supports, as well as the pore system, which prevents aggregation of the active species.

Several ways to use MCM-41 materials for catalytic applications have been developed. MCM-41 can be used as support for metal particles or metal oxides, the supported species being located inside the pores, as represented in Fig. 4, or on the surface. Modifications can be performed by the isomorphous substitution of Si atoms in the framework as described above, resulting in acidic or redox-active catalysts. Organic molecules or organometallic complexes can be anchored directly in the pores via Si-O- bonds, possibly involving organic spacers, creating specific catalytic functions. The flexibility can be increased by wall functionalization with organic molecules which changes the hydrophobicity, especially if they are introduced as an integral part of the inorganic framework[109], the polarity or the acidity of the materials. The presence of anchored transition metal complexes has led to interesting results in many catalytic reactions (see 4.2.2).
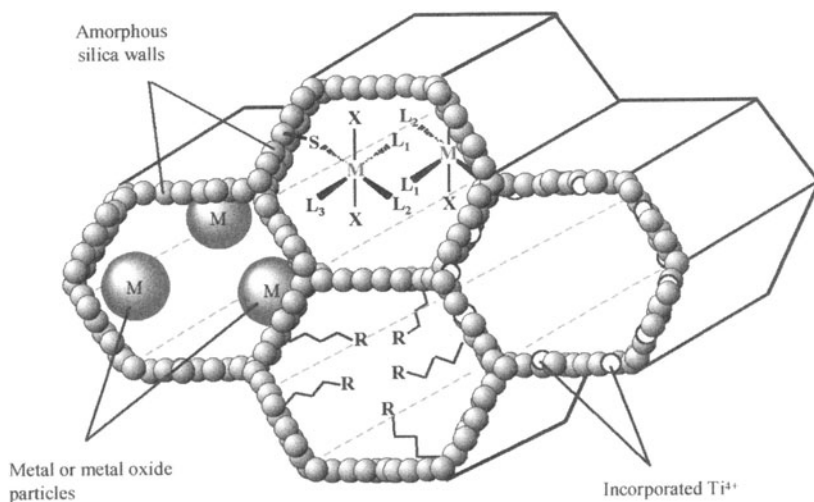
Fig. 4: Schematic representation of different possibilities for the use of the mesoporous structure. Left: supported metal or metal oxide particles, located on the surface or within the pores. Right: metal cations (ex: Ti 4+ in white) incorporated by isomorphous substitution. Top: organometallic complexes grafted onto the surface and inside the pores via organic spacer (S) (6-, 5- or 4-coordinated complexes, metallocenes or metal salts). Bottom: surface modified by organic molecules with functionality (R = CH3, Ph, OAc, Cl, SH, NH2)

In the following sections 4.1 and 4.2 we will distinguish between the so-called direct catalytic applications, namely the catalytic possibilities offered by mesoporous silica and metallosilicates themselves, and their applications as support, in a second part (4.2).

4.1   Direct Catalytic Applications

The direct catalytic applications mainly comprise acid-base catalyzed reactions, redox catalysis, and polymerisation catalysis, although some overlap, especially between the first two and the latter exist. In addition, for some acid or base catalyzed reactions and also for polymerisation reactions supported systems have been used.

4.1.1   Acid-Base Catalysis

As described previously, acid sites in mesoporous materials can be generated either by silicon substitution with trivalent cations such as aluminum, or by adding an acidic component such as a heteropolyacid or an acidic zeolite.

Initially, the use of mesoporous materials in FCC catalysis was envisaged, but their limited hydrothermal stability and the relatively low acid site strength limits their suitability in this field. However, other reactions that require milder acidity and involve bulky reactants and products, such as mild hydrocracking reactions, seem more promising. In this way, substantial efforts have focused on the potential activity of Al-MCM-41 in processing bulky hydrocarbon molecules. Applications studied comprise fuel refining, isomerisation and oligomerisation of hydrocarbons and olefins, hydrodesulfurization and hydrodenitrogenation reactions (HDS and HDN), where especially transition metals supported on mesoporous materials have been used.

In addition to these bulk processes several reactions directed to the production of fine chemicals have been studied. In particular, the preparation of acetals, used in the fragrance industry, demonstrates, that MCM-41 type materials can advantageously be used in such applications.

4.1.1.1 Surface Properties

Adsorption of bases such as ammonium[15,97] and pyridine[97] on Al-MCM-41 allows to determine the strength of acid sites via temperature programmed desorption (TPD) and FTIR[110,111]. One can distinguish with these methods between Lewis and Brønsted acidity and recognize weak and strong acid sites, depending on the Si:Al ratio and the nature of the trivalent element (Al, Fe, Ga). Also, weak silanol Brønsted acidity is detected. Yiu et al.[112] evaluated the Lewis and Brønsted acidities of Al^{3+}, Fe^{3+}, Ga^{3+} and H^+ containing mesoporous silica, by comparing the respective activities in the Lewis-catalyzed alkylation of toluene with benzylchloride and the Brønsted-catalyzed alkylation of toluene with benzyl alcohol, as test reactions.

In general, the strength of acid sites was found to be similar to that of amorphous aluminosilicates. Also ^{29}Si-NMR results indicate the amorphous nature of the pore walls. The T-O-T bond angles are widely distributed. Since the O-Al-O angle is less flexible than the O-Si-O angle, Al-MCM-41 materials are commonly less well ordered and show a broader pore size distribution than their pure silica analogues[31].

The nature and concentration of the acid sites of MCM-41 materials as a function of Si/Al ratio have been investigated by FTIR spectroscopy using pyridine as a probe molecule[113]. The tetrahedral to octahedral aluminum ratio is found to increase with higher aluminum incorporation. The sample with the lowest Si/Al ra-

tio is found to exhibit higher acidity compared to the other samples. Al-MCM-41 has been synthesized using colloidal silica (Ludox AS) and either Al(OH)$_3$, or Al(iPrO)$_3$, or NaAlO$_2$ as a aluminum source[114]. Samples prepared with Al(OH)$_3$ contain a wide distribution of acid site strengths, indicating the absence of pre-ferred locations of Si-O-Al groups within the pore walls. In contrast, distinct populations of acid sites appear in materials prepared with Al(iPrO)$_3$ or with NaAlO$_2$. For aluminosilicate MCM-41 mesophases prepared at room temperature, 2D heteronuclear chemical shift correlation NMR spectra show that tetrahedrally coordinated aluminum and silicon intra-framework species are in close spatial proximity to the trimethylammonium head groups of the cationic surfactants in the as-synthesized materials and to ammonium cations following calcination and ion exchange[115]. For MCM-41 materials synthesized under hydrothermal conditions, the same technique shows that the appearance of six-coordinate aluminum species results from strongly bound water molecules coordinated to aluminum atoms that are also in the vicinity of the surfactant species. Furthermore, the detection of couplings between ^{27}Al or ^{29}Si species and protons associated with the structure-directing surfactant molecules or exchangeable ammonium counterions establishes that a significant fraction of the aluminum atoms are present in the inorganic frameworks of these materials[116].

The investigation of the adsorption of polar and nonpolar molecules on a sur-face is a suitable tool for measuring its hydrophilic or hydrophobic character. The adsorption studies of cyclohexane[15], benzene[32] and water[117] on MCM-41 revealed that the surface is relatively hydrophobic. The silanol density corresponds only to about half of that usually found in conventional silica. Even Al-MCM-41 is quite hydrophobic[118]. Information about surface OH-sites is important for surface modifications such as silylations[32]. Single, (SiO)$_3$Si-OH, hydrogen-bonded, (SiO)$_3$Si-OH-OH-Si(SiO)$_3$, and geminal, (SiO)$_2$Si(OH)$_2$, silanol groups could be distinguished by spectroscopic examinations[119] (^{29}Si CP/MAS/NMR, FTIR) and a fourth silanol group was reported as well[116]. However, only single and geminal si-lanols are accessible to the silylating agent, trimethylchlorosilane (TMCl)[115]. Sev-eral NMR, FTIR and TG/DTA experiments carried out on MCM-41 and MCM-48 showed that in both mesoporous materials 26-30 % of the Si atoms carry OH-groups. MCM-48 contains more associated terminal OH-groups than MCM-41. Exchange experiments with D$_2$ and NH$_3$ adsorption studies show that these silanol groups are freely accessible and not acidic[120].

To evaluate the catalytic activity, test reactions can be carried out. For instance, in microactivity tests with hexadecane as a model feed, Al-MCM-41 produced a higher amount of gaseous products as well as more olefins and a lower amount of branched hydrocarbons[121] than commercial FCC catalysts. Another test reaction is the conversion of 1,3,5-triisopropylbenzene. Platinum loaded MCM-41 alumi-nosilicate proved here to be highly active in the conversion of 1,3,5-triisopropyl-benzene to mainly mono- and di-substituted isopropylbenzene[122]. Cumene cracking is also one possible catalytic test reaction. For example, FSM-16 was impregnated with an alcohol solution of aluminum isopropoxide. The resulting mesoporous silica-alumina catalysts exhibited activities for cumene cracking, though the activities are lower than that of an amorphous silica-alumina catalyst[123].

Summarizing, virtually all reports on the acidity of MCM-41 type materials agree, that the acidity resembles much more that of amorphous aluminosilicates than that of zeolites.

4.1.1.2 Refinery Catalysis

Mesoporous materials have been extensively investigated with regard to their use in cracking and hydrocracking reactions. The patent literature contains many examples, but cannot be reviewed in detail here. Unfortunately, the disadvantages of low acid strength and low hydrothermal stability of MCM-41 catalysts are a counterbalance to the advantage of the accessibility of the pores even for large molecules. For small molecules, such as n-heptane, the cracking activity of MCM-41 is much lower than that of ultra-stabilized Y zeolite and comparable with that of amorphous aluminosilicate[98]. For crude oil cracking, the difference in activity decreases. Steam treatment, used as a way to simulate fluidized catalytic cracking, results in a collapse of the mesopore structure and a decrease in activity far below that of steam-treated aluminosilicate. Nevertheless, fuel was successfully processed over a hydrocracking catalyst composed of Ni and W or Pt loaded MCM-41, compounds for the hydrogenation reaction and the cracking reaction, respectively[124]. For the conversion of low-density polyethylene to hydrocarbon feedstock, MCM-41 was found to be more active than amorphous aluminosilicate, but due to its greater acidity, the activity of ZSM-5 was even higher. Moreover, the products obtained from reactions over MCM-41 contained more liquid hydrocarbons in the gasoline and middle distillates range with a decrease in aromatic content[125,126].

There are scattered reports[127] on comparable cracking activities of Al-MCM-41 and zeolite Y using long-chain hydrocarbons and increased cracking activities of MCM-41, when using bulky hydrocarbon molecules. Aluminum chlorohydrate which contains Al polycations, such as the Al_{13}^{7+} Keggin ion, has been used as a source of Al for post-synthesis alumination of MCM-41[128]. As confirmed by ^{27}Al MAS NMR, a large proportion of the Al is substituted into tetrahedral positions within the framework, whereas no separate surface alumina phases could be detected with TEM and XPS. These materials exhibit considerable catalytic activity for cumene cracking and their activity is superior to that of a $AlCl_3$-grafted MCM-41 or aluminum chlorohydrate-grafted amorphous silica.

Mesoporous materials with pores too large to expect any shape selectivity have been used in the skeletal isomerisation of 1-butene[129]. The conversion of 1-butene increases with higher aluminum content in mesoporous materials, while the selectivity for isobutene decreases. Ammonia TPD, IR measurement of 1-butene adsorption, and TG analysis were performed to confirm that the high concentration of activated 1-butene molecules on the mesoporous material with high aluminum content accelerates the multimolecular oligomerisation and, thus, reduces the selectivity.

The oligomerisation of butene at 423 K and 1.5-2 MPa has been investigated over zeolites, amorphous silica-alumina and ordered mesoporous alumosilicate with uniform 3 nm pores. The mesoporous catalyst exhibited high selectivity and good stability with time for the production of branched dimers while olefin oligomerisation into strongly adsorbed residue and fast deactivation prevailed on microporous catalysts and amorphous silica-alumina[130]. Phosphated mesoporous zirconium oxide (Zr-TMS) was used as a mild acidic catalyst. It has been found to be active for the gas-phase double-bond isomerisation of 1-butene at temperatures of $100 - 350°C$[131]. Recently, Pater et al.[132] showed in a comparative study, that MCM-41 is a suitable catalyst to perform selective hex-1-ene dimerization in octane. Owing to the mesopores, the dimerization cracking reactions, which produce isohexene and cracked products, are avoided.

As the catalytic hydrotreating of petroleum fractions is of crucial importance due to increasingly strict environmental legislation, numerous materials were developed aiming to applications in hydrodesulfurization reactions and hydrodenitrogenation. Al-MCM-41 was co-impregnated with $Co(NO_3)_2 \cdot 6H_2O$ and $(NH_4)_6Mo_7O_{24}$ followed by calcination and sulfidation[133,134]. At 350-375 °C under 6.9 MPa H_2 pressure, sulfided Co-Mo/MCM-41 catalysts show higher hydrogenation and hydrocracking activities in hydrodesulfurization of a model fuel containing 3.5 wt% sulfur as dibenzothiophene in n-tridecane, whereas Co-Mo/Al_2O_3 catalysts show higher selectivity to desulfurization. Co-Mo/MCM-41 catalyst with a high metal loading level is substantially more active than the Co-Mo/Al_2O_3 catalysts. It was, however, not as good as commercial Co-Mo/Al_2O_3 for the desulfurization of petroleum residues with large-sized molecules, such as asphaltene. A similar catalyst system with Co replaced by Ni was used for gasoil hydrocracking, and showed higher hydrodesulfurization and hydrodenitrogenation activity than the oxides supported on USY and amorphous aluminosilicate[98]. Increase of HDS activity after introduction of Ni has also been observed for HMS materials, which are active for acid-catalyzed reactions, such as cumene cracking and isopropanol dehydration in unmodified form[135].

Acidity in mesoporous compounds can also be generated by addition of heteropolyacids or acid zeolites to mesoporous materials. However, since in this approach the mesoporous oxide is rather used as a support, we will cover this topic in a later section.

4.1.1.3 Catalysis for fine Chemicals Production

Acetal compounds find important uses for pharmaceuticals and fragrances and can be obtained via acetalization of carbonyl functions. For the acetalization of aldehydes, zeolites were found to be more active than MCM-41, as long as small molecules were processed. For larger reactants, the restriction of pore size became decisive, and MCM-41 appeared to be interesting despite its low acid strength[136].

A good example of this type of reactions is the synthesis of alpha-n-amylcinnamaldehyde (jasminaldehyde) (**4**). The product has been prepared with high selectivity via a process involving the acetalization of heptanal (**1**) with methanol, followed, in the same pot, by a slow hydrolysis of dimethylacetal (**2**) and then the aldolic condensation of the two aldehydes (Figure 5)[137]. In this interesting work, the authors made a comparison of several catalysts including a large pore zeolite (Beta) and mesoporous silica-alumina with various Si/Al ratios. They investigated the influence of the catalysts structure on its performance, concluding that the suitable catalysts have to present mild acidity with large regular pores in a narrow range of pore diameter, which enables fast diffusion of the jasminaldehyde. This reduces the probability for undesired consecutive reactions (oxidation of (**4**) followed by decarboxylation or intramolecular acid-catalyzed cyclization of the hemiacetal function of (**4**)). It was also shown that, in the case of MCM-41, the deacetalyzation process (slow hydrolysis + condensation) of the heptanal dimethylacetal (**2**) proceeds slowly, maintaining a low concentration of heptanal on the catalysts surface, helping to inhibit the formation of the secondary product (**5**).
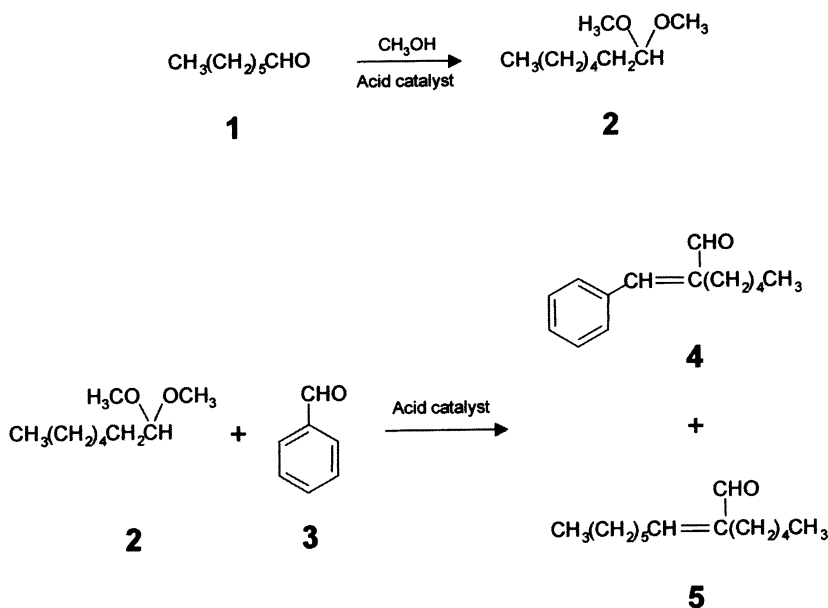
Fig. 5. Jasminaldehyde (**4**) one pot synthesis via heptanal (**1**) acetalization, proceeded with Al-MCM-41 as acid catalyst (M.J. Climent, A. Corma, R. Guil-López, S. Iborra and J. Primo, J. Catal. **175**, 70, 1998)

With high global reaction rates it is possible to have a low concentration of heptanal at the surface, decreasing the self-condensation of heptanal (**1**), and, thus, achieving a high selectivity for jasminaldehyde. The influence of the concentration of acid sites on H-MCM-41 has also been investigated, indicating that the activity is directly proportional to the amount of acid sites and the activity per site is the same for different amounts of Al. Increasing the Si/Al ratio leads to an increase of the selectivity towards the jasminaldehyde. This fact is due to a higher hydrophobicity of MCM-41, that will favor the elimination of methanol which occures during the conversion of an unstable intermediate product (giving (**4**)). Conversions beyond 90% were achieved with selectivity being higher at 373K than at higher temperatures. One can assume that the different results obtained with zeolite β are mostly caused by the faster diffusion of heptanal with respect to benzaldehyde.

There are many other examples for specific conversions over ordered mesoporous oxides. Much work focused on applying mesoporous catalysts to various well-known alkylation reactions. For example, Friedel-Crafts alkylation of 2,4-di-tert-butyl-phenol with 3-phenylpropenol (cinnamyl alcohol) was carried out over MCM-41[138]. Al-MCM-41 proved to be superior to the commercial aluminosilicate catalysts, when bulky alcohols including cholesterol, adamantan-1-ol, 2-naphthol and dihydropyran were converted to the corresponding tetrahydropyranyl ethers with remarkable catalytic activity and selectivity[139]. The synthesis of alkylgluco-sides from glucose and n-butanol has been carried out on Al-MCM-41 mesopor-

ous materials[140]. It has been found that a higher concentration of acid sites does not guarantee a better catalytic performance. The adsorption-desorption properties of the material play a determinant role in this reaction. Therefore, the larger the diameter of the pore at the same level of Al contents, the more active is the final catalyst.

Moreover, amorphous mesoporous silica-aluminas (MSA) and MCM-41 show alkylation activities comparable with zeolite β in the liquid-phase alkylation of toluene with propylene, while their isomerisation and transalkylation activities are lower than those of zeolite β and $AlCl_3$-HCl, but similar to that of supported phosphoric acid[141]. Alkylation is a stage in the production of sulfonated linear alkylbenzenes, which are an important class of detergents. Nowadays, either aluminum chloride or hydrogen fluoride are used as catalysts for this reaction. However, the use of these catalysts presents serious problems in terms of both environmental impact and lack of selectivity towards the desired product. Aluminum chloride on MCM-41 proved to be a catalyst that can be easily separated from the products and is environmentally friendly. In addition, it exhibits significant improvements in selectivity towards both the monoalkylated product and the preferred 2-phenyl isomer[142].

MCM-41 and Al-MCM-41 were tested in various other alkylation reactions. They have, for example, catalytic activity for the alkylation of benzene with isopropanol, cumene being the major product[143], and for the isopropylation of toluene[144]. Separate studies showed that Al-MCM-48 exhibited higher activity for the isopropylation of naphthalene and for the isopropylation of pyrene than Al-MCM-41. This is attributed to its larger pore size and the three-dimensional pore system, which is more advantageous for molecular diffusion than the relatively narrow and one-dimensional pore system of Al-MCM-41[145]. Compared with the yields of 2,6-diisopropylnaphthalene on large-pore zeolites, those on Al-MCM-41 and Al-MCM-48 are not high. However, isopropylation of pyrene occurs inside the mesopores of Al-MCM-41 and Al-MCM-48, while pyrene derivatives cannot be produced inside the micropores of zeolite Y. Therefore, a much higher activity is achieved for the mesoporous materials, but coke formation and adsorption of both the reactant and the product caused catalyst deactivation. The product distributions indicate that shape selectivity occurs inside the regular mesopores of the materials. In general, for processing bulky molecules mesoporous materials are advantageous. Since such molecules are difficult to evaporate, reactions can be carried out in the liquid phase, such as tert-butylation of anthracene, naphthalene and thianthrene with tert-butyl alcohol in isooctane or carbon tetrachloride[146].

β-Naphthyl methyl ether was synthesized from b-naphthol and methanol at 200°C and 3.5 · 10^6 Pa over Al-MCM-41 and sulfated Al-MCM-41 in a batch autoclave reactor[147]. The sulfated Al-MCM-41 catalyst formed exclusively β-naphthyl methyl ether and had much higher yields than sulfuric acid, amorphous silica-alumina, γ-alumina and H-ZSM-5, which was attributed to the extra-framework aluminum within the intra-channel space.

Recently, Lindlar et al.[148] tested the activity of Al-MCM-41 in Friedel-Craft acylation of 2-methoxynaphtalene. They found that pH adjustment of the synthesis gel during formation of MCM-41 leads to increased activity, mostly due to a better accessibility of the active sites.

Base catalysis is not as well investigated as acid catalysis over mesoporous materials, but they can be adapted for several applications in specific reactions. For instance, Al-MCM-41 cation exchanged with sodium and cesium have been

used for the base-catalyzed Knoevenagel condensation[149]. In the presence of Na-MCM-41, the reaction of benzaldehyde and ethyl cyanoacetate carried out in aqueous solution, led to a selectivity of almost 100 % and conversion of 90 %. Both H-MCM-41 and Na-MCM-41 further catalyze the condensation of benzaldehyde with acetophenone yielding chalcone. Al-FSM-16 was used in the synthesis of meso-tetraarylporphyrins from the corresponding aromatic aldehydes and pyrrole. Except for o-methylbenzaldehyde this catalyst was preferable compared to the liquid acid $BF_3 OEt_2$, and it could also be regenerated by calcination[150].

One last example detailing the increased conversion over MCM-41 in comparison to zeolite β, is the conversion of linalool into cyclic furan and pyran hydroxyl ethers[151]. The reaction is carried out over framework substituted Ti-catalysts. It consists of an epoxidation reaction, catalyzed over the titanium sites, and an acid catalyzed nucleophilic substitution reaction, proceeding via ring opening of the epoxide going along with ring closure for furan or pyran formation.

4.1.2   Redox Catalysis

As previously detailed, metal containing MCM-41 analogues are expected to be promising oxidation catalysts, particularly those based on early transition metals (Ti, Zr, V, Cr, Mo, W, Mn).

Previously, isolated titanium ions have been incorporated into microporous silica materials. The best known is TS-1 with a MFI zeolite topology in which silicon is substituted by Ti cations. TS-1 and several other titanium-containing zeolites have shown good performances in selective partial oxidation reactions of various organic compounds with hydrogen peroxides or organic hydroperoxides as oxidants. Catalytic oxidation was carried out successfully on alkanes, alkenes, alcohol and arylamines[152,153,154].

However, the catalytic activity of these microporous materials are limited to reactants and products that can diffuse in their relatively narrow pores. Ti-MCM-41 present the clear advantage of a large pore system enabling the oxidation of much larger hydrocarbon chains, cycloalkanes and branched alkanes. To date, only Ti-Beta, a large pore zeolite, allowed bulky alkyl peroxides, such as TBHP, to be used as oxidants. Ti-MCM-41 widened the range of catalysts available for such reactions. When alkylhydroperoxides are used as oxidants, a better hydrophobic interaction with the substrates, competing with water, is expected. Moreover, in Ti-MCM-41, the alkylhydroperoxide can easily penetrate the mesopore system, avoiding diffusion limitations or steric hindrance.

The further examples will show that MCM-41 materials with incorporated transition metal centers can be very effective catalysts, depending on the role played by their pore diameter, the organization of the channel system, the nature of the oxidant, the nature of the metal and the hydrophobic/hydrophilic properties.

The first publications on titanium modified mesoporous silicas appeared in 1994. Tanev et al. investigated the selective oxidation of 2,6-di-tert-butylphenol (2,6-DTBP) with H_2O_2 to the corresponding quinone[155]. They compared the activity over Ti-MCM-41, synthesized with ionic surfactants under hydrothermal conditions, with that over Ti-HMS, synthesized with neutral primary amine surfactants at room temperature. The latter was more active, probably due to a higher textural mesoporosity along with less diffusional limitations. Corma et al.[156] compared Ti-Beta, Ti-ZSM-5, and Ti-containing MCM-41, which showed good activities in the catalytic partial oxidation of hex-1-ene with H_2O_2. Ti-MCM-41 also

showed a high catalytic activity in the epoxidation of norbornene using tert-butyl hydroperoxide (TBHP) as an oxidant. The incorporation of Ti-MCM-41 into a partially polymerized polymethylsiloxane matrix led to an even higher catalytic activity in the epoxidation of cis-cyclooctene with TBHP than that observed over the free catalyst[157]. Zr-MS[158], synthesized with hexadecylamine and zirconium iso-propoxide at room temperature, showed a similar activity for this reaction, but had a higher selectivity for alcohol in the epoxidation of norbornylene. Framework Ti-substituted and Ti-grafted MCM-41 prepared by direct hydrothermal synthesis and a post-synthesis grafting method have been tested as catalysts for cyclohexene oxidation with aqueous H_2O_2 and tert-butylhydroperoxide[159]. With aqueous H_2O_2 in methanol, the major products were cyclohexene diol and its methyl ethers, but no cyclohexene oxide was produced. Titanium leaching was a serious problem. In contrast, with tert-butylhydroperoxide the selectivity for cyclohexene oxide was nearly 100 % and titanium leaching was negligible. However, the reaction rate was lower than with H_2O_2. The Ti-grafted MCM-41 was shown to be somewhat more active than the Ti-substituted material. Substituted mesoporous molecular sieves were also prepared post-synthetically by applying Ti-butoxide in ethanol solutions of different concentrations to MCM-41, MCM-48 and KIT-1[160]. The resultant catalysts were active for the selective oxidation of 2,6-di-tert-butylphenol with H_2O_2. Ti-Beta and Ti-MCM-41 catalysts are able to epoxidize methyl oleate using hydrogen peroxide or tert-butyl hydroperoxide as oxygen donors with high conversions and epoxide selectivities[161].

Ti containing zeolites as well as Ti-MCM-41 catalytic systems present tunable hydrophobic/hydrophilic properties, which are, indeed, as important as the number of active sites. Several studies have shown that a control of the hydrophobicity of the surface is necessary to optimize the adsorption of reactants and products [161,162]. This is particularly true in the case of olefin epoxidation, where the epoxide has a higher polarity than the olefin reactant. As pointed out by Corma et al.[163], the presence of silanol and Ti-OH groups allows the favored adsorption of the epoxide on the hydroxylated surface. This leads to ring opening of the epoxide and formation of diols. Diols are known to strongly adsorb on the titanium sites and, thus, deactivate the catalyst. As a solution, one can increase the catalysts surface hydrophobicity to diminish the catalysts poisoning by reducing the formation of the diols. The increase of hydrophobicity could also, depending on the system, improve the access of the olefin to the active sites or reduce the inhibitory effect of water.

Such routes were shown to be successful for the epoxidation of cyclohexene with TBHP, with improved catalytic activity[163]. Ti-MCM-41 materials were created in a more hydrophobic form by methylating silicon centers. They are highly stable and present high activity and selectivity for the epoxidation of olefins using organic peroxides[164]. Despite the fact that Ti-MCM-41 was found to be almost inactive in the epoxidation of propylene with aqueous hydrogen peroxide[165], Ti-MCM-41 and Ti-MCM-48, have been successfully modified by trimethylsilylation to exhibit enhanced catalytic activity in the oxidation of alkenes and alkanes with H_2O_2[166]. An effective method for trimethylsylilation of micro- and mesoporous titanosilicates using [N,O-bis(trimethylsilyl)trifluoroacetamide], renders Ti-MCM-41 and SiO_2/TiO_2 aerogels active for olefin epoxidation with aqueous H_2O_2[167].

Recently, Bhaumik et al.[168] synthesized organically modified Ti-rich Ti-MCM-41 with Si:Ti molar ratios from 33.6 to 53 to produce efficient catalysts in epoxidation and oxidative cyclization using TBHP. Methyl-, vinyl-, allyl-, chloropropyl-, pentyl-, and phenyl- modified materials were obtained. The authors showed

that the efficiency of Ti incorporation is higher when organosilane is used as Si source in conjunction with TEOS. The highest Ti incorporation was achieved when 3-chloropropyl-modification was used, with larger pores and high surface area (1218 m^2/g). The more hydrophobic materials exhibited high activity in catalytic epoxidation of unsaturated alcohols followed by cyclization to cyclic ethers. The oxidation activity increased extremely when TBHP was used instead of aqueous H$_2$O$_2$. A recent study showed that modifications of Ti-MCM-41 by 3-chloropropyl-groups and methyl-groups generated efficient catalysts for epoxidation of cyclododecene. The modifications were performed simultaneously on the same Si atom to achieve materials with higher surface hydrophobicity and very high surface area (>1400 m^2/g. Due to the problems with surface area analysis, this value should be considered with care)[169].

In an attempt to modify catalytic performance, the simultaneous incorporation of trivalent metal cations with Ti^{4+} led to bifunctional catalysts. This method enables fine tuning the acidity and the nature of the active sites. Bifunctional Ti-mesoporous molecular sieves containing different trivalent ions, e.g. B^{3+}, Al^{3+} or Fe^{3+}, were tested and were found to be active in epoxidation of bulky olefins such as alpha-pinene and highly selective in diol formation[170].

By changing the nature of the incorporated metal, several other redox catalysts were achieved. These systems, however, appear to be less studied and have inferior catalytic performance. Gontier and Tuel were able to overcome diffusion limitations, that occur when using conventional catalysts like TS-1 or ZSM-48, by characterizing the activity of titanium and vanadium substituted MCM-41 in the liquid-phase oxidation of aniline[171]. V-HMS was shown to be active in selectively converting aniline to nitrobenzene in presence of TBHP only. V-MCM-41 was also investigated for the partial oxidation of cyclododecane and 1-naphthol with H$_2$O$_2$ as an oxidant and proved to be highly active and selective[172].

Ti, V, Cr, Mn, Fe and Co containing MCM-41 were active as catalysts for the liquid phase oxidation of cyclohexane with aqueous H$_2$O$_2$ or tert-butyl hydroperoxide[173]. Ti-, V-, Cr-, Mo- and Mn-substituted MCM-41 and HMS materials were prepared via an electrostatic and neutral templating pathway, respectively, and were found to be active in the peroxide hydroxylation of benzene[174]. For the selective peroxide oxidation of styrene and methyl methacrylate to benzaldehyde and methyl pyruvate, Ti-, V- and Cr substituted MCM-48 were successfully used[175]. Mo-incorporated MCM-41 materials, prepared by direct hydrothermal synthesis, were found to be stable and active for cyclohexanol and cyclohexane oxidation reactions with H$_2$O$_2$ as oxidant[176]. Cho et al. [177] provided recently a study on several Mo containing MCM-41 catalysts with various Si:Mo ratios. They characterized the catalysts containing Mo incorporated in the silica framework by standard techniques (XRD, N$_2$-sorption, ESR, FTIR and UV-vis analyses). The catalytic performance was investigated in the propylene oxidation for producing acrolein (at conversions of propylene 0.9%-4.2%). Mo-MCM-41 showed a higher selectivity than pure Si-MCM-41. The highest selectivity to oxygenated products was achieved with hexagonally structured materials having Si:Mo = 20 (initial ratio). The authors suggest, on the basis of ESR measurements, that Mo^{5+} species are the ones included in the hexagonal MCM-41 framework and could be the active site of these catalysts. Higashimoto et al.[178] synthesized Mo-MCM-41 using TEOS, (NH$_4$)$_6$Mo$_7$O$_{24}$.4H$_2$O and CTAB as starting materials. UV-irradiation of the Mo-MCM-41 in presence of NO led to the evolution of N$_2$, N$_2$O and NO$_2$. When the photocatalytic reaction is carried out in the presence of propane, high efficiency is

observed, leading also to the formation of propylene and oxygen containing compounds (CH_3COCH_3 and CO_2). W-MCM-41, synthesized *in situ* in acidic medium with ammonium tungstate as precursor, was found to be more active than the conventional WO_3 catalyst with respect to the hydroxylation of cyclohexene using H_2O_2 as oxidant[179]. Tungsten-containing MCM-41 showed high activity in hydrogen peroxide hydroxylation of cyclohexene in acetic acid[180]. Mn-MCM-41, prepared by the template ion exchange method, has a higher activity for the catalytic epoxidation of aromatic olefins than Mn-SiO_2 and Mn-Al_2O_3, prepared by conventional impregnation methods, or Mn-ZSM-5 prepared by an ion exchange method[181]. Even olefins with bulky substituents such as 4-tert-butylphenyl and 2-naphthyl could be processed. Cr-containing MCM-41 was prepared by introduction of chromium chloride during gel-preparation for the hydrothermal synthesis. Cr-MCM-41 was very active for benzylic oxidation of alkylarenes to the corresponding carbonyl compounds with TBHP[182]. Cr-MCM-48, prepared by similar means, was very efficient in the oxidative destruction of trichloroethylene, which is a typical chlorinated volatile organic compound (CVOC)[183].

Fu et al.[184] synthesized copper substituted mesoporous silica, denoted Cu-HMS, using dodecylamine as template. They showed that this material has relatively high activity for the hydroxylation of phenol using H_2O_2 in aqueous solution (38.7% max. phenol conversion and selectivity for dihydroxybenzene isomers reaching 95%). The liquid-phase oxygenation of benzene to phenol over Cu-MCM-41, synthesized by impregnation and by ion exchange, was studied using molecular oxygen as an oxidant and ascorbic acid as a reducing reagent for the Cu species[185]. Cu-MCM-41 catalysts were more active than the corresponding Cu catalysts supported on SiO_2, TiO_2, MgO, Na-ZSM-5, Na-Y, or K-L zeolites.

As last examples of catalyzed oxidation reactions, it has been shown, based on the photocatalytic properties of silica, that FSM-16 can catalyze metathesis reactions of propene by photoirradation and propene photooxidation with gaseous oxygen. In both cases, much higher activity than for amorphous silica was observed[186,187].

Finally, it should be mentioned that mesoporous materials have found some applications as reduction catalysts. For instance, Ti-MCM-41 and Ti-MCM-48 prepared by a hydrothermal synthesis exhibited high photocatalytic reactivity for the reduction of CO_2 with H_2O at 328 K to produce CH_4 and CH_3OH in the gas phase[188]. Pt and tungstophosphoric acid supported on MCM-41 type materials showed a pronounced increase in the activity during the catalytic reduction of NO_x with propene in the presence of water vapor[189]. Aluminum alkoxide moieties were grafted onto purely siliceous mesoporous MCM-41 via siloxide linkages, producing materials which reveal enhanced catalytic activity in the MPV reduction of cyclic ketones[190]. And, Fe^{3+} exchanged mesoporous Al-HMS and Al-MCM-41 catalyze the selective reduction of NO with NH_3[191].

4.1.3   Polymerisation Catalysis

Many reasearch groups focused on applications for the mesoporous systems in polymerisation chemistry[192,193]. Sn-HMS was shown to yield higher conversion for the lactide ring-opening polymerisation than tin-doped silica and pure tin oxide[194]. Poly(L-lactic acid) (PLA) was produced with a polydispersity near 1. Compared to homogeneous catalysts, the average molecular weight and polydispersity of the polymers was improved. Polymerisation of lactones such as delta-valerolactone

and epsilon-caprolactone with protic compounds proceeded in the presence of Al-MCM-41 to give polyesters with a narrow molecular weight distribution[195]. A sequential two-stage polymerisation of both lactones with Al-MCM-41 in butanol gave a block copolymer.

Free radical polymerisation of methyl methacrylate within the uniform channels of MCM-41 proceeds at 100°C to give a high molecular weight polymer[196]. Al-MCM-41 was found to be active in the degradation of high density polyethylene at a rate similar to that observed over H-ZSM-5 catalyst. This reaction is interesting with regard to the selective recovery of useful chemical fractions[197].

Efficient polymerisation catalysts can also be generated by supporting Ziegler catalysts or single size polymerisation catalysts on the surface of ordered mesoporous oxides. MCM-41 has, thus, been grafted with methylalumoxane, to obtain a support for Ziegler polymerisation catalysts[198,199,200]. The molecular weight and the physical properties of the polymers are influenced by the support[199,200]. Van Looveren et al.[201] also hydrolyzed trimethylaluminum in situ to anchor alumoxane on the pore walls of MCM-41 in order to avoid clustering of the alumoxane that was observed in the case of physisorption. A remarkable reaction was reported to lead to polymers with unusual properties: Crystalline polyethylene fibers with a diameter of 30 – 50 nm were formed by the polymerisation of ethylene with titanocene supported on mesoporous silica-fiber and MAO as a cocatalyst. The mesoporous silica fibers with mesopores arranged in a parallel direction to the fiber axis act as nano-extruders in this template-assisted extrusion polymerisation[202]. However, in most of the fibers the pores are not oriented parallel to the fiber axis which sheds some doubt on the proposed mechanism[203]. Chromium acetylacetonate [Cr(acac)$_3$] complexes have been grafted onto the surface of Al-MCM-41, yielding materials that were found to be active for the polymerisation of ethylene[204].

4.2   Support Applications

Ordered mesoporous oxides have been used as supports for metals, metal oxides and as a substrate for grafting catalytically active species. Such uses will be covered in this part. However, bifunctional catalysts, as used in HDS and HDN, or grafted catalysts for polymerisation have already been mentioned in the previous sections and will therefore not be discussed here.

4.2.1   Support for Metals and Metal Oxides

One of the most important properties of ordered mesoporous oxides is their exceptionally high surface area. This can be exploited to highly disperse active species on interacting and non-interacting support materials. Several pathways for depositing the active compound on the mesoporous support are available. In order to prepare supported metal and metaloxide catalysts, even simple routes such as incipient wetness impregnation can be chosen. Since for many materials the primary particle size is very low and the pores thus short, pore blockage is not an important issue up to relatively high loadings. Furthermore, the mesoporous materials have an additional advantage in that they can stabilize the metal and metaloxide particles inside the pores.

Pd-MCM-41, synthesized by the incipient wetness method with $[Pd(NH_3)_4](NO_3)_2$ as a precursor, was used for the hydrogenation of 1-hexene[205] and crotonaldehyde[206]. In case of the hydrogenation of crotonaldehyde, also ion exchange with $[Pd(NH_3)_4]Cl_2$ as a precursor and direct incorporation of Pd during the synthesis utilizing $[Pd(NH_3)_4]Cl_2$ and Pd(acac) were performed. Another approach is the introduction of palladium species, such as $[CpPd(\eta^3\text{-}C_3H_5)]$, via the vapor phase[207]. After reduction under hydrogen, this catalyst showed higher activity in a variety of Heck reactions than other heterogeneous Heck catalysts and even some homogeneous catalysts. Au nanoparticles, deposited on MCM-41 by chemical vapor deposition of dimethyl gold acetylacetonate, exhibit high catalytic activities for the oxidation of CO and of H_2, below and above 273K, respectively[208]. Metal clusters like Pd_{561} and Au_{55}, stabilized by hydrophobic ligands, have been used as precursors in the in situ synthesis of MCM-41[209]. Both surfactant and ligands can be removed by calcination, resulting in highly dispersed metal clusters on the inner and outer surface. Pt-MCM-41, synthesized via the incipient wetness technique with hexachloroplatinic acid as a precursor, showed high activity in the hydrogenation of naphthalene, however, higher turnover frequencies were obtained for Pt-USY[210]. As compared with other supports, Pt-MCM-41 was also found to provide the highest specific NO reduction rates in the selective catalytic reduction of NO by hydrocarbons in the presence of O_2[211]. $[Pt(CO)_6]_5^{2-}$ and $[Pt(CO)_6]_6^{2-}$ were synthesized in the hexagonal channels of FSM-16 and ZrO_2-modified FSM-16 by reductive carbonylation of H_2PtCl_6 with CO and H_2O[212]. The controlled removal of CO by thermal evacuation yielded highly dispersed Pt clusters[213]. Dependant on the temperature, $[Pt(CO)_6]_5^{2-}$ decomposed to Pt-15 clusters or naked Pt. Both showed marked catalytic activities for hydrogenation of ethene and 1,3-butadiene at 300 K. Whereas the latter is selectively hydrogenated to 1-butene on the partially decarbonylated Pt carbonyl clusters, it is preferentially converted to n-butane on the naked Pt particles. Via thermal decomposition of $[Ru_6C(CO)_{16}]^{2-}$ or $[H_2Ru_{10}(CO)_{25}]^{2-}$ that were incorporated into MCM-41 from solution, nanoparticles of ruthenium were obtained, showing good activity as hydrogenation catalysts for hexene and cyclooctene[214]. Al-MCM-41, ion exchanged with $Rh(NO_3)_3$, leads to a Rh(I)-Al-MCM-41 catalyst suitable for a selective catalytic reduction (SCR). It shows a high low temperature activity in converting NO to N_2 and N_2O with C_3H_6 in the presence of excess oxygen[215]. High-performance Ru-Cu[216] and Ag-Ru[217] bimetallic nanoparticle catalysts were produced from their metal-cluster carbonylates, anchored inside MCM-41, by gentle thermolysis. The Ru-Cu nanoparticles were successfully tested in several catalytic hydrogenation reactions. The catalytic properties of Pt, Rh and Co supported on MCM-41 and hexagonal Al_2O_3 were studied for the reduction of NO with propene. The samples were prepared by incipient wetness impregnation utilizing $Rh(NO_3)_3$, $Co(NO_3)_3$ and $PtCl_4$. Pt-MCM-41 was the most active catalyst and showed in contrast to Rh- and Co-containing catalysts a minor decrease in the activity when water vapor was added to the reactant gas mixture, whereas Pt supported on mesoporous Al_2O_3 and Rh supported on MCM-41 as well as mesoporous Al_2O_3 gave an improved selectivity towards N_2. The activity of Fe-MCM-41 as a catalyst for sulfur dioxide oxidation in highly concentrated gases was found to be much higher than that observed for an industrial iron reference catalyst, as shown in Figure 6. The catalysts were remarkably stable at temperatures up to 750 °C, and are therefore promising for the conversion of highly concentrated gases. Highly concentrated

gases mean high reaction temperatures and can thus not be processed by conventional vanadium based catalysts due to thermal breakdown[218].
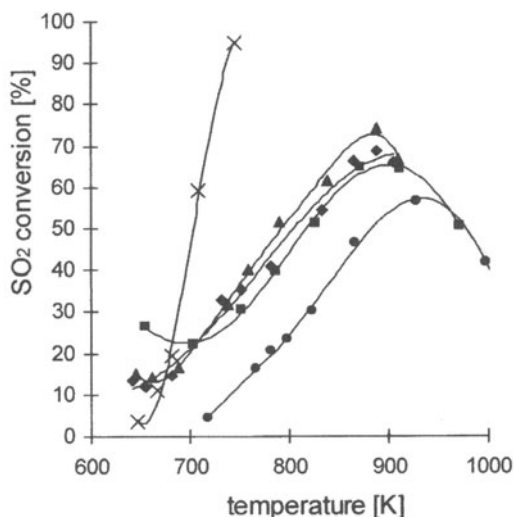
Fig. 6: SO$_2$ conversion vs T for Fe-MCM-41 catalysts (prepared by incipient wetness impregnation ▲, solid state impregnation ◆, and in situ synthesis ■) as compared to a V1605 Fe-reference ● and a V4-111 V-reference ✕. The connecting lines are just a guide for the eyes. The dotted line shows the equilibrium conversion.

Ru, supported on mesoporous sulfated zirconia by incipient wetness impregnation with $RuCl_3 \cdot 3H_2O$ solutions, was significantly more active for the liquid phase hydrogenation of $n\text{-}C_{17}H_{35}CN$ than Ru supported on microporous sulfated zirconia[219]. Both catalysts show a good stability and a high selectivity towards formation of the primary amine. Mesoporous aluminosilicate, ion-exchanged with $ZnCl_2$, has been found to be more effective in the Diels-Alder reaction between cyclopentadiene and dienophiles, such as methyl acrylate and methyl methacrylate, than a catalyst with irregular pore structure and broad mesopore size distribution[220]. The oligomerisation of olefins was carried out over chromia loaded MCM-41, treated with carbon monoxide to reduce the chromium prior to catalysis[221], and over nickel impregnated MCM-41[222]. Over the former catalyst the oligomerisation of 1-decene results in a wide variety of lubricants with viscosities higher than that obtained over chromia on silica. The nickel impregnated MCM-41 showed high activity and selectivity for the formation of trimers and tetramers of propylene. Furthermore, the degree of branching could be controlled via variations in the synthesis conditions. Isolated Mo(VI) active sites have been grafted onto the inner surfaces of MCM-41 via a molybdocene dichloride precursor[223]. After calcination, at low Mo loadings, isolated MoO_4 species are generated on the surface, whereas at higher loadings there is some evidence for the formation of polymeric oxo-molybdenum species. The lower Mo loading leads to a higher selectivity for the production of formaldehyde in the oxidative dehydrogenation of methanol.

Recently, Choudhary et al.[224] compared the catalytic activity of amphoteric and basic metal oxides supported on Si-MCM-41, silica-alumina, γ-alumina, ZrO_2 or zeolites. They showed that Ga_2O_3 (amphoteric) and In_2O_3 (basic) supported on Si-MCM-41 have a very high activity for Friedel-Craft type benzene benzylation and acylation of aromatic compounds, even in the presence of moisture. The authors indicated in this work that the support acidity does not play a significant role in the benzylation reaction over these catalysts. As these metaloxides are supported on mesopores solids, the catalysts can be used for reaction with large aromatic compounds and since they are poorly acidic or basic, these catalysts are suitable for reactions with acid-sensitive organic compounds.

Stable basic catalysts have been prepared by wet or solid-state impregnation of MCM-41 with cesium acetate and lanthanum nitrate followed by thermal decomposition[225]. This CsLa-oxide/MCM-41 system catalyzes the liquid-phase Michael addition of ethyl cyanoacetate to ethyl acrylate and the Knoevenagel addition of enolates to benzaldehyde in aqueous media.

Wong et al.[226] studied recently the morphological effect of MCM-41 on the catalytic performance. In this direction, they reported various syntheses and the characterization of transition metal oxide catalysts supported on tubular MCM-41. They tested the catalytic performance of several molybdenum oxide catalysts for ethylbenzene dehydrogenation and showed that Mo supported on tubular MCM-41, synthesized by physical mixture, presents a higher activity ($3.07 \ 10^{-3}$ mol/h g after 24 h) than Mo supported on MCM-41 with an usual particulate morphology ($2.6 \ 10^{-3}$ mol/h g) and has the lowest decay rate. The high porosity of the tubular MCM-41 and the presence of defects are believed to be responsible for the better catalytic performances, by improving the inter-channel diffusion of reactants and products.

Various metal elements were further grafted onto siliceous frameworks with different structures, such as MCM-41, MCM-48, SBA-1 and disordered mesoporous materials, using non-aqueous solutions of $AlCl_3$, $Al(NO_3)_3$, $SnCl_2$, $Zn(O_2CMe)_2$ and $Mn(O_2CMe)_2$[227]. Also, strong Brønsted basic sites could be introduced into the MCM-41 structure by anchoring 3-trimethoxysilylpropyl (trimethyl) ammonium on the surface and exchanging with hydroxide. The resulting strong solid base catalyst is a useful alternative to soluble bases in reactions such as Knoevenagel condensations, Michael additions and aldol condensations because of the high catalytic activity under mild conditions and the good stability[228].

4.2.2   Support for Organometallic Complexes

Due to the pore size of mesoporous materials even the grafting of complete metal complexes and organometallic moieties is possible, enabling the formation of shape-selective catalysts with a large concentration of accessible and well spaced active sites. Species known to be active in homogeneous catalysis can, thus, be used, utilizing the advantages of heterogeneous catalysis.

Usually, complexes are anchored to the mesoporous support via silylation of silanol groups, so that the support and active component are covalently linked via an organic spacer. In this way leaching of the complexes is overcome.

The fixation of organometallic complexes of titanium[229], vanadium[230] and manganese[231] on the walls of MCM-41 followed by removal of the ligands has turned out to be a good method to obtain highly dispersed metal oxide. In the case of titanium, for instance, solutions of [Cp_2TiCl_2] in the presence of NEt_3 have been

used. Most of the time, however, the complexes are maintained. One example for a ship-in-the-bottle synthesis is the immobilization of ruthenium perfluorophthalo-cyanine complexes in the channels of MCM-41[232]. The carbonyl ligands of ruthenium carbonyl are replaced by phthalocyanine ligands via reaction with tetra-fluorophthalocyanine. *In situ* incorporation of the preformed complex during the synthesis and grafting of the complex to the functionalized surface were performed as well. The resultant catalysts were tested for the oxidation of n-hexane and cyclohexane in the liquid phase under ambient conditions. In general, the activity of the catalysts was very low, however, the catalyst prepared by the ship-in-the-bottle route showed high turnover frequencies, which are one order of magnitude higher than that of the free complex in homogeneous solution and they are regenerable by simple extraction methods. [Fe{(η-C$_5$H$_4$)$_2$SiMe$_2$}] was fixed inside the pores of MCM-41 via ring opening in the ferrocenophane structure[233]. MCM-41 ion-exchanged with [Fe(phenanthroline)$_3$]Cl$_2$ [234] or [Fe(8-quinolinol)$_3$]Cl$_2$[235] showed high activity in phenol hydroxylation with H$_2$O$_2$. In case of [Fe(phenanthroline)$_3$]Cl$_2$ leaching could be overcome by anchoring the complex with an organic linker. Also MCM-41 grafted with [Co$_3$(μ_3-O)(OAc)$_5$(μ_2-OH)(py)$_3$]PF$_6$ was stable against leaching when previously modified with 3-bromopropyltrichlorsilane and glycine to substitute hydroxyl with carboxylic acid groups[236]. The resultant catalyst was used for the oxidation of cyclohexane. This functionalized MCM-41 showed conversions up to 38% after 4 days of reaction with a selectivity reaching 95 % towards cyclohexanone and cyclohexanol (TOF after 4 days: 216 mol$_{cyclohexane}$/(mol$_{cat}$ x h), TOF max after 4 h: 352 mol$_{cyclohexane}$/(mol$_{cat}$ x h)). These values are substantially superior to that recorded when non-functionalized MCM-41 is used as catalyst. It is believed that the better life time, activity and selectivity observed are caused by a better isolation of the active centers via the functionalized surface. Cobalt(II) complexes have also been immobilized on MCM-41 by functionalizing the surface of MCM-41 with alkoxysilyl compounds with donor amine groups for the complexation of cobalt(II), which was introduced via CoCl$_2$.[237] A ruthenium porphyrin complex was anchored on MCM-41 modified with (3-aminopropyl)triethoxysilane. It was shown to result not only in high activity in the oxidation of olefins, but even in a high selectivity towards trans-stilbene oxide in the oxidation of cis-stilbene[238]. Ion-exchange of Al-MCM-41 with [Mn(bpy)$_2$]NO$_3$ led to a catalyst exhibiting higher activity for the oxidation of styrene than the corresponding homogeneous catalyst[239].

Several different epoxidation catalysts have been synthesized based on grafted metal complexes, especially for stereoselective reactions. An epoxidation Mn(III) Shiff-base complex was attached to MCM-41 by first functionalizing the surface with (MeO)$_3$Si(CH$_2$)$_3$Cl, then treating the MCM-41 with an excess of bis-3-(3,5-di-*tert*-butylsalicylidenaminopropyl) amine (pentadentate ligand)[240]. The introduction of metal atoms was achieved via a solution of [Mn^{II}(acetylacetone)$_2$] in methanol, followed by oxidation of the resultant complex to yield Mn^{III}. Up to now, no catalytic data are available. Another epoxidation catalyst was synthesized by anchoring 1,4,7-triazacyclononane on MCM-41 modified with (3-glycidyloxypropyl)trimethoxysilane. The reaction takes place via oxirane ring opening and is followed by doping with MnSO$_4$H$_2$O[241]. Manganese (III) 3-[*N,N'*-bis-3-salicyldenamino propylamine] ("Salpr") and 3-[*N,N'*-bis-3-(3,5-di-*tert*-butylsalicyldenamino) propylamine] ("tSalpr") complexes linked to the MCM-41 surface catalyzed styrene epoxidation. Al-MCM-41, ion exchanged with Mn(OAc)$_2$ and subsequently modified with a chiral salen, (*R,R*)-(-)-*N,N'*-bis(3,5-

di-*tert*-butylsalicylidene)-1,2-cyclohexadiamine, is an effective enantioselective solid epoxidation catalyst for cis-stilbene[242]. Chiral Mn(salen) complexes immobilized on MCM-41 by either ion exchange with (Mn-salen)$^+$PF$_6^-$ or ion exchange with Mn(OAc)$_2$ followed by calcination and subsequent mixing with the chiral ligand were stable during the asymmetric epoxidation of styrene without any leaching and exhibited relatively high enantioselectivity as compared with homogeneous complexes[243]. Solid-phase immobilization of [{(c-C$_6$H$_{11}$)$_7$Si$_7$O$_{12}$}Ti(η^5-C$_5$H$_5$)] on MCM-41 was achieved after the support was pretreated with SiCl$_2$Ph$_2$ or SiCl$_2$(CH$_3$)$_2$. The catalyst was successfully tested in the epoxidation of cyclooctene with tert-butylhydroperoxide[244]. Significant effects on catalytic activity in the epoxidation of cyclohexene with alkyl hydroperoxides are observed when the surface of MCM-41 is modified with either Ge(IV) or Sn(IV) prior to the grafting of TiCp$_2$Cl$_2$[245].

Dichlorobis(benzylcyano)palladium(II) grafted on MCM-41 pretreated with 3-triethoxysilylpropyl amine was used in the reduction of aromatic nitro compounds to the corresponding amino compounds[246] and for the hydrodehalogenation of 1-bromonaphthalene by molecular hydrogen[247].

The acid-base catalysis over unmodified mesoporous oxides has been addressed in a previous section (4.1.1). However, it is possible to improve acid-base properties by grafting suitable species on the oxide surface.

Functionalization of MCM-41 to yield basic catalysts was achieved by silanation with either 3-amino-propyl alkoxysilane or 3-halogeno-propyl alkoxysilane followed by halogen substitution by piperidine, tetraalkyl guanidine, (-)-ephedrine, Salpr and tSalpr[248]. The primary and tertiary amine functions were efficient immobilized catalysts for Knoevenagel condensations and the selective monoglyceride synthesis. 1,5,7-triazabicyclo[4.4.0]dec-5-ene was an efficient base catalyst for performing transesterification reaction. High activity and regioselectivity was found when MCM-41 functionalized with (-OSi)$_3$Si(CH$_2$)$_3$NH$_2$ or the corresponding 3-piperidinopropyl moiety was used as a catalyst for the glycidol ring-opening with fatty acids under mild conditions[249].

Van Bekkum and coworkers developed in 1996 the first heteropolyacids H$_3$PW$_{12}$O$_{40}$ supported on MCM-41 molecular sieves[250]. MCM-41 was impregnated with phosphotungstic acid H$_3$PW$_{12}$O$_{40}$ and tested in catalytic conversions[251]. In n-butane conversion, isobutane was obtained with a selectivity substantially higher than that achieved over ZSM-5. For the conversion of n-hexane, the selectivity was comparable to that over Pt-MCM-41, however, the activity was higher. For comparison, 12-tungstophosphoric acid has been supported on a commercial silica, a high surface area amorphous aluminosilicate and on an all-silica mesoporous MCM-41[252]. A maximum in activity in the alkylation of 2-butene with isobutane, a high selectivity to trimethylpentane and stability with time-on-stream was found for the commercial silica, despite the higher acid dispersions achieved with the high surface area MCM-41 and amorphous aluminosilicate supports. Supporting the heteropolyacid species H$_3$PW$_{12}$O$_{40}$ on HMS resulted in a catalyst highly active in the methanol conversion, which is a bulk-type reaction, and in the n-butane isomerisation, a surface-type reaction[253]. H$_3$PW$_{12}$O$_{40}$ and H$_4$SiW$_{12}$O$_{40}$ further proved to be active catalysts in the liquid-phase esterification of 1-propanol and hexanoic acid, and in the gas-phase esterification of acetic acid and 1-butanol[254]. When subjected to the esterification conditions, however, the catalysts have the tendency to form large heteropolyacid clusters on the external surface of the supporting material, and when re-used after one reaction cycle, the activity decreases sig-

nificantly. In a recent work, Jentys et al.[255] studied the catalytic activity of Pt and tungstophosphoric acid supported on MCM-41 for the reduction of NO_x with propene in the presence of water vapor. Pt/MCM-41 was the most active catalyst, but loading of Pt/MCM-41 with $H_3PW_{12}O_{40}$ led to an increase in the selectivity towards N_2, and to an enhanced activity in the presence of water vapor, which is opposite to most of the catalysts reported[256]. This study shows that it is possible to develop new catalysts by achieving high loading of the MCM-41 large pores with metallic and acidic clusters, without great limitations of the accessibility of these sites.

Van Rhijn et al. prepared acid catalysts by anchoring 3-mercaptopropyltrimeth-oxysilane on MCM-41 and HMS, followed by a mild oxidation and acidification to obtain covalently attached alkylsulfonic acid groups[257].

$[M\{N(SiHMe_2)_2\}_3(THF)_x]$ (M = Sc, Y, La, Al) was grafted onto MCM-41, generating stable metal siloxide linkages. Subsequent surface-confined ligand exchange with Hfod (fod=1,1,1,2,2,3,3-heptafluoro-7,7-dimethyl-4,6-octanedionate) yields materials with promising activity in the catalytic hetero Diels-Alder cyclization of trans-1-methoxy-3-trimethylsilyloxy-1,3-butadiene and benzaldehyde[258]. The performance of the immobilized catalyst species was found to be superior to known homogeneous systems, and to materials obtained from the reaction of $[Ln(fod)_3]$ with the dehydrated MCM-41, particularly in its deactivation behavior and reusability. After grafting of 3-chloro- or 3-iodopropyltrialkoxysilane mesoporous templated silicas were linked to chiral ephedrine, used as heterogeneous chiral auxiliaries. Promising results are obtained in the enantioselective alkylation of benzaldehyde by diethylzinc[259] with enantiomeric excess up to 38-41% in the best cases. Finally, nitroalkenes are synthesized in a one-pot liquid-phase procedure from carbonyl compounds and nitroalkanes using $(-OSi)_3(CH_2)_3NH(CH_2)_2NH_2$ anchored on MCM-41[260].

5.   Conclusions

We have shown here the wide range of possibilities that could be offered by ordered mesoporous materials. The great diversity of synthesis pathways allows control over morphology, structure and pore size, and further enables the production of materials designed for specific applications. Furthermore, the understanding of the formation of such materials is crucial. External (time, temperature, pressure) and internal parameters (co-solvents effects, pH variations, modifiers or dyes added) play important roles in materials syntheses and must be characterized. However, a high level of understanding regarding the formation and the control of material properties has already been achieved.

Research applications in heterogeneous catalysis are numerous and ordered materials show many interesting features in terms of activity and selectivity compared with zeolites, amorphous silica-alumina, or other types of inorganic catalysts or catalysts supports. Still, it must be stated that in a number of the publications available no suitable benchmark, such as amorphous high surface area silica or alumosilicate, has been used and the data presented are often difficult to judge. However, a wide range of reactions were tested, ranging from fine chemicals production to petrochemical catalysis, and generally, MCM-41-type compounds gave promising results. The major advantages of the mesoporous materials are their

high surface area and their pore size in the mesopore range, allowing diffusing of bulky molecules. These essential qualities are combined with tunable acid/base, redox and hydrophobic/hydrophilic properties of the porous environment, providing novel catalytic centers and a wide range of new opportunities. Moreover, MCM-41 and other members of this family have been demonstrated as good supports for metals or anchored organometallic complexes with a good activity and selectivity in various reactions. The sharp pore size distribution and the regular pore system, on the other hand, seem to be less important for most catalytic applications discussed.

Especially interesting, although used to a much lesser extent, seem to be ordered transition metal mesoporous oxides. Other than for silica, for such materials alternative synthesis routes resulting in very high surface areas are often not available. However, they are up to now still poorly investigated, and the metal mesoporous oxides still remain problematic with regard to their thermal and hydrothermal stability. Work to further improve the materials is in progress, and new applications in catalysis are currently being explored, mainly for titanium and zirconium oxides[261]. It is anticipated that transition metal mesoporous oxides should develop into future commercial catalysts.

Reactions such as hydrocarbon cracking or olefin epoxidation have been extensively investigated. However, the mesoporous materials still present some limitations, such as their low hydrothermal stability and their relatively high costs, which makes it difficult to replace the established materials. There are still major improvements to be made in the development of mesoporous materials before they can be used as catalysts in commercial processes. Nevertheless, it is anticipated, that ordered mesoporous oxides, whether they are silicas, substituted silicas or transition metal oxides, will become one of the standard materials the catalysis chemist can resort to when a novel catalyst or support is needed.

References

1   K.S.W. Sing, D.H. Everett, R.A.W. Haul, L. Moscou, R.A. Pierotti, J. Rouquerol and T. Siemieniewska, Pure Appl. Chem. **57**, 603, 1985
2   V. Chiola, J.E. Ritsko and C.D. Vanderpool, US Patent No. 3 556 725, 1971
3   F. DiRenzo, H. Cambon and R. Dutartre, Microporous Materials **10**, 283, 1997
4   J.S. Beck and N.Y. Princeton, US Patent No. 5 057 296, 1991
5   T.Yanagisawa, T. Shimizu, K. Kuroda and C. Kato, Bull. Chem. Soc. Jpn. **63**, 988, 1990
6   A. Sayari, Chem. Mater. **8**, 1840, 1996
7   A. Corma, Chem. Rev. **97**, 2373, 1997
8   M. Linden, S. Schacht, F. Schüth, A. Steel and K.K. Unger, J. Por. Mat. **5**, 177, 1998
9   J.Y. Ying, C.P. Mehnert and M.S. Wong, Angew. Chem. Int. Ed. Engl. **38**, 56, 1999
10   U. Ciesla and F. Schüth, Microporous Mesoporous Mater. **27**, 131, 1999
11   P.J. Branton, P.G. Hall, K.S.W. Sing, H. Reichert, F. Schüth and K.K. Unger, J. Chem. Soc., Faraday Trans. **90**, 2965, 1994
12   O. Franke, G. Schulz-Ekloff, J. Rathousky, J. Starek and A. Zukal, J. Chem. Soc. Chem. Commun. 724, 1993
13   R. Schmidt, M. Stöcker, E. Hansen, D. Akporiaye and O.H. Ellestad, Microporous Mater. **3**, 443, 1995

14   S.J. Gregg and K.S.W. Sing, *Adsorption, Surface Area and Porosity*, 2nd Ed, Academic Press, London, 1995

15   C.Y. Chen, H.X. Li and M.E. Davis, Microporous Mater. **2**, 17, 1993

16   P.I. Ravikovitch, D. Wei, W.T. Chueh, G.L. Haller, and A.V. Neimark, J. Phys. Chem. B **101**, 3671, 1997

17   E.P. Barrett, L.G. Joyner and P.P. Halenda, J. Am. Chem. Soc. **73**, 373, 1951

18   M. Kruk, M. Jaroniec and A. Sayari, Langmuir **13**, 6267, 1997

19   P.I. Ravikovitch, S.C. O'Domhnaill, A.V. Neimark, F. Schüth and K.K. Unger, Langmuir **11**, 4765, 1995

20   M.W. Maddox, J.P. Olivier and K.E. Gubbins, Langmuir **13**, 1737, 1997

21   A. Galarneau, D. Desplantier, R. Dutartre and F. Di Renzo, Microporous Mesoporous Mat. **27**, 297, 1999

22   K.S.W. Sing, Adv. Colloid Interface Sci. **77**, 3, 1998

23   Q.S. Huo, D.I. Margolese and G.D. Stucky, Chem. Mater. **8**, 1147, 1996

24   D. Khushalani, A. Kuperman, N. Coombs and G.A. Ozin, Chem. Mater. **8**, 2188, 1996

25   R. Ryoo and J.M. Kim, J. Chem. Soc. Chem. Comm. 711, 1995

26   S. Schacht, M.T. Janicke and F. Schüth, Microporous Mesoporous Mater. **22**, 485, 1998

27   V. Alfredsson, M. Keung, A. Monnier, G.D. Stucky, K.K. Unger and F. Schüth, J. Chem. Soc. Chem. Commun. 921,1994

28   J. Feng, Q. Huo, P.M. Petroff and G.D. Stucky, Appl. Phys. Lett. **71**, 620, 1997

29   A. Chenite, Y. LePage and A. Sayari, Chem. Mater. **7**, 1015, 1995

30   C.Y. Chen, S.-Q. Xiao and M.E. Davis, Microporous Mater. **4**, 1, 1995

31   J.S. Beck, J.C. Vartuli, W.J. Roth, M.E. Leonowicz, C.T. Kresge, K.D. Schmitt, C.T.-W. Chu, D.H. Olson, E.W. Sheppard, S.B. McCullen, J.B. Higgins and J.L. Schlenker, J. Am. Chem. Soc. **114**, 10834, 1992

32   P.A. Windsor, in *Liquid Crystals and Plastic Crystals*, G.W. Gray and P.A. Windsor (Eds.) vol.1, Ellis Horwood, Chichester, 1974

33   P. Ekwall, in *Advances in Liquid Crystals*, G.H. Brown (Ed.) vol.1, Academic, New York, 1975

34   C.F. Cheng, Z.H. Chan and J. Klinowski, Langmuir **11**, 2815, 1995

35   A. Monnier, F. Schüth, Q.S. Huo, D. Kumar, D.I. Margolese, R.S. Maxwell, G.D. Stucky, M. Krishnamurty, P. Petroff, A. Firouzi, M. Janicke and B.F. Chmelka, Science **261**, 1299, 1993

36   Q.S. Huo, D.I. Margolese, U. Ciesla, D.G. Demuth, P.Y. Feng, T.E. Gier, P. Sieger, A. Firouzi, B.F. Chmelka, F. Schüth and G.D. Stucky, Chem. Mater. **6**, 1176, 1994

37   A. Firouzi, F. Atef, A.G. Oertli, G.D. Stucky and B.F. Chmelka, J. Am. Chem. Soc. **119**, 3596, 1997

38   J.N. Israelachvili, D.J. Mitchell and B.W. Ninham, J. Chem. Soc. Faraday Trans. **72**, 1525, 1976

39   J.N. Israelachvili, *Intermolecular and Surface Forces*, Academic Press, London, 1991

40   G.D. Stucky, A. Monnier, F. Schüth, Q. Huo, D. Margolese, D. Kumar, M. Krishnamurty, P. Petroff, A. Firouzi, M. Janicke and B.F. Chmelka, Mol. Cryst. Liq. Cryst. **240**, 187, 1994

41   A. Firouzi, D. Kumar, L.M. Bull, T. Besier, P. Sieger, Q. Huo, S.A. Walker, J.A. Zasadzinski, C. Glinka, J. Nicol, D.I. Margolese, G.D. Stucky and B.F. Chmelka, Science **267**, 1138, 1995

42   J.C. Vartuli, K.D. Schmitt, C.T. Kresge, W.J. Roth, M.E. Leonowicz, S.B. McCullen, S.D. Hellring, J.S. Beck, J.L. Schlenker, D.H. Olson and E.W. Sheppard, Chem. Mater. **6**, 2317, 1994

43   Q.S. Huo, D.I. Margolese, U. Ciesla, P.Y. Feng, T.E. Gier, P. Sieger, R. Leon, P.M. Petroff, F. Schüth and G.D. Stucky, Nature **368**, 317, 1994

44   U. Ciesla, D.G. Demuth, R. Leon, P.M. Petroff, G.D. Stucky, K.K. Unger and F. Schüth, J. Chem. Soc. Chem. Commun. 1387, 1994
45   A. Stein, M. Fendorf, T.P. Jarvie, K.T. Mueller, A.J. Benesi and T.E. Mallouk, Chem. Mater. 7, **304**, 1995
46   D.M. Antonelli and J.Y. Ying, Angew. Chem. Int. Ed. Engl. **34**, 2014, 1995
47   U. Ciesla, S. Schacht, G.D. Stucky, K.K. Unger and F. Schüth, Angew. Chem. Int. Ed. Engl. **35**, 541, 1996
48   U. Ciesla, M. Fröba, G.D. Stucky and F. Schüth, Chem. Mater. **11**, 227, 1999
49   J.M. Kim, C.H. Shin and R. Ryoo, Catal. Today **38**, 221, 1997
50   J.O. Perez, R.B. Borade and A. Clearfield, J. Mol. Struct. 470, 221, 1998
51   M.J. MacLachlan, N. Coombs and G.A. Ozin, Nature **397**, 681, 1999
52   K.M. McGrath, D.M. Dabbs, N. Yao, I.A. Aksay and S.M. Gruner, Science **277**, 552, 1997
53   P.T. Tanev and T.J. Pinnavaia, Science **267**, 865, 1995
54   S.A. Bagshaw, E. Prouzet and T.J. Pinnavaia, Science **269**, 1242, 1995
55   P.T. Tanev and T.J. Pinnavaia, Chem. Mater. **8**, 2068, 1996
56   P.T. Tanev and T.J. Pinnavaia, Science **271**, 1267, 1996
57   P.T. Tanev, Y. Liang and T.J. Pinnavaia, J. Am. Chem. Soc. **119**, 8616, 1997
58   E. Prouzet and T.J. Pinnavaia, Angew. Chem. Int. Ed. Engl. **36**, 516, 1997
59   S.A. Bagshaw and T.J. Pinnavaia, Angew. Chem. Int. Ed. Engl. **35**, 1102, 1996
60   P.D. Yang, D.Y. Zhao, D.I. Margolese, B.F. Chmelka and G.D. Stucky, Nature **396**, 152, 1998
61   G.S. Attard, J.C. Glyde and C.G. Göltner, Nature **378**, 366, 1995
62   M. Antonietti and C.G. Göltner, Angew. Chem. Int. Ed. Engl. **36**, 910, 1997
63   C.G. Göltner and M. Antonietti, Adv. Mater. **9**, 431, 1997
64   G.S. Attard, C.G. Göltner, J.M. Corker, S. Henke and R.H. Templer, Angew. Chem. Int. Ed. Engl. **36**, 1315, 1997
65   G.S. Attard, P.N. Bartlett, N.R.B. Coleman, J.M. Elliott, J.R. Owen and J.H. Wang, Science **278**, 838, 1997
66   T.M. Nenoff, S.G. Thoma, P. Provencio and R.S. Maxwell, Chem. Mater. **10**, 3077, 1998
67   M. Thieme and F. Schüth, Microporous Mesoporous Mater. **27**, 193, 1999
68   D.M. Antonelli and J.Y. Ying, Angew. Chem. Int. Ed. Engl. **35**, 426, 1996
69   D.M. Antonelli and J.Y. Ying, Chem. Mater. **8**, 874, 1996
70   D.M. Antonelli, A. Nakahira and J.Y. Ying, Inorg. Chem. **35**, 3126, 1996
71   B.T. Holland, C.F. Blanford, T. Do and A. Stein, Chem. Mater. **11**, 795, 1999
72   D.H. Gray and D.L. Gin, Chem. Mater. **10**, 1827, 1998
73   P.D. Yang, T. Deng, D.Y. Zhao, P.Y. Feng, D. Pine, B.F. Chmelka, G.M. Whitesides and G.D. Stucky, Science **282**, 2244, 1998
74   H.Yang, A. Kuperman, N. Coombs, S. Mamiche-Afara and G.A. Ozin, Nature **379**, 703, 1996
75   I.A. Aksay, M. Trau, S. Manne, I. Honma, N. Yao, L. Zhou, P. Fenter, P.M. Eisenberger and S.M. Gruner, Science **273**, 892, 1996
76   Q.S. Huo, D.Y. Zhao, J.L. Feng, K. Weston, S.K. Buratto, G.D. Stucky, S. Schacht and F. Schüth, Adv. Mater. **9**, 974, 1997
77   P.D. Yang, D.Y. Zhao, B.F. Chmelka and G.D. Stucky, Chem. Mater. **10**, 2033, 1998
78   P.J. Bruinsma, A.Y. Kim, J. Liu and S. Baskaran, Chem. Mater. **9**, 2507, 1997
79   H.P. Lin and C.Y. Mou, Science **273**, 765, 1996
80   S. Schacht, Q. Huo, I.G. Voigt-Martin, G.D. Stucky and F. Schüth, Science **273**, 768, 1996
81   M. Grün, I. Lauer and K.K. Unger, Adv. Mater. **9**, 254, 1997
82   M. Grün, K.K. Unger, A. Matsumoto and K. Tsutsumi, Microporous Mesoporous Mater. **27**, 207, 1999

83   H. Izutsu, F. Mizukami, P.K. Nair, Y. Kiyozumi and K. Maeda, J. Mater. Chem. **7**, 767, 1997

84   Y.F. Lu, H.Y. Fan, A. Stump, T.L. Ward, T. Rieker and C.J. Brinker, Nature **398**, 223, 1999

85   A. Firouzi, D.J. Schaefer, S.H. Tolbert, G.D. Stucky and B.F. Chmelka, J. Am. Chem. Soc. **119**, 9466, 1997

86   S.H. Tolbert, A. Firouzi, G.D. Stucky and B.F. Chmelka, Science **278**, 264, 1997

87   (a) M. Ogawa, Chem. Comm. 1149, 1996. (b) J.E. Martin, M.T. Anderson, J. Odinek and P. Newcomer, Langmuir **13**, 4133, 1997 (c) Y. Lu, R. Ganguli, C.A. Drewien, M.T. Anderson, C.J. Brinker, W. Gong, Y. Guo, H. Soyez, B. Dunn, M.H. Huang and J.I. Zink, Nature **389**, 364, 1997

88   D. Zhao, P. Yang, N. Melosh, J. Feng, B.F. Chmelka and G.D. Stucky, Adv. Mater. **10**, 1380, 1998

89   W. Kolodziejski, A. Corma, M.T. Navarro and J. Pérez-Pariente, Solid State Nucl. Magn. Reson. **2**, 253, 1993

90   R. Ryoo, C.H. Ko and R.F Howe, Chem. Mater. **9**, 1607, 1997

91   U. Oberhagemann, I. Kinski, I. Dierdorf, B. Marler and H. Gies, J. Noncryt. Solids **197**, 1451, 1996

92   Z.Y. Yuan, S. Q. Liu, T.H. Chen, J. Z. Wang and H. X. Li, Chem Commun. 973, 1995

93   T. Takeguchi, J.B. Kim, M. Kang, T. Inui, W.T. Cheuh and G.L. Haller, J. Catal. **175**, 1, 1998

94   H. Kosslick, G. Lischke, B. Parlitz, W. Storek and R. Fricke, Appl. Catal. A Gen **184**, 49, 1999

95   S.-C. Shen and S. Kawi, Chem. Lett. 1293, 1999

96   A. Corma, M.S. Grande, V. Gonzalez-Alfaro and A.V. Orchilles, J. Catal. **159**, 375, 1996

97   A. Corma, V. Fornes, M.T. Navarro and J.Perez-Pariente, J. Catal. **148**, 569, 1994

98   A. Corma, A. Martínez, V. Martínez-Soria and J.B. Montón, J. Catal. **153**, 25, 1995

99   D.W. Breck in *Zeolite Molecular Sieves : Structure, Chemistry, and Use*; Robert E. Kreiger Publishing Co., Malabar, FL, 1994

100 Z. Luan, C.F. Chen, W. Zhou and J. Klinowski, J. Phys. Chem. B **99**, 10590, 1995

101 R. Schmidt, D. Akporiaye, M. Stöcker and O.H. Ellestad, Chem. Commun. 1493, 1994

102 R.B. Borade and A. Clearfield, Catal. Lett. **31**, 267, 1995

103 M.T. Janicke , C.C. Landry, S.C. Christiansen , S. Birtalan, G.D. Stucky and B.F. Chmelka, Chem. Mater. **11**, 1342, 1999

104 G.Y. Fu, C.A. Fyfe, W. Schwieger and G.T. Kokotailo, Angew. Chem. Int. Ed. Eng. **34**, 1499, 1995

105   K.R. Kloetstra, H.W. Zandbergen and H. van Bekkum, Catal. Lett. **33**, 157, 1995

106 A. Araujo and M. Jarionec, J. Colloid and Interface Sci. **218**, 462, 1999

107 M.D. Alba, Z. Luan and J. Klinowski, J. Phys. Chem. B **102**, 857, 1996

108 B.J. Aronson, C.F. Blanford and A. Stein, Chem. Mater. **9**, 2842, 1997

109 (a) B.J. Melde, B.T. Holland, C.F. Blanford and A. Stein, Chem. Mater. **11**, 3302, 1999. (b) T. Asefa, M.J. MacLachlan, N. Coombs and G.A. Ozin, Nature **402**, 867, 1999. (c) C. Yoshina-Ishii, T. Asefa, N. Coombs, M.J. MacLachlan and G.A. Ozin, Chem. Comm. 2539, 1999 (d) S. Inagaki, S. Guan, Y. Fukushima, T. Ohsuna and O. Terasaki, J. Am. Chem. Soc. **121**, 9611, 1999. (e) S. Guan, S. Inagaki, T. Ohsuna and O. Terasaki, J. Am. Chem. Soc. **122**, 5660, 2000

110 A. Jentys, K. Kleestorfer and H. Vinek, Microporous Mesoporous Mater. **27**, 321, 1999

111 M. Hunger, U. Schenk, M. Breuninger, R. Glaser and J. Weitkamp, Microporous Mesoporous Mater. **27**, 261, 1999

112 H.H.P. Yiu and D. R. Brown, Catal. Lett. **56**, 57, 1998
113 B. Chakraborty and B. Viswanathan, Catal. Today **49**, 253, 1999
114 M.L. Occelli, S. Biz, A. Auroux and G.J. Ray, Microporous Mesoporous Mater. **26**, 193, 1998
115 M.T. Janicke, C.C. Landry, S.C. Christiansen, D. Kumar, G.D. Stucky and B.F. Chmelka, J. Am. Chem. Soc. **120**, 6940, 1998
116 K.R. Kloetstra, H. van Bekkum and J.C. Jansen, Chem. Commun. 2281, 1997
117 P.L. Llewellyn, Y. Grillet, F. Schüth, H. Reichert and K.K. Unger, Microporous Mater. **3**, 345, 1994
118 T. Boger, R. Roesky, R. Gläser, S. Ernst, G. Eigenberger and J. Weitkamp, Microporous Mater. **8**, 79, 1997
119 X.S. Zhao, G.Q. Lu, A.K. Whittaker, G.J. Millar and H.Y. Zhu, J. Phys. Chem. B **101**, 6525, 1997
120 H. Landmesser, H. Kosslick, W. Storek and R. Fricke, Solid State Ion. **101**, 271, 1997
121 K. Roos, A. Liepold, W. Reschetilowski, R. Schmidt, A. Karlsson and M. Stöcker, Stud. Surf. Sci. Catal. **94**, 389, 1995
122 K.M. Reddy and C. S. Song, Catal. Today **31**, 137, 1996
123 K. Hamaguchi and H. Hattori, React. Kinet. Catal. Lett. **61**, 13, 1997
124 T.F. Degnan Jr, K.M. Keville, M.E. Landis, D.O. Marler and D.N. Mazzone, Mobil Oil Corp., USA 5183557, 1993 (Chem. Abstr. **119**, 31376, 1993)
125 J. Aguado, D.P. Serrano, M.D. Romero and J.M. Escola, Chem. Commun. 725, 1996
126 J. Aguado, J. L. Sotelo, D.P. Serrano, J. A. Calles and J. M. Escola, Energy and Fuels **11**, 1225, 1997
127 H. Koch and W. Reschetilowski, Microporous Mesoporous Mater. **25**, 127, 1998
128 R. Mokaya and W. Jones, J. Mater. Chem. **9**, 555, 1999
129 G. Seo, N.H. Kim, Y.H. Lee and J.H. Kim, Catal. Lett. **57**, 209, 1999
130 B. Chiche, E. Sauvage, F. Di Renzo, I.I. Ivanova and F. Fajula, J. Mol. Catal. A-Chem. **134**, 145, 1998
131 M.S. Wong, D.M. Antonelli and J.Y. Ying, Nanostr. Mater. **9**, 165, 1997
132 J.P.G. Pater, P.A. Jacobs and J.A. Martens, J. Catal. **184**, 262, 1999
133 K.M. Reddy, B.L. Wei and C.S. Song, Catal. Today **43**, 261, 1998
134 C.S. Song and K.M. Reddy, Appl. Catal. A-Gen. **176**, 1, 1999
135 Y.H. Yue, Y. Sun, Q. Xu and Z. Gao, Appl. Catal. A-Gen. **175**, 131, 1998
136 M.J. Climent, A. Corma, S. Iborra, M.C. Navarro and J. Primo, J. Catal. **161**, 783, 1996
137 M.J. Climent, A. Corma, R. Guil-Lopez, S. Iborra and J. Primo, J. Catal. **175**, 70, 1998
138 E. Armengol, M.L. Cano, A. Corma, H. Garcia and M.T. Navarro, Chem. Commun. 519, 1995
139. K.R. Kloetstra and H. van Bekkum, J. Chem. Res. (S), 26, 1995
140 M.J. Climent, A. Corma, S. Iborra, S. Miquel and J. Primo, F. Rey, J. Catal. **183**, 76, 1999
141 C. Perego, S. Amarilli, A. Carati, C. Flego, G. Pazzuconi, C. Rizzo and G. Bellussi, Microporous Mesoporous Mater. **27**, 345, 1999
142 P.M. Price, J.H. Clark, K. Martin, D.J. Macquarrie and T.W. Bastock, Org. Process Res. Dev. **2**, 221, 1998
143 J. Medina-Valtierra, O. Zaldivar, M.A. Sanchez, J.A. Montoya, J. Navarrete and J.A. de los Reyes, Appl. Catal. A-Gen. **166**, 387, 1998
144 J. Medina-Valtierra, M.A. Sanchez, J.A. Montoya, J. Navarrete and J.A. de los Reyes, Appl. Catal. A-Gen. **158**, L1, 1997
145 S.B. Pu, J.B. Kim, M. Seno and T. Inui, Microporous Mater. **10**, 25, 1997
146 E. Armengol, A. Corma, H. Garcia and J. Primo, Appl. Catal. A-Gen. **149**, 411, 1997
147 L.W. Chen, C.Y. Chou and A.N. Ko, Appl. Catal. A-Gen. **178**, L1, 1999

148 B. Lindlar, A. Kogelbauer and R. Prins, Microprous Mesoporous Mater. **38**, 167, 2000

149 K.R. Kloetstra and H. van Bekkum, Chem. Commun. 1005, 1995

150 T. Shinoda, Y. Izumi and M. Onaka, Chem. Commun. 1801, 1995

151 A. Corma, M. Iglesias and F. Sanchez, Chem. Commun. 1635, 1995

152 D. R. C. Huybrechts, L. De Bruycher and P. A. Jacobs, Nature **345**, 240, 1990

153 G. Bellusi, A. Carati, M. G. Clerici, G. Meddinelli and R. Millini, J. Catal. **133**, 220, 1992

154 S. Gontier and A. Tuel, Appl. Catal. **118**, 173, 1994

155 P.T. Tanev, M. Chibwe and T.J. Pinnavaia, Nature **368**, 321, 1994

156 A. Corma, M.T. Navarro and J. Pérez Pariente, Chem. Commun. 147, 1994

157 I. Vankelecom, K. Vercruysse, N. Moens, R. Parton, J.S. Reddy and P. Jacobs, Chem. Commun. 137, 1997

158 A. Tuel, S. Gontier and R. Teissier, Chem. Commun. 651, 1996

159 L.Y. Chen, G.K. Chuah and S. Jaenicke, Catal. Lett. **50**, 107, 1998

160 W.S. Ahn, D.H. Lee, T.J. Kim, J.H. Kim, G. Seo and R. Ryoo, Appl. Catal. A-Gen. **181**, 39, 1999

161 M.A. Camblor, A. Corma, P. Esteve, A. Martinez and S. Valencia, Chem Commun. 795, 1997

162 T. Blasco, M.A. Camblor, A. Corma P. Esteve, J.M. Guil, A. Martínez, J.A. Perdigón-Melón and S. Valencia, J. Phys. Chem. B, **102**, 75, 1998

163 A. Corma, M. Domine, J.A. Gaona, J.L. Jorda, M.T. Navarro, F. Rey, J. Perez-Pariente, J. Tsuji, B. McCulloch and L.T. Nemeth, Chem. Commun. 2211, 1998

164 A. Corma, J.L. Jorda, M.T. Navarro and F. Rey, Chem. Commun. 1899, 1998

165 L.Y. Chen, G.K. Chuah and S. Jaenicke, J. Mol. Catal. A-Chem. **132**, 281, 1998

166 T. Tatsumi, K.A. Koyano and N. Igarashi. Chem. Commun. 325, 1998

167 M.B. D'Amore and S. Schwarz, Chem. Commun. 121, 1999

168 A. Bhaumik and T. Tatsumi, J. Catal. **189**, 31, 2000

169 A. Bhaumik and T. Tatsumi, Catal. Lett. **66**, 181, 2000

170 D.T. On, M.P. Kapoor, P.N. Joshi, L. Bonneviot and S. Kaliaguine, Catal. Lett. **44**, 171, 1997

171 S. Gontier and A. Tuel, J. Catal. **157**, 124, 1995

172 K.M. Reddy, I. Moudrakovski and A. Sayari, Chem. Commun. 1059, 1994

173 W.A. Carvalho, P.B. Varaldo, M. Wallau and U. Schuchardt, Zeolites **18**, 408, 1997

174 W.Z. Zhang, J.L. Wang, P.T. Tanev and T.J. Pinnavaia, Chem. Commun. 979, 1996

175 W.Z. Zhang and T.J. Pinnavaia, Catal. Lett. **38**, 261, 1996

176 R.K. Rana and B. Viswanathan, Catal. Lett. **52**, 25, 1998

177 D.H. Cho, T.S. Chang, S.K. Ryu and Y.K. Lee, Catal. Lett. **64**, 227, 2000

178 S. Higashimoto, R. Tsumura, S.G. Zhang, M. Matsuoka, H. Yamashita, C. Louis, M. Che and M. Anpo, Chem. Lett. 408, 2000

179 Z.R. Zhang, J.S. Sue, X.M. Zhang and S.B. Li, Chem. Commun. 241, 1998

180 Z.R. Zhang, J.S. Sue, X.M. Zhang and S.B. Li, Appl. Catal. A-Gen. **179**, 11, 1999

181 M. Yonemitsu, Y. Tanaka and M. Iwamoto, J. Catal. **178**, 207, 1998

182 T.K. Das, K. Chaudhari, E. Nandanan, A.J. Chandwadkar, A. Sudalai, T. Ravindranathan and S. Sivasanker, Tetrahedron Lett. **38**, 3631, 1997

183 S. Kawi and M.Te, Catal. Today **44**, 101, 1998

184 Z. Fu, J. Chen, D. Yin, D. Yin, L. Zhang and Y. Zhang, Catal. Lett. **66**, 105, 2000

185 J. Okamura, S. Nishiyama, S. Tsuruya and M. Masai, J. Mol. Catal. A-Chem. **135**, 133,1998

186 H. Yoshida, K. Kimura, Y. Inaki and T. Hattori, Chem. Comm. 129, 1999.

187 H. Yoshida, C. Murata, Y. Inaki and T Hattori, Chem. Lett. 1121, 1998

188 M. Anpo, H. Yamashita, K. Ikeue, Y. Fujii, S.G. Zhang, Y. Ichihashi, D.R. Park, Y. Suzuki, K. Koyano and T. Tatsumi, Catal. Today **44**, 327, 1998

189 A. Jentys, W. Schiesser and H. Vinek, Chem. Commun. 335, 1999
190 R. Anwander, C. Palm, G. Gerstberger, O. Groeger and G. Engelhardt, Chem. Commun. 1811, 1998
191 R.T. Yang, T.J. Pinnavaia, W.B. Li and W.Z. Zhang, J. Catal. **172**, 488, 1997
192 C.G. Wu and T. Bein, Chem. Mater. **6**, 1109, 1994
193 C.G. Wu and T. Bein, Science **264**, 1757, 1994
194 T.M. Abdel-Fattah and T.J. Pinnavaia, Chem. Commun. 665, 1996
195 K. Kageyama, S. Ogino, T. Aida and T. Tatsumi, Macromolecules **31**, 4069, 1998
196 S.M. Ng, S. Ogino, T. Aida, K.A. Koyano and T.Tatsumi, Macromol. Rapid Commun. **18**, 991, 1997
197 A. Garforth, S. Fiddy, Y.-H. Lin, A. Ghanbari-Siakhali, P.N. Sharratt and J. Dwyer, Thermochim. Acta **294**, 65, 1997
198 Y.S. Ko, T.K. Han, J.W. Park and S.I. Woo, Macromol. Rapid Commun. **17**, 749, 1996
199 J. Tudor and D. O'Hare, Chem. Commun. 603, 1997
200 L.K. Van Looveren, D.F. Geysen, K.A. Vercruysse, B.H. Wouters, P.J. Grobet and P.A. Jacobs, Angew. Chem. Int. Edit. Engl. **37**, 517, 1998
201 L.K. Van Looveren, D.E. De Vos, K.A. Vercruysse, D.F. Geysen, B. Janssen and P.A. Jacobs, Catal. Lett. **56**, 53, 1998
202 K. Kageyama, J. Tamazawa and T. Aida, Science **285**, 2113, 1999
203 F. Kleitz, F. Schüth, G.D. Stucky, F. Marlow, Chem.Mater. **13**, 3587, 2001
204 R.R. Rao, B.M. Weckhuysen and R.A. Schoonheydt, Chem. Commun. 445, 1999
205 C.A. Koh, R. Nooney and S. Tahir, Catal. Lett. **47**, 199, 1997
206 U. Junges, S. Disser, G. Schmid and F. Schüth, Stud. Surf. Sci. Catal. **117**, 391, 1998
207 C.P. Mehnert, D.W. Weaver and J.Y. Ying, J. Am. Chem. Soc. **120**, 12289, 1998
208 M. Okumura, S. Tsubota, M. Iwamoto and M. Haruta, Chem. Lett. 315, 1998
209 U. Junges, F. Schüth, G. Schmid, Y. Uchida and R. Schlögl, Ber. Bunsenges. Physikal. Chem. **101**, 1631, 1997
210 A. Corma, A. Martinez, V. Martinez-Soria, J. Catal. **169**, 480, 1997
211 R.Q. Long and R.T. Yang, Catal. Lett. **52**, 91, 1998
212 M. Sasaki, M. Osada, N. Sugimoto, S. Inagaki, Y. Fukushima, A. Fukuoka and M. Ichikawa, Microporous Mesoporous Mater. **21**, 597, 1998
213 T. Yamamoto, T. Shido, S. Inagaki, Y. Fukushima and M. Ichikawa, J. Phys. Chem. B **102**, 3866, 1998
214 W.Z. Zhou, J.M. Thomas, D.S. Shephard, B.F.G. Johnson, D. Ozkaya, T. Maschmeyer, R.G. Bell and Q.F. Ge, Science **280**, 705, 1998
215 R.Q. Long and R.T. Yang, J. Phys. Chem. B **103**, 2232, 1999
216 D.S. Shephard, T. Maschmeyer, G. Sankar, J.M. Thomas, D. Ozkaya, B.F.G. Johnson, R. Raja, R.D. Oldroyd and R.G. Bell, Chem.-Eur. J. **4**, 1214, 1998
217 D.S. Shepard, T. Maschmeyer, B.F.G. Johnson, J.M. Thomas, G. Sankar, D. Ozkaya, W.Z. Zhou, R.D. Oldroyd and R.G. Bell, Angew. Chem. Int. Edit. Engl. **36**, 2242, 1997
218 A. Wingen, N. Anastasievi•, A. Hollnagel, D. Werner and F. Schüth, Stud. Surf. Sci. Catal. **193**, 248, 2000
219 Y.Y. Huang and W.M.H. Sachtler, Appl. Catal. A-Gen. **163**, 245, 1997
220 M. Onaka and R. Yamasaki, Chem. Lett. 259, 1998
221 B.P. Pelrine, K.D. Schmitt and J.C. Vartuli, Mobil Oil Corp., USA 5105051, 1992 (Chem. Abstr. **117**, 154327,1992)
222 N.A. Bhore, I.D. Johnson, K.M. Keville, Q.N. Le and G.H. Yokomizo, US Patent No. 5260501, 1993
223 I.J. Shannon, T. Maschmeyer, R.D. Oldroyd, G. Sankar, J.M. Thomas, H. Pernot, J.P. Balikdjian and M. Che, J. Chem. Soc., Faraday Trans. **94**, 1495, 1998
224 V. Choudhary, S.K. Jana and B.P. Kiran, J. Catal. **192**, 257, 2000

225 K.R. Kloetstra, M. van Laren and H. van Bekkum, J. Chem. Soc., Faraday Trans. **93**, 1211, 1997

226 S.T. Wong, H.P. Lin and C.Y. Mou, Appl. Catal. A-Gen. **198**, 103, 2000

227 R. Ryoo, S. Jun, J.M. Kim and M.J. Kim, Chem. Commun. 2225, 1997

228 I. Rodriguez, S. Iborra, A. Corma, F. Rey and J.L. Jorda, Chem. Commun. 593, 1999

229 T. Maschmeyer, F. Rey, G. Sankar and J.M. Thomas, Nature **378**, 159, 1995

230 R. Neumann and A.M. Khenkin, Chem. Commun. 2643, 1996

231 R. Burch, N. Cruise, D. Gleeson and S.C. Tsang, Chem. Commun. 951, 1996

232 S. Ernst and M. Selle, Microporous Mesoporous Mater. **27**, 355, 1999

233 S. O'Brien, J. Tudor, S. Barlow, M.J. Drewitt, S.J. Heyes and D. O'Hare, Chem. Commun. 641, 1997

234 C.B. Liu, X.K. Ye and Y. Wu, Catal. Lett. **36**, 263, 1996

235 C.B. Liu, Y.J. Shan, X.G. Yang, X.K. Ye and Y. Wu, J. Catal. **168**, 35, 1997

236 T. Maschmeyer, R.D. Oldroyd, G. Sankar, J.M. Thomas, I.J. Shannon, J.A. Klepetko, A.F. Masters, J.K. Beattie and C.R.A. Catlow, Angew. Chem. Int. Ed. Engl. **36**, 1639, 1997

237 J.F. Diaz, K.J. Balkus, F. Bedioui, V. Kushev and L. Kevan, Chem. Mater. **9**, 61, 1997

238 C.J. Liu, S.G. Li, W.Q. Pang and C.M. Che, Chem. Commun. 65, 1997

239 S.S. Kim, W.Z. Zhang, T.J. Pinnavaia, Catal. Lett. **43**, 149, 1997

240 P. Sutra and D. Brunel, Chem. Commun. 2485, 1996

241 Y.V.S. Rao, D.E. De Vos, T. Bein and P.A. Jacobs, Chem. Commun. 355, 1997

242. P. Piaggio, P. McMorn, C. Langham, D. Bethell, P.C. Bulman-Page, F.E. Hancock and G.J. Hutchings, New J. Chem. 1167, 1998

243 (a) G.J. Kim and S.H. Kim, Catal. Lett. **57**, 139, 1999. (b) G.J. Kim, Reac. Kin. Catal. Lett. **67**, 295, 1999

244. S. Krijnen, H.C.L. Abbenhuis, R.W.J.M. Hanssen, J.H.C. van Hooff and R.A. van Santen, Angew. Chem. Int. Ed. Engl. **37**, 356, 1998

245 R.D. Oldroyd, G. Sankar, J.M. Thomas and D. Ozkaya, J. Phys. Chem. B **102**, 1849, 1998

246 M.L. Kantam, T. Bandyopadhyay, A. Rahman, N.M. Reddy and B.M. Choudary, J. Mol. Catal. A-Chem. **133**, 293, 1998

247 M.L. Kantam, A. Rahman, T. Bandyopadhyay and Y. Haritha, Synth. Commun. **29**, 691, 1999

248 D. Brunel, Microporous Mesoporous. Mater. **27**, 329, 1999

249 A. Cauvel, G. Renard and D. Brunel, J. Org. Chem. **62**, 749, 1997

250 I.V. Kozhevnikov, K.R. Kloetstra, A. Sinnema, H.W. Zandbergen and H. Van Bekkum, J. Mol. Cat. A-Chem. **114**, 287, 1996

251 C.T. Kresge, D.O. Marler, G.S. Rav and B.H. Rose, US Patent No. 5366945, 1994

252 T. Blasco, A. Corma, A. Martinez and P. Martinez-Escolano, J. Catal. **177**, 306, 1998

253 F. Marme, G. Coudurier and J.C. Vedrine, Microporous Mesoporous Mat. **22**, 151, 1998

254 M.J. Verhoef, P.J. Kooyman, J.A. Peters and H. van Bekkum, Microporous Mesoporous Mater. **27**, 365, 1999

255 A. Jentys, W. Schießer and H. Vinek, Catal. Today **59**, 313, 2000

256 H.Y. Chen and W.M.H. Sachtler, Catal. Lett. **50**, 125, 1998

257 W.M. Van Rhijn, D.E. De Vos, B.F. Sels, W.D. Bossaert and P.A. Jacobs, Chem. Commun. 317, 1998

258 G. Gerstberger, C. Palm and R. Anwander, Chem.-Eur. J. **5**, 997, 1999

259 M. Lasperas, N. Bellocq, D. Brunel, and P. Moreau, Tetrahedron-Asymmetry **9**, 3053, 1998

260 M.L. Kantam and P. Sreekanth, Catal. Lett. **57**, 227, 1999

261 D. J. McIntosh and R.A. Kydd, Microporous Mesoporous Mater. **37**, 281, 2000

In situ Characterisation
of Practical Heterogeneous Catalysts

Contents

In situ Characterisation
of Practical Heterogeneous Catalysts

Robert Schlögl

Fritz-Haber-Institut der MPG
Faradayweg 4-6
14195 Berlin
www.fhi-berlin.mpg.de

Abstract. In situ methods are considered as a curiosity within the standard methodology of practical catalyst characterisation. The methods are not commercially available and need to be adapted and validated for each specific problem. The great advantage of these methods is, however, that they deliver immediately relevant characteristics of the working state of a heterogeneous catalyst and allow justified structure-function relations to be deduced. To achieve this it is essential that the experiments are planned and conducted in such a way that the proven to be active state of the catalyst is investigated. This can only be ascertained if simultaneous kinetic and spectroscopic data are acquired. The contribution lists a selection of methods with their main characteristics that allows to choose from the wide spectrum of information those that are most relevant for the given problem. A tabulated selection of case studies from the literature gives some insight in the current practice.

1.   Introduction

1.1   Catalyst Characterisation

The characterisation of heterogeneous catalysts is still a major challenge to physical chemistry despite the enormous progress in this area and the large arsenal of methods that are available for this purpose. The challenge resides in the identification of analytical characteristics that are directly related to the function of a catalytic material.

The typical situation is the characterisation of a prepared catalyst by the standard suite of methods that are powder X-ray diffraction, BET surface analysis and SEM/EDX or elemental analytical techniques. These data are all obtained usually from the fresh parent material stored in air or activated under non-reacting conditions (e.g. "in-situ" reduced) and are then empirically related to the catalytic function. Heuristic arguments such as "structure sensitivity" "particle size effects" "metal support interactions" or others are derived form these correlations allowing to justify the choice of catalytic materials or specific preparation conditions.

Unfortunately, these arguments are not based on physically traceable and theoretically founded correlations nor do these correlations take into account the solid state and surface dynamics of well-active catalytic materials. So it is little surprise that the transferability of the heuristic rules and their predictive power are rather limited and do often not even apply to sets of materials of the nominal same composition but prepared under different conditions or by different persons.

The general disappointment of the seemingly poor ratio between analytical effort and functional value of physical characterisation of catalysts has led to critical assessments of the role of characterisation in catalyst development efforts in general and to the development of high throughput testing procedures that promise to solve problems without all the analytical "overhead".

For the case of "in-situ" analysis the general view that this methodology is of insignificant value to practical problems holds the more as the technical effort is very significantly larger than for ex-situ analytics and the required equipment is not available commercially and hence difficult to operate and to validate. It is the purpose of this work to define and to justify in-situ analysis as an essential tool also for practical problems, to collect some literature examples in an overview and to introduce specific experimental requirements. For case studies the reader is referred to the tabulated original references. The work relates predominantly to heterogeneous catalysis but includes in the tabulated examples several typical examples from homogeneous catalysis, where "in-situ" analysis stands often for mechanistic considerations on the atomic level even when no-reaction is actually taking place during analytical assessment.

1.2   Definition of "in-situ" Analysis

The request for in-situ catalyst characterisation has often been made and was systematically expressed first in a book edited by Sir John Thomas. The definition there was that characterisation should be conducted of catalysts in their working state. This definition was often relaxed to an experiment that is done in the presence of a gas phase similar to the educt gas phase of an operating system. The conflicting requirements for chemical kinetics on one side and geometric requirements of the in-situ cell together with compromises in gas pressure, composition and reaction temperature on the other side led to wide definitions of "working state". In many experiments no proof of the working state is given, it is simply *a priory* assumed that the provision of some reaction environment brings a catalytic material into the same active state where it is used in conventional reactor experiments.

Good catalysts are, however, responding dynamically to their environment and occur hence in states highly specific to the testing conditions. In order to correlate in-situ analytical data to performance data it has thus to the ascertained that the differences in testing conditions exert no qualitative effect on the catalyst, or the conditions have to be chosen identically to technical conditions. Such conditions cannot be chosen, however, in most cases due to the physical boundary conditions imposed by the experiment.

It should be pointed out that in–situ studies on so-called model systems are usually forgiving for not maintaining realistic testing conditions. The sensitivity of a catalyst to changes in its reaction environment is closely related to its efficiency. Highly effective catalysts are materials far from their equilibrium state. They

contain much "chemical energy" and transform easily into less reactive or differently active materials. Model systems prepared with the emphasis on a rigorous structural definition are, on the other hand, per definition equilibrium materials with the exception of the inevitable surface defect. Hence, their bulk is often non-reactive and stable to modifications of the reaction environment or the structural response is slow within the time window of in-situ observation. These comments hold both for homogeneous and for heterogeneous catalysts.

True in-situ experiments on practical systems must thus be conducted in such a way that the catalytic performance is measured simultaneously with the spectroscopic or structural property of the experiment. Reliable in-situ experiments are performed at multiple steady states and a quantitative correlation between catalytic function (activity, selectivity) and spectroscopic/structural property is established. The preferred way of doing this should be a periodic modulation of the reaction conditions coupled with observation of the same periodicity in the spectroscopic signal. Only then it is proven that a direct and physically meaningful correlation exists between structure/spectral property and catalytic function.

1.3   Why is in-situ Analysis Essential?
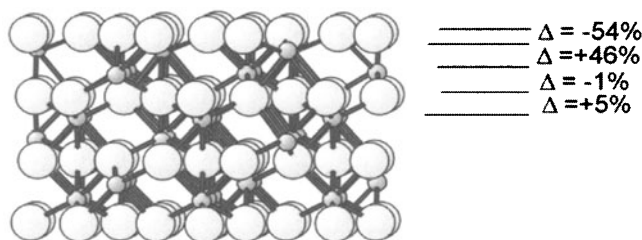
Fig. 1.1: Surface relaxation of single crystalline and oxygen terminated Fe_2O_3 prepared at 1 mbar oxygen pressure. The figures denote the deviation of the atomic layer distances from the expected bulk values.

Many negative experiences with the relation of characterisation results to functional performance have their origin in the fact that a "non-relevant" property of the catalyst has been analysed that is not clearly related to the function. The typical example is the application of powder diffraction phase analysis in correlation with catalytic performance. In general, there exists a relation between bulk structure and surface properties that is, however, difficult to unravel as reconstructions that minimise the free energy tend to grossly modify the bulk structure in the surface-near region. In Figure 1.1 the example of an oxide system is shown[1]. It should be noted that the layer distances between the top atomic layers deviate in both directions from the respective bulk values by a factor of 2. It is the great virtue of surface science of catalytic model systems to provide such data that cannot otherwise be obtained As these reconstructions are usually controlled by the reaction variables, there exists not only no correlation between bulk and

surface structure but also no correlation between surface structures at different testing conditions (at room temperature in air versus high temperature-reacting atmosphere). The same governance of surface energy minimisation may mislead particle size effect analysis by the fact that particles under X-ray diffraction or TEM conditions or even in the selective chemisorption test experiment may be of quite different size and shape than under reaction conditions.

In other cases the analytical tool may probe the relevant surface property of the material but the test conditions are so vastly different from the reaction conditions that a non-relevant state of the system is probed. The only moderate success of surface analysis with its arsenal of methods is the archetype example of this phenomenon. In Figure 1.2 this is illustrated for the NEXAFS spectrum of a (001) single crystal surface of MoO_3 prepared by standard UHV conditions and annealed in-situ at 10 mbar oxygen pressure and at a temperature of 673 K. The average bonding state of oxygen is different in the two cases with the spectra indicating a substantial chemical reduction of the surface under UHV condition that was re-oxidised at moderate oxygen pressure[2]. It is obvious that two different materials are studied under two different partial pressures of oxygen. As for most studies the in-situ preparation is not accessible, these studied deal with oxygen deficient and partly reduced oxide surfaces although they are considered to be intact MoO_3 surfaces. This discrepancy has serious consequences when for example bulk-sensitive experiments, catalytic data on nominally MoO_3 samples or theoretical results are compared with such "faulted" data.

The only way around these for the catalytic problem irrelevant efforts in describing the functional state of the material is the investigation of a given property proven to be related to the catalytic function under test conditions typical

Fig. 1.2. Figure 1.2: Oxygen K-edge NEXAFS spectra of single crystalline MoO_3 under two different oxygen partial pressures

for the practical application. This ideal request can, however, not be fulfilled in most cases.

The compromise between the practical application conditions and the physical requirements of the analytical tool has to be made such as that the testing conditions are shown to deliver the same qualitative behaviour in the analytical mode and in the practical mode. A safe test for this is the analysis of a series of catalysts that show the same sequence of performance under the different testing condition in the in-situ cell and in a kinetically well-defined reactor. In Figure 1.3 the example of such a comparison is shown for a series of four catalysts for the selective oxidation of butane to maleic anhydride. Four different samples of bulk vanadyl pyrophosphate (VPP) were obtained by different preparative protocols and exhibit different steady state catalytic performances under the same test conditions at atmospheric pressure of the reactants and after a sufficient time of continuous operation (equilibration). These materials were then tested under conditions required for an in-situ high pressure NEXAFS experiment that was performed at 2 mbar pressure at the same temperature and with same gas fed composition that was used in the tubular flow reactor. The kinetic conditions between this reactor and the in-sit cell that is a flow through reactor with a large dead volume and no forced flow through the sample are significantly different and it cannot e expected to observe the same macrokinetic behaviour. Yet it can be seen that the same relative sequence of productivity to maleic anhydride and hence the same relative selectivity can be achieved in the in-situ cell and in the kinetically well-defined reactor. In such a case it can be expected that the "chemical lock-in experiment" will be meaningful.

The proof of the relevance of the analytical property for the function can be always achieved by the detection of the effect of a forced excursion from steady state operation on the spectroscopic property. This chemical lock-in test has to reproduce the temporal pattern of the kinetic perturbation in the spectral property under study. An illustration of this technique is shown in Figure 1.4 performed with the in-situ NEXAFS technique of one of the VPP catalysts used for the experiments in Figure 1.3. In this example the perturbation was a fast change of the sample temperature at constant gas flow that switched off and on again the production of maleic anhydride. The spectral property that follows the catalytic operation is the intensity of a particular resonance in the V L3 edge NEXAFS signal of the VPP sample. This reversible change in intensity indicates a change in the local electron density (partial chemical reduction) in the particular vanadium-oxygen bond that gives rise to that resonance[3].
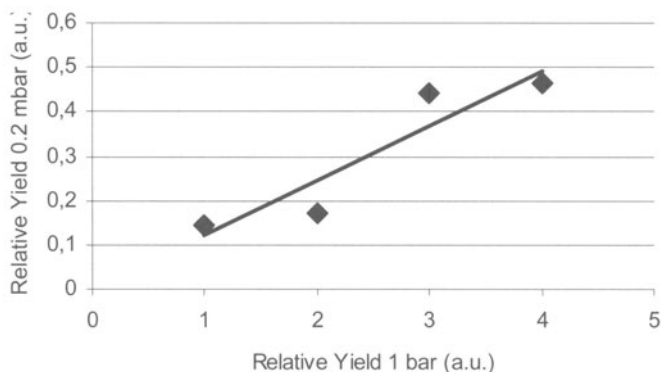
Fig. 1.3. Correlation between the catalytic activity Figure 1.3: Correlation between the catalytic activity of four VPP catalysts at atmospheric pressure (abscissa) and in the in-situ cell of a NEXAFS experiment (ordinate) at 2 mbar. Test conditions were: 673 K, O_2:n-butane 1.2% in He.

The methodology of in-situ testing has to be adaptable to the form of the functional material. This means that methods only applicable to model systems such as planar samples or single crystals are of limited value for catalysis research if they cannot be brought to bear on polycrystalline "practical" catalysts. The
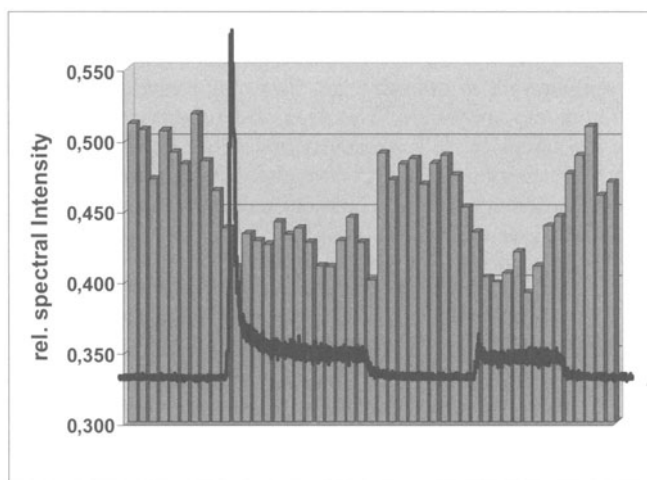
Fig. 1.4: Correlation of catalytic performance of a VPP system in butane oxidation to maleic anhydride (black curve m/e 99 mass spectrometric trace) with the NEXAFS intensity change of a V-O-V anti-bonding state.

corresponding adaptation has usually the consequence that part of the rigorous data analysis becomes uncertain or even impossible. All physicochemical methods require well-defined samples for results that can be interpreted to the limit of the theoretical understanding of the method. This rigor has to be abandoned partly for the benefit of obtaining information from real world systems. A multiple analytical approach and frequent comparison with results obtained from nominally similar model systems can minimise the discrepancy between the two worlds of analysis that prohibits to a good deal the efficient exploitation of the arsenal of methods for in-situ characterisation. There is -in principle- no excuses for not doing in-situ analysis on technical catalytic materials other than these experiments are intrinsically difficult. The argument of the intolerable effort for in-situ characterisation would found to be invalid would the wasted effort on characterisation of with the catalytic function unrelated properties be taken into account.

2. Performing in-situ Analysis

2.1 Choice of Methods, Work Flow

The analytical effort for in-situ characterisation can be minimised by the choice of the appropriate method. The following section lists a selection of useful techniques. In Table 1 a compilation of methodical acronyms is given together with its principal characteristics as referred to surface sensitivity, probe species, sample requirements and principal in-situ capability. For the sake of complete information a selection of ex-situ techniques frequently used in characterisation work is included. All in-situ techniques are implicitly capable of analysing samples ex-situ, which is not case vice versa. The following abbreviations are used in the table: **L**=local information, **I**=integral information, **b**=bulk informations=surface sensitive information, **Ex**=ex-situ method, **In**=in-situ method, **D**=destructive to the sample, **Nd**=non-destructive method, **(Nd)**=principally non-destructive but stability problems of catalyst samples under examination conditions.

It is absolutely essential for the successful application of in-situ methods to know important ex-situ characteristics of a given catalyst system in order to select the appropriate in-situ method and more importantly to correctly define the conditions for the in-situ experiment. Typical information that is prerequisite is collected in the following "check-list":

1. Type of catalyst (supported, massive, nanostructured), morphology
2. Complete chemical composition, including if possible trace elements
3. Catalytic activity, selectivity, Arrhenius parameters
4. Specific surface area, density, porosity
5. Structural phase composition, crystallinity, amorphous components
6. Thermal behaviour, thermostability, phase transitions
7. Kinetic behaviour in the in-situ cell, effects of specimen preparation
8. Irreversible reactions with the feed (carbon deposition, exothermic excursions during intentional or unintentional oxidation

Info 1 is essential to know about the ratio of surface–near atoms in relation to bulk atoms. This helps to decide how relevant for catalysis are bulk structural techniques and how severe complications may become with the data analysis of diffraction techniques having to deal with small particles and interface regions. It is highly advisable to have electron microscopic information both by SEM and TEM in order to know the textural disposition of the starting sample. It is also good practice to re-examine the texture after the in-situ experiment checking for eventual changes

Info 2 is essential for planning the spectroscopic observations. For high-sensitivity experiments it is crucial to know about additives, promoters or un-intentional foreign elements as they can produce "spurious" signals or ruin e.g. EXAFS energy scans and require often a change in the energy levels to be observed. For magnetic resonance experiment it is also of relevance to know about paramagnetic impurities that can either spoil NMR observations or help the analysis as EPR-active centres.

Info 3 is of central relevance as only the comparison between catalytic behaviour in proper reaction environments and under the in-situ conditions allows concluding that the relevant state of material is being investigated. In many systems even the observation of some catalytic activity is not sufficient as one and the same reaction may proceed under different conditions with differing pathways and hence produce different spectroscopic signatures. As the performance in terms of activity and selectivity will be very difficult to obtain in identical figures in the two reaction environments it is important to compare the Arrhenius parameters and, if possible, reaction orders of key components in the feed. If these parameters agree reasonably one is safe to assume that the reaction is the same in normal operation and under in-situ conditions.

Info 4 is important to determine how much active surface is in an in-situ cell and how much products or adsorbates can be expected to be analysed. Porous materials require in general considerations for out gassing under reduced pressure and for extended time profiles in observation to allow equilibration of the solid with the gas phase.

Info 5 is a prerequisite to select the analysis strategy. The phase information should be checked after the in-situ experiment if it is not subject of analysis. The degree of crystallinity decides over many spectral properties and may require specific techniques to be applied if poor crystallinity (nanostructured) or even amorphous components can be of relevance for the function. This is almost always the case when solid-state reactivity or phase transformations occur during catalytic function. Knowledge about phase composition and average local co-ordinations is required to model EXAFS data and to define experiments sensitive to hyperfine coupling that is so sensitive to the local symmetry around the atomic probe.

Info 6 refers to structural stability of the bulk and eventually present adsorbates. Thermoanalysis and temperature-programmed desorption techniques should always be applied prior to in-situ investigation. The signatures of phase transformations must be found in the in-situ experiment at temperatures that resemble the ex-situ studies. If significant deviations occur or if transformations occur differently from the ex-situ analysis, then important conclusions can be drawn about the role of in-situ reaction conditions on the stability and constitution of a catalyst. Detailed knowledge about thermostability of the sample is required as often high temperature clean-up procedures or extended ranges of reaction temperatures are chosen to find relevant changes in the in-situ experiments. Such

experimental procedures should always be limited to temperature ranges where it is known that no stability problems of the starting materials occur.

Info 7 is advisable to have prior to the in-situ experiment. It is useful to test the sample after its preparation (e.g. pelletising or filling into a capillary) in the in-situ cell for catalytic function. A balance of stoichiometry between feed and product stream should be constructed giving hints to losses of molecules either at the catalyst or at the reaction environment (reactor wall, windows, tubing) being often at temperatures allowing condensation or thermal decomposition. Such losses must be avoided under all circumstances during the hot in-situ experiment as the deposits may interfere with the course of the reaction (clogging), destroy the windows or result in non-typical deactivation phenomena of the catalyst (deposition during re-circulation operation of a process normally operated in the flow-through mode).

Info 8 is related to these topics and is of crucial importance for safety consideration during in-situ operation. Unattended operation or operation at large-scale facilities requires a high safety standard. To assess the chemical risk during experimentation any excursions in temperature or pressure that may occur with the activated sample by intentional or unintentional contact with environmental or reactant gases must be known.

If the necessary pre-information is collected then in-situ experiments can be considered. In order to allow the reader to choose from the large selection of possible methods the Table 1 provides basic information about the probe species and the response of the sample under study. This information has implications on choice of partial pressures (interactions between probe and reaction atmosphere) of reactants and products, on the choice of window materials and on sample requirements.
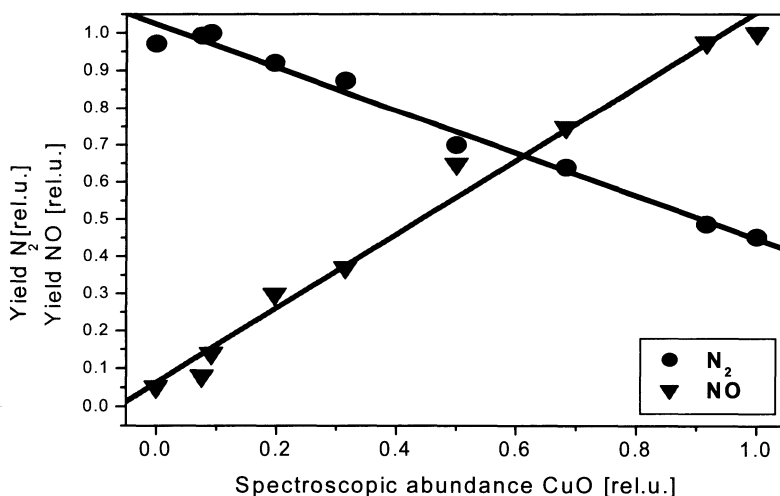
Fig. 2.1: Spectroscopy-function correlation for the partial oxidation of ammonia over polycrystalline Cu foil. Conditions: 0.8 mbar pressure, 50:1 O_2:NH_3 and 673 K

There is no universal in-situ method. Each catalytic problem requires usually a set of in-situ experiments that is tailored to the question under study. Never should be only a single in-situ experiment be carried out as the often extreme demands in experimentation tend to lead to artefacts that are effectively only discovered by contradictions between experimental data. In several families of methods the examination of several independent properties of a sample under the same conditions can fulfil this request.

Figure 2.1 gives a worked example of a quantitative structure-function relationship from in-situ analysis. NEXAFS data were obtained from a polycrystalline Cu foil in the selective oxidation of ammonia to di-nitrogen. This reaction is of interest for tail gas cleaning after SCR systems. The formation of total oxidation products NO_x is thus to be avoided even in the typical enormous excess of oxygen over ammonia. The correlation shows the yields of nitrogen and NO measured by calibrated mass spectrometry as function of the normalised abundance of CuO covering the surface together with Cu_2O.

It is evident that the unwanted deep oxidation is correlated with the copper II oxide abundance at the surface whereas the desired partial oxidation reaction requires the presence of copper I oxide. It is interesting to note that the specific site requirement of copper I oxide and copper II oxide for the formation of one product molecule is the same as occurs from the difference in slopes reflecting the different stoichiometry of the products. The co-existence of the two oxides at the surface under these harsh reaction conditions is quite unexpected and would not have been predicted from ex-situ analysis. Quench experiments showed after cooling to 300 K only the presence of copper II oxide that was expected from the excess of oxygen and the temperature.

The method was also suitable to prove that the same reaction pathway was adopted when Cu clusters deposited on carbon were used instead of the Cu foil. The reaction proceeded to completion at about 150 K lower temperatures than with the foil indicating that small metal particles seem to form the required oxides at more moderate conditions than the extended solid[4].

Table 1: List of commonly used characterisation techniques. The ordering follows the acronyms. Multiple acronyms for the same technique are cross-referenced. For the meaning of the abbreviations see text.

Acronym	Full text	Type of information	Application for	Probe	Response	Conditions
AAS	Atomic absorption spectroscopy	I, b, ex	Elemental composition	Photons	Photons	D, dissolution of solid samples
AEM	Analytical electron microscopy	L ,b, ex	Elemental composition	Electrons	Photons	Nd, transparent for TEM, beam damage, high vacuum
AES	Auger electron spectroscopy	I ,s, ex	Surface composition, chemical bonding	Electrons	Electrons	Nd, UHV, conducting sample, beam stability, see SAM
AFM	Atomic force microscopy	L, s, ex, in	Morphology,atomic structure	Electrostatic force	Topography, friction	(Nd), Needs flat surfaces, artefacts possible, see NC-AFM
AP-MS	Appearance potential mass spectrometry	Kinetics	Metastable intermediates	Sample gas	Ions	With line of sight reactor under atmospheric pressure
AS	Atom scattering	L, s, ex	Surface atomic structure	Atoms	Atoms	Nd, UHV, single crystals
ASA	Active surface area	Kinetics	See Chem			
BET	BET method	L, s, ex	Surface area, porosity, texture	Gas	Pressure change	Nd, Very flexible, see Chem, TSA
BF	Bright field imaging	See TEM, HRTEM, AEM, CTEM	Contrast formation mode using all diffracted beams	Electrons	Electrons	Nd, Normal imaging mode in TEM
CEMS	Conversion electron Mössbauer spectroscopy	I, s, ex, in	Surface chemical constitution	γ-rays	Electrons	Nd, restricted to few elements (Fe, Sn, Au)
Chem.	Chemisorption	I, s, in	Surface reactivity, active surface area, analysis via Langmuir formalism	Gas, or molecules in solution	Pressure change, or concentration change	(Nd), Versatile routine method for determination of active site abundance in complex catalysts

Acronym	Full text	Type of infor- mation	Application for	Probe	Response	Conditions
CI-MS	Chemical ionisation mass spectros- copy	Kinetics	Gas phase composition, time resolved, isotope labelling	Sample gas, reactive auxiliary gas, electrostatic field	Ion	D, Catalytic process monitoring, gas phase
CPD	Contact potential difference measureme nts	I,s,ex, in	Qualitative and quantitative chemisorption analysis	Surface charge	Capacitance	Nd, Surface potential, extremely sensitive to impurities
CP-MAS	Cross pola- risation magic angle spinning NMR	I, b ,s, ex, in	Local bulk structure, adsorbate structure	High frequency radiation (MHz) external magnetic field, mechanical sample rotation	High- frequency electrostatic field, variations in	Nd, Wide range of nucleii, (H,C,P, Al, Si and metals), only for diamagnetic samples, in-situ limited
CTEM	Conven- tional trans- mission electron microscopy	L, b, ex	Local struc- ture, defects, nanostructures	Electrons	Electrons	Nd, Only thin samples, beam- stability pro- blems, high va- cuum, see TEM
CV	Cyclovolta- metry	I, s, in	Redox proper- ties, reaction kinetics, ele- mentary reac- tion steps, electrocata- lysis	Electrons at varying potential	Current	Nd, Requires condensed phases, electro- lyte problem, surface - sensitive
DF	Dark field imaging	See TEM, HRTEM, AEM, CTEM	Contrast formation using selected diffracted beam	Electrons	Electrons	Nd, Imaging mode resolving abundance and distribution of a selected struc- tural element (lattice plane) in TEM
DR	Diffuse reflectance		Mode of spectroscopy with photons for "dark" solid samples	Photons	Photons	Nd, works for IR and UV spectroscopic methods
DRIFTS	Diffuse reflectance Fourier transform infrared spectros- copy	I, b, ex, in	Vibrational analysis of catalysts and adsorbates	IR- light	IR-light	Nd, Wide range of applications with gas, solid, liquid samples, Critical inten- sity analysis,

Acronym	Full text	Type of infor-mation	Application for	Probe	Response	Conditions
DSC	Differential scanning calorimetry	I, b, ex	Solid state structure by specific reactions, phase transfor-mations	Heat, linear variation of temperature	Heat	(D), Polymorph analysis, requires solid state samples, wide range of applications
DTA	Differential thermal analysis	I, s, b, ex, in	Heat flow during solid-state reactions and gas-solid reactions,	Heat at variable temperature	Heat	D, Wide range of application, phase transi-tions, extremely sensitive to chemical reactions
DTG	Differential Thermogra-vimetry	I, b, ex, in	Reaction monitoring by weight changes of solid sample	Gas, variable tempera-ture, con-trolled tem-perature profile	Derivative of sample weight vs temperature or time	D, solid powder samples, see TGA
ED	Electron Diffraction	L, b, ex	Local crys-tallographic analysis of solid particles and thin films	Electrons	Electrons	Nd, Sample good for TEM, good for metric and symmetry, difficult for atom positions (intensity analysis), see also SAD
EDX	Energy-dispersive X-ray emission analysis	L ,b, ex	Local elemen-tal composi-tion, analysis of nanostruc-tures (suppor-ted metal par-ticles) analy-sis of phase mixtures, la-teral distribu-tion analysis	Electrons	X-ray Photons Synonym: EDAX	Nd, Solid samples, beam stability, problems with light elements, attachment to SEM and AEM, CTEM instruments
EELS	Electron energy loss spectros-copy	L, b, ex	Chemical bonding of light ele-ments, lateral distribution analysis with atomic resolu-tion, (solid-solid inter-faces)	Electrons (highly monochrom atic)	Electrons	(Nd), Solid samples, suitable for TEM, high vacuum, beam stability
Ellip.	Ellipso-metry	I, s, in	Thin film properties	Photons (visible light)	Photons	Nd, Solid samples, flat, model catalysts

Acronym	Full text	Type of information	Application for	Probe	Response	Conditions
EPMA	Electron probe micro-analysis	L, b, ex	Elemental composition in flat hetero-geneous samples	Electrons	X-ray photons	Nd, Flat solid samples, high vacuum, similar to EDX
EPR	Electron paramagne-tic reso-nance spec-troscopy	Same as ESR				
ESCA	Electron spectros-copy for chemical analysis	Same as XPS				
ESEM	Environ-mental scanning electron microscopy	L, s, in	Morphology in reactive atmosphere	Electrons	Electrons	Nd, Excellent for insulating samples, works in water and air at ca. 50 mbar pressure
ESR	Electron spin resonance spectros-copy	L, b, ex, in	Paramagnetic centres and radicals in and on catalysts	High fre-quency radiation (GHz) external magnetic field	High Frequency radiation	Nd, Solid, liquid samples, very sensitive, limited in-situ capabilities
EXAFS	Extended X-ray absorption fine structure	L, b, ex, in	Local atomic structure, see also NEXAFS	X-ray photons	X-ray photons, (conversion electrons)	Nd, Works for amorphous and crystalline samples, very flexible, com-plex data ana-lysis, good for in-situ studies, requires synchrotron
FEM	Field emission microscopy	L, s, ex	Single atoms on metals	El. Static field	Electrons	Nd, UHV, very limited in mate-rials and sample (tip), extreme resolution, dynamics of atoms, model reactions
FIM	Field ion microscopy	L, s, ex	Single atoms on metals	El. Static field, gas atoms	Ions	Nd, See FEM

Acronym	Full text	Type of information	Application for	Probe	Response	Conditions
FT-IR	Fourier-transform infrared spectroscopy	I, s, b, ex, in	Vibrational analysis of catalysts and adsorbates	IR- light	IR light	Nd, Extremely versatile method, excellent in interpretation, chemical and structural information, numerous methods for all types of samples, good in-situ capabilities
FT-R	Fourier-transform Raman spectroscopy	I, s, b, ex, in	Vibrational analysis of catalysts and adsorbates	Light (IR, visible)	Light	(Nd), Solid liquid samples, beam stability, intensity difficult to analyse, good in-situ capabilities
GC	Gas chromatography	Kinetics	Qualitative and quantitative gas analysis	Gas	Detector responses (conductivity, ionisation MS, alight absorption, electron capture etc)	Nd, Extremely versatile family of methods for separation and quantification of all gas mixtures, advanced instrumentation and analysis, routine method in all catalytic problems
GC-MS	Gas chromatography coupled mass spectroscopy	Kinetics	Qualitative and quantitative analysis of complex gas mixtures	Gas	Ion current	D, See GC, excellent for identification of molecules, isotope labelling studies
GR-XPD	Grazing incidence X-ray powder diffraction	I, s, ex	Phase analysis, film thickness and roughness analysis of thin film solid samples	X-ray photons	X-ray photons	Nd, surface-sensitive variety of powder diffraction, requires flat samples, morphology analysis difficult for complex film compositions, model studies

Acronym	Full text	Type of infor-mation	Application for	Probe	Response	Conditions
HPLC	High pressure liquid chromato-graphy	Kinetics	Quantitative analysis of liquid samples	Liquid	Detector signals (light ab-sorption, electrical conductivi-ty, spectros-copy)	Nd, See GC Universal for all liquid mixture analysis problems
HREELS	High-resolution electron energy loss spectros-copy	I, s, ex	Vibrational analysis of adsorbates on flat surfaces	Electrons (low energy), extremely mono-chromatic	Electrons	Nd, UHV method, single crystal, electro-nic conductivi-ty, mind selec-tion rules, inter-pretation similar to FT-IR
HREM	High resolution electron microscopy	Same as HRTEM				
HRTEM	High resolution electron microscopy	L, b, ex	Projection of atomic struc-ture into two dimensions, visualisation of lattice fringes analy-sis of solid interfaces and defect struc-tures	Electrons (high energy)	Electrons	Nd, Solid samples, high vacuum, transparent for electrons, interpretation only with model calculations and crystallographic model, see ED
ICP-MS	Inductively coupled Plasma mass spectro-metry	I, b, ex	Elemental chemical analysis, trace analysis	Atoms in solutions	Ions	D, liquid samples, ex-tremely sensi-tive, requires extensive che-mical prepa-ration of solids
IMP	Ion microprobe	L, s, ex	Surface elemental mapping , speciation by fragments, see SIMS	Imaging Ions (high energy)	Sample Ions	D, Solid sample, extremely sensitive, UHV quantification difficult
IMR-MS	Ion molecule reaction mass spectros-copy	Kinetics	Gas phase analysis with MS reducing the fragmen-tation of analyte ions	Primary ions	Product ions	Nd, Very mild ionisation reduces frag-mentation to analyse strongly overlapping mass spectra of small molecules

Acronym	Full text	Type of information	Application for	Probe	Response	Conditions
IR	Infrared spectroscopy	L ,i, s, b, ex, in	Vibrational analysis	See FT-IR, DRIFTS		Nd, Family of spectroscopic methods giving a wealth of chemical structure information on catalyst and adsorbates, in solid, liquid and gaseous states numerous in-situ capabilities, microspectroscopy for lateral inhomogeneous samples
ISS	Ion scattering spectroscopy	I, s, ex	Elemental analysis of the topmost atomic layer	Ions (noble gases)	ions	D, UHV, solid samples quantification difficult
LEED	Low-energy electron diffraction	I, s, ex	Surface crystallography	Electrons (low energy)	Electrons	Nd, UHV, single crystal, ordered surface structure, electrical conductivity
LEIS	Low-energy ion scattering spectroscopy	Same as ISS				
LIF	Laser-induced fluorescence spectroscopy	Kinetics	In-situ analysis of traces in gs phase, no sampling	Light (IR, visible)	Light	Nd, Gas phase, lateral resolution in reaction volume, very specific, large molecules
LMMS	Laser microprobe mass spectrometry	L, s, b, ex	Local surface and bulk composition	Laser light	Ions	D, Solid samples, high vacuum, complex data analysis, Syn. LAMMA
LRS	Laser Raman spectroscopy	I, b, ex, in	Vibrational analysis of catalysts	Laser-Light (IR, visible)	Light	(Nd), Solid samples, beam stability, microspectroscopy, good in-situ capabilities
Magn.	Magnetic susceptibility measurements	I, b, ex, in	Bulk electronic structure, Redox state	Magnetic field	Force, magnetic field	Nd, Measured with magnetic balances or SQUID devices

Acronym	Full text	Type of information	Application for	Probe	Response	Conditions
MAS	Mössbauer absorption spectroscopy	I, b, ex, in	Geometric and electronic structure	γ-rays, mechanical motion	γ-rays	Nd, Solid samples crystalline or amorphous, limited to few practically measurable elements (Fe, Sn, Au, I), good in-situ capabilities, advanced analysis
MAS-NMR	Magic angle spinning nuclear magnetic resonance	See CP-MAS, NMR				
MBS	Molecular beam scattering	Kinetics, surface structure	Kinetics of elementary step processes, atom scattering for surface crystallography	Molecules (in defined energetic states)	Molecules, scattered or reacted	UHV, single crystal, model experiments
Merc.	Mercury porosimetry	I, b, ex	Porosity and pore shape in Solids	mercury	Pressure	D, widely used routine technique, best for larger pores, complementary to BET analysis
MS	Mass spectrometry	Kinetics, detector for secondary and scattered ions	Many applications in gas analysis, secondary ion spectrometry and isotope-labelling methods	Gas plus ionisation source (electrons, ions)	Ions and ionised fragments	Many instrument types, quadrupoles , TOF and magnetic focussing instrumentation
NC-AFM	Non-contact AFM	See AFM				Nd, Special mode avoids artefacts through strong forces between sample and tip
NEXAFS	Near-edge X-ray absorption fine structure spectroscopy	L, s, b, ex, in	Local electronic structure of solids	X-rays, variable wavelength	X-rays	Nd, solid samples, fingerprint technique, difficult analysis, good for in-situ studies, requires synchrotron, see EXAFS

Acronym	Full text	Type of information	Application for	Probe	Response	Conditions
NMR	Nuclear magnetic resonance	I, b, ex, in	Local structure of catalysts , model compounds and of adsorbates, dynamic motion of molecules, in-situ imaging	Magnetic filed, high frequency (MHz) radiation	High frequency radiation	Nd, Very wide application for liquid and solid samples, wide range of nucleii, limited to diamagnetic samples, see also CP-MAS, MAS-NMR, limited in-situ capability, excellent interpretation
NS	Neutron scattering	I, b, ex	Structure of solid and liquids, magnetic ordering, hydrogen structures	neutrons	neutrons	Insensitive, requires nuclear reactor, versatile for many structural aspects, scattering law different from X-ray scattering
OM	Optical microscopy	I, b, ex, in	Morphology, phase transformation , in situ reaction monitoring	Visible light	Visible light	Nd, Polarisation analysis, suitable for solids and liquids, good in-situ capabilities
PAS	Photoacoustic spectroscopy	I, s, b, ex, in	Vibrational analysis of strongly absorbing systems	IR-light	Sound waves	Nd, versatile solid sample environment, difficult to analyse data
PES	Photoelectron spectroscopy	Designates XPS and UPS				
Physisorp.	Physisorption	L, s, ex	Integral surface area determination, see BET	Gas	Pressure	Nd, Weak interaction of probe molecule with solid samples,
PIXE	Proton-induced X-ray emission	I, b, ex	Trace elemental analysis	High energy protons	X-rays	D, requires accelerator

Acronym	Full text	Type of infor-mation	Application for	Probe	Response	Conditions
Raman	Raman spectros-copy	I, s, b, ex, in	Vibrational analysis, complemen-tary selection rules to IR	Light (IR, visible)	Light	Beam damage problem with solid samples, very versatile, intensity diffi-cult to analyse, excellent in-situ technique for catalyst struc-ture, not very surface-sensitive
RBS	Rutherford back-scattering	I, b, ex	Elemental analysis, depth resolved	Ions (high energy)	Ions	Nd, solid samples, requires accelerator
RED	Radial electron distribution	I, b, ex	Description of geometric structure in non-crystal-line solids	Can be determined by several methods	See: EXAFS, ND, XRD, SAX, ED	Nd, Synonym: RDF (radial distribution function)
REMPI	Resonance-enhanced multi-photon ionisation spectros-copy	Kinetics	In-situ detection of small concentrations of product species	Photons	Ions	Nd, Space-time resolved mecha-nistic studies, high throughput testing, model reactions with single crystals, complex experiment
SAD	Selected area electron diffraction	L, b, ex	Crystallogra-phic infor-mation from nanostructures in solids	Electrons	Electrons	Nd, TEM samples, high vacuum, inten-sity analysis difficult,
SAM	Scanning Auger Microscopy	L, s, ex	Morphology with elemen-tal resolution	Electrons	Electrons	Nd, UHV, flat samples, model systems, see AES
SAX	Small-angle X-ray scattering	I, b, ex, in	Micromor-phology and porosity of powder samples	X-ray photons	X-ray photons	Nd, analysis difficult, re-quires structural model, comple-mentary to Merc. and BET, also for amor-phous and col-loidal samples

Acronym	Full text	Type of infor-mation	Application for	Probe	Response	Conditions
SEM	Scanning electron microscopy	I, s, b, ex	Morphology, particle size. Pore size	Electrons	Electrons	Nd, solid samples, high vacuum, conductivity necessary, wide range of samples, often in combination with EDX, see also ESEM
SERS	Surface enhanced Raman scattering	See LRS, Ft-R				Nd, Extreme enhancement for adsorbate vibrations on certain metals (Ag) with special structures
SEXAFS	Surface-sensitive extended X-ray absorption fine structure	L, s, ex	Local atomic bonding geometry of adsorbates	X-rays (variable wavelength)	Electrons (X-rays for fluorescence detection)	Nd, UHV, single crystal, model systems
SFG	Sum frequency generation	I, s, in	In situ vibrational analysis of small adsorbed molecules	Laser light, two sources	Light	Nd, requires flat surface, non-linear optical effect, interpretation like IR, complex experiment
SHG	Second harmonics generation	I, s, in	In –situ analysis of gas-solid interfaces	Laser light	Light	Nd, requires flat surfaces, non-linear optical effect, difficult in interpretation, model experiment
SIMS	Secondary ion mass spectroscopy	I, s, b, ex	Local elemental and chemical composition, depth profiling	Primary ions	Sample ions	D, Solid, flat samples, complex information, quantification difficult, see also IMP, SNMS
SNMS	Secondary neutral mass spectroscopy	I, s, b, ex	Local elemental and chemical composition, depth profiling	Plasma and electron impact ionisation	Sample ions	D, Solid flat samples, good for insulators, complex information, quantification difficult, see also IMP, and SIMS

Acronym	Full text	Type of infor-mation	Application for	Probe	Response	Conditions
SPM	Scanning probe microscopy	See also STM, AFM				Nd, Family of methods using a variety of probes other than tunnelling current or atomic forces. These probes are scanned by the same technique as in STM over the solid sample.
SSITKA	Steady state isotope transient kinetics analysis	Kinetics	Reaction mechanism	Isotope-labelled educts as pulse in steady state feed	Scrambled isotope labels in all components, MS analysis	Nd, Time resolved gas phase analysis required
STEM	Scanning transmission electron microscopy	L, b, ex	High resolution structural and compositional analysis of discontinuous solids (interfaces, supported particles)	Electrons (scanned beam)	Electrons, usually combined with EELS	Nd, flat thin solid samples, best for designed interfaces allowing atomic resolution
STM	Scanning tunnelling microscopy	I, s, ex, in	Surface imaging with atomic resolution and limited chemical contrast. Sensitive to regular and defective structures, surface topography on all length scales from atoms to microns	Electrostatic potential	Current	Nd, Very versatile for all kinds of solid conducting samples, UHV, in-situ capabilities, also at solid-liquid interfaces, limited range of temperature variation
STS	Scanning Tunnelling spectroscopy	L, s, ex	Local electronic structure near the Fermi edge with atomic lateral resolution	Electrostatic potential (gap voltage, scanned)	Current (derivative vs. gap voltage)	Nd, Ideal for active site analysis, problems with sample drift and interpretation due to tip effects
TA	Thermal analysis methods	I, b, ex, in	Reaction monitoring for gas-solid and solid-solid processes	Gas, variable temperature, linear heating	Weight change, heat flow	D, powdered solids, versatile method, fingerprinting technique

Acronym	Full text	Type of information	Application for	Probe	Response	Conditions
TDS	Thermal desorption spectroscopy	I, s, ex	Thermodynamic and kinetic parameters of sorption processes	Pre-adsorbed gas, variable temperature, linear heating	Partial pressure changes	D, UHV method, best for single crystals, requires multiple experiments for data analysis, yields no information about reaction, no equilibrium between gas and solid
TEM	Transmission electron microscopy	L, i, b, ex	Regular and defective bulk structure with varying resolution	Electrons	Electrons	Nd, versatile family of methods for bulk structural analysis, sensitive to chemical and structural defects, solid samples, transmission condition requires thin samples (nm), beam stability problems
TGA	Thermogravimetric analysis	I, b, ex, in	Reaction monitoring by weight changes of solid sample	Gas, variable temperature, controlled temperature profile	Weight change	D, excellent in-situ capability, versatile for many solid-state reaction problems, problems with transport limitations in gas-solid reactions (kinetics)
TPD	Temperature-programmed desorption	I, s, in	Thermodynamic and species analysis of chemisorbed molecules on an activated catalyst	Gas, temperature rise with defined time profile	Molecules desorbed and/or converted detection with GC, MS	D, works in continuos gas-solid equilibrium, with powders complementary to TDS, yields reaction parameters not chemisorption parameters
TPN	Temperature-programmed nitridation	I, s, in	Thermodynamic and kinetic parameters of solid state nitridation reactions	Gas, temperature rise with defined time profile	Consumption of ammonia gas	D, solid powders, follows formation of metastable nitride catalysts (HDS, HDN)

Acronym	Full text	Type of information	Application for	Probe	Response	Conditions
TPO	Temperature-programmed oxidation	I, s, in	Thermodynamic and kinetic parameters of solid state oxidation reactions	Gas, temperature rise with defined time profile	Consumption of oxygen gas	D, solid powders
TPR	Temperature-programmed reduction	I, s, in	Thermodynamic and kinetic parameters of solid state reduction reactions	Gas, temperature rise with defined time profile	Consumption of hydrogen gas	D, solid powders
TPRS	Temperature-programmed reaction spectroscopy	I, s, in	Temperature profile of gas – solid reactions	Gas, temperature rise with defined time profile	Reaction products, detection by MS	Nd, solid powders or single crystals reduced pressure
TPS	Temperature-programmed sulfidation	I, s, in	Thermodynamic and kinetic parameters of solid state sulfidation reactions	Gas, temperature rise with defined time profile	Consumption of hydrogen disulfide gas	D, solid powders, follows formation of metastable sulfide catalysts (HDS, HDN)
UPS	UV photoelectron spectroscopy	I, s, ex	Electronic structure near the Fermi edge	UV photons	Electrons	Nd, all conducting solids, UHV, clean solid surface and adsorbate analysis
UV-NIR	UV-near infrared spectroscopy	I, s, b, ex, in	Electronic structure, redox state	Visible- IR Light	Visible-IR Light	Nd, all solid samples, good in-situ capabilities, interpretation difficult, transmission and reflection geometry
UV-vis	UV-visible spectroscopy	See UV-NIR				Limited frequency range
WAX	Wide angle X-ray scattering	Same as XRD				
XAS	X-ray absorption spectroscopy	Same as NEXAFS				Term used for low-energy NEXAFS/EXAFS
XES	X-ray emission spectroscopy	I, s, b, ex, in	Electronic structure of solids and adsorbates	White X-ray photons	Characteristic X-ray photons	Nd, requires synchrotron, UHV, complex experiment, model studies

Acronym	Full text	Type of infor-mation	Application for	Probe	Response	Conditions
XPD	X-ray powder diffraction	Same as XRD				
XPD	a) X-ray powder diffraction b) X-ray photoelec-tron diffrac-tion	a) Sam e as XRD b) I, s, ex	Local geometry of disordered adsorbates	X-ray photons	Photo-electrons	Nd, UHV, single crystal, model studies requires syn-chrotron, com-plementary to LEED
XPS	X-ray photo-electron spectros-copy	I, s, b. ex	Surface composition, electronic structure	X-ray photons	Electrons	Nd, UHV, ver-satile for solid samples, ad-vanced interpre-tation, surface sensitivity varies, charging phenomena and spectroscopic artefacts hamper proper analysis
XRD	X-ray diffraction	I, b, ex, in	Bulk struc-ture, phase analysis, phase trans-formations, real structure	X-ray photons	X-ray photons	Nd, very ver-satile universal method, works for solids and liquids, powder and single crys-tal methods, good in-situ capabilities, high resolution at synchrotrons
XRF	X-ray fluores-cence spec-troscopy	I, b, ex	Elemental chemical analysis, detection for EXAFS	Electrons, X-ray photons	X-ray photons	Nd, high sen-sitivity, see also EDX and EXAFS, multi-purpose detec-tion technique

2.2   Characteristics of in-situ Cells

All in-situ experiments are most sensitive in their validity to the choice and construction of the reactor that is used for the experiment. A catalyst is always to be seen as unity with its reaction apparatus. Due to the massive influence of heat and mass transport phenomena on one side and of reactions of the gas phase components with the solid catalyst on the other side, the choice of the gas flow, the accuracy of temperature control, the dynamics of heat and mass transport and the presence of detectors, heaters and windows of unusual materials will affect the catalytic performance. In addition, many reactors are built such that their surface is equal or even larger than that of the surface of the active material. Thus reactions and condensation processes have to be considered carefully when interpreting the catalytic data that inevitably are not identical to those of the same catalyst in a conventional microreactor.

In-situ cells have also to accommodate to the physical requirements of the analytical experiment. These conditions often impose stringent conditions on e.g. transmittance of a sample wafer or on a small distance of a hot catalyst from a cold window or of the size of a sample in relation to the cell size. The presence of the reaction atmosphere almost always deteriorates the performance of the technique. For this reason as well as for the ease of the kinetic analysis it is prerequisite to minimise the cell volume and so to minimise the dead volume of the reactor and of its connection lines.

A critical practice is often applied in structural research where the spectral resolution of an experiment is enhanced by "quenching" the sample from reaction conditions to low temperatures (300 K or even cryogenic temperatures). Such "in-situ" cells are built around a low temperature cryostat and either can counter-heat the sample or move the sample to a reaction stage mounted usually above the line of sight of the analytical instrument. In surface analysis all "in-situ" experiments are carried out in this mode, in EXAFS it is custom to quench samples with small particles to enhance structural definition (signal), in Mössbauer spectroscopy real in-situ operation is rare as compared to "off situ" operation and also in probe molecule vibrational spectroscopy the off-situ mode is very common.

These assemblies are to be considered very critical as during temperature and/or gas quench uncontrollable transformations of surface and bulk of the catalyst may happen. If the "off-situ" mode is unavoidable then every effort should be made to minimise the volume of the assembly and to move the sample rather than to control the temperature of a fixed sample by brute force. Bulky coolant lines and high-power heating systems are quite incompatible with real catalytic performance.

When reduced pressure between a few millibars and atmospheric pressure has to be used great care should be paid to the way of reducing the pressure. The usual method of pumping versus a gas flow provided at atmospheric pressure needs to be controlled for:

☐ Contamination by pumping fluids (use dry pumps whenever possible)
☐ Stability of the pumping speed (valve system, capillary flow restrictors, apertures for pump regulation)

☐ Avoiding of preferential pumping (happens when condensable and non-condensable molecules are mixed)
☐ Oscillatory behaviour induced by the regulating systems of the mass flow controllers (use correct flow restrictors)

Otherwise substantial problems with sloping reactant partial or total pressures will occur not only in the spectroscopy data (absorption changes) but also in the kinetic data and eventually also in the catalyst lifetime and stability.
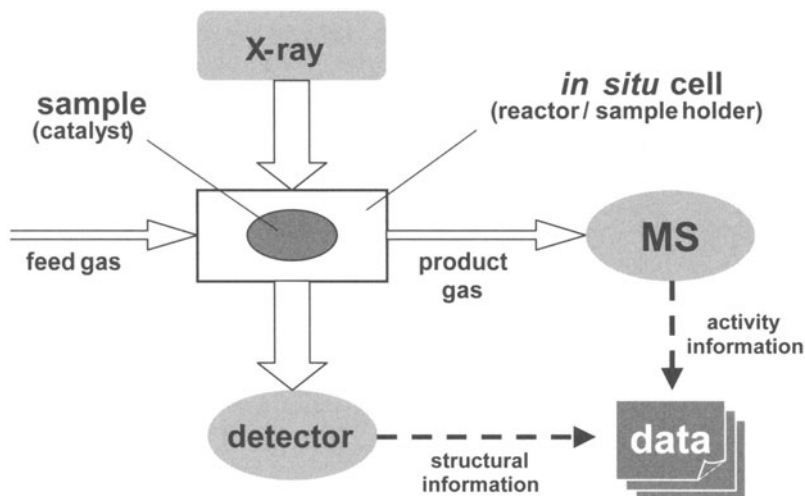
Fig. 2.1: Schematic representation of an in-situ cell for structural evaluation (XRD, EXAFS, XAS).

A typical in-situ cell system that may be used for structural work but would look very similar for vibrational or UV-vis experiments is depicted in Figure 2.1. The cell is the crossing point of two streams of molecules and of photons meeting at the sample position. The feed needs to be carefully controlled (via bypass not shown in the scheme). It is good practice to use a guard reactor filled with the catalyst material in the feed stream. At low temperatures the guard material cleans the gas stream. At intermediate temperatures the guard reactor can be used to simulate a plug flow reactor situation in which the typical catalyst sees a mixture of educt and products. Such studies with varying levels of product content can be used for simulations of deactivation processes (coke formation).

The scheme illustrates evidently that it is difficult to control the energy flow to and from the catalyst as it sits in the centre of the cell. Heater systems within the gas flow are best for temperature control but require very careful shielding from the gas phase. As the heater is always and often substantially hotter than the catalyst a large number of side reactions can modify the gas phase composition (decomposition, radicals etc). In addition, corrosion of the heater tends to inhibit the heat flow to the catalyst and produces secondary catalytic material (heater

metal oxides). Thus light heating by e.g. diode laser systems or external heating with a transfer gas (educts mixed with He) are safe alternatives.

Substantial attention should be paid to the temperature control. It is essential to have a micro-thermocouple as close as possible at the sample site. As the mass of the sample is usually very small, the thermal response of the regulator system must be fast requiring a non-damped input signal. External thermocouples or over-protected sensors (in quartz tubes or ceramic hulls) must be avoided whenever the chemistry allows it. It is not acceptable to ignore the thermal gradient of the in-situ cell and to measure the temperature only at the outer wall of the cell. Even when this location is calibrated in the laboratory, the variation in gas flow conditions and the varying sample contact (after sample change) are constant sources of error. It is good practice to use the catalytic performance itself as in-situ thermometer. If the kinetics is well-enough known it is possible to deduce the sample surface temperature from conversion and selectivity data. Structural techniques analysing the lattice constant or cell volume of crystalline materials as function of temperature can also check the temperature control.

The product gas stream needs to be analysed with high sensitivity and suitable temporal resolution on line with the data acquisition. The calibrated mass spectrometer is a widely used detector, gas chromatography (modern micro GC) are not always applicable as the total pressure of the experiment may be too low. Whenever possible it should be avoided to operate in-situ cells in a batch re-circulation mode. This enhances the products for analysis but leads often to ill defined and not typical deactivation phenomena, as the equivalent of the residence time is critical to many hydrocarbon molecular products. The use of GC-MS couplings fed with suitable make-up gasses is a precise and preferable detection mode. Gas-phase IR spectrometry with long-pathway cuvetts as used e.g. in environmental catalysis testing is a suitable alternative.
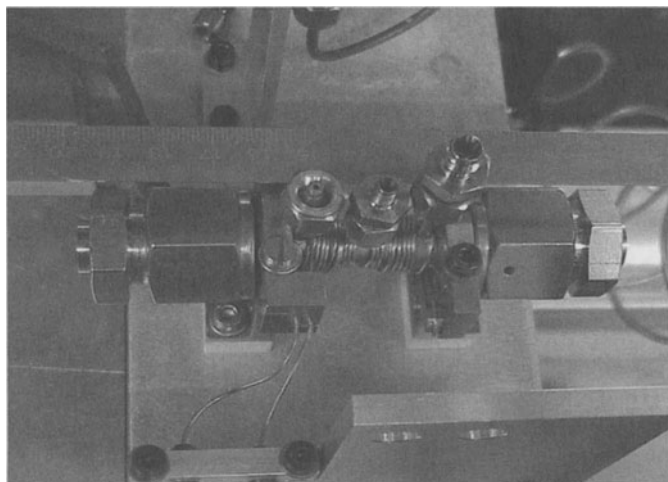
Fig. 2.2: Realisation of a transmission in-situ cell. The gas in- and outlets (top, edges) use 3 mm o.d. gas pipes. The central swagelock connector fixes the thermo-couple.

In Figure 2.2 the realisation is shown of a small in-situ cell for transmission work[5]. The cell is based around standard tube fittings that fix the windows (Al foil, light tight) and hold the sample block in place. The sample is a pressed wafer of the catalyst mixed with typical diluents to ensure sufficient transmission, to provide porosity and to reduce

overheating in highly exothermic (oxidation) reactions. A heating capillary provides external heating wound in such a way as to provide a temperature gradient symmetric with respect to the position of the sample marked by the thermocouple fixation. The reactor is overpowered with heating in order to minimize thermal insulation that would spoil the response time of the temperature regulator. A fast response time is essential when exothermic reactions are studied as otherwise the sample is easily ruined by rapid overheating if the reaction sets in with an ignition-type behaviour.

As cleaning of such systems is difficult it is important to design the cell such that all materials which come in contact with the catalyst (windows, holders etc) may be discarded after a single use. The internal screw set holding the sample wafer in position and providing thermal contact should be replaced at least when the catalyst system is changed.
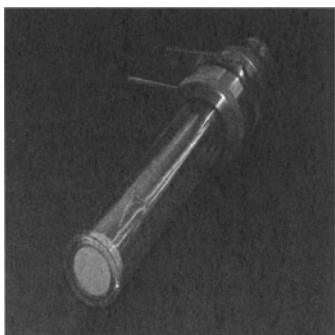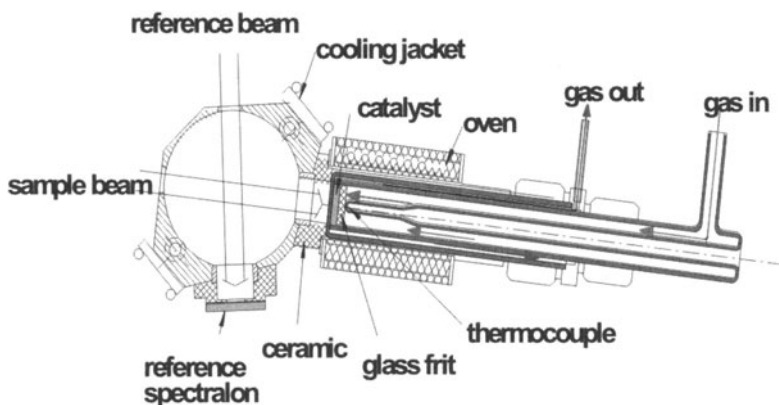
Fig. 2.3: Realisation of typical cell for reflectance work. The photo shows the cell from its optical window side with a catalyst (yellow material) loaded.. A typical diameter is 20 mm, the cell length about 20 cm. Note the concentric class capillary for the gas inlet.

In Figure 2.3 a typical reflectance cell is shown used here for UV-vis experiments[6]. The problem is to bring the sample as close as possible to the window, to master the temperature gradient and to provide uniform gas flow. The same problems hold for many commercial cells used for FT-IR and UV-vis studies. In the schematic diagram the problem is obvious of the temperature gradient from the cell furnace heating also the integration sphere and thus creating spurious

reflectivity losses. The cooling jacket at the integration sphere reduces the effects on the spectrometer but enhances the thermal asymmetry of the reactor and requires thus careful adjustment of the coolant flow. The sample is pressed to the optical window by a quartz frit that also provides a radially uniform gas flow. Due to the size of the sample diameter (required to maximise the sensitivity of the spectroscopy) radial gradients of temperature and gas flow in opposite directions are unavoidable. By using a coloured sample (heteropoly acid) the gradients were made visible and minimised by adjusting heating power and gas cooling effects. Positive is the amount of catalyst usable in the cell allowing to accurately detect the catalytic performance in-situ. With many small-sized cells the minimal amount of catalyst sample allows no sufficient catalytic conversion to be reached.

3.   Case Studies from the Literature

Within the last 7 years about 250 case studies were devoted to the application of in-situ studies to heterogeneous catalysis. About 3 times as many studies were published in the field of homogeneous catalysis. The non-critical bibliometry is erroneous in this case as the term "in-situ" is used by many preparative chemists not only to designate analytical methods but also to indicate the intermediate generation of activated reactants that are postulated to exist from particular reaction product structures.

In the large area of surface science a substantial number of reaction studies are carried out "in-situ" but these references describe single crystal work that is conducted at low pressures exclusively and thus is not so instructive in the context of this compilation. The Table 2 gives an impression of the state of the art in the field and refers back to some milestones in the development. The selection is neither comprehensive nor does it cover all experimental possibilities. It does, however, provide sufficient data to enable the reader to interrogate the current methodology for its suitability in a given research strategy.

The reader will also notice that a wide definition of in-situ is required extending over the definition given above in order to justify the paper selection. Within the strict limit of the definition only a small number of papers would qualify for the table. The prevailing definition of in-situ is still "under conditions somewhat close to catalytic reaction" without validation or even kinetic verification of the function of the specimen investigated.

Table 2: Selected literature references to frequently used methods and techniques in the characterisation of practical catalysts with in-situ methods

Topic	References
Reviews	7-29, 29 a
In-situ cell designs	30-43
Extended X-ray absorption and near-edge X-ray absorption spectroscopy	5;34;44-57
X-ray diffraction	42;58-69
Nuclear magnetic resonance spectroscopies	13;19;30;38;58;63;70-96
Fourier-Transform-infrared spectroscopy and DRIFTS	17;40;97-115
Thermal methods	112;116-121
Raman spectroscopy	10;103;122-129
Electron paramagnetic resonance	9;19;33;130-136
Sum frequency generation	28;101;105;137-139
Surface science of real and model systems. High-pressure modifications of surface-science methods.	140;141;141-156 4;157-159
Scanning tunnelling methods	16;39;142;144;160-170
UV-VIS spectroscopy	132;171-175
Electron microscopy	18;162;176-179
Mössbauer spectroscopy	51;180-183
Molecular species in heterogeneous catalysis	17;28;82;184-190
Model systems	16;39;144;145;162-166;191-206
Kinetics	32;41;131;142;187;207-222

References

1   X. G. Wang et al., *Physical Review Letters* 81, 1038-1041 (1998).
2   R. Schlogl et al., *Topics in Catalysis* 15, 219-228 (2001).
3   G. J. Hutchings et al., *Journal of Catalysis* 208, 197-210 (2002).
4   R. W. Mayer, M. Havecker, A. Knop-Gericke, R. Schlogl, *Catalysis Letters* 74, 115-119 (2001).
5   T. Ressler et al., *Journal of Catalysis* 191, 75-85 (2000).
6   J. Melsheimer, S. S. Mahmoud, G. Mestl, R. Schlogl, *Catalysis Letters* 60, 103-111 (1999).
7   E. Bourgeat-Lami, *Journal of Nanoscience & Nanotechnology* 2, 1-24 (2002).
8   D. Bazin, L. Guczi, J. Lynch, *Applied Catalysis A-General* 226, 87-113 (2002).
9   M. Labanowska, *Chemphyschem* 2, 712-731 (2001).
10   P. C. Stair, Current Opinion in Solid State & Materials Science 5, 365-369 (2001).
11   V. B. Kazansky, *Catalysis Reviews-Science & Engineering* 43, 199-232 (2001).

12   J. Ryczkowski, *Catalysis Today* 68, 263-381 (2001).

13   W. O. Parker, *Comments on Inorganic Chemistry* 22, 31-73 (2000).

14   K. I. Hadjiivanov, *Catalysis Reviews-Science & Engineering* 42, 71-144 (2000).

15   F. Atamny and A. Baiker, *Applied Catalysis A-General* 173, 201-230 (1998).

16   C. R. Henry, *Surface Science Reports* 31, 235-325 (1998).

17   G. Busca, *Catalysis Today* 27, 457-496 (1996).

18   P. L. Gai, *Current Opinion in Solid State & Materials Science* 5, 371-380 (2001).

19   M. Hunger and J. Weitkamp, Angewandte Chemie-International Edition 40, 2954-2971 (2001).

20   D. M. Murphy and C. C. Rowlands, Current Opinion in Solid State & Materials Science 5, 97-104 (2001).

21   D. Bazin and L. Guczi, *Applied Catalysis A-General* 213, 147-162 (2001).

22   I. W. C. E. Arends and R. A. Sheldon, Applied Catalysis A-General 212, 175-187 (2001).

23   T. Mallat and A. Baiker, *Applied Catalysis A-General* 200, 3-22 (2000).

24   J. M. Thomas, *Angewandte Chemie-International Edition* 38, 3589-3628 (1999).

25   V. A. Matyshak and O. V. Krylov, *Catalysis Today* 25, 1-87 (1995).

26   J. M. Thomas and G. Sankar, Accounts of Chemical Research 34, 571-581 (2001).

27   J. M. Thomas, *Chemistry-A European Journal* 3, 1557-1562 (1997).

28   P. S. Cremer, B. J. Mcintyre, M. Salmeron, Y. R. Shen, G. A. Somorjai, Catalysis Letters 34, 11-18 (1995).

29   G. A. Somorjai, Zeitschrift fur Physikalische Chemie-International Journal of Research in Physical Chemistry & Chemical Physics 197, 1-19 (1996).

29a   A. Brückner, Catal. Rev. Sci. Eng. 45, 97-151, 2003

30   A. J. Pardey et al., Reaction Kinetics & Catalysis Letters 70, 293-301 (2000).

31   C. M. Finnerty, R. H. Cunningham, R. M. Ormerod, Catalysis Letters 66, 221-226 (2000).

32   C. Longo et al., *Polyhedron* 19, 487-493 (2000).

33.   W. Reichl, G. Rosina, G. Rupprechter, C. Zimmermann, K. Hayek, Review of Scientific Instruments 71, 1495-1499 (2000).

34   I. Pettiti et al., *Journal of Synchrotron Radiation* 6, 1120-1124 (1999).

35   J. A. van Bokhoven, A. M. J. van der Eerden, A. D. Smith, D. C. Koningsberger, Journal of Synchrotron Radiation 6, 201-203 (1999).

36   S. Gaemers, H. Luyten, J. M. Ernsting, C. J. Elsevier, Magnetic Resonance in Chemistry 37, 25-30 (1999).

37   B. G. Li and R. D. Gonzalez, *Applied Spectroscopy* 52, 1488-1491 (1998).

38   J. A. Iggo, D. Shirley, N. C. Tong, New Journal of Chemistry 22, 1043-1045 (1998).

39   W. Weiss, M. Ritter, D. Zscherpel, M. Swoboda, R. Schlogl, Journal of Vacuum Science & Technology A-Vacuum Surfaces & Films 16, 21-29 (1998).

40   M. Komiyama and Y. Obi, Review of Scientific Instruments 67, 1590-1592 (1996).

41   M. M. Schubert, T. P. Haring, G. Brath, H. A. Gasteiger, R. J. Behm, Applied Spectroscopy 55, 1537-1543 (2001).

42   G. D. Moggridge, S. L. M. Schroeder, R. M. Lambert, T. Rayment, Nuclear Instruments & Methods in Physics Research Section B-Beam Interactions with Materials & Atoms 97, 28-32 (1995).

43   S. Johansson, E. Fridell, B. Kasemo, Journal of Vacuum Science & Technology A-Vacuum Surfaces & Films 18, 1514-1519 (2000).

44   A. J. Dent, *Topics in Catalysis* 18, 27-35 (2002).

45   J. D. Grunwaldt and B. S. Clausen, *Topics in Catalysis* 18, 37-43 (2002).

46   J. D. Grunwaldt, P. Kappen, B. S. Hammershoi, L. Troger, B. S. Clausen, Journal of
      Synchrotron Radiation 8, 572-574 (2001).
47   S. T. Wong, J. F. Lee, S. F. Cheng, C. Y. Mou, Applied Catalysis A-General 198,
      115-126 (2000).
48   A. P. Markusse, B. F. M. Kuster, D. C. Koningsberger, G. B. Marin, Catalysis Letters
      55, 141-145 (1998).
49   B. S. Clausen, *Catalysis Today* 39, 293-300 (1998).
50   T. Ressler et al., *Journal of Catalysis* 191, 75-85 (2000).
51   M. Benz, A. M. Vanderkraan, R. Prins, Applied Catalysis A-General 172, 149-157
      (1998).
52   U. Hatje, T. Ressler, S. Petersen, H. Forster, Journal de Physique IV 4, 141-144
      (1994).
53   T. Ressler, M. Hagelstein, U. Hatje, W. Metz, Journal de Physique IV 7, 731-733
      (1997).
54   T. Ressler et al., *Journal of Catalysis* 191, 75-85 (2000).
55   T. Ressler, R. E. Jentoft, J. Wienold, M. M. Gunter, O. Timpe, Journal of Physical
      Chemistry B 104, 6360-6370 (2000).
56   S. L. M. Schroeder, G. D. Moggridge, R. M. Ormerod, R. M. Lambert, T. Rayment,
      Physica B 209, 215-216 (1995).
57   S. L. M. Schroeder, G. D. Moggridge, T. Rayment, R. M. Lambert, Journal of
      Molecular Catalysis A-Chemical 119, 357-365 (1997).
58   H. Klein, H. Fuess, M. Hunger, Journal of the Chemical Society-Faraday
      Transactions 91, 1813-1824 (1995).
59   A. J. Dent et al., Nuclear Instruments & Methods in Physics Research Section B-
      Beam Interactions with Materials & Atoms 97, 20-22 (1995).
60   R. Schnell and H. Fuess, Berichte der Bunsen Gesellschaft fur Physikalische Chemie-
      An International Journal of Physical Chemistry 100, 578-584 (1996).
61   C. J. Kepert, D. Hesek, P. D. Beer, M. J. Rosseinsky, Angewandte Chemie
      International Ed. in English. 37, 3158-3160 (1998).
62   G. Sankar, J. M. Thomas, C. R. A. Catlow, Topics in Catalysis 10, 255-264 (2000).
63   P. J. Chupas, M. F. Ciraolo, J. C. Hanson, C. P. Grey, Journal of the American
      Chemical Society 123, 1694-1702 (2001).
64   B. Herzog, D. Herein, R. Schlogl, Applied Catalysis A-General 141, 71-104 (1996).
65   M. M. Gunter et al., *Catalysis Letters* 71, 37-44 (2001).
66   T. Ressler, J. Wienold, R. E. Jentoft, O. Timpe, T. Neisius, Solid State
      Communications 119, 169-174 (2001).
67   M. M. Gunter, T. Ressler, R. E. Jentoft, B. Bems, Journal of Catalysis 203, 133-149
      (2001).
68   R. Schlogl et al., Topics in Catalysis 15, 219-228 (2001).
69   G. Weinberg et al., Applied Catalysis A-General 163, 83-99 (1997).
70   A. G. Stepanov, M. V. Luzgin, V. N. Sidelnikov, Catalysis Letters 78, 153-156
      (2002).
71   A. Eichhorn, A. Koch, J. Bargon, Journal of Molecular Catalysis A-Chemical 174,
      293-295 (2001).
72   E. G. Derouane, H. Y. He, S. B. D. A. Hamid, D. Lambert, I. Ivanova, Journal of
      Molecular Catalysis A-Chemical 158, 5-17 (2000).
73   D. Ma et al., Angewandte Chemie-International Edition 39, 2928-2931 (2000).
74   L. K. Carlson, P. K. Isbester, E. J. Munson, Solid State Nuclear Magnetic Resonance
      16, 93-102 (2000).
75   C. Bianchini, H. M. Lee, A. Meli, F. Vizza, Organometallics 19, 849-853 (2000).

76   P. S. Pregosin and M. Valentini, Enantiomer 4, 529-539 (1999).

77   C. Ulrich and J. Bargon, Magnetic Resonance in Chemistry 38, 33-37 (2000).

78   I. I. Ivanova, Colloids & Surfaces A-Physicochemical & Engineering Aspects 158, 189-200 (1999).

79   M. Hunger, M. Seiler, T. Horvath, Catalysis Letters 57, 199-204 (1999).

80   C. Keeler et al., Catalysis Today 49, 377-383 (1999).

81   T. R. Krawietz, D. K. Murray, J. F. Haw, Journal of Physical Chemistry 102, 8779-8785 (1998).

82   T. Mildner and D. Freude, *Journal of Catalysis* 178, 309-314 (1998).

83   J. F. Haw et al., Angewandte Chemie (International Edition in English) 37, 948-949 (1998).

84   J. C. Linehan, S. L. Wallen, C. R. Yonker, T. E. Bitterwolf, J. T. Bays, Journal of the American Chemical Society 119, 10170-10177 (1997).

85   H. B. Schwarz et al., Journal of Catalysis 167, 248-255 (1997).

86   H. Ernst, D. Freude, T. Mildner, I. Wolf, Solid State Nuclear Magnetic Resonance 6, 147-156 (1996).

87   V. B. Kazansky and R. A. Vansanten, Catalysis Letters 38, 115-121 (1996).

88   H. Ernst, D. Freude, T. Mildner, I. Wolf, Zeitschrift fur Physikalische Chemie-International Journal of Research in Physical Chemistry & Chemical Physics 189, 221-228 (1995).

89   W. Wang, M. Seiler, I. I. Ivanova, J. Weitkamp, M. Hunger, Chemical Communications 1362-1363 (2001).

90   T. Mildner, H. Ernst, D. Freude, J. Karger, U. Winkler, Magnetic Resonance in Chemistry 37, S38-S42 (1999).

91   M. Seiler, U. Schenk, M. Hunger, *Catalysis Letters* 62, 139-145 (1999).

92   J. F. Haw, *Topics in Catalysis* 8, 81-86 (1999).

93   E. G. Derouane, H. Y. He, S. B. Derouane-Abd Hamid, I. I. Ivanova, Catalysis Letters 58, 1-19 (1999).

94   P. K. Isbester et al., Catalysis Today 49, 363-375 (1999).

95   E. Macnamara and D. Raftery, Journal of Catalysis 175, 135-137 (1998).

96   R. C. Matthews et al., Angewandte Chemie International Ed. in English. 35, 2253-2256 (1996).

97   C. J. Hirschmugl, Surface Science 500, 577-604 (2002).

98   H. Y. N. Holman et al., Environmental Science & Technology 36, 1276-1280 (2002).

99   S. Csihony, H. Mehdi, I. T. Horvath, Green Chemistry 3, 307-309 (2001).

100   L. J. Burcham, L. E. Briand, I. E. Wachs, Langmuir 17, 6164-6174 (2001).

101   U. Metka, M. G. Schweitzer, H. R. Volpp, J. Wolfrum, Zeitschrift fur Physikalische Chemie-International Journal of Research in Physical Chemistry & Chemical Physics 214, 865-888 (2000).

102   T. C. Schilke, I. A. Fisher, A. T. Bell, Journal of Catalysis 184, 144-156 (1999).

103   M. J. Weaver, Topics in Catalysis 8, 65-73 (1999).

104   R. J. H. Clark, P. J. Dyson, D. G. Humphrey, B. F. G. Johnson, Polyhedron 17, 2985-2991 (1998).

105   P. S. Cremer, X. C. Su, G. A. Somorjai, Y. R. Shen, Journal of Molecular Catalysis A-Chemical 131, 225-241 (1998).

106   A. M. Herring and R. L. Mccormick, Journal of Physical Chemistry B 102, 3175-3184 (1998).

107   X. Z. Liang et al., Chemical Journal of Chinese Universities-Chinese 18, 777-781 (1997).

108 S. S. C. Chuang, M. A. Brundage, M. W. Balakos, Applied Catalysis A-General 151, 333-354 (1997).

109 K. Ogura, M. Nakayama, C. Kusumoto, Journal of the Electrochemical Society 143, 3606-3615 (1996).

110 J. A. Anderson and M. M. Khader, Journal of Molecular Catalysis A-Chemical 105, 175-183 (1996).

111 S. S. C. Chuang, M. A. Brundage, M. W. Balakos, G. Srinivas, Applied Spectroscopy 49, 1151-1163 (1995).

112 B. W. L. Southward, J. S. Vaughan, C. T. Oconnor, Journal of Catalysis 153, 293-303 (1995).

113 D. Ferri and T. Burgi, Journal of the American Chemical Society 123, 12074-12084 (2001).

114 J. C. Lavalley, S. Jollyfeaugas, A. Janin, J. Saussey, Mikrochimica Acta 51-56 (1997).

115 G. A. Beitel, A. Laskov, H. Oosterbeek, E. W. Kuipers, Journal of Physical Chemistry 100, 12494-12502 (1996).

116 T. E. Caldwell, I. M. Abdelrehim, D. P. Land, Journal of Physical Chemistry B 102, 562-568 (1998).

117 L. Bencze, G. Szalai, T. L. Overton, Inorganica Chimica Acta 254, 5-7 (1997).

118 I. Pitsch et al., Journal of Materials Chemistry 11, 2498-2503 (2001).

119 J. K. Lee, V. Russo, J. Melsheimer, K. Kohler, R. Schlogl, Physical Chemistry Chemical Physics 2, 2977-2983 (2000).

120 G. Mestl et al., Journal of Molecular Catalysis A-Chemical 162, 455-484 (2000).

121 G. Mestl et al., Applied Catalysis A-General 210, 13-34 (2001).

122 C. Fokas and V. Deckert, Applied Spectroscopy 56, 192-199 (2002).

123 Y. Zeng, Z. L. Li, M. Ma, S. M. Zhou, Electrochemistry Communications 2, 36-38 (2000).

124 S. B. Xie, M. P. Rosynek, J. H. Lunsford, Applied Spectroscopy 53, 1183-1187 (1999).

125 I. E. Wachs, Topics in Catalysis 8, 57-63 (1999).

126 H. Knozinger, Catalysis Today 32, 71-80 (1996).

127 S. T. Oyama and W. Zhang, Journal of the American Chemical Society 118, 7173-7177 (1996).

128 G. Mestl and T. K. K. Srinivasan, Catalysis Reviews-Science & Engineering 40, 451-570 (1998).

129 H. Knozinger and G. Mestl, Topics in Catalysis 8, 45-55 (1999).

130 Z. Sojka and M. Che, Comptes Rendus de l Academie des Sciences Serie II Fascicule C-Chimie 3, 163-174 (2000).

131 F. P. Ballistreri, R. Bianchini, C. Pinzino, G. A. Tomaselli, R. M. Toscano, Journal of Physical Chemistry 104, 2710-2715 (2000).

132 A. Bruckner, Chemical Communications 2122-2123 (2001).

133 U. Bentrup, A. Bruckner, M. Richter, R. Fricke, Applied Catalysis B-Environmental 32, 229-241 (2001).

134 A. Brückner, Appl. Catal. A: General 200, 287-297 (2000)

135 A. Bruckner and H. W. Zanthoff, Colloids & Surfaces A-Physicochemical & Engineering Aspects 158, 107-113 (1999).

136 A. Bruckner, A. Martin, N. Steinfeldt, G. U. Wolf, B. Lucke, Journal of the Chemical Society-Faraday Transactions 92, 4257-4263 (1996).

137 G. Rupprechter, T. Dellwig, H. Unterhalt, H. J. Freund, Journal of Physical Chemistry B 105, 3797-3802 (2001).

138 S. J. Lin, A. Oldfield, D. Klenerman, Surface Science 464, 1-7 (2000).

139 C. T. Williams, Y. Yang, C. D. Bain, Langmuir 16, 2343-2350 (2000).

140 B. E. Spiewak and J. A. Dumesic, Thermochimica Acta 290, 43-53 (1997).

141 S. Chinta, T. V. Choudhary, L. L. Daemen, J. Eckert, D. W. Goodman, Angewandte Chemie-International Edition 41, 144-146 (2002).

142 Y. Iwasawa, H. Onishi, K. Fukui, S. Suzuki, T. Sasaki, Faraday Discussions 259-266 (1999).

143 T. Burgi et al., Catalysis Letters 66, 109-112 (2000).

144 T. Dellwig et al., Journal of Molecular Catalysis A-Chemical 162, 51-66 (2000).

145 H. Nishimura, J. Ogawa, J. Nakamura, Surface Science 482, 215-219 (2001).

146 H. Mehner, W. Meisel, A. Bruckner, A. York, Hyperfine Interactions 111, 51-56 (1998).

147 M. Wark, M. Koch, A. Bruckner, W. Grunert, Journal of the Chemical Society-Faraday Transactions 94, 2033-2041 (1998).

148 W. Zipprich, H. D. Wiemhofer, U. Vohrer, W. Gopel, Berichte der Bunsen Gesellschaft fur Physikalische Chemie-An International Journal of Physical Chemistry 99, 1406-1413 (1995).

149 Q. Guo and R. W. Joyner, Applied Surface Science 145, 375-379 (1999).

150 A. Kolmakov and D. W. Goodman, Surface Science 490, L597-L601 (2001).

151 M. Grunze et al., Physical Review Letters 53, 850-853 (1984).

152 K. Homann, H. Kuhlenbeck, H. J. Freund, Surface Science 327, 216-224 (1995).

153 K. Homann, H. Kuhlenbeck, H. J. Freund, Zeitschrift fur Physikalische Chemie-International Journal of Research in Physical Chemistry & Chemical Physics 198, 135-147 (1997).

154 R. Schlogl et al., Topics in Catalysis 15, 219-228 (2001).

155 M. Havecker, A. Knop-Gericke, T. Schedel-Niedrig, Applied Surface Science 142, 438-442 (1999).

156 G. J. Hutchings et al., Journal of Catalysis 208, 197-210 (2002).

157 M. Havecker, A. Knopgericke, T. Schedelniedrig, R. Schlogl, Angewandte Chemie International Ed. in English. 37, 1939-1942 (1998).

158 A. Knop-Gericke, M. Havecker, T. Schedel-Niedrig, R. Schlogl, Topics in Catalysis 10, 187-198 (2000).

159 V. I. Bukhtiyarov et al., Catalysis Letters 74, 121-125 (2001).

160 Y. Iwasawa, H. Onishi, K. Fukui, Topics in Catalysis 14, 163-172 (2001).

161 R. A. Bennett, P. Stone, M. Bowker, Catalysis Letters 59, 99-105 (1999).

162 G. Rupprechter, K. Hayek, L. Rendon, M. Joseyacaman, Thin Solid Films 260, 148-155 (1995).

163 B. F. Bartlett and W. T. Tysoe, Catalysis Letters 46, 101-106 (1997).

164 Y. Iwasawa, Journal de Physique IV 7, 67-81 (1997).

165 R. M. Lambert, F. Williams, A. Palermo, M. S. Tikhov, Topics in Catalysis 13, 91-98 (2000).

166 R. Imbihl, Journal of Molecular Catalysis A-Chemical 158, 101-106 (2000).

167 C. Kuhrs, Y. Arita, W. Weiss, W. Ranke, R. Schlogl, Topics in Catalysis 14, 111-123 (2001).

168 A. Kolmakov and D. W. Goodman, Catalysis Letters 70, 93-97 (2000).

169 A. Kolmakov and D. W. Goodman, Surface Science 490, L597-L601 (2001).

170 P. S. Cremer, B. J. Mcintyre, M. Salmeron, Y. R. Shen, G. A. Somorjai, Catalysis Letters 34, 11-18 (1995).

171 B. M. Weckhuysen et al., Journal of Molecular Catalysis A-Chemical 151, 115-131 (2000).

172 J. Melsheimer, S. S. Mahmoud, G. Mestl, R. Schlogl, Catalysis Letters 60, 103-111 (1999).
173 C. S. Jin and Y. B. Shim, Bulletin of the Korean Chemical Society 20, 381-383 (1999).
174 A. Malinauskas and R. Holze, Berichte der Bunsen Gesellschaft fur Physikalische Chemie-An International Journal of Physical Chemistry 102, 982-984 (1998).
175 J. Melsheimer, M. C. Bohm, J. K. Lee, R. Schlog, Berichte der Bunsen Gesellschaft fur Physikalische Chemie-An International Journal of Physical Chemistry 101, 726-732 (1997).
176 P. L. Gai, Topics in Catalysis 8, 97-113 (1999).
177 T. W. Hansen et al., Science 294, 1508-1510 (2001).
178 E. D. Boyes and P. L. Gai, Ultramicroscopy 67, 219-232 (1997).
179 D. S. Su et al., Catalysis Letters 75, 81-86 (2001).
180 W. Meisel, H. Mehner, A. Bruckner, Fresenius Journal of Analytical Chemistry 352, 483-485 (1995).
181 J. W. Niemantsverdriet and W. N. Delgass, Topics in Catalysis 8, 133-140 (1999).
182 J. Sanchez-Valente, J. M. M. Millet, F. Figueras, L. Fournes, Hyperfine Interactions 131, 43-50 (2000).
183 F. Bodker, I. Chorkendorff, S. Morup, Zeitschrift fur Physik D-Atoms Molecules & Clusters 40, 152-154 (1997).
184 O. V. Krylov and V. A. Matyshak, Uspekhi Khimii 64, 177-197 (1995).
185 G. A. Somorjai, Progress in Surface Science 50, 3-29 (1995).
186 D. S. Shephard et al., Chemistry-A European Journal 4, 1214-1224 (1998).
187 J. Cejka, N. Zilkova, J. E. Sponer, B. Wichterlova, Collection of Czechoslovak Chemical Communications 63, 1769-1780 (1998).
188 M. K. Carter, Journal of Molecular Catalysis A-Chemical 172, 193-206 (2001).
189 R. A. Vansanten, Chemical Engineering Science 50, 4027-4044 (1995).
190 R. Ugo, C. Dossi, R. Psaro, Journal of Molecular Catalysis A-Chemical 107, 13-22 (1996).
191 J. Find, Z. Paal, R. Schlogl, U. Wild, Catalysis Letters 65, 19-23 (2000).
192 Y. Joseph et al., Physical Chemistry Chemical Physics 3, 4141-4153 (2001).
193 K. A. Davis and D. W. Goodman, Journal of Physical Chemistry B 104, 8557-8562 (2000).
194 C. C. Chusuei et al., Langmuir 17, 4113-4117 (2001).
195 Z. X. Yang, R. Q. Wu, Q. M. Zhang, D. W. Goodman, Physical Review B 6515, 5407 (2002).
196 A. Fischer et al., Journal of Materials Research 14, 3725-3733 (1999).
197 V. V. Roddatis, D. S. Su, C. Kuhrs, W. Ranke, R. Schlogl, Thin Solid Films 396, 78-83 (2001).
198 V. V. Roddatis et al., Surface & Coatings Technology 151, 63-66 (2002).
199 H. Colfen et al., Langmuir 18, 3500-3509 (2002).
200 M. Klimenkov et al., Surface Science 391, 27-36 (1997).
201 S. A. Nepijko et al., Surface Science 413, 192-201 (1998).
202 S. A. Nepijko et al., Langmuir 15, 5309-5313 (1999).
203 N. Nilius, N. Ernst, H. J. Freund, Physical Review B 6511, 5421 (2002).
204 S. Dahl, J. Sehested, C. J. H. Jacobsen, E. Tornqvist, I. Chorkendorff, Journal of Catalysis 192, 391-399 (2000).
205 C. J. H. Jacobsen et al., Journal of Molecular Catalysis A-Chemical 163, 19-26 (2000).
206 J. H. Larsen and I. Chorkendorff, Surface Science Reports 35, 165-222 (1999).

207 G. J. Li, M. Ichikawa, X. X. Guo, Reaction Kinetics & Catalysis Letters 59, 75-86 (1996).
208 G. W. Coulston et al., Science 275, 191-193 (1997).
209 N. A. Alekar et al., Journal of Molecular Catalysis A-Chemical 164, 181-189 (2000).
210 H. Bielawa, M. Kurtz, T. Genger, O. Hinrichsen, Industrial & Engineering Chemistry Research 40, 2793-2800 (2001).
211 T. V. de Bocarme and N. Kruse, Chaos 12, 118-130 (2002).
212 T. E. Caldwell, I. M. Abdelrehim, D. P. Land, Journal of Physical Chemistry B 102, 562-568 (1998).
213 P. M. Dentinger and J. W. Taylor, Journal of Vacuum Science & Technology B 16, 3759-3766 (1998).
214 O. A. Kholdeeva, L. A. Kovaleva, R. I. Maksimovskaya, G. M. Maksimov, Journal of Molecular Catalysis A-Chemical 158, 223-229 (2000).
215 N. M. Markovic, C. A. Lucas, V. Climent, V. Stamenkovic, P. N. Ross, Surface Science 465, 103-114 (2000).
216 T. Ressler, J. Wienold, R. E. Jentoft, T. Neisius, M. M. Gunter, Topics in Catalysis 18, 45-52 (2002).
217 S. Besselmann, C. Freitag, O. Hinrichsen, M. Muhler, Physical Chemistry Chemical Physics 3, 4633-4638 (2001).
218 Z. Paal et al., Journal of Catalysis 152, 252-263 (1995).
219 O. Hinrichsen, A. Hornung, M. Muhler, Chemical Engineering & Technology 22, 1039-1042 (1999).
220 H. Bielawa, O. Hinrichsen, A. Birkner, M. Muhler, Angewandte Chemie-International Edition 40, 1061-+ (2001).
221 P. Rybarczyk et al., Journal of Catalysis 202, 45-58 (2001).
222 C. V. Ovesen et al., Journal of Catalysis 158, 170-180 (1996).

A Personal View on Important Developments in Homogeneous Catalysis

Contents

A Personal View on Important Developments in Homogeneous Catalysis

Matthias Beller

Leibniz-Institut für Organische Katalyse an der Universität Rostock e.V. (IfOK), Buchbinderstr. 5-6, 18055 Rostock, Germany, matthias.beller@ifok.uni-rostock.de

Abstract. This chapter represents a personal view on selected important achievements of the past as well as some new developments in homogeneous catalysis, which might be important in the future. Special focus is given on sub-areas of homogeneous catalysis such as carbonylations and transition metal-catalyzed coupling reactions for fine chemicals. It is intended to stimulate the reader´s appetite for more homogeneous catalysis.

1. Introduction

Basically homogeneous catalysts are characterized by the fact that catalyst, starting materials and products are staying within the same reaction phase. Comparing homogenous and heterogeneous catalysis, both have common characteristics, but also significant differences are visible:

- Homogeneous catalysts (most often the pre-catalyst) are molecularly defined in nature. This fact combined with the possibility to synthesize potential intermediates of a given catalytic cycle allows an easier understanding of the reaction mechanism. Based on this mechanistic understanding in general a more rational development of improved catalysts is possible.
- Most often homogeneous catalysis takes place under much milder reaction conditions compared to heterogeneous catalysis. Typically reactions are performed in between room temperature and 120°C. Also the reaction pressure is comparably low, in general reactions are run at atmospheric pressure. If gases or low boiling starting materials are used reactions are performed in between 1-60 bar pressure. Nevertheless also high pressure processes are known. Hence, the conversion of more complicated organic building blocks with different functional groups is favorably done with homogeneous catalysts. On the other hand the temperature based stability of heterogeneous catalysts is increased compared to their homogeneous counterparts. Hence, reactions such as CH-activation processes, which need higher temperatures (> 250°C) in order to take place with significant rate, are based on heterogeneous catalysts.

- It is important to note that most reactions using homogeneous catalysts are run in liquid phase in a batch wise mode. Especially in academic research laboratories homogeneous catalysis is attributed to batch reactions using organic solvents. However, in industry large scale processes, e.g. carbonylation reactions, oxidations, are performed in a continuos mode.
- Due to the advancements in organometallic chemistry and organic ligand synthesis, nowadays a plethora of ligands [P-, N-, and recently C-ligands) is theoretically available (10.000 – 100.000). These ligands are extremely important in determining the activity, productivity and selectivity of a homogeneous catalyst. In fact "ligand-tailoring" constitutes an extremely powerful tool to control all kinds of selectivity in a given catalytic reaction and to influence catalyst stability and activity. A selection of important ligands for homogeneous catalysis is shown in Scheme 1. Apart from the well-known aryl and alkyl phosphines and amines, recently also carbenes [1] have become more and more important. In addition mixed ligand systems with two different chelating groups, as well as hemilabile ligands find increasing interest.
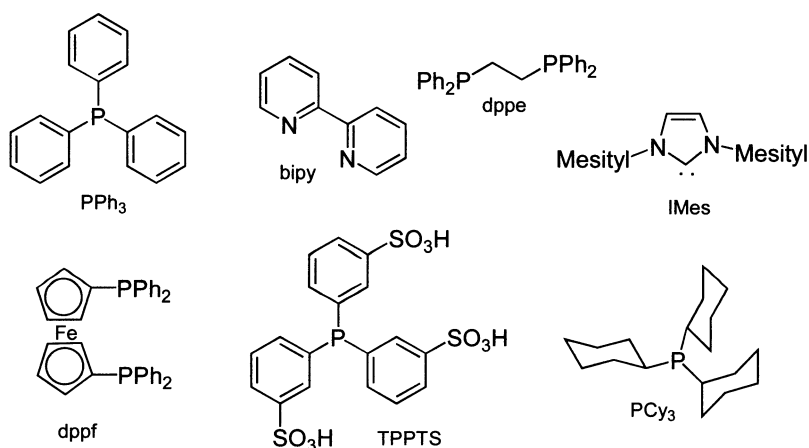
Scheme 1: Typical ligands for homogeneous catalysis.

- In asymmetric catalysis [2] the stereoselectivity of a given reaction is induced by a soluble chiral phosphine or amine ligand. Although in general not recognized there exist an interesting analogy of ligands for homogeneous catalysis and supports and modifiers used in heterogeneous catalysis.
- Importantly, the separation of the catalyst is straightforward done in heterogeneous catalysis via filtration. In homogeneous catalysis, either distillation of starting materials and products, chromatography, crystallization, or modern techniques of multiphasic catalysis have to be applied.

Due to the specific characteristics of homogeneous and heterogeneous catalysis the application and use of these systems are most often performed in different

chemistry communities. Although noteworthy efforts are undertaken to bridge this gap, still a lot of work has to be done in order to make full use of the synergism of the two fields.

Until to date the application of homogeneous catalysts is dominating in organic synthesis and the fine chemical industry. However, also bulk processes are run in industry. Basically all industrial carbonylation reactions are done with homogeneous catalysts. Important examples include the production of aliphatic aldehydes and acetic acid. Despite enormous efforts the leaching of volatile carbonyl clusters and complexes from heterogeneous catalysts prevent the technical use of this class of compounds. Other large scale processes run with homogeneous catalysts are oxidation reactions, which are performed with low molecular weight transition metal salts.

Clearly, homogeneous catalysis can not be discussed comprehensively within the frame of this one chapter. Therefore this chapter represents a personal view on selected important achievements of the past as well as some new developments in homogeneous catalysis, which might be important in the future. Special focus is given on sub-areas of homogeneous catalysis such as carbonylations and transition metal-catalyzed coupling reactions for fine chemicals. Clearly other homogeneous catalytic reactions such as oxidations, cyanations, olefin dimerizations and oligomerizations, hydrogenations, asymmetric catalysis as well as "simple" acid and base catalysis constitute also important areas in academic and industrial chemistry, but will be treated here only on the surface. Here, it is intended to stimulate the reader´s appetite for more homogeneous catalysis.

The broad area of hydrogenation reaction is excluded at all due to space limitations. However, there are excellent recent textbooks on the market, which provide the reader with a more comprehensive insight into this lively and fascinating topic [3].

2.   Carbonylation Reactions

2.1   General Aspects

At its beginning and still today homogeneous catalysis benefits significantly from advancements in the area of organometallic chemistry. Here, mechanistic understanding of elementary steps and the synthesis of new organometallic compounds provide a valuable source for inspiration regarding new catalytic reactions. In addition to metal hydrides especially metal oxo complexes have been proven important catalysts and intermediates in homogeneous reactions. Due to the industrial importance of catalytic carbonylations this type of reaction is first discussed. The term carbonylation [4, 5] is used for a large number of closely related reactions that all have in common that carbon monoxide is incorporated into a substrate by addition of CO to unsaturated compounds such as alkynes or alkenes in presence of nucleophiles (NuH) (Scheme 2).

$$R\text{—}\!\!\equiv\ +\ CO\ +\ NuH\ \xrightarrow{\text{catalyst}}\ $$

$$R\diagdown\!\!\diagup\ +\ CO\ +\ NuH\ \xrightarrow{\text{catalyst}}\ $$

$$R\diagdown\!\!\diagup\ +\ CO\ +\ H_2\ \xrightarrow{\text{catalyst}}\ $$

$$RCH_2\text{-}X\ +\ CO\ +\ NuH\ \xrightarrow{\text{catalyst}}\ RCH_2\text{-}CONu$$
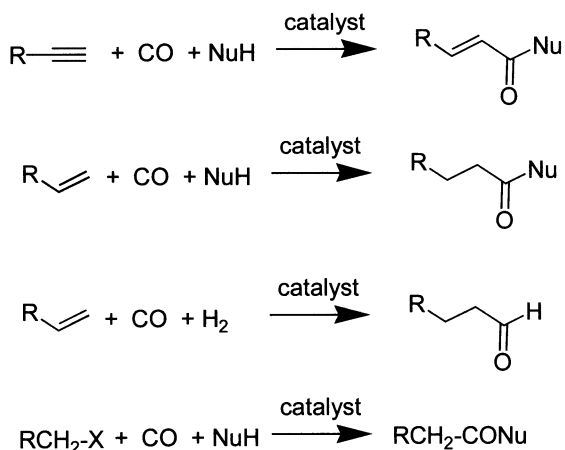
Scheme 2: Different types of industrially important carbonylation reactions.

These reactions are closely related to the hydroformylation process (oxo-synthesis) by which a formyl group and a hydrogen atom are attached to a olefinic double bond (see below). Apart from the carbonylation of unsaturated compounds the reaction of carbon monoxide with activated C-X compounds (X = OH, halide) is of industrial interest. Here, CO is inserted into an existing C-X bond leading to aliphatic or aromatic carboxylic acid derivatives. The most important industrial example of this type of chemistry is the carbonylation of methanol to give acetic acid.

Because most late and middle transition metal metals are capable to undergo the required elementary steps for carbonylation catalysis (e.g. coordination of CO and olefins, ligand exchange reactions) there exists a number of different catalysts based on Co, Rh, Ir, Ni, Pd, Pt, Fe, Mo, W, and others. However, the rate of ligand exchange reactions, insertion into CX-bonds, addition of CO to unsaturated bonds is different by orders of magnitude. Hence, catalyst performance of the different metals is quite diverse.

2.2   Hydroformylation

Today, from an industrial point of view, one of the most important homogeneously catalyzed reactions is the hydroformylation of olefins (Scheme 3) [6]. In this reaction discovered in 1938 by Otto Roelen at Ruhrchemie/Oberhausen olefins and synthesis gas (hydrogen and carbon monoxide) react to form aldehydes.
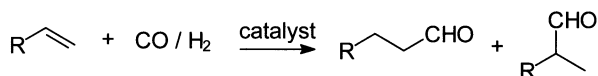
Scheme 3: Linear and branched aldehydes formed by hydroformylation of terminal olefins.

Despite investigations for more than 40 years still some mechanistic issues remain open; e.g. the hydrogenolysis of the metal acyl complex at different conditions.
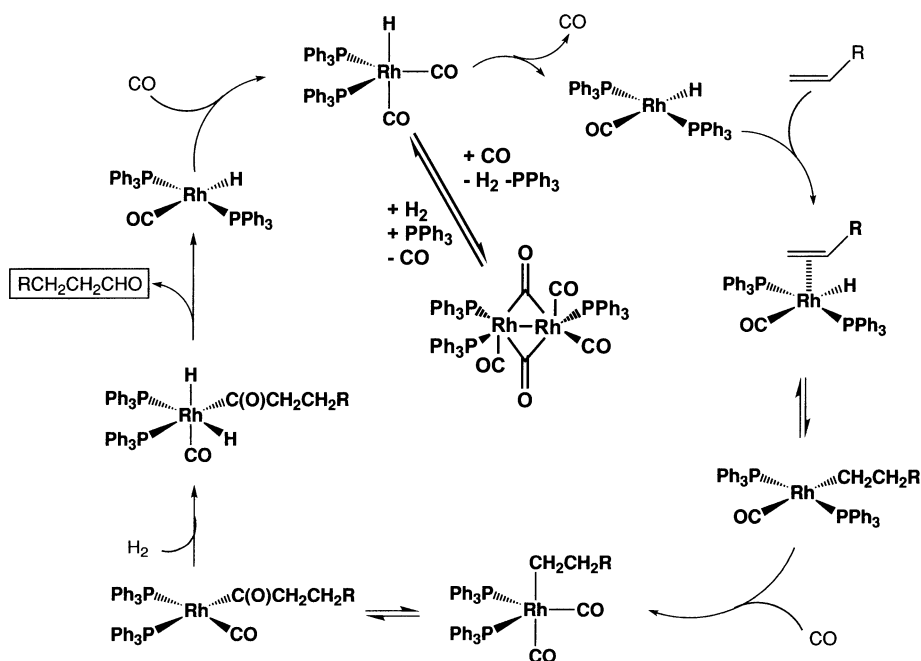
Scheme 4: General mechanism of the rhodium-catalyzed hydroformylation.

Although various transition metal based complexes (e.g. Ru, Ir, Co, Rh, Fe, ...) are known to catalyze hydroformylation reactions, mainly rhodium and (less) cobalt-based systems are used because of their superior activity. The generally accepted mechanism of the reaction using a triphenylphosphine rhodium based catalyst is depicted in Scheme 4. The major share of the produced aldehydes is applied as starting material for the production of alcohols, e.g. 2-ethylhexanol (made by aldol réaction of butyraldehyde and subsequent reduction), which in turn is used for the production of the corresponding terephthalic esters. These esters are used as plasticizers for polyvinylchloride (PVC) and therefore are produced on a

large scale (ca. 7-8 million tons in 2000). It is estimated that the volume of these products increase each year by 3%.

Nowadays commercial hydroformylation plants are run exclusively with catalysts based on either rhodium or cobalt as central metal. The first generation of hydroformylation processes (BASF, ICI, Ruhrchemie) using cobalt carbonyl complexes was run at relatively high temperature (150-180°C) and pressure (200-350 bar). Later on, Shell introduced a phosphine modified cobalt carbonyl process for the synthesis of detergent alcohols, which is still in use today.

Since the technical and economical success of the homogeneous low-pressure-oxo-processes (LPO) by Union Carbide and Celanese in the mid seventies a substitution of cobalt catalysts by rhodium catalysts is taking place. Therefore most of the hydroformylation studies in the last decade focused there attention on rhodium catalysts. Nevertheless, a significant amount of oxo products (> 2.5 Mio tons/a) is still produced using cobalt catalysts, especially, $HCo(CO)_4$ and $HCo(CO)_3PR_3$ complexes. Looking at the hydroformylation of propene which amounts for the major share of hydroformylation capacity, the technology of the cobalt-based processes has remained unchanged over the years, whereas in case of rhodium novel hydroformylation processes have been introduced. An important industrial development in this area was the Ruhrchemie/Rhône-Poulenc process [7], whereby a water-soluble rhodium catalyst is employed in a two-phase hydro-formylation process. Based on the original idea of Kuntz [8] a Rh/TPPTS complex (TPPTS = tris sodium salt of *meta* trisulfonated triphenylphosphine) is used as catalyst for this process which reached a production level of more than 500.000 tons per year nowadays. The economical competitiveness of the Ruhrchemie/Rhône-Poulenc process are based on the simple principle of catalyst recycling and the low-cost catalyst/product separation. Despite the advantages the Rh/TPPTS catalyst has also limitations, e.g. it is not possible to hydroformylate internal olefins or long chain olefins in water with sufficient catalyst activity.

What are recent trends in hydroformylation reactions? On the one hand industry is interested to substitute the more expensive terminal olefin feedstock by cheaper olefinic mixtures. Additional impetus for the development of alternative hydroformylation processes is provided by the discussion about new and more environmentally friendly plasticizer products [9]. Thus, hydroformylation of low-price internal olefins to longer-chain linear aldehydes represents an important and actual task in industry. In fact P. W. N. M. van Leeuwen stated in 2000 in his excellent recent book *"The selective formation of linear aldehydes starting from internal alkenes is still one of the greater challenges in hydroformylation chemistry"* [10]. For example hydroformylation of *E*-2-butene and *Z*-2-butene to *n*-valeraldehyde is of industrial interest due to the economic advantage using raffinate II as feedstock. The product *n*-valeraldehyde may partly substitute *n*-butyraldehyde for the production of plasticizers. Also upon oxidation *n*-valeric acid is produced, which is the basis of new ester-type lubricants for CFC-substituents in refrigeration systems.

In order to obtain linear aldehydes from internal olefins the catalyst has to perform a fast isomerization between the internal and terminal olefin (Scheme 5: reaction a).
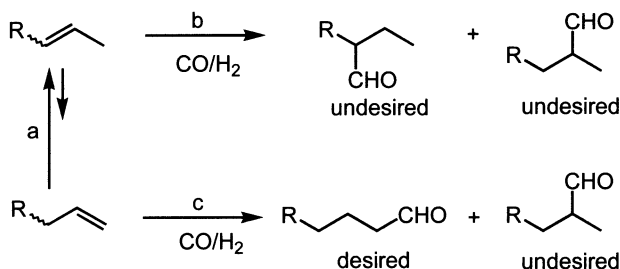
Scheme 5: Selective hydroformylation of internal olefins to give linear aldehydes: a) isomerizaton, b) hydroformylation of internal olefin, c) hydroformylation of terminal olefin.

Unfortunately the thermodynamic equilibrium mixture contains in general less than 5 % of the terminal olefin (for this reason isomerization should be avoided if terminal olefins are used as starting material). In addition, the hydroformylation of the terminal olefin (Scheme 5: reaction c) must occur many times faster (and with high n-selectivity) compared to the reaction of the internal olefin (Scheme 5: reaction b).

To date different homogeneous catalysts have been tested for use in the hydroformylation of internal olefins. In general cobalt-based homogenous systems show the same hydroformylation activity for terminal and internal olefins. However, these catalysts need high temperatures and pressures (up to 190 °C and 250 bar) which is not desirable for industry. The selectivity towards the linear products, which is reported as n/i-ratio, is typically in between 1:1 and 7:1 even if phosphine-modified systems are used. In the presence of cobalt catalysts it is often observed that the selectivity does not depend on whether the terminal or internal isomer is reacted olefins. Interestingly, not only is the rate of olefin isomerization faster than hydroformylation with cobalt catalysts but also the CO insertion step is faster than olefin dissociation. Thus the internal olefins are converted to aldehydes without leaving the metal. In contrast to cobalt catalysts rhodium phosphine systems show a much higher activity for terminal olefins and internal olefins are converted only very slowly to branched aldehydes with little isomerization. Similar to cobalt catalysts coordinatively unsaturated rhodium species exhibit activity towards isomerization of the olefinic substrate.

Such unsaturated rhodium species are formed either due to a lack of CO in the liquid phase or in the presence of sterically demanding ligands which prevent the coordination of more than one phosphorous-containing ligand [11].

In this respect Billig *et al.* reported excellent selectivities for the rhodium-catalyzed hydroformylation of internal olefins using chelating bulky phosphites as ligands. Here, n/i-ratios up to 96:4 have been obtained for the hydroformylation of 2-butene by using the chelating, but sterically demanding phosphites [12]. More recently, also phosphonites, phosphinites and even phosphines have been developed [13]. This area clearly demonstrates that catalyst improvement in

homogeneous catalysis still is based to a large extent on the synthesis of new organic ligands. Despite progress in the area of molecular modeling, successful ligand synthesis relies on experience, intuition and trial and error.

Phosphite derivative (UCC 1)

☞ *Bryant et al., EP 213639, 1987 (UCC)*

☞ *Burke et al., WO 97/33854, 1997 (DSM/DuPont)*

R = t-Bu

☞ *Börner et al., Angew. Chem. Int. Edn., 2001, 40, 1696*

NAPHOS derivative

☞ *Beller et al., Angew. Chem. Int. Ed. 2001, 40, 3408.*

XANTPHOS derivative

☞ *van Leeuwen et al., Angew. Chem. Int. Ed. 1999, 38, 336.*
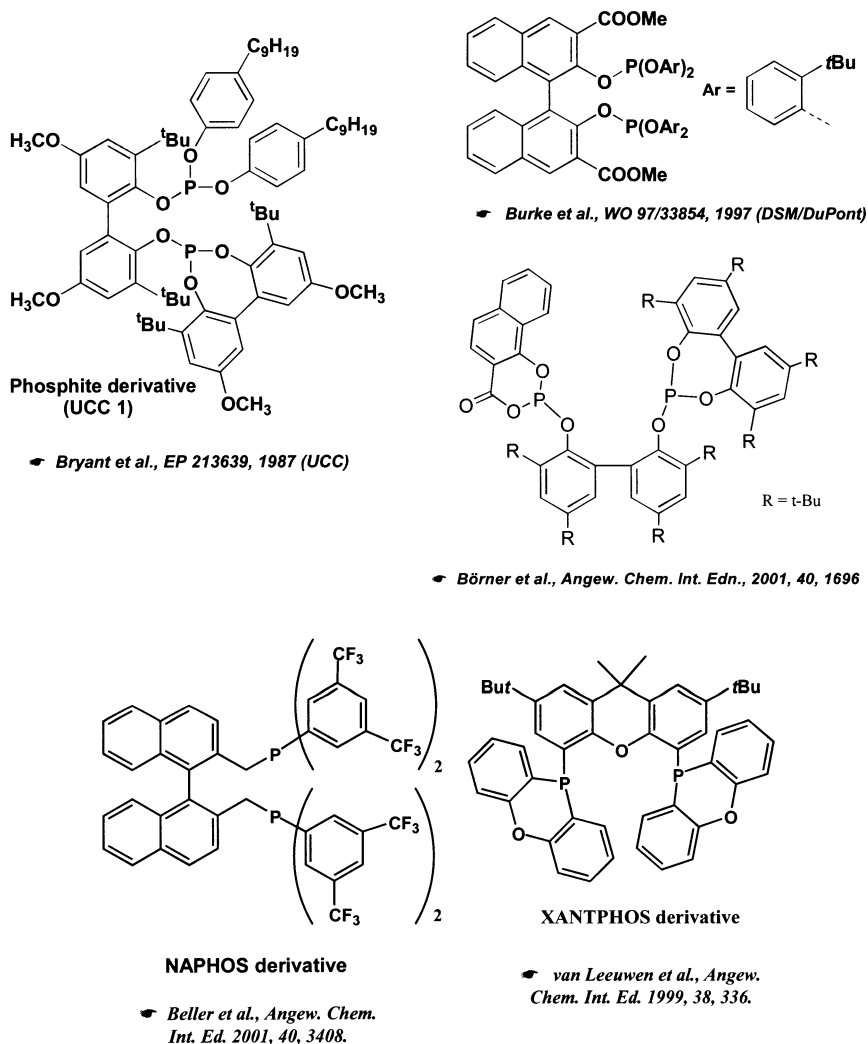
Scheme 6: Ligands for hydroformylation of internal olefins to linear aldehydes.

Unfortunately, most the ligands shown in Scheme 6 have a rather complicated structure which makes them difficult to synthesize. In addition P-O based ligands are susceptible towards Arbuzov-type degradation reactions, which is bad for long term stability. Hence, further improvements are needed for large scale application. Nevertheless new industrial applications are predicted to take place in the next 5 years.

An environmentally benign (atom efficient, one pot) synthesis of amines from olefins using an in situ hydroformylation is the so-called hydroaminomethylation reaction [14]. After initial hydroformylation of the olefin subsequent formation of an enamine (or imine) followed by hydrogenation takes place. Since its discovery by Reppe at BASF the hydroaminomethylation reaction has been mainly studied in industry. Only in recent years especially Eilbracht and co-workers developed new methodologies based on tandem sequences using the hydroaminomethylation reaction. Interestingly, the synthesis of linear amines from internal olefins via hydroaminomethylation has been described very recently [15].

2.3   Other Carbonylations of Olefins and Alkynes

Pioneering work in the field of carbonylations was done by W. Reppe at BASF in the thirties and forties of the 20th century. He coined the term carbonylations for the addition of carbon monoxide to unsaturated compounds in the presence of nucleophiles. In Scheme 7 typical carbonylation reactions of olefins are depicted. In these reactions similar to hydroformylations, selectivity of linear versus branched products is an important issue. Often mixtures of isomeric carboxylic acids are obtained, owing not only the occurrence of both Markovnikov and *anti*-Markovnikov addition of the alkene to the metal hydride, but also to the metal-catalyzed alkene isomerization. If the nucleophile NuH is water or an alcohol the reaction is usually called hydrocarboxylation or hydroesterification. Furtheron thiols, amines, acids and even CH-acidic compunds can be applied as nucleophiles in these reactions.

$$R{-}CH{=}CH_2 \; + \; CO \; + \; H_2O \; \longrightarrow \; R{-}CH_2{-}CH_2{-}COOH$$

$$R{-}CH{=}CH_2 \; + \; CO \; + \; ROH \; \longrightarrow \; R{-}CH_2{-}CH_2{-}COOR$$

$$R{-}CH{=}CH_2 \; + \; CO \; + \; RSH \; \longrightarrow \; R{-}CH_2{-}CH_2{-}COSR$$

$$R{-}CH{=}CH_2 \; + \; CO \; + \; HNR^1R^2 \; \longrightarrow \; R{-}CH_2{-}CH_2{-}CONR^1R^2$$

$$R{-}CH{=}CH_2 \; + \; CO \; + \; HOOCR' \; \longrightarrow \; R{-}CH_2{-}CH_2{-}COOCOR'$$
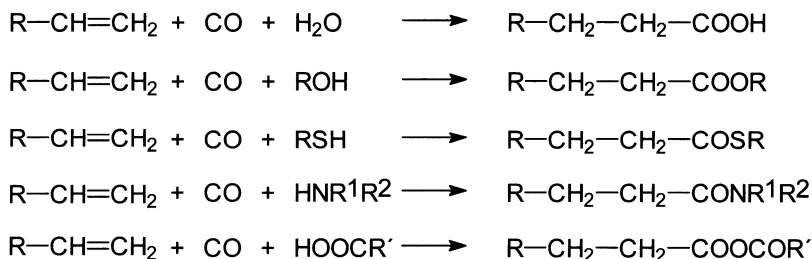
Scheme 7: Typical carbonylations of alkenes in presence of various nucleophiles.

In addition to olefins also alkynes can be converted into α,β-unsaturated compounds. Formally, a hydrogen and a CONu group are attached to the C-C triple bond. In principle the formation of *E* and *Z* double bond isomers is observed. In contrast to the carbonylations of alkynes, the carbonylation of alkenes is slower and therefore often higher pressures and temperatures are required to reach acceptable rates.

Among the different carbonylation reactions the hydrocarboxylation has attracted most industrial interest. Importantly, this method provides a route to monocarboxylic acids, e.g. ethylene to propanoic acid, acetylene to acrylic acid or 1-olefins (readily available from oligomerisation of ethylene) to higher carboxylic

acids. In addition, the alkoxy carbonylation of 1,3-butadiene to give methyl 3-pentenoate (intermediate for ε-caprolactam) [16] and propyne to give methyl methacrylate (MMA) [17] were investigated intensively by industry in the last decade.

Catalysts for the hydrocarboxylation are complexes of the transition metals Ni, Co, Fe, Rh, Ru, Pd, Pt, and Ir. Under reactions conditions the corresponding metal carbonyls or hydridocarbonyls are formed from various catalyst precursors which can be metal salts (halides preferred), complex salts, oxides, or in some special cases even fine metal powders. In case of metal halides the nature of the anion plays an important role. Most important catalyst metals from an industrial point of view are Ni and Co. However, these catalysts require harsh conditions as can be seen from Table 1.

The $Co_2(CO)_8$-catalyzed hydrocarboxylation of linear α-olefins usually gives 50–60 % linear carboxylic acids, the total carboxylic acid yield being 80–90 %. Typical conditions are: 150–200 °C, 150–250 bar.

Table 1: Hydrocarboxylations of olefins with various catalysts.

Catalyst	$Co_2(CO)_8$	$Ni(CO)_4$	PdX_2L_2	$PtX_2L_2+SnX_2$	RhX_3
Temperature [°C]	150–200	200–320	70–120	80–100	100–130
Pressure [bar]	150–250	150–300	1–150	1–200	1–100

A special feature of cobalt catalysts is that if internal olefins are used predominantly the linear products are formed. This effect is very similar to what is observed in Co-catalyzed hydroformylations. In case of Co catalysts addition of hydrogen (5–10 vol%) is beneficial and accelerates the reaction. Also the presence of 3–8 mol equiv. pyridine as ligand accelerates the reaction. The cobalt-carbonyl/pyridine catalyst system is applied industrially for the synthesis of higher alkanoic acids, e.g. the hydrocarboxylation of isomers of undecene yields dodecanoic acid with approximately 80 % selectivity. The cobalt catalyst can be recovered on distilling over the products of the reaction.

It is commonly assumed for cobalt-catalyzed carbonylations that $Co_2(CO)_8$ reacts with hydrogen or an nucleophile (NuH) with an acidic proton to form the catalytically active species $HCo(CO)_4$ [18]. After replacement of one CO ligand by the olefin which could occur either by an associative or an dissociative mechanism, olefin insertion into the Co-H bond takes place (Scheme 8).

Subsequent coordination and insertion of CO into the metal-alkyl bond leads to the corresponding acyl complex. Finally, hydrolysis of the acyl complex with the nucleophile NuH gives the corresponding carboxylic acid or carboxylic acid derivative and completes the catalytic cycle. Presumably, the acyl cleavage takes place by a nucleophilic attack on the carbonyl carbon of the acyl group.

Nickel catalysts are more suitable for the carbonylation of alkynes, whereas for olefins, Co, Rh, Pd, Pt, and Ru are equally good if not better. Characteristic for nickel catalysts in the hydrocarboxylation of α-olefins is that as main product (60–70 %) the branched carboxylic acid is formed. With internal olefins branched products are formed exclusively.
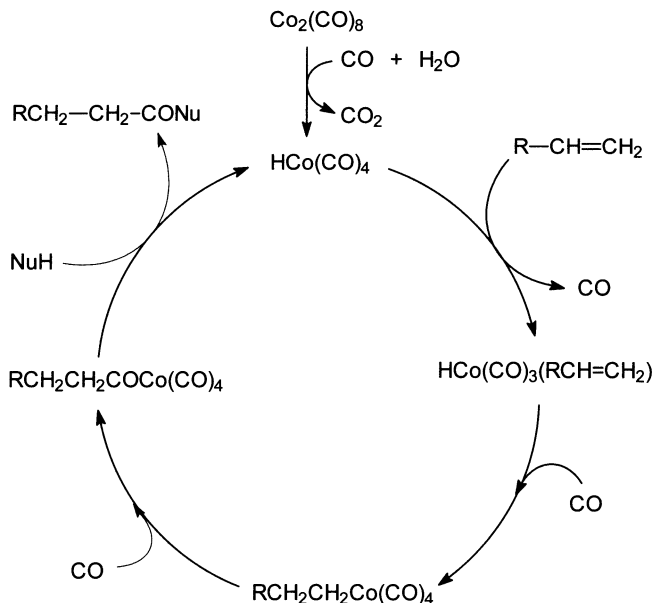
Scheme 8: Mechanism of the Co-catalyzed carbonylation.

More recently, Pd, Pt, Rh, and Ru found widespread use due to their better performance under milder conditions [19]. Platinum catalysts are superior concerning the regioselectivity, especially with tin compounds as co-catalysts. However, the rates remain quite low even under high pressure. As in hydroformylation the catalysts may be ligand modified or not. Co and Ni catalysts are usually used in an unmodified way, whereas ligands are used with Pd and Pt. Due to the milder reaction conditions substrates like butadiene and styrene can be efficiently carbonylated with Pd catalysts. Otherwise polymerization or other side reactions are problematic. The regioselectivity of hydroesterification of alkyl acrylates or aromatic olefins catalyzed by L_mPdX_n can be largely controlled by variation of the ligands. Triphenylphosphine promotes preferential carboxylation to the branched isomer, wheras with bidentate bisphoshines the linear product is produced overwhelmingly.

In case of Pd-catalyzed carbonylations, there is support for the involvement of $HPdCl(PPh_3)_2$ as the acitve species under acidic conditions. Evidence for this comes from the isolation of *trans*-Pd-(COPr)Cl(PPh$_3$)$_2$ from propene hydroformylation,[20] while $Pd(CO)(PPh_3)_3$ is inactive as a catalyst in the absence of HCl. In the case of PdX_2L_2/SnX_2 catalyst systems olefins seem to be the hydrogen source for the formation of the active Pd-H species. Under neutral or basic conditions, another mechanism involving a alkoxycarbonyl complex may operate (Scheme 9).
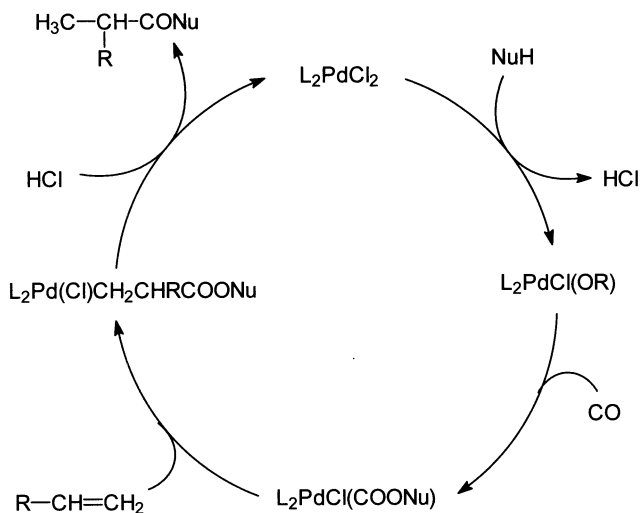
Scheme 9: Mechanism of the palladium-catalyzed carbonylation under neutral or basic reaction conditions.

Future challenges for carbonylation reactions of olefins and alkynes remain the improvement of catalyst activity and generality of the reactions. Still a number of functionalized olefins (interesting for fine chemicals) can not be efficiently (and selectively) carbonylated. Other challenging topics constitute carbonylations in water [21] or "novel" solvents, e.g. supercritical fluids and ionic liquids as well as asymmetric carbonylations. While progress in controlling the regiochemistry of hydrocarboxylations has been made, stereoselective carboxylations which are of interest for intermediates for pharmaceuticals and agrochemicals are clearly underdeveloped. Valuable representatives of higher-value acids are the commercially important 2-arylpropionic acids. Despite reasonable research efforts which led to progress in this area,[22] better catalysts systems which fulfill technical needs have yet to be developed. Best optical yields were reported to be 84 % ee with a turnover number (TON) of 7–8 for the synthesis of ibuprofen with $PdCl_2/CuCl_2$ as catalyst and 1,1´-binaphthyl-2,2´-diyl hydrogen phosphate (BNPPA) as ligand.

Interestingly, there is only little information available regarding the recycling of olefin or alkyne carbonylation catalysts. Similar to hydroformylation heterogeneous or heterogenized catalysts always face the problem of leaching via the formation of volatile metal carbonyl complexes or clusters. However, immobilization by a second soluble phase might be a more feasible approach, which has not been studied in detail for these reactions up to now.

Of current industrial interest is the methoxycarbonylation of 1,3-butadiene as a potential reaction step for a new ε-caprolactam synthesis. Therefor carbonylation reactions of butadiene shall be discussed in a little bit more detail. 1,3-Butadiene

can be functionalized by carbonylation reations in several ways. Depending on reaction conditions, monocarboxylate, dicarboxylate, or telomerized products can be obtained (Scheme 10).
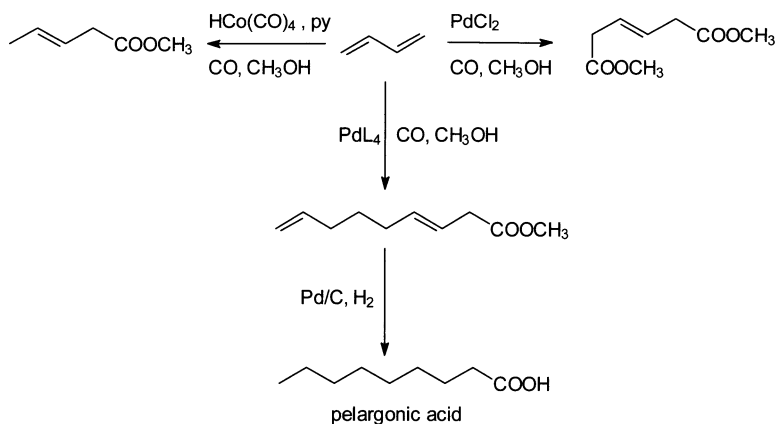
Scheme 10: Carbonylation reactions of 1,3-butadiene.

Telomerization of 1,3-butadiene occurs in the presence of methanol and CO using halide-free Pd as catalyst to give 3,8-nonadienoate ester [23]. Hydrogenation of the telomerization product provides pelargonic acid in good yields. Halide ions seem to inhibit dimerization because they occupy the coordination site on palladium and thus block the coordination of a second diene group required for the dimerization. Thus, palladium acetate solubilized by tert. amines gives the best yield of dimerization products. In contrast, oxidative carbonylation of 1,3-butadiene in methanol catalyzed by $PdCl_2$ gives dimethyl-2-butene-1,4-dicarboxylate, while palladium complexes operating under non-oxidative conditions catalyze the hydrocarboxylation to yield preliminary 3-pentenoates. This latter reaction has been optimized considerably by DSM. Earlier on BASF developed a three stage process for the synthesis of adipic acid from the butadiene-containing C_4 cut. Here, cobalt was the catalyst metal of choice for this process.
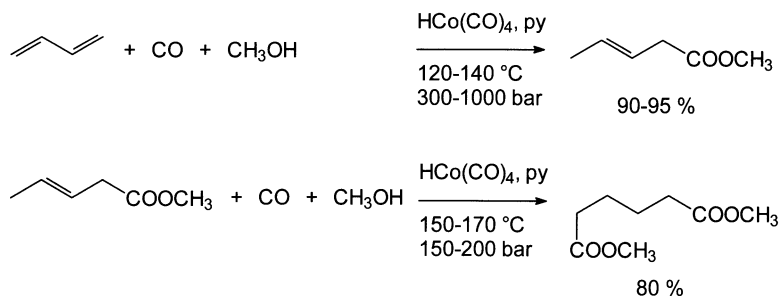
Scheme 11: BASF´s pilot-plant process for carbonylation of 1,3-butadiene.

The reaction takes place in two steps; the first stage which involves a lower temperature (100–140°C), uses a fairly high concentration of HCo(CO)$_4$ and pyridine as catalyst system to ensure rapid carbonylation of butadiene to give methyl pent-3-enoate in 90 % selectivity, thus avoiding typical side reactions such as dimerization and oligomerization. In the second step, the concentration of pyridine as a ligand must be low because it has an inhibitory effect on the isomerization reaction. In situ isomerization to the 4-pentenoic acid ester is a prerequisite for the subsequent carbonylation which provides dimethyl adipate. To ensure internal double-bond rearrangement, the temperature of the reaction is increased to 160–200 °C to give dimethyl adipate with 80 % selectivity. After hydrolysis of the ester, adipic acid is obtained with an overall selectivity of about 70 %.

A special type of carbonylation reaction is the so-called Pausen-Khand reaction. Here, an olefin and alkyne is reacted with CO to give directly cyclopentenones. Apart from cobalt also rhodium is a catalyst metal for this carbonylation reaction.

2.4   Carbonylations of Alcohols and Aryl Halides

Alcohols, amines, ethers, carboxylic acids and alkyl and aryl halides can be carbonylated to give the corresponding acids, amides, esters, anhydrides and acid halides for instance. Typically these reactions are catalyzed by either Pd, Rh, Co, Ir complexes under relatively drastic conditions (acid presence, > 100°C). While the carbonylation of aryl and benzyl halides attracted considerable interest from the organic synthesis community, the reaction of methanol to acetic acid constitutes the most important industrial example. Traditionally, rhodium or cobalt have been used for the carbonylation of methanol.

The mechanism of the rhodium-catalyzed carbonylation of methanol (generally referred as Montsanto process), is depicted in Scheme 12 [24]. The active species [Rh^I(CO)$_2$I$_2$]$^-$ can be easily formed from various Rh compounds. The rate determining step is the oxidative addition of methyl iodide (formed from methanol and HI) to [Rh^I(CO)$_2$I$_2$]$^-$ explaining the independence of the reaction rate on the CO pressure. After the oxidative addition, CO insertion into the alkyl-Rh bond takes place. CO up-take gives an 18 electron complex that decomposes under reductive elimination of acetic acid iodide into [Rh^I(CO)$_2$I$_2$]$^-$. In a second half cycle the iodide reacts with methanol producing acetic acid and methyl iodide. Although the acetic acid selectivity in this process is 99 % at low CO pressure (as low as 1 bar), in the last decade a new improved methanol carbonylation process emerged based on Ir as catalyst metal (Cativa™ process). Starting in the early 1990´s researchers of BP discovered that Ir catalysts provide high carbonylation activity even at low water content. This is a significant advantage compared to the Rh-based process because the catalyst is more stable and fewer by-products are formed. In addition also CO efficiency is advantageous compared to the Montsanto process. The active catalyst in the Cativa™ process is [Ir^I(CO)$_2$I$_2$]$^-$. The catalytic cycle is similar to the Rh process, however a different rate determining step is involved. Interestingly the performance of the Ir catalyst is improved by adding promotors such as Zn, Cd, In iodides or carbonyl complexes of Re, Ru, Os, W. Apparently these ·promoters abstract iodide from [IrCH$_3$(CO)$_2$I$_3$]$^-$ thereby

facilitating the formation of the corresponding acyl complex. So far 4 acetic acid plants of BP use this new technology.
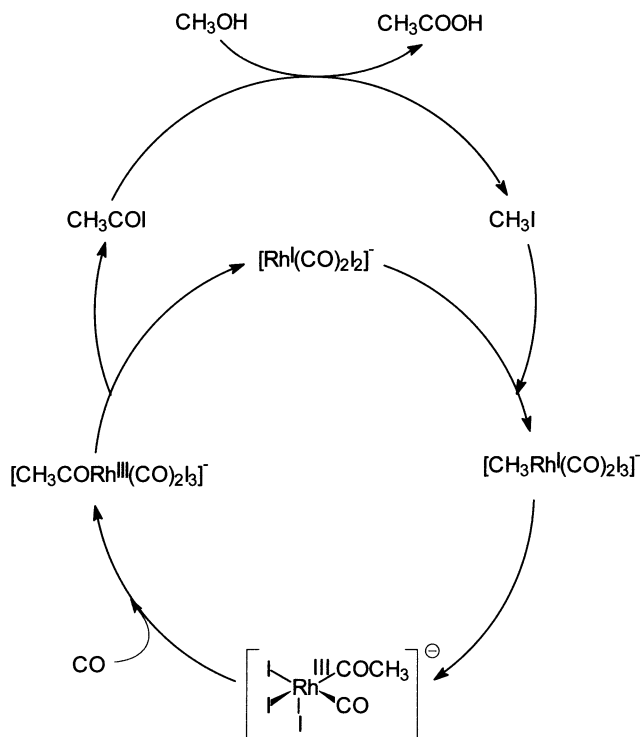
Scheme 12: Rhodium-catalyzed carbonylation of methanol.

Apart from bulk production, carbonylation reactions of aryl and benzyl halides have attracted interest of the fine chemical industry. Basically, these three component coupling reactions offer numerous possibilities for the selective synthesis of aromatic carbonyl compounds, especially carboxylic acid derivatives (acids, esters, amides). Additionally, aldehydes and ketones are accessible in a similar way (Scheme 13) [25].

n = 1, 2

X = I, Br, Cl, N_2^+, OSO_2R, ArI^+, IO_2, SO_2Cl

M = Na, K, BR_2, AlR_2, SnR_3, SiR_3

Nu^1 = OH, OR, NR_2, F, Cl; Nu^2 = H, alkyl, aryl, alkenyl, alkynyl, CN, RCO_2
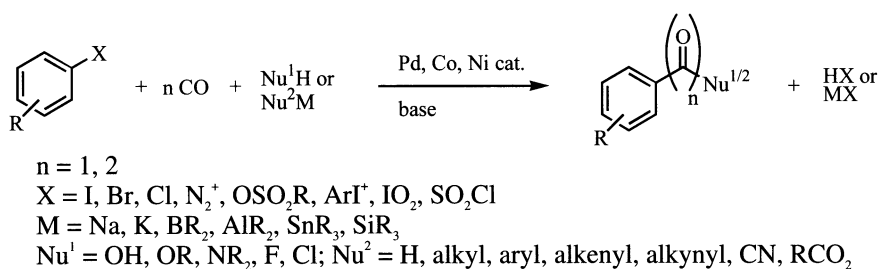
Scheme 13. Carbonylation of aryl–X derivatives.

An example for a carbonylation reaction applied for fine chemical production is Hoechst-Celanese's synthesis of Ibuprofen which is one of the important non-steroidal anti-inflammatory agents. The reaction sequence consists of the *p*-acetylation of *iso*-butylbenzene in liquid HF, reduction of the resulting acetophenone to the corresponding benzylic alcohol in the presence of a Pd/C catalyst and subsequent palladium-catalyzed carbonylation in conc. HCl to yield the target molecule (Scheme 14) [26].

This catalytic route is nowadays the main industrial production process (> 3500 t/a) for Ibuprofen due to the greatly reduced number of steps and the lower amount of by-products compared to the original Boots process.
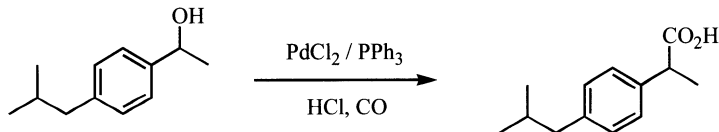
Scheme 14. Synthesis of Ibuprofen.

Among the carbonylation reactions of aryl halides, those of heteroaryl halides were of special interest to industrial research groups. This methodology provides an easy access to valuable intermediates for the manufacture of herbicides and pharmaceuticals. One example for the industrial application of a palladium-catalyzed carbonylation reaction is the synthesis of Lazabemide, a monoamine oxidase B inhibitor by Hoffmann-La Roche. The original 8-step laboratory synthesis of Lazabemide could be replaced by a one step protocol starting from 2,5-dichloropyridine (Scheme 15) [27]. The product was isolated in 65 % yield. Traces of palladium in the product could be removed by appropriate work-up, because only small amounts of catalyst have to be used (TON = 3000).

In addition to aryl– and vinyl–X starting materials palladium-catalyzed carbonylations take place smoothly with allyl– and benzyl–X (X = Cl, Br, I, OAc, OC(O)R, etc.) compounds. Apart from the synthesis of Ibuprofen the industrially interesting carbonylations of benzyl chloride to give phenyl acetic acid [28] or *N*-acetyl phenyl alanine [29] have been studied.
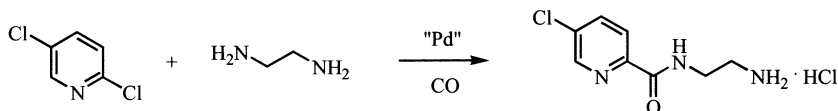
Scheme 15. Synthesis of Lazabemide.

The most recent successful example of this chemistry is Clariant´s process for the production of isochroman-3-one starting from o-xylylene dichloride (Scheme 16). In the highly efficient one step reaction sequence a palladium/ phosphine-catalyzed carbonylation and subsequent lactonization is performed in the presence of water in NMP as the solvent. Advantageously in this reaction a suitable (tertiary) alkanol instead of a base can be used for neutralization of hydrochloric acid resulting in the formation of the corresponding alkyl chloride [30].
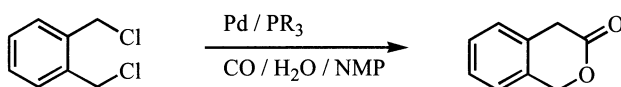
Scheme 16. Synthesis of isochroman-3-one by Clariant.

Future challenges for C-X carbonylations include direct reactions of alcohols. Even better would be the selective carbonylation of C-H bonds. Although some special examples demonstrate that such reactions are indeed possible, still general methodologies have to be developed.

3.   Other (Bulk) Olefin Refinement Reactions

Similar to the carbonylation other important homogeneous catalytic reactions of olefins involve the addition of olefin to a transition metal hydride complex. The resulting alkyl complex can then undergo various functionalization reactions. Important examples include dimerization and oligomerization of olefins, cyclodimerization, telomerizations, hydrocyanation, catalytic hydroborations, hydroaminations and of cause hydrogenation and hydrosilylation.

Due to the limited space of this chapter only few important industrial examples will be mentioned. For more detailed information the reader is referred to an excellent monograph of homogeneous catalysis.

Low molecular weight olefins are dimerized in the presence of cationic nickel complexes [31]. The general reactivity decreases in the order ethylene > propylene > butene. The reactions proceed via olefin addition into Ni-H complexes and subsequent ß-hydride elimination. In the presence of sterically demanding phosphines the formation of tail-to-tail dimers is favored. Today the regioselective dimerization of propene is done on commercial scale by Sumitomo and BP. The selective dimerization of ethylene to give 1-butene is observed in the presence of titanium catalysts. The high selectivity obtained is due to the formation of a titanacyclopentane. This reaction (Alphabutol® process of IFP) does not involve hydride intermediates, hence double bond isomerization is not taking place.

Related to olefin dimerization reactions is the oligomerization of olefins. Here, the reaction of ethylene to give α-olefins is of significant importance, because the products are versatile intermediates for the chemical industry. Ethylene

oligomerization is performed as one step of the Shell Higher Olefin Process (SHOP), which was basically developed to produce α-olefins for detergents. The SHOP constitute of ethylene oligomerization, isomerization of the resulting C_4-C_{10} and C_{20+} olefins and metathesis of the lower and higher internal olefins. The oligomerization reaction is run preferentially in 1,4-butanediol in which the catalyst, but not the resulting products are soluble. This was probably the first commercial example of a liquid/liquid biphasic reaction system. As catalyst nickel complexes such as the ones shown in Scheme 17 are employed [32]. Nowadays approximately 1 million tons of α-olefins per year are produced by this process.
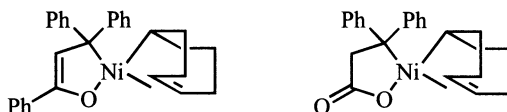
Scheme 17. Nickel complexes for ethylene oligomerization.

Olefin dimerization and oligomerization reactions can also be performed in an intramolecular manner. This reactions are called cyclodimerization or cyclo-oligomerization reactions [33]. For application the cyclodimerization and -trimerization of 1,3-butadiene in the presence of nickel/phosphine or phosphite catalysts to give cyclooctadienes and cyclododecatrienes, respectively are prominent examples.

A special type of olefin dimerization in the presence of nucleophiles is the so-called the telomerization. This reaction assembles simple starting materials in a 100 % atom efficient manner to give octadienes [34]. In general, the telomerization reaction is the dimerization of two molecules of a 1,3-diene in the presence of an appropriate nucleophile HX, *e.g.* alcohols,[35] to give substituted octadienes (1-substituted 2,7-octadiene, 3-substituted 1,7-octadiene). The resulting compounds are useful as intermediates in the total synthesis of several natural products as well as in industry, especially as precursors for plasticizer alcohols,[36] important monomers, solvents, corrosion inhibitors and non-volatile herbicides [37]. For industry 1,3-butadiene and methanol are the most attractive starting materials due to their ready availability and their exceedingly low price. Apart from the desired product 1-methoxyocta-2,7-diene (1), the 3-substituted octa-1,7-diene (2) (*iso*-product), 1,3,7-octatriene (3) (formed by the linear dimerization of butadiene) and – less importantly – 4-vinylcyclohexene (4) (formed by the Diels-Alder reaction of two molecules of butadiene) are observed as major by-products in this reaction (Scheme 18).
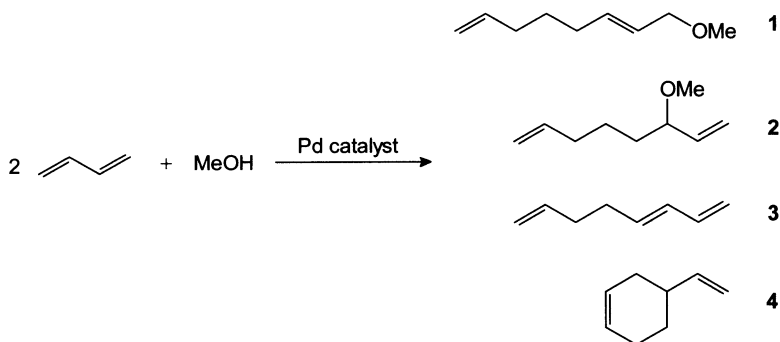
Scheme 18. Telomerization reaction of 1,3-butadiene with methanol.

The mechanism of the palladium-catalyzed telomerization reaction has been carefully examined (Scheme 19) [38]. Recently, it has been shown that the main principle which governs the *n / iso* (l/b) selectivity of the octadienyl products is an internal coordination of the olefinic side-chain. Hence, one should avoid a large excess of coordinating ligands. Unfortunately using phoshines as ligands it is necessary to use an excess of phosphine in order to stabilize the palladium catalyst appropriately at low catalyst concentration. Recently, palladium complexes based on carbene ligands, which are more strongly bound to the metal center, led to improved catalysts for this reaction [39].

Industrially applied is the telomerization reaction by Kuraray. The company produces *ca.* 5000 t/a of 1-octanol in a two step procedure consisting of telomerization of 1,3-butadiene with water to yield 2,7-octadien-1-ol and subsequent heterogeneous nickel-catalyzed hydrogenation of both double bonds [40]. Here, for stabilization of the palladium catalyst not a phosphine ligand itself is employed in the process but an alkyl phosphonium salt which is believed to be in equilibrium with the corresponding tertiary phosphine under reactions conditions. Remarkable selectivities of more than 90 % are observed. However, the catalyst activity and productivity are relatively low, preventing the use of this chemistry in the synthesis of commodities.

384   M. Beller
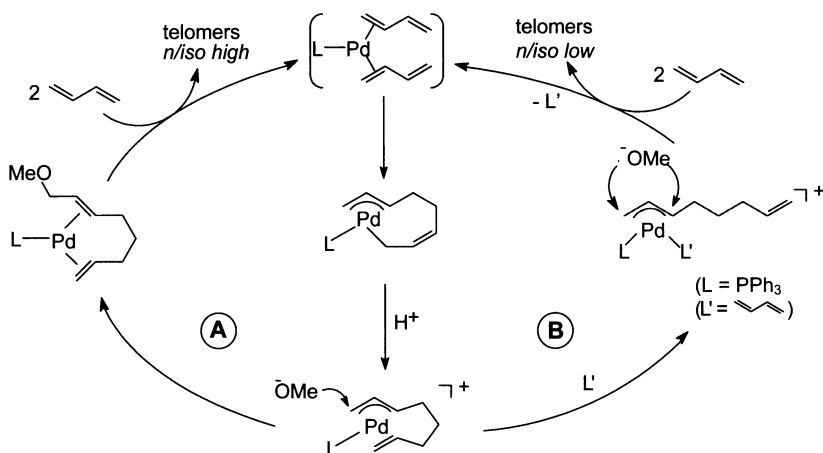
Scheme 19. Mechanism of the palladium-catalyzed telomerization reaction.

A different type of olefin refinement reaction represent the addition of nucleophiles to olefins. Examples include the catalytic hydroamination, hydrocyanation, hydroboration and Wacker reaction of olefins. However, in general carbon-heteroatom bond forming reactions are only used rarely in industrial laboratories. Hence, practical methods for the direct transformation of unfunctionalized olefins to alcohols or amines particularly to industrially important linear *anti*-Markovnikov products are rare. Catalysis is obligatory for such conversions and hence the functionalization of olefins with *anti*-Markovnikov regioselectivity is viewed as one of the major challenges of catalysis [41]. Active research work in this field for the past years shows possibilities of a few catalytic routes for this transformation [42]. For instance, the amine can be activated by oxidative addition to a transition metal, which allows insertion of the alkene into the M–N or M–H bond, thereby promoting the hydroamination catalytically (Scheme 20).
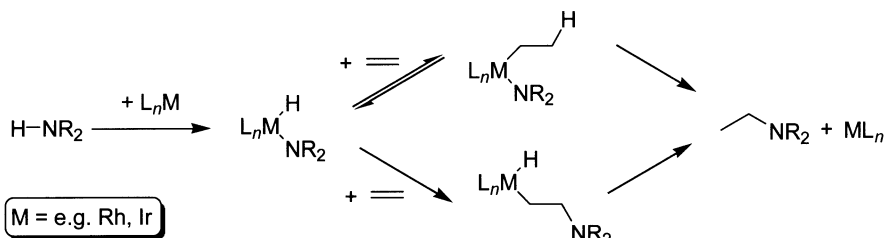
Scheme 20. Catalytic hydroamination of olefins via oxidative addition of the amine to a transition metal.

Actinides [43] and early transition metal complexes [44] can activate the amine by converting it into the coordinated imide M=NR and enable the reaction of C–C multiple bonds with the M–N bond (Scheme 21).

$$H_2NR \xrightarrow[\text{- 2 R'H}]{\text{+ } L_nMR'_2} L_nM=NR \xrightarrow{\text{+ }\equiv} L_nM\overset{R}{\underset{N}{\diagup}} \xrightarrow[\text{- } L_nM=NR]{\text{+ } H_2NR} \diagdown NR$$

$$\boxed{M = \text{e.g. U, Zr, Ti}}$$
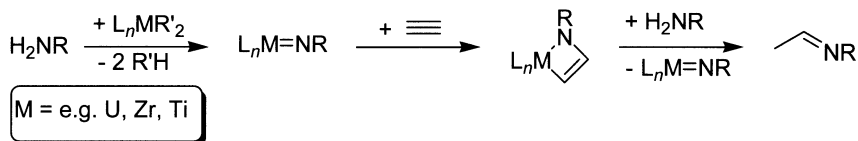
Scheme 21. Catalytic hydroamination of alkynes via metal imide species.

Also strong bases or strongly electropositive metals like alkali, alkaline earth or the lanthanide group elements,[45] can deprotonate amines to give more nucleophilic amides, which can undergo addition to certain olefins. In addition to the activation of the amino group, C–C multiple bonds can also be activated towards hydroamination by late transition metals [46]. Here, the nucleophilic attack of amines on the unsaturated C–C bond is facilitated by coordination of the olefin (alkyne) to an electrophilic transition metal center: β-hydride elimination from the resulting 2-aminoalkylmetal complex leads to the oxidative amination product and protonolysis leads to the hydroamination product (Scheme 22).

$$\equiv \xrightarrow[\text{- L}]{\text{+ } L_nM} L_{n-1}M\text{- -}\| \xrightarrow[\text{- H}^+]{\text{+ HNR}_2} \left[L_{n-1}M \diagdown NR_2 \right]^-$$

Oxidative Amination

$$\diagup NR_2 \quad + \quad L_{n-1}M\text{--}\overline{H}\rceil^-$$

$$\overset{H^+, L}{\searrow} \diagdown NR_2 \quad + \quad ML_n$$

Hydroamination

$$\boxed{M = \text{e.g. Pd, Pt}}$$
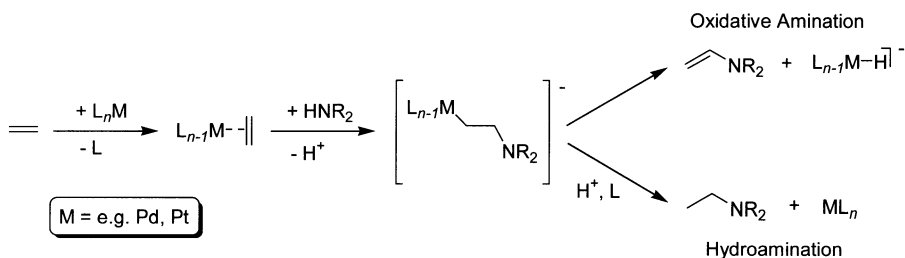
Scheme 22. Amination via activation of olefins.

Aliphatic nitriles are easily produced via hydrocyanation of olefins. The commercial interest in this methodology mainly stems from the DuPont´s adiponitrile process. Here, 1,3-butadiene is first monocyanated in the presence of a nickel phosphite complex into a mixture of 3-pentenenitrile and 2-methyl-3-butenenitrile (70:30). Subsequent isomerization in the presence of a nickel catalyst and a Lewis acid give 3- and 4-pentenenitriles. The final step consists of a second nickel-catalyzed hydrocyanation in the presence boron compounds (Scheme 23).
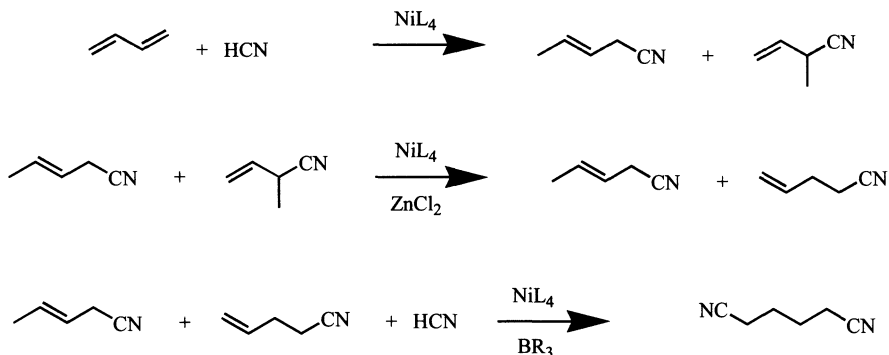
Scheme 23. DuPont´s adiponitrile process.

Recently, asymmetric hydrocyanation reactions, e.g. of substituted styrenes to give valuable intermediates for chiral aryl propionic acids, have been studied in more detail. Chelating bisphosphinites based on carbohydrates and phosphoramidites were found to be excellent ligands for these reactions.

4.   Selected Catalytic CC-coupling Reactions for the fine Chemical Industry

Compared to the petrochemistry and the bulk chemical industry the area of fine chemical synthesis is expected to grow more rapidly in the future because fine chemicals are essential feed stocks for pharmaceuticals, agrochemicals and "life style" products, all manufactured by the emerging "life science" companies. Hence, the interest in fine chemicals has been increased both in industry and academic laboratories. In general two different definitions are used commonly for fine chemicals. On the one hand fine chemicals are defined through their production volume (less than 1 t up to *ca.* 10,000 t per year), on the other hand it is a product related specification (intermediates for active substances, food additives, fragrances, special tensides, dyes, etc.). In general, fine chemicals are characterized by a comparatively complex molecular structure containing various functionalities and often stereogenic centers. Their syntheses include several steps resulting in a significant increase in value. Often product life times (< 10 up to 30 years) are significantly lower compared to those of bulk chemicals.

Palladium-catalyzed coupling reactions offer numerous interesting possibilities for fine chemicals synthesis [47]. Based on methodological developments achieved by a number of academic (and industrial) groups since the early 1970´s a number of new processes has been introduced. It is interesting to note that at the end of the 1980´s only one or two refinement reactions of aryl halides (Scheme 24) have been commercialized, while actually much more than 15 processes are currently applied in industry.
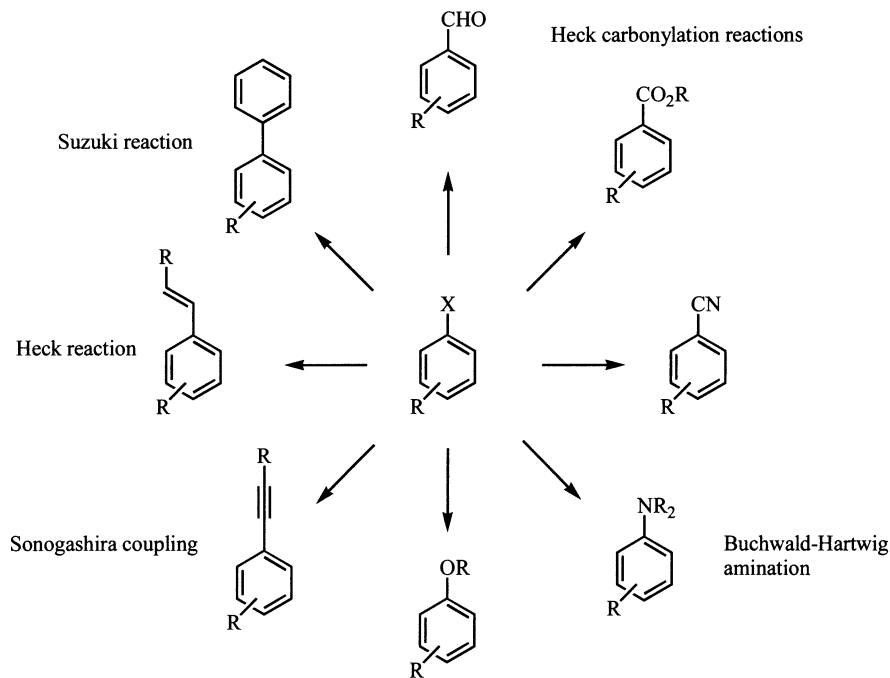
Scheme 24. Selected examples of palladium-catalyzed coupling reactions of aryl–X.

After the original discovery of a couple of novel catalytic reactions (Heck,[48] Suzuki,[49] Stille, Sonogashira, Negishi, etc.) starting from aryl iodides and bromides for constructing relatively simple molecules, it has been shown in the last 15 years that these reactions can be applied efficiently to the synthesis of numerous organic building blocks, natural products, monomers for functionalized polymers and biologically important molecules. The main advantages of these coupling processes compared to classical synthetic methods are the ready avai- lability of the different starting materials, the generality of the methods and the broad tolerance of the palladium catalysts with various functional groups.

In order to apply more and more of these reactions in the fine chemical industry still significant cost reductions of the generally developed lab-scale syntheses must occur. Efforts to substitute costly iodides or triflates by economically more attractive chlorides, reduction of catalyst concentration etc are to be seen in this respect. Typical examples of palladium-catalyzed CC coupling reactions are shown in Schemes 26-30.
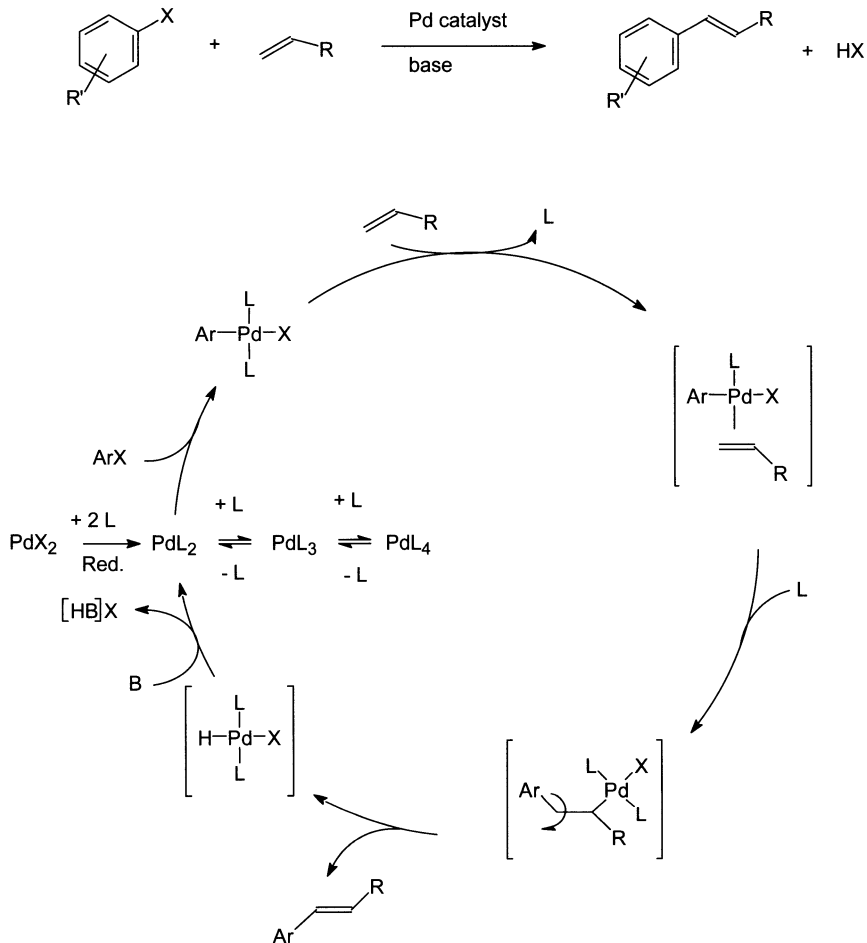
Scheme 25. Mechanism of the Heck reaction.

As an example of the mechanism of these reactions the simplified catalytic cycle of the palladium-catalyzed olefinations of aryl halides (Heck reaction) is shown in Scheme 25. Depending on the substrate and the reaction conditions the rate determining step is varying. Apart from aryl chlorides, which require special nucleophilic palladium catalysts, a variety of palladium complexes (both homogeneous and heterogeneous), even colloidal systems can be applied.

The Matsuda-Heck reaction of an aryl diazonium salt with 1,1,1-trifluoropropene is one of the earliest examples of a palladium-catalyzed coupling reaction realized on an industrial scale. The reaction sequence was developed elegantly by Baumeister, Blaser and co-workers from Ciba-Geigy and is performed on a multi-ton scale by Novartis for the synthesis of the herbicide Prosulfuron [50].

This process was made economically feasible by combining diazotization of 2-aminobenzene sulfonic acid, subsequent palladium-catalyzed olefination and hy-

drogenation in a one pot sequence with an overall yield of more than 93 % (i. e., an average yield of 98 % per step; Scheme 26).
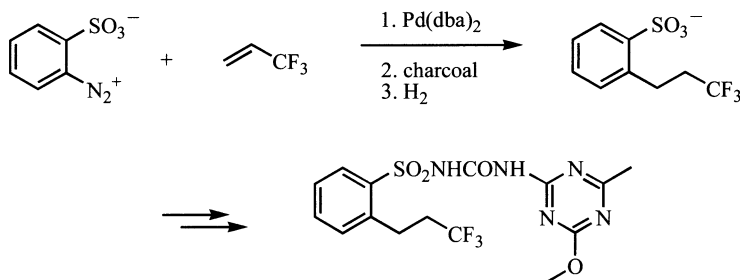
Scheme 26. The industrial synthesis of Prosulfuron.

Another interesting example of an industrial Heck reaction is the recently announced synthesis of Naproxen by Albermarle [51]. Here, 2-bromo-6-methoxynaphthalene is coupled with ethylene in the presence of a palladium catalyst with a sterically hindered basic phosphine ligand [52]. Known palladium-catalyzed hydrocarboxylation of 2-methoxy-6-vinylnaphthalene and subsequent resolution gives access to Naproxen (Scheme 27). Other profenes, e. g. Ketoprofen, can be produced by a similar reaction sequence.
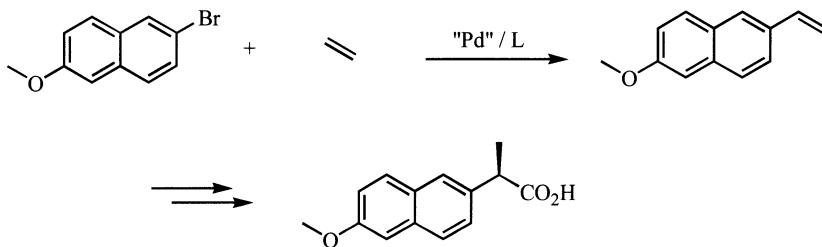
Scheme 27. Naproxen synthesis by Albermarle.

Similar alkenylations of aryl bromides with ethylene have been studied by de Vries from Dow Chemical in order to make high-purity 2- and 4-vinyltoluenes which are of interest as co-monomers for styrene polymers [53].

In the area of pharmaceuticals such palladium-catalyzed Heck reactions are increasingly applied. An example include a practical route to a new class of LTD$_4$ receptor antagonists, which was developed at Merck [54]. In the synthesis of a very similar active compound, the asthma drug Montelukast Sodium (Singulair, MK-0476 by MSD),[55] the intermediate phenethyl moiety (which is subsequently transformed to the thioether) is built up by the Heck coupling of methyl *o*-iodobenzoate with the substituted 3-arylpropene-3-ol and *in situ* isomerization of the primarily formed unsaturated alcohol (Scheme 28).
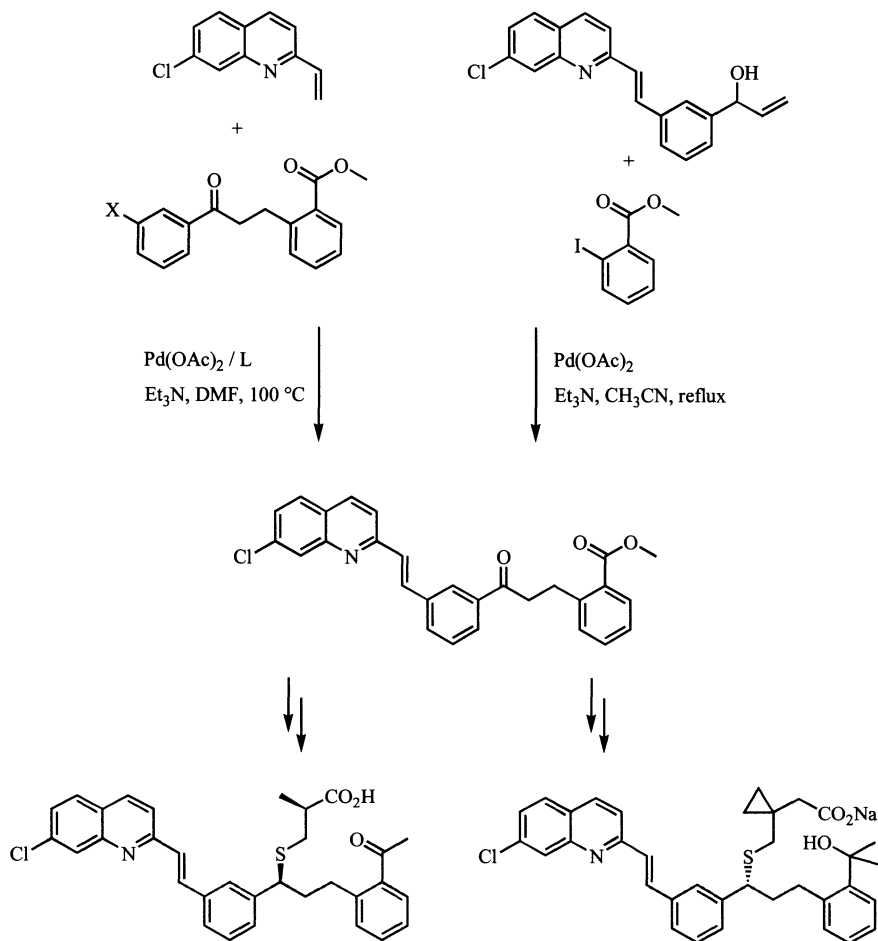
Scheme 28. Syntheses of L-699,392 and Montelukast Sodium.

Pfizer's Eletriptan,[56] a potent 5-HT$_{1D\text{-like}}$ partial agonist for the treatment of migraine, has completed Phase III trials. As in the case of Prosulfuron, aromatic alkylation is realized by a combination of Heck alkenylation and following hydrogenation of the resulting styrene derivative. Palladium(II) acetate and tri(o-tolyl)phosphine are used as the catalyst system.

In the area of Suzuki couplings the coupling of 4-tolylboronic acid and 2-chlorobenzonitrile to yield 2-cyano-4•-methylbiphenyl was applied at Clariant. This process was originally developed in the Central Research laboratories of Hoechst AG[57] but then has been transferred to Clariant. Surprisingly, the use of a simple palladium/sulfonated triphenylphosphine (TPPTS) catalyst gives high yield (> 90 %) of the desired biphenyl derivative (Scheme 29). The polar catalyst can easily be recycled by separating the two phases which form at the end of the reaction. The product 2-cyano-4•-methylbiphenyl that forms the organic layer is

used as a building block for the commercial synthesis of AT II antagonists. Merck also uses the Suzuki coupling as a key step in its synthesis of Losartan, but the synthesis strategy is a more convergent one [58].
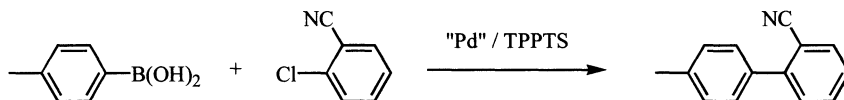
Scheme 29. Hoechst (Clariant) process for 2-cyano-4•-methylbiphenyl.

Other examples of industrial Suzuki reactions have been developed by Merck KG (Germany) for the synthesis of NLO materials [59]. In addition to Heck and Suzuki reactions, alkyne coupling reactions with aryl or vinyl halides (Sonogashira coupling reactions) have been realized on an industrial scale as well. Examples are members of a new class of LTD_4 receptor antagonists and Terbinafin,[60] which is the active agent of Sandoz's broad-spectrum antimycotic Lamisil. An important step in the synthesis of Terbinafin is the palladium-catalyzed coupling of a substituted alkenyl chloride with *tert*-butylacetylene (Scheme 30).
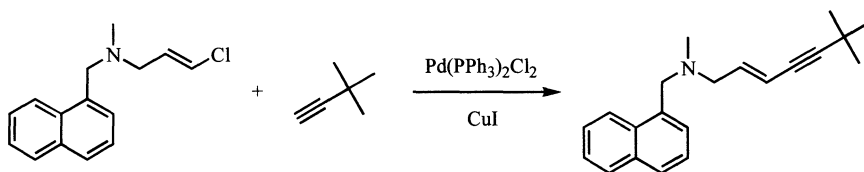
Scheme 30. Sandoz (Novartis) process for Terbinafin.

In addition to already realized processes there is an enormous demand for efficient transition metal-catalyzed processes for the manufacture of fine chemicals in the future.

In addition, relatively new coupling procedures such as the amination of aryl halides[61] may find application in industrial fine chemical synthesis. But also double carbonylations,[62] cyanations,[63] Grignard couplings[64] and other palladium-catalyzed reactions which have received only little attention in industrial organic synthesis so far may become interesting to fine chemical synthesis after significant improvements. As starting materials are aryl chlorides especially attractive. Significant advancements towards efficient activation of C-Cl bonds have been reported [65, 66, 67].

5.   Oxidation Reactions

5.1   Oxidations of Aromatic Compounds Aspects

The transition metal catalyzed oxidation of alkyl aromatics repesent one of the largest industrial-scale applications of homogeneous catalysis. Here, of special importance is the oxidation of p-xylene to give terephthalic acid derivatives.
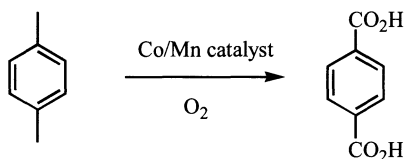
Scheme 31. Air oxidation of p-xylene.

Originally nitric acid was used for this oxidation. The Witten process developed in the 1950´s displaced this reaction. In the Witten process p-xylene is initially oxidized using air at 140-180° in the presence of cobalt/manganese catalyst systems to give the mono carboxylic acid. After esterification with methanol, subsequent oxidation and esterification leads to dimethyl terephthalate (DMT) in approximately 90%. The mechanism of these air oxidations involve radical chain reactions. Primarily a benzyl radical is formed by the electron transfer from xylene to cobalt(III). In contrast to the Witten process the Amoco process for terephthalic acid uses acetic acid as solvent. Here, the diacid is obtained in 95% yield in one step directly from p-xylene at 175-230°C. As a free radical source bromide ions are applied in the Amoco process.

In the area of fine chemicals different substituted toluenes (e.g. p-nitrotoluene, chlorotoluenes) are oxidized to a variety of substituted benzoic acids, which serve as intermediates for pharmaceuticals, agrochemicals and advanced materials.

5.2   Epoxidation and Dihydroxylation Reactions

The oxidative functionalization of olefins is of major importance for both organic synthesis and the industrial production of bulk and fine chemicals [68]. Among the different oxidation products of olefins, epoxides and 1,2-diols are used in a wide variety of applications. Epoxides, e.g. propylene oxide serve as starting material for bulk polymers. Approximately 45% of the 3 million tons of propylene epoxide produced annually are made by the so-called Oxirane process (Halcon or Arco process). The oxidation reaction uses an alkyl hydroperoxide in the presence homogeneous catalysts based on molybdenum, vanadium, tungsten, titanium, and other metals. In general molybdenum catalysts give the best selectivity and highest rate. In the commercial process the alkyl hydroperoxide is in situ generated from either isobutane or ethylbenzene. Hence, as co-products tert. butanol (which is converted further on to MTBE) or 1-methylbenzylalcohol (which is converted to styrene) are generated.

Also, ethylene- and propylene glycol are produced on a multi million ton scale per annum, due to their importance as polyester monomers and anti-freeze agents [69]. A number of epoxides and 1,2-diols such as styrene epoxide, glycidol, 2,3-

dimethyl-2,3-butanediol, 1,2-octanediol, 1,2-hexanediol, 1,2-pentanediol, 1,2- and 2,3-butanediol are of interest for the fine chemical industry. Chiral epoxides and 1,2-diols are employed as intermediates for pharmaceuticals and agrochemicals. The synthetic utility of asymmetric epoxidations is nicely demonstrated by the Sharpless epoxidation of allylic alcohols (Scheme 32) [70]. As oxidant tert. butyl hydroperoxide (TBHP) is employed in the presence of titanium tetraisopropoxide and diethyl tartrate (DET) as chiral ligand. While the original procedure required stoichiometric amounts of titanium alkoxides and chiral ligand, the addition of molecular sieves allowed a catalytic reaction.
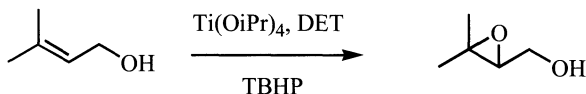
Scheme 32. Sharpless epoxidation of allylic alcohols.

Apparently this method is used for producing (*R*)- and (*S*)-glycidol on a commercial scale.

It is interesting to note that asymmetric epoxidations of unfunctionalized olefins proceed in a general way only with chiral manganese salen complexes, which were independently developed by Jacobsen and Katsuki et al. (Jacobsen epoxidation) [71]. There is still a need for more general and improved catalysts in this area. Importantly, similar salen complexes of other metals have been used as catalysts in efficient kinetic resolution reactions of epoxides.

The dihydroxylation of olefins is catalyzed by osmium, ruthenium or manganese oxo species. The osmium-catalyzed variant is the most reliable and efficient method for the synthesis of *cis*-1,2-diols [72]. Using osmium in catalytic amounts together with a stoichiometrically used secondary oxidant various olefins, including mono-, di-, and trisubstituted unfunctionalized as well as many functionalized olefins, can be converted to the corresponding diols. Since OsO_4 as an electrophilic reagent reacts only slowly with electron-deficient olefins, higher amounts of catalyst and ligand are necessary in these cases. Recent studies have revealed, that these substrates react much more efficiently when the pH of the reaction medium is maintained on the acidic side [73]. On the other hand it was found, that providing a constant pH value of 12.0 leads to improved reaction rates for internal olefins [74]. Since its discovery by Sharpless and co-workers the catalytic asymmetric dihydroxylation (AD) has significantly enhanced the utility of osmium-catalyzed dihydroxylation (Scheme 33) [75].
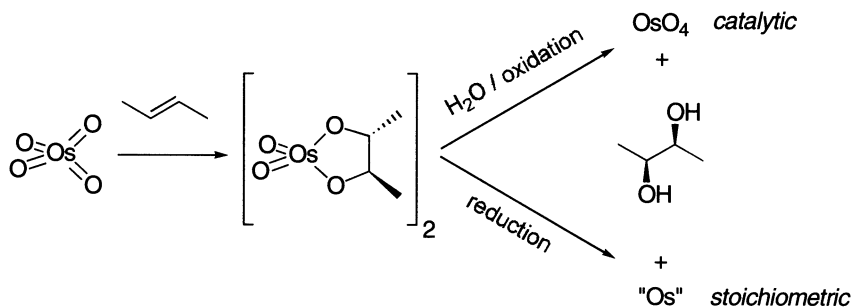
Scheme 33. Osmylation of olefins.

The problem of (enantio)selectivity has largely been solved through extensive synthesis and screening of cinchona alkaloid ligands by the Sharpless group. In the past several reoxidation processes for osmium(VI) glycolates or other osmium(VI) species have been developed. Historically, chlorates [76] and hydrogen peroxide [77] were first applied as stoichiometric oxidants, however in both cases the dihydroxylation often proceeds with low chemoselectivity. Other reoxidants for osmium(VI) are *tert*-butyl hydroperoxide in the presence of Et₄NOH [78] and a range of *N*-oxides such as *N*-methylmorpholine *N*-oxide (NMO) [79] (Upjohn process) and trimethylamine *N*-oxide. K₃[Fe(CN)₆] gave a substantial improvement in the enantioselectivities in asymmetric dihydroxylations when it was introduced as a reoxidant for osmium(VI) species in 1975. Today the "AD-mix", containing the catalyst precursor K₂[OsO₂(OH)₄], the cooxidant K₃[Fe(CN)₆], the base K₂CO₃, and the chiral ligand, is commercially available and the dihydroxylation reaction is easy to carry out. But the production of overstoichiometric amounts of waste remains as a significant disadvantage of the reaction protocol. More recently it was reported that the osmium-catalyzed dihydroxylation of aliphatic and aromatic olefins also proceeds efficiently in the presence of dioxygen at ambient conditions. As shown in Table 2 the new dihydroxylation procedure constitutes a significant advancement compared to other reoxidation procedures.

It should be noted that only salts and by-products formed from the oxidant have been included in the calculation. Other waste products have not been considered. Nevertheless the numbers presented in Table 2 give a rough estimation of the environmental impact of the reaction.

Table 2. Comparison of the dihydroxylation of α-methylstyrene in the presence of different oxidants.

Entry	Oxidant	Yield [%]	Reaction conditions	ee [%]	TON	Waste [kg/kg diol]
1 [80]	$K_3[Fe(CN)_6]$	90	0°C $K_2[OsO_2(OH)_4]$ ^{t}BuOH/H$_2$O	94[a]	450	8.1[c]
2 [81]	NMO	90	0°C OsO$_4$ Acetone/H$_2$O	33[b]	225	0.88[d]
3 [82]	PhSeCH$_2$Ph/ O$_2$ PhSeCH$_2$Ph/air	89 87	12°C $K_2[OsO_2(OH)_4]$ ^{t}BuOH/H$_2$O	96[a] 93[a]	222 48	0.16[e] 0.16[e]
4 [83]	NMM/Flavin/H$_2$O$_2$	93	RT OsO$_4$ Acetone/H$_2$O	-	46	0.33[f]
5 [84]	O$_2$	96	50°C $K_2[OsO_2(OH)_4]$ ^{t}BuOH/aq.	80[a]	192	-
6 [85]	NaOCl	99	0°C $K_2[OsO_2(OH)_4]$ ^{t}BuOH/H$_2$O	91[a]	247	0.58[g]

[a] Ligand: Hydroquinidine 1,4-phtalazinediyl diether. [b] Hydroquinidine p-chlorobenzoate. [c] $K_4[Fe(CN)_6]$ [d] N-Methylmorpholine (NMM). [e] PhSe(O)CH$_2$Ph. [f] NMO/Flavin-OOH. [g] NaCl.

5.3. Other Oxidation Reactions

In addition to the aforementioned reactions numerous other oxidation reactions play an important role in homogeneous catalysis. Due to the scope of this chapter only a few other examples should be named. Historically the oxidations of olefins to aldehydes or ketones represent an key development. Especially the oxidation of ethylene to acetaldehyde in the presence of palladium(II) salts and copper(II) chloride (Wacker process). As terminal oxidant oxygen is used which reoxidizes Cu(I) to Cu(II), which in turn oxidizes Pd(0) to Pd(II). The produced acetaldehyde served as starting material for acetic acid, which is nowadays produced more economically via carbonylation from methanol.

In the area of more specialized products the oxidation of functional groups represent a powerful tool for synthesis. Important methods include the selective oxidation of alcohols to aldehydes in the presence of perruthenate, the direct oxidation of alcohols to carboxylic acid derivatives in the presence of a variety of metal complexes, and the selective oxidative cleavage of double bonds in the presence of ruthenium complexes. Most of these oxidation reactions proceed under remarkably mild reaction conditions with high selectivity compared to heterogeneous catalysis. Clearly both disciplines could benefit from a closer collaboration within this area.

References

1   a) W. A. Herrmann: Angew. Chem. Int. Ed. **41**, 1290 (2002); b) A. C. Hillier, S. P. Nolan: Plat. Met. Rev. **46**, 50 (2002)

2   See for example: *Comprehensive Asymmetric Catalysis*, E. N. Jacobsen, A. Pfaltz, H. Yamamoto (Eds.) (Springer, Berlin 1999)

3   See for example: a) *Applied Homogeneous Catalysis with Organometallic Compounds*, B. Cornils, W. A. Herrmann (Eds.), 2nd Ed. (Wiley-VCH, Weinheim 2002) Vol. 1-3; b) *Transition Metals for Organic Synthesis*, M. Beller, C. Bolm (Eds.) (Wiley-VCH, Weinheim 2000) Vol. 1-2

4   A. Mullen, in *New Syntheses with Carbon Monoxide*, J. Falbe (Ed.) (Springer, Berlin 1980) p. 243

5   W. Bertleff, in *Ullmann´s Encycl. Ind. Chem.*, 5th Ed., (VCH, Weinheim 1986), Vol. A5, p. 217

6   For an excellent book see: a) *Rhodium Catalyzed Hydroformylation*, P. W. N. M. van Leeuwen, C. Claver (Eds.) (Kluwer, Dordrecht 2000); for major reviews see: b) C. D. Frohning, C. W. Kohlpaintner, H.-W. Bohnen, in *Applied Homogeneous Catalysis with Organometallic Compounds*, B. Cornils, W. A. Herrmann (Eds.), 2nd Ed. (Wiley-VCH, Weinheim 2002), Vol. 1, p. 30; c) M. Lenarda, L. Storaro, R. Ganzerla: J. Mol. Catal. **111**, 203 (1996); d) M. Beller, B. Cornils, C. D. Frohning, C. W. Kohlpaintner: J. Mol. Catal. **104**, 17 (1995)

7   a) B. Cornils: Industrial Catalysis News **2**, 7 (1998); b) B. Cornils, E. Wiebus: CHEMTECH **25**, 33 (1995); c) B. Cornils, E. Wiebus: Recl. Trav. Chim. Pays-Bas **115**, 211 (1996)

8   a) E. G. Kuntz: CHEMTECH **17**, 570 (1987); b) B. Cornils, E. G. Kuntz: J. Organomet. Chem. **502**, 177 (1995)

9   Chem. & Ind., 379 (May 18, 1998)

10   P. W. N. M. van Leeuwen, in *Rhodium Catalyzed Hydroformylation*, P. W. N. M. van Leeuwen, C. Claver (Eds.) (Kluwer, Dordrecht 2000) p. 57

11   a) P. W. N. M. van Leeuwen, C. F. Roobeek: J. Organomet. Chem. *258*, 343 (1983); b) A. van Rooy, E. N. Orij, P. C. Kamer, F. v. d. Aardweg, P. W. N. M. van Leeuwen: J. Chem. Soc., Chem. Comm. 1096 (1991)

12   a) E. Billig, A. G. Abatjoglou, D. R. Bryant: US 4769498 (1988); b) E. Billig, A. G. Abatjoglou, D. R. Bryant: EP 0213639 (1991); c) E. Billig, A. G. Abatjoglou, D. R. Bryant: EP 0214622 (1992)

13   a) M. Beller, B. Zimmermann, H. Geissler: Chem. Eur. J. **5**, 1301 (1999); b) D. Selent, K.-D. Wiese, D. Röttger, A. Börner: Angew. Chem. **112**, 1694 (2000); Angew. Chem. Int. Ed. **39**, 1639 (2000); c) B. Breit, W. Seiche: Synthesis 1 (2001); d) D. Selent, D. Hess, K.-D. Wiese, D. Röttger, C. Kunze, A. Börner: Angew. Chem. **113**, 1739 (2001); Angew. Chem. Int. Ed. **40**, 1696 (2001); e) L. A. van der Veen, P. C. J. Kamer, P. W. N. M. van Leeuwen: Angew. Chem. **111**, 349 (1999); Angew. Chem. Int. Ed. **38**, 336 (1999); f) H. Klein, R. Jackstell, K.-D. Wiese, M. Beller: Angew. Chem. **113**, 3505 (2001); Angew. Chem. Int. Ed. **40**, 3408 (2001)

14   P. Eilbracht, L. Bärfacker, C. Buss, C. Hollmann, B. E. Kitsos-Rzychon, C. L. Kranemann, T. Rische, R. Roggenbuck, A. Schmidt: Chem. Rev. **99**, 3329 (1999)

15   A. Seayad, M. Ahmed, H. Klein, R. Jackstell, T. Gross, M. Beller: Science 297, 1676 (2002)

16   M. Beller, A. Krotz, W. Baumann: Adv. Synth. Catal. **344**, 517 (2002) and references therein

17   E. Drent, P. Arnoldy, P. H. M. Budzelaar: J. Organomet. Chem. **475**, 57 (1994)

18   B. Cornils, in *New Syntheses with Carbon Monoxide*, J. Falbe (Ed.) (Springer, Berlin 1980) p. 1

19   Reviews: a) M. Beller, B. Cornils, C. D. Frohning, C. W. Kohlpaintner: J. Mol. Catal. **104**, 17 (1995); b) H. M. Colquhoun, D. J. Thompson, M. V. Twigg: *Carbonylation, Direct Synthesis of Carbonyl Compounds* (Plenum Press, New York 1991); c) R. F. Heck: *Palladium Reagents in Organic Syntheses* (Academic Press, New York 1985); d) M. Röper: Stud. Surf. Sci. Catal. **64**, 381 (1991)

20   R. Bardi, A. del Pra, A. M. Piazzesi, L. Toniolo: Inorg. Chim. Acta **35**, L345 (1979)

21   *Aqueous-Phase Organometallic Catalysis*, B. Cornils, W. A. Herrmann (Eds.) (Wiley-VCH, Weinheim 1998)

22   a) Chelucci, M. A. Cabras, C. Botteghi, M. Marchetti: Tetrahedron Asymm. **5**, 299 (1994); b) G. Consiglio, L. Roncetti: Chirality **3**, 341 (1991); c) T. Hiyama, N. Wakasa, T. Kusumoto: Synlett 569 (1991)

23   D. Neibecker, B. Stitou, I. Tkatcher: J. Org. Chem. **54**, 2459 (1989)

24   D. Forster: J. Am. Chem. Soc. **98**, 846 (1976)

25   a) M. Beller, B. Cornils, C. D. Frohning, C. W. Kohlpaintner: J. Mol. Catal. **104**, 17 (1995)

26   a) M. Beller, in *Applied Homogeneous Catalysis with Organometallic Compounds*, B. Cornils, W. A. Herrmann (Eds.), 2nd Ed. (VCH, Weinheim 1996) and references therein

27   a) R. Schmid: Chimia **50**, 110 (1996); b) M. Scalone, P. Vogt (Hoffmann-La Roche): EP 385210 (1990)

28   C. W. Kohlpaintner, M. Beller: J. Mol. Catal. **116**, 259 (1997) and references therein

29   J. G. de Vries, R. P. de Boer, M. Hogeweg and E. E. C. G. Gielens: J. Org. Chem. **61**, 1842 (1996)

30   a) H. Geissler, R. Pfirmann (Clariant): DE 19815323 (1998); b) H. Geissler, R. Pfirmann (Clariant): EP 1086949 (2000)

31   J. Skupinska: Chem. Rev. **91**, 613 (1991)

32   W. Keim, A. Behr, B. Limbäcker, C. Krüger: Angew. Chem. **95**, 505 (1983); Angew. Chem. Int. Ed. **22**, 503 (1983)

33   G. Wilke, A. Eckerle, in *Applied Homogeneous Catalysis with Organometallic Compounds*, B. Cornils, W. A. Herrmann (Eds.), 2nd Ed. (Wiley-VCH, Weinheim 2002) Vol. 1, p. 368

34   For recent reviews on telomerization reactions see: a) J. M. Takacs, in *Comprehensive Organometallic Chemistry II*, E. W. Abel, F. G. A. Stone, G. Wilkinson (Eds.) (Pergamon Press, Oxford, 1995) Vol. 12, p. 785; b) J. Tsuji: *Palladium Reagents and Catalysts: Innovations in Organic Synthesis* (John Wiley & Sons, Chichester, 1995) p. 422; c) N. Yoshimura, in *Applied Homogeneous Catalysis with Organometallic Compounds,* B. Cornils, W. A. Herrmann (Eds.) (Wiley-VCH, Weinheim, 1996) Vol. 1, p. 351

35   a) P. Grenouillet, D. Neibecker, J. Poirier, I. Tkatchenko: Angew. Chem. **94**, 796 (1982); Angew. Chem. Int. Ed. **21**, 767 (1982); b) R. Patrini, M. Lami, M. Marchionna, F. Benvenuti, A. M. R. Galletti, G. Sbrana: J. Mol. Catal. **129**, 179 (1998); c) F. Benvenuti, C. Carlini, M. Lami, M. Marchionna, R. Patrini, A. M. R. Galletti, G. Sbrana: J. Mol. Catal. **144**, 27 (1999); d) M. Basato, L. Crociani, F. Benvenuti, A. M. R: Galletti, G. Sbrana: J. Mol. Catal. **145**, 313 (1999)

36   N. Yoshimura, M. Tamura, (Kuraray Company, Ltd.): US 4.356.333 (1981)

37   J. Falbe, H. Bahrmann, W. Lipps, D. Mayer, *in Ullmann's Encyclopedia of Industrial Chemistry*, W. Gerhartz, Y. S. Yamamoto, F. T. Campbell, R. Pfefferkorn, J. F. Rounsaville (Eds.) (VCH, Weinheim 1985) Vol. A1, p. 279

38   For an excellent review see: a) P. W. Jolly: Angew. Chem. **97**, 279 (1985); Angew. Chem. Int. Ed. **24**, 283 (1985); b) F. Vollmüller, J. Krause, S. Klein, W. Mägerlein, M. Beller: Eur. J. Inorg. Chem. 1825 (2000); c) P. W. Jolly, R. Mynott, B. Raspel, K.-P. Schick: Organometallics **5**, 473 (1986); d) A. Behr, G. v. Ilsemann, W. Keim, C. Krüger, Y.-H. Tsay: Organometallics **5**, 514 (1986); e) R. Benn, P. W. Jolly, T. Joswig, R. Mynott, K.-P. Schick: Z. Naturforschung **41b**, 680 (1986); f) R. Benn, P. W. Jolly, R. Mynott, B. Raspel, G. Schenker, K.-P. Schick, G. Schroth: Organometallics **4**, 1945 (1985); g) A. Döhring, P. W. Jolly, R. Mynott, K.-P. Schick, G. Wilke: Z. Naturforschung *36b*, 1198 (1981)

39   R. Jackstell, M. Gomez Andreu, A. Frisch, H. Klein, K. Selvakumar, A. Zapf, A. Spannenberg, D. Röttger, O. Briel, R. Karch, M. Beller: Angew. Chem. Int. Ed. **41**, 986 (2002)

40   N. Yoshimura, in *Aqueous-Phase Organometallic Catalysis*, B. Cornils, W.A. Herrmann (Eds.) (Wiley-VCH, Weinheim 1998) p. 408

41   J. Haggin: *Chem. Eng. News* **71**, 23 (May 31, 1993)

42   For leading reviews see: a) J. J. Brunet, D. Neibecker, in *Catalytic Heterofunctionalization from Hydroamination to Hydrozirconation*, A. Togni, H. Grützmacher (Eds.) (Wiley-VCH, Weinheim 2001) p. 98; b) M. Nobis, B. Drießen-Hölscher: Angew. Chem. Int. Ed. **40**, 3983 (2001); Angew. Chem. **113**, 4105 (2001); c) T. E. Müller, M. Beller: Chem. Rev. **98**, 675 (1998); d) T. E. Müller, M. Beller, in *Transition Metals for Organic Synthesis*, M. Beller, C. Bolm (Eds.) (Wiley-VCH, Weinheim 1998) Vol. 2, p. 316

43   a) T. Straub, A. Haskel, T. G. Neyroud, M. Kapon, M. Botoshansky, M. S. Eisen: Organometallics **20**, 5017 (2001); b) M. S. Eisen, T. Straub, A. Haskel: J. Alloys Compd. **271-273**, 116 (1998); c) A. Haskel, T. Straub, M. S. Eisen: Organometallics **15**, 3773 (1996); d) Y. Li, T. J. Marks: Organometallics **15**, 3370 (1996)

44   a) A. Tillack, I. Garcia Castro, C. G. Hartung, M. Beller: Angew. Chem. **114**, 2646 (2002); Angew. Chem. Int. Ed. **41**, 2541 (2002); b) E. Haak, I. Bytschkov, S. Doye: Eur. J. Org. Chem. 457 (2002); c) H. Siebeneicher, S. Doye: Eur. J. Org. Chem. 1213 (2002); d) A. Heutling, S. Doye: J. Org. Chem., *67*, 1961 (2002); e) F. Pohlki, A. Heutling, I. Bytschkov, T. Hotopp, S. Doye: Synlett 799 (2002); f) B. F. Straub, R. G. Bergman: Angew. Chem. **113**, 4768 (2001); Angew. Chem. Int. Ed. **40**, 4632 (2001); g) J. S. Johnson, R. G. Bergman: J. Am. Chem. Soc. **123**, 2923 (2001); h) I. Bytschkov, S. Doye: Eur. J. Org. Chem. 4411 (2001); i) F. Pohlki, S. Doye: Angew. Chem. **113**, 2361 (2001); Angew. Chem., Int. Ed. **40**, 2305 (2001); j) Y. Shi, J. T. Ciszewski, A. L. Odom: Organometallics **20**, 3967 (2001); k) C. Cao, J. T. Ciszewski, A. L. Odom: Organometallics **20**, 5011 (2001); l) E. Haak, H. Siebeneicher, S. Doye: Org. Lett. **2**, 1935 (2000); m) E. Haak, I. Bytschkov, S. Doye: Angew. Chem. **111**, 3584 (1999); Angew. Chem. Int. Ed. **38**, 3389 (1999)

45   a) J. Ryu, T. J. Marks, F. E. McDonald: Organic Lett. **3**, 3091 (2001); b) V. M. Arredondo, F. E. McDonald, T. J. Marks: Organometallics **18**, 1949 (1999); c) V. M. Arredondo, S. Tian, F. E. McDonald, T. J. Marks: J. Am. Chem. Soc. **121**, 3633 (1999); d) Y. Li, T. J. Marks: J. Am. Chem. Soc. **120**, 1757 (1998)

46   a) J. Pawlas, Y. Nakao, M. Kawatsura, J. F. Hartwig: J. Am. Chem. Soc. **124**, 3669 (2002); b) U. Nettekoven, J. F. Hartwig: J. Am. Chem. Soc. **124**, 1166 (2002); c) O. Löber, M. Kawatsura, J. F. Hartwig: J. Am. Chem. Soc. **123**, 4366 (2001); d) M. Beller, H. Trauthwein, M. Eichberger, C. Breindl, J. Herwig, T. E. Müller, O. R. Thiel: Chem. Eur. J. **5**, 1306 (1999)

47   a) *Applied Homogeneous Catalysis with Organometallic Compounds*, B. Cornils, W. A. Herrmann (Eds.), 2nd Ed. (Wiley-VCH, Weinheim 2002); b) M. Beller, C. Bolm: *Transition Metals for Organic Synthesis* (Wiley-VCH, Weinheim 1998); c)

F. Diederich and P. J. Stang: *Metal-catalyzed Cross-coupling Reactions* (Wiley-VCH, Weinheim 1997)

48 a) R. F. Heck and J. P. Nolley, Jr.: J. Org. Chem. **37**, 2320 (1972); b) T. Mizoroki, K. Mori, A. Ozaki: Bull. Chem. Soc. Jpn. **44**, 581 (1971); c) J. Tsuji: *Palladium Reagents and Catalysts* (Wiley, Chichester 1995); d) T. Jeffery: Adv. Met. Org. Chem. **5**, 153 (1996); e) W. A. Herrmann, in *Applied Homogeneous Catalysis with Organometallic Compounds*, B. Cornils, W. A. Herrmann (Eds.) (VCH, Weinheim 1996), Vol. 2, p. 712; f) A. de Meijere, F. E. Meyer: Angew. Chem. **106**, 2473 (1994); Angew. Chem. Int. Ed. **33**, 2379 (1994); g) S. Bräse and A. de Meijere, in *Metal-catalyzed Cross-coupling Reactions*, F. Diederich and P.J. Stang (Eds.) (Wiley-VCH, Weinheim 1998) p. 99; h) I. P. Beletskaya and A. V. Cheprakov: Chem. Rev. **100**, 3009 (2000)

49 a) N. Miyaura, A. Suzuki: Chem. Rev. **95**, 2457 (1995); b) H. Geissler, in *Transition Metals for Organic Synthesis*, M. Beller, C. Bolm (Wiley-VCH, Weinheim 1998), Vol. 1; c) A. Suzuki, in *Metal-catalyzed Cross-coupling Reactions*, F. Diederich and P. J. Stang (Eds.) (Wiley-VCH, Weinheim 1998)

50 a) R. R. Bader, P. Baumeister and H.-U. Blaser: Chimia **50**, 99 (1996); b) P. Baumeister, G. Seifert and H. Steiner (Ciba-Geigy AG): EP 584043 (1992) [Chem. Abstr. 120, 322 928n (1994)]

51 For further information see http://www.dmg.co.uk/specchem; T.-C. Wu (Albermarle): US 5315026 (1994)

52 T.-C. Wu (Albermarle): US 5536870 (1996)

53 R. A. DeVries and A. Mendoza: Organometallics **13**, 2405 (1994)

54 R. D. Larsen, E. G. Corley, A. O. King, J. D. Carroll, P. Davis, T. R. Verhoeven, P. J. Reider, M. Labelle, J. Y. Gauthier, Y. B. Xiang, R. J. Zamboni: J. Org. Chem. **61**, 3398 (1996)

55 a) I. Shinkai, A. O. King and R. D. Larsen: Pure Appl. Chem. **66**, 1551 (1994); b) A. O. King, E. G. Corley, R. K. Anderson, R. D. Larsen, T. R. Verhoeven, P. J. Reider, Y. B. Xiang, M. Belley, Y. Leblanc, M. Labelle, P. Prasit, R. J. Zamboni: J. Org. Chem. 58, 3731 (1993); c) G. Higgs: Chem. Ind. 827 (1997)

56 a) J. F. Perkins (Pfizer Ltd.): EP 1088817 (2001); b) J. E. Macor, M. J. Wythes (Pfizer Inc.): WO 9206973 (1992); c) C. Q. Meng: Curr. Opin. Cent. Peripher. Nerv. Syst. Invest. Drugs **2**, 186 (2000)

57 S. Haber, in *Aqueous-Phase Organometallic Catalysis*, B. Cornils and W. A. Herrmann (Eds.) (VCH-Wiley, Weinheim 1998) p. 444

58 R. D. Larsen, A. O. King, C. Y. Chen, E. G. Corley, B. S. Foster, F. E. Roberts, C. Yang, D. R. Lieberman, R. A. Reamer, D. M. Tschaen, T. R. Verhoeven, P. J. Reider, Y. S. Lo, L. T. Rossano, A. S. Brookes, D. Meloni, J. R. Moore, J. F. Arnett: J. Org. Chem. **59**, 6391 (1994)

59 E. Poetsch: Kontakte (Darmstadt 1988) p. 15

60 U. Beutler, J. Mazacek, G. Penn, B. Schenkel, D. Wasmuth: Chimia **50**, 154 (1996)

61 a) M. Kosugi, M. Kameyama, T. Migita: Chem. Lett. 927 (1983); b) M. Beller: Angew. Chem. **107**, 1436 (1995); Angew. Chem. Int. Ed. **34**, 1316 (1995); c) M. Beller, T. H. Riermeier, C.-P. Reisinger, W. A. Herrmann: Tetrahedron Lett. **38**, 2073 (1997); d) J. F. Hartwig: Synlett 329 (1997); e) N. P. Reddy, M. Tanaka: Tetrahedron Lett. **38**, 4807 (1997); f) M. Beller, T. H. Riermeier, in *Organic Synthesis Highlights III*, J. Mulzer and H. Waldmann (Eds.) (Wiley-VCH, Weinheim 1998); g) T. Yamamoto, M. Nishiyama, Y. Koie: Tetrahedron Lett. **39**, 2367 (1998); h) J. F. Hartwig, M. Kawatsura, S. I. Hauck, K. H. Shaughnessy, L. M. Alcazar-Roman: J. Org. Chem. **64** (1999) 5575; i) X. Bei, T. Uno, J. Norris, H. W. Turner, W. H. Weinberg, A. S. Guram, J. L. Petersen: Organometallics **18**, 1840 (1999); j) J. Huang, G. Grasa, S. Nolan: Org. Lett. **1**, 1307 (1999); k) S. R.

Stauffer, S. Lee, J. P. Stambuli, S. I. Hauck, J. F. Hartwig: Org. Lett. **2**, 1423 (2000)

62   S. Couve-Bonnaire, J. F. Carpentier, Y. Castanet, A. Mortreux: Tetrahedron Lett. **40**, 3717 (1999)

63   a) F. Jin, P. N. Confalone: Tetrahedron Lett. **41**, 3271 (2000); b) M. Sundermeier, A. Zapf, M. Beller, J. Sans: Tetrahedron Lett. **42** (2001) in press

64   a) J. Huang, S. P. Nolan: J. Am. Chem. Soc. **121**, 9889 (1999); b) V. P. W. Böhm, T. Weskamp, C. W. K. Gstöttmayr, W. A. Herrmann: Angew. Chem. **112**, 1672 (2000); Angew. Chem. Int. Ed. **39**, 1602 (2000)

65   W. A. Herrmann, C. Broßmer, K. Öfele, C.-P. Reisinger, T. Priermeier, M. Beller, H. Fischer: Angew. Chem. **107**, 1989 (1995); Angew. Chem. Int. Ed. **34**, 1844 (1995)

66   a) M. Beller, H. Fischer, W. A. Herrmann, K. Öfele, C. Broßmer: Angew. Chem. **107**, 1992 (1995); Angew. Chem. Int. Ed. **34**, 1848 (1995); b) A. F. Littke, G.C. Fu: Angew. Chem. **110**, 3586 (1998); Angew. Chem. Int. Ed. **37**, 3387 (1998); c) D. W. Old, J. P. Wolfe, S. L. Buchwald: J. Am. Chem. Soc. **120**, 9722 (1998); d) J. P. Wolfe, S. L. Buchwald: Angew. Chem. **111**, 2570 (1999); Angew. Chem. Int. Ed. **38**, 2413 (1999); e) C. Zhang, J. Huang, M. L. Trudell, S. P. Nolan: J. Org. Chem. **64**, 3804 (1999); f) X. Bei, H. W. Turner, W. H. Weinberg, A. S. Guram, J. L. Petersen, J. Org. Chem. 64 (1999) 6797; g) X. Bei, T. Crevier, A.S. Guram, B. Jandeleit, T. S. Powers, H. W. Turner, T. Uno, W. H. Weinberg: Tetrahedron Lett. **40**, 3855 (1999); h) H. Gröger: J. Prakt. Chem. **342**, 334 (2000); i) A. Zapf, A. Ehrentraut, M. Beller: Angew. Chem. **112**, 4315 (2000); Angew. Chem. Int. Ed. **39**, 4153 (2000); j) C. Zhang, M. L. Trudell: Tetrahedron Lett. **41**, 595 (2000); k) A. F. Littke, C. Dai, G. C. Fu: J. Am. Chem. Soc. **122**, 4020 (2000); l) V. P. W. Böhm, C. W. K. Gstöttmayr, T. Weskamp, W. A. Herrmann: J. Organomet. Chem. **595**, 186 (2000); m) W. A. Herrmann, V. P. W. Böhm, C. W. K. Gstöttmayr, M. Grosche, C.-P. Reisinger, T. Weskamp: J. Organomet. Chem. **617-618**, 616 (2001)

67   A. Zapf, M. Beller: Chem. Eur. J. **6**, 1830 (2000)

68   M. Beller, C. Bolm: *Transition Metals for Organic Synthesis* (Wiley-VCH, Weinheim 1998)

69   Worldwide production capacities for ethylene glycol in 1995: 9.7 Mio to/a; worldwide production of 1,2-propylene glycol in 1994: 1.1 Mio to/a; K. Weissermel, H. J. Arpe: *Industrielle Organische Chemie*, 5th Ed. (Wiley-VCH Weinheim 1998) p. 167, p. 302

70   a) T. Katsuki, K. B. Sharpless: J. Am. Chem. Soc. **102**, 5974 (1980); b) R. A. Johnson, K. B. Sharpless, in *Catalytic Asymmetric Synthesis*, I. Ojima (Ed.) (VCH, Weinheim 1993) p. 101

71   W. Zhang, J. L. Loebach, S. R. Wilson, E. N. Jacobsen: J. Am. Chem. Soc. **112**, 2801 (1990)

72   Reviews: a) M. Schröder: Chem. Rev. **80**, 187 (1980); b) H. C. Kolb, M. S. Van Nieuwenhze, K. B. Sharpless: Chem. Rev. **94**, 2483 (1994); c) M. Beller, K. B. Sharpless, in *Applied Homogeneous Catalysis*, B. Cornils, W. A. Herrmann (Eds.) (VCH, Weinheim 1996) p. 1009; d) H. C. Kolb, K. B. Sharpless, in *Transition Metals for Organic Synthesis*, M. Beller, C. Bolm (Eds.) (Wiley-VCH, Weinheim 1998), Vol. 2, 219; e) I. E. Marko, J. S. Svendsen, in *Comprehensive Asymmetric Catalysis II*, E. N. Jacobsen, A. Pfaltz, H. Yamamoto (Eds.) (Springer, Berlin 1999), p. 713

73   P. Dupau, R. Epple, A. A. Thomas, V. V. Fokin, K. B. Sharpless: Adv. Synth. Catal. **344**, 421 (2002)

74   G. M. Mehltretter, C. Döbler, U. Sundermeier, M. Beller: Tetrahedron Lett. **41**, 8083 (2000)

75 a) S. G. Hentges, K. B. Sharpless: J. Am. Chem. Soc. **192**, 4263 (1980); b) K. B. Sharpless, W. Amberg, Y. L. Bennani, G. A. Crispino, J. Hartung, K.-S. Jeong, H.-L. Kwong, K. Morikawa, Z.-M. Whang, D. Xu, X.-L. Zhang: J. Org. Chem. **57**, 2768 (1992)
76 K. A. Hofmann: Chem. Ber. **45**, 3329 (1912)
77 a) N. A. Milas, S. Sussmann: J. Am. Chem. Soc. **58**, 1302 (1936); b) N. A. Milas, J.-H. Trepagnier, J. T. Nolan, M. I. Iliopulos: J. Am. Chem. Soc. **81**, 4730 (1959)
78 K. B. Sharpless, K. Akashi: J. Am. Chem. Soc. **98**, 1986 (1976)
79 a) W. P. Schneider, A. V. McIntosh (Upjohn): US-2.769.824 (1956), Chem. Abstr. **51**, 8822e (1957); b) V. Van Rheenen, R. C. Kelly, D. Y. Cha: Tetrahedron Lett. **17**, 1973 (1976); c) R. Ray, D. S. Matteson: Tetrahedron Lett. **21**, 449 (1980)
80 K. B. Sharpless, W. Amberg, Y. L. Bennani, G. A. Crispino, J. Hartung, K.-S. Jeong, H.-L. Kwong, K. Morikawa, Z.-M. Whang, D. Xu, X.-L. Zhang: J. Org. Chem. **57**, 2768 (1992)
81 E. N. Jacobsen, I. Marko, W. S. Mungall, G. Schröder, K. B. Sharpless: J. Am. Chem. Soc. **110**, 1968 (1988)
82 A. Krief, C. Colaux-Castillo: Tetrahedron Lett. **40**, 4189 (1999)
83 K. Bergstad, S. Y. Jonsson, J.-E. Bäckvall: J. Am. Chem. Soc. **121**, 10424 (1999)
84 C. Döbler, G. Mehltretter, M. Beller: Angew. Chem. Int. Ed. **38**, 3026 (1999)
85 G. M. Mehltretter, S. Bhor, M. Klawonn, C. Döbler, U. Sundermeier, M. Eckert, H.-C. Militzer, M. Beller: Synthesis (2003) in press

Polymerisation Catalysis

Contents

Polymerisation Catalysis

W. Kaminsky

Institute for Technical and Macromolecular Chemistry
University of Hamburg
Bundesstr. 45, 20146 Hamburg

Abstract. About 50 % of all plastics are produced by catalytic processes. Organometallic compounds such a lithiumbutyl, titanium iodides are used for the polymerisation of 1,3-butadiene and styrene. Great industrial importance has the production of polyethylene and polypropylene by Phillipps- and Ziegler-Natta catalysis. Beside these classical catalysts, catalysts such as metallocenes, half-sandwich, nickel, palladium, and iron complexes have been synthesized – that give tailored polymers of totally different structures and allow to control the polymer tacticity, molar mass and molar mass distribution more efficient. New kinds of copolymers and elastomers can be synthesized. It has become possible to polymerize cyclic olefins with different zirconocenes or nickel and palladium catalysts without any ring opening reaction.

1.   Introduction, Importance

Polymers are materials with an annual growth rate of 5 to 7 % which is high as compared to other materials. While 1990 the world plastics production was 100 million tons, in 1997 it was 150 million tons, and is estimated to reach 220 million tons in 2005 [1,2]. More than 50 % of all plastics are produced by a catalytic processes. The polymerisation of olefins by organometallic catalysts is the most important catalytic process in the organic chemical industry. It accounts for more than 10 % of all profits made with these catalysts. In 1999 the production of linear low-density polyethylene (LLDPE), high density polyethylene (HDPE) and isotactic polypropylene (PP) reached 65 million tons including 5 million tons of HDPE produced by Phillips catalysts.

Anionic catalysts such as lithium butyl and sodium naphthyl have a long tradition for polybutadiene production.

Cationic and metathesis catalysts are used for the production of polyisobutylene or other elastomers [3]. In some aspects, even free radical polymerisation processes using peroxides, butyronitriles and other compounds as initiators can be discussed as catalytic processes. In this case, over 80 % of the industrial plastic production is based on catalytic processes. Due to the different mechanism of the free radical polymerisation, this reaction is not a part of the following chapter.

One of the first industrial catalytic polymerisation processes was the production of polybutadiene (butadiene-rubber, BR) by sodium naphthyl in the years 1918 to 1925 (BUNA, Germany). The synthesis of neoprene starting from 2-chloro-butadiene by DuPont, USA, followed. 1954 the cationic polymerisation of isobutene led to a new rubber material (IR) with a low permeability for oxygen and air which can be used in the production of tubeless tires. In the following years, poly-

butadienes with new microstructures and other elastomers (ethylene-propylene rubber, EPR), made by different catalysts, followed. The world production of synthetic rubber reached eleven million tons, including about 1,5 million tons of BR, in 1998.

Karl Ziegler's use of transition metal halides and organoaluminium compounds as catalysts for the polymerisation of ethylene and Giulio Natta's extension of these systems to the synthesis of stereoregular poly(α-olefins) are two of the major achievements in the areas of catalysis and polymerisation in the last 50 years. They led to the development of a new branch of the chemical industry. For their work, K. Ziegler and G. Natta were awarded the Nobel prize in 1963.

Since the first generation of Ziegler-Natta catalysts based on $TiCl_3/AlEt_2Cl$, which were characterized by their low polymerisation activities, thousands of papers and patents have been published related to this subject (for reviews see [3-11]). A highly active second generation of catalysts has been generated and commercialized supporting the titanium compound by $MgCl_2$, SiO_2 or Al_2O_3. Recently, a new generation of Ziegler-Natta catalysts based on group 4 metallocenes or other transition metal compounds and methylaluminoxane or perfluorinated phenylborate as cocatalysts are on their way to commercialisation.

2.   Anionic Polymerisation

The anionic polymerisation plays an important role in the rubber synthesis and in the ring opening polymerisation of lactones and of alkylene oxides. These reactions proceed via metal organic sites such as carbanions or oxanions with their metallic counterions. Carbanion catalysts are nucleophiles and the attack onto a monomer bearing an electro-attractive substituent for the propagation reaction. Thus, a new carb-anionic site is formed at the chain end [6, 12].

$$
\text{pol-CH}_2\text{-CH}|^- + \text{CH}_2 = \text{CH} \rightarrow \text{pol-CH}_2\text{-CH-CH}_2\text{-CH}|^-
$$
$$
\begin{array}{cccc}
| & | & | & | \\
R & R & R & R
\end{array}
\tag{1}
$$
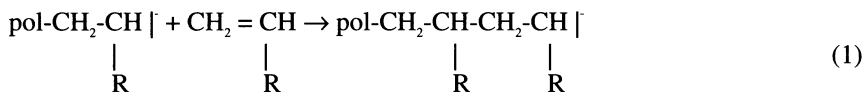
The same happens for the ring opening polymerisation of cyclic monomers containing some functions such as oxiranes or lactones.

Industrial polymers made by anionic polymerisation are polybutadiene (BR), styrene-butadiene copolymers, acrylonitrile-butadiene copolymers, polychloroprene, polyisoprene, polyamide 6 (PA6), polylactones, polyethers, etc.

2.1   Polybutadiene

The anionic polymerisation of 1,3-butadiene by butyl lithium is the most used industrial process for the production of BR [13]. About 40 % of the total BR production is based on this process. The rest quantity of BR is manufactured using different Ziegler catalysts (see 5.2.3).

Butadiene can polymerize via 1,4 cis, 1,4-trans or 1,2-linkage:

| 1,4 - cis | 1,4 - trans | 1,2 (vinyl) |
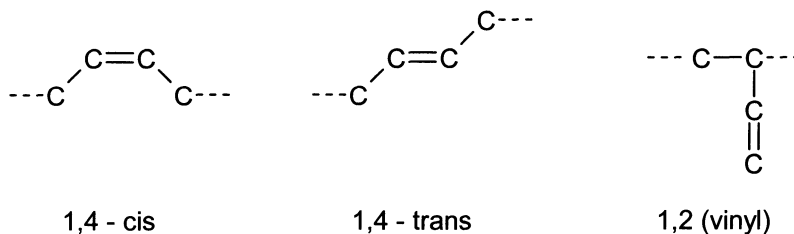
The 1,2-linkage yields a tertiary carbon atom, which allows the formation of isotactic, syndiotactic, and atactic structure units in analogy to polypropylene. Metal alkyls, preferably of alkali metals, catalyze as an initiator the anionic polymerisation of butadiene. The polarisations of the catalyst and of the solvent have a strong influence on the stereospecificity of the formation of different polybutadiene microstructures (Table 1) [14]. Lithium alkyls in hexane give a

Table 1. Selectivities for various microstructures of Poly(1,3-butadiene) in relation to the Initiator

Initiator	Solvent	Microstructure selectivity (%)		
		cis	trans	1,2
C_2H_5Li	Hexane	43	50	7
C_2H_5Li	THF	0	9	91
CH_4H_9Li	Hexane	35	55	10
$C_{10}H_8Li$	THF	0	3,6	96,4
$C_{10}H_8Na$	THF	0	9,2	90,8
$C_{10}H_8K$	THF	0	17,5	82,5
$C_{10}H_8Rb$	THF	0	24,7	75,3

polymer with the greatest trans-1,4 portion. The stereospecificity is also influenced by the catalyst concentration, the temperatures, and the associative behavior. In more concentrated solutions, alkyllithium, especially butyllithium, which is a preferred initiator, forms hexameric associates that are dissociated in several steps to give finally monomers [15-20]. Only monomeric butyllithium is suitable for the insertion. Isobutyllithium shows an association grade of 4 in cyclohexane. Branched alkyl groups show higher activities than n-alkyl groups. As postulated by the kinetic model for a very low initiator concentration, the reaction order is 1 and decreases with increasing concentration. Following reactions take place [21]:

Dissociation: $(CH_3-(CH_2)_3-Li)_6 \longrightarrow 6\ CH_3-(CH_2)_3-Li$ (2)

Start: $CH_3-(CH_2)_3-Li+CH_2=CH-CH=CH_2 \longrightarrow$ (3)
$CH_3-(CH_2)_3-CH_2-CH=CH-CH_2-Li$

Propagation: $CH_3-(CH_2)_4-CH=CH-CH_2-Li+CH_2=CH-CH=CH_2$ (4)
$\longrightarrow CH_3-(CH_2)_3-(CH_2-CH=CH-CH_2)_2-Li$
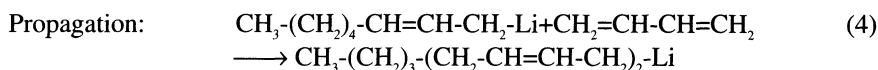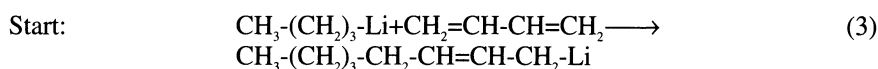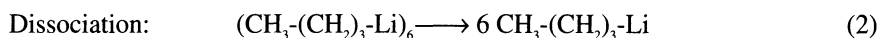
With hydrocarbons as solvents such as hexane, heptane, the rate of the starting reaction is up by a factor of 0.01 smaller than that of the propagation step. This difference is caused by the absence of a double bond in conjugation to lithium in butyllithium while octenyl lithium (see reaction 3) has such a double bond. The use of ether accelerates the starting reaction in such a way that propagation becomes the rate-determining step [22].

In the absence of chain transfer reagents, the molecular weight increases steadily with increasing the conversion of the monomer. Thus, living polymers with very narrow molecular weight distribution $M_w/M_n=1,03$ are obtained when the starting reaction is fast or when lithium octenyl is used as a starter (Poisson distribution). The average degree of polymerisation is equal to the ratio of the converted moles of monomer (starting concentration $[M]_0$) to the number of moles of initiator reacted. At the end of the polymerisation when all initiator has reacted, this ratio is similar to the total initiator concentration I.

The average molecular weight can be calculated as follows:

$$\overline{M}_n = \frac{[M]_0}{[I]_0} \times 54 \tag{5}$$

The monomer consumption is then governed by the following rate equation:

$$\frac{-d[M]}{dt} = kp\,[I]_o\,[M] \tag{6}$$
$$(kp = \text{propagation rate constant})$$

To improve the processability of linear polybutadiene with a narrow molecular weight distribution, one can continuously add initiator in the course of the polymerisation, vary the reaction temperature, or force long-chain branching by addition of divinyl compounds [23]. Addition of small amounts of ethers or tertiary amines alters the vinyl content from some 12 % to more than 70 %. [17]. The microstructures of the polybutadienes can be determinated by IR-NMR spectroscopy, X-ray diffraction, and other methods. The polymerisation in ethers requires low temperatures because of the high reactivity and low stability of the lithium alkyl in this solvent. Using n-hexane as a solvent, a butadiene concentration of 25 wt % and an adiabatic process starting by 20 °C will reach an end temperature of 130 °C.

2.2   Other Polydienes

The homopolymerisation of isoprene

$$\overset{\displaystyle \underset{|}{CH_3}}{H_2C=C-CH=CH_2}$$
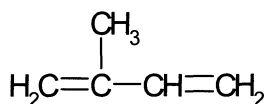
can take place with a cis-1,4-, trans-1,4-, -1,2-, or 3,4-connection.

cis - 1,4   trans - 1,4   1,2   3,4
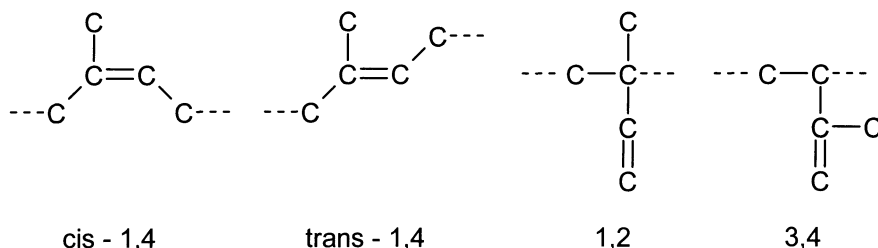
In addition, both 3,4- and 1,2-polyisoprenes can exist in three forms: isotactic, syndiotactic, and atactic. Thus, there are eight possible structures if head-to-head possibilities are disregarded. The part of the structure elements in the polymer depends on the catalysts. The same catalyst could also be used for the polymerisation of polybutadiene. In general, the polymerisation activity is lower.

Highly cis-oriented polyisoprene (similar to natural rubber) can be synthesized by anionic polymerisation with alkyllithium compounds. The cis fraction is about 93 %, the other 7 % are 3,4 connections. Up to 97 % cis content is possible by Ziegler-Natta catalysis. The cis content depends on the initiator and the monomer concentrations as well as on the temperature. Impurities such as acetylenes, carbonyl compounds, hydrogen sulfide and water have to be removed.

The polymer prepared by anionic polymerisation is highly linear without branching. Vacuum or seeding technique could be used for the synthesis of polyisoprenes with an extremely narrow molecular weight distribution (M_w/M_n = 1,05) [24]. In the case of the seeding technique the polymerisation is started with separately prepared polyisoprene of low molecular weight. Polar solvents such as ethers and amines have an influence on the microstructure, too [25].

Anionic polymerisation leads to polymers with an active lithium end group. This can be used for further reactions. By treatment with chlorsilanes, such as 1,2-bis(dichloromethylsilyl)ethane, a four-branched star-shaped polymer results; with 1,2-bis(trichlorosilyl)ethane, a six-branched star-shaped polymer results.

Polymers of some of the higher 2-alkyl-1,3-butadienes result in vulcanizates with tensile strength and elasticity comparable to that of natural rubber. Poly(2-ethylbutadiene) and poly(2-phenyl-butadiene) are most important. 2-Ethyl-1,3-butadiene can be polymerized in the same way as isoprene [26]. The polymer has a glass transition temperature of - 76 °C. A polymer enriched with trans-1,4 structures is obtained by catalysis with VCl3/TIBA. In contrast to trans-1,4-

polyisoprene, the product can be used as rubber, due to its reduced tendency to crystallize.

2.3   Polyethers and Polyesters

Oxiranes such as ethylene oxide, propylene oxide, and isobutylene oxide can be polymerized to polyethers by ring opening polymerisation initiated by alcoholates or other anionic compounds. In a similar reaction lactones, such as propiolactone or butyrolactone, are ring opened to polyesters.

Polyethers are very useful polymer materials of great industrial importance. Poly- and oligoethers derived from oxiranes have been widely used as surfactants, plasticizer, adhesives, coatings, and as prepolymers for the production of polyurethanes. Polymerisation of cyclic ethers is historically one of the oldest examples of the formation of macromolecules. The formation of oligomers of oxiranes was first reported by Wurtz in 1863 [27] and investigated systematically by Staudinger in 1929 [28]. The polymerisation of oxiranes with anionic initiators ($X'M^+$) proceeds via metal alkoxides acting as the growing species [29].

$$X^-M^+ + n\; \underset{\underset{\displaystyle O}{\diagdown\;\diagup}}{C\!-\!\overset{\displaystyle \overset{R}{|}}{C}\!-\!R} \longrightarrow X\text{-}(C\!-\!C\!-\!O)_n\text{-}M \tag{7}$$
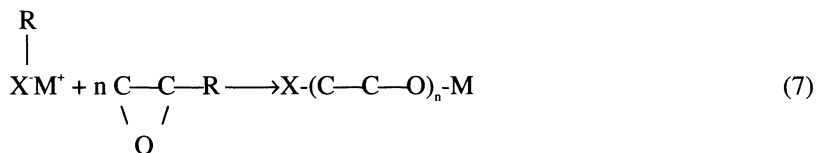
In the case of a mono-substituted oxirane, such as propylene oxide, the oxirane ring is opened mostly at the oxygen atom-methylene carbon bond to produce a secondary alkoxide, leading to the formation of polymers consisting of regular head-to-tail linkages.

The ring opening polymerisation of lactones by anionic initiators constitutes a convenient method of synthesis of main-chain polyesters possessing an aliphatic structure. This process is of importance because it is difficult to obtain some of these polymers by classical polyesterification methods. Some of the polyesters produced by ring opening polymerisation from lactones and diester lactones (e.g., glycolide) exhibit some unique properties as biodegradability, bioresorbability, and non-immunogenity, and, therefore, they are considered to be very interesting materials for medical applications [30]. Lactones are highly polar compounds that possess both nucleophilic and electrophilic sites in their molecules. Thus, numerous polyesters exhibiting a great variety of properties can be produced via ring opening polymerisation using a score of anionic, cationic, and complexation initiators. The same initiators as for the polymerisation of oxiranes can also be used.

3.   Cationic Polymerisation

The cationic polymerisation of vinyl monomers has been known for a long time. All monomers with electron donating substituents, because of the polarisation of the double bond are sensitive to an electrophilic attack by a carbenium site and can therefore undergo cationic polymerisation.

Activation $HCl + AlCl_3 \rightleftharpoons H^+ [AlCl_4]^-$

Start $H^+ [AlCl_4]^- + H_2C{=}\underset{CH_3}{\overset{CH_3}{C}} \longrightarrow H_3C{-}\underset{CH_3}{\overset{CH_3}{C^+}} [AlCl_4]^-$

Propagation $H_3C{-}\underset{CH_3}{\overset{CH_3}{C^+}} [AlCl_4]^- + n\ H_2C{=}\underset{CH_3}{\overset{CH_3}{C}} \longrightarrow H{-}\left[CH_2{-}\underset{CH_3}{\overset{CH_3}{C}}\right]_n CH_2{-}\underset{CH_3}{\overset{CH_3}{C^+}} [AlCl_4]^-$

Deactivation $H{-}\left[CH_2{-}\underset{CH_3}{\overset{CH_3}{C}}\right]_n CH_2{-}\underset{CH_3}{\overset{CH_3}{C^+}} [AlCl_4]^- \longrightarrow H{-}\left[CH_2{-}\underset{CH_3}{\overset{CH_3}{C}}\right]_n CH_2{-}\underset{CH_3}{\overset{CH_2}{C}} + H^+ [AlCl_4]^-$
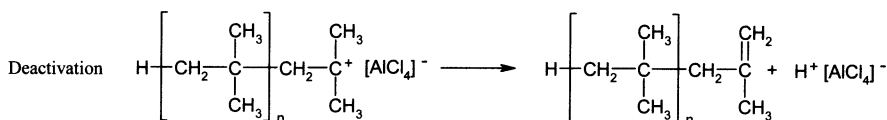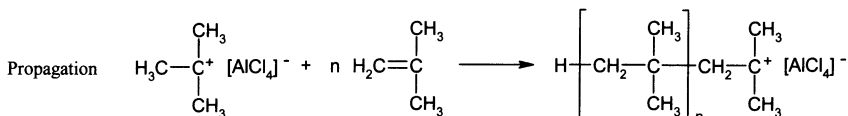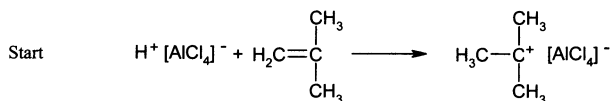
Such monomers are, for example, isobutylene, vinylethers, vinyl acetals, styrene, N-vinyl pyrrolidone. In industrial cationic polymerisation processes isobutylene is mainly used as monomer. The solvents should be stable towards acids and should not react with electrophiles.

3.1   Polyisobutylene

The cationic polymerisation of isobutylene can be carried out as a precipitation reaction at temperatures below 0 °C with Friedel-Crafts catalysts (e.g., $AlCl_3$, BF_3) in chloromethane or other solvents [31]. The mechanism includes the following reactions:

The molecular weights differs over a wide range from 3000 for viscous oily liquids up to 2 500 000 for elastic rubbery materials. To obtain high molecular weights, the polymerisation temperature and, along with it, the rate of the transfer reactions must be lowered. For example, at a temperature of 100 °C, poly(isobutylene) of molecular weight 300 000 g/mol is obtained [32].

The reaction is strongly exothermic with a reaction enthalpy of 356 kJ/mol and is usually finished from seconds to a few minutes, even at low temperatures. The molecular mass is kept low by adding α-olefins and diisobutene. Addition of 0.25 % of diisobutene, for instance, reduces the molecular weight from 260 000 to 45 000. In contrast, the addition of organometallic amides [e.g., zinc bis(diethylamide), titanium tetra(diethylamide)] has the opposite effect, raising the molecular weight to more than 1 million [33]. Poly(isobutylenes) have low glass transition temperatures and thermal conductivity as well as high electrical resistivity and chemical resistance. They are soluble in hydrocarbons but insoluble in alcohols.

Copolymers of Isobutene

Isobutene can be copolymerised with numerous unsaturated compounds, such as butadiene, isoprene, styrene or indene, via a cationic route [34]. The isobutene portion in the copolymers usually exceeds 90 %. The use of aluminium organic compounds (e.g., $AlEt_2Cl$) instead of aluminium trichloride permits a better control of the copolymerisation as the former are weaker Lewis acids. Hydrogen chloride or halogens must be added as cocatalysts capable of regenerating the carbocations. The organoaluminium catalysts are used at - 78 °C with boron trifluoride.

Isobutene/isoprene copolymers (butyl rubbers) are the technically most important copolymers. The polymerisation is carried out as a continuous suspension polymerisation with 0,8 to 3 mol % isoprene in chloromethane. The isoprene is incorporated with a trans 1,4-linkage.

4.   Ring Opening Metathesis Polymerisation (ROMP)

The metathesis polymerisation of cycloolefins as a ring opening reaction yields unsaturated polyhydrocarbons called polyalkenamers. Since several cycloolefins are inexpensive starting materials, their ring opening polymerisation has found commercial interest. The resulting polyalkenamers possess flexible chains and can be used as elastomers, which, after cross-linking of double bonds with sulfur. Examples of such technically produced commercially available elastomers are polypentenamer, polyoctenamer (Vestamer), polynorbornene (Norsorex), and cross-linked dicyclopentadiene (Metton or Telene). Numerous reviews dealing with reaction mechanisms and preparative application of metathesis polymerisations have been published [35,36].

For the ROMP tungsten hexachloride/alkylaluminium/activator. Alkylaluminium compounds, such as triisobutylaluminium, Et_3Al, Et_2AlCl are used as catalysts; they are mixed with WCl_6, which is pretreated by activators such as alcohols, phenols, or oxiranes to form W=0 bonds. The best effect is obtained at a W/0 ratio of 1:2. Table 2 shows some conditions of the ROMP for cyclopentene and norbornen [37,38]. Yields of up to 80 % are reached. The polymers have a high trans content.

Table 2. Reaction conditions, yield and product selectivities of the polymerisation of cyclopentene (C) and norbornene (N) by ringopening metathesis polymerisation (ROMP) (conditions and polymer properties)

Monomer	Catalyst	Solvent	Temp. °C	Yield %	cis %	trans %
C	$MoCl_5/Et_3Al$	-	- 30	-	99	1
C	WCl_6/iBu_3Al	Toluene	0	35	9	91
C	$WCl_6/Et_2AlCl/EtOH$ + aromatic ether	Hexane	0	83	17	83
C	$WCl_6/EtAlCl/C_6H_5OH$	Toluene	20	80	<20	>80
N	$MoCl_5/iBu_3Al$	Heptane	- 20		high cis	
N	$WCl_6/(\pi\text{-}C_3H_5)3Cr$	Toluene	30	100	47	53

The reaction mechanism of the metathesis of cycloolefins has been an object of numerous studies. It is generally accepted that there is an initial formation of a metal-carbene complex that reacts with one olefin via a metallocyclobutane transition state to a new olefin and a complex with a new carbene ligand (Fig. 1).

The ROMP of cyclopentene leads to a technically used polypentenamer with a high trans content. The polypentenamer can vulcanize with sulfur in analogy to polyisoprene or polybutadiene, but is less sensitive to oxidation. Also cyclooctene, which is available on dimerisation of butene, is used by ROMP forming a polyoctenamer. The polymer has between 50-80 % of trans bonds and contains a considerable fraction of cyclic oligomers and macrocycles. The trans content consists on the Al/W ratio.
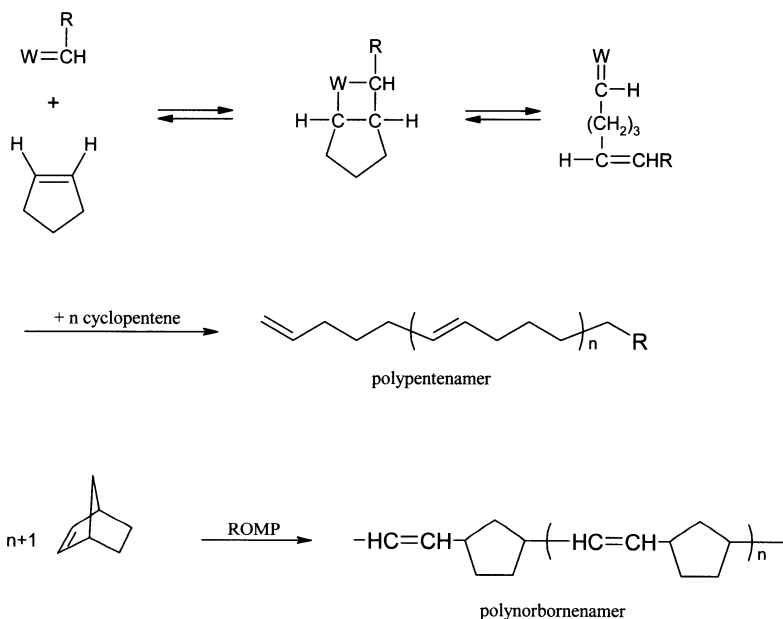
Fig. 1.   Ring opening metathesis polymerisation

5.   Catalytic Olefin Polymerisation

Activated organometallic compounds are able to insert 1-olefins into the transition metal carbon bond. This step can be repeated up to 100 000 times until a transition metal hydride (alkyl) and a non-bonded polymer chain are formed by a hydrogen transfer reaction. The ethylene polymerisation using these catalysts results in a polymer exhibiting a greater density (high density polyethylene, HDPE) and crystallinity than the polymer obtained via radical high pressure polymerisation (low density polyethylene, LDPE) [8].

The coordination catalysts for the polymerisation of olefins can be of very different nature. They all contain a transition metal that is soluble or insoluble in hydrocarbons, supported on silica, alumina, or magnesium chloride [39]. In most cases cocatalysts are used as activators. These are organometallic compounds containing elements of the groups I to III: e.g., $AlEt_3$, $AlEt_2Cl$, $Al(i\text{-}Bu)_3$, $ZnEt_2$.[40].

1. Catalysts based on titanium or zirconium halogenides or hydrides in connection with aluminium organic compounds (Ziegler catalysts).
2. Catalysts based on chromium supported by silica or alumina without a coactivator (Phillips catalysts).
3. Catalysts based on metallocenes or other transition metal complexes in connection with aluminoxane or perfluorinated phenylborate.

Propylene and higher 1-olefins can only be polymerized by Ziegler-Natta catalysts. By copolymerisation of ethylene, propylene, other 1-olefins cyclic olefins, or polar monomers, the product properties can be varied considerably, thus extending the field of possible applications. The polyolefins are used for the production of packing materials, receptacles, pipes, films, domestic articles, car plastics, fails, and fibers.

In the past only Ziegler and Phillips catalysts were used. In the recent years industrial polymerisation is catalyzed also by metallocene and other transition metal complexes to produce polyolefins with a tailored microstructure.

5.1   Phillips Catalysts

In 1951 Hogan and Banks developed the Phillips process for ethylene polymerisation [41]. Commercialisation of this process over the following 5 years provided the first linear polyethylene. Phillips began with the first commercial production of HDPE in 1956. Because there is no possibility to separate polymer from the catalyst; the process requires high catalysts - activity so that the minor amounts of the catalyst can remain in the final product. Today in most of the processes using the Phillips catalyst, a pipe loop reactor is applied to maximize the heat-transfer area and to minimize fauling tendencies. The polymer and the catalyst are circulated through the loop in a hydrocarbon slurry in which the reactant alkenes are dissolved. The hydrocarbon diluent must be a poor solvent for the polymer and the temperatures must be maintained below the „swelling point" of the polymer. Otherwise it can become gelatinous and cause the fouling of the reactor. Light hydrocarbons have been used as diluents; operating temperatures are typically 75 – 110 °C and reactor pressure less than 70 bar [42].

The Phillips catalyst is usually made by impregnation of a chromium compound onto a porous, high-surface-area silicate carrier (200 - 600 m^2/g), followed by a calcination in dry air at temperatures from 500 to 900 °C (Fig. 2).
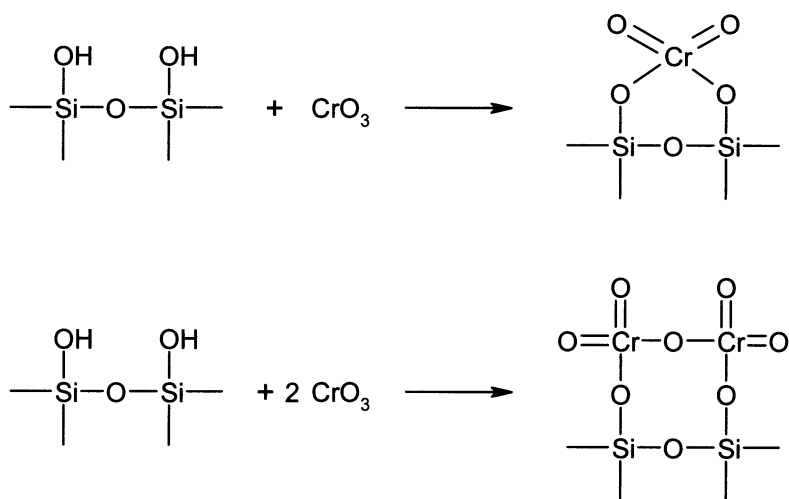
Fig. 2. Formation of the Phillips catalyst by reaction of chromium trioxide with hydroxyl groups on silica

The activation step converts the chromium into a hexavalent surface chromate, or perhaps dichromate ester, because each Cr atom is individually attached to the surface. The carrier is not inert but exerts a strong influence on the polymerisation behavior of the site. Hexavalent Cr is reduced by ethylene or other hydrocarbons in the reactor, probably to a Cr^{II} or Cr^{III} which acts as active species. Since Cr^{VI} is tetrahedrally coordinated, and the reduced species can be octahedral, the active site is thus coordinatively unsaturated and accepts readily alkenes. However, this same trait makes the catalyst very sensitive to small amounts of polar impurities in the feed stream, such as alcohols, water, amines, etc. Commercial catalysts usually contain 0,5 - 1,0 wt% Cr, but only a small fraction of this, perhaps 10-20 % or even less, is actually active in polymerisation reactions [42]. Alternatively, the reduction can be accomplished prior to the contact of the catalyst with ethylene, by exposure to carbon monoxide at 350 °C. In this case, the reduced species has definitely been identified as Cr^{II}.

In another variation of the catalyst, lower-valent organochromium compounds can be deposited onto an already calcined support to produce very active catalysts [43]. These compounds react with surface hydroxyls to become attached to the support, often losing one or more ligands. Examples are bis(arene)-Cr^{0}, bis(cyclopentadienyl)-Cr^{II}, and allyl-Cr^{II} and -Cr^{III}. Organochromium catalysts differ from those based on chromium oxide. The activity of these catalysts is quite high, and the obtained polymer is particularly different, usually much broader in molecular weight distribution.

As described, the catalyst ethylene is reduced by ethylene and alkylated to the active species.

$$Cr(II) + C_2H_4 \rightarrow Cr - R \qquad\qquad\qquad \text{Initiation} \qquad (8)$$

$$Cr - R + nC_2H_4 \rightarrow Cr\text{-}(CH_2\text{-}CH2)n - R \qquad \text{Propagation} \qquad (9)$$

$$Cr\text{-}(CH_2 - CH_2)_n - R + C_2H_4$$

$$\rightarrow Cr - C_2H_5 + CH_2 = H\text{-}(CH_2\text{-}CH_2)_{n\text{-}1} - R \qquad \text{Chain transfer} \qquad (10)$$
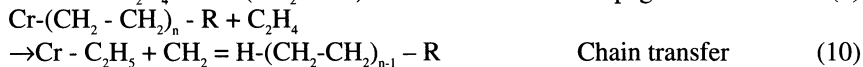
This alkylated species inserts ethylene molecules [42] and forms the growing polymer chain. A hydrogen transfer to usually an ethylene molecule gives the polyethylene chain and an alkylated Cr species again, which starts a new polymer chain. The length to which a chain grows is determined by the rate of propagation lative to transfer. A typical chain length can vary from 100 to over 35 000 units, depending on the choice of the catalyst and the reactor conditions. The lifetime of a chain on an active site is probably around 0.1 seconds or less. Since the catalyst spends about an hour in the reactor, each site produces several thousand chains during its active life.

As the silica surface is heterogeneous, not all the sites behave in a similar way. The propagation and transfer rate constants seem to vary considerably from one site to another, influenced by the local geometry and chemistry. Thus, each site produces its own characteristic chain length, and the total molecular weight distribution (MWD) of the resultant polymer is with values of Mw/Mn = 10-30 broad which each individual site produces a narrow MWD of 2. In comparison with Ziegler catalysts it is difficult to influence the molecular weight of the obtained polyethylene by adding hydrogen. The molecular weight must be controlled by the catalyst preparation and the process parameters and is usually between 100 000 and 30 000.

5.2   Ziegler-Natta Catalysts

The first generation of Ziegler-Natta catalysts, based on $TiCl_3$/AlEt$_2$Cl, was characterized by low polymerisation activity. Thus, a large amount of catalyst was needed, which contaminated the raw product. A washing step that increased the production costs was necessary. Since the first Ziegler-Natta catalysts were developed thousands of papers and patents related to this subject have been published [3-12,44,]. By supporting the titanium compound on $MgCl_2$, SiO_2, Al_2O_3 a highly active second generation of catalysts has been developed and commercialized.. The product obtained by using these catalysts contains only traces of residues which may remain in the polymer. Therefore, most Ziegler-Natta catalysts are therefore heterogeneous. Only some vanadium-based systems for the production of ethylene/propylene copolymers (EP) or ethylene/propylene diene terpolymers (EPDM) are homogeneous.

Ziegler-Natta catalysts are highly sensitive to oxygen, moisture, and a large number of chemical compounds. Therefore, very stringent requirements of reagent purity and most care in all manipulations of catalysts and polymerisation reactions themselves are mandatory for achieving experimental reproducibility and reliability. Special care must be taken to ensure that solvents and monomers are extremely pure. Alkanes and aromatic compounds have no substantial effect on the polymerisation and can therefore be used as solvents.

A two-step mechanism is commonly accepted. First, the monomer is adsorbed onto the transition metal. During this step the adsorbed monomer may be activated

by the formation of an active complex. Afterwards, the activated monomer is inserted into the metal-carbon bond.

5.2.1   Polyethylenes and Copolymers

Two different processes for the production of polyethylene are being applied: the slurry process and the gas-phase process [5].

1. *Slurry process.* For the slurry process, hydrocarbons are used, e.g., isobutane, hexane, and n-alkane in which the polyethylene is insoluble. Fig. 3 shows the scheme of a slurry process [45].
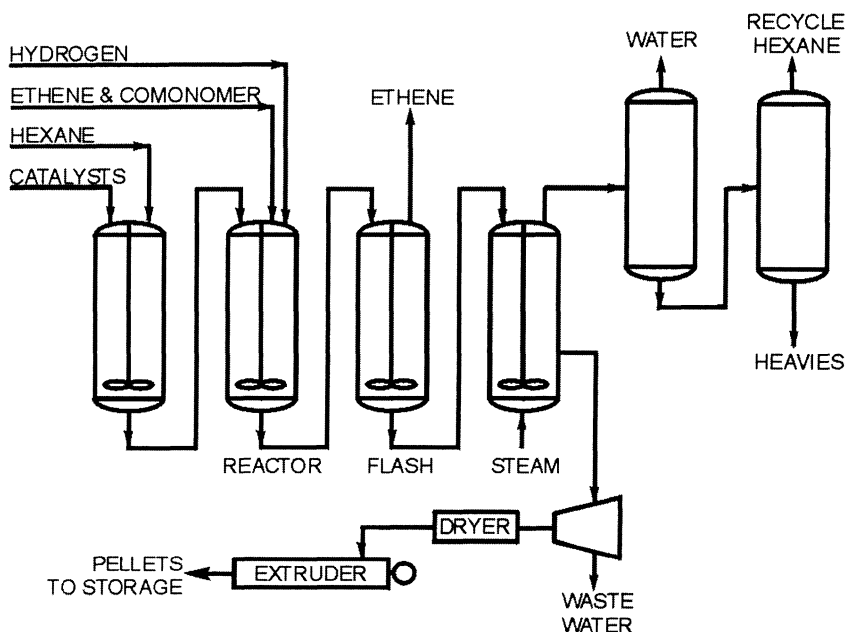
Fig. 3.   Scheme of the slurry process for the production of polyethylene

The polymerisation temperature ranges from 70 to 90 °C, with ethylene pressure varying between 0.7 and 3 Ma. The polymerisation time is 1 to 3 h and the yield is 95 to 98 %. The produced polyethylene is obtained in the form of fine particles in the diluent and can be separated by filtration. The molecular weight can be controlled by addition of hydrogen which increased the chain transfer reactions. The molecular weight distribution is regulated by variation of the catalyst design or by conducting the polymerisation in several steps under different conditions [46,47]. The best results are obtained in stirred vessels or loop reactors. In some cases the polymerisation is carried out in a series of cascade reactors to allow the variation of the hydrogen and comonomer concentration in different reactors in order to control the distribution of the molecular weights. The slurry contains

about 40 % by weight polymer. In some processes the diluent is recovered after centrifugation and recycled without purification.

2. *Gas-phase polymerisation.* Compared to the slurry process, the polymerisation in the gas phase has the advantage that no diluent is used, which simplifies the process [48]. A fluidized bed that can be stirred is used with supported catalyst. The polymerisation is carried out at 2 to 2.5 Mpa and 85 to 100 °C. The ethylene monomer circulates, thus removing the heat of the polymerisation and fluidizing the bed. To keep the temperature at values below 100 °C, gas conversion is maintained at 2 to 3 per pass. The polymer is withdrawn periodically from the reactor.

In contrast to the high-pressure polyethylene, which is characterized by long-chain branches, the polyethylene produced with coordination catalysts has a more or less linear structure. The density of homopolyethylenes is high but it can be lowered by copolymerisation. Polymers produced with unmodified Ziegler catalysts showed extremely high molecular weight (some millions) and broad molecular weight distribution (MWD = 5-20) [49]. In fact, there is no reason for any termination step, except for consecutive reaction.

As already pointed out, the major drawback of the first generation of catalysts is their low activity. In order to increase the amount of the active Ti from 0.1 - 1 % to 2 - 60 %, supported catalysts with inorganic carriers for $TiCl_4$ have been investigated. Commonly, $CoCl_2$, $MgCl_2$ or other Mg-salts are used because of their ionic radii (Mg^{2+} 0.066 nm, Co^{2+} 0.072 nm) being similar to the one of Ti^{4+} (0.068 nm). The major advantage of these catalysts is the high activity. Thus, only low concentrations of the catalysts are needed. Therefore residues can remain in the polymer.

A wide range of procedures has been developed to prepare supported Ziegler-Natta catalysts. A typical route is the mixing and ball milling of carefully dried „anhydrous" $MgCl_2$ with an „activating agent" which is an electron donor, typically ethyl benzoate or another aromatic ester, to produce the catalyst support [50]. In a second step $TiCl_4$ is fixed on the „active $MgCl_2$" either by suspending the support in hot $TiCl_4$ or by ball milling of the support with $TiCl_4$. Finally, the soluble part of the catalyst is removed by washing with hydrocarbons.

The role of the electron donors in the preparation of the support is to stabilize very small $MgCl_2$ particles produced during the ball milling by adsorption on the freshly prepared surfaces. Thereby reaggregation of the crystallites is prevented [51].

A typical composition of a supported Ziegler catalyst is 95 % wt $MgCl_2$, 5 % wt $TiCl_4$, $TiCl_4$: $AlEt_3$ ratio = 1 : 10.

The triethylaluminium alkylates the titanium, and inserts the ethylene into the titanium carbon bondethylene. Table 3 shows some kinetic data for the polymerisation of ethylene by unsupported and supported Ziegler-Natta catalyst [52].

The density of polyethylene (PE) can be lowered from 0,97 g/cm^3 up to 0,87 g/cm by a copolymerisation with longer-chained 1-olefins such as propylene, 1-butene, 1-hexene, 1-octene. Depending on the density, different types of PE are produced with increasing parts of comonomers:

High density PE	HDPE	$\delta = 0,95$	g/cm^3
Linear low density PE	LLDPE	$\delta = 0,91 - 0,93$	„
Very low density PE	VLDPE	$\delta = 0,87 - 0,90$	„

For the production of high module fibers, ultra high molecular weight PE (PE-UHMW) is used.

In heterogeneous processes the polymerisation reaction takes place only at the beginning inside the catalyst particle. Afterwards the reaction proceeds in the growing polymer particle. Each of these polymer particles is a small reactor with own energy and mass balance. The catalyst is fragmentated into small parts up to 1 μm. When the particle expands in the process of polymerisation, the rate of polymerisation can also increase because of a heat transfer. The monomer flow increases simultaneously. To reach a high catalyst productivity, the polymerisation rate must stay at a high level as long as the polymerizing particle remains in the reactor [53].

Table 3. A comparison of Kinetic Data for Ethylene Polymerisation Using Supported and Unsupported Ziegler-Natta Catalysts. The Number of Active Centers as well as the Rate Constant of Polymerisation are Responsible for the Higher Activities Observed in Supported Catalysts (adapted from Ref. 52)

Catalyst	T(°)	Efficiency[a]	Rate constant[b]	Molecular Weight[c] (kg mol^{-1})	
TiCl$_3$/AlEt$_2$Cl	50	0,005	540	2 000	(M$_n$)
TiCl$_4$/MgBuBr/AlEt$_3$	50	0,6	580	2 000	(Mn)
TiCl$_4$/Al(i-Bu)$_3$	30	0,03	33	1 000	(Mw)
TiCl$_4$/Mg(Oet)$_2$/Al(i-Bu)$_3$	30	0,016	2000	10 000	(Mw)
	60	0,023	12000		

[a] Efficiency = molar amount of active species per mol Ti. [b] Rate constant in liter d per mol Ti per second. [c] M$_n$ = number average molecular weight; M$_w$ weight average molecular weight.

Applying the detailed knowledge about the relation between the polyethylene structure and the polymer properties, tailored products can be produced for various applications. Bimodal molecular weight distribution of the polyethylene is advantageous for the production of special properties useful for pipes and films. In this case the catalyst is introduced into two reactors; the first reactor produces a homopolymer with a very low molecular mass, the second reactor with the same catalyst forms a very high molecular mass copolymer under different conditions. Each catalyst fragment is covered by layers of the low molecular mass homopolymer and the high molecular mass copolymer. These polymers have an outstanding combination of desired properties as high stiffness, toughness, stress crack resistance, and better processability [53].

The properties of polyethylene could be varied within a wide range by copolymerisation of ethylene with other comonomers. Most commercial products contain small amounts of other monomers. In general, adding comonomers during the polymerisation reduces the polyethylenes crystallinity, thereby reducing the melting point, the freezing point, and, in many cases, the tensile strength and odulus. At the same time, the optical properties are improved and the polarity is increased. Titanium- and vanadium-based catalysts have been used to synthesize copolymers that have a prevailingly random, block, or alternating structure. Only with Ziegler catalysts, long-chain α-olefins can be used as a comonomer (e.g., propylene, 1-butene, 1-hexene, 1-octene). Depending on the comonomer content, LLDPE or

VLDPE is formed. Thus, LLDPE or VLDPE is formed upon the addition of 2-5 mol% or 5-20 mol%, respectively. The comonomer decreases the melting point and the crystallinity of the polyethylene. Longer-chained monomers, such as 1-hexene, are more effective at the same weight concentration than smaller olefins such as propylene. The copolymerisation results in a branched polyethylene with methyl branching if propylene is used, ethyl if butene is used.

Important for the copolymerisation are the different reactivities of the olefins. [54]: ethylene > propylene > 1-butene > linear α-olefins >branched α-olefins.

In contrast to LDPE, produced with the high-pressure process, LLDPE exhibits much higher tensile strength . Therefore, there has been a considerable boost in the production of LLDPE [55].

5.2.2 Isotactic Polypropylene

In contrast to ethylene, propylene is converted to a crystalline polymer only using coordination catalysts propylene. The catalyst played a key role for the development and the innovation of the industrial technologies. The first catalysts were based on $TiCl_3/AlEt_2Cl$ systems and were characterized by low productivity and stereospecifity [56]. It was necessary to remove the catalyst residue and the atactic polymer fraction.

If the polymerisation is conducted with Ziegler-Natta catalysts, propylene or longer-chained α-olefins are inserted into the growing chain in a head-to-tail fashion with high selectivity. Every CH_2 group (head) is followed by a CH(R) group (tail) with a tertiary carbon atom bearing a methyl or an even larger alkyl group:

$$Cat — CH_2 — CH — CH_2 — CH — \qquad\qquad (11)$$
$$\qquad\qquad\quad | \qquad\qquad\quad |$$
$$\qquad\qquad CH_3 \qquad\quad CH_3$$
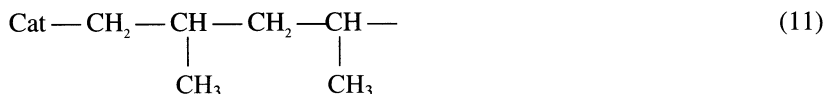
This construction principle is mandatory for the stereoregular structure of the polypropylene molecule. In addition, head-to-head

$$Cat — CH — CH_2 — CH_2 — CH — \qquad\qquad (12)$$
$$\qquad\quad | \qquad\qquad\qquad\quad |$$
$$\qquad CH_3 \qquad\qquad\qquad CH_3$$

and tail-to-tail

$$Cat — CH_2 — CH — CH — CH_2 \qquad\qquad (13)$$
$$\qquad\qquad\quad | \quad\quad |$$
$$\qquad\qquad CH_3 \quad CH_3$$
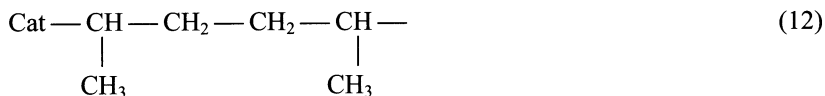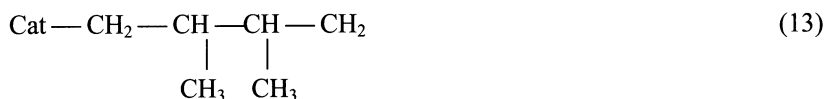
arrangements occur. An exclusive head-to-tail bonding is a mandatory but not a sufficient condition for stereoregularity. Another important detail is the sterical orientation of the pendant methyl groups with respect to the main C-C axis of the polymer molecule. Natta [57] formulated three different structures: isotactic, syndioactic, atactic (see Fig.9).

The most widely used catalyst for the stereospecific polymerisation of propylene consists of titanium halogenides and alkylaluminum compounds.A large num-

ber of other systems have been tested. Table 4 lists some important heterogeneous systems. The nature of the ligands and the valency of the transition metal atoms are the determining factors for the activity, productivity, and stereospecifity. Another strong influence on the stereospecifity is exerted by the nature of the cocatalyst.

The breakthrough in the development of the high-active supported catalysts was the discovery of „activated" $MgCl_2$ able to support $TiCl_4$ [58] and the subsequent discovery of electron donors (Lewis bases) capable of increasing the stereospecificity of the catalyst so that highly isotactic polypropylene could be obtained [59] High-active Ziegler-Natta catalysts on the basis of $MgCl_2$, $TiCl_4$ and an „internal" electron donor are typically used in combination with an aluminum alkyl cocatalyst such as $AlEt_3$ and an „external" electron donor added in polymerisation.

Table 4. Heterogeneous Catalysts for the Propylene Polymerisation

Catalyst [a]	Activity (g PP/g Ti · h · atm)	Isotacticity PP (%)
$TiCl_4/Al(C_2H_5)_3$ (1:3)	30	27
a-$TiCl_3/AlCl_3Al/(C_2H_5)_2Cl$	120	80
$TiCl_3/LiAl_2H7/NaF$	70	90
ß-$TiCl_3/Al(C_2H_5)2Cl/LB^1$	99	95
ß-$TiCl_3/AlCl_3/Al(C_2H_5)_2Cl/LB^2$	520	98
$MgCl_2/TiCl_4donors/AlEt_3$	1 600 000	99

[a]LB^1 = Lewis base 1, methyl methacrylate; LB^2 = Lewis base 2, diisoanyl ether

These catalyst systems contained ethyl benzoate as an internal donor and a second aromatic ester as an external donor. The catalysts most widely used in polypropylene manufacture currently contain, however, a diester (e.g. diisobutyl phthalate) as internal donor and are used in combination with an alkoxysilane external donor of the type $RR'Si(OMe)_2$ or $RSi(OMe)_3$ [60]. The functions of the internal donor in $MgCl_2$-supported catalysts were already mentioned (see Chapt. 5.2). One of the functions is to stabilize small primary crystallites of magnesium chloride; the other is to control the amount and distribution of $TiCl_4$ in the final catalyst. Activated magnesium chloride has a disordered structure comprising very small lamellae with (110) and (100) faces. It is discussed that $TiCl_4$ coordinated to the (100) face creates isotactic active sites, while, the coordination to the (110) face creates atactic sites. The donor now blocks the atactic (110) sites forming strong chelating complexes with tetra-coordinated Mg atoms.

The requirement for an external donor when using catalysts containing an ester as an internal donor is due to the fact that, when the catalyst is brought into contact with the cocatalyst, a large proportion of the internal donor is lost as a result of alkylation and/or complexation reactions. The absence of an external donor, results in a lower stereospecificity due to the increased mobility of the titanium species on the catalyst surface. When present, the external donor replaces the internal one.

Recently, research on $MgCl_2$-supported catalysts has led to systems which can be used without an external donor. This required the identification of bidentate internal donors, which not only had the right oxygen-oxygen distance for effective coordination with $MgCl_2$ but which, unlike esters, were not removed from the upport on contact with $AlEt_3$ and which, in contrast to alkoxysilanes, were unreactive with $TiCl_4$ during catalyst preparation. It was found that 2,2-disubstituted-1,3-dimethoxypropanes met all these criteria [61,62]. The following $MgCl_2$-supported catalysts show an activity up to 80 000 kg PP/g catalyst.

CATALYST TYPE	COCATALYST	EXTERNAL DONOR
$MgCl_2/TiCl_4$/ethyl benzoate	AlR_3	aromatic ester
$MgCl_2/TiCl_4$/dialkyl phthalate	AlR_3	alkoxysilane
$MgCl_2/TiCl_4$/diether	AlR_3	

The morphology of the obtained polypropylene particle plays an important role for the processing of the polypropylene and depends mainly on the catalyst structure. The Spheripol process is beside the Novolen- and Unipol-process is the one mostly used for the gas-phase polymerisation [60]. A multistep polymerisation allows the production of polymers with a wide range of molecular weight, crystallinity and stereoregularity. Separated and not agglomerated polypropylen granules are formed with a high bulk density and melting points up to 162 °C.

5.2.3   EPDM-Elastomers

Copolymers of ethylene and propylene with 20 to 80 mol % of propylene units are amorphous materials and can be produced using Ziegler-Natta or single site catalysts. Such amorphous ethylene-propylene-monomer copolymers (EPM) have some valuable elastomeric properties such as high stability against oxydation. This copolymer has gained some potential as an inexpensive elastomer. When small amounts of a non-conjugated diene are added to the reaction mixture ethylene-propylene-diene monomers (EPDM) are obtained [63-66]. EPDM is a commercially important synthetic rubber. The terpolymers are curable with sulfur. This rubber shows a higher growth rate than the other synthetic rubbers [67]. The most outstanding property of the ethylene-propylene rubber is its weather resistance. The latter is due to the fact, that this rubber has no double bonds in the backbone of the polymer chain and is, thus less sensitive to oxygen and ozone. Other excellent properties of this rubber are its resistance to acids and alkalis, its electrical insulation and its low-temperature performance [68].

It is important for the quality of the elastomer that the unsaturation of the added diene should not be located in the main chain, because this would decrease the stability against oxidation. Many non-conjugated dienes, such as 1,4-hexadiene, dicyclopentadiene, and ethylidene norbornene which polymerize only through one of the double bonds, are most suitable.
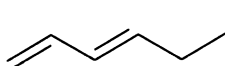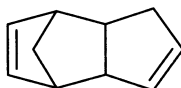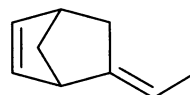
1,4-hexadiene   dicyclopentadiene   ethylidene norbornene

The properties of the copolymers depend to a great extent on several structural features of the copolymer chains, e.g. on the relative content of comonomer units, the way the comonomer units are distributed in the chain, the molecular mass and molecular mass distribution, and the relative content of normal head-to-tail addition or head-to-head/tail-to-tail addition.

For commercial processes, mainly vanadium-based catalysts are used for the synthesis of EPM or EPDM [69]. Catalysts typically applied for a solution process are: $VOCl_3/AlEt_3$, $VCl_3/Al(C_6H_{13})_3$, $VCl_4/AlEt_3$, $VO(OR)_3/AlEt_2Cl$.

The solvent is removed by distillation in the flash. Some catalysts contain $TiCl_3$ and $AlEt_2Cl$. More recently, supported $MgCl_2TiCl_4/AlEt_3$ and homogeneous aluminoxane-containing catalysts have also been used. For example, the molecular weights of copolymers increase if the ethen/-propylene ratio is increased, the concentration of catalyst is decreased, and the polymerisation temperature is lowered. Molecular weights increase in the order [70]

$$AlEt_2Cl > Al_2Et_3Cl_3 > AlEtCl_2 > AlEt_3.$$
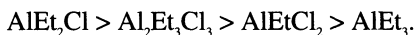
For technical uses the molecular mass (M_w) is in the range 100,000 to 200,000 g/mol. EPDM-rubber synthesized with vanadium catalyst show a molecular mass distribution between 3 and 10, indicating that two or more active centers are present.

5.2.4 Polydienes

Most polybutadiene is produced by Ziegler catalysts and late transition metal complexes, the remainder by lithium butyl. Especially cobalt, nickel and titanium (in few cases also neodym) compounds are used in combination with trialkylaluminium and some donors (Tab. 5) [71,72].

These catalysts produce polybutadienes with a high cis-content. As in the case of Ziegler-Natta catalysis of propylene, the active centers are transition metal-carbon bonds. They normally form an η^3-allyl bond (Fig. 4).

Table 5. Production Conditions of Different Polybutadiene Types

Type	Ti-BR	Co-BR	Ni-BR		Nd-BR
Solvent	aromatic	aromatic	aliphatic		aliphatic
atalyst	TiJ_4	Co-octanoate	Ni-naphthenate		Nd-carboxylate
	AlR_3	AlR_3	BF_3-etherate		$Al_2Et_3Cl_3$
	H_2O	AlR_3	AlR_3		
Temperature (°C)	5-35	5-50	50-60	50-100	
Reaction time (h)	3	2-4	3	2-4	
Conversion (%)	>90	>90	>90		100
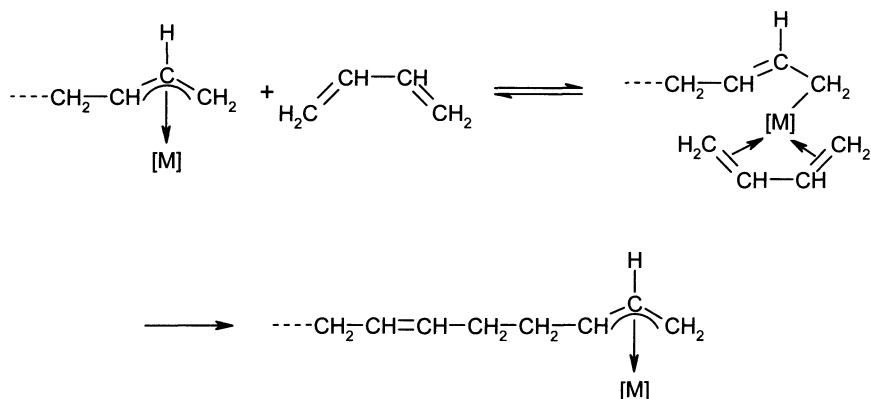
Fig. 4.   Insertion of butadiene into a transition metal (M) allyl bond

The propagation reaction proceeds via insertion into this carbon-transition metal bond after the diene has been coordinated as a π-complex. In the transition state a short-lived σ-allyl bond is formed, which restores in the case of a cis-migration the alkyl-transition metal bond.

In the case of titanium catalysts for achieving a high cis content of the products, it is essentiel that the catalyst contains iodine. $TiCl_4/AlEt_3$ produces a polybutadiene with 65 % cis and 35 % trans structures [73]. Regulation of the molecular masses can be achieved by the addition of 1,5-cyclooctadiene.

Supported Ziegler catalysts are also used for the production of polydienes [74]. High cis contents, up to 98 %, can be obtained with cobalt salts (cobalt octanoate, cobalt naphthenate) in combination with alumoxanes, which are synthesized in situ by hydrolysis of chlorodiethylaluminum or ethylaluminum sesquichloride. Only 0.005 to 0.02 mmol of the cobalt salt is needed for the polymerisation of 1 mol of 1,3-butadiene [75].

Water modifies the reaction rate and the polymer properties. The polymerisation activity has a maximum for a 0.03 : 0.2 ratio of water to Et_2AlCl, while the cis-1,4-content is 95 to 96 % at ratios higher than 0.1. For a 50:50 benzene/butane solvent the molecular mass approaches 800,000 g/mol at a 0,2 water/aluminum ratio. With a 30:70 solvent mixture the molecular mass approaches 400,000 at a ratio of 0,2. Also, systems of $AlCl_3/CoCl_2$ and thiophene produce a high cis-1,4 polymer. Nickel compounds can be applied as catalysts as well. A three-component system consisting of nickel naphthenate, triethylaluminum, and boron trifluoride diethyletherate is used technically. The activity of this system is similar to that of cobalt systems. The molar Al/B ratio varies between 0,7 to 1,4. Polymerisation temperatures range from -5 to 40 °C.

5.2.5   Mechanism of Ziegler-Natta Catalysis

Three main reaction steps take place during the polymerisation:

- *Formation of active centers* - the active centers comprise metal-C σ bonds, which are generated by the reaction of the metalhalide with the alkylaluminum

species (although the active center is believed to have a coordination vacancy or a ligand, which is easily replaced by the monomer).

- *Chain growth (propagation)* - based on a mechanism proposed by Cossee and Arlman [76,77], the monomer is believed to be coordinated to the active center prior to the insertion (more recently molecular orbital calculations implicate to real π complex of themonomer approaching and inserting [78]. The polymer chain is built up by rapid repetitions of the insertion step.
- *Chain termination or transfer* - hydrogen elimination, chain transfer to the co-catalyst, or a chain transfer reagent, such as hydrogen, are the main mechanisms to eliminate the polymer chain from the active center (Fig. 5) [5].

The mechanisms of chain propagation can be divided into two groups according to the role of the cocatalyst. In monometallic mechanisms the cocatalyst generates the active species from the transition metal but is not involved in the chain growth reaction itself. Bimetallic mechanisms favour the propagation at a cocatalyst alkyl group.

Early examples of bimetallic mechanisms were proposed by Natta and Mazzonti [79] and by Patat and Sinn [80]. In the Patat-Sinn mechanism the alkene is partially bonded between the transition metal and the methylene carbon of the last inserted monomer unit that is bonded to the aluminum. There is experimental evidence that insertion takes place at a transition metal-alkyl bond rather than at an Al-alkyl bond [81].

The mechanism of Cossee and Arlman is the most widely accepted one and a lot of other monometallic mechanisms being variations of its basic assumptions have been developed. Their model of the active species is the conclusion of Arlman's recognition of the existence of coordinative vacancies on the surface of theTiCl$_3$. These vacancies must exist to ensure the electroneutrality of the crystallite. Cossee derived an octahedral configuration for the active titanium centers - these have a vacancy, four chlorine ligands of the crystal and an alkyl group formed by alkyl transfer from the cocatalyst (Fig. 6).
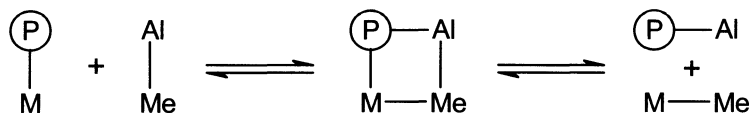
Exchange of alkyl groups
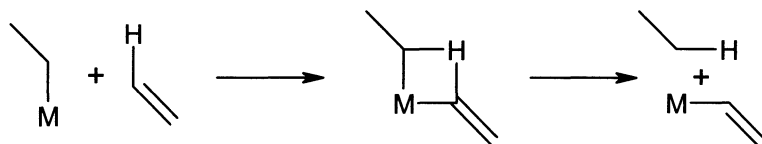
σ-bond methathesis
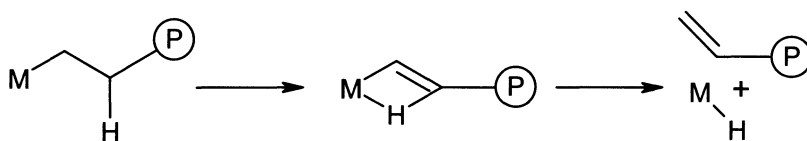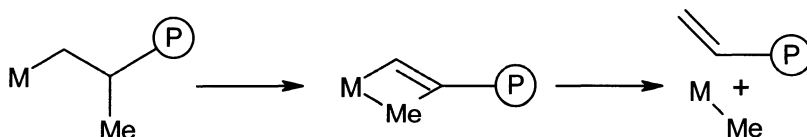
β-H elimination

β-methyl elimination

Fig. 5.   Chain termination reactions in Ziegler-Natta catalysis; P = polymer chain, M = transition metal, Me = methyl

The alkene is complexed to the vacancy and inserts into the Ti-alkyl bond via a four-membered transition state forming a new Ti-alkyl σ bond. After the insertion the growing polymer chain flips back into its old position, exchanging its place with the vacancy. This step is necessary to explain the stereospecificity observed in α-alkene polymerisation.

A lot of modifications of the Cossee-Arlman mechanism has been proposed to explain a different monomer coordination and the stereospecific propylene insertion. The structure of the active site is more complex and is investigated in the last years by the metallocene catalysts. The mechanism of Cossee and Arlman suggests that the polymerisation takes place at exposed Ti atoms at lateral faces of the TiCl$_3$ crystal, which is formed by close-packed anion layers. Electron microscopy studies support this view, showing polymer growth at defects and spiral dislocations of the surface.
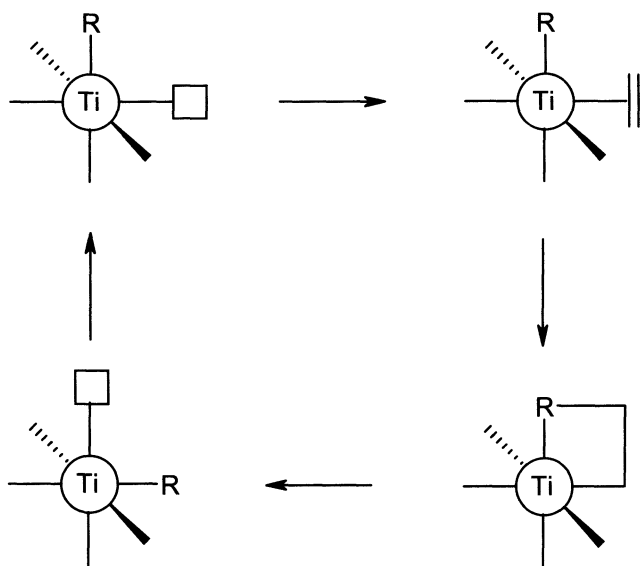
Fig. 6.   Cossee-Arlman mechanism of alkene polymerisation

The commercially important supported catalysts have been investigated extensively. The titanium IV is at least partially reduced to titanium III and II. Chien et al [82] detected Ti^{II} (8 %), Ti^{III} (38 %) and Ti^{IV} (54 %) in a catalyst prepared by ball milling $MgCl_2$ in the presence of ethyl benzoate as the internal donor and by washing with p-cresol and reaction with AlEt3 and TiCl4. At least, in supported Ziegler-Natta catalysts there are doubts if Ti(III) rather than Ti(IV) forms the active species.

5.3   Metallocenes and Single Site Catalysts

The manufacture of polyolefins by metallocene catalysts represents a new push in the polymer industry [83-95]. Metallocene catalysts are soluble in hydrocarbons, they have only one type of active sites (single site catalysts) and their chemical structure can be easily changed. New polymers, from ethylene copolymers with special properties up to transparent polypropylene fibers, cycloolefin copolymers and syndiotactic polystyrene, are industrially produced by single site catalysts.ethylene. The metallocenes single site catalysts allow an accurate prediction of the properties of the resulting polyolefins by knowing the structure of the catalyst used during their manufacture and to control the resulting molecular mass distribution, comonomer content and tacticity by careful selection of the appropriate reactor conditions. In addition, the activity of these catalysts is 10-100 times higher than of the classic Ziegler-Natta systems.

Metallocenes, in combination with the conventional aluminium alkyl cocatalysts used in Ziegler systems, are indeed capable of polymerizing ethylene, but only at a very low activity. Only with the discovery and application of methylalu-

minoxane (MAO) in our institute in Hamburg in 1977 it was possible to enhance the activity, surprisingly, by a factor of 10 000 [83]. Therefore, MAO plays a crucial part in catalysis with metallocenes. Methylaluminoxane is a compound in which aluminium and oxygen atoms are arranged alternately and free valences are saturated by methyl substituents. It is gained by careful partial hydrolysis of trimethylaluminium and, according to investigations by Sinn [84] and Barron [85], it consists mainly of units of the basic structure $(Al_4O_3Me_6)$, which contains four aluminium, three oxygen atoms and six methyl groups. As the aluminium atoms in this structure are coordinatively unsaturated, the basic units join together forming clusters and cages; these have molecular masses from 1 200 to 1 600 and are soluble in hydrocarbons.

If metallocenes, especially zirconocenes (Fig. 7), are treated with MAO, then catalysts are available that allow the polymerisation of up to 100 tons of ethylene per g of zirconium. At such high activities only extremely small amounts of the catalyst are needed which then can remain in the product. The insertion time for one molecule of ethylene into the growing chain amounts only to the order of 10^{-5} s. A comparison with enzymes is not far-fetched.

It is generally assumed that the primary function of MAO is to facilitate a fast ligand exchange reaction with the metallocene dichloride, thus rendering the metallocene methyl and dimethyl aluminium compound (Fig. 8).

In a further step, either Cl^- or CH_3^- is abstracted from the metallocene compound by an Al-centre in MAO, thus forming a metallocene cation and a MAO anion [86,87]. An equilibrium exists between the ion pair of the cationic metallocene and the anionic MAO and the resulting complex. Although both systems show polymerisation activity, the cationic complex is significantly more active. The two types of active centers show differences in the molecular masses of the obtained polymers [88].

An important side reaction is the α-hydrogen transfer which causes the production of methane. Condensation of the metallocene molecule and MAO takes place forming $Zr-CH_2-Al$ or $Zr-CH_2-Zr$ structures. These compounds are inactive and one of the reasons for the deactivation of metallocene catalysts [89]. The condensation rate depends on the structure of the zirconocene, the temperature, the Al/Zr ratio and the concentration of the zirconocene. The methane formation occurs much faster with MAO than with the Lewis-acidic trimethylaluminium. More than 50 moles of methane are eliminated per mol of zirconium in 2 h. The picture is complicated by a self-condensation of MAO. Due to the high methane production and the high amount of $Zr-CH_2-Al$ structures the catalyst ought to be inactive after some minutes. As the metallocene catalyst is active for hours or even days, there has to be a reactivation step.
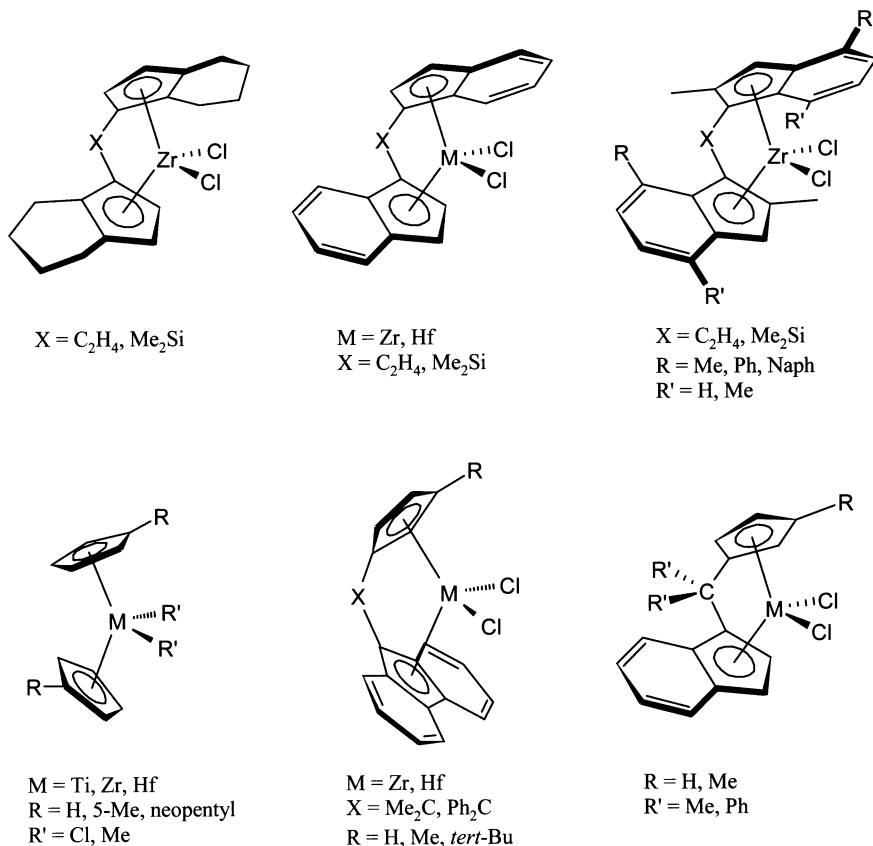
Fig. 7.   Structures of metallocenes used for olefin polymerisation

It was observed that inactive Zr-CH$_2$-Al structures could be activated by an excess of MAO, forming L$_2$ZrCH$_3$(Cl) (the active compound) and Al-CH$_2$-Al structures. After 5 to 20 min, thus, an equilibrium is established between deactivation and reactivation.

Meanwhile, other weakly coordinating cocatalysts, such as tetra(perfluoro-phenyl)borate anions [(C$_6$F$_5$)$_4$B]$^-$ have been successfully applied to the activation of metallocenes [90,91].

A further milestone was reached when Brintzinger [92] synthesized chiral bridged metallocenes in 1982 at the University of Konstanz and in 1984, when Ewen [93] at the Exxon Company (USA) was able to demonstrate that appropriate titanocenes render partially isotactic polypropylene. Nearly at the same time, highly isotactic material was obtained with analogous zirconocenes in our institute [94]. After this discovery, a fervent development of industrial and scientific research in the metallocene sector commenced [95].

Complexation

$$L_2ZrCl_2 + MAO \rightleftharpoons L_2ZrCl_2 MAO$$

Methylation

$$L_2ZrCl_2 MAO \rightleftharpoons L_2Zr(CH_3)Cl + \underset{Cl}{\overset{CH_3}{Al}}-O-$$

$$L_2Zr(CH_3)Cl\ MAO \rightleftharpoons L_2Zr(CH_3)_2 + MAO\text{-}Cl$$

Activation

$$L_2Zr(CH_3)Cl + MAO \rightleftharpoons L_2Zr(CH_3)Cl\ MAO \rightleftharpoons [L_2ZrCH_3]^+ + [MAO\text{-}Cl]^-$$
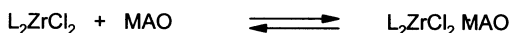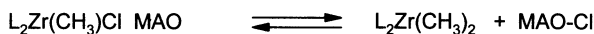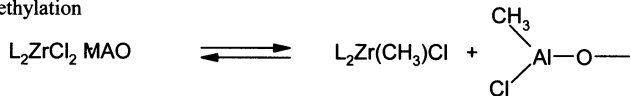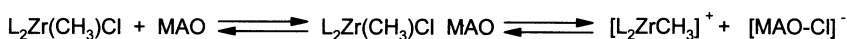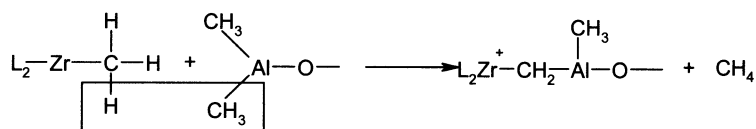
Deactivation

Reactivation
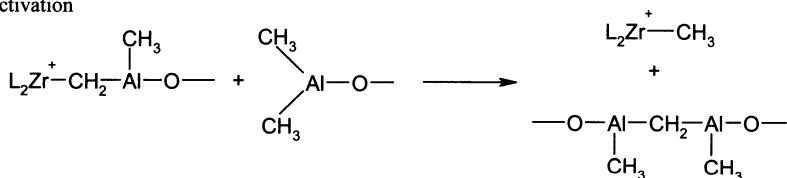
Fig. 8. Reactions of zirconocenes with MAO; L = cyclopentadienyl ligand

Polyolefins with different microstructures and characteristics can be custom-made just by varying the ligands on the metallocene (see Fig. 7) [96-101]. By combining different olefins and cycloolefins , the range of characteristics can be further broadened. The production of polyolefins with narrow molecular weight distributions ($M_w/M_n = 2$), of syndiotactic polymers and of chemically uniform co-polymers has not yet been achieved by conventional heterogeneous catalysts.

Using metallocene catalysts, it was possible for the first time to produce poly-ethylenes, polypropylenes, and copolymers with narrow molecular mass distributions [102], syndiotactic polypropylene (in technical scale amounts) [103], syndio-tactic polystyrene [104], cyclopolymerisates of 1,5-hexadiene [105], cycloolefin copolymers (COC) with high catalytic activity [106], optically active oligomers [107] and composite materials with biomass and powdered metals with polyole-fins. Organic or inorganic particles (starch, cellulose, quartz sand or powdered metal) can be coated with a hydrocarbon soluble metallocene catalyst and in turn, after polymerisation, with a polyolefin film of variable thickness [108].

5.3.1 Polyethylenes and Copolymers

Titanocene, zirconocene, or hafnocene together with methylaluminoxane as the cocatalyst form highly active catalysts for the polymerisation of ethylene. Using bis(cyclopentadienyl)zirconium dichloride-MAO catalysts, activities of 600 000 kg PE per mole Zr per hour may be obtained. Experimental results show that almost every zirconium atom forms an active species producing more than 46 000 polymer chains per hour [109]. The catalysts have a very long lifetime. Thus after more than 100 h of polymerisation there is still some activity left. The activities of

Table 6. Homopolymerisation of ethylene in toluene at 30 °C; 2,5 bar ethylene pressure; $6,25 \cdot 10^{-6}$ mol/l zirconocene concentration; molar ratio MAO/Zr = 250

Catalyst	Activity (kg PE/mol Zr $\cdot$ h $\cdot$ C$_E$)	Molecular weight viscosity (g/mol)
Cp$_2$ZrCl$_2$	60 900	620 000
C$_5$Me$_5$ZrCl$_2$	1 300	1 500 000
[En(Ind)$_2$]ZrCl$_2$	41 100	140 000
[Me$_2$Si(Ind)$_2$]ZrCl$_2$	36 900	260 000
[Me$_2$Si(2,4,7Me$_3$Ind)$_2$]ZrCl$_2$	111 900	250 000
[Me$_2$C(Flu)(Cp)]ZrCl$_2$	2 000	500 000

Polyethylene produced by metallocene-MAO catalysts features narrow molecular weight distributions with $M_w/M_n \approx 2$ to 2.5. Polydispersity may be controlled by mixing different metallocenes. The molecular mass can easily be lowered by increasing the temperature, increasing the metallocene: ethylene ratio, or by addition of hydrogen, acting as a chain transfer agent. Chain transfer to hydrogen and β-H elimination are 2-3 orders of magnitude greater than the corresponding value for MgCl$_2$-supported heterogeneous Ziegler-Natta catalysts.

An unique feature of metallocene catalysts is their copolymerisation behavior. Contrary to conventional Ziegler-Natta catalysts, which produce „heterogeneous" copolymers with the highest incorporation rates in the short chains and less co-monomer content in the longer chains due to the different active species in these catalysts, metallocenes produce copolymers with a statistical distribution of the comonomer sequences. By tuning the metallocene ligands the copolymerisation behavior can be varied from random to almost alternating [110].

Metallocenes are highly useful for the copolymerisation of ethylene with propylene, 1-butene, 1-pentene, 1-hexene and 1-octene forming linear low density polyethylene (LLDPE). These copolymers have a great industrial potential and show a higher growth rate than the homopolymer. Due to the short branching from the incorporated α-olefin, the copolymers show lower melting points, lower crystallinities, and lower densities. The main part of the comonomers is randomly distributed over the polymer chain. The amount of extractables is much lower than in polymers synthesized with Ziegler catalysts.

Under the same conditions, syndiospecific (C$_s$-symmetric) metallocenes insert more effectively in inserting α-olefins into an ethylene copolymer than isospecific

working (C_2-symmetric) metallocenes or unbridged metallocenes. In this particular case, hafnocenes are also more efficient than zirconocenes.

The copolymerisation of ethylene with other olefins is effected by the variation of the Al/Zr ratio, temperature and catalyst concentration. These variations change the molecular mass and the ethylene content. Higher temperatures increase the ethylene content and lower the molecular mass. The copolymers of ethylene and propylene with a molar ratio of 1:0,5 up to 1:2 are of great industrial interest. These EP-polymers show elastic properties and, together with 2-5 wt-% of dienes as third monomers, they are used as elastomers (EPDM).

The regiospecificity of the metallocene catalysts towards propylene leads exclusively to the formation of head-to-tail enchainments. Ethylidenenorbornene polymerizes via vinyl polymerisation of the cyclic double bond and the tendency of branching is low. The molecular mass distribution of about 2 is narrow [111].

$$
\begin{array}{c}
CH_3 \\
| \\
H_2C{=}CH
\end{array}
\qquad
\begin{array}{c}
CH_3 \\
| \\
H_2C{=}CH
\end{array}
\qquad \longrightarrow \qquad
\begin{array}{c}
CH_3 \quad\quad CH_3 \\
| \quad\quad\quad | \\
\cdots CH_2{-}CH_2{-}CH\cdots
\end{array}
$$

head   tail   **or**   1   2
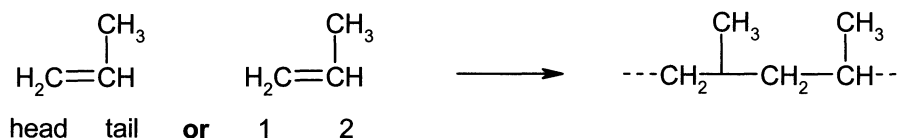
5.3.2 Polypropylene

Using metallocene catalysts, the microstructure of polypropylene and higher α-alkanes can be varied over a wide range. In addition to the main structures, isotactic, atactic and syndiotactic stereoblock, isoblock and hemiisotactic polypropylenes can be produced (Fig. 9).

The stereospecificity of the polymerisation depends on the metallocene used. Two basic mechanisms are found: enantiomorphic site control and chain end control [93]. If a prochiral monomer coordinates to the transition metal centre of a chiral metallocenium ion two diastereometric transition states exist, one of which is favored. This type of stereocontrol is called enantiomorphic site control: the chirality of the metallocene determines the stereochemistry of the insertion. If the monomer is coordinated to an achiral metallocenium ion, the two possible transition states are energetically equivalent; if there is no influence from chirality, an atactic polymer is formed in the growing polymerchain (chain end control).

The first chiral bridged zirconocene (ethylene-bis(4,5,6,7-tetrahydro-1-indenyl) zirconium dichloride) was synthesized by Brintzinger [92] and gives by an enantiomorphic site control isotactic polypropylene. Ewen and Razavi [103] showed that a C_s-symmetric bridged cyclopentadienyl fluorenyl zirconocene produces syndiotactic polypropylen. The activity, the molecular mass and the ^{13}C-NMR spectroscopically measured isotacticity of polypropylene obtained by different catalysts is given in Table 7 for comparison.

By inserting a silyl bridge and substituting the indenyl ligands in zirconocene, Spaleck was able to enhance the activity and stereoselectivity of the isotactic functioning catalyst considerably. These catalysts give isotactic PP of high mole-

isotactic

isoblock

stereoblock

syndiotactic

atactic
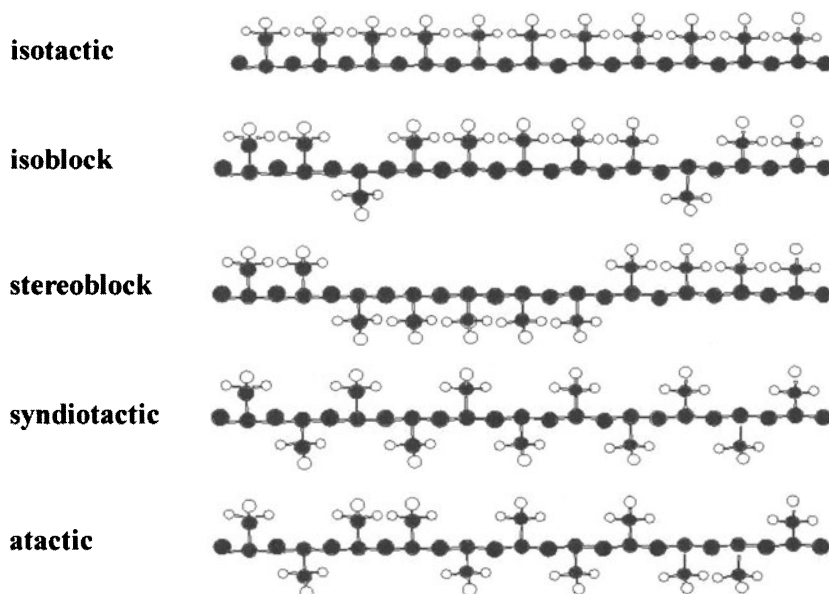
Fig. 9.   Microstructures of polypropylene

cular mass and with a melting point of 161 °C [96]. Polypropylenes made by met-allocenes exhibit distinct differences to conventionally produced polypropylenes, such as narrow molecular mass distribution, higher stiffness and greater tensile strength. This is caused not only by the more uniform structure, but

Table 7. Polymerisation of propylene with different zirconocenes in toluene at 30 °C; 2,5 bar propylene pressure; $6{,}25 \cdot 10^{-6}$ mol/l zirconocene concentration; MAO/Zr = 250

Catalyst	Activity (kg PP/mol Zr x h x cp)	Molecular (viscosity) (%)	Isotacticity mmmm-pentades (%)
Cp_2ZrCl_2	140	2 000	7
$[En(Ind)_2]ZrCl_2$	1 690	32 000	91
$[En(2,4,7Me_3Ind)_2]ZrCl_2$	750	418 000	> 99
$[Me_2Si(Ind)_2]ZrCl_2$	1 940	79 000	96
$[Me_2Si(2Me-4PhInd)_2]ZrCl_2$	15 000	650 000	99
$[Me_2Si(2Me-4,5BenzInd)_2]ZrCl_2$	6 100	380 000	98
$[Me_2C(Flu)(Cp)ZrCl_2$	1 550	159 000	0,6

also by the extremely small fractions of oligomeric products of low molecular mass. These fractions amount to less than 0,1 %, compared to 2-4 % in Ziegler-Natta PP.

5.3.3 Polycycloolefins

Metallocene catalysts are particularly important for the polymerisation of cyclo-olefins (cyclopentene, norbornene and their substituted compounds). In this process, only the double bond is opened and not the ring. Crystalline polycycloolefins with extremely high melting points of at least 380 °C, sometimes being higher than the decomposition temperature, are obtained [112].

While homopolymerisation of cyclopentene results in 1,3-enchainment of the monomer units, norbornene is inserted in 1,2-enchainment, as usual for olefin polymerisation. The problems of processing that arise from the high melting temperatures of the homopolymers can be solved by copolymerizing cycloolefins with ethylene [106].

The insertion of norbornene units into the growing polymer chain is very easy and only two to four times slower than the ethylene insertion. $Me_2C(t$-BuCp,Flu)]ZrCl$_2$ shows not only high activities for the copolymerisation of ethylene with norbornene, but gives an alternating structure with a melting point of 320 °C. Most metallocenes produce polymers with a statistical structure.

Such materials have characteristically an excellent transparency and a very high continuous service temperature. From cycloolefin insertion rates of 10 mol % upwards, these cycloolefin copolymers (COC) are no longer crystalline but amorphous. They are very resistant towards solvents and chemicals, they exhibit high softening temperatures (glass temperatures of up to 200 °C) and can be processed on a thermoplastic basis [113].

5.3.4 High Branched Polyolefins

High branching, which is caused by the incorporation of long chain olefins into the growing polymer chain, is obtained with a new class of silyl bridged amido-cyclopentadienyltitanium compounds (Fig. 10) [114-116].

These catalysts, used by Dow and Exxon, in combination with MAO or borates, incorporate oligomers with vinyl endgroups, which are formed during polymerisation by ß-hydrogen transfer. As a result, long chain branched polyolefins are formed. In contrast, structurally linear polymers are obtained when catalyzed by other metallocenes. Copolymers of ethylene with 1-octene are very flexible materials as long as the comonomer content is less than 10 %. Upon reaching 20 %, the long branched polymers show elastic properties.
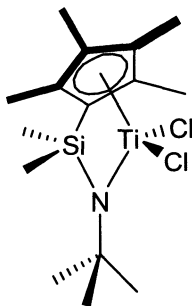
Fig. 10.   Structure of dimethylsilylamido-cyclopentadienyl-titaniumdichloride

5.3.5 Syndiotactic Polystyrene

Idemitsu was able to demonstrate that titanium compounds combined with MAO are capable of polymerizing styrene in a syndiotactical manner [104]. Moreover, trichloro(cyclopentadienyl)titanium (CpTiCl₃) has been proved to be remarkably active [117]. Syndiotactic polystyrene is crystalline and shows a melting point of 275 °C, which nearly makes it a high performance plastic.

Previously, it was already possible to produce isotactic polystyrene with classical Ziegler-Natta catalysts with very low polymerisation activities. However, it crystallized so slowly that technical usages were unthinkable. Furthermore, the polymerisation activity of CpTiCl₃-MAO catalysts was also unsatisfactory for technical usage. If fluorinated complexes, such as trifluoro(pentamethylcyclopentadienyl)titanium are employed, the activity can be improved by a factor of 30 (Table 8) [118]. At the same time the molecular weight rises from 169 000 to 660 000.

Table 8. Synthesis of Syndiotactic Polystyrene with „Half sandwich Metallocene/MAO Catalysts". M_n: molecular mass, M_wM_n: molecular mass distribution

Catalyst	Temperature (°C)	Activity*	M.p./°C	M_n	M_w/M_n
CpTiCl₃	50	1 100	258	140 000	1,9
CpTiF₃	50	3 000	265	100 000	2,0
C₅Me₅TiF₃	30	0,01	249	20 000	2,2
C₅Me₅TiF₃	50	15	275	169 000	3,6
C₅Me₅TiF₃	50	690	275	660 000	2,0

*Measured in kg PS per mol metallocene per h

The copolymerisation of styrene with ethylene, as examined by Mülhaupt [119], expands the property domains and employment areas. Syndiotactic polystyrene has already been produced in technical amounts by Idemitsu [104].

5.3.6   Supporting of Metallocene Catalysts

Metallocene catalysts are soluble in hydrocarbons and these dissolved form un-
suitable for the production of polyethylene or isotactic polypropylene on an indus-
trial scale. In order to use them in existing technical processes (drop-in technol-
ogy) instead of the conventional Ziegler-Natta catalysts, the metallocenes have to
be applied to a powdery, insoluble substrate. One way to do so is supporting met-
alloceneson silica, alumina, magnesium dichloride or other supports. Different
methods are possible [120]. Two of them are:

(1) initial absorption of MAO on the support with addition of metallocenes in a
second step. These washed catalysts are used in the polymerisation in combination
with additional MAO or other aluminum alkyls.

(2) Another way of the immobilisation of the metallocene is the absorption or
the covalent bonding by a spacer to the support surface. After addition of MAO,
this catalytic system is used in the polymerisation process. Both procedures afford
different catalysts and these in turn produce polyolefins with different properties
[121].

The polymers obtained by method (1) are very similar to those obtained by the
homogeneous system. Each metallocene on the support forms an active center and
the starting point for the growth of a polymer chain. As the active sites on the sur-
face of each catalyst grain are identical, all chains grow uniformly resulting in
polymers with narrow molecular mass distributions [122].

If the metallocene is first linked to the support, different states of absorptions
occur. Moreover, a large part of the metallocene is destroyed by acid centers. This
different bonding leads to different active sites. Therefore, the activity is much
lower than in the case of the homogeneous system and the molecular mass distri-
bution of the produced polymer is much broader.

References

1   B. Schmitt, W. Prätorius, K. Mühlbach, T. Plesning, Kur
        (1999).
2   T.E. Clayfield, Kunststoffe-Plast Europe **85**, 9 (1995)
3   P. Rempp, E.W. Merrill, Polymer Synthesis, Hüthig u. Wepf, Heidelberg
        1986
4   P. Pino, R. Mühlhaupt, Angew. Chem. Int. Ed. Engl. **19**, 857 (1980)
5   H. Sinn, W. Kaminsky, Adv. Organomet. Chem. **18**, 99 (1980)
6   R.P. Quirk (ed.), Transition Metal Catalyzed Polymerisation: Ziegler-
        Natta and Metathesis Polymerisations, Cambridge University Press,
        Cambridge 1988
7   T. Keii, K. Soga (eds.) Studies in Surface Science and Catalysis, El-
        sevier-Kodansha, Tokyo 1986, Vol. 25
8   J. Boor, Ziegler-Natta Catalysts and Polymerisation, Academy Press,
        New York 1979
9   G. Fink, R. Mülhaupt, H.H. Brintzinger (eds.), Ziegler Catalysts: Recent
        Scientific Innovations and Technological Improvements, Springer,
        Berlin 1995

10   W. Kaminsky, H. Sinn (eds.), Transition Metals and Organometallics as Catalysts for Olefin Polymerisation, Springer, Berlin 1988

11   W. Kaminsky (ed.), Metalorganic Catalysts for Synthesis and Polymerisation, Springer, Berlin 1990

12   W. Dittrich, P.C. Schulz, Makromol. Chem. **15**, 109 (1971).

13   J.N. Henderson, M.C. Throckmorton, Encycl. Polym. Sci. Eng. **10**, 811 (1987)

14   M. Morton, Anionic Polymerisation: Principles and Practice, Academic Press, New York 1983

15   A. Guyot, J. Vialle, J. Macromol. Sci. Chem., Part A, **4**, 79 (1970)

16   D. Margerison, D.M. Bishop, G.C. East, P. McBride, Trans. Faraday Soc. **64**, 1872 (1968)

17   D.J. Worsfold, S. Bywater, Can. J. Chem. **42**, 2884 (1964)

18   D.J. Worsfold, J. Polym. Sci. Part A-1, **5**, 2783 (1967)

19   A.F. Johnson, D.J. Worsfold, J. Polym. Sci. Part A, **3**, 449 (1965)

20   H. Sinn, C. Lundborg, O.T. Onsager, Makromol. Chem. **70**, 222 (1964)

21   H. Hernandez, J. Semel, H.Ch. Bröcker, H.-G. Zachmann, H. Sinn, Makromol. Chem. **70**, 222 (1964)

22   J.F. Eastman, G.W. Gibson, J. Am. Chem. Soc. **81**, 2171 (1963)

23   H. Hsieh, R.C. Farrar, K. Udipi, Chem. Tech. **11**, 626 (1981)

24   L.J. Fetters, M. Morton, Rubber Chem. Technol. **48**, 359 (1975)

25   J.E.L. Roovers, S.Bywater, Macromolecules **8**, 251 (1975)

26   R. Ohno, Y. Tanaka, M. Kawakami, J. Polym. **4**, 56 (1973)

27   A. Wurtz, Ann. Chem. Phys. **69**, 330 (1863)

28   H. Staudinger, O. Schweitzer, Ber. **62**, 2395 (1929)

29   M. Bednarek, P. Kubisa, Macro. Chem. Phys. **200**, 2429 (1999)

30   H.R. Kricheldorf, S. Eggerstedt, Macromolecules **30**, 5693 (1997)

31   G. Kaszas, J.E. Puskas, J.P. Kennedy, J. Macromol. Sci. Chem. Part A, **26**, 1099 (1989)

32   J.P. Kennedy, R.M. Thomas, Adv. Chem. Ser. **34**, 111 (1962)

33   O. Wichterle, M. Marek, J. Trekoval, J. Polym. Sci. **53**, 281 (1961)

34   J. Foundet, A. Gandini, Makromol. Chem. Rapid. Commun. **10**, 277 (1989)

35   F. Haas, G. Nutzel, G. Pampus. D. Theisen, Rubber Chem. Technol. **43**, 1116 (1970)

36   J.J. Ivin, T. Saegusa (eds.), Ring opening Polymerisation, Elsevier, New York 1985

37   G. Natta, G. Dall'Asta, I.W. Bassi, G. Carella, Makromol. Chem. **91**, 87 (1966)

38   R. Streck, J. Mol. Catal. **15**, 3 (1982)

39   K. Choi, W.H. Ray, Rev. Macromol. Chem. Phys. Part C, **25**, 18 (1985)

40   G. Natta, I. Pasquon, A. Zambelli, G. Gatti, J. Polymer Sci. **51**, 387 (1961)

41   A. Clark, J.P. Hogan, R.L. Banks, W.C. Lanning, Ind. Eng. Chem. **48**, 1152 (1956)

42   M.P. McDaniel, in: Handbook of Heterogeneous Catalysis, G. Ertl, H. Knözinger, J. Weitkamp (eds.), Wiley-VCH, Weinheim 1997, p. 2400

43   M.P. McDaniel, Advances in Catalysis, **33**, 47 (1985)

44   K. Ziegler, E. Holzkamp, H. Martin, H. Breil, Angew. Chem. **67**, 541 (1955)

45   W.H. Ray, Symposium documents

46   L. Böhm, Angew. Makromol. Chem. **89**, 1 (1980)

47   E. Heath, Chem. Engl. Apr. **3**, 66 (1972)

48   D.M. Rasmussen, Chem. Eng. Feb. **2**, 104 (1972)

49   H. Wesslau, Makromol. Chem. **20**, 111 (1956)

50   N. Kashima, in: Transition Metal Catalyzed Polymerisations, (ed.: R.P. Quirk), Harwood, New York 1983, p. 379

51   F.W. Locher, H.M.V. Seebach, Ind. Eng. Chem. Process Res. Dev. **11**, 190 (1972)

52   K.H. Reichert, Angew. Makromol. Chem. **94**, 1 (1981)

53   L. Böhm, in 11 (1999), p. 3

54   Y.V. Kissin, Adv. Polym. Sci. **15**, 91 (1974)

55   W. Glenz, Kunststoffe **76**, 834 (1986)

56   G. Natta, J. Am. Chem. Soc. **77**, 1708 (1955)

57   G. Natta, J. Polym. Sci. **16**, 143 (1955)

58   P. Galli, L. Luciani, G. Cecchin, Angew. Makromol. Chem. **94**, 63 (1981)

59   P.C. Barbé, G. Cecchin, L. Noristi, Adv. Polym. Sci. **81**, 1 (1987)

60   P. Galli, in 11 (1999) p. 14

61   E. Albizzati, U. Giannini, G. Morini, C.A. Smith, R.C. Zeiger, in 9 (1995), p. 413

62   L. Barino, R. Scordamaglia, Macromol. Symp. **89**, 101 (1995)

63   W. Marconi, A. Mazzei, S. Cucinella, M. de Malde, Makromol. Chem. **71**, 118 (1964)

64   A. Mazzei, S. Cucinella, W. Marconi, Makromol. Chem. **122**, 168 (1969)

65   D.H. Lee, J.K. Jang, T.O. Ahn, J. Polym. Sci. Part A. Polym. Chem. 25, 1457 (1987)

66   U. Gebauer, S. Engelmann, K. Gehrke, Acta Polym. **40**,. 341 (1989)

67   U. Zucchini, Data of Himont and Parpinelli Technon presented at Intern. Symp. on Advances in Olefin, Cycloolefin and Diolefin Polymerisation, Lyon 12-17 April, 1992

68   J.S. Lasky, H.K. Garner, R.H. Ewart, Ind. Eng. Chem. Prod. Res. Develop. **1**, 82 (1962)

69   P. Racanelli, L. Porri, Eur. Polym. J. **6**, 751 (1970)

70   E. Junghans, A. Gumboldt, G. Bier, Macromol. Chem. **58**, 18 (1962)

71   G. Natta, L. Porri, A. Mazzei, Chim. Ind. (Milan) **41**, 398 (1959)

72   G. Kraus, J. Short, V. Thornton, Rubber Plast Age **38**, 880 (1957)

73   M. Harwarth, K. Gehrke, M. Ringel, Plaste Kautschuk **22**, 1233 (1975)

74   R.P. Chaplin, R. Burford, G.J. Tory, S. Kirby, Polymer **28**, 1418 (1987)

75   W.M. Saltman, L.J. Kuzma, Rubber Chem. Technol. **46**, 1055 (1973)

76   P. Cossee, J. Catal. **3**, 80 (1964)

77   E.J. Arlman, J. Catal. **3**, 89 (1964)

78   T.K. Woo, L. Fan, T. Ziegler, Organometallics **13** (1994)

79   G. Natta, G. Mazzanti, Tetrahedron **8**, 86 (1960)

80   P. Patat, H. Sinn, Angew. Chem. **70**, 496 (1958)

81   A. Schindler, J. Polym. Sci. B **3**, 147 (1965)

82   J.C.W. Chien, J.-C. Wu, C.-I. Kuo, J. Polym. Sci. Polym. Chem. Ed. **20**, 2019; 2461 (1982)

83   H. Sinn, W. Kaminsky, H.J. Vollmer, R. Woldt, Angew. Chem. **92**, 396 (1980); Angew. Chem., Int. Ed. Engl. **19**, 390 (1980)

84   H. Sinn, I. Schimmel, M. Ott, N. v. Thienen, A. Harder, W. Hagendorf, B. Heitmann, E. Haupt, in: 11 (1999), p. 105

85   A.R. Barron, Macromol. Symp. **97**, 15 (1995)

86   J.J. Eisch, S.I. Pombrick, G.X. Zheng, Organometallics **12**, 3856 (1993)

87   P.G. Gassmann, M.R. Callstrom, J. Am. Chem. Soc. **109**, 7875 (1987)

88   R. Mülhaupt, T. Duschek, D. Fischer, S. Setz, Polym. Adv. Technol. **4**, 439 (1993)

89   W. Kaminsky, R. Steiger, Polyhedron **7**, 2375 (1988)

90   C. Sishta, R.M. Hathorn, T.J. Marks, J. Am. Chem. Soc. **114**, 1112 (1992)

91   M. Bochmann, J. Chem. Soc. Dalton Trans. **255** (1996)

92   F.R.W.P. Wild, L. Zsolnai, G. Huttner, H.H. Brintzinger, J. Organomet. Chem. **232**, 233 (1982)

93   J.A. Ewen, J. Am. Chem. Soc., **106**, 6355 (1984)

94   W. Kaminsky, K. Külper, H.H. Brintzinger, F.R.W.P. Wild, Angew. Chem., Int. Ed. Engl. **24**, 507 (1985)

95   J. Scheirs, W. Kaminsky (eds.), Metallocene-Based Polyolefins, Wiley, New York 2000

96   W. Spaleck, F. Küber, A. Winter, J. Rohrmann, B. Bachmann, M. Antberg, V. Dolle, E.F. Raulus, Organometallics, **13**, 954 (1994)

97   R. Mülhaupt, T. Ruschek, B. Rieger, Makromol. Chem., Macromol. Symp., **48/49**, 317 (1991)

98   J.K.G. Erker, R. Fröhlich, J. Am. Chem. Soc. **119**, 11 165 (1997)

99   H. Schumann, M. Glanz. E.C.E. Rosenthal, H. Hemling, Z. Anorg. Allg. Chem. **622**, 1865 (1996)

100   H.G. Alt, J.S. Han, U. Thewalt, J. Organomet. Chem. **456**, 89 (1993)

101   V. Busico, R. Cipullo, G. Monaco, M. Vacatello, Macromolecules **30**, 6251 (1997)

102   H. Sinn, W. Kaminsky, Adv. Organomet. Chem. **18**, 99 (1980)

103   J.A. Ewen, R.L. Jones, A. Razavi, J.P. Ferrara, J. Am. Chem. Soc. **110**, 6255 (1988)

104   N. Ishihara, M. Kuromoto, M. Uol, Macromolecules **21**, 3356 (1988)

105   G.W. Coates, R.M. Waymouth, J. Am. Chem. Soc. **113**, 6270 (1991)

106   W. Kaminsky, R. Spiehl, Makromol. Chem. **190**, 515 (1989)

107   W. Kaminsky, A. Ahlers, N. Möller-Lindenhof, Angew. Chem. **101**, 1304 (1989); Angew. Chem., Int. Ed. Engl. **28**, 1216 (1989)

108   W. Kaminsky, H. Zielonka, Polym. Adv. Technol. **4**, 415 (193)

109   P.J.T. Tait, in: 10 (1988), p. 309

110   M. Arndt, W. Kaminsky, A.-M. Schauwienold, U. Weingarten, Macromol. Chem. Phys. **199**, 1135 (1999)

111   N. Herfert, P. Montag, G. Fink, Makromol. Chem. **194**, 3167 (1993)

112   W. Kaminsky, A. Bark, M. Arndt, Makromol. Chem., Macromol. Symp. **47**, 83 (1991)

113   H. Cherdron, M.-J. Brekner, F. Osan, Angew. Makromol. Chem. **223**, 121 (1994)

114   A. Torres, K. Swogger, C. Kao, S. Chum, in: 95 (2000), p. 143
115   P.J. Shapiro, E. Bunel, W.P. Schaefer, J.E. Bercaw, Organometallics **9**, 867 (1990)
116   J. Okuda, K.E. du Plooy, W. Massa, H.-C. Kang, U. Rose, Chem. Ber. **129**, 275 (1996)
117   A. Zambelli, L. Olivia, C. Pellecchia, Macromolecules **22**, 2129 (1989)
118   W. Kaminsky, S. Lenk, V. Scholz, H.W. Roesky, A. Herzog, Macromolecules **30**, 7647 (1997)
119   S. Jüngling, R. Mülhaupt, D. Fischer, F. Langhauser, Angew. Makromol. Chem. **229**, 93 (1995)
120   W. Kaminsky, F. Renner, Makromol. Chem., Rapid Commun. **14**, 239 (1993)
121   K. Soga, M. Kaminaka, Makromol. Chem., Rapid Commun., **13**, 221 (1992)
122   C. Przybyla, J. Zechlin, B. Steinmetz, B. Tesche, G. Fink, in: 11 (1999), p. 32

Biocatalysis

Biocatalysis

Udo Kragl

Rostock University, Department of Chemistry,
18051 Rostock, Germany
udo.kragl@chemie.uni-rostock.de

Abstract. Biocatalysis is an established method not only for lab scale but also for industrial scale synthesis of fine or speciality chemicals as well as for bulk chemicals. One has to distinguish between fermentation processes and biotransformation or biocatalysis. For the latter the biocatalyst is either a whole cell or a (partly) purified enzyme catalysing only one step. Whereas oxidations and reductions are most often performed with whole cells, for hydrolytic reactions purified enzymes are used. These are often immobilized on various supports enhancing their stability and facilitating their recovery. Some examples highlight the potential and importance of biocatalysis as useful method besides heterogeneous and homogeneous catalysis.

1   Introduction

A discussion of modern aspects of catalysis has to consider biocatalysis besides homogeneous and heterogeneous catalysis as well. The treatment of biocatalysis as a third area might be justified by the special properties of the biocatalyst as discussed below. On the other hand, biocatalysts can be used either as homogeneous or as heterogeneous catalysts.

When speaking about biotechnological processes one has to distinguish between fermentation processes where products are synthesized by microorganisms (bacteria, yeasts) or higher cells (animal cells, plant cells) from components in the fermentation broth (carbohydrates, amino acids and trace elements). Product examples are amino acids such as L-lysine or L-threonine[1], vitamines (eg vitamin B12), penicillin and cephalosporin derivatives or recombinant pharma proteins such as erythropoetin or Factor VIII [2]. But also for simple products such as 1,3-propanediol or polymers such as polylactide fermentation processes are investigated at least at pilot scale [3]. In food industry many fermentation processes are used such as brewing of beer, production of vinegar or soy sauce [4]. On the other hand the term biocatalysis or biotransformation is used for processes where a starting material is converted into the desired product by one step only. This can be done either using whole cells or (partly) purified enzymes (Fig. 1). Product examples range from bulk chemicals such as acrylamide, fine chemicals and chiral synthons such as chiral alcohols to food ingredients such as high fructose corn sirup. Also in daily life enzymes play an important role: they are ingredients in washing powders, "stone washed jeans" are obtained by biobleaching, or citrus fruits are peeled with the help of pectinases.

One Step Biotransformations Use

educt $\xrightarrow{\text{biocatalyst}}$ product

· **whole cells**   · **enzymes, (partly) purified**

· Prokaryonts
  - bacteria

· Eukaryonts
  - funghi, yeasts
  (- higher cells)
  (plant, animal)
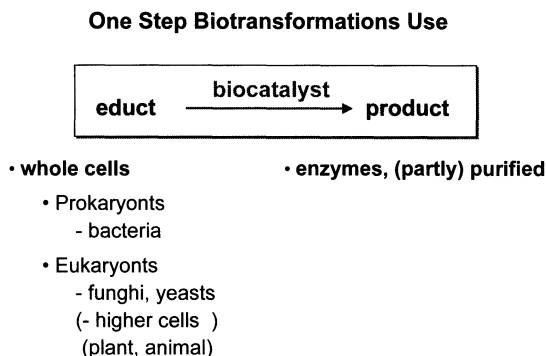
Fig. 1. Biotransformations using either whole cells or purified enzymes

There are several books and reviews dealing with the use of biotransformations either on lab scale or industrial scale [5-13]. Some examples are given in section 3.

2   Handling of Biocatalysts

2.1   Recovery of Biocatalysts by Immobilization

Depending on the type of biocatalyst used a specific handling including specific reactor requirements is necessary. For reactions where cofactor regeneration is necessary - this is the case in most reduction or oxidation processes - mostly whole cell processes are used. In these cases supply of oxygen is often a limiting factor, but also foaming, clogging etc has to be addressed. This is discussed in more detail in the textbooks about biochemical reaction engineering [14, 15]. When whole cell processes are used the biocatalyst may be either separated from the reaction medium by centrifugation or by microfiltration. Both unit operations can be used on a large scale and in continuously operated equipment. But also entrapment in gels or adsorption to carriers for use in fixed or fluidized bed reactors is possible.

For hydrolytic reactions often purified enzymes are used. These are - depending on the solvent - homogeneously soluble and therefore show the same advantages as other homogeneous catalysts such as no mass transfer limitations, easy control of pH etc. Compared to chemocatalysts, enzymes as macromolecules inherit the advantage of an easy recovery by ultrafiltration. This is used on an industrial scale by Degussa for the synthesis of chiral amino acids [16, 17], but it is valuable for lab scale synthesis as well. Examples are the production of N-acetylneuraminic acid and derivatives [18, 19] or nucleotide sugars [20]. The concept of the membrane reactor has been transferred to chemocatalysts as well [21-24].

In the majority enzymes are used as immobilized catalysts. It is beyond the scope of this short introduction, to list all the different supports, coupling methods

or enzymes already investigated. A survey can be found in [4, 25-30]. In the following some important points to consider are summarised:

- The easiest way to immobilise a soluble enzyme - besides the use of an ultra-filtration membrane - is the entrapment into a hydrogel such as alginate or carragenan. This can be easily achieved by mixing the appropriate solutions [31]. The resulting particles however are soft and therefore are of limited use in large scale industrial reactors.

- The greatest benefit can be achieved when the enzyme is covalently attached to an insoluble support. By fixation of its tertiary structure the thermal stability is often increased dramatically leading to a catalyst with high operational stability. Examples for this are Penicillin G amidase in the synthesis of 6-aminopenicillinic acid, a building block for semisynthetic penicillins. The enzyme was used in more than 1000 reaction cycles [26]. Another example is the glucose-fructose isomerase which is used for the production of high fructose corn sirup. The record for the longest lifetime of a column containing the immobilized enzyme is 687 days at pH 7.5 and 55 °C [5].

- The support used for covalent or adsorptive attachment may be inorganic material such as porous glas or organic polymers [27]. The attachment can be either by electrostatic interactions when ion exchange resins are used. For a covalent attachment suitable groups of the protein - mostly amino functions - have to be coupled to the support which has to bear appropriate functional groups. A very common method is the use of amino groups on the support as well which can be coupled by glutardialdehyde to amino groups on the surface of the enzyme [37]. Another very simple method is the use of oxirane groups on the support which react in water with amino and sulfhydryl groups on the surface of the enzyme. Such material has been introduced under the name Eupergit® by Röhm. It is used for example for industrial preparations of Penicillin acylase [25, 32]. In this case a catalyst consumption of less than 1000 U per kg of product has been achieved [33]. If the enzyme consumption is in this order of magnitude and the enzyme is reasonable cheap, than the catalyst costs are not longer the limiting factor.

- Crystallisation is a good method for purification of enzymes. If the enzyme molecules in a crystal are crosslinked by inter- and intramolecular bondings, the protein becomes insoluble in water and mechanically more stable. This technique of cross-linked enzyme crystalls (CLEC's) has been introduced by Altus Biologics [34-36]. Due to the high density of active enzyme in the catalyst particle mass transport limitations may occur. But also direct crosslinking of the protein in solution, eventually in the presence of an inert protein, is possible. This approach is used for many enzymes used for industrial applications. The enzyme is purified only to that extent that side activities are removed.

- In all cases, the advantages of easier separation or prolonged operational stability have to be balanced against immobilization yield and the costs of the support and the procedure. The immobilization yield might be improved by performing the reaction in the presence of a substrate preserving the enzyme in its most active form and, more important, blocking the active centre and

therefore preventing reactions at this place. On the other hand enzymes are becoming more readily available by modern methods of genetic engineering. But not only the access is simplified, also the activity and selectivity for a given reaction can be improved or the stability can be enhanced [38-41].

2.2   Special Requirements of Biocatalysts

Nature has designed its biocatalysts to perform best in an aqueous surrounding, neutral pH and temperatures below 40 °C. This conditions sometimes are contrary to the requirements of the chemist or process engineer to optimise a reaction with respect to space-time yield or high product concentration in order to facilitate downstream processing. Furthermore, enzymes as well as whole cells often show inhibition of product or substrates. These might easily overcome by continuously operated stirred reactors, fed-batch reactors or reactors with *in situ* product removal. Examples for the latter are the removal of organic acids by electrodialysis [42, 43] or of alcohols by pervaporation [44, 45]. A very clever method introduced by coworkers of Eli Lilly is shown in the examples.

To increase solubility of substrates and/or products the addition of organic cosolvents is common practise [46]. However, it should be noted, that despite all success there is no general rule which solvent is "enzyme friendly". To a certain extent, the log P concept, based on the distribution coefficient between water and octanol, can be used as guideline [47]. In general, solvents with a log P >3 such as xylene (3.1) or hexane (3.9) are less deactivating than those with a low log P such as ethanol (-0.24). Surprisingly, *tert*-butanol (0.35) stabilises enzymes [48]. Certainly the hydrophilicity of the cosolvent is important as it allows interaction and breaking of hydrogen bonds which are stabilizing the tertiary structure of the enzyme. But not only common organic solvents have been used for biocatalysis, also supercritical CO_2 [49] and recently even ionic liquids have been shown to be compatible with enzymes or whole cells. [50-53].

Hydrolytic enzymes and amongst them lipases are the work horses of biocatalysis [9]. From nature designed to work at aqueous/organic interfaces for the cleavage of fats and oils to make the cleavage product accessible as nutrients lipases in general tolerate and are active in pure organic solvents. This concept has pioneered by Klibanov and coworkers [46, 54]. BASF introduced recently several processes for the kinetic resolution of racemic amines (compare example section). The enzyme is immobilized on polyacrylate and the reaction is performed in methyl-*tert*-butylether (MTBE) as solvent [5, 55].

For biocatalysts the same rules apply as for other catalysts: "Reactor and catalyst can not be treated separately". Therefore at least some basic information about kinetic and thermodynamic data is required in order to identify and get rid of bottlenecks. Especially the already mentioned substrate and product inhibition can cause problems when not properly taken into consideration. Some examples are discussed in detail in [56, 57].

3   Examples

Today, more than 100 one-step biotransformations making use of whole cells or isolated enzymes are employed at an industrial scale. At lab scale, more than

13,000 enzyme catalysed reactions have been described. There are numerous books and reviews covering various aspects such as stereoselective biotrans-formations, special classes of enzymes such as hydrolases or food technology. A very recent example listing not only the different reactions but also giving details about the processes is [5]. Due to limitations in space, only a few examples can be given here.

Biotransformations in the meaning as discussed here go back to the beginning of the 20th century. The term enzyme was already keyed in in 1867 by Kühne, 15 years before Ostwald gave his famous definition of a catalyst. The first asymmetric catalysis most probably has been performed by an enzyme: Rosenthaler described the HCN addition to aldehydes using (R)-Oxynitrilase (EC 4.1.1.10) yielding chiral cyanohydrins [58]. This reaction was again investigated in the second half in the 20th century by different groups finally leading to an industrial process recently established by DSM Linz in Austria for the synthesis of (S)-phenoxybenzaldehyde cyanohydrin **3** (Fig. 2) [59, 60]. The (S)-specific enzyme (EC 4.1.1.11) has been cloned from *Havea brasiliensis*. The reaction is performed in a two phase system with the substrate dissolved in an organic solvent. The process yields high-quality cyanohydrin (enantiomeric excess >97%) in almost quantitative yield. The resulting (S)-cyanohydrins are versatile building blocks for synthetic pyrethroids used as insectizides.

Fig. 3. Oxynitrilase catalysed synthesis of chiral cyanohydrins

But also "old processes" like the Reichstein-process for the oxidation of D-sorbitol to L-sorbose using *Acetobacter suboxidans* as key step in the synthesis of ascorbic acid, which has been established in 1934, are still in use. In some cases biotechnology offers advantages over established processes therefore replacing them. The reasons may be better regio-, stereo- or chemoselectivity or a better product purity or a simplified downstream processing. Often the incorporation of biocatalytic steps reduces the amount or toxicity of waste. The most popular example is the use of a nitrile hydratase (EC 4.2.1.84) from *Rhodococcus rhodochrous* for the production of acrylamide **6** starting from acrylnitrile **4** (Fig. 3). This process replaces the older copper-catalysed process. Meanwhile more than 30,000 t a^{-1} are produced by this process which is about 30% of the acrylamide worldwide [61, 62]. Another example is the production of 7-amino cephalosporinic acid (7-ACA). A two step enzymatic process consisting of a D-amino acid oxidase (EC 1.4.3.3) and a Glutaryl acylase (EC 3.1.1.41) has replaced the old chemical process for cleaving Cephalosporine C obtained from a fer-mentation process. Both enzymes are immobilized on a support [26, 63]. The enzymatic process drastically reduces the amount of waste: 0.3 t per ton of product compared to 31 t for the chemical method. Thus the costs for waste disposal could be reduced by 20%.

For the enantioselective ketone reduction very often whole cells are used to get rid of the problem of cofactor regeneration. Zmijewski and coworkers have

described the reduction of 3,4-methylenedioxyacetophenone **7** to the corresponding (S)-alcohol **8** by using whole cells of *Zygosaccharomyces rouxii* (Fig. 3) [64, 65]. As the substrate is toxic to the cells at higher concentrations it is adsorbed on a hydrophobic XAD-7 resin (80 g L^{-1} resin) and added to the reaction mixture. The substrate is desorbed into the aqueous phase to its maximum solubility of 2 g L^{-1}. The formed alcohol is also adsorbed to the resin thus simplifying downstream processing. Due to the size of the resin particles and the much smaller cells the resin can be recovered easily by filtration. The alcohol is liberated by washing the resin with acetone: 96% yield, >99.9% ee. The productivity of this process is 75 g L^{-1} d^{-1}.

BASF has introduced recently a process for the kinetic resolution of racemic amines **9** by transesterification. The lipase (EC 3.1.1.3) from *Burkholderia plantarii* is immobilized on polyacrylate and the reaction is performed in MTBE [46, 54]. Ethylmethoxyacetate **10** is used as second substrate. But the key step during process development was the discovery that freeze drying the lipase together with fatty acid increases its activity in the organic solvent by several orders of magnitude. The process is now operated at a >100 t a^{-1} scale. The residence time is 5-7 h. Due to the kinetic resolution the conversion is limited to 50%. The yield is 90% and the ee >99%.

It is likely that an increasing number of processes which are either using bio- or chemocatalytic steps will compete. One example is the synthesis of L-DOPA which is used for treatment of Parkinson. Monsanto had commercialised the process using a Rh-catalysed enantioselective hydrogenation of the corresponding unsaturated amino acid derivative [6, 66, 67]. The competing biocatalytic process, commercialised by Ajinomoto, starts from catechol **12** and pyruvic acid **13** (Fig. 3). Whole cells of *Erwinia herbicola* are used containing a tyrosine phenol lyase (EC 4.1.99.2) [5, 68]. The reaction is performed as fed batch process at a reactor volume of 60 m^3 at a scale of 250 t a^{-1}.

Finally, two examples shall be used to highlight that integrated processes using both, chemical and biocatalytic steps, can be of great interest and use, even when the biocatalytic step is only used to remove a byproduct as in the second example.

Lonza has introduced a process for the production of nicotinamide **21** starting from 2-methylpentane-1,5-diamine **17**. This starting material is obtained by hydrogenation of 2-methylglutarnitril, a byproduct of the Nylon-6,6 production. The overall process contains gas-phase cyclisation, a Pd-catalysed dehydrogenation, an ammonoxidation and the enzymatic hydrolysis (Fig. 4) [69, 70]. For the biocatalytic step the same enzyme is used as for the production of acrylamide. The yield and selectivity of the biocatalytic step is >99%, whereas the alkaline hydrolysis of 3-cyanopyridine gives 4% of nicotinic acid as byproduct.

Novartis is using catalase (EC 1.11.1.6) from a microbial source to decompose hydrogen peroxide **24** which is formed as a byproduct during synthesis of dinitrobenzyl **23** (Fig. 5) [5, 71]. Decomposition using a heavy-metal catalyst does only yield in incomplete conversion. Furthermore, following steps for converting dinitrobenzyl are sensitive to contamination with heavy metals. By this enzymatic treatment the H_2O_2 content is reduced from 7,000 ppm to <200 ppm.

Nitto Chemical Industry

4   5   6

Eli Lilly

7   8

BASF

(R,S)-9   10   (S)-9   (R)-11

Ajinomoto Co.

12   13   14   L-15   16
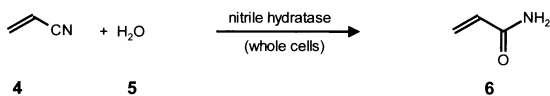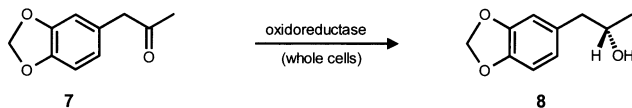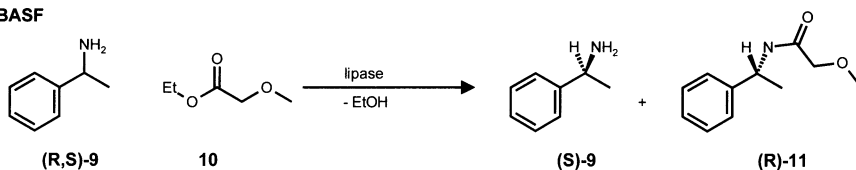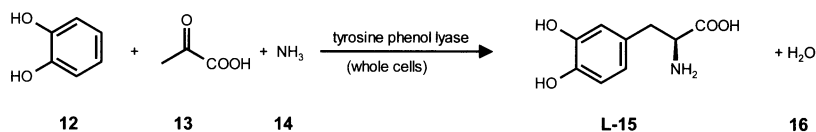
Fig. 3. Examples for biocatalytic processes (details see text)

17   18   19

20   21
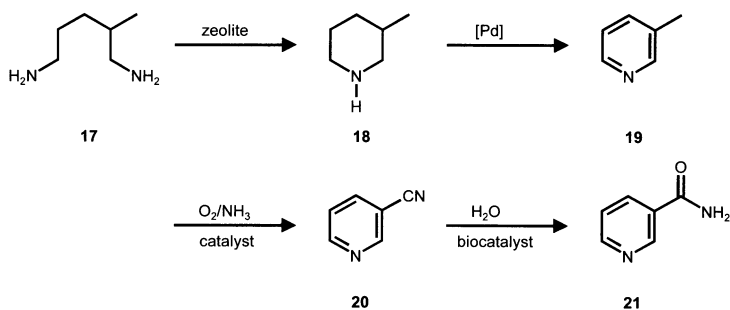
Fig. 4. Process for production of nicotinamide **21** (details see text)

22   23

$H_2O + 0.5 O_2$
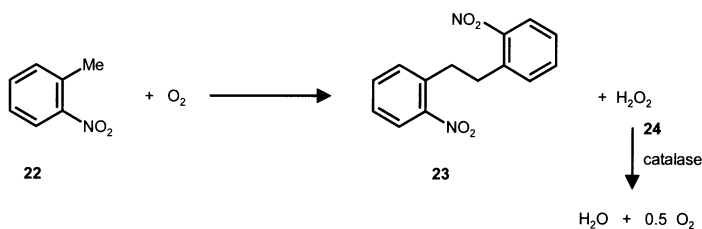
Fig. 5. Catalase for decomposition of the byproduct hydrogen peroxide (details see text)

4   Conclusions

Biocatalysis has established itself as useful method. It took some decades to bring the vision of Sir Cyril Hinshelwood into life: "Bacteria are capable of bringing about chemical reactions of amazing variety and subtley in an extremely short time. Many bacteria are of very great importance to industry where they perform tasks which would take much time and trouble by ordinary chemical methods." [72]. Important for the success of biocatalysis are several factors:

- An interdisziplinary approach combining the expertise of chemists, microbiologists and engineers at an early stage of process development to test biocatalytic steps from the beginning, not when all other methods have been failed.
- The methods of genetic engineering for better production of enzymes and altering their properties. This will be of increasing importance for the future when metabolic engineering is used to create new metabolic pathways in bacteria to synthesize the desired product [73]. There are first examples of this type of "designer bugs" eg for synthesis of indigo [5], antibiotics [74] or nucleotide sugars [75, 76].

References

1   H. Kumagai, Adv. Biochem. Eng. **69**, 71 2000.
2   J. M. Reichert, Trends Biotechnol. 18, 364, 2000.
3   P. L. Meredith, J. Polymer Sci. 38, 667 2000.
4   A. Tanaka, T. Tosa and T. Kobayashi (eds.), Industrial Application of Immobilized Biocatalysts, Marcel Dekker, New York, 1993.
5   A. Liese, K. Seelbach and C. Wandrey, Industrial Biotransformations, VCH-Wiley, Weinheim, 2000.
6   B. Cornils, W. A. Herrmann, R. Schlögl and C.-H. Wong, Catalysis from A to Z, Wiley-VCH, Weinheim, 2000.
7   K. Faber, Biotransformations in Organic Chemistry, Springer, Berlin, 2000.
8   R. N. Patel, Stereoselective Biocatalysis, Marcel Dekker, New York, 2000.VCH, Weinheim, 1999.
10   U. T. Bornscheuer, Enzymes in Lipid Modification, Wiley-VCH, Weinheim, 2000.
11   A. Liese and M. Villela Filho, Curr. Op. Biotech. 10, 595, 1999.
12   A. Schmid, J. S. Dordick, B. Hauer, A. Kiener, M. Wubbolts and B. Witholt, Nature 409, 258, 2001.
13   H. Griengl, Biocatalysis, Springer, Berlin, 2000.
14   J. E. Bailey and D. F. Ollis, Biochemical Engineering Fundamentals, McGraw-Hill, New York, 1986.
15   H. Chmiel (Ed.), Bioprozeßtechnik 1 & 2, Gustav Fischer Verlag, Stuttgart, 1991.
16   A. S. Bommarius, in Biotechnology, Vol 3, Edited by H.-J. Rehm, G. Reed, A. Pühler, P. Stadler, G. Stephanopoulus, VCH, Weinheim, 427, 1993.
17   A. S. Bommarius, M. Schwarm, K. Stingl, M. Kottenhahn, K. Huthmacher and K. Drauz, Tetrahedron: Asymmetry 6, 2851, 1995.
18   U. Kragl, A. Gödde, C. Wandrey, W. Kinzy, J. J. Cappon and J. Lugtenburg, Tetrahedron: Asymmetry 4, 1193, 1993.
19   C. Salagnad, A. Gödde, B. Ernst and U. Kragl, Biotechnol. Progress 13, 810, 1997.

20   S. Fey, L. Elling and U. Kragl, Carbohydr. Res. 305, 475, 1997.

21   U. Kragl and C. Dreisbach, Angew. Chem. Int. Ed. Engl. 35, 642, 1996.

22   G. Giffels, J. Beliczey, M. Felder and U. Kragl, Tetrahedron: Asymmetry 9, 691, 1998.

23   N. Brinkmann, D. Giebel, G. Lohmer, M. T. Reetz and U. Kragl, J. Catal. 183, 163, 1999.

24   T. Dwars, J. Haberland, I. Grassert, G. Oehme and U. Kragl, J. Mol. Cat. A 168, 81, 2001.

25   E. Katchalski-Katzir and D. M. Kraemer, J. Mol. Cat. B 10, 157, 2000.

26   P. Rasor, in Chiral Catalyst Immobilization and Recycling, Edited by D. E. De Vos, I. F. J Vankelecom, P. A. Jacobs, Wiley-VCH, Weinheim, 96, 2000.

27   W. Keim and B. Drießen-Hölscher in Handbook of Heterogeneous Catalysis Edited by G. Ertl, H. Knözinger and J. Weitkamp, Wiley-VCH, Weinheim, 231, 1997.

28   U. Kragl, L. Greiner and C. Wandrey, in Encyclopedia of Bioprocess Technology, Edited by M. C. Flickinger and S. W. Drew, Wiley, New York, 1064, 2000.

29   W. Tischer and V. Kasche, Trends Biotechnol. 17, 326, 1999.

30   V. M. Balcao, A. L. Paiva and F. X. Malcata, Enzyme Microb. Technol. 18, 392, 1996.

31   M. Jekel, A. Buhr, T. Willke and K. D. Vorlop, Chem. Eng. Technol. 21, 275, 1998.

32   Product Information Eupergit, Röhm, Darmstadt.

33   1 U means conversion of 1µmol of substrate per minute at given conditions. It is still very often used besides the SI-unit of enzyme activity katal with 1 kat = 1 mol s-1.

34   R. A. Persichetti, N. L. S. Clair, J. P. Griffith, M. A. Navia and A. L. Margolin, J. Am. Chem. Soc. **117**, 2732, 1995.

35   J. Lalonde, C. Govardhan, N. Khalaf, A. G. Martinez, K. Visuri and A. L. Margolin, J. Am. Chem. Soc. 117, 6845, 1995.

36   Y.-F. Wang, K. Yakovlevsky, B. Zhang and A. L. Margolin, J. Org. Chem. 62, 3488, 1997.

37   D. R. Walt and V. I. Agayn, Trends Anal. Chem. 13, 425, 1994.

38   U. T. Bornscheuer, Chimica Oggi 18, 65, 2000.

39   M. Pohl, Chem.-Ing.-Tech, 72, 883, 2000.

40   F. Arnold, Nature 409, 253, 2001.

41   M. T. Reetz and K.-E. Jäger, Chem Eur. J. 6, 407, 2000.

42   Y. H. Kim and S. H. Moon, J. Chem. Technol Biotechnol. 76, 169, 2001.

43   K. Suga, T. Sorai, S. Shioya and F. Ishimura, J. Chem. Eng. Jap. 26, 709, 1993.

44   F. Lipnizki, S. Hausmanns, G. Laufenberg, R. Field and B. Kunz, Chem. Eng. Technol, 23, 569, 2000.

45   K. Jitesh, V. G. Pangarkar and K. Niranjan, Bioseparation 9, 145, 2000.

46   A. Klibanov, Nature 409, 241, 2001.

47   C. Laane, S. Boeren, R. Hilhorst and C. Veeger, in Biocatalysis in organic media Edited by C. Laane, J. Tramper and M. D. Lilly, Elsevier, Amsterdam, 1987.

48   M. P. J. van Deurzen, I. J. Remkes, F. van Rantwijk and R. A. Sheldon, J. Mol. Catal. A 117, 329, 1997.

49   T. Hartmann, E. Schwabe and T. Scheper, in Stereoselective Biocatalysis Edited by R. Pathel, Marcel Dekker, New York, 799, 2000.

50   S. G. Cull, J. D. Holbrey, V. Vargas-Mora, K. R. Seddon and G. J. Lye, Biotechnol. Bioeng. 69, 227, 2000.

51   M. Erbeldinger, A. J. Mesiano and A. J. Russel, Biotechnol. Prog. 16, 1129, 2000.

52   R. Madeira Lau, F. van Rantwijk, K. R. Seddon and R. A. Sheldon, Org. Lett. 2, 4189, 2000.

53   S. H. Schöfer, N. Kaftzik, P. Wasserscheid and U. Kragl, Chem. Comm., 425, 2001.

54   A. M. Klibanov, CHEMTECH 16, 354, 1986.

55   F. Balkenhohl, K. Ditrich, B. Hauer and W. Lander, J. prakt. Chem. 339, 381, 1987.

56   U. Kragl, and A. Liese, in Encyclopedia of Bioprocess Technology, Edited by M. C. Flickinger and S. W. Drew, Wiley, New York, 454, 2000.

57   M. Biselli, U. Kragl and C. Wandrey, in Handbook of Enzyme Catalysis in Organic Synthesis Edited by K. Drauz and H. Waldmann, VCH, Weinheim, 89, 1995.

58   L. Rosenthaler, Biochem. Z. 14, 238, 1908.

59   H. Griengl, N. Klempier, P. Pöchlauer, M. Schmid, N. Shi and A. Mackowa, Tetrahedron 54, 14477, 1998.

60   P. Pöchlauer, Chimica Oggi 16, 15, 1998.

61   H. Yamada and M. Kobayashi, Biosci. Biotech. Biochem. 60, 1391, 1996.

62   T. Nagasawa, H. Shimizu and H. Yamada, Appl. Microb. Biotechnol. 40, 189, 1993.

63   C. Christ, Chem.-Ing.-Tech., 72, 42, 2000.

64   B. A. Anderson, M. M. Hansen, A. R. Harkness, C. L. Henry, J. T. Vicenzi and M. J. Zmijewski, J. Am. Chem. Soc. 117, 12358, 1995.

65   J. T. Vicenzi, M. J. Zmijewski, M. R. Reinhard, B. E. Landen, W. L. Muth and P. G. Marler, Enzyme Microb. Technol. 20, 494, 1997.

66   D. J. Ager, Handbook of Chiral Chemicals, Marcel Dekker, New York, 1999.

67   W. Knowles, M. Sabacky, B. Vineyard and D. Weinkauff, J. Am. Chem. Soc. 97, 2567, 1975.

68   H. Kumagai in Encyclopedia of Bioprocess Technology, Edited by M. C. Flickinger and S. W. Drew, Wiley, New York, 821, 2000.

69   J. Heveling, Chimia 50, 114, 1996.

70   M. Petersen and A. Kiener, Green Chem. 2, 99, 1999.

71   U. Onken, E. Schmidt and T. Weissenrieder, International conference on biotechnology for industrial production of fine chemicals, 93rd event of the EFB; Zermatt, Schweiz, 29.09.1996.

72   The New Scientist, 1st issue 22 Nov. 1956.

73   M. Chartrain, P. M. Salmon, D. K. Robinson and B. C. Buckland,, Curr. Opin. Biotechnol. 11, 209, 2000.

74   W. M. van Gulik, W. T. A. M. de Laat, J. L. Vinke and J. J. Heijnen, Biotechnol. Bioeng. 68, 602, 2000.

75   T. Endo, S. Koizumi, K. Tabata and A. Ozaki, Appl. Microb. Biotech. 53, 257, 2000.

76   K. Tabata, S. Koizumi, T. Endo and A. Ozaki, Biotechnol. Lett. 22, 479, 2000.

Kinetics of Heterogeneous Catalytic Reactions

Contents

Kinetics of Heterogeneous Catalytic Reactions

Dorit Wolf

Institut für Angewandte Chemie Berlin-Adlershof e. V.
Richard-Willstätter-Str. 12, 12489 Berlin, Germany
dwolf@aca-berlin.de

Abstract. Aspects of kinetic analysis are reviewed taking into account different scopes of applied heterogeneous catalysis: the micro-kinetic analysis for reaction synthesis, i.e. analysis of rate determining steps and derivation of optimised catalyst design; the kinetic analysis of complex reactions under closed-to-process conditions for optimisation of catalysts and reactor operation; the analysis of the interplay of kinetics and transport processes for optimisation reactor design as well as experimental methods of kinetic data acquisition as a basis of kinetic modelling.

1. Introduction

Kinetic analysis of catalytic reactions includes a diversity of goals. Depending on the aspect on which a certain kinetic study is focused different theoretical and experimental method are preferred. Accordingly, this chapter will focus on three typical scopes of kinetic analysis in the field of applied catalysis and will describe state-of-the-art strategies to achieve desired information and results:

- *Micro-kinetic analysis for catalytic reaction synthesis*

According to Dumesic [1] the term "catalytic reaction synthesis" is defined as a coherent description of how a catalyst in a catalytic-reaction cycle influences the concentration of reactants depending on their initial concentration and on temperature. If fundamental knowledge (specification of surface intermediates structure and elementary steps) is used for catalytic reaction synthesis the catalyst and process development are expected to become more targeted than conventional screening of kinetic data together with subsequent data fitting. In this context, micro-kinetic analysis reveals an innovative field of catalysis since it takes up newest developments in theoretical chemistry, surface science, coordination and solid-state chemistry.

In the section 2, experimental and theoretical principles, which were suggested for deriving micro-kinetic parameters such as sticking coefficients, activation energies of single reaction steps and heats of adsorption based on theoretical as well as microscopic and macroscopic semi-empirical correlations are briefly reviewed.

- *Kinetic analysis of complex reaction systems under close-to-process conditions*

As a result of catalytic reaction synthesis by micro-kinetic modeling crucial steps which affect the overall rate and selectivity can be identified, their rates can

be determined, and their changes due to gradual modifications of catalyst properties can be determined. Hereby, feedback to catalyst design (elemental composition and/or surface structure) and optimal reaction conditions are obtained.

This approach is a straight forward one in homogeneous catalysis, where the sphere of catalytic activity is clearly marked off by the catalytic complexes [2].

In heterogeneous catalysis up to now, catalytic reaction synthesis based on micro-kinetic approach was most successful when applied to metal catalysts where information about electronic and atomic surface processes can be obtained by modern experimental tools of surface science [3]. However, for catalysts of polycrystalline or amorphous nature and complex composition (e. g., mixed oxides), the identification of surface and bulk structures which are relevant for catalysis and the estimation of kinetic parameters on an elementary-step level are still unsolved problems, since the contributions of surface and bulk to catalytic reactions cannot easily be separated and, moreover, catalyst structure might successively change with increasing degree of conversion as well [4].

Accordingly, section 3 in which the state of the art in kinetic analysis is analyzed presents an overview on present activities in the field of modeling complex catalytic processes.

- *Analysis of the interplay between reaction kinetics and transport processes*

The substantial aim of the analysis of the interplay between reaction kinetics, catalyst morphology and fluid-dynamic conditions is the proper choice of a reactor design for technical application. In this field, the application of micro-kinetic models might give new insight especially in processes where homogeneous and heterogeneous reactions are coupled via common reaction intermediates. Here, the interplay of reaction kinetics, pore-structure of catalyst particles and fluid dynamics plays a decisive role and determines the reactor performance. Thus, section 4 considers especially these challenging aspects of reaction-engineering kinetics.

Irrespective the purpose of kinetic analysis, the derivation of kinetic models requires a suitable basis of experimental data under steady-state as well as unsteady-state conditions. The state-of-the-art of experimental techniques will be presented in section 5.

For further reading in the field some selected books [1], [5], [6], [7] and articles are recommended [8], [9], [10].

2.   Micro-Kinetic Analysis for Catalytic Reaction Synthesis

At the present state of understanding, micro-kinetics models consist of rate expressions describing rates of elementary steps (see equ. (1)) without assuming a certain rate determining step within a full catalytic reaction cycle. It is supposed that all elementary steps (forward and reverse) are included explicitly into the model. A further demand of micro-kinetic models concerns the kinetic parameters, which have to be accurate and consistent with respect to experimental observations, thermodynamics as well as to electronic structure calculations. From

this approach, a large predictive power of micro-kinetic models is expected allowing the coverage of a large range of reaction conditions. Accordingly, the derivation of kinetic parameters being constituents of rate equations like equ. (1) requires the compilation of information from different theoretical and experimental investigations. Such constituents are numbers of active sites Z_j, pre-exponential factors A_j, activation energies E_A as well as a surface site heterogeneity function $\Phi(a_j)$ which describes the fact that sites of different affinity exist with respect to a species j.

$$
\bar{r} = \prod_i p_i^m \left(\frac{\int\limits_{a_{j,1}(\theta_j=1)}^{a_{j,0}(\theta_j=0)} \left(A_j(a_j) \cdot e^{-\frac{E_A(a_j)}{k_B T}} \prod_j \theta_j(a_j,p)^r Z_j \Phi(a_j) \right) da_j}{\int\limits_{a_{j,1}(\theta_j=1)}^{a_{j,0}(\theta_j=0)} \Phi(a_j)\, da_j} \right)
\tag{1}
$$

a_j	affinity of species j to the surface
$A_j(a_j)$	pre-exponential factor referring to a particular affinity a_j
$E_{A,j}(a_j)$	activation energy referring to a particular affinity a_j
k_B	Bolzmann constant
p_i^m	partial pressure of gas-phase species i
T	temperature
Z_j	number of active centres for adsorption of species j
$\theta_j^n(a_j)$	degree of surface coverage by species j referring to a particular affinity a_j
$\Phi(a_j)$	function describing surface non-uniformity for a surface species j

In this context, equ. (1) expresses a mean reaction rate accounting for the average site affinity resulting from the normalized integral

$$
\bar{r} = \int (r(a)\Phi(a))\, da / \int \Phi(a)\, da .
\tag{2}
$$

In the subsequent paragraphs tools to determine the particular constituents of equation (1) are summarized. Moreover, limitations of the established paradigm of micro-kinetics which became obvious from new insights into catalytic processes based on theoretical calculations and surface-science findings will be touched.

Determination of Numbers of Active Centers Z_j

For homogeneous catalysts, Z_j can be easily determined since it is equivalent to the number of catalytic complexes solved in a solution of substrates and additives. For solid catalytic surfaces, however, the number of active sites, cannot be determined in a straightforward way if the catalytic surface does not consist of a particular single-crystal surface where the types of catalytically active sites are known. For surfaces of polycrystalline catalysts as applied in technical processes, only a part of surface atoms might act as catalytic centers (atoms at steps or edges, atoms in the near of defects or belonging to certain crystallographic surfaces) [5].

As an experimental approach for the determination of Z_j, chemisorption experiments are generally employed. For example, hydrogen and carbon monoxide are typically used to measure metallic surface area on supported catalysts [11]. The resulting equilibrium data reveal all sites, which have a potential to be covered by a respective gas-phase species. However, under reaction conditions, there exist sites, which bond molecules very strongly and which are, consequently, occupied during the whole catalytic cycle without taking part in the catalytic process(so-called "spectators"). On the other hand sites might exist, which reveal a very weak bonding to a specific gas-phase molecule A_i. Hence, the respective molecule would be displaced by other gas-phase reactants which have a stronger affinity to these sites and the respective site would not play a role in activating that molecule A_i at all. The presence of sites related to different adsorption energies can be taken into account by the term $\Phi(a_j)$ which describes the surface non-uniformity.

Determination of pre-Exponential Factors A_j

Orders of magnitudes of pre-exponential factors can be estimated by collision theory or transition state theory [1]. For both models, the mathematical description is based on the assumption that the rate of a reaction between molecules A and B is determined by the number of collisions and the probability that these collisions lead to a chemical reaction. In contrast to collision theory, the transition state theory in its microscopic formulation allows to take into account for details of the molecular structure of reactants. For this purpose, it is assumed that an equilibrium between reactants and an activated complex $AB^{\#}$ is established. This activated complex can be understood by means of the potential energy diagram, which describes the relationship between potential energy and atomic coordinates of reactants and products. The saddle point within this potential energy diagram corresponds to the lowest energy barrier that must be surmounted to form the products. The molecular configuration of the active species at this saddle point is defined as the transition state.

Transition state theory allows rapid initial insight into the reaction kinetic processes since the equilibrium constant for the step from reactants to the activated complex can be derived based on molecular partition functions of statistical thermodynamics. Depending on the reaction type (homogeneous gas-phase reaction or surface reaction step), different degrees of freedom of reactive species result. For instance, for adsorbed species, the degrees of freedom are, of course, restricted. Dumesic gave an overview on orders of magnitudes of pre-exponential factors of rate constants depending on the reaction type and the adsorption state of reacting species [1].

Determination of Activation Energies

In contrast to pre-exponential factors which can be derived based on the partition function assuming equilibrated states of the considered molecules, for the estimation of activation energies, one still cannot proceed completely without experimental information since non-uniform surface structure influence the energetic relationships. A single molecular process can be studied either by performing a molecular dynamics simulation or by using transition state theory

(calculating energy barriers and pre-exponential factors by DFT, [12], [13]). However, presently, still due to computer limitations it seems unlikely that complete heterogeneous processes can be treated by molecular dynamics since statistical sampling for the non-uniform surfaces leading to competing processes becomes crucial. Handling of statistics is the essence of kinetic Monte-Carlo methods. Their usage requires high computational effort (see paragraph "Consideration of heterogeneity of active sites in kinetic rate equations").

Based on experiments, activation energies can be derived from sets of kinetic data obtained at different temperatures. To determine activation parameters of particular reaction steps, experiments focusing on certain surface process such as adsorption, desorption and surface reactions of certain reactant molecules are required. Accordingly, temperature programmed desorption and surface reaction experiments lead to the desired information [14] , [15], [16], [6].

The differential heat of adsorption obtained by micro-calorimetry [17] provides information about enthalpy values, i. e., strength of interaction between adsorbates and the adsorption site. Entropy values of adsorption can be determined by combining calorimetry with volumetric adsorption measurements. Such data reveal information about the mobility of the adsorbed species and, hence, about the role of energetic versus steric effects in controlling the kinetic rate constants over a series of catalysts [18], [19], [20], [21].

If no direct experimental information on activation energies is available, semi-empirical estimates based on microscopic or macroscopic correlations can be used which provide the bridge between (surface) thermodynamic quantities and (surface) kinetic properties [1]. Microscopic correlations involve a description of the catalytic process in terms of the geometry of active sites and the surface species on these sites. Typical microscopic correlations include molecular orbital calculations and bond-order conservation correlations for the estimation of surface bond energies. Molecular orbital correlations based on quantum chemical calculations may be used to capture the essential bonding properties of known molecules and estimate the chemical bonding properties of related unknown surface species. Accordingly, an effective strategy is to calibrate a semi-empirical quantum mechanical method (e. g. molecular orbital calculations) for stable molecules that possess structures and chemical bonds believed to be important in the critical reaction intermediates of the catalytic cycle. Bond-order conservation theory according to Shustorovich [22], [23], [24] is based on the assumption that two-center bond interaction between one atom of an adsorbed molecule and a surface atom can be described using a Morse potential. The total energy of the adsorbate complex results from the sum of all interactions between the atoms of the adsorbed molecule and surface atoms while the bond order is maintained and normalized to unity. This correlation can be used to estimate surface-bond energies of reaction intermediates in terms of measured heats of adsorption of various probe molecules and bond energies of gas-phase molecules.

Even if no information on the structure of the adsorbates is available, phenomena, which are macroscopically observable (e. g., electronegativity of atoms involved in a heterolytic bond, acid-base interactions and ionization potential) may be correlated with the strength of the chemical bonding of reaction intermediates believed to be important. This approach corresponds to the so-called empirical macroscopic correlations. An overview on microscopic and macroscopic correlations is presented in Tables 1a and 1b.

Table 1a: Microscopic empirical correlations [1]

Correlation	Theoretical/empirical bases; Underlying assumptions	Examples of Application
	Empirical methods	
bond-order-conservation [22], [23], [24]	Estimation of surface bond energies of reaction intermediates based on information or assumption about adsorption stoichiometry and adsorbate structure	CO oxidation over metal surfaces
Evans-Polanyi correlation [1]	Correlation between activation energies for formation of chemical bonds (e. g., C-H, O-H, C-O, C-C) and heats of adsorption of reactants: $$E_A = E_A^0 + \gamma_P \Delta_R H$$ with E_A^0 - intrinsic activation barrier, γ_p – transition coefficient	complex mechanisms treated by grouping elementary steps into families of reactions such as hydrogenation, dehydrogenation and isomerization reactions of paraffines catalyzed by metal surfaces
	Semi-empirical methods	
Extended Hückel-approximation / Atomic Superposition and delocalization [25], [26], [27]	Semi-empirical calculations of adsorption geometry and energy	Methane oxidation over vanadium and molybdenum oxide [1]
Molecular Orbital correlation [25] [28], [29]	a) Calibrating molecular orbital calculations for stable molecules that possess structures and chemical bonds believed to be important in the critical reaction intermediates of the catalytic cycle b) Transferring known ratios of intrinsic activation barriers of gas-phase reactions calculated by quantum mechanics to those of catalytic reactions in order to estimate probabilities of alternative catalytic reaction pathways	Methane oxidation over vanadium and molybdenum oxide [1] Interaction of gas-phase molecules with noble metal surfaces (Pt, Rh) [30], [31].

Table 1b: Macroscopic empirical correlations

Correlation	Theoretical/empirical bases; Underlying assumptions	Examples of Application
Drago-correlations [32], [33], [34]	Correlation between electronegativity of atoms and heat of acid-base reactions	Systematization of silica-alumina catalysts with respect to acid-base properties [1]
Proton affinity and ionization potential correlations [1]	Correlation between proton affinity of bases and heat of adsorption on acid catalysts	Prediction of surface acidity based on elemental catalyst composition

Consideration of Heterogeneity of Active Sites in Kinetic Rate Equations

Surface non-uniformity with respect to activity of catalytic sites may result either from energy distribution of different surface sites, from adsorbate induced restructuring of catalytic surfaces or from adsorbate-adsorbate interactions. At the present state of art inclusion of surface non-uniformity in micro-kinetics is still considered as a challenging task [9].

- Energy distribution of different surface sites

Site heterogeneity may result from different coordination states of surface atoms acting as adsorption site. This effect can be considered within rate equations by definition of a heterogeneity function $\Phi(a)$ (see equ. (1)) which defines the probability that an arbitrary site is characterized by an adsorption affinity a.

In principle, one can find mathematical expressions for $\Phi(a)$ to describe each type of adsorption isotherms exactly by fitting the $\Phi(a)$ functions to experimental data [35]. However, the physical meaning remains questionable in most of the cases of arbitrary usage and fitting of $\Phi(a)$ functions. To define proper heterogeneity functions experimental evidences from measured differential heat of adsorption [9] are required which can be obtained from microcalorimetry using small increments of gas to progressively saturate the surface sites. The respective sensitive experimental equipment (Calvet microcalorimeters) is described in [17]. A typical micro-calorimetric experiment involves the measurement of the differential heat of adsorption vs. surface coverage. After each dose of a small amount of probe molecules the thermal and pressure equilibration of the system must take place before a subsequent dose of gas can be introduced. The sum of heats involved in the various doses to reach a certain surface coverage is the integral heat of adsorption at the corresponding surface coverage. The derivative of the integral heat with respect to coverage gives the differential heat of adsorption. In general, the differential heat varies with surface coverage. The surface coverage is determined from the adsorption isotherm, which has to be recorded simultaneously. Based on these experiments, $\Phi(a)$ can be determined and be built into the micro-kinetic model relating the surface bond energies to the surface coverage.

- Lateral adsorbate interactions

Catalytic surfaces may appear to be non-uniform because of adsorbate-adsorbate interactions. Lateral interactions between adsorbed species can lead to phenomena such as two-dimensional phase transition (e. g., formation of adsorbate islands on metal surfaces). In such cases which are inherently difficult to treat by analytical rate expressions, the rate constants for reactions between two surface species will depend on their local environment (e. g., edges or surfaces islands of adsorbed species).

The underlying physical processes can be studied based on Monte Carlo simulations of the surface processes using statistical mechanics as the theoretical basis. The calculation starts with a particular configuration of surface entities. Consequently, reactive processes such as adsorption, desorption, combination of species on the surface, their repulsion and surface diffusion are simulated using the potentials of intermolecular interactions. An overview on applications of Monte-Carlo methods was given e. g. in [36], [37].

- Adsorbate induced restructuring of catalytic surfaces

Several spectroscopic and microscopic studies combined with molecular beam techniques [38] indicated that catalytic surfaces can change their structure and hence their number of active sites during a surface reaction. Such surface reconstruction processes can be reflected realistically by quantum chemical calculations. These calculations are presently performed on different levels of complexity [9]: Cluster models use a small number of atoms to represent the catalyst and capture only the local environment around the active site [27]; embedding schemes treat a small region of the catalyst quantum mechanically and use classical methods to incorporate long-range interactions [39]. To enable even more direct comparison with experimental results ab initio methods that treat the infinite solid with periodic boundary conditions are being used with increasing frequency mostly for metal surface but also for bimetallic systems [9]. Systems that have been examined in detail, e. g., were the nitrogen adsorption on Fe(111), (100) and (110) surfaces [40], [41], and the CO oxidation over a Ru surface [12].

Nevertheless, the present incomplete quantitative understanding of surface processes on a microscopic scale and the computer limitations restrict the ab-initio investigation of sustained heterogeneous processes combined with statistical mechanics calculation. As fare as that goes, the mean-field approximation which describes the influence of surface coverage on the rate of surface reactions based on assumptions of a homogeneous surface, a random distribution of surface species and certain parameters for lateral interaction of species is still the preferred micro-kinetic approach. Examples of the application of mean field approximation were given by Stoltze and Norskov [42].

Elucidation of Rate Determining Steps (RDS)

The elucidation of the reaction step determining the overall rate in a sustained catalytic reaction cycle is one of the main aims of micro-kinetic analysis for reaction synthesis since it reveals information on how to decrease the free-energy barrier of a catalytic process by modifying the catalytic surface. Criteria on how to determine the RDS based on give a reaction scheme and rate constants were suggested by Boudart [43], Baranski [44], Dumesic [45] and in their most general form by Campell [46].

3. Kinetic Analysis of Complex Reaction Systems Under Close-to-Process Conditions

As mentioned above micro-kinetic analysis for reaction synthesis includes elementary steps and uses rate constants derived either from theoretical calculations or from direct measurements. As far as all information required to fulfil the paradigm of micro-kinetic modelling is available this approach can be applied to predict optimal catalyst design at a very precise and detailed level. Until now, this rigorous approach requires a tremendous effort in theory and experiments including catalyst preparation and observation techniques to complete the picture of kinetics of catalytic processes as it was demonstrated by Freund et al. [47] for CO oxidation on model catalysts consisting of defined Pd clusters supported on an alumina film.

In most of the cases where polycrystalline/polymorphous catalysts are considered for applied purposes (i. e., development and optimisation of catalytic processes) the gap of microscopic information has to be covered either by model simplifications and/or by deriving kinetic constants from numerical fitting of model responses to appropriate experimental data which yield significant information on the kinetic processes of interest. Usually, the experimental data result either from transient studies, particular of adsorption, desorption and reaction processes [48], [49] or from steady state measurements which reveal information of the sustained catalytic reaction cycle [50], [51].

For transient kinetic data, partial differential equations must be solved for calculating mass balances for both surface and gas-phase species along a catalytic reactor whereas for the steady-state approximation, the rate molar rate of change

Thus, in the steady-state case, the coverage is calculated from a system of nonlinear equations. It must be emphasized that this approximation eliminates the possibility to describe transient behavior but it can be well used to describe steady-state conversion and selectivity of an equilibrated catalyst bed. The simplest example for the steady-state approach is the Mars-van-Krevelen type rate equation which was derived in its original form to describe redox-type reactions where the lattice oxygen of oxide catalysts is involved in the catalytic reaction cycle [52].

The success of micro-kinetic analysis based on fitting model responses to experimental data depends strongly on the availability of proper software. Meanwhile, various programs are available [53], [54], [55], [56].

Besides the solution of large sets of coupled differential equations, tools for estimation of kinetic constants are required. The procedure of parameter estimation, of course, has to be supported by the preliminary estimation of the likely range of the kinetic parameters that describe the elementary reactions. Id est, the background of micro-kinetic analysis is an essential requirement.

Studies dealing with numerical and statistical aspects of kinetic parameter estimation are presented in [53], [56].

The usability of parameter estimation for analysis of relationships between solid and catalytic properties based on kinetic models without supposing rate determining steps was demonstrated for different complex catalytic processes such oxidative coupling of methane to C_2 hydrocarbons and partial oxidation of ethane to acetic acid, water-gas shift reaction and DENOX processes [50], [51], [57], [58].

For analysis of reactions in the traditional way, different strategies of simplifications of kinetic models exist. If model simplifications are used, rate expressions with effective kinetic rate constants have to be derived resulting from fitting of model predictions to experimental data. The physical meaning of the remaining rate expressions and rate constants depends on the degree of simplification. In general, the degree of simplification has to be adapted to the aim of kinetic modeling, but also depends on the complexity of the reaction systems under consideration. Thus, simplifications are very much used when difficulties in formulating a kinetic model for a complicated reaction mechanism arise and when an analytical form of a kinetic model is required to simulate chemical reactors (see further below).

Strategies of simplification are:
-   Boudart´s concept of most abundant surface reaction intermediates [5]

The first step of simplification concerning the underlying reaction mechanism is the estimation of the simplest set of chemically realistic elementary reactions that are likely to include enough detail to fit and predict the experimental data. Often, the true reaction mechanism consists of a sequence of reaction steps among which one is the rate determining and determines the overall rate. Accordingly, the reaction intermediate, which is converted in the rate-determining step, appears as most abundant (MASI) surface intermediate. For instance, all other intermediates except the MASI and the free sites are less abundant. If the most abundant intermediate could be unambiguously identified, the sequence of reaction steps can be reduced to the rate-determining step. The application of this concept has been firstly demonstrated by Boudart for various examples [5], [8]. The limitation of the usability of this concept concerns the fact that the MASI might change depending on reaction conditions.

Langmuir-Hinshelwood kinetics; Hougen-Watson formalism [59]

For the derivation of rate expressions it is assumed that reactants adsorb on a catalytic surface according to Langmuir-adsorption isotherms.For instance, all adsorption sites are energetically equivalent, no lateral interaction exist between the molecules and the total number of active sites is independent on reaction conditions. Moreover, the catalyst surface attains its steady-state. Depending on the strength of adsorption of the different reactants and products as well as the rate of surface reaction, different functional relationships between reactant concentration and rate of molar change of reactants can be discriminated supposing a differential range of conversion. Thus, kinetic analysis based on Langmuir-Hinshelwood kinetics allows the derivation of the underlying reaction mechanism of heterogeneous reactions to a certain extent. Hougen and Watson extended the scheme of derivation of rate equation by the explicit consideration of the reverse reaction. An overview about the different types of rate equation and their application was given by Tschernitz et al. [60]. A general problem in applying the required experimental approach results from the fact that a differential conversion cannot be ascertained even if the range of conversion is low, since both adsorption of products as well as very fast consecutive reactions of intermediates cannot be excluded [61]. In principle, concepts based on a set-up of rate-determining steps (MASI and Langmuir-Hinshelwood and Hougen-Watson kinetics) are limited to certain experimental conditions since the rate-determining step might change depending on concentration of reactants, temperature or degree of conversion, respectively.

However, until now, the Hougen-Watson concept was very successfully applied since a large variety of catalytic reactions [62] could be described under the steady-state conditions. Usually, different rate equations of the Langmuir-Hinshelwood-type are able to describe the experimental data with similar quality, which results from the large number of kinetic parameters making the mathematical expressions very flexible. This, in turn, implies that an adequate fit of experimental data by these rate expressions does not give any final evidence for a certain reaction mechanism. If more detailed information on the reaction mechanism is desired for the purpose of interpreting the behavior of catalysts, the steady-state experiments to which the Langmuir-Hinshelwood equations exclusively can be applied must be supplemented by non-steady-state experiments.

Due to the flexibility of the Langmuir-Hinshelwood/Hougen-Watson rate equations in describing different reactions, they are mostly used for simulation and optimisation of industrial reactors operated under steady-state conditions.

Lumping of reaction groups / reactant groups

If very complex reaction processes including large numbers of reactants shall be described special methods were developed which lump reactants with similar properties into groups of pseudo species representing essential chemical properties of groups of reactants. This approach leads to a reduction of the number of rate equations and plays an important role in analyzing kinetic processes in oil refinery such as fluid catalytic cracking (FCC) [63], [64], [65], [66]. An overview over these methods was given in [67].

4. Analysis of the Interplay Between Reaction Kinetics and Transport Processes

Optimisation of reactor performance including scale-up of catalytic processes to industrial sizes deals with complex interactions of transport phenomena and chemical kinetics.

Until now, the huge amount of scale-up studies, is, however, based only on little knowledge of reaction kinetics [10].

In process optimisation it turns out that only in the minority of cases the catalyst activity is the decisive factor for sizing the industrial reactor [10]. The catalyst volume is often determined by heat transfer restrictions or aging or poisoning of catalysts. Thus, industrial reactor concepts have to take into account the catalyst life time and the method of regeneration [68]. Considering especially this latter aspect which is related to complex non-steady-state catalytic processes, one becomes aware of the usefulness of detailed micro-kinetic analysis (see above).

For so-called "ppm-reactions" aiming at complete conversion at ppm-level such as SCR reaction, HDS or trace-CO methanation [10], [69], [70], the interaction between diffusion restrictions and intrinsic kinetics becomes complex as the concentration of reactants approaches zero [71] and poor mixing and possible by-pass effects may have an important impact on reactor performance [69].

Both, aging/poisoning processes and "ppm-reactions" are strongly influenced by external and internal transport processes, i. e., mass and heat transfer between gas-phase and catalyst surface and inside porous catalyst pellets.

The simulation of the intrinsic kinetic processes and of pore diffusion phenomena with the aim of optimization pore-size and shape of catalyst particles received a large impact due to the developments of fast computers on one hand and due to the development of molecular-dynamic, Monte-Carlo and quantum chemical methods on the other hand [72], [73], [74]. A comprehensive overview on this topic was given by Keil [6]. The interplay between diffusion processes in micro-porous media and on catalytic surfaces can be described meanwhile by methods of statistical mechanics as well. Reactant molecules can hop between sorption sites with probabilities governed by activation barriers which can be derived from transition state theory.

Recently, the numerical simulation of catalytic reactors obtained new impact due to the rapid developments in the field of computational fluid-dynamics (CFD) where the flow field inside the reactor is described based on the multi-dimensional Navier-Stokes equations. Meanwhile a variety of commercial CFD codes exist (e. g., FLUENT, CFX ACE, Star CD) [75] which allow the simulation of very complex flow configurations. While homogeneous reactions can be conveniently treated by these commercial tools, the implementation of complex surface reaction processes into the codes is still difficult. For this purpose, the software package DETCHEM has been developed [76] which consists of a basic module for modeling chemical reaction kinetics and CFD applications including single monoliths channels and entire monoliths. The package can be coupled with commercial CFD codes as well. This tool was already applied to simulation of gaseous chemically reacting flow and heterogeneous reactions. Until now, the flow-field simulation was coupled with models for the temperature and composition dependent transport coefficients, heat transfer and complex reaction mechanism for different catalytic oxidation-reaction processes such as partial oxidation of methane and ethane [77]. Moreover, ignition processes in flameless catalytic burners as well as catalytic monoliths such as automotive catalytic converters where investigated based on the application of DETCHEM.

5. Experimental Methods for Kinetic Data Acquisition

The different levels of details of kinetic models do require a different extend of data basis. If the intention of kinetic modeling is a pragmatic one, i. e. the behavior of steady-state reactor performance in a certain range of conditions shall be described, the usage of Langmuir-Hinshelwood/Hougen Watson models or models with the MASI approximation would be sufficient. For this type of kinetic modeling, in turn, steady-state kinetic data obtained in conventional steady-state lab-scale reactors allows the derivation of kinetic parameters. The only requirement, which has to be fulfilled by the catalytic reactors, is the realization of defined (ideal) fluid dynamic conditions with respect to the contact time distribution (either plug-flow or continuous stirred tank reactor allowing an easy derivation of molar rate of changes of reactants). As soon as more detailed information on the reaction mechanism as well as on transient states of the catalytic surface (or reactor) are desired, steady-state kinetic experiments are often not sufficient. Consequently, equipment allowing transient studies is required for this purpose.

Summaries on the design and application of reactors for kinetic data acquisition were for example written by Weekman [78], Christoffel [79] Anderson and Pratt [80] and Baerns, Hofmann, Renken [7]. Reactors for transient studies were described in several papers [81], [82], [83], [84], [85], [86], [87].

5.1 Steady-State Reactors

Steady-state reactors are operated either in an integral or differential mode. The advantage of the differential mode of reactor operation is the direct derivation of molar rates of changes of reactants. However, differential conditions can be

ascertained only in a narrow range of conversion of reactants. For the plug-flow-type reactor, the criterion for the differential range of conversion is the appearance of an linear relationship between concentration and contact time. Than, the molar rate of change can be simply derived by the quotient $\Delta c/\tau$ where Δc is the difference of inlet and exit concentration of a reaction component and τ is the contact time in the reactor. This criterion is often fulfilled for low contact time values leading to reactant conversions lower than 10 %. However, there are cases, where very fast consecutive reactions take place even in this low conversion range (this happens for instance in combustion reactions of partial oxidation of stable alkanes where the reaction intermediates (alkenes or oxygenates) are converted to carbon oxides much faster than they were formed). In such cases, the rule of thumb that differential conditions are obtained below a conversion of 10 % might lead to misleading data evaluation.

A possibility to establish experimental conditions allowing the direct derivation of molar rate of changes based on simple $\Delta c/\tau$ ratios even for larger ranges of conversion is the use of gradient-free reactors corresponding to fluid-dynamic conditions of continuous stirred tank reactors.

While for homogeneous catalytic reactions this operation can be realized simply by stirring, for heterogeneous catalytic reactions, special designs for complete gas mixing within the catalyst bed is required. Typical designs for this purpose are the Berty reactor with its different modifications [88], [89] and the Carberry reactor [90], [91]. In the Berty reactor, the catalyst is contained in tubular fixed-bed reactor through which gas is passed as a fast internal recycle forced by a turbine. The gas stirring in the Carberry reactor is realized by a rotating basket.

Gradient-free reactor types do reveal neither concentration nor temperature gradients (difference between reactor entrance exit < 2 K) and hence, they can be operated isothermally even if reactions with significant heat generation or consumption have to be studied.

If isothermal conditions cannot be warranted during kinetic measurements the heat balance of the reactor system must be solved besides the mass balance. Unfortunately, this situation is related to several disadvantages:

a) Except for adiabatic reactor operation, a precise solution of heat balances is difficult. Local rate of heat exchange between reactor and its surrounding and local temperature are interrelated and depend on the fluid-dynamic conditions inside the reactor. A correct prediction of the respective heat transport co-efficient is difficult and still a matter of research in reaction engineering [92], [93].

b) Kinetic studies under non-isothermal conditions suffer from the fact that both pre-exponential factors and activation energies cannot be separately determined. Thus, the number of free parameters to be estimated by numerical methods increases.

These circumstances indicate that isothermal modes of reactor operation should be realized for kinetic data acquisition.

For plug-flow operation, the realization of isothermal conditions is much more difficult than for the continuous tank or recycle reactor. Here, one possibility is the dilution of the catalyst by inert material in order to decrease the heat generation per volume element of the fixed bed. However, there are limits of bed dilution since too high proportions of inert material might lead to the effect that reactant molecules bypass the catalyst surface. Criteria for proper dilution of fixed beds were suggested by van den Bleek et al. [94].

An advanced tool for guaranteeing isothermicity along a catalytic reaction zone might be provided by micro-structured reactors [95], [96]. This reactor concept is based on a multi-channel unit with channel dimensions in the range from 50 to 200 μm width and depth. Meanwhile there is a large variety of technologies to produce these structures for different materials (metals, ceramics, glass etc.). Besides the small channel dimension another characteristics of such micro-reactor structures is the high ratio of wall/channel volume. Thus, the heat transport within these structures is mainly determined by axial heat conductivity through the reactor wall which allows isothermal reactor operation even for highly exothermic reactions as was demonstrated by Steinfeldt et al. [97].

A method for pseudo steady-state kinetic data acquisition under non-isothermal conditions was suggested by Wojciechowski et al. [98], [99]. The basic principle of this method is the following:

Polythermal temperature ramping (PTR) experiments comprise the measuring of reactant concentration and temperature at the reactor exit for a number of different contact time values. For further data evaluation of the experiments it is necessary that the changes of particular contact time values lead only to differential changes of exit concentration and temperature. With this precondition, the relationship between concentration and contact time is describable by a simple interpolation function, which can be analytically differentiated. Thus, molar rate of changes of each reactant component can be obtained which refers to the measured temperature at the reactor exit. Besides the boundary condition the changes of residence time must be in an differential range; further, a second boundary condition has to be fulfilled – i. e., radial temperature profiles must not exist. In the experimental set up suggested by Wojciechowski this is ascertained by keeping the external heat transfer of the reactor principally at a low value.

In order to accelerate the kinetic data acquisition, Wojciechowski suggested to ramp the temperature of the feed gases up or down with increasing space time according to a time-program. Here, an additional boundary condition of the procedure must be emphasized - the heating rate must be slow enough to guarantee the steady-state of the catalyst.. Until now, the applicability, speed and precision of this method was analysed for CO oxidation and dehydrogenation of ethyl benzene [99], [100] and for ammonia synthesis [101].

5.2   Non-Steady-State Reactors

In non-steady-state reactors, reaction conditions such as temperature or reactant concentrations are temporarily changed [81] – [85]. Temperature programmed Surface Reaction Experiments (TPSR), temperature programmed desorption (TPD), temperature programmed reduction and oxidation (TPR, TPO) [102], [103], Temporal Analysis of Products Reactor (TAP) and Steady-State Isotopic Transient Kinetic Analysis (SSITKA) [84], [104], [105] are established methods dealing with non-steady-state reactor operation. Among these methods, TPSR and SSITKA are techniques, which can directly be applied under reaction conditions relevant for catalytic processes. They allow determination of the number of active sites depending on the steady-state established for different temperatures and partial pressures of reactants.

Temperature programmed methods are frequently used for surface science studies. Starting from a defined initial state of the catalyst surface (certain coverage and temperature) the temperature is raised and the response of reactant concentration or pressure at the reactor outlet is recorded by analytical methods with high time resolution. The variation of heating rates allows to draw conclusions with respect to mechanisms of desorption and reaction as well as the determination of activation energies of these processes.

The other group of methods is based on sudden jump-like disturbance of the concentration of reactants after establishing a defined steady-state of the whole reactor system [83], [106]. From the different shapes of responses at the reactor outlet conclusions can be drawn concerning the reaction mechanism such as rate determining steps and catalyst restructuring phenomena 81], [107]. A more complex evaluation of the experimental data is performed by the wave-front analysis where besides the concentration response also the temperature response is recorded for reactions with significant heat generation and consumption [108].

Pulse methods are based on the principle that a sequence of concentration pulses passes the catalyst bed until no change of the shape of the pulse response is observed. Depending on the pulse frequency one can attain near steady-state conditions for kinetic data analysis [109].

The Temporal Analysis of Products (TAP)-reactor is a special type of a pulse method which was introduced by Gleaves $et\ al.$ [84]. The catalyst is usually under vacuum conditions (p $\approx 10^{-6}$ to 10^{-4} Pa) and small amounts of gas molecules are pulsed over the bed of catalyst particles (ca. 10^{15} molecules per pulse). The responses at the outlet of the reactor are measured by a mass spectrometer with high time-resolution (around 10 µs). The reactant transport through the reactor occurs only by Knudsen diffusion. Hence, gas-phase reactions are suppressed under high-vacuum operation. Therefore, reactive intermediates like radicals can be detected if they desorb from the surface. The small amounts of molecules pulsed over the surface occupy only a small part of the active sites. One disadvantage of the TAP method results from the fact that it is operated under vacuum condition. Therefore, one should be aware, that co-adsorption processes and surface reconstruction due to higher pressure of gas-phase species might not be observed under these conditions although they play an important role under steady-state operation. Nevertheless, the method can provide quantitative insight into particular surface processes.

Meanwhile kinetic data evaluation from TAP experiments for particular surface reaction steps becomes a standard procedure performed by several groups [86], [110], [111].

Reverse chromatography [112] describes a method where small amounts of reactants are pulsed into a carrier gas. As for the TAP method, the state of the catalyst surface is not changed significantly and the pulse shape at the reactor exit indicates the interaction of the reactant molecules with the catalytic surface. In this way reverse chromatography is a complimentary method related to larger pulse sizes. In contrast to the TAP method where transport occurs by diffusion only, for quantitative evaluation of the reverse chromatography, gas transport by convection has to be taken into account as well.

Transient methods based on isotopic labeling experiments allow the detailed elucidation of particular reaction pathways. For steady-state isotopic transient analysis (SSITKA) first the steady-state operation of the reactor is established with non-labeled reactant feed. Afterwards, a certain reactant is substituted by the

respective labeled component and its response is observed at the reactor outlet. The shape of the outlet signal shows the extent of accumulation and lifetime of reactants on the surface. The method was introduced by Biloen [82]. A description on how kinetic data evaluation proceeds for SSITKA was illustrated by Goodwin et al. [104] for the example of CO hydrogenation, ammonia synthesis and methanol synthesis.

Novel techniques such as positron emission tomography and profiling can be used for in situ studies of mass transport processes and reactions with molecules labeled by ^{11}C, ^{13}N, ^{15}O inside fixed-reactors [113], [114], [115]. The measured concentration distribution, as a function of location and time can be used as input data for coupled (non-steady-state) kinetic models and reactor models.

6.   Concluding Remarks

The usability of micro-kinetic analysis profited from both the significant advances in quantum chemical methods and experimental methods in the field of surface science. As a result, several catalytic reactions have been analyzed based on micro-kinetic approaches. Future challenges are the improvement of precision of kinetic parameters determined by ab-initio methods, the speed of their calculation and the treatment of complex reaction mechanisms in which many reaction pathways and intermediates are involved. Due to the limitations still remaining in modeling complex systems under close-to-process conditions by micro-kinetic means fitting of kinetic parameters to experimental data appears to be still an unavoidable requisite.

Thus, for optimization of industrial reactors and their operation, empirical kinetic modeling by fitting parameters is still preferred. Here, the range of reaction conditions which has to be taken into account from technological as well as economical point of view is often narrow and allows the application of the established strategies of approximations (assumption of rate determining steps, MASI, Hougen-Watson-formalism). However, practice has also shown that the respective models do not stand up to several cases of catalytic reactions. Hence, kinetic models based on mechanistic considerations without pre-assumption of rate determining steps have meanwhile made its arrival at industrial reactor simulation as well and are coupled with detailed models of mass and heat transport using molecular-dynamic, Monte-Carlo and quantum chemical methods for description of pore diffusion and computational fluid dynamics for description of external transport processes.

For both micro-kinetic analysis of catalyst performance as well as kinetic modeling for reactor optimization, further advances in method development and extension of methods application in practice are directly related to the continued development of computational power.

A further challenge in the field of reactor optimization is the acquisition of reliable experimental data. This is especially important for reaction processes accompanied by strong heat generation or consumption. Here, reactor concepts allowing a large range of conversion and industrial pressure and temperature operation on one hand and either isothermicity or near adiabatic conditions on the other hand are required to obtain proper data as a basis of parameter fitting.

Suitable solutions are provided by micro-structured reactors (isothermal operation mode) and the polythermal ramping reactor concept (non-isothermal operation mode).

Often the acquisition of data is very time consuming. Therefore, the acceleration of data measurement will help to promote the application of kinetic methods in practice. Here, transient methods do have a potential since the time period until establishing of the steady-state leads to a large reservoir of data including several informations on catalytic processes. Although the evaluation of transient data requires a higher numerical effort, the availability of numerical tools meanwhile allows application of these methods by a broad user community. Finally, parallelization of experiments is an additional step in speeding up kinetic data acquisition.

References

1   J. A. Dumesic, D. F. Rudd, L. M. Aparicio, J. E. Rekoske, A. A. Treviño, in The Microkinetics of Heterogeneous Catalysis, American Chemical Society, Washington DC, 1993.

2   R. Schlögl, Angew. Chem. Int. Ed. 37, No. 17, 2333, 1998.

3   G. Ertl, H. Knözinger, J. Weitkampb (Eds.), *Handbook of Heterogeneous Catalysis*, VCH, Weinheim 1997.

4   T. Ilkenhans, T., B. Herzog, T. Braun, R. Schlögl, *J. Catal.,* **153**, 275, 1995.

5   M. Boudart and G. Djega-Mariadassou, in *Kinetics of Heterogeneous Catalytic Reactions*, Princeton University Press, Princeton, N. J., 1984.

6   F. Keil, *Diffusion und Chemische Reaktion in der Gas/Feststoff-Katalyse,* Springer, Berlin-Heidelberg-New York, 1999.

7   M. Baerns, H. Hofmann, A. Renken, *Chemische Reaktionstechnik*, Georg Thieme Verlag Stuttgart-New York 1992

8   P. Stoltze, *Surface Science.* **65,** 65, 2000.

9   L. J. Broadbelt, R. Q. Snurr, *Appl. Catal A.,* **200,** 23 , 2000.

10   J. R. Rostrup-Nielsen, *J. Mol. Catal.*, A **163**, 157, 2000.

11   J. R. Anderson, *Structure of Metallic Catalysts*, Academic Press, New York, 1975.

12   C. Stampfl, M. . Ganduglia-Pirovano, K. Reuter, M. Scheffler, *Surface Science*, **500**, , 368, 2001.

13   A. Eichler, *Surface Science*, **498**, , 314, 2002.

14   D. P. Woodruff, T. A. Delchar, *Modern Techniques of Surface Science,* Cambridge University Press, Cambridge 1994.

15   J. W. Niemandsverdriet, *Spectroscopy in Catalysis*, VCH Weinheim, 1995.

16   H. Bielawa, M. Kurtz, T. Genger, O. Hinrichsen, *Ind. Eng. Res.,* **40**, 2793, 2001.

17   N. Cardona-Martinez, J. A. Dumesic, *Adv. Catal.* **38**, 149, 1992.

18   M. G. Evans, M. J. Polanyi, *J. Chem. Soc., Farad. Trans.* **1(34)**, 11, 1938.

19   J. N. Bronstedt, K. J. Pederson,, *Z. Phys. Chem.* **108**, 185, 1923.

20   L. P. Hammet, Physical Organic Chemistry: Reaction Rates, Equilbia,and Mechanism, McGraw-Hill, New York, 1940.

21 R. W. Taft, *J. Am. Chem. Soc.* **74** 2729, 1952.
22 E. Shustorovich, *Surf. Sci. Rep.*, **6**, 1, 1986.
23 E. Shustorovich, *Surf. Sci.*, **176**, L863, 1986.
24 E. Shustorivich (Ed.), *Metal-Surface Reaction Energetics*, VCH Weinheim, 1991.
25 A. B. Anderson, *J. Phys. Chem.*, **62**, 1187, 1975.
26 A. B. Anderson, R. W. Grimes, S. Y. Hong, *J. Phys. Chem.*, **91**, 4250, 1987.
27 R. A. van Santen, M. Neurock, *Catal. Rev.-Sci. Eng.*, **37**, 557, 1995.
28 R. I. Masel, R. I.: Principles of Adsorption and Reaction on Solid Surfaces, Wiley, New York, 1996.
29 R. I. Masel, W. T. Lee, *J. Catal.*, **165**, 80, 1997.
30 E. Yagasaki, R. I. Masel, *Catalysis*, **111**, 1, 1994.
31 A. B. Anderson, R. W. Grimes, S. Y. Hong, *J. Phys. Chem.*, **91**, 4250, 1987.
32 R. S. Drago, B. B. Wayland, *J. Am. Chem. Soc.*, **87**, 3571, 1965.
33 R. S. Drago, N. Wong, C. Brigrien, G. C. Vogel, *Inorg. Chem.*, 26, 9, 1987.
34 in: James E. Huheey, Inorganic Chemistry, 1074 – 1077, Walter de Gruyter, Berlin – New York 1988.
35 R. J. Sips, *J. Phys. Chem.* **16**, 490 (1948).
36 H. C. Kang, W. H. Weinberg, *Chem. Rev.* **95**, 667, 1995.
37 V. P. Zhdanov, B. Kasemo, *Surf. Sci. Rep.* **39**, 25, 2000.
38 G. A. Somorjai, G. Rupprechter in: G. F. Froment, G. C. Waugh (Eds.) *Stud. Surf. Catal.* **109**, 35 (1997).
39 J. Gao in: K. B. Lipkowitz, D. B. Boyd (Eds.) *Reviews in Computational Chemistry*, **7**, 119, VCH New York 1996.
40 J. J. Mortensen, M. V. Ganduglia-Pirovano, L. B. Hansen, B. Hammer, P. Stoltze, J. K. Norskov, *Surf. Sci.*, **422**, 8, 1999.
41 J. J. Mortensen, L. B. Hansen, B. Hammer, J. K. Norskov, *J. Catal.*, **182**, 479, 1999.
42 P. Stoltze, J. K. Norskov, *J. Catal.*, **110**, 1, 1988.
43 M. Boudart, K. Tamaru, *Catal. Lett..*, **9**, 15, 1991.
44 Baranski, *Solid State Ionics.*, **117**, 123, 1999.
45 J. A. Dumesic, *J. Catal.*, **185**, 496, 1999.
46 C. T. Campbell, *Topics Catal.*, **1**, 353, 1994.
47 J. Hoffmann, I. Meusel, J. Libuda, H.-J. Freund, *J. Catal.*, **204**, 378, 2001.
48 M. Soick, D. Wolf, M. Baerns, *Chem. Eng. Sci.*, **55**, 2875, 2000.
49 E. P. J. Mallens, J. H. B. J. Hoebink, G. B. Marin, *Catal. Lett.* **33**, 291, 1995.
50 D. Wolf, M. Heber, W. Grünert, M. Muhler, *J. Catal.*, **199** , 92, 2001.
51 D. Linke, D. Wolf, M. Baerns, U. Dingerdissen, S. Zeyss, *J. Catal.*, **205(1)**, 32, 2002.
52 P. Mars, D. W. van Krevelen, *Chem. Eng. Sci.* (Sec. Suppl.) **3**, 41, 1954.
53 J. A. Dumesic, A. A. Trevino, B. A. Milligan, L. A. Greppi, V. R. Balse, K. T. Sarnowski, C. E.Beall, T. Kataoka, D. F. Rudd, *Ind. Eng. Chem. Res.*, **26**, 1399, 1987.
54 H.G. Bock in K. H. Eberet, P. Deufelhard, W. Jäger (Eds.) *Modelling of Chemical Reaction Systems*, Springer, Heidleberg 1981.
55 F. J. Keil,, *Chem.-Ing.-Techn.* **68**, 639, 1996.
56 D. Wolf, R. Moros, *Chem. Eng. Sci.*, **52** (7), 1189, 1997.

57 N.-Y. Topsoe, *Science.*, **265**, 1217, 1994

58 D. Wolf, M. Barré-Chassonnery, M. Höhenberger, A. van Veen, M. Baerns, *Catal. Today,* **40**, (2-3), 147, 1998.

59 K. H., Yang, O. A. Hougen, *Chem. Eng. Prog.* **46,** 146, 1950.

60 J. L. Tschernitz, S. Bornstein, R. B. Beckmann, O. A. Hougen,, *Trans. AIChE.*, **42**, 883, 1946.

61 M. Boudart, *Chem. Eng. Sci.*, **22**, 1387, 1967.

62 R. Mezaki, H. Inoue, *Rate equations of Solid-Catalyzed Reactions.*, University of Tokyo Press, 1991.

63 M. Larocca, S. Ng. H. de Lasa, *Ind. Eng. Chem. Res.,* **29**, 171, 1990.

64 R. R. D. Kemp, B. W. Wojciechowski, N.-Y. Topsoe, , *Ind. Eng. Chem. Fundam.*, **13**, 332, 1974

65 S. M. Jacob, B. Gross, S. E. Voltz, V. W. Weekman Jr., *Am. Inst. Chem. Eng. J.*, **22**, 701, 1976.

66 P. Hagelberg, I. Eilos, J. Hiltunen, K. Lipiäninen, V. M. Niemi, J. Aittamaa, A. O. I. Krause, *Appl. Catal. A*, **223**, 73, 2002.

67 M. S. Okino, M. L. Mavrovouniotis, *Chem. Rev.*, **98**, 391, 1998.

68 J. R. Rostrup-Nielsen, *Catal. Today,* **37**, 225, 1997.

69 J. R. Rostrup-Nielsen, P. S. Schoubye, L. J. Christiansen, P. E.Nielsen, *Chem. Eng. Sci.*, **49**, 3995, 1992

70 J. R. Rostrup-Nielsen, *Chem. Eng. Sci.*, **50**, 4061, 1995

71 J. R. Rostrup-Nielsen, in: R. W. Joyner, R. A. van Santen (Eds.) *Elementary Steps in Heterogeneous Catalysis*, 144, Kluwer Academic Publishers, Dordrecht 1993

72 C. Rödenbeck, J. Kärger, K. Hahn, *J. Catal..*, **157,** 656, 1995

73 B. L. Trout, A. K. Chakraborty, A. T. Bell, *Chem. Eng. Sci.*, **52**, 2265, 1997

74 E. Klemm, J. Wang, G. Emig, *Chem. Eng. Sci.*, **52**, 3173, 1997

75 A. Birtigh, C. Y. Werninger, G. Lauschke, W. F. Schierholz, D. Beck, C. Maul, N. Gilbert, H.-G. Wagner, *Chem.-Ing.-Tech.,* **72**, *No. 3*, 175-193, 2000.

76 O. Deutschmann, C. Correa, S. Tischer, D. Chatterjee, J. Warnatz. DETCHEM, User Manual, Version 1.4.1 http://reaflow.iwr.uniheidelberg.de\~dmann/DETCHEM.html, 2001

77 O. Deutschmann, *Chem.-Ing.-Tech,* **72**, *No. 9*, 987, 2000.

78 V. W. Weekman, *AIChE. J.*, **20**, 833, 1974

79 E. G. Christoffel, Laboratory Studies of Heterogeneous Catalytic Processes, Elsevier, Amsterdam, 1989

80 J. R. Anderson, K. C. Pratt, *Introduction to Characterization and Testing of Catalysts*, Academic Press, New York, 1985.

81 C. O. Bennett, *Catal. Rev.-Sci. Eng.*, **13**, 121, 1976..

82 P. Biloen, *J. Molec. Catal.*, **21**, 17, (1983)

83 H. Kobayashi, M. Kobayashi, *Catal. Rev.-Sci. Eng.*, **10**, 139, 1974.

84 J. T. Gleaves, J. R. Ebner, T. C. Kueckler, *Catal. Rev.-Sci. Eng.*, **30**, 49, 1988.

85 F. H. M. Dekker, G. Klopper, G. Bliek, F. Kapteijn, J. A. Moulijn, *Chem. Eng. Sci.,* **49**, 4375, (1994).

86 M. Rothaemel, M. Baerns, *Ind. Eng. Chem. Res.*, **35**, 1556, 1996.

87   O. Keipert, M. Baerns, M., *Chem. Eng. Sci.*, **53** No. 20, 3623, 1998.

88   J. M. Berty, *Chem. Eng. Progr.*, **70**, 121, 1974.

89   J. Nelles, *Chem. Techn.*, **39**, 328, 1987.

90   J. J. Carberry in: R. Anderson, M. Boudart (Eds.), *Catalysis, Science and Technology*, Springer, Heidelberg, 1980.

91   P. C. Borman, A. N. R. Bos, *AIChE J.*, **40**, 862, 1994.

92   R. Adler, *Chem.-Ing.-Techn.* **72**, No. 6, 555; No. 7, 688, 2000.

93   M. Winterberg, *Modellierung des Wärme- und Stofftransports in durchströmten Festbetten mit homogenen Einphasenmodellen*, Fortschrittsberichte VDI, Reihe 3, Verfahrenstechnik, Nr. 654, VDI-Verlag, Düsseldorf 2000.

94   C. M. van den Bleek, K. van der Wielke, P. J. van den Berg *Chem. Eng. Sci.*, **24**, 681, 1969.

95   W. Ehrfeld, H. Löwe, V. Hessel, T. Richter, Chem.-Ing.-Techn. 69, 931, 1997.

96   W. Ehrfeld, V. Hessel, H. Löwe, *Microreactors: New Technology for Modern Chemistry*, John Wiley & Sons Ltd., 2000

97   N. Steinfeldt, O. Buyevskaya, D. Wolf, M. Baerns, *Stud. Surf. Sci. Catal.*, **136**, 185, 2001.

98   Rice, Wojciechowski, *Catal. Today*, **36**, 191, 1997.

99   Wojciechowski, B. W., Asprey, S. P., Appl. Catal. A **190**, 1, 2000.

100   S. B. Domke, R. F. Pogue, F. J. R. van Neer, C. M. Smith, B.W. Wojciechowski, *Ind. Eng. Chem. Res.*, **40**, 5878, 2001.

101   C. Liebner, D. Wolf, M. Baerns, M. Kolkowski, F. Keil, *Appl. Catal. A*, in press, 2002.

102   D. P. Woodruff, T. A. Delchar, Modern Techniques in Surface Science, Cambridge University Press, Cambridge, 1994.

103   J. W. Niemandsverdriet, Spectroscopy in Catalysis, VCH, Weinheim, 1995.

104   S. L. Shannon, J. G. Goodwin, Catal.-Rev., **95**, 677, 1995.

105   C. Mirodatos, Catal. Today, **9**, 83, 1991.

106   C. O. Bennett, AIChE J., **13**, 891, 1967.

107   M. Kobayashi, Chem. Eng. Sci., **37**, 403.

108   E. Müller-Erlwein, H. Hofmann, Chem-Eng.-Techn., **59**, 956, 1987.

109   A. R. Garayhi, F. J. Keil, Chem. Eng. Sci., **56** (4), 2001.

110   G. S. Yablonskii, S. O. Shekhtman, S. Chen, J. T. Gleaves, Ind. Eng. Chem. Res., **37**, 2193, 1998.

111   M. Soick, D. Wolf, M. Baerns, Chem. Eng. Sci., **55**, 2875, 2000.

112   A. R. Garayhi , F. J. Keil, Chem. Techn. **52**, 80, 2000.

113   B. G. Anderson, N. J. Noordhoek, D. Schuring, F. J. M. M. de Gauw, A. M. de Jong, M. J. A. de Voigt, R. A. van Santen, Catal. Lett., **56**, 137, 1998.

114   B. G. Anderson, F. J. M. M. de Gauw, N. J. Noordhoek, L. J. van Ijzendoorn, R. A. van Santen, M. J. A. de Voigt, Ind. Eng. Chem. Res., **37**, 815, 1998.

115   B. G. Anderson, R. A. van Santen, A. M. de Jong,, *Topics in Catalysis*, **8**, 125, 1999.

Catalyst Deactivation

Contents

Catalyst Deactivation

Goran Boskovic[1] and Manfred Baerns

ACA-Institute for Applied Chemistry Berlin-Adlershof,
Richard-Willstaetter-Str. 12, 12489 Berlin, Germany

Abstract. An overview of deactivation mechanisms, their causes and consequences, as well as of methods and techniques of investigation of deactivation is presented. There are three fundamental reasons for catalyst deactivation, i.e. poisoning, coking or fouling and ageing. Poisoning can be reversible or irreversible, and with geometric or electronic effect. It can also be selective, nonselective and antiselective, depending on catalyst/poison affinity and kinetics. The action of coke is by direct active sites coverage, or by pore plugging, and depends on reaction conditions, pore's type and catalyst acidity. Kinetics of coking is determined by both mechanism of the coking reaction and its diffusion restrictions. Sintering is the main cause for catalyst ageing. It appears in two forms: thermal or chemical, depending on prevailing reaction parameters, i.e., temperature or concentration. To cope with deactivation two approaches are offered: either to avoid it when possible, like in the case of feed purification, or accept it but with an effort to minimize its effects. Accelerated deactivation tests can be a powerful tools for studying catalyst deactivation in a relatively short time. By proper selection of reaction parameters and applying deactivation compensation approach, reaction and deactivation kinetics can be separated. Based on obtained deactivation kinetics parameters, and by applying appropriate modeling and simulation, the life time of a catalyst and its performance in the commercial reactor at any time can be predicted.

1.   Introduction

During their life time catalysts undergo usually deactivation. This happens in the time frame of seconds (fluid catalytic cracking on zeolites), or years (iron catalyst in ammonia synthesis). This phenomenon may significantly contribute to the economy of a catalytic process. The economic impact of catalyst deactivation expressed as revenue loss is, in general, not due to the cost of the catalyst itself, but to the lower production rate as a result of the decrease in space-time yield of the desired product with time-on-stream, and intermittent process shut-down in order to load the new catalyst or to regenerate the deactivated one. Moreover, additional costs may arise from poorer utilization of a feedstock due to a decrease in selectivity and from additional energy required for catalyst regeneration. These circumstances have led to extensive studies aimed at unveiling the mechanism of deactivation and finding measures of reducing deactivation [1]. Quite extensive monographs [2,3] and reviews [4-10] covered this area of catalysis, and there are continuing efforts in the field [11-16].

---

[1] University of Novi Sad, Faculty of Technology, 21000 Novi Sad, Yugoslavia

2. Deactivation Mechanisms

Basically catalyst deactivation is a temporal or permanent loss of active sites, caused by chemical and physical reasons. Deactivation occurs by: (i) chemical poisoning due to chemisorption or reaction of a certain substrate on the surface, like H_2S on Pt in hydrogenation reactions; (ii) coking as a result of coke deposition due to hydrocarbon decomposition to hydrogen-poor compounds, i.e. coke; (iii) fouling as a result of solids deposition due to dusty materials within the feed; (iv) sintering and crystallization or segregation of the catalytic material due to thermal effects [17]. Although these are individual effects, it is possible that several deactivating processes take place simultaneously, or that the dominating deactivation process can be initiated by another one.

2.1 Chemisorption of Poison

Deactivation of catalysts by chemical adsorption of some substance is known as *poisoning*. A poison is a molecule of reactant, product, or impurity in the feed with a certain affinity towards the catalyst; the magnitude of interaction defines the character of *reversible* or *irreversible* poisoning. When the affinity of a poison is equal to all active sites than this is *uniform poisoning*, where all active sites have the same chance of being poisoned. In the opposite case, when a poison preferentially chemisorbs on one category of active sites, *selective poisoning* occurs.

   A poison may act by blocking the active sites - *geometric effect*, or by changing their electronic properties - *electronic effect*. In the first case the adsorption of the poison is often arranged by some geometric rule, which is defined by both the catalyst and the poison. Sometimes for the same combination of catalyst and poison different geometrical arrangements are possible, as it is the case of the well known example of Pt (100) poisoned by sulphur [18]. Sulphur is adsorbed on Pt in two different geometric arrangements, as c(2x2) and p(2x2), corresponding to one-half, and one-quarter of a monolayer of S at full coverage of active sites, respectively (Figure 1). At first glance the second geometry is preferential from the viewpoint of catalyst activity, since one vacant adsorption site exist at the center of p(2x2). For bimolecular reactions, however, being the majority of processes where Pt catalysts are used, the possibility of an isolated molecule adsorption is useless. Therefore, the c(2x2) geometric arrangement is beneficial from a practical viewpoint, since for a certain activity level the catalyst is capable of accepting more sulphur.

a   b
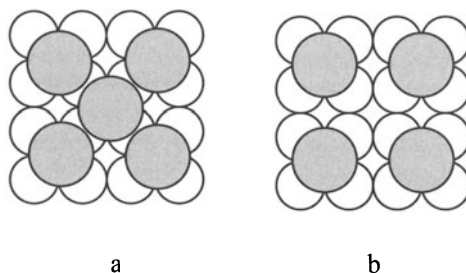
Fig. 1. Two geometric structures of S adsorption on Pt(100): a) c(2x2), and b) p(2x2)

Due to the exchange of electrons for strong chemisorption, the poison can change the electronic properties of the catalyst. Electronic and geometric effects may be coupled, however, as is the case of poisoning of Ni-catalysts by S, Cl, C, N and P [19]. These poisons block the active sites on which they are adsorbed, but they also decrease the adsorption abilities of neighboring active sites for adsorption of reactants by electronic interaction. The poisoning effect of S and Cl is more pronounced due to their higher electronegativities and sizes relative to C, N and P [19].

For heterogeneous catalytic surfaces, the most common case is selective poisoning [3]. Due to the different energy and geometry of active sites different mechanisms of poisoning occur. The poisoning usually starts with preferential adsorption on sites with higher affinity towards the poison, and once the adsorption reaches the point of saturation, it is followed by the additional adsorption of poison over the rest of the sites. In the case of bifunctional catalysts, poisoning may affect their activity and/or selectivity, depending on the reaction mechanism. For illustration, the reaction of methyl-cyclopropane (MCP) hydrogenolysis on Pt/Al_2O_3 catalyst is possible through two main routes, involving: (i) metallic sites only, and (ii) both acidic and metallic sites. In the case of unpromoted catalysts the first mechanism prevails, leading to high selectivity to i-butane. When chlorine is added to the rection mixture, however, only metallic sites are selectively poisoned, resulting in a minor activity decrease, but dramatic selectivity changes [20]. As shown in Figure 2, the extent and profile of these changes depend on the precursor of the poison, CCl_4 or HCl, used to introduce the chlorine. A quite different result of poisoning is obtained for a reaction with a consecutive mechanism, like isomerisation of n-hexane. Here, poisoning of metallic sites would rather be expressed as an activity drop, than a selectivity change; due to the absence of a dehydrogenation function, olefin production is stopped, and straight isomerisation of paraffin on acidic sites is quite difficult when these are of moderate acidity [21].
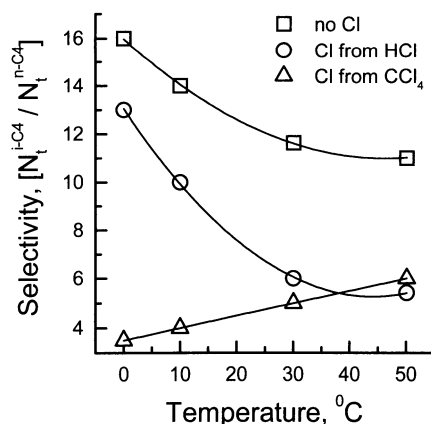
Fig.2. Influence of addition of 0.82 % Cl from different precursors, on selectivity of 0.31%-Pt/Al_2O_3 catalyst (47.6 % Pt dispersion) in MCP hydrogenolysis reaction [20]

The rate of catalyst deactivation may depend on the size of the catalytic sites, which means that deactivation can be *structure sensitive* [22]. The effect sometimes interferes with the structure sensitivity of the catalytic reaction, making it difficult to decouple these two phenomena. It was found, e.g., that sympathetic behavior of the n-hexane reforming reaction on Pt/SiO_2 is rather due to the higher rate of coke deposition on larger particles (deactivation reaction), than to the catalytic reaction turn-over frequency increase due to dispersivity increase [22]. Thus, when the catalytic reaction and the deactivation reaction belong to different types of structure sensitivity, the effect of catalyst dispersivity on the catalytic reaction is masked by marked structure sensitivity of deactivation. Even a more dramatic effect occurs in the case of a hydrogenolysis reaction, where poisoning by coke can even change the original type of structure sensitivity of the catalytic reaction [23]. Since this type of reaction involves destruction of one or several C-C bonds, multibonding of a reactant onto the catalyst surface is the most appropriate mechanism. Accordingly, an antipathetic behavior of the catalyst is expected, since the particle size increase will result in high-coordinated plain sites close to each other being favorable for this kind of hydrocarbon adsorption. However, the opposite was noticed during time on stream, showing a higher rate increase with smaller particles, i.e. particles having a larger number of lower coordinated active sites. This might be the result of preferential poisoning of sites with high coordination number, and the reaction is forced to "switch" from sites on the plain (poisoned) to those which sit on edges of crystals (still unpoisoned). This phenomenon is known as *secondary structure sensitivity* [23].

Structure sensitivity of the deactivation reaction depends on catalyst support as well. In the case of two Pt-based catalysts with the same metal loading and dispersion, and having the same history of preparation and usage, the type of poisoning by CO was found to be different for alumina and silica supports. In both cases structure sensitive poisoning takes place, however its patterns are different (Figure 3). The uniform poisoning in the case of alumina [24], in contrast to the selective poisoning observed for silica [25], was explained by stronger metal-support-interaction for alumina, leading to more stable Pt particles with constant deactivating behavior [3].
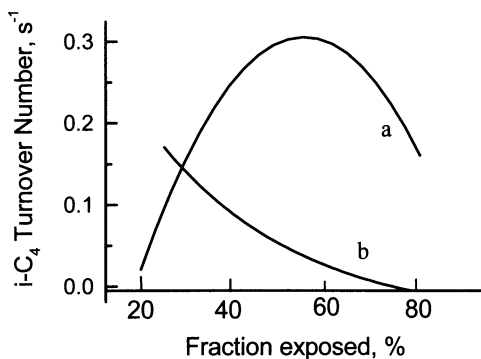
Fig. 3. Structure sensitivity patterns of Pt/SiO_2 (a) [25], and Pt/Al_2O_3 (b) [24] catalysts, having the same CO coverage of 40%

2.2   Coking and Fouling

Formation of hydrocarbon deposits on catalyst surfaces is the common mechanism of deactivation in processes dealing with conversion of hydrocarbons in oxygen-lean conditions. The mechanism is known as *coking*, or *fouling*, although the last expression has sometimes the broader meaning for all kinds of deposition, such as of iron or ceramic particles displaced originating from the reactor material [11].

The chemical nature of coke is not easy to define since, in principle, every hydrocarbon molecule which has a deficit in hydrogen can be considered as a coke precursor. The nature of coke deposits and the mechanisms of their formation depend on the feed and the nature of the catalyst employed. In the case of a bi-functional catalyst it even depends on which part of the catalyst coking occurs [26]. Finally, the mechanism of coking is a function of time since the nature of coke can change with time-on-stream [3]. It is believed that aromatics and/or ole-fins are the main precursors of coke formation, which by reactions of dehydroge-nation, condensation, and oligomerization finally result in coke-like products [3]. Coking by decomposition of hydrocarbons, which may result in similar species, is in principle different, since hydrocarbons are likely to produce various H-containing species of general formula CH_X, or C_nH_m [27].

To some extent the mechanism of coking is a single property of every catalyst. Thus, it was suggested that for a bifunctional Pt-based catalyst coking starts on metallic sites by adsorption of coke precursors like monocyclic diolefins, which than migrate to acidic sites and polymerize to form a polycyclic molecule with several double bonds [3]. In the case of Ni-based catalysts for steam reforming, it seems that coke formation starts as a result of hydrocarbon decomposition on the catalyst surface resulting in C_α. This coke species can be gasified, but also polym-erize to more stable C_β which can form carbidic carbon [11,28]. Similarly, decom-position of CH_4 on Co-based catalysts leads to species with different quality of carbon relative to its further reactivity. Transformation from the most reactive C_α to less reactive C_β, and finally to the most stable C_γ follows the increase in both surface coverage and temperature of decomposition [29].

In principle, coke can lead to catalyst deactivation by *active sites coverage* and by *pore blockage*. The first occurs when both the catalytic and coking reactions are of a single site mechanism, and the higher the density of active sites the more effective is coking. When catalytic and coking reactions do not compete for the same sites, deactivation by coking is only due to pore blockage [30]. The effi-ciency of the process of pore plugging by coke depends on catalyst texture, and may be rather high for a favorable pore shape, e.g. ink-bottle necks. In that case quite a small amount of adsorbed coke may bring a high activity decline. But sometimes the amount of coke can rise to a significant fraction of the total mass of the catalyst due to an *avalanche effect*, when initial coke particles act as a "glue" for new coke particles [31].

Coking on zeolites is a shape selective process since both the rate of deposit build-up and its nature depend on pore dimensions [32]. The prevailing mecha-nism of zeolite deactivation by coke depends on operating conditions, zeolite acidity and its topology. Pore size and structure are probably the most important parameters as shown in Figure 4 [32]. In systems consisting of non-intercon-necting channels, like in the case of mordenite (Fig. 4a), coking occurs through pore blockage and is very effective in terms of deactivation. Similarly, tri-dimensional zeolites with small apertures and large cavities, like erionite, are very

sensitive to deactivation by pore plugging (Fig. 4b). Contrary, in systems with tri-dimensional channels without cavities, like HZSM-5, deactivation initially starts as acid sites coverage, but with time-on-stream and amount of coke increasing, deactivation is due to blocking of the sites in the channel intersections, and finally due to blocking of pores by exterior deposits (Fig. 4c,d,e). The amount of coke formed in the last case, and hence the dynamics of changes in the deactivation mode, are proportional to the severity of operating conditions [32].

a   **b**   **c**   **d**   **e**
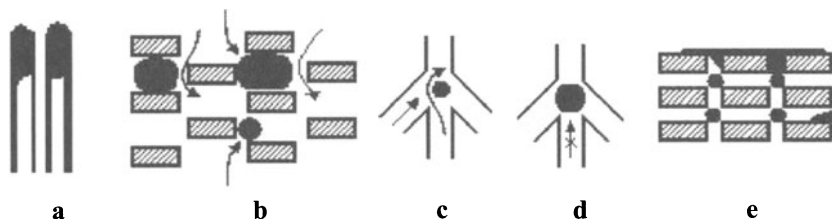
Fig. 4. Different mode of deactivation by coke: pore blocking in monodimenzional mordenite (a), and tridimenzional erionite (b); site coverage (c), sites accessibility hindered by channel blocking (d), and pore blocking by exterior deposits (e), all in HZSM-5 [after 32]

2.3   Ageing

Catalyst ageing is due to slow processes of physical and chemical solid-state transformations as a result of the catalyst being exposed to the reaction environment. These transformations can proceed without or with a change of catalyst overall composition [33]. Sintering of the active phase and/or support, segregation and transformation of phases, and all kinds of metal-support interactions are frequent phenomena belonging to the first group, while changes of oxidation state, formation of carbide, and loss of catalyst component are those resulting in a change of catalyst composition. While one of these processes may dominate under specific conditions, more often they occur simultaneously.

Sintering is an important and frequent reason for catalyst deactivation [14,34-36]. In metal supported catalysts it is usually manifested either as loss of active metal area, or decrease of catalyst support area. It includes, however, several other phenomena like dissociation of metal atoms, diffusion of metal atoms and crystals, spreading of particles, nucleation of particles, coalescence, etc. [36]. Depending on its cause *thermal* and *chemical* sintering are known. In the first case a decrease of surface area occurs simply by particle enlargement due to high reaction temperatures. Thermal sintering is strongly influenced by the height of temperature, and it is believed that it has to be at least as high as the *Tamman* temperature for the phenomena to occur. But it might not be a general case since the real mechanism of sintering is not known. For example, if diffusion of atoms through the particle volume is the mechanism of sintering, then the *Tamman* temperature probably must be reached for sintering to occur. But if surface diffusion of atoms is the mechanism, than the *Hüttig* temperature (one third of the melting temperature) is probably enough. Even assuming high temperature as the main cause of thermal sintering other factors should not be excluded. These are the size and the shape of particles, surface roughness, metal-support interaction, the presence of promoters and the gaseous environment [14,15,36]. The combination of factors

results sometimes in an unexpected behavior, like in the case of the presence of different gasses, which might influence sintering depending on the particular metal and conditions applied [36]. Time is also an important variable since sintering, like all other solid-state transformations, is a time consuming process. In the case of zeolite based catalysts, sintering of the active metal depends on the preparation method, metal loading, zeolite framework, and thermal conditions determining the position of the metal in the zeolite structure. In Pt-exchanged Y zeolites the chance of Pt sintering depends on calcination temperature, determining either particle migration to more stable positions, or their settling in the largecavities. In the reduction following preparation, these particles which missed stabilization in the previous calcination step, migrate and agglomerate on the external surface of the zeolite [37].

Basically, two models have been proposed to explain the growth of supported metal particles: a) *particle/crystallite migration* [38], and *atoms migration* [39] (Figure 5). The basis of the first one is the assumption that week metal-support interaction and a high temperature lead to migration of crystallites which are in a quasi-liquid state. On their way the crystallites collide and agglomerate. The atoms-migration model assumes that movement of atoms is important for sintering. The process can be assumed to occur in three stages: transport of atoms from the crystallite to the surface of the support, their migration over the support and finally their collision with bigger crystals. The two models do not exclude each other, but most probably occur in sequence, i.e., at lower temperatures sintering starts by migration of atoms, and once the higher temperature is reached movement of particles occur. At a very high temperature, when particles are of bigger size, volatilization of atoms is the prevailing mechanism responsible for transport and sintering [14]. Apart from these traditional models, an additional mechanism of sintering has been proposed including wetting and spreading [40]. This has been portrayed as a consequence of the formation of films between deposited metal particles in O_2, and subsequent rupture of this film in H_2. The explanation for this lies in the different strengths of metal-substrate interactions in different atmospheres, and the driving force for both phenomena is the decrease of free energy of the system [40].
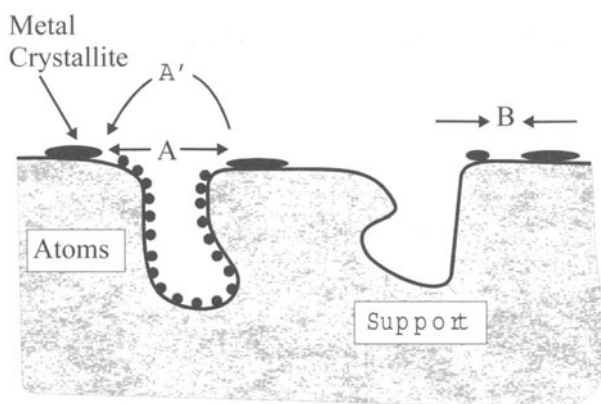
Fig. 5. Two models for crystallite growth due to sintering: Movement of atoms by migration (A), or by volatilization (A'), and migration of particles (B) [after 36]

Chemical sintering is caused by a chemical reaction between an active metal and a molecule in the feed, resulting in a new compound forming particles of larger size. The subsequent reverse reaction will result in the active component again, but the size of the particle may stay unchanged [41]. Similarly, in alternating conditions of oxidation-reduction reactions [42], active metals are forced to change from one compound to another usually having particles of different size. These frequent and fast rearrangements of structure in the metal lattice cannot be followed by all atoms, therefore they occupy thermodynamically more stable positions resulting in enlarged particles.

As already mentioned there are several other catalyst deactivation phenomena belonging to the category of ageing, and most of them are caused by high temperature. Phase transformation of the often used active γ-Al_2O_3 support to its inactive α-phase is, for example, very common in catalysts exposed to high temperature for extended periods of time. The process is usually promoted by an active metal sitting on the support, like in the case of a Ni/Al_2O_3 catalyst where migration of Ni and formation of Ni-nucleation sites play a decisive role for phase transformation of the support [43]. In addition, alumina often undergoes reactions with M^{2+}-type active metals, forming spinel-like structures, like $CoAl_2O_4$, $NiAl_2O_4$, etc. [21]. Both the transformation of atomic to graphitic carbon, and active-carbon-rich carbides to inactive carbon-poor carbides, occur often in Fe-based catalysts used in the Fischer-Tropsch process; these are examples of catalyst composition changes due to reaction [44]. Sublimation of Mo from a CoO-MoO_3-Al_2O_3 HDS catalyst is a typical example for a loss of a catalytic active component [45]. For zeolites exposed to severe hydrothermal conditions, dealumination is a frequent reason for their acidity change [46]. One of the processes often accompanying sintering is a change of particle morphology. In the case of a Pt/Al_2O_3 catalyst transformations of cubic to spherical particles, and vice-versa, were found to be dependent on both temperature and gas environment [47]. A similar change of particle morphology due to sintering was observed for an Ag/Al_2O_3 epoxidation catalyst [48].

3. Catalyst Deactivation in Important Industrial Processes

3.1 Fluid Catalytic Cracking

Fluid catalytic cracking (FCC) is designed to process heavy, i.e., high boiling hydrocarbon feed at rather high temperatures; FCC catalysts used are subject to excessive coking [49]. Coke is a reversible poison of chemical structure determined by its precursor. This can be an olefin, or diolefin, preferentially of cyclic structure, which leads via a mechanism of cyclodimerisation and hydrogen transfer to heavier products, like decaline or naphthalene [50]. Coke is the cause for catalyst-porosity changes due to its deposition inside pores or blocking their entrance. In such a way coke can dramatically change the selectivity of the catalyst by preventing larger hydrocarbon molecules to enter or leave the pore. For modern zeolite FCC catalysts the mode of deactivation by coke depends mainly on their pore structure: monodimensional zeolites and zeolites with large cavities are deactivated mainly by pore blocking, while for threedimensional zeolites active sites

coverage is a predominant cause for deactivation [32,51]. Different basic mole-cules, e.g. nitrogen compounds are a frequent reversible poison of FCC catalysts. Their presence is highly undesirable since they are strongly adsorbed on the cata-lyst surface and can produce coke which is more difficult to remove in the follow-ing regeneration cycle, requiring more severe conditions [52]. Among the irre-versible poisons the most important ones are heavy metals like V and Ni. They damage the catalyst by destroying its active sites and blocking the pores, but they can as well promote some undesirable reactions, like dehydrogenation [49]. The deactivation mechanism by V is believed to occur via its migration and formation of metal silicates and aluminates in both the reduction and oxidation cycles finally leading to destruction of the zeolite matrix [49,52]. Vanadium is a critical poison, its effect reaching the maximum for V^{+5}; this might be related to the high mobility of this ion [53]. Deactivation by Na is mainly due to poisoning of acid sites, and accelerated sintering of the zeolite framework [54]. During its life a FCC catalyst undergoes several ten thousands alternating reaction and regeneration cycles [52]. Regeneration usually occurs under severe conditions of coke burning, resulting in catalyst ageing, i.e., surface area and porosity collapse. For zeolite catalysts the process includes dealumination, leading to an acidity change and reduction of unit cell size [49].

3.2   Catalytic Hydrogenation Processes in the Oil Industry

Processes for hydrotreating of oil fractions on $CoMo/Al_2O_3$ or $NiMo/Al_2O_3$ cata-lysts are very essential in petroleum industry. The increasing attention to deactiva-tion of hydroprocessing catalysts is in line with growing interest in the utilization of heavy oil fractions. Both, the severe conditions required for processing of such feeds, and the high content of potentially dangerous species contained in them, make these catalysts rather vulnerable. Deactivation occurs by a number of differ-ent mechanisms: sintering and solid state transformation of the active phase, de-composition of the active phase, adsorption of N-containing components, coking and deposition of metals and metal-sulphides [55,56]. Since several types of reac-tions which occur in hydroprocessing (HDS, HDN, HDO, and HDM) take place on different active sites, some reactions will be effected more than others by the same deactivation mechanism [56]. Thus, for the HDS function the most impor-tant deactivation mechanisms are coking and metal-sulphide depositions [49], but which one will prevail in any particular situation depends on the combination of various factors. Coking and metal deposition, e.g., are greatly influenced by feed-stock properties and reaction conditions. Commercial experience says that the quality of asphalthenes in the feed residue, i.e., their aromaticity, is more impor-tant than their quantity [57]. A different conclusion has been drawn from an ex-periment where a commercial Ni-Mo catalyst was deactivated by pyrene and dibenzothiophene as a model feed, showing the quantity of coke being the deci-sive factor [58]. Among reaction conditions, temperature is the most important one, since the increase of reaction temperature enhances both coke and metal deposition. Increasing hydrogen pressure decreases coking but increases metal deposition [59]. Olefins as well as aromatic and heterocyclic components are most subject to coking; this occurs basically through polymerization or polycondensa-tion mechanisms involving products from the cracking reactions [55,56]. Besides, involvement of coke precursors containing N usually results in more severe cok-

ing. In hydroprocessing of residues, in which the content of coke leading precursors and heavy metals is usually high, two distinct mechanisms of catalyst deactivation play a role: an initial rapid deactivation due to coking is followed by more gradual decline due to fouling by metals, especially V, Ni and Fe [49,60]. A common feature of deactivation of HDS catalysts by coke, as an initial activity decline followed by constant catalyst activity, indicates that only a fraction of the HDS catalyst sites undergo coking, while another part stays with the same intrinsic activity as in the uncoked catalyst [55]. Nitrogen compounds are the most frequent poisons; the degree of poisoning increases with the basicity of these compounds. The poisoning effect of piperidine, e.g., is more pronounced than that one of 2,6-lutidine, and the difference in magnitude is higher for HDO than for HDS [56]. Water, which is formed by HDO reactions, is also considered as a poison, but its effect varies from strong inhibition of HDS functions, to weak inhibition, or even a promoting effect on the HDO function [56]. Commonly deactivation of $CoMo/Al_2O_3$ catalysts is related to sintering of the MoS_2 phase. The process is usually a consequence of local overheating, and leads to a decrease of the number of MoS_2 edge sites. As a result Co edge atoms are less stable and they segregate as Co_9S_8. Thus by decreasing the Co/Mo ratio it is possible to tailor a catalyst with higher resistance to sintering, due to the higher saturation point related to edge MoS_2 sites. However, lower initial activity of such a catalyst has to be accepted [55].

Since catalytic reforming is one of the most important processes in the field of petroleum refining, deactivation of related catalysts is an important issue [61-63]. Reversible poisons for bifunctional reforming catalysts are S, N, O, and Cl-derivatives, of which the first is responsible for active metal poisoning, and the rest for modification of catalyst acidity [62]. At process conditions with high hydrogen pressure, S is present as H_2S, and once the S-containing impurity is removed from the feed, the hydrogenation/dehydrogenation function of the catalysts is gradually recovered. Although acting as a reversible poison S yet can cause a permanent damage to the catalyst reducing its life expectancy. There are direct and indirect causes for this: almost irreversible adsorption of S on the second metal, and need for a higher reaction temperature due to poisoning by S, which in turn brings more coking [62]. The effect depends, however, on the amount of S in the feed, thus catalysts having more than 2ppm of S show a marked tendency to reduced life expectancy [62]. Nitrogen poisons the acidic catalytic function shifting selectivity to less isomers as products. An additional problem for catalysts exposed to N-containing substances for a longer period of time is the formation of NH_4Cl, which precipitates and takes away Chlorine necessary for maintaining a balance in catalyst acidity [61].

Coking is an unavoidable cause for deactivation of reforming catalysts since both high temperature and low hydrogen pressure, which are desirable for the catalytic reactions, favor also coke formation [62,63]. Basically, the reactions occurring on metallic sites are more effected by coking than those on acidic sites [62]. The extent of coking depends on catalyst properties, feed properties, and reaction conditions. Thus, it is known that larger metal particles on more acidic supports are proner to coking. Introduction of a second metal like Re to Pt-containing catalysts decreases the chance of coking by promoting the coke graphitisation. Graphitic coke is denser but less toxic for the metallic function [63]. Basically, second metals added to Pt-based catalyst may be divided into two groups with respect to their mechanisms towards coking restriction: they either

diminish the coke deposit on Pt (Re added), or isolate small clusters of Pt to protect them from coking and direct the coke to deposit on the support (Sn added) [62]. The increase of total pressure decreases coking, but the magnitude of this effect depends on the H_2/hydrocarbon ratio as well; by lowering the hydrogen partial pressure the formation of unsaturated species, considered as coke precursor, is increased [62]. Elevated total pressure changes also the coke quality by changing the location of coke deposition from metal to support. The coke produced on the former is easier to hydrogenate and consequently less dangerous to the catalyst [63].

One of the reasons for deactivation of reforming catalysts is sintering of its metallic phase. In the presence of an optimal chlorine concentration in the feed, however, sintering is not pronounced due to the redispersion effect of chlorine on Pt. In the presence of an oxidizing agent, the process proceeds with the formation of some oxychloroplatinum complexes which are strongly bonded to the support, leaving redispersed Pt particles after decomposition and evaporation [64]. In hydrogen atmosphere, however, when Pt is present as atoms, their mobility is suppressed by decreased volatility, preventing in such a way atoms from escaping from the crystallite [64]. These mechanisms are in line with the observation that sintering of platinum is more marked in nitrogen atmosphere than in air [62].

3.3   Ethylene Epoxidation

Epoxidation of ethylene to ethylene oxide is an important process in petrochemical industry. The uniquely effective Ag-based catalyst undergoes deactivation during time-on-stream; therefore it has been a subject of extensive research in order to improve its stability [65]. Under industrial operating conditions deactivation of Ag-catalysts is compensated by increasing reaction temperature, which in turn leads to more rapid deactivation, followed by a selectivity decay. As a consequence the life expectancy of the catalyst is decreasing. Thus, the catalyst utilization in the process can be seen as a compromise between its current activity and predicted life, which should result in maximal yield over the total catalyst life.

Much of the work performed on the mechanism of the reaction of ethylene oxidation on Ag catalysts has been aimed at unveiling causes and mechanisms of catalyst deactivation. It has been clarified that the existence of both subsurface and atomic oxygen is essential for the selective ethylene oxidation [66-68]. Recently, the reduced ability of oxygen adsorption upon catalyst ageing in industrial conditions was recognized as the possible reason for the loss of catalyst activity and selectivity [69]. The reason for the lower oxygen adsorption ability may be ascribed to any one of the phenomena which have been related to Ag-catalyst deactivation: catalyst poisoning either by impurities in the feed [70], or by chlorine [71-73], and an accumulation of carbonaceous deposits on the catalyst surface [68,74-76], increase in Ag particle size [42,70,77,78], as well as of the support, possibly followed by redistribution of promoters [78]. Despite of such a wide list of possible causes, however, it is widely accepted that silver sintering, resulting in a change of particle size distribution and decrease of active area, is the reason for deactivation. Very often, however, these changes were not found to be proportional to the extent of deactivation, pointing out that several other phenomena might contribute to deactivation, like the rearrangement of faces [77], changes of morphology of Ag particles followed by changes in MSI [48,77-79].

3.4   Reduction of NO_X in Exhaust Gases from Automotive Engines

Since catalysts for automotive exhaust gases are very extensively used and contain expensive precious metals, the request for their long life is a basic requirement.

In platinum based three-way catalysts for the cleaning of exhaust gases from gasoline engines, the deactivation problem is related to both poisoning and sintering. From a historical point of view, the first effort to overcome the problem of poisoning of the catalytic active component by lead-based antiknocking agent, was done by complete exclusion of Pb-compounds; this is as much a benefit to the environment as it was to the catalyst. Besides, the usage of unleaded gasoline made it possible to replace the very expensive Pt by Pd in Pt-Rh catalyst [80]. However, in order to avoid formation of bimetallic Pd-Rh particles, a special technology had to be used by which the existence of separate layers of two active metals on a high-surface area "wash coat" was possible. The sintering of CeO_2, which has the role for oxygen storage in noble-metal catalyzed oxidation of CO, is an additional deactivation process of three-way catalysts. Achievement of higher ceria dispersion and higher stability of smaller particles was accomplished by introduction of an additional metal oxide, such as zirconia, forming a solid solution with CeO_2 [80].

Deactivation of exhaust-gas catalysts is even more demanding for fuel-lean gasoline and for diesel engines. As a matter of fact there is no catalyst up to date which completely satisfies activity and selectivity requirements. Deactivation is especially prominent in the presence of H_2O vapor and SO_2, which are commonly associated with exhaust gases [81], and which have a synergistic character [82]. The mechanism of poisoning by SO_2 is either by simply blocking active sites due to poison dissociation, or by its interaction with the oxidized catalyst surface leading to sulphates and sulphites [83]. In the case of selective catalytic reduction, accumulation of coke from an added hydrocarbon reductant might be an additional reason for catalyst deactivation [84]. For the most-investigated Cu-ZSM-5 catalyst which is, however, not a suitable catalyst for diesel-engine exhaust, the activity loss is the consequence of dealumination, especially in the presence of water. The loss of tetrahedral Al atoms affects the population of Cu^{2+} active sites responsible for $DeNO_X$, but it is also seen as a cause for failed hydrocarbons oxidation due to the decline of the rest of Bronsted sites [85]. At very high temperatures, i.e., between 600 ^0C and 800 ^0C, it is believed that substantial deactivation of Cu-ZSM-5 is due to a significant loss in microporosity [86]. Since there are no other effects which could be responsible for this textural change, like dealumination or/and coking, the formation of an active-metal compound is most likely to be the reason. The existence of Cu_2O particles indeed has been confirmed by XRD [86] and TEM [87]. In contrast, recent investigation on deactivation of Cu-ZSM-5 catalyst at 400 ^0C in the presence of water, showed irreversible deactivation only due to a change of Cu^{2+} distribution, with neither additional framework changes nor formation of Cu-compounds [88].

4. Prevention of Catalyst Deactivation and Regeneration of Deactivated Catalysts

To overcome catalyst deactivation two approaches are possible: (1) trying to avoid or to minimize possible causes for deactivation, or (2) to accept it, but minimizing its effect both by both process and catalyst tuning. If the first approach is a choice, than feed purification, or the selection of more appropriate feed is what can be done. The process tuning related to catalyst deactivation can be approached in two different ways: i) careful selection of process parameters in order to avoid initiation of some deactivation phenomena, and ii) careful monitoring of parameters in the process of catalyst production in order to obtain a product with desirable and reproducible properties [33]. Among the process parameters reaction temperature is the most important one when sintering is concerned. In order to minimize the chances for sintering the temperature must be chosen in such a way that severe temperature gradients are avoided throughout the bed of catalyst particles. The last measure can be only achieved, however, when the catalyst itself is of uniform physical and chemical properties. By ascertaining that the chance of appearance of hot spots is low, thermal sintering may be avoided to a certain degree. Generally, production of catalysts of constant quality is very important from the point of view of deactivation. The reason for this is that many catalysts, like all other solid materials, might have a *memory effect*, i. e., the history of catalyst preparation affects its behavior during its life-time [33]. Quite often catalyst and process imperfections are interrelated, the first being sometimes passive as long as there is no excessive change in desired process conditions. Once this is provoked by some accident in the process, the result can be a prominent deactivation due to a synergistic effect of these two imperfections.

In order to improve catalyst resistance to poisoning the distribution of the active sites in and on a catalyst particle is of primary importance. The preferred active metal location depends on the mechanism of poisoning, i. e., uniform distribution through the particle is favored in the case of a parallel mechanism, and metal deposition on the catalyst surface is preferred for the case of consecutive poisoning. An additional tailoring of pore structure in the first case might be seen as a compromise between catalyst life and its activity, resulting in maximal total catalyst efficiency [2,3]. Besides this, several other techniques in catalyst preparation are used to increase its resistance to all kinds of deactivation phenomena. The second metal may sometimes serve as a guard to the primary active metal, protecting it from poison. The addition of Re to Pt/Al_2O_3 catalysts, e.g., which results in increased resistance to coking, was explained by the ability of Re to remove the coke precursors, like cyclopentane, e.g., from Pt [89]. Taking the fact into account, however, that a physical mixture of Pt/Al_2O_3 and Re/Al_2O_3 does not result in the same deactivation suppression as in the case of bimetallic Pt-Re/Al_2O_3 catalyst, the question of the real role of Re is still open [90]. Similarly, the addition of K to a Ni/Al_2O_3 catalyst for steam reforming of hydrocarbons was found to suppress coke formation. The promotion effect of K is explained by both a decrease of the rate of hydrocarbon decomposition on the catalyst surface, and an increase of the rate of removing the coke deposits from the surface [91]. A beneficial influence of a second metal related to deactivation is known in practice of zeolite preparation; an inactive metal may force the active one to stay in a certain position in the zeolite matrix, thus protecting it from sintering. This kind of stabilization,

which was observed for Pt promoted by Fe^{2+} and Cr^{3+} in a Y zeolite is known as *chemical anchoring* [92]. Besides previously mentioned redispersion effects of chlorine on Pt [64], there is also a chlorine effect on the reduction of coke deposition. It is believed that Cl optimizes H_2 chemisorption, and subsequent H-spillover, which consequently leads to self-regeneration of the coked Pt-reforming catalyst [93]. Similarly, addition of α-Sb_2O_4 to an active phase of MoO_3 promotes spillover of O_2, which reacts with a reduced location on the surface of MoO_3, hence creating an active site [94].

Accumulation of coke on zeolite-based catalysts doubles the negative effect: it decreases activity due to active sites coverage, and requires subsequent oxidative treatment to burn-off the coke. Consequently, some rules have to be followed in order to decrease chances of coking in a hydrogenation process: a) if possible tridimensional zeolites with small apertures and large cavities have to be avoided, b) acid strength and density have to be adjusted to the lowest values necessary for the reaction, c) operating conditions have to be tuned in order to avoid formation of coke precursors [95]. In some cases, however, a beneficial effect of coke deposits has been also demonstrated, like for n-butane skeletal isomerisation to isobutene over ferrierite [96]. An initial low selectivity, followed by a selectivity increase with time-on-stream, can be explained by preferential poisoning of the non-selective strongest active sites located inside of the 10-member ring channels. At the same time shape selective Bronsted acid sites located at the pore mouth are not too vulnerable to the medium level of coking as long as the formation of poly-aromatic compounds which may block the pore mouth is avoided [96].

Catalyst regeneration is the least desirable approach to catalyst deactivation. It requires both process time and man power, and it usually does not result in the original activity of the fresh catalyst [97]. Catalyst regeneration typically consists of either removal of poison/coke, or catalyst particles redispersion, although sometimes both processes occur simultaneously. In principle, the removal of coke is possible by gasification with oxygen, steam, hydrogen, and carbon dioxide [98]. Since catalyst regeneration by coke burning starts with hydrogen oxidation and H_2O production, the process is performed in two steps, i. e., at low and high reaction temperature. The approach is of special interest for zeolite catalyst regeneration, avoiding a coupling effect of high temperature and water [95].

A simulation of steam regeneration of deactivated commercial catalysts for HDS shows all the complexity of choosing the right agent for coke removal [45]. Since the removal of coke by water vapor is an endothermic reaction, the use of steam is supposed to be a more saver approach to catalyst regeneration than using oxygen. Under laboratory conditions, however, an activity loss of a commercial Co-Mo/Al_2O_3 catalyst previously regenerated in steam was found. The results were attributed to both Mo redispersion and a molybdenum loss of the active phase comprising molybdena; this was due to reaction of water vapor with MoO_3 at temperatures from 600 to700 ^0C [45]. This model describes the details of deactivation of a hydrotreating Ni-Mo/Al_2O_3 commercial catalyst well [99]. After regeneration in steam at a rather mild temperature of 400 ^0C, the catalyst showed substantial loss of activity when afterwards exposed to a feed stock with higher S level. The loss of active component by MoO_3 segregation and vaporization of MoO_3, proved by SEM investigation of discharged catalyst samples, was identified as the primary cause for deactivation. This might have happened as the result of hot spots forming in the period of catalyst regeneration. In addition, an intensive sintering caused by a liquid MoO_3 phase was identified as the secondary

cause for the catalyst deactivation. The BET surface area decrease and average pore diameter increase by a factor of 5 and 10, respectively, support this conclusion [99].

Finally, not being directly connected to coping with catalyst deactivation, but more as a consequence of it, the handling of deactivated catalysts is often important. Even the deactivated catalysts are mostly still pyrophoric, and passivation by appropriate methods is required before catalyst discharge. In the case of CuO-ZnO/Al$_2$O$_3$ catalysts for methanol synthesis, *wet* passivation of the spent catalyst, has been exchanged by *in situ* oxidation. However, due to the extremely exothermal reaction this regeneration process is difficult to control. DSC analysis of a deactivated commercial catalyst sample in controlled oxidizing atmosphere revealed that the total heat released in cyclic operation is much less than for a one-step catalyst oxidation in air [100].The latter procedure applied on large-scale could result in thermal reactor runaway.

5.   Kinetics of Catalyst Deactivation

5.1   Temporal Deactivation Phenomena

Since shape and size of both catalyst pores and poison molecules are often different, various types of poisoning occur depending on the rates of the catalytic reaction and the poisoning process [3]. When the affinity between poison and catalyst is not very strong, mainly the interior of pores is poisoned; the type of poisoning is then determined by the value of the Thiele modulus. With no, or very low diffusional restrictions, uniform or *nonselective* poisoning occurs (Figure 6, curve a). If the catalytic reaction is strongly diffusion limited and the deactivation rate is not, *antiselective* poisoning occurs (Figure 6, curves b and c). The higher activity obtained at a higher Thiele modulus is partly due to adsorption of poison on that fraction of active sites which, as a result of strong diffusion, do not contribute to the reaction anyway. In reality, however, this type of poisoning does not occur, as poisons usually tend to adsorb at the pore inlet [13]. As a matter of fact the affinity between poison and catalyst is often so high that they react as soon as contact is achieved. In this case the majority of poisoning molecules hardly enters the pore interior and is mainly adsorbed at the pore mouth. This is called *selective* or *pore mouth* poisoning; the activity profile then depends on the diffusion regime. In the kinetic regime the remaining activity will be proportional to the fraction of the not-deactivated surface (Figure 6, curve d). If the catalytic reaction is strongly limited by diffusion a dramatic effect of poison on catalyst activity may happen (Figure 6, curve e). This is due to the fact that even small concentrations of poison adsorbed on the pore entrance deactivate de facto the only available active sites for the reaction, since due to strong diffusion restrains the rest of the sites stays out of the domain of the catalytic reaction.
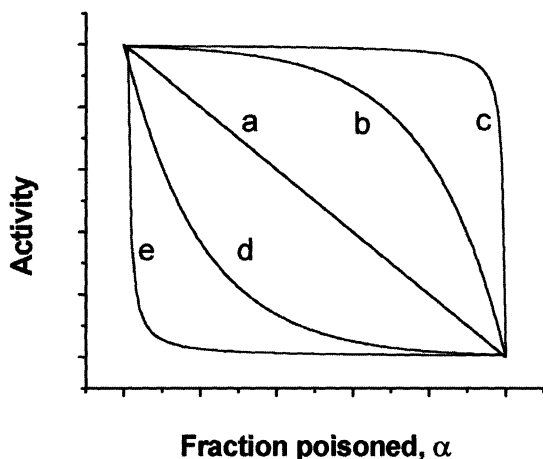
Fig. 6. Different type of poisoning in porous catalyst: a- uniform; b,c- antiselective; d,e-selective

There is similarity in poisoning and coking kinetics, although the latter one is specific to certain properties of the coke. Mainly, coke particles tend to stick to-gether and to agglomerate, making deactivation by pore blockage sometimes very effective. Distribution of coke in the catalyst particle reflects both mechanisms of coking, which could be in parallel or in series, and the kinetics of the catalytic reaction (Figure 7). For the parallel coking mechanism, the coke distribution can be either uniform, if no strong diffusion limitation exists, or the coke can cover the internal surface of the catalyst, if fast diffusion prevails (7a and 7b, respectively). In the case of the later, the thickness of the coke layer is defined by the extent of diffusion. For both, series mechanism and low-value of Thiele modulus, again uniform distribution of coke is obtained, with the only difference to case *a* being the direction of coke growth within the pore (7c). For strong diffusion limitations, pboth consecutive reactions occur predominantly close to the surface and the coke layer is forming similarly to the previous case of parallel coking (7d) [3].
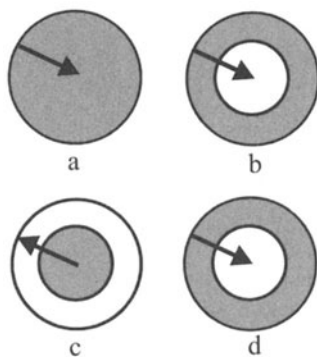
Fig. 7. Distribution of coke inside catalyst particle for: parallel (a, b), and consecutive (c,d) fouling mechanism; arrows indicate direction of spreading of the coke

5.2   Kinetics

A general attempt in deriving deactivation kinetics is to determine catalyst activity as a function of time. This is the basis of predicting catalyst life time. Catalyst activity is defined by the ratio of reaction rate for one of the key feed molecules at time, t, and the rate at the beginning of the process, i. e., with the fresh catalyst (t = 0) [101]:

$$a = \frac{R_i^{\,t}}{R_i^{\,t=0}} \tag{1}$$

The activity term may be applied to the catalytic reaction rate equation in such a way that two independent terms f_1 and f_2 exist:

$$r_i = f_1(T, C_i) \cdot f_2[a_i(t, T, C_i)] \tag{2}$$

Equation (2) is the core of so called *separability:* the kinetic term f_1, which is constant with time-on-stream, and the activity term f_2, which is by its definition the time dependent function, are separated [101,102]. This approach clearly defines the function describing the decay of the rate of the catalytic reaction with time-on-stream [3]. Mainly, by knowing catalyst activity as a function of time, the deactivation rate prevailing at any time can be easily calculated. However, not in all situations of deactivation the two processes, i. e., their rates are separable; only those where deactivation is due to a decrease of active sites are separable. [103]. This can happen as the result of poisoning, or sintering. The turn-over-frequency (TOF) may stay constant or change 14]. Therefore, by tracking the TOF along the decrease of the reaction rate, the deactivation mechanism taking place might be revealed.

The experimental approach for catalyst activity determination requires several concerns. Besides the requirement for selecting appropriate variables (which is in detail explained in section 6), the problem of decoupling catalytic and deactivation kinetics is the real issue for concentration dependent deactivation. Mainly, due to deactivation of the catalyst with time-on-stream, concentration of its gaseous environment changes, which in turn affects the catalytic reaction kinetics (function f_1 in the equation (2)). As a result of the decay the catalytic rate is not only a function of catalyst activity change. To achieve "separable" deactivation conditions *deactivation compensation* has to be applied in order to keep concentrations of the reactants to which the catalyst is exposed constant. This can be done either by changing the concentration of key components, or by changing the total inlet flow [101,102]. Performing the test in a gradientless well-mixed flow reactor, the concentration of the reactant/product stays both uniform and constant as long as the flow change follows the decrease of the catalyst conversion.

A kinetic equation describing a deactivation process, leading finally to a = 0, is given by the following expression [3,101,102]:

$$-r_d = -\frac{da}{dt} = k_d \cdot C_i^{\,\alpha} \cdot a^{\,d} \tag{3}$$

By integration of equation (3), catalyst activity *a* can be expressed as a function of the deactivation rate order *d*, the deactivation rate constant k_d, and the exponent

α determining the dependence of the deactivation rate on the concentration of the key component i affecting deactivation. The analytical solution, however, depends on the order of the deactivation rate. For a first-order deactivation reaction ($d = 1$), the following solution is obtained:

$$a = \exp\left(-k_d^0 \cdot e^{\frac{-E_{a,d}}{RT}} \cdot C_i^{\alpha} \cdot t\right) \tag{4}$$

Once the kinetic parameters of deactivation ($d = 1$, α, k^0_d, $E_{a,d}$) are estimated by applying a regression analysis [104], from equation (4) the catalyst activity decay can be predicted as a function of time-on-stream for a set of experimental parameters, i.e. different temperatures T, and concentrations C_i. Finally, after additional optimization of the objective function, the integrity of the model has to be validated by applying the real process parameters [105].

A practical approach to deactivation stands only for an implicit dependence of activity on time, while its real, explicit dependence is related to the population of active sites which decreases with time-on-stream. The information on the number of active sites is, however, not always available, but by applying a kinetic analysis assuring a probable mechanism it is possible to derive kinetic mechanism parameters [3]. In the case of parallel poisoning with the single site mechanism, e.g., and assuming Langmuir-Hinshelwood kinetics with the rate of deactivation much slower than the catalytic reaction rate, the fraction of active sites ζ is defined as:

$$\zeta = \frac{N_t}{N_0} = \frac{X_0 - X_D}{X_0} = e^{\frac{-k_d K_A C_A}{1 + K_A C_A + K_B C_B} \cdot t} \tag{5}$$

In the equation (5) X_0 and X_D are relative concentrations of the total amount of sites, and deactivated sites, respectively, k_d is the deactivation rate constant, and K_i and C_i are corresponding adsorption constants and concentrations of both the reactant A and the product B. Since the activity dependence on active sites has the identical form to that one on the left-hand side of equation (5), the catalyst activity a (equation (1)) can be replaced by ζ, and it follows [3]:

$$R_r^t = R_r^{t=0} \cdot e^{\frac{-k_d K_A C_A}{1 + K_A C_A + K_B C_B} \cdot t} \tag{6}$$

For sintering, the decrease of the remaining active area S is a good basis for describing the kinetics of sintering:

$$-\frac{dS}{dt} = k_d (S - S_{SS})^d \tag{7}$$

In equation (7), S_{SS} is the active area at a steady state when no further deactivation occurs. d is the order of sintering which is usually 1 or 2 [34,35,106]. A more general approach to modeling of sintering kinetics, however, must include concentration of gaseous environment:

$$-\frac{da}{dt} = k_d (p_i)^{m_1} \dots \cdot p_j^{m_2} (a - a_{SS})^{m_3} \tag{8}$$

where m_i shows dependence of deactivation rate on components of different partial pressures p_i *to* p_j, and a is a measure of sintering which corresponds to S in equation 7 assuming that a is proportional to S [107].

6.   Strategies in Catalyst Deactivation Studies

6.1   Accelerated Deactivation Test

In principle, two main approaches for studying catalyst deactivation are offered: a) the deactivation process is followed in the real process during commercial catalyst operation, or b) the deactivation is mimicked by some experimental means on a smaller scale. Although the first approach always leads to a deactivated catalyst, the information which can be elucidated from its *post mortem* examination after unloading is limited [1]. There is usually an activity profile in flow reactor unless it is a gradientless one which is usually not true. From catalytic fixed-bed it is difficult to derive any kinetics. In addition, deactivation studies in a commercial plant are limited due to narrow operating conditions, imposed to avoid high operational risks and expenses. Therefore, deactivation studies on bench, or laboratory-scale, offering a variety of possibilities for establishing well-defined conditions of deactivation are highly preferential.

    To investigate catalyst deactivation on a smaller scale again two approaches are possible: a) to continuously investigate the catalyst under reaction conditions, or b) to alter catalyst activity by some treatment outside the reaction conditions, and to measure the effect, before and after the treatment [41]. Long-time pilot plant investigation belonging to the first, however, cause high costs for time of manpower and of equipment operation. They are justified only for experimental studies of catalyst lifetime. Preferred to the previous procedures are accelerated deactivation studies, either on pilot-plant, bench, or laboratory level. Such a test has to provide deactivation which will mimic the temporal profile, the rate and the extent of deactivation in the real process. This is a challenging task requiring the identification of deactivation mechanism and kinetics [1,97]. However, due to the scale-up problems these parameters often must not be the same as in industrial conditions, but they have to lead to results by which these conditions responsible for the decay on the big plant can be correlated with the deactivation process. [108]. Conditions chosen for an accelerated deactivation test should not be too far from those in the commercial unit, unless it is of interest to investigate the catalyst ability to tolerate plant malfunction [41].

    The selection of variables for an accelerated study of deactivation depends on its mechanism. For poisoning or coking, variations in temporal and local activity are caused by the concentration of feed molecules influencing deactivation [108]. For sintering, however, increased temperature sometimes is not sufficient, but the concentration of surrounding atmosphere must be considered as well. This is due to differences in mechanisms of thermal and chemical sintering. The later is altered by both variables but with a prevailing influence of the concentration of the reactive components. It is difficult to discriminate between these two mechanisms, but an increase of space velocity in order to obtain high degrees of conversion and hence, to minimize the concentration influence, might be an additional strategy in accelerated catalyst deactivation by sintering [108,109]. Sometimes the selection

of variables is related to a certain catalyst property, such as the ability for regeneration, e.g., in the case of reforming catalysts [110]. For hydrotreating catalysts the resistance to coke might be the clue for choosing either straight-chain or aromatic compounds in order to accelerate deactivation by coking [111].

From a fundamental point of view accelerated catalyst deactivation requires the use of a suitable type of reactor. The selection depends mainly on the specific objective of catalyst research, i.e. whether it is to improve productivity, selectivity, or catalyst life [112]. Preliminary catalyst screening is often performed in a small laboratory fixed-bed reactor of different designs [113]. It may be performed in a gradientless reactor, either of the Berty type [112], or in a fixed-bed reactor with a high external recycle [114]. However, due to mixing the result obtained from back-mixed laboratory reactors is, of course, only representative of a certain local part of the catalyst bed in the commercial plant. It may be required, therefore, in the laboratory to repeat the experiment for several different feed concentrations, or to perform fixed-bed investigations on a pilot-plant level with different bed lengths of the same catalyst type [108]. When using fixed-bed reactors one must be aware of possible non-diabatic conditions as a result of non-uniform concentration of coke along catalyst bed. Only an appropriate reactor design, with independently controlled heaters around the isolation cover, may simulate commercial reactor performance and an adequate heat compensation and hence, reliably information on deactivation phenomena [107,115,116].

6.2   Experimental Strategy for Deactivation Kinetics Investigations, Ag/Al$_2$O$_3$ Catalyst for Ethylene Epoxidation

Sintering is the broadly accepted mechanism of deactivation of Ag-based catalysts for ethylene epoxidation. Therefore both elevated reaction temperature and a broad range of O$_2$ concentration were chosen as parameters to accelerate deactivation of commercial catalyst samples in its original size [109]. This is justified by the fact that in many other cases the rate of sintering does depend on oxygen concentration [15,35,36]. Both reaction temperature and initial O$_2$ concentration were varied in the range from 260 to 280 ^{0}C and from 1.5 to 7.5 vol.% O$_2$; one of these variables was kept constant during a single run: The remaining variables were total pressure 25 bar, 25 vol.% C$_2$H$_4$, 5.5 vol.% CO$_2$, 1.8 ppm of chlorine (as ethyl chloride), the balance to 100 vol.% being N$_2$. In order to avoid interference of sintering with any concomitant deactivation mechanism, conversion was kept at a level common for commercial units.

The experiments were performed in an internally back-mixed reactor (Berty) providing no temperature and concentration gradients throughout the reactor volume, and a high mass flow of reactants through the catalyst bed. The unit was equipped with automatic process control [109]. An experimental procedure aimed to measure solely deactivation kinetics must ascertain that only catalyst activity is time dependent. Therefore, the method of *deactivation compensation* was applied [101,102], by means of contact time variation, i. e., increase with progressing deactivation, resulted in a constant conversion and hence constant concentration of components [109]. Since it is known that a reduced capacity of oxygen adsorption on a commercial Ag/Al$_2$O$_3$ catalyst may be directly correlated to its decayed activity [69], the concentration of O$_2$ in the effluent was chosen as the key variable to

which the degree of catalyst deactivation was related besides temperature. Therefore, O_2 concentration was varied for various deactivation experiments [109].

The outcome of experiments are rates of ethylene consumption and C_2H_4O and CO_2 formation, which then can be converted to the activity function $\mathbf{a} = (t)$. This then allows to correlate the rate of deactivation with the various process variables.

7. Conclusions

Deactivation mechanisms differ by their causes and consequences. Although having separated reasons for their appearance and different impacts on the catalyst, they are often interconnected, even one mechanism being initiated by another. This makes situation fuzzy since the main deactivation mechanism can be a secondary one by order of appearing. Sometimes the main deactivation mechanism can even be masked by another, more benign one.

While poisoning changes the character of active sites, coking or fouling mainly leave the active sites unchanged but suppress their availability to reactants. The influence of ageing on active sites is different, depending on which particular mechanism of ageing occurs, i.e. with or without change of catalyst composition.

Different factors determine the particular mechanism of deactivation: the type of substrate responsible for deactivation (poison, coke), the substrate/catalyst affinity, main and deactivation reaction mechanisms and kinetics, reaction parameters like temperature, concentration and pressure, and finally textural properties of the catalyst and its acidity.

In effort to control deactivation as much as possible, two approaches are offered: either to avoid it when possible, like feed purification, or accept it but minimizing its effects. For the second approach catalyst memory effects have to be acknowledged, by preventing process irregularities as early as in the phase of catalysts fabrication.

Accelerated deactivation tests are powerful tools for studying catalyst deactivation in a relatively short time and at a suitable reactor scale. With properly selected reaction variables and by applying e.g. a deactivation compensation approach in a gradientless reactor, deactivation kinetics can be determined. This can be the basis for further modeling, with the final goal of predicting the catalyst life and its performance in commercial conditions at any time of operation for a given time of reactor.

References

1   B.Delmon, Appl.Catal. **15**, 1, 1985.
2   R.Hughes, *Deactivation of Catalysts*, Academic Press, Inc., London, 1984.
3   J.B.Butt and E.E.Petersen, *Activation, Deactivation and Poisoning of Catalysts*, Academic Press, Inc., New York, 1988.
4   *Catalyst Deactivation*, Edited by B.Delmon and G.F.Froment, Stud.Surf.Sci.Catal. Vol. **6**, 1980.
5   J.B.Butt, in *Catalysis – Science and Technology*, Edited by J.R.Anderson and M.Boudart, Vol **6**, 1, 1985.

6   *Deactivation and Poisoning of Catalysts*, Edited by J.Oudar and H.Wise, Chemical Industries Vol. **20**, 1985.

7   *Catalyst Deactivation 1987*, Edited by B.Delmon and G.F.Froment, Stud.Surf.Sci.Catal. Vol. **34**, 1987.

8   *Catalyst Deactivation*, Edited by E.E.Petersen and A.T.Bell, Chemical Industries Vol. **30**, 1987.

9   *Catalyst Deactivation 1994*, Edited by B.Delmon and G.F.Froment, Stud.Surf.Sci.Catal. Vol. **88**, 1994.

10   *Deactivation and Testing of Hydrocarbon-Processing Catalysts*, Edited by P.O'Connor, T.Takatsuka, and G.L.Woolery, ACS Symposium Series **634**, 1996.

11   D.L.Trimm, in *Handbook of Heterogeneous Catalysis*, Vol. 3, Edited by G.Ertl, H.Knözinger, and J.Weitkamp, VCH Verlagsgesellschaft mbH, Weinheim, 1263, 1997.

12   *Catalyst Deactivation 1999*, Edited by B.Delmon and G.F.Froment, Stud.Surf.Sci.Catal. Vol. **126**, 1999.

13   P. Forzatti and L.Lietti, Catal. Today, **52**, 165, 1999.

14   J.A.Moulijn, A.E.van Diepen, and F.Kapteijn, Appl.Catal. A: General **212**, 3, 2001.

15   H.Bartholomew, Appl.Catal. A: General **212**, 17, 2001.

16   G.F.Froment, Appl.Catal. A: General **212**, 117, 2001.

17   M.Baerns, H.Hofmann, and A.Renken, *Chemische Reaktionstechnik*, Georg Thieme Verlag, Stuttgart, 1999.

18   T.E.Fischer and S.R.Kelemen, J.Catal. **53**, 24, 1978.

19   C.H.Bartholomew, in *Catalyst Deactivation 1987*, Edited by B.Delmon and G.F.Froment, Stud.Surf.Sci.Catal. Vol. **34**, 81, 1987.

20   R.L.Ollendorf, G.Boskovic, J.B.Butt, Appl.Catal. **62**, 85, 1990.

21   B.C.Gates, J.R.Katzer, and G.C.A.Schuit, *Chemistry of Catalytic Processes*, McGraw-Hill Book Company, p.282, New York 1979.

22   P.Lankhorst, H.C.de Jongste, and V.Ponec, in *Catalyst Deactivation*, Edited by B.Delmon and G.F.Froment, Stud.Surf.Sci.Catal. Vol. **6**, 43, 1980.

23   M.Che and C.O.Bennett, Advan.Catal. **36**, 55, 1989.

24   D.E.Damiani and J.B.Butt, J.Catal. **94**, 203, 1985.

25   I.Önal and J.B.Butt, J.C.S.Faraday I, **78**, 1887, 1982.

26   E.E.Petersen, in *Catalyst Deactivation*, Edited by E.E.Petersen and A.T.Bell, Chemical Industries Vol. **30**, 39, 1987.

27   A.T.Bell, in *Catalyst Deactivation*, Edited by E.E.Petersen and A.T.Bell, Chemical Indutries Vol. **30**, 235, 1987.

28   D.L.Trim, in *Deactivation and Poisoning of Catalysts*, Chemical Industries Vol. **20**, 151, 1985.

29   T.Koerts, M.J.A.G.Deelen, and R.A.van Santen, J.Catal. **138**, 399, 1992.

30   G.F.Froment, in *Catalyst Deactivation*, Edited by B.Delmon and G.F.Froment, Stud.Surf.Sci.Catal. Vol. **6**, 1, 1980.

31   D.McCalloh, in *Applied Industrial Catalysis-1*, 69, Edited by B.E.Leach, Academic Press, New York, 1983.

32   M.Guisnet and P.Magnoux, Appl.Catal. 54, 1, 1989.

33   B.Delmon and P.Grange, in *Catalyst Deactivation*, Edited by B.Delmon and G.F.Froment, Stud.Surf.Sci.Catal. Vol. **6**, 507, 1980.

34   G.A.Fuentes and E.D.Gamas, in *Catalyst Deactivation 1991*, Edited by C.H.Bartholomew and J.B.Butt, Stud.Surf.Sci.Catal. Vol. **68**, 637, 1991.

35   C.H.Bartholomew, Appl.Catal. A: General **107**, 1, 1993.

36   C.H.Bartholomew, in *Catalyst Deactivation 1994*, Edited by B.Delmon and G.F.Froment, Stud.Surf.Sci.Catal. Vol. **88**, 1, 1994.

37   S.H.Park, M.S.Tzou, and W.M.H.Sachtler, Appl.Catal. **24**, 85, 1986.

38   E.Ruckenstein and B.Pulvermacher, AIChE J. **19**, 356, 1973.

39   P.C.Flynn and S.E.Wanke, J.Catal. **34**, 390, 400, 1974.

40   E.Ruckenstein, in *Catalyst Deactivation 1991*, Edited by C.H.Bartholomew and J.B.Butt, Stud.Surf.Sci.Catal. Vol. **68**, 585, 1991.

41   N.Pernicone, Appl.Catal. **15**, 17, 1985.

42   Y.Murakami, S.Komai, and T.Hattori, in *Catalyst Deactivation 1991*, Edited by C.H.Bartholomew and J.B.Butt, Stud.Surf.Sci.Catal. Vol. **68**, 645, 1991.

43   D.J.Young, P.Udaja, and D.L.Trimm, in *Catalyst Deactivation*, Edited by B.Delmon and G.F.Froment, Stud.Surf.Sci.Catal. Vol. **6**, 331, 1980.

44   S.A.Eliason and C.H.Barholomew, Appl.Catal. A: General **186**, 229, 1999.

45   A.Arteaga, J.L.G.Fierro, P.Grange, and B.Delmon, in *Catalyst Deactivation 1987*, Edited by B.Delmon and G.F.Froment, Stud.Surf.Sci.Catal. Vol. **34**, 59, 1987.

46   J.H.C.van Hooff and J.W.Roelofsen, in *Introduction to Zeolite Science and Practice*, Stud.Surf.Sci.Catal. Vol. **58**, 241, 1991.

47   T.Wang, C.Lee, and L.D.Schmidt, Surf.Sci. **163**, 181, 1985.

48   X.E.Verikios, E.P.Stein, and R.W.Coughlin, J.Catal. **66**, 368, 1980.

49   J.W.Gosselink and J.A.R.van Veen in *Catalyst Deactivation 1999*, Edited by B.Delmon and G.F.Froment, Stud.Surf.Sci.Catal. Vol. **126**, 3, 1999.

50   B.Mercier des Rochettes, C.Marcilly, C.Gueguen, and J.Bousquet, in *Catalyst Deactivation 1987*, Edited by B.Delmon and G.F.Froment, Stud.Surf.Sci.Catal. Vol. **34**, 589, 1987.

51   M.Guisnet and P.Magnoux, in *Catalyst Deactivation 1994*, Edited by B.Delmon and G.F.Froment, Stud.Surf.Sci.Catal. Vol. **88**, 53, 1994.

52   P.O'Connor and A.C.Pouwels in *Catalyst Deactivation 1994*, Edited by B.Delmon and G.F.Froment, Stud.Surf.Sci.Catal. Vol. **88**, 129, 1994.

53   L.T.Boock, T.F.Petti, and J.A.Rudesil, ASC Div.Petrol.Chem., **40**, 3, 421, 1995.

54   X.Zhao and W.C.Cheng, in *Deactivation and Testing of Hydrocarbon-Processing Catalysts*, Edited by P.O'Connor, T.Takatsuka, and G.L.Woolery, ACS Symposium Series **634**, 159, 1996.

55   H.Topsoe, B.S.Clausen, and F.E.Massoth, in *Hydrotreating Catalyst*, Edited by J.R.Anderson and M.Boudart, Catal.Sci&Techn. Vol.**11**, 1, 1996.

56   E.Furimsky and F.E.Massoth, Catal.Today **52**, 381, 1999.

57   H.Seki and M.Yoshimoto, Fuel Proc.Techn., **69**, 229, 2001.

58   P.Zeuthen, J.Bartholdy, P.Wiwel, and B.H.Cooper in *Catalyst Deactivation 1994*, Edited by B.Delmon and G.F.Froment, Stud.Surf.Sci.Catal. Vol. **88**, 199, 1994.

59   M.Absi-Halabi and A.Stanislaus, in *Deactivation and Testing of Hydrocarbon-Processing Catalysts*, Edited by P.O'Connor, T.Takatsuka, and G.L.Woolery, ACS Symposium Series **634**, 229, 1996.

60   S.T.Sie, in *Catalyst Deactivation*, Edited by B.Delmon and G.F.Froment, Stud.Surf.Sci.Catal. Vol. **6**, 545, 1980.

61   M.D.Edgar in *Applied Industrial Catalysis -1*, Edited by B.E.Leach, Academic Press, 123, New York 1983.

62   J.-P.Franck and G.P.Martino, in *Deactivation and Poisoning of Catalysts*, Edited by J.Oudar and H.Wise, Chemical Industries Vol. **20**, 205, 1985.

63   J.Barbier, in *Catalyst Deactivation 1987*, Edited by B.Delmon and G.F.Froment, Stud.Surf.Sci.Catal. Vol. **34**, 1, 1987.

64   J.P.Bournoville and G.Martino, in *Catalyst Deactivation*, Edited by B.Delmon and G.F.Froment, Stud.Surf.Sci.Catal. Vol. **6**, 159, 1980.

65   See for example: US 4740493; US 5374748; US 4994588; US 2279470; US 2194602; EP 207550A1; EP 243996B1; EP 255975

66   R.B.Grant and R.M.Lambert, J.Catal. **92**, 364, 1985.

67   R.A.van Santen and C.P.M. de Groot, J.Catal. **98**, 530, 1986.

68   J.T.Gleaves, A.G.Sault, R.J.Madix, and J.R.Ebner, J.Catal. **121**, 202, 1990.

69   A.Bruckner, E.Kondratenko, H.Berndt, D.Muller and M.Baerns, Proc. North Amer.Catal.Society, Toronto 2001, Book of Abstracts

70   G.L.Montrasi, G.R.Tauszik, M.Solari, and G.Leofanti, Appl.Catal. **5**, 359, 1983.

71   E.T.McBee, H.B.Hass, and P.A.Wiseman, Ind.Eng.Chem. Vol.**37**, 3, 432, 1945.

72   S.A.Tan, R.B.Grant, and R.M.Lambert, J.Catal. **100**, 383, 1986.

73   K.L.Yeung, A.Gavriilidis, A.Varma, and M.M.Bhasin, J.Catal. **174**, 1, 1998.

74   I.E.Wachs and S.R.Kelemen, in *New Horizons in Catalysis*, Edited by T.Seiyama and K.Tanabe, Elsevier, 682, Tokyo, 1981.

75   B.Grife, E.Blues, and D.B.Smith, Appl.Catal. **10**, 303, 1984.

76   S.A.Tan, R.B.Grant, and R.M.Lambert, Appl.Catal. **31**, 159, 1987.

77   A.E.B.Presland, G.L.Price, and D.L.Trimm, J.Catal. **26**, 313, 1972.

78   G.B.Hoflund and D.M.Minahan, J.Catal. **162**, 48, 1996.

79   J.C.Wu and P.Harriot, J.Catal. **39**, 395, 1975.

80   M.Shelef and R.W.McCabe, Catal.Today **62**, 35, 2000.

81   M.Ivamoto, N.Mizuno, and H.Yahiro, in *New Frontiers in Catalysis*, Edited by L.Guczi, F.Solymosi, and P.Tetenyi, Elsevier Sci.Publ. and Akademiai Kiado, Budapest, 1258, 1993.

82   A.Obuchi, A.Ohi, M.Nakamura, A.Ogata, K.Mizuno, and H.Ohuchi, Appl.Catal. B: Environ. **2**, 71, 1993.

83   C.M.Pradier, H.Lu, and P.Dubot, in *Catalyst Deactivation 1999*, Edited by B.Delmon and G.F.Froment, Stud.Surf.Sci.Catal. Vol. **126**, 249, 1999.

84   J.L.d'Itri and W.M.H.Sachtler, Appl.Catal. B: Environ. **2**, L7, 1993.

85   R.A.Grinsted, H.-W.Jen, C.N.Montreuil, M.J.Rokosz, and M.Shelef, Zeolites **13**, 602, 1993.

86   K.C.C.Kharas, H.J.Robota, and D.J.Liu, Appl.Catal. B: Environ. **2**, 225, 1993.

87   K.C.C.Kharas, H.J.Robota, and A.Datye, in *Environmental Catalysis*, ACS Symposium Series **552**, 39, 1994.

88   S.A.Gomez, A.Campero, A.Martinez-Hernandez, and G.A.Fuentes, Appl. Catal., **197**, 157, 2000.

89   R.J.Bertolacini and R.J.Pelet, in *Catalyst Deactivation*, Edited by B.Delmon and G.F.Froment, Stud.Surf.Sci.Catal. Vol. **6**, 73, 1980.

90   E.E.Petersen in *Catalyst Deactivation 1997*, Edited by C.H.Bartholomew and G.A.Fuentes, Stud.Surf.Sci.Catal.Vol.**111**, 87, 1997

91   R.A.Hadden, J.C.Howe, and K.C.Waugh, in *Catalyst Deactivation 1991*, Edited by C.H.Bartholomew and J.B.Butt, Stud.Surf.Sci.Catal. Vol. **68**, 177, 1991.

92   M.S.Tzou, H.J.Jiang, and W.M.H.Sachtler, Appl.Catal. **20**, 231, 1986.

93   A.Parmaliana, F.Frusteri, G.A.Nesterov, E.A.Paukshtis, and N.Giordano, in *Catalyst Deactivation 1987*, Edited by B.Delmon and G.F.Froment, Stud.Surf.Sci.Catal. Vol. **34**, 197, 1987.

94   B.Delmon, in *Catalyst Deactivation 1994*, Edited by B.Delmon and G.F.Froment, Stud.Surf.Sci.Catal. Vol. **88**, 113, 1994.

95   M.Guisnet, P.Magnoux, Catal.Today, **36**, 477, 1997.

96   S.v.Donk, J.H.Bitter, and K.P.d.Jong, Appl.Catal. A: General **212**, 97 2001.

97   J.Haber, J.H.Block, and B.Delmon, Pure&Appl.Chem. Vol. **67**, 8/9, 1257, 1995.

98   D.L.Trimm in *Deactivation and Poisoning of Catalysts*, Edited by J.Oudar and H.Wise, Chemical Industries Vol. **20**, 151, 1985.

99   R.M.Neducin, G.Boskovic, E.Kis, G.Lomic, H.Hantsche, R.Micic, and P.Pavlovic, Appl.Catal. A: General **107**, 133, 1994.

100 E.Kis, G.Lomic, G.Boskovic, R.M.Neducin, and P.Putanov, J.Therm.Anal. **44**, 1367, 1995.

101 O.Levespiel, J.Catal. **25**, 265, 1972.

102 O.Levenspiel, *Omnibook*, Corvallis, Oregon 1984.

103 J.Klose, M.Baerns, J.Catal. **85**, 105, 1984.

104 F.Kapteijn and J.A.Moulijn in *Handbook of Heterogeneous Cataly*sis, Edited by G.Ertl, H.Knözinger, and J.Weitkamp, VCH Verlagsgesellschaft mbH, Weinheim, 1189, 1997.

105 G.Boskovic, N.Dropka, D.Wolf, A.Bruckner, and M.Baerns, submitted to Appl. Catal.

106 G.A.Fuentes, Appl.Catal. **15**, 33, 1985.

107 R.Christoph and M.Baerns, in *Catalyst deactivation 1987*, Edited by B.Delmon and G.F.Froment, Stud.Surf.Sci.Catal. Stud.Surf.Sci.Catal. Vol. **34**, 355, 1987.

108 J.J.Birtill in *Catalyst Deactivation*, Edited by B.Delmon and G.F.Froment, Stud.Surf.Sci.Catal. Vol. **126**, 43, 1999.

109 G.Boskovic, D.Wolf, A.Bruckner, and M.Baerns, submitted to Appl. Catal.

110 P.Sarrazin, JP.Boitiaux, M.Berthelin, and J.C.Plumail, Catal.Today **11**, 93, 1991.

111 B.Dabyburjor, Z.Liu, S.Matoba, S.Osanai, and T.Shirooka, in *Catalyst Deactivation 1994*, Edited by B.Delmon and G.F.Froment, Stud.Surf.Sci.Catal. Vol. **88**, 273, 1994.

112 J.V.Porcelli, Catal.Rev.-Sci.Eng., **23**(1&2),151, 1981.

113 L.Forni, Catal.Today 34, 353, 1997.

114 J.M.Oelderik, S.T.Sie, and D.Bode, Appl.Catal. **47**, 1, 1989.

115 J.R. Rostrup-Nielsen, A.Skov, and J.Christiansen, Appl.Catal. **22**, 71, 1986.

116 S.T.Sie and P.M.M.Blauwhoff, Catal.Today, **11**, 103, 1991.

Divided Catalytic Processes

Contents

Divided Catalytic Processes

Harald Seiler[1] and Gerhard Emig[2]

[1] Degussa AG, Verfahrens- & Prozesstechnik, Paul-Baumann-Str. 1,
45764 Marl, Germany
harald.seiler@degussa.com
[2] Universität Erlangen-Nürnberg, Technische Chemie I, Egerlandstr. 3,
91058 Erlangen, Germany
emig@tc.uni-erlangen.de

Abstract. This chapter is concerned with *divided catalytic processes*, a topic which is still an innovative concept in chemical reaction engineering, but which has meanwhile become a known and applied one. *Divided catalytic processes* belong to the class of unsteady state reaction processes, specifically to the class of forced periodic processes (see for example [1,2]). They are an extreme form of modulation of initial concentrations and can only be used in heterogeneous catalysis. A description of the principle and history of divided catalytic processes will be given, together with specific examples. After a short view on reactor designs with industrial potential, advantages and disadvantages of the processes will also be considered. Finally, industrial application of this concept in reaction engineering will be described. Not only scientific research associations assume that, with increasing research, thus increasing knowledge and experience, periodic operation of chemical reactors will establish itself as a possible method of operation which promises success [3].

1   Principle

Divided catalytic processes as a concept in reaction engineering can be employed to heterogeneously catalysed gas-phase reactions which have more than one feed component and one or more chemical elements which are transferred between gas-phase and solid-phase (= catalyst). During a non-divided (i.e. steady-state) catalytic process, this transfer continuously takes place, so it cannot be recognised in an integral manner. A well investigated class of these reactions are those where reduction and oxidation of the solid catalyst proceed simultaneously under steady-state reaction conditions (mechanism as specified by Mars and van Krevelen [4])[1].

---

[1] The term *reduction* or *oxidation* here refers to the solid catalyst or, more precisely, to the relevant metal component(s).

The principle of divided catalytic processes is to divide such heterogeneously catalysed gas-phase reactions into two individual steps (e.g. reduction and oxidation) which proceed separately in space or time. Hence, the solid acts no longer as a catalyst, but as a reactant; the heterogeneously catalysed gas-phase reaction breaks down into two independent gas-solid reactions (see Fig. 1).

$$\text{in. comp.} + \langle O \rangle \xrightarrow{\text{(cat.)}} \text{prod. 1 (+ prod. 2)} \qquad \text{(Catalysis)}$$

$$\text{in. comp.} + \text{"cat."}_{ox.} \longrightarrow \text{prod. 1} + \text{"cat."}_{red} \qquad \text{(Reduction)}$$

$$\text{"cat."}_{red} + \langle O \rangle \longrightarrow \text{"cat."}_{ox} (+ \text{ prod. 2}) \qquad \text{(Oxidation)}$$
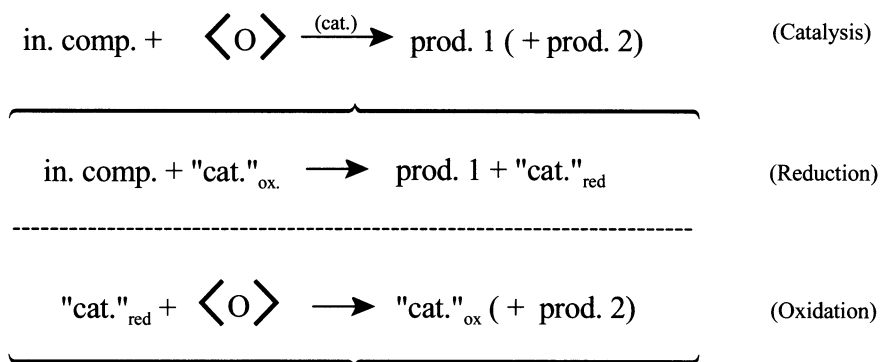
Fig. 1. A divided catalytic process using the example of a partial oxidation of the gas-phase initial component "in. comp." to the main product "prod. 1" with the catalyst "cat.", whereby a side-product "prod. 2" can be formed. ("cat."$_{ox}$ and "cat."$_{red}$ dedicate the oxidised and reduced form of the solid; <O> stands for an oxygen source)

A more general classification of divided catalytic processes as dynamic operated catalytic processes will describe them as forced unsteady state processes with periodic modulation of the initial concentrations [1,2,5]. This is because during a periodic repetition of a divided catalytic process, the change of inlet components between two successive steps is like an extreme variation of the concentrations in the inlet stream. The concentrations are varied so greatly, that only some or one of the initial components are fed to the reactor, respectively.

2   History and Examples

It is usually assumed that the concept of divided catalytic processes was first proposed by Lewis et al. [6] in 1949. The authors studied the reaction of methane reforming in the presence of copper(II) oxide (CuO) as a divided catalytic process.

$$CuO + CH_4 \longrightarrow Cu + CO + 2 H_2 \qquad \text{(Step 1)}$$

$$Cu + \tfrac{1}{2} O_2 \longrightarrow CuO \qquad \text{(Step 2)}$$

The advantages specified for this system were the use of air as oxidising agent and the improved thermal balance. For partial oxidation reactions where reduction

and oxidation processes proceed on the solid, the commonly given historical data are correct. But if *divided catalytic processes* are considered to be a general principle – where other elements beside oxygen can be transferred between gas and solid phase –, the first reference was as early as 1889. The invention by Mond [7], which was published at this time, included splitting the Deacon process [8] (Eq. (1)) for the recovery of chlorine (Cl_2) from hydrogen chloride (HCl)

$$2\,HCl + \frac{1}{2}\,O_2 \quad \longleftrightarrow \quad Cl_2 + H_2O \tag{1}$$

into a chlorination step and a dechlorination step in the presence of doped magnesium oxide (MgO/KCl). This two-step process variant was further developed and was finally applied by Minet et al. [9-12] to the catalyst favoured by Deacon containing copper (Cu) as active component [2] (for the history and chemistry see also Pan et al. [10]).

$$CuO + HCl \quad \rightleftharpoons \quad Cu(OH)Cl \tag{Step 1}$$

$$2\,Cu(OH)Cl \quad \rightleftharpoons \quad Cu_2OCl_2 + H_2O \tag{Step 1}$$

$$Cu_2OCl_2 \quad \rightleftharpoons \quad CuO + CuCl_2 \tag{Step 1}$$

$$CuCl_2 \quad \rightleftharpoons \quad CuCl + \frac{1}{2}\,Cl_2 \tag{Step 2}$$

$$2\,CuCl + \frac{1}{2}\,O_2 \quad \rightleftharpoons \quad CuCl_2 + CuO \tag{Step 2}$$
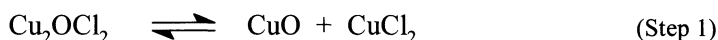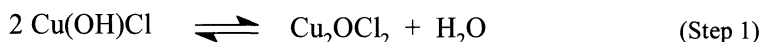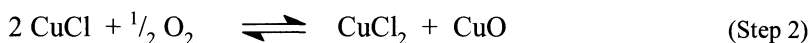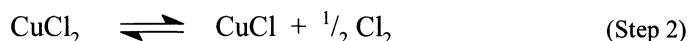
The advantages resulting from dividing the chlorination and dechlorination step are significantly decreased corrosion problems in the chlorine work-up section owing to the lack of hydrogen chloride, and overcoming the thermodynamic equilibrium of the reaction (1)[3] (see also [13]).

Relatively soon after the divided catalytic process concept had been published for methane reforming, it was considered for industrial use. In 1956 Krönig et al. [14] filed a patent claiming the beneficial use of divided catalytic oxidehydrogenation processes for dehydrogenation reactions. Improvements in partial oxidations, using the examples of the oxidation and ammoxidation of propene, were promised by *SOHIO* (= *Standard Oil Co. of Ohio*; since 1987, *BP America*), which had made a detailed study of these systems in the 1960s on a laboratory scale [15]. This concept was later successfully applied to other reactions:

---

[2] Although the reaction mechanism shown here also contains a reduction-oxidation cycle, with respect to the solid, this cycle takes place completely in step 2, so it is not divided. Divided is the absorption and release of chlorine atoms as well as of oxygen atoms.

[3] The thermodynamic equilibrium is overcome in this open system as a result of different temperature regions for the independent steps 1 and 2, where certain reactions of the solids proceed preferentially.

- Ammoxidation of toluene and of xylene isomers to benzonitrile and dicyanobenzene isomers, respectively (*C-E Lummus*, USA [16][2])
- Oxidation of n-butane to maleic anhydride (*DuPont*, USA [17,18] [1,2,3])
- Oxidehydrogenation of isobutyraldehyde to methacrolein (*University of Erlangen-Nürnberg*, Germany [19] [1])
- Oxidehydrogenation of ethane to ethene (*University of Reading*, United Kingdom [20] [1])
- Oxidehydrogenation of ethylbenzene to styrene (*BASF*, Germany [21-24] [1])
- Oxidehydrogenation of isobutyric acid to methacrylic acid (*University of Erlangen-Nürnberg*, Germany [25, 26] [1])
- Oxidehydrogenation of propane to propene (*Polish Academy of Sciences*, Poland, [27] [1] and *University of Waterloo*, Canada [28,29] [1] and the *Institut de Recherches sur la Catalyse, Villeurbanne*, France [30] [1])
- Oxidative coupling of toluene to 1,2-diphenylethane (*Ecole Polytechnique Fédérale de Lausanne*, Switzerland [31] [1])
- Oxidative coupling of isobutene to 2,5-dimethyl-1,5-hexadiene (*University of Erlangen-Nürnberg*, Germany [32,33] [1])
- Oxidation of propene to acrolein (*DuPont*, USA, and *AtoChem*, France [34] [2])
- Oxidation of acrolein to acrylic acid (*Technical University of Darmstadt*, Germany [35] [1])

Key: [1] = laboratory scale; [2] = pilot scale; [3] = production

3   Reaction Equipment

In order to implement divided catalytic processes in industrial production, special reactor designs are required which enable a periodic sequence of gas-phase feed change to the solid catalyst. In principle, it is possible to separate the individual steps either in time or in space.

When the catalytic process is separated in time, a fixed-bed reactor will be used. The latter is operated in the unsteady state by periodically changing the feed stream, so the solid remains in the reactor (see Fig. 2a). For industrial applications, downstream units should be supplied with a continuous, rather than a discontinuous, product stream. This may be achieved by connecting an appropriate number of periodically operated fixed-bed reactors with a phase shift in parallel. Purge steps have to be taken into account where applicable.

The oxidehydrogenation of ethylbenzene as mentioned above may serve as an example of a process in periodically operated fixed-bed reactors. Approximately 22 % of elemental oxygen (O) which are theoretically available (completely oxidised state) are exchanged between the gas and the solid per individual step in one fixed-bed reactor. With this amount 53 $g_{product}/kg_{cat}$ or with respect to the cycle time 2.65 $g_{product}/kg_{cat}/h_{cyc}$ can be produced (data used from [24]). The advantages of fixed-bed reactors over fluidized beds are especially the adjustable narrow residence time distribution[4] and the purely static mechanical strain on the solid.

---

[4] Narrow residence time distributions permit more optimised reaction times for all molecules, so a higher global selectivity can be reached.
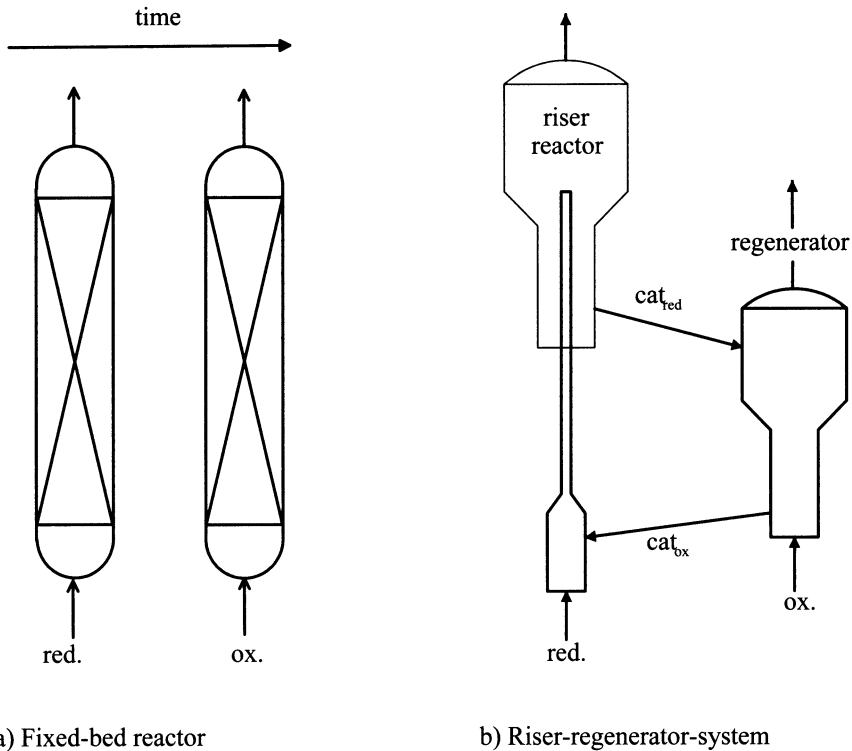
Fig. 2. Reactor designs for divided catalytic processes with reduction and oxidation of the catalyst as example:
a) separation in time in a periodically operated fixed-bed reactor;
b) separation in space in the riser-regenerator system;
(red = feed reducing agent; ox = feed oxidising agent; cat = transported solid catalyst)

Riser-regenerator systems (see Fig. 2 b) operate with a spatial separation of the reduction and oxidation steps, and these systems are commonly used for fluid-catalytic-cracking (= FCC) (see e.g. [36]). This type of reactor is used especially in the case of very fast reactions which release a lot of energy or have a tendency towards overreduction of the catalyst[5]. A well-known example is the synthesis of maleic anhydride where approximately 2.6 % of elemental oxygen (O) which is theoretically available (completely oxidised state) are exchanged between the gas and the solid per pass through the riser reactor. With this amount, 0.63 $g_{product}/kg_{cat}$ or, with respect to the cycle time, 24 $g_{product}/kg_{cat}/h_{cyc}$ can be produced (data used from [18]). For the synthesis of acrolein, data are available [34] which yield

---

[5] Overreduction: The amount of oxygen removed from the solid catalyst is so high that the original structure cannot be reconstituted during (re-)oxidation and the process becomes irreversible [37] (see also Section 5.4, page 10).

0.05 % exchangeable oxygen (O) and 0.062 $g_{product}/kg_{cat}$ or 0.44 $g_{product}/kg_{cat}/h_{cyc}$ product. Further advantages of fluidized-beds or riser-regenerator systems are the higher effective reaction rate, which depends on the degree of pore efficiency, and the easier introduction and removal of the solid.

If the riser reactor is replaced by a (second) fluidised bed, this also leads to a spatial separation between reaction and regeneration, but then both steps are operated with longer residence times (see e.g. [12]). The Deacon process is an example: here, the reactor concept permits 9 % of the theoretically available chlorine atoms (Cl) to be exchanged. Hence, the amount of Cl_2 which can be produced is 20 $g_{product}/kg_{cat}$ or, with respect to the cycle time, 34 $g_{product}/kg_{cat}/h_{cyc}$ (data used from [11]).

Moving-bed reactors reveal a further possibility of spatial separation in reactions during which the oxygen in the solid is consumed very slowly, or the available amount is correspondingly large [38]. These have been applied especially to the periodic reduction and oxidation of iron in the steam-iron process (see Casper [39], Chapters 2 and 5).

The choice of reactor type is affected to a great extent by energetic and, thus, economic aspects as well as safety reasons, as discussed by Cavani and Trifirò [40] for selective oxidations of alkanes. Both principles of reactor design (separation in time or space) have already been successfully applied to divide the reaction and regeneration steps. The majority of applications going beyond the laboratory scale involve riser-regenerator systems, as shown by the examples of the ammoxidation of toluene [16] or the oxidation of n-butane [18,41-46]. The approach of periodically operated fixed-bed reactors has been studied extensively for the oxidehydrogenation of ethylbenzene [22,24] and of isobutyric acid [25].

For completing the description of reactor types used for reduction-oxidation cycles, the pulse reactor has to be mentioned, too. This reactor type has repeatedly been described in literature. The experiments in the pulse reactor have been carried out to study the behaviour of the catalyst [27,30,47,48], to explain reaction mechanisms [28,29,37,38] or to assess in a fundamental manner the possible application of divided catalytic processes [20,23,25,28,29,35,49]. However, this reactor design seems not to be suitable for the production scale.

4   Advantages

The advantages of all or some of the processes listed in Section 2 are discussed in separate subsections below:

4.1   Increased Selectivity

The application of the concept of divided catalytic processes for all of the systems listed in Section 2 results in a decrease of the total oxidation and, thus, in a noticeable increase (by 5 through 40 percent relatively) of the product selectivity with regard to the reactant to be converted. However, the yield can be increased only for some of the processes. The reasons are the decreased activity of lattice oxygen, or either the slow diffusion of oxygen from the bulk of the solid phase to the surface becomes rate determining, as well as a decrease in time of the oxygen

supply (= conversion decreases with time during a single reaction step). Therefore, the measured time-averaged yields are mostly increased by only about 1 - 30 % relative to the yield of a conventional process – and only in exceptional cases by up to 100 % [31].

A number of possible reasons for the selectivity improvement have been discussed in literature. Originally, it was assumed that the absence of oxygen molecules as free radicals prevented total oxidation [15,16]. Subsequently, it was found that adsorbed oxygen species (O_2^- or O^-) especially promote the total oxidation [50]. Since total oxidation has repeatedly been observed to be unavoidable in processes which have been carried out as divided catalytic processes [25,33,51], the discussion which steps are selective or non-selective has not come to a conclusion [51,52]. For example, Creaser et al. [28,29] have found for the oxidehydrogenation of propane that both, adsorbed oxygen and lattice oxygen, lead to total oxidation.

A further approach explaining the increased selectivity is based on the mechanism for heterogeneous catalysis of oxidation reactions in the presence of oxygen-transfer metal catalysts, proposed by Mars and van Krevelen [4]. The reduction-oxidation cycle of the metal must settle during the conventional mode of steady-state operation such that the slower of the two reaction steps is rate-determining. The metal catalyst is thus in an oxidation state which may not be optimal for the reaction to yield the target product (see also [2]). In contrast, during the divided process, the ideal oxidation state for the reaction to the target product can be utilised [17,26,28,29,41,42]. Pugsley et al. [43] pursue a similar approach, which explains the improved selectivity as due to changes in concentration ratios and thus to different reaction rates (= purely kinetic aspects).

4.2   Optimum Control of the Separate Processes

The separation of the reduction and oxidation steps in space or time makes the independent optimisation of the conditions for the two separate processes possible. This involves optimising pressure, temperature, initial concentrations and residence time. The advantages which can be achieved by proper control of the separate processes have been shown by Hagemeyer, Watzenberger et al., using as examples the parameters *temperature* [21,24] and *residence time* [22].

4.3   Increased Initial Concentrations in the Feed Stream

Depending on the reaction system, divided catalytic processes offer the advantage of markedly increasing the concentration of the component which is to be reacted in the feed stream. Due to the absence of oxygen, firstly, explosive mixtures cannot be formed [16,41] and, secondly, runaways in the adiabatic or approximately adiabatic state cannot occur [16]. Runaways can be substantially avoided because the reaction automatically comes to a standstill when the active lattice oxygen in the solid has been consumed. The increase in the concentration of the reactive component results in a higher conversion rate, reduces the separation requirements downstream of the reactor and requires smaller units for gas transportation.

4.4   Decreased Separation Effort

In addition to higher concentrations in the product stream, other aspects play an important role here. Increases in selectivity and increased conversion rates (see paragraphs 4.1 and 4.2) minimise the separation requirement. Since the oxidation step takes place independently, the offgas from the oxidation step need not be passed on to the product purification. If air is used as the oxidising agent, this prevents passing huge amounts of nitrogen (as present in the air) through the separation units [15]. Depending on the product spectrum, downstream of the production step there is the possibility that – after removing the main product – the residual gas stream need not be cleaned further. Unwanted by-products could be oxidised completely within a subsequent oxidation step and the gas stream discharged as exhaust gas [16]. It can also be advantageous for the downstream separation to have additionally installed nitrogen purge steps, during which adsorbed carbon dioxide CO_2 from the oxidation step, for example, is removed from the system and thus does not enter the product purification steps [53].

4.5   Reduced Catalyst Mass

In addition to the increase in selectivity, the optimised mode of operating the individual separated steps (see paragraphs 4.1 and 4.2) leads to higher space-time yields (STY = mass product/(mass of catalyst × reaction time))[6], so that the mass of catalyst required can be reduced by up to 50 % [42]. Here, the total mass of the catalyst in the whole equipment, dedicated to reduction and oxidation steps, must be taken into account. For processes separated in time in a single apparatus, the same applies with respect to the reaction time, which is than the whole time of all single steps. In addition, the deactivation of the catalyst by progressive coking can be prevented. The reason is that species adsorbed on the solid catalyst – reacting in a conventional process further to form coke precursors or coke – are completely oxidised during the separate oxidation step and, thus, are removed from the catalyst's surface [26,44].

5   Disadvantages

In addition to the above mentioned advantages of divided catalytic processes, other aspects which may appear to be disadvantageous must be considered.

5.1   Additional Equipment Requirements

Depending on the design of the reaction apparatus, additional components such as switching valves to change the feed stream or additional equipment such as

---

[6] The term *space-time yield* is correct only indirectly in this context, since catalyst mass and reactor volume are not directly proportional to each other. The term *mass-time yield* would be logically correct, but is not common. W*eight hourly space velocity* (= WHSV) is often used, but WHSV can also rely on the mass of the materials fed.

regenerators or other fixed-bed reactors must be installed (see also Section 3). This additional expense is acceptable under some circumstances owing to higher selectivities and yields (see e.g. [41]) or higher space-time yields (see e.g. [16]).

5.2 Increased Energy Consumption

Especially using a riser-regenerator system is accompanied by an increased energy consumption. This is due to the continuous pneumatic transport of the high mass of solid which depends both on the number of oxygen atoms required per formula conversion and on the amount of oxygen released per mass of solid catalyst (see e.g. [24,32,33]). The purpose here is to find optimised catalysts which – in addition to high yields – also ensure high, controlled oxygen release over a long period[7].

5.3 Increased Material Consumption

The high abrasion of solids in riser-regenerator systems leads to a more rapid consumption of the solid, so this must be replaced batchwise or continuously. However, specific research and further development of the solid catalyst can lead to very stable and thus longer-living catalysts. As example Contractor et al. [44] introduced a highly suitable catalyst for oxidising n-butane to maleic anhydride.

Particularly when fixed-bed reactors are used, it might be necessary to install additional purge steps (usually applying nitrogen N_2) [22,53]. These act to remove adsorbed components which may decrease selectivity or prevent reoxidation [53], as well as to avoid explosive mixtures during the switch from reducing gas to oxidising gas.

5.4 Required Cycle Stability of the Solid Catalyst

The fundamental criterion with which every solid catalyst must comply if it is to be used in divided catalytic processes, is the ability to undergo a large number of reduction-oxidation cycles without loss of activity or selectivity (= cycle stability). The cycle stability is only ensured if both the chemical and mechanical preconditions are satisfied.

Chemically, the cycle stability is ensured when the reduction and oxidation steps are completely reversible. This is not always the case, as shown by the studies of Ilkenhans et al. [37] on heteropoly acids which decompose under strong reduction, forming stable MoO_3 phases. The tendency towards deactivation because of reduction of the solid below a certain oxygen content (= overreduction) is also known with other catalysts such as vanadium(V) oxide V_2O_5 [42] and pure as well as modified bismuth oxide Bi_2O_3 [32,33]. Permanent deactivation can be prevented in the case of heteropoly acids by constant addition of steam to the feed [26] (an explanation is given in [37]).

---

[7] The parameter which should be used here is the mass-specific space-time yield as *(mass of product)/(mass of catalyst)/(contact time* or *cycle time,* respectively).

Mechanical impairment of the cycle stability is caused by the constant change in solid structures during the individual, separated steps [16,54]. Changes in volume due to different densities in the reduced and oxidised state and changes in the crystal structure are particularly noticeable here. This problem may be circumvented by using supported catalysts, for example, since the active phase is stabilised by an inert support – at least in its basic structure – and mechanical strains are absorbed by the support.

Adequate cycle stability of the solid catalyst is therefore considered crucial for implementing a given divided catalytic process in industrial production. Therefore, intensive studies of the cycle-dependent behaviour are the fundamental basis for further action. Detailed studies of the processes during reduction and oxidation as have been carried out, for example, by Ilkenhans et al. [37,48] or in an introductory manner by Hiltner [32,33], must not be underestimated here.

5.5   Overreactive Behaviour After the Oxidation Step

Hagemeyer et al. [21,22] observed increased total oxidation of ethylbenzene at the beginning of the dehydrogenation step (reduction) during the divided catalytic oxidative dehydrogenation to styrene over a bismuth oxide catalyst. This is due to the high activity after the (complete) catalyst (re-)oxidation. The higher activity can be counteracted by the modes of operation patented by *BASF*, Germany. Thus Hagemeyer et al. propose as a solution varying the temperature between reduction and oxidation [21] or changing the temperature profile during the reduction by varying the inert gas content [22].

6   Industrial Application

It is definitely useful to survey the known existing industrial applications of a new technique under investigation, because if this technique has already been used for industrial production, it meets the usual requirements (such as economic efficiency, availability of materials and operational reliability).

Generally, the only unsteady state processes with short duration times which have potential for industrial use are those which can be repeated in the same way in high numbers – means they can be operated periodically [55,56]. Only in this way can the advantages of the unsteady state operation mode be combined with steady-state production. The discussed divided catalytic processes can be periodically operated, so that corresponding potential may be expected. Unfortunately, information on the use of new technologies in industry is relatively difficult to obtain, so that only a few examples can be mentioned.

Divided catalytic processes in which the catalyst is cyclically reduced and oxidised have appeared in industrial production only slowly. The first application was planned towards the end of the 1960s by *SOHIO* (now *BP America*) in the oxidation of propene [15]. Its introduction as a production process was prevented shortly before the planning stage by an improvement in the catalyst for the (non-divided) steady-state process.

Another attempt to use divided catalytic processes in a production process was made at *DuPont* for producing maleic anhydride from n-butane at the beginning of

the 1990s [57]. A recent article gives some insight into the current state of the production process [18]. It was found that despite thorough preliminary testing and moderate scale-up factors, the implementation of the novel process design in the production scale raises additional problems. However, it is also shown that after three years of intensive work, the production plant is now achieving its nominal capacity. For this reason it is not surprising that *DuPont* is making new attempts in applying the divided catalytic processes also to further selective oxidations, as shown by the patent of *DuPont* and *AtoChem* [34] for preparing acrolein from propene.

In principle, one would expect *divided catalytic processes* <u>to</u> be a technology which can be handled on a industrial scale, because cyclic operation modes of catalysts have been successfully used for years in the form of periodic regeneration processes, for example, in fluid-catalytic-cracking (FCC).

7 Summary

As this contribution shows, in addition to the chemical and engineering aspects, owing to the various advantages and disadvantages of divided catalytic processes, an economic consideration is always necessary, too. Only this comprehensive evaluation can indicate whether carrying out heterogeneously catalysed gas-phase reactions as divided and periodic processes is an industrially viable alternative to existing or known processes. A fundamental study of the system including microscopic level (intrinsic kinetics, cycle stability) and macroscopic level (simulation of the overall process) can act as a basis for this. This assessment is facilitated by the increasing amount of research work in the sector of unsteady-state heterogeneous catalysis [2].

References

1   P. Silveston, R. Hudgins, and A. Renken, *Periodic operation of catalytic reactors – introduction and overview*, Catal. Today, Vol. 25, pp. 91-112, 1995.
2   C. Bennett, Experiments and processes in the transient regime for heterogeneous catalysis, Adv. Catal., Vol. 44, pp. 329-416, 1999.
3   A. Stankiewicz and M. Kuczynski, An industrial view on the dynamic operation of chemical converters, Chem. Engng. Proc., Vol. 34, pp. 367-377, 1995.
4   P. Mars and D. van Krevelen, Oxidations carried out by means of vanadium oxide catalysts, Chem. Eng. Sci.; Spec. Suppl., Vol. 3, pp. 41-59, 1954.
5   P. Silveston and M. Forrisier, Influence of composition modulation on product yields and selectivity in the partial oxidation of propylene over an antimony-tin oxide catalyst, Ind. Eng. Chem. Process Des. Dev., Vol. 24, pp. 320-325, 1985.
6   W. Lewis, E. Gilliland, and W. Reed, Reaction of methane with copper oxide in a fluidized bed, Ind. Eng. Chem., Vol. 41, No. 6, pp. 1227-1237, 1949.

7   L. Mond and G. Eschellmann, Process of obtaining chlorine, Patent US 416,038, Nov., 1889.

8   H. Deacon, Improvement in manufacture of chlorine, Patent US 165,802, Jul., 1875.

9   R. Minet, S. Benson, and T. Tsotsis, Recovery of chlorine from hydrogen chloride by carrier catalyst process, Patent US 4,994,256, Feb., 1991.

10   H. Pan, R. Minet, S. Benson, and T. Tsotsis, Process for converting hydrogen chloride to chlorine, Ind. Eng. Chem. Res., Vol. 33, pp. 2996-3003, 1994.

11   M. Mortensen, R. Minet, T. Tsotsis, and S. Benson, A two-stage cyclic fluidized bed process for converting hydrogen chloride to chlorine, Chem. Eng. Sci., Vol. 51, No. 10, pp. 2031-2039, 1996.

12   M. Mortensen, R. Minet, T. Tsotsis, and S. Benson, The development of a dual fluidized-bed reactor system for the conversion of hydrogen chloride to chlorine, Chem. Engng. Sci., Vol. 54, pp. 2131-2139, 1999.

13   U. Nieken and O. Watzenberger, Periodic operation of the Deacon process, Chem. Engng. Sci., Vol. 54, pp. 2619-2626, 1999.

14   W. Krönig, O. Tegtmeyer, and W. Schmidt, Verfahren zur Dehydrierung von Kohlenwasserstoffen, Patent DE 1 161 257, 24.09.56, Bayer AG, 1956.

15   J. Callahan, R. Grasselli, E. Milberger, and H. Strecker, Oxidation and ammoxidation of propylene over bismuth molybdate catalyst, Ind. Eng. Chem. Prod. Res. Develop., Vol. 9, No. 2, pp. 134-142, 1970.

16   M. Sze and A. Gelbein, Make aromatic nitriles this way, Hydrocarbon Processing, pp. 103-106, Feb., 1976.

17   R. Contractor, H. Bergna, H. Horowitz, C. Blackstone, C. Malone, C. Torardi, B. Griffiths, U. Chowdhry, and A. Sleight, Butane oxidation to maleic anhydride over vanadium phosphate catalysts, Catal. Today, Vol. 1, pp. 49-58, 1987.

18   R. Contractor, Du Pont's CFB technology for maleic anhydride, Chem. Engng. Sci., Vol. 54, pp. 5627-5632, 1999.

19   E. Müller-Erlwein and J. Guba, Experimentelle Untersuchung zum periodischen Reaktorbetrieb bei der heterogen katalysierten Oxidehydrierung von Isobutyraldehyd zu Methacrolein, Chem.-Ing.-Tech., Vol. 60, No. 12, pp. 1072-1073, 1988.

20   R. Burch and R. Swarnakar, Oxidative dehydrogenation of ethane on vanadium-molybdenum oxide and vanadium-niobium-molybdenum oxide catalysts, Appl. Catal., Vol. 70, pp. 129-148, 1991.

21   A. Hagemeyer, O. Watzenberger, and A. Deimling, Katalysator und Verfahren für die katalytische oxidative Dehydrierung von Alkylaromaten und Paraffinen, Patent DE 44 37 252 A1, 18.10.94, BASF AG, 1994.

22   A. Hagemeyer, Th. Lautensack, O. Watzenberger, and A. Deimling, Verfahren zur katalytischen oxidativen Dehydrierung von Alkylaromaten und Paraffinen, Patent DE 44 36 385 A1, 12.10.94, BASF AG, 1994.

23   O. Watzenberger and A. Hagemeyer, Verfahren zur Herstellung von Styrol aus Ethylbenzol und Xylole enthaltenden C8-Gemischen, Patent DE 195 45 095 A1, 04.12.95, BASF AG, 1995.

24   O. Watzenberger, E. Ströfer, and A. Anderlohr, Instationär-oxidative Dehydrierung von Ethylbenzol zu Styrol, Chem.-Ing.-Tech., Vol. 71, No. 1+2, pp. 150-152, 1999.

25   L. Weismantel, Zweistufige Reaktionsführung bei heterogen katalysierten Oxidationsreaktionen am Beispiel der Methacrylsäuresynthese an Heteropolyverbindungen, Dissertation, Universität Erlangen-Nürnberg, 1996.

26   L. Weismantel, J. Stöckel, and G. Emig, Improvement of selectivity with a two-step process for the oxidation of isobutyric acid, Appl. Catal. A, Vol. 137, pp. 129-147, 1996.

27   J. Sloczynski, Kinetics and mechanism of reduction and reoxidation of the alkali metal promoted vanadia-titania catalysts, Appl. Catal. A, Vol. 146, pp. 401-423, 1996.

28   D. Creaser, B. Andersson, R. Hudgins, and P. Silveston, Transient kinetic analysis of the oxidative dehydrogenation of propane, J. Catal., Vol. 182, pp. 264-269, 1999.

29   D. Creaser, B. Andersson, R. Hudgins, and P. Silveston, Transient study of oxidative dehydrogenation of propane, Appl. Catal. A, Vol. 187, pp. 147-160, 1999.

30   H.-W. Zanthoff, J.-C. Jalibert, Y. Schuurmann, P. Slama, J.-M. Herrmann, and C. Mirodatos, Dynamics of the oxidative dehydrogenation of propane over VMgO catalysts studied by in situ electrical conductivity and step transients. In: A. Corma and F. Melo and S. Mensioros and J. Fierro (Ed.), 12th Int. Congress Catal., Granada, E, June 2000, Studies in Surface Science and Catalysis, Elsevier, Amsterdam, 2000.

31   S. Dubuis, M. Lorenzi, R. Doepper, and A. Renken, Oxidative coupling of toluene under periodic conditions on Pb/Li/MgO: A selective path to 1,2-diphenylethane. In: G. Froment and K. Waugh, (Eds.), Dynamics of Surfaces and Reaction Kinetics in Heterogeneous Catalysis, pp. 469-477, Elsevier, Amsterdam, 1997.

32   H. Hiltner and G. Emig, Oxidative coupling of isobutene in a two step process. In: 3rd World Congress on Oxidation Catalysis, pp.593-603, Elsevier, Amsterdam, 1997.

33   H. Hiltner, Reaktionstechnische Untersuchungen zur oxidativen Kopplung von Isobuten zu 2,5-Dimethyl-1,5-Hexadien, Dissertation, Universität Erlangen-Nürnberg, 1998.

34   R. Contractor, M. Anderson, D. Campos, G. Hecquet, R. Kotwica, C. Pham, and M. Simon, Improved vapor phase oxidation of propylene to acrolein, Patent WO 99/03809, 28.01.99, E.I. Du Pont de Nemours and Elf Atochem S.A., 1999.

35   R. Böhling, A. Drochner, M. Fehlings, D. König, and H. Vogel, Konzentrationsprogrammierte Reaktionstechnik –- Eine Methode zur Beurteilung des Anwendungspotentials instationärer Prozeßführungen bei Partialoxidationen, Chem. Ing. Tech., Vol. 71, No. 3, pp. 226-230, 1999.

36   Yu Zhiqing, Application collocation. In: M. Kwauk, (Ed.), Fast fluidization, Vol. 20 in Advances in Chemical Engineering, pp. 39-63, Academic Press, 1994.

37   T. Ilkenhans, H. Siegert, and R. Schlögl, The mechanism of the synthesis in connection with assignments for a solid reaction cycle of the HPA catalyst during catalytic reactions, Catal. Today, Vol. 32, pp. 337-347, 1996.

38   K. Westerterp, W. van Swaaij, and H. Beenackers, Chemical Reactor-Design and Operation, rev. ed., John Wiley, Chichester, 1984.

39   M. Casper, (Ed.), Hydrogen manufacture by electrolysis, thermal decomposition and unusual techniques, Vol. 102 in Chemical Technology Review, Noyes Data Corp., Park Ridge, NJ, USA, 1978.

40   F. Cavani and F. Trifirò, Some aspects that affect the selective oxidation of paraffins, Catal. Today, Vol. 36, pp. 431-439, 1997.

41   R. Contractor and A. Sleight, Maleic anhydride from C-4 feedstocks using fluidized bed reactors, Catal. Today, Vol. 1, pp. 587-607, 1987.

42   R. Contractor and A. Sleight, Selective oxidation in a riser reactor, Catal. Today, Vol. 3, pp. 175-184, 1988.

43   T. Pugsley, G. Patience, F. Berruti, and J. Chaouki, Modeling the catalytic oxidation of n-butane to maleic anhydride in a circulation fluidized bed reactor, Ind. Eng. Chem. Res., Vol. 31, pp. 2652-2660, 1992.

44   R. Contractor, H. Bergna, H. Horowitz, C. Blackstone, U. Chowdry, and A. Sleight, Butane oxidation to maleic anhydride in a recirculating solids reactor.

In: J. Ward, (Ed.), Catalysis 1987, pp. 645-654, Elsevier, Amsterdam, 1988.

45   R. Contractor, H. Horowitz, G. Sisler, and E. Bordes, The effects of steam on n-butane oxidation over VPO as studied in a riser reactor, Catal. Today, Vol. 37, pp. 51-57, 1997.

46   K. Golbig and J. Werther, Selective synthesis of maleic anhydride by spatial separation of n-butane oxidation and catalyst reoxidation, Chem. Eng. Sci., Vol. 52, No. 4, pp. 583-595, 1997.

47   Y. Schuurman and J. Gleaves, Activation of vanadium phosphorus oxide catalysts for alkane oxidation: The influence of the oxidation state on catalyst selectivity, Ind. Eng. Chem. Res., Vol. 33, pp. 2935-2941, 1994.

48   Th. Ilkenhans, B. Herzog, Th. Braun, and R. Schlögl, The nature of the active phase in the heteropoly acid catalyst $H_4PVMo_{11}O_{40} \bullet 32\ H_2O$ used for the selective oxidation of isobutyric acid, J. Catal., Vol. 153, pp. 275-292, 1995.

49   G. Emig, K. Uihlein, and C.-J. Häcker, Separation of catalyst oxidation and reduction – An alternative to the conventional oxidation of n-butane to maleic anhydride.
     In: V. Cortés Corberán and X. Victor Bellón, (Eds.), New Developments in Selective Oxidation II, pp. 243-251, Elsevier, Amsterdam, 1994.

50   A. Bielanski and J. Haber, Oxygen in catalysis on transition metal oxides, Catal. Rev.-Sci. Eng., Vol. 19, No. 1, pp. 1-41, 1979.

51   U. Rodemerck, B. Kubias, H.-W. Zanthoff, and M. Baerns, The reaction mechanism of the selective oxidation of butane on $(VO)_2P_2O_7$ catalysts: The role of oxygen in the reaction chain to maleic anhydride, Appl. Catal. A, Vol. 153, pp. 203-216, 1997.

52   M. Abon, K. Béré, and P. Delichère, Nature of active oxygen in the n-butane selective oxidation over well defined V-P-O catalysts: an oxygen isotopic labelling study, Catal. Today, Vol. 33, pp. 15-23, 1997.

53   Xiaosu Lang, R. Hudgins, and P. Silveston, Application of periodic operation to maleic anhydride production, Can. J. Chem. Eng., Vol. 67, pp. 635-645, 1989.

54   H. Seiler, and G. Emig, Reduction-oxidation cycles in a fixed-bed reactor with periodic flow reversal, Chem. Eng. Technol., Vol. 21, No. 6, pp. 479-484, 1999.

55   A. Zwijnenburg, A. Stankiewicz, and J. Moulijn, Dynamic operation of chemical reactors: Friend or foe?, Chem. Eng. Progr., pp. 39-47, Nov., 1998.

56   P. Silveston. In: R. Mashelkar and R. Kumar, (Eds.), Reactors and Reaction Engineering. Indian Academy of Sciences, Bangalore, India, 1987.

57   R. Contractor, Du Pont's new process for n-butane to tetrahydrofuran, Appl. Catal. B, Vol. 6, No. 1, pp. N3, 1995.

Microstructured Reactors for Heterogeneous Catalytic Processes

Contents

Microstructured Reactors for Heterogeneous Catalytic Processes

Albert Renken

Laboratoire de genie de la réaction chimique
Ecole polytechnique fédérale de Lausanne, LGRC-EPFL
1015 Lausanne, Switzerland
albert.renken@epfl.ch

Abstract. Microstructured reactors are mainly characterized by their very high surface to volume ratio compared to traditional chemical reactors. Multichannel microreactors having channel diameters in the order of ten to several hundred micrometers have specific surface areas up to 50'000 m^2/m^3. This value is roughly two orders of magnitude higher compared to conventional production vessels.

Due to the small reactor dimensions diffusion times are short and the influence of mass transfer on the rate of reaction can be efficiently reduced. As the heat transfer performance is greatly improved compared to conventional systems, higher reaction temperatures are admissible leading to reduced reaction volumes and amount of catalyst. Therefore, microstructured reactors are especially predestinated for fast, highly exothermic or endothermic chemical reactions.

1   Introduction

Microreaction technology became an important issue in Chemical Reaction Engineering within the last 6 years. In Europe the development started mainly with a workshop on "Microsystem technology for chemical and biological microreactors" held in Germany in the year 1995 [1]. This first workshop was followed by five International Conferences on Microreaction Technology (IMRET) organized up-to-now alternatively in Europe and North America. As a consequence of the rather new and rapidly growing developments, most of the literature in the domain of microtechnology can be found in the proceedings of the mentioned international conferences.

Microstructured reactors are characterized by three-dimensional structures in the sub-millimeter range. Mainly multichannel reactors are currently used with channel diameters between ten and several hundred micrometers. Therefore, one of the main features of microstructured reactors is their high surface to volume ratio compared to traditional chemical reactors. The specific surface in microchannels lays in the range of 10'000 to 50'000 m^2/m^3, whereas the specific

surface in typical laboratory and production vessels is about 100 m^2/m^3 and seldom exceeds 1000 m^2/m^3.

Usually, microstructured reactors work under laminar flow conditions. Therefore, the Nusselt number reaches a constant value. As the heat transfer coefficient is inversely proportional to the channel diameter, their values for micro-reactors are in the order of 10 kW/(m^2·K) being roughly one order of magnitude higher than those found for the traditional heat exchangers [2]. Schubert et al. reported values for heat transfer coefficients determined experimentally of up-to 25 kW/(m^2·K) [3].

The high heat transfer performance allows very fast heating and cooling of reaction mixtures in open reactor systems [4, 5]. Therefore, reactions can be carried out under isothermal conditions for short, well defined residence times in the reactor, and the decomposition of unstable products can be efficiently avoided. An example is the catalytic dehydrogenation of methanol to water-free formaldehyde. The reaction takes place in the range of 1000-1200K to get complete conversion of methanol. As the produced formaldehyde is unstable under the reaction conditions and decomposes to carbon monoxide and hydrogen, the reaction mixture has to be quenched rapidly at the reactor outlet. Using a microstructured, heat exchanger temperature gradients of up to 6400K/s could be obtained leading to formaldehyde yields of more than 80% at nearly complete conversion of methanol [6].

Besides heat transfer, mass transfer is also considerably enhanced in micro-structured reactors. In special configurations mixing times in the order of milliseconds or even nanoseconds are reported [7, 8].

Due to the small reactor dimensions diffusion times are short and the influence of mass transfer on the rate of reaction can be efficiently reduced. As the heat transfer performance is greatly improved compared to conventional systems, higher reaction temperatures are admissible leading to reduced reaction volumes and amount of catalysts [9]. Therefore, micro-structured reactors are especially predestinated for fast, highly exothermic or endothermic chemical reactions.

Small inventory of reactants and products leads to an increased inherent safety of the reactor. In addition, it was demonstrated that the reactor can be operated safely under conditions, which lay in the explosion regime [10-12]. The small reactor dimensions facilitates the use of distributed production units at the place of consumption thus avoiding the transportation and storage of dangerous materials.

Finally, using of microstructured reactors can lead to an efficient process development since the step of scale-up is replaced by simple "numbering-up" [13].

The potential benefits of micro-structured reactors can be summarized as follows:

- Process intensification
- Inherent reactor safety
- Broader reaction conditions including the explosion regimes
- Distributed production
- Faster process development

2   Packed bed Reactors

One of the main problems in using microstructured reactors for heterogeneously catalyzed reactions is the introduction of catalytic active phase. The easiest way is to fill microchannels with catalyst powder. The "micro-packed-bed" is commonly used for catalyst screening [14, 15]. But there are also examples for the use of micro-packed-beds for the distributed production of chemicals. The advantage of packed-bed microreactors stems from the fact that traditional and optimised catalytic systems can be easily implemented in the microsystem. Typically, the catalyst particles have diameters in the range of 35 to 75 µm [16]. At these dimensions, the reactor operates in laminar flow.

Tonkovich and coworkers used packed bed microreactors for the production of hydrogen [17-22]. For the partial oxidation of methane the authors constructed a reactor consisting of stacked stainless steel sheets [18]. The microchannels (254 µm wide, 1500 µm deep and 35 mm long) are cut either by conventional or electrodischarge machining and filled with a mesoporous silica impregnated with Rh. The reactor plates are sandwiched between two integrated heat exchanger plates. A similar reactor system is used for fuel processing [19, 23]. The fuel processor produces hydrogen-rich streams from hydrocarbon-based feedstocks in a multi-step process including fuel vaporizer, primary conversion reactor producing CO-rich synthesis gas, a water gas shift reactor, and finally a CO clean-up reactor. Microchannel reactors can be used to reduce the size of conventional reactors without lowering the throughput as limitations of the global reaction rates by heat and mass transfer can be efficiently avoided. A critical step of the fuel processor is the CO elimination. As PEM fuel cells are sensitive to carbon monoxide, its concentration should not exceed 50 ppm. Tonkovich et al. [19] demonstrated that CO can be transformed by the water gas shift reaction to CO_2 with a conversion of 99.8% within 25ms at 300°C in a microchannel reactor over a Ru/ZrO_2 powder.

An example for the inherently safe production of phosgene in a microsystem is given by Ajmera et al. [24]. The used microreactor was fabricated out of single crystal silicon. The reactor consisted of a 20mm long, 625µm wide and 300µm deep reaction channel capped with Pyrex glass. At the outlet of the microchannels
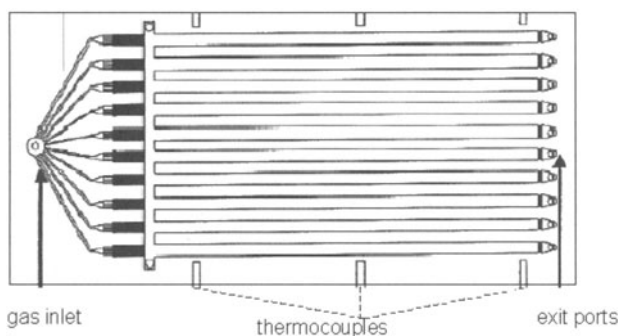
Fig. 1: Multichannel reactor design [25]
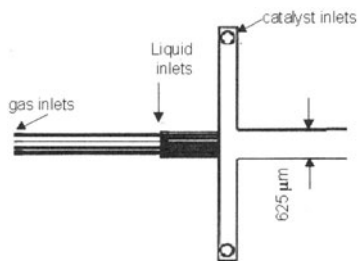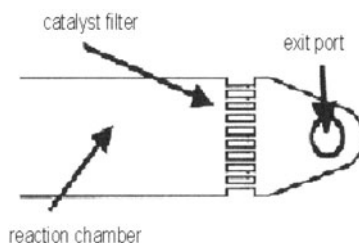
a filter with 25μm holes were placed to retain the catalyst powder. Experiments were carried out with ca. 1.3mg activated carbon with a particle diameter of 53-73 μm. The reactor was operated with a stoichiometric mixture of CO and Cl_2 at a total flow rate of 4.5 cm^3/min (STP). At atmospheric pressure and a temperature of 200°C complete conversion was achieved, corresponding to a productivity of 0.4 g/h (3.5kg/a) phosgene from a single channel.

The design of the used micro-packed-bed reactor was initially developed for multiphase reactions [25]. Besides a one-channel reactor a bundle of ten parallel microchannels were used as shown schematically in Fig. 1. The micro multi-tubular reactor consists of a microfluidic distribution manifold, a microchannel array, and a 25μm microfilter at the channel exit to retain the catalyst powder. Details of the reactor inlet and outlet are shown on Fig. 2 and 3.

The microreactor was used for the catalytic hydrogenation of cyclohexen as a model reaction. Hydrogenations are highly exothermic. Consequently thermal uniformity and efficient temperature control is important to prevent reactor runaway. In addition, the reaction rate is often limited by gas-liquid mass transfer. For the mentioned test reaction the reactor channels were packed with platinum supported on alumina powder. Catalyst loading was in the order of 4 g/channel. Experimental results show that the volumetric mass transfer lies in the range of $5<k_La<15$ s^{-1}. This values are roughly two orders of magnitude higher than those reported for classical trickle beds. Analysis of the power dissipation for a given mass transfer rate showed that the microreactor operates with an efficiency corresponding to traditional multiphase reactors.

The drawback of micro-packed-bed reactors is the high pressure drop. In addition, each channel must be packed identically to avoid maldistribution, which is known to lead to a broad residence time distribution in the reactor system. To avoid problems related to the use of randomly packed beds, structured catalytic beds were recently proposed [26-28]. The novel concept of a microreactor is based on a structured catalytic bed arranged with parallel filaments of a few micrometers in diameter (3-10 μm). The arrangement gives flow hydrodynamics similar to multi-channel microreactors, known to have a narrow residence time distribution (RTD). The channels for gas flow between the filaments (see Fig.4) have an equivalent hydraulic diameter in the range of few microns ensuring laminar flow and short diffusion times in the radial direction.
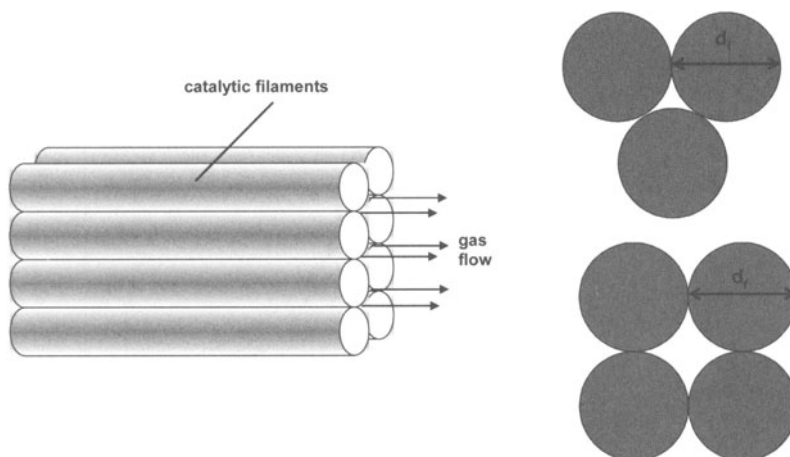
Fig. 4 : Schematic presentation of gas flow between catalytic filaments [30]

The microstructured catalyst was used in a membrane reactor specially developed for the continuous production of propene from propane via non-oxydative dehydrogenation. The catalytic filaments with a diameter of ca. 7μm consisted of a silica core covered by γ-alumina porous layer on which an active phase of Pt/Sn is supported (Fig. 5) [29, 30].

The catalytic filaments were introduced into the tubular reactor in the form of threads. Each thread with a diameter of about 0.5 mm consists of a bundle of ~100 filaments, with a diameter of ~7 μm. The catalytic threads were placed in parallel into the tube to form a cylindrical catalytic bed of several centimetres length. The catalytic bed arranged in this manner has about 300 threads per cm^2 within the tube cross-section. The porosity of the filamentous packed bed is ε=0.8. The specific surface per volume is in the order of 108 m^2/m^3 and thus, about 50 times higher compared to washcoated tubes of the same inner diameter [27]. The hydrodynamics of gas flow through the microstructured catalytic bed were studied and compared to different conventional packings. The residence time distribution (RTD) was measured in a tube packed with the filamentous catalyst and with particles of silica and γ-alumina of different shapes and sizes. Experimental results are presented in Figure 6. Under identical experimental conditions, randomly packed beds showed significantly broader RTD compared to the structured
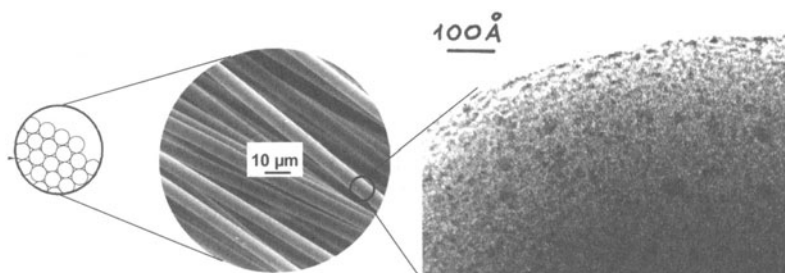
Fig. 5 : SEM and TEM images of Pt/glass fibrous catalyst [30]
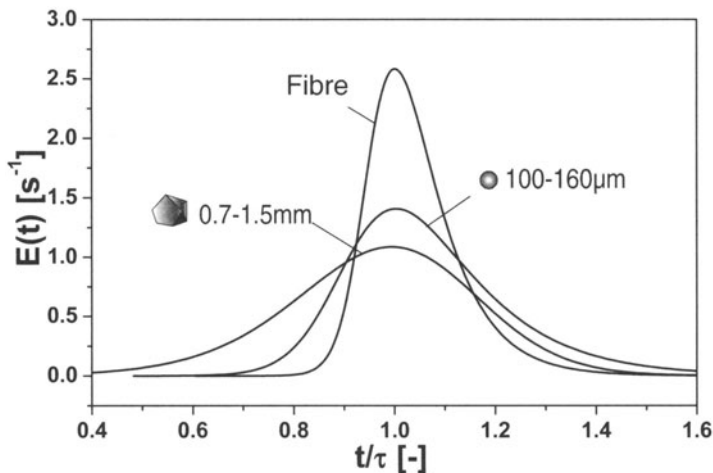
Fig.6: Residence time distribution in randomly packed beds compared to a structured filamenteous bed [27]

filamentous packing. A further advantage of the structured filamentous packed bed is the ca. 5 times lower pressure drop compared to the randomly packed bed for the same hydraulic diameter and comparable gas flow rates.

3   Catalytic Wall Reactors

To avoid high pressure drop in randomly packed microstructured reactors multichannel reactors with catalytically active walls were proposed. In most cases the reactors are based on micro heat exchangers [3, 31] as shown in Fig. 7. Typical channel diameters are in the range of 50 to 500 μm with a length between 20 and 100 mm. About 200 to 2000 channels are assembled in one unit. Due to the small channel diameters the reactor operates under laminar flow conditions. Whereas, the pressure drop in the channels can be estimated from the Hagen-Poisseuille law, the prediction of the pressure drop in the whole system can only be calculated on the basis of a detailed flow model taking into account the inlet and outlet zones [32-34].

Besides the kinetic parameters, the mean residence time and the residence time distribution (RTD) in the reactor influence strongly the product yield and selectivity. To get the maximal yield of the intermediate product for consecutive reactions, RTD in the reactor should be suppressed. Microchannel reactors work under laminar flow conditions. At first glance, a laminar flow profile seems to provoke a vast distribution of residence times. But Taylor and Aris [35] showed that radial diffusion can counteract the RTD broadening influence of the parabolic flow profile. For circular tubes the axial dispersion coefficient, D_{ax}, is given by:

$$D_{ax} = D + \frac{d_t^2 \cdot u^2}{192 \cdot D}$$
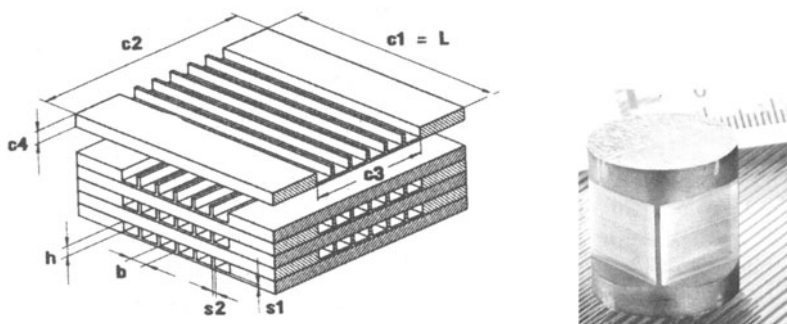
Fig. 7: Micro heat exchanger: foil length (c1):14 mm; foil width (c2): 14mm; width of patterning (c3): 10mm; foil thickness (c4): 100µm; channel length (L): 14mm; channel width (b): 100µm; channel height (h): 75 µm; [31]

where D is molecular diffusion coefficient; u- average linear velocity; d_t- tube diameter.

Due to the small tube diameters of the microchannels the radial diffusion time of gases is in the order of milliseconds and the axial dispersion can be efficiently suppressed, as shown by theoretical and experimental studies [36, 37]. The optimal design for flow uniformity in microchannel reactors was recently discussed in detail by Matlosz et al. [38]. Industrial examples for the efficient use of microchannel reactors to suppress consecutive reactions are discussed by Wörz [13, 39].

To use microstructured wall reactors for heterogeneously catalysed reactions a catalytically active layer has to be introduced. The catalyst can be deposited on the interior wall of the channels by various techniques, like physical vapour deposition (PVD), chemical vapour deposition (CVD) of catalytic thin films, or deposition of microporous catalyst layers on microstructured surfaces. Finally the microreactor can be entirely constructed from the catalytic active material or of its precursor. This method was used for one of the first reactions studied in a microstructured wallreactor: the partial oxidation of propene to acrolein [40]. The reactor consisted of a stack of 100 copper foils of 14x14mm containing 80 microchannels. To obtain a catalytic active surface of copper oxides the walls of the microchannels were oxidized by di-oxygen. Under the chosen reaction conditions (350-375°C, reactant concentrations <1vol%) acrolein selectivities of up to 50% could be observed.

Hönicke and coworkers chose aluminium as construction material. The developed microstructured reactor consisted of 672 parallel rectangular channels of 200x200 μm^2. The specific surface of the micro channels was increased by anodic oxidation of the aluminium surface resulting in a thin porous layer of Al_2O_3. The obtained oxide layer had a very regular pore structure oriented perpendicularly to the flow direction. This porous layer served as support for the catalytically active components [40-42].

The reactor concept was tested for several complex consecutive reactions:

- Selective hydrogenation of benzene to cyclohexene [43, 44]
- Partial gas phase hydrogenation of cyclodecatriene and cyclooctadiene [44]
- Selective oxidation of 1-butene to maleic anhydride [43]
- Selective oxidation of ethene to ethane-oxide (oxiran) [43, 45, 46]

Whereas in the above mentioned examples the catalytic layer was developed within the micrchannels, the reactor can be constructed directly from the catalytic active material. Kestenbaum et al. [47] used silver foils for the construction of a microchannel reactor for the partial oxidation of ethen to oxiran. A similar concept was recently proposed by Fichtner et al. [48, 49]. The authors used a microstructured rhodium catalyst for the partial oxidation of methane to syngas. The partial oxidation of methane can be considered as a coupling of the exothermic oxidation and endothermic reforming, which occur at different reaction rates. Therefore, the use of a material with high thermal conductivity can avoid pronounced axial temperature profiles. The reactor was operated under autothermal conditions at 0.17-0.6 MPa and temperatures of ca. 1100°C. The observed temperature difference between inlet and outlet of the reactor was in the order of 100°C. For a ratio of $CH_4/O_2=2$ a methane conversion of 50% and a selectivity towards hydrogen of 70% could be obtained.

If the reactor material is not catalytically active or can be used as precursor for the development of an active layer, the catalyst must be deposited on the reactor walls. Different methods are described in the literature. Sol-gel methods [50-53] are commonly proposed to obtain a porous support layer on the wall of the microchannel. The catalytically active phase can be deposited on the porous layer by classical methods like precipitation or impregnation. Rouge et al. [34] used the sol-gel or wash-coating method to get uniform layers of γ-alumina. The initial solutions for wash-coating are either colloidal suspensions of boemithe in water or solutions of aluminium alkoxides [54]. By subsequent heating of the deposited film to 450-500°C, a layer of porous γ-Al_2O_3 is obtained. The method was reported to be satisfactory for films up to 2µm. [52, 53]. To get thicker films, γ-alumina powder was added to the aqueous suspension of boemithe. Boemithe acts as a binder for the particles [55]. For the coating of rectangular stainless steel microchannels (300×240 µm^2, 20mm length) Rouge developed a six step procedure to ensure a homogeneous deposition of γ-aluminia [34, 36]. The loading was in the order of 0.4 mg/channel.

Besides wash-coating physical vapor deposition (PVD) [56], chemical vapor deposition [57], or aerosol techniques [58] are known. An interesting approach was reported by Fichtner et al. [59]. The authors used dispersions of commercially available nano-particle powders for the catalytically active coatings. The advantage of this method is that no further procedures like impregnation or precipitations are necessary. The final pore structure depends on the type of nano-particles used and the thermal treatment. First experimental results were reported for the steam reforming of methanol [60]. Reuse et al. [61] developed a coating method for the direct use of commercially available catalysts. The activity of the catalyst layer was found to exceed the values of the original formulation. By the proposed method a sometimes tedious and time consuming procedure for the development of an active catalytic layer can be shortened or even avoided.

4   Membrane Reactors

The concept of membrane reactors is mainly proposed to overcome equilibrium limitations in chemical processes [62]. Different membrane materials for the use in microstructured devices were recently developed. Wegner et al. [63, 64] developed ultrathin polymeric membranes for the separation of ethylene oxide from ethylene. It has been shown that polymer layers with a thickness of only 50 to 100nm can be used efficiently in separation processes and resist large pressure changes.

Hydrogen can be selectively separated with Palladium membranes [65]. Therefore, Pd membrane reactors are used in hydrogenation and dehydrogenation processes. But the extensive use of Pd membranes is limited by their high cost, due to the thick Pd films of 10-25μm employed in traditional membrane fabrication [65]. In addition, thick Pd films greatly reduce efficiency, since the hydrogen flux through the film is inversely proportional to its thickness. Microfabrication methods offer an opportunity to produce membranes with much lower film thickness [66]. Cui et al. [67] developed a micro membrane reactor on silicon for the catalytic dehydrogenation of cyclohexane to benzene. The reaction chamber consisted of 80 microchannels 50μm wide, 400mm deep and 8μm long.
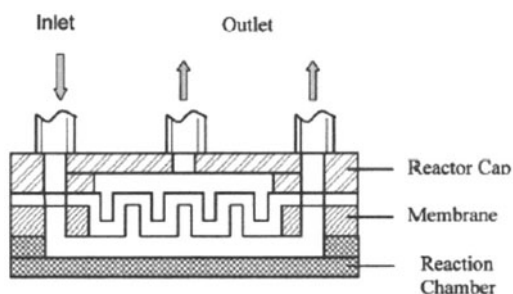
Fig. 8: Design of the micro membrane reactor [67]
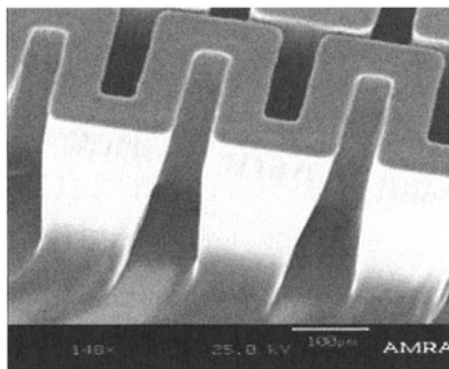
Fig. 9 : Separation membrane [67]

The separation membrane is 6mm by 8mm, with 80 folded rectangular 4μm thick

Pd foil structures 50 µm wide, 200 µm high and 6mm long anchored on silicon (Fig. 8 and 9).

The design and fabrication of zeolite based microreactors and membrane microseparators was reported by Yeung et al. [68, 69]. Four different strategies for the manufacture of the microreactors were presented: zeolite powder coating, uniform zeolite film growth, localized zeolite growth, and etching of zeolite-silicon composite film. The zeolites were deposited either as film or dicrete islands with controlled particle size, crystal morphology and a layer thickness of 3-16µm.

5   Microreactors for Periodic Operation

Forced periodic concentration oscillations in continuously operated reactors can lead to a considerable increase of selectivity and reactor performance compared to the optimal steady state [70, 71]. In particular, the reactor performance can be drastically increased for catalytic reactions with educt inhibition, as shown in experimental and theoretical studies [72, 73]. The obtainable performance depends strongly on the amplitude and frequency of the imposed parameter variations. The optimal cycle period depends on the reaction kinetics and the reactor behaviour and may be in the range of seconds up to hours. Due to the high inertia of conventional reactors the attainable frequencies are in the order of 10^{-4} to 10^{-2} Hz. To increase the frequency microstructured reactors were recently proposed [57]. Microstructured multichannel reactors allow forced concentration variations of up to 1 Hz [36].

One of the examples for the increased reaction rate by periodic variation of reactant concentration in the reactor is the dehydration of alcohols over amphoteric oxides, e.g. Al_2O_3 [74, 75].

$$RCH_2CH_2OH \rightarrow RCHCH_2 + H_2O$$
$$2ROH \qquad \rightarrow ROR \qquad + H_2O$$
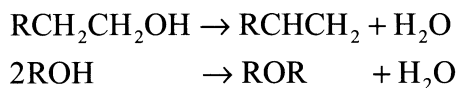
The kinetics of this reaction can be described by considering a model with two different active sites i involved in the catalytic action. The supposed reaction scheme and the resulting kinetic equations are as follows:

<table>
<tr><td align="center"><i>Model</i></td><td align="center"><i>Kinetic equations</i></td></tr>
<tr><td>$A + S_1 \xrightleftharpoons[k_{-1}]{k_1} AS_1$</td><td>$r_1 = k_1 C_A (1 - \theta_1) - k_{-1}\theta_1$</td></tr>
<tr><td>$A + S_2 \xrightleftharpoons[k_{-2}]{k_2} AS_2$</td><td>$r_2 = k_2 C_A (1 - \theta_2) - k_{-2}\theta_2$</td></tr>
<tr><td>$AS_1 + S_2 \xrightarrow{k_3} B + C + S_1 + S_2$</td><td>$r_3 = k_3 \theta_1 (1 - \theta_2)$</td></tr>
<tr><td>$AS_1 + AS_2 \xrightarrow{k_4} D + C + S_1 + S_2$</td><td>$r_4 = k_4 \theta_1 \theta_2$</td></tr>
</table>
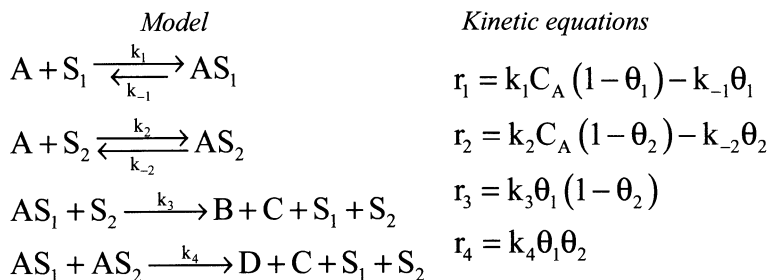
Alcohol (A) is strongly adsorbed on an acid site (S_1) and weakly on the basic S_2. An adjacent empty basic site (S_2) is required for the formation of an olefin,

while the production of ether necessitates two occupied sites (AS_1 and AS_2). Under steady state conditions the rate of olefin formation increases with the reactant concentration C_A up to a maximum value. A further concentration increase leads to a decrease of the reaction rate due to the blocking of free S_2 sites (Fig. 10). In order to increase the yield of the olefin it was proposed to stop periodically the feed of alcohol in the reactor inlet. After a feed stop, the alcohol desorbs rapidly from S_2 but almost not from S_1. As a consequence, the surface concentration of empty S_2-sites rises quickly, which results in an increase of the instantaneous reaction rate of olefin formation until the accumulated surface compound (AS_1) has been consumed.

At the same time ether formation is suppressed. The obtainable reactor performance and olefin selectivity depends strongly on the amplitude and
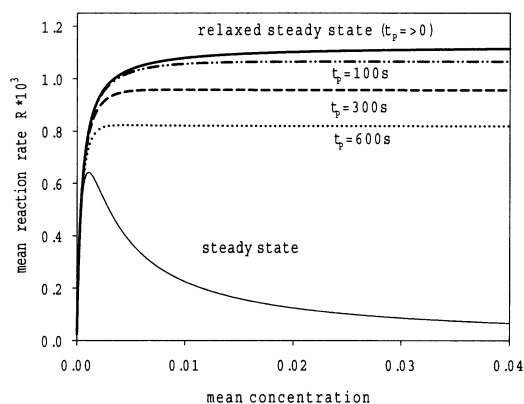
Fig. 10 : Mean reaction rate over a period as function of the feed concentration for different length of period and cycle split of γ=0.9 [76]

frequency of the imposed concentration variations. The optimal cycle period is related the adsorption capacity of the catalyst and must be in the range of the characteristic time of the surface processes.
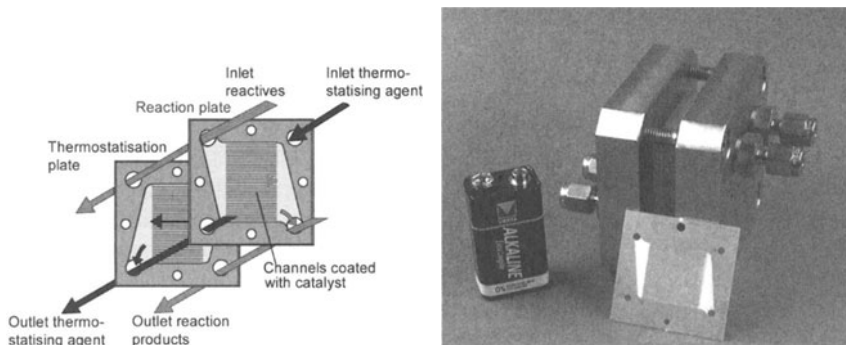
Fig. 11 :Photo and sketch of fluid flows in the microstructured reactor (Institut für Mikrotechnik, Mainz) [77]

When the forced cycling is repeated sufficiently often, the results within the periods become identical. For this cycle invariant conditions the predicted mean production rate as a function of the reactant concentration and length of period is shown in Fig. 10 for a constant cycle split of $\gamma=0.9$ [76]. The mean reaction rates are considerably higher compared to the maximum at steady state for concentrations exceeding the optimal steady state value. If the adsorption equilibrium for sites 2 is attained rapidly, high frequencies for the concentration oscillations are required to get a maximal average reaction rate. If instantaneous adsorption equilibrium is supposed, the optimal length of period approaches zero ($t_p=>0$).

Compared to conventional randomly packed beds microchannel reactors are much more suitable for periodic operation at high frequencies, due to their small dimensions and well defined structure. As the channel diameters are in the order of several micrometers, microstructured multichannel reactors operate under laminar flow conditions. But, due to the short radial diffusion times the radial concentration profile is flat, leading to a narrow residence time distribution of the reactants. The latter characteristic is of crucial importance for non steady state operation. Only reactors with a uniform residence time can be used to get the full advantage of forced concentration variations [77].

For the catalytic dehydration of isopropanol a special microchannel reactor consisting of microstructured stacked plates was designed and constructed (Fig 11) [36]. The geometry of the plates and of the stack itself was optimised to avoid mixing in the entrance and outlet area and to distribute evenly the flow between the different channels [37].

The reactor, plates as well as the housing, was constructed of stainless steel. Each plate contains rectangular channels of 300 µm width, 240 µm depth and 20 mm length. The developed microchannel reactor can be operated efficiently at frequencies up to 1 Hz.
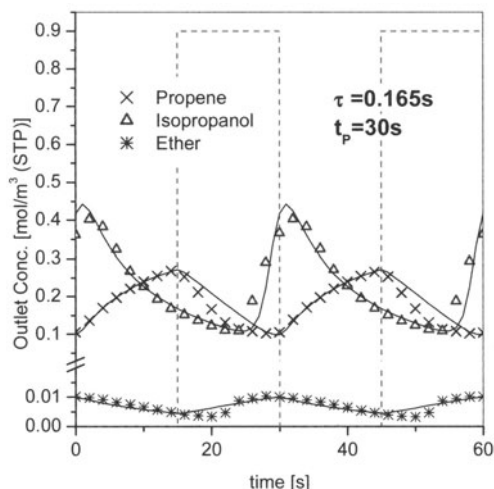
Fig. 12 : Outlet concentrations as function of time. T=200°C, P_1.26 bar, $C_{iPrOH,average}$=0.45 mol/m^3 (STP). Symbols: experimental values; lines: model simulation [77]
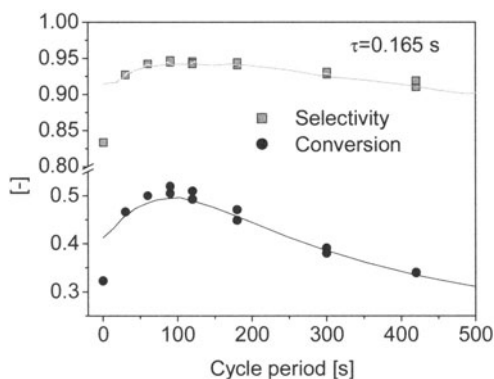
Fig. 13 : Mean selectivity and conversion as function of cycle period. T=200°C, P_1.26 bar, $C_{iPrOH,average}$= 0.45 mol/m^3 (STP). Symbols: experimental values; lines: model simulation [77]

In Fig. 12 the instantaneous outlet concentrations of the reactant, isopropanol and the products, propene and diisopropylether are shown for a cycle period of t_p=30 s and a space time of τ=0.165s. An important phase shift between the concentration oscillations of isopropanol and the propene is observed, whereas the formation rate of ether is proportional to the reactant concentration. This results in considerable changes in the conversion and the product selectivity (Fig. 13).

Depending on the length of period, the conversion increases from 32% at steady state up to 51% under forced periodic operation. At the same time the

olefin selectivity reaches 95% compared to 83% at steady state. In addition, the productivity for the target product could be nearly doubled (Fig. 14).
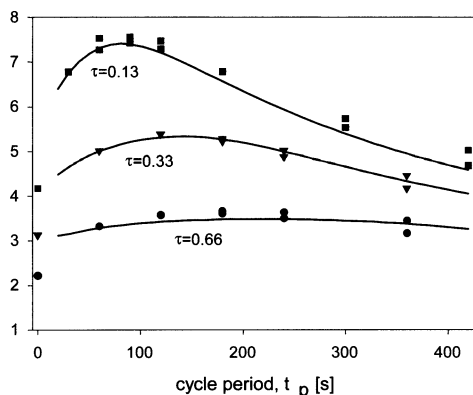
Fig. 14: Average reactor performance as function of cycle period and space time. T=200°C, P_1.26 bar, $C_{iPrOH,average}$=0.45 mol/m^3 (STP). Symbols: experimental values; lines: model simulation [77]

The variables generally investigated are the fluid-flow and/or the inlet concentrations. Theoretical studies suggest that periodic changes of the reactor temperature can help to get useful informations on the catalyst behaviour as well as reaction mechanism and should be considered for reactor optimisation [78].

Investigation on the dehydration of ethanol to diethylether over cation exchange resins showed that for heterogeneously catalysed reactions the adsorption and desorption constant may influence greatly the transient reactor behaviour [79]. However, the published results highlight the difficulty for experimental investigations in this domain, due to the high inertia of conventional systems. Hence, no further studies with conventional reactors were reported in the field.

Quiram et al. [80] showed that very fast temperature jumps can be obtained in single channel microsystems. Brandner et al. [81] studied the transient behaviour of an electrically heated microreactor and found a characteristic response time of about 30 s. In order to reduce the response time, thermo-fluids were used by Rouge and Renken [82] for fast heating and cooling of the system. A proper design of the temperature control allows fast temperature changes or a periodic variation of the temperature in a multi-channel microreactor. The catalytic dehydration of isopropanol to propene was studied as a model reaction.

6   Conclusions

Microstructured reactors are characterized by their high heat and mass transfer performances compared to conventional reactor systems. Therefore, fast and highly exothermic reactions can be safely carried out. microstructured reactors

allow an efficient process intensification and to work under conditions not attainable in traditional reactors.

Although the flow in micro multichannels is laminar, a uniform radial concentration profile and consequently a narrow residence time distribution is obtained. This allows to optimize the contact time in the reactor and to avoid unwanted consecutive reactions. The main problem for the use of microstructured reactors in heterogeneous catalysis is the introduction of catalytically active micro-porous materials. The catalytic materials should have high activity/-selectivity and mechanical stability under reaction conditions. Therefore, the development of catalyst layers which can be strongly anchored on the reactor walls remains a challenge for the future.

References

1   Ehrfeld, W., *Microsystem technology for chemical and biological bioreactors*. DECHEMA-Monographs, ed. DECHEMA. Vol. 132. 1995.
2   Ehrfeld, W., V. Hessel and V. Haverkamp, *Microreactors*, in *Ullman'sEncyclopedia of Industrial Chemistry*. 1999, Wiley-VCH: Weinheim.
3   Schubert, K., W. Bier, J. Brandner, M. Fichtner, C. Franz and G. Linder. *Realization and testing of microstructure reactors, micro heat exchangers and micromixers for industrial application in chemical engineering.* in Proceedings of 2nd International conference on microreaction technology (IMRET2). 1998. New Orleans, USA: AIChE; 88-95.
4   Alépée, C., L. Paratte, P. Renaud, R. Maurer and A. Renken, *Fast heating and cooling for high temperature chemical microreactors*, in *Proceedings of the 4th International Conference on Microreaction Engineering*, W. Ehrfeld, Editor. 2000, Springer: Berlin. p. 514-525.
5   Alépée, C., L. Vulpescu, P. Cousseau, P. Renaud, R. Maurer and A. Renken, *Microsystem for high temperature gas phase reactions*, in *Proceedings of the 4th International Conference on Microreaction Technology (IMRET 4)*, W. Ehrfeld, U. Eul, and R.S. Wegeng, Editors. 2000, AIChE: Atlanta. p. 71-77.
6   Maurer, R., M. Fichtner, K. Schubert and A.Renken, *A microstructured reactor system for the methanol dehydrogenation to water-free formaldehyde*, in *Proceedings of the 4th International Conference on Microreaction Technology (IMRET 4)*, W. Ehrfeld, U. Eul, and R.S. Wegeng, Editors. 2000, AIChE: Atlanta. p. 100-105.
7   Ehrfeld, W., V. Hessel and H. Löwe, *Microreactors*. 2000, Weinheim: Wiley-VCH.
8   Knight, J.B., A. Vishwanath, J.P. Brody and R.H. Austin, *Hydrodynamic focussing on a silicon chip: mixing nanoliters in milliseconds*. Phys. Rev. Lett., 1996. **80**: p. 3863.
9   Hardt, S., W. Ehrfeld and K.M.v.d. Bussche, *Strategies for size reduction of microreactors by heat transfer enhancement effects*, in *4th International conference on microreaction technology (IMRET4)*, W. Ehrfeld, U. Eul, and R.S. Wegeng, Editors. 2000, AIChE: Atlanta, USA. p. 432-440.
10   Ehrfeld, W., V. Hessel and H. Löwe, *Extending the knowledge base in microfabrication towards chemical engineering and fluid dynamic simulation*, in *Proceedings of the 4th International Conference on Microreaction Technology (IMRET 4)*, W. Ehrfeld, U. Eul, and R.S. Wegeng, Editors. 2000, AIChE: Atlanta, USA. p. 3-20.

11   Hagendorf, U., M. Janicke, F. Schüth, K. Schubert and M. Fichtner. *A Et/Al2O3 coated microstructured reactor/heat exchanger for the controlled H2/O2-reaction in the explosive regime*. in 2nd International conference on microreaction technology (IMRET2). 1998. New Orleans, USA: AIChE; 81-87.

12   Veser, G., G. Friedrich, M. Freygang and R. Zengerle, *A modular microreactor design for high-temperature catalytic oxidation reactions*, in *Proceedings of the 3nd International conference on microreaction technology (IMRET3)*, W. Ehrfeld, Editor. 2000, Springer: Berlin. p. 81-87.

13   Wörz, O., K.-P. Jäckel, T. Richter and A. Wolf, *Microreactors-A new efficient tool for reactor development*. Chem. Eng. Technol., 2001. **24**: p. 138-142.

14   Rodemerck, U., P. Ignaszewski, M. Lucas, P. Claus and M. Baerns. *Parallel synthesis and testing of heterogeneous catalysts*. in Proceedings of the 3rd International Conference on Microreaction Technology, IMRET 3. 2000. Frankfurt: Springer; 287-293.

15   Jensen, K.F., *Microreaction engineering - is small better?* Chemical Engineering Science, 2001. **56**(2): p. 293-303.

16   Losey, M.W., S. Isogai, M.A. Schmidt and K.F. Jensen. *Microfabricatad devices for multiphase catalytic processes*. in Proceedings of the 4th International Conference on Microreaction Technology (IMRET 4). 2000. Atlanta: AIChE; 416-422.

17   Tonkovich, A.L.Y., D.M. Jimenez, J.L. Zilka, L. M.J., Y. Wang and R.S. Wegeng. *Microchannel Chemical Reactors for Fuel Processing*. in Proceedings of the 2nd International Conference on Microreaction Technology (IMRET 2). 1998. New Orleans, USA: AIChE; 186-195.

18   Tonkovich, A.L.Y., J.L. Zilka, M.R. Powell and C.J. Call. *The catalytic partial oxidation of methane in a microchannel chemical reactor*. in Proceedings of the 2nd International Conference on Microreaction Technology (IMRET 2). 1998. New Orleans, USA: AIChE; 45-53.

19   Tonkovich, A.Y., J.L. Zilka, M.J. LaMont, Y. Wang and R.S. Wegeng, *Microchannel reactors for fuel processing applications. I. Water gas shift reactor*. Chemical Engineering Science, 1999. **54**(13-14): p. 2947-2951.

20   VanderWiel, D.P., J.L. Zilka-Marco, Y. Wang, A.Y. Tonkovich and R.S. Wegeng, *Carbon dioxide conversions in microreactors*, in *Proceedings of the 4th International Conference on Microreaction Technology (IMRET 4)*, W. Ehrfeld, U. Eul, and R.S. Wegeng, Editors. 2000, AIChE: Atlanta. p. 187-193.

21   Fitzgerald, S.P., R.S. Wegeng, A.Y. Tonkovich, Y. Wang, H.D. Freeman, J.L. Marco, G.L. Roberts and D.P. VanderWiel, *A compact steam reforming reactor for use in automotive fuel processor*, in *Proceedings of the 4th International Conference on Microreaction Technology (IMRET 4)*, W. Ehrfeld, U. Eul, and R.S. Wegeng, Editors. 2000, AIChE: Atlanta. p. 358-363.

22   Daym, E.A., D.P. VanderWiel, S.P. Fitzgerald, Y. Wang, R.T. Rozmiarek, M.J. LaMont and A.Y. Tonkovich, *Microchannel fuel processing for man portable power*, in *Proceedings of the 4th International Conference on Microreaction Technology (IMRET 4)*, W. Ehrfeld, U. Eul, and R.S. Wegeng, Editors. 2000, AIChE: Atlanta. p. 364-369.

23   Tonkovich, A.L.Y., S.P. Fitzgerald, J.L. Zilka, M.J. LaMont, Y. Wang and R.S. Wegeng. *Microchannel Chemical Reactors for Fuel Processing Applications II: Compact Fuel Vaporization*. in Proceedings of the 3rd International Conference on Microreaction Technology, IMRET 3. 2000. Frankfurt, D: Springer Verlag; 364-371.

24   Ajmera, S.K., M.W. Losey, K.F. Jensen and M.A. Schmidt, *Microfabricated packed-bed reactor for phosgene synthesis*. Aiche Journal, 2001. **47**(7): p. 1639-1647.

25   Losey, M.W., M.A. Schmidt and K.F. Jensen, *Microfabricated multiphase packed-bed reactors: Characterization of mass transfer and reactions*. Industrial & Engineering Chemistry Research, 2001. **40**(12): p. 2555-2562.

26   Kiwi-Minsker, L., O. Wolfrath and A. Renken, *Membranereactor microstructured by filamentous catalyst*. Chem. Eng. Sci., 2001: p. in press.

27   Wolfrath, O., L. Kiwi-Minsker and A. Renken, *Filamenteous catalytic beds for the design of membrane micro-reactor: propane dehydrogenation as a case study*, in *Proceedings of the 5th International Conference on Microreaction Engineering (IMRET 5)*, W. Ehrfeld, Editor. 2001, Springer: Strasbourg. p. 191-201.

28   Wolfrath, O., L. Kiwi-Minsker, P. Reuse and A. Renken, *Novel membrane reactor with filamentous catalytic bed for propane dehydrogenation*. Industrial & Engineering Chemistry Research, 2001. **40**: p. 5234-5239.

29   Kiwi-Minsker, L., I. Yuranov, E. Slavinskaia, V. Zaikovskii and A. Renken, *Pt and Pd supported on glass fibers as effective combustion catalysts*. Catalysis Today, 2000. **59**: p. 61-68.

30   Kiwi-Minsker, L., *Novel structured materials for structured catalytic reactors*. Chimia, 2002. **56**(4): p. 143-147.

31   Bier, W., W. Keller, G. Linder, D. Seidel, K. Schubert and H. Martin, *Gas to Gas Heat-Transfer in Micro Heat-Exchangers*. Chem Eng Process, 1993. **32**(1): p. 33-43.

32   Commenge, J.M., *Modélisation de microréacteurs en génie des procédés*. 2001, Ph-D thesis, ENSIC, INPL Nancy: Nancy.

33   Commenge, J.M., L. Falk, J.P. Corriou and M. Matlosz, *Optimal design for flow uniformity in microchannel reactors*, in *Proceedings of the 4th International Conference on Microreaction Technology (IMRET 4)*, W. Ehrfeld, U. Eul, and R.S. Wegeng, Editors. 2000: Atlanta. p. 23-30.

34   Rouge, A., *Periodic operation of a micro-reactor for heterogeneously catalysed reactions: -The dehydration of iso-propanol-*. 2001, Ph-D, EPF-Lausanne.

35   Baerns, M., H. Hofmann and A. Renken, *Chemische Reaktionstechnik*. 3 Edition ed. Lehrbuch der Technischen Chemie, ed. J.F. M.Baerns, F.Fetting, H.Hofmann, W. Keim, U. Onken. Vol. Bd. 1. 1999, Stuttgart - New York: Georg Thieme Verlag. 444 pages; 215 figures; 41 tables.

36   Rouge, A., B. Spoetzl, K. Gebauer, R. Schenk and A. Renken, *Microchannel reactors for fast periodic operation: the catalytic dehydrogenation of isopropanol*. Chem. Eng. Sci., 2001. **56**: p. 1419-1427.

37   Commenge, J.M., A. Rouge, A. Renken, J.P. Corriou and M. Matlosz, *Dispersion dans un microréacteur multitubulaire: Etude expérimentale et modélisation*. Récents Progrés en Génie des Procédés, 2001. **15**: p. 329-336.

38   Commenge, J.M., L. Falk, J.P. Corriou and M. Matlosz, *Optimal design for flow uniformity in microchannel reactors*. AIChE Journal, 2002. **48**(2): p. 345-358.

39   Wörz, O., *Wozu Mikroreaktoren ?* Chemie in unserer Zeit, 2000. **34**(1): p. 24-29.

40   Hönicke, D. and G. Wiessmeier, *Heterogeneously catalized reactions in a microreactor*. DECHEMA Monographs, Microsystem Technology for Chemical and Biological Microreactors, 1996. **132**: p. 93-107.

41   Wiessmeier, G., K. Schubert and D. Hönicke, *Monolithic microstructure reactors possessing regular mesopore systems for the successful performance of heterogeneously catalyzed reactions*, in *Proceedings of the 1st International Conference on Microreaction Technology (IMRET 1)*, W. Ehrfeld, Editor. 1997, Springer: Berlin. p. 20-26.

42   Wiessmeier, G. and D. Hönicke. *Strategy for the development of micro channel reactors for heterogeneously catalyzed reactions.* in 2nd International Conference on Microreaction Technology (IMRET 2). 1998. New Orleans, USA: AIChE; 24-32.

43   Kursawe, A., E. Dietzsch, S. Kah, D. Hönicke, M. Fichtner, K. Schubert and G. Wiessmeier, *Selective reactions in microchannel reactors*, in *Proceedings of the 3nd International conference on microreaction technology (IMRET3)*, W. Ehrfeld, Editor. 2000, Springer: Berlin. p. 213-223.

44   Dietzsch, E., D. Hönicke, M. Fichtner, K. Schubert and G. Wiessmeier, *The formation of cycloalkenes in the partial gas phase hydrogenation of C,T,T-1,5,9,-cyclodecatriene, 1,5-cyclooctadiene and benzene in microchannel reactors*, in *Proceedings of the 4th International Conference on Microreaction Technology (IMRET 4)*, W. Ehrfeld, U. Eul, and R.S. Wegeng, Editors. 2000, AIChE: Atlanta. p. 89-99.

45   Kursawe, A. and D. Hönicke, *Epoxidation of ethene with pure oxygen as a model reaction for evaluating the performance of microchannel reactors*, in *Proceedings of the 4th International Conference on Microreaction Technology (IMRET 4)*, W. Ehrfeld, U. Eul, and R.S. Wegeng, Editors. 2000, AIChE: Atlanta. p. 153-166.

46   Kursawe, A. and D. Hönicke, *Comparison of Ag/Al- and Ag/ -Al2O3 catalytic surfaces for the partial oxidation of ethene in microchannel reactors*, in *Proceedings of the 5th International Conference on Microreaction Engineering (IMRET 5)*, W. Ehrfeld, Editor. 2001, Springer: Strasbourg. p. 240-251.

47   Kestenbaum, H., A.L.d. Oliveira, W. Schmidt, F. Schüth, W. Ehrfeld, K. Gebauer, H. Löwe and T. Richter, *Synthesis of ethylenen oxide in a microreaction system*, in *Proceedings of the 3nd International conference on microreaction technology (IMRET3)*, W. Ehrfeld, Editor. 2000, Springer: Berlin. p. 207-212.

48   Mayer, J., M. Fichtner, D. Wolf and K. Schubert, *A microstructured reactor for the catalytic partial oxidation of methane to syngas*, in *Proceedings of the 3nd International conference on microreaction technology (IMRET3)*, W. Ehrfeld, Editor. 2000, Springer: Berlin. p. 187-196.

49   Fichtner, M., J. Mayer, D. Wolf and K. Schubert, *Microstructured rhodium catalysts for the partial oxidation of methane to syngas under pressure.* Industrial & Engineering Chemistry Research, 2001. **40**(16): p. 3475-3483.

50   Frye, G.C., C.J. Brinker, T. Bein, C.S. Ashley and S.L. Martinez. *Controlled microstructure oxide coatings for chemical sensors.* in Solid-state sensor and actuator workshop. 1990. Hilton Head Island; 61-64.

51   Harizanov, O.A. and M. Surtchev, *Glycerol Treated Aluminium Trihydroxide Sol for Coatings.* Materials Letters, 1997(32): p. 25-28.

52   Lombardi, T. and L.C. Klein, *Processing alumina gels: Effects on surface area and pore volume.* Advanced Ceramic Materials, 1988. **3**(2): p. 167-170.

53   Nass, R. and H. Schmidt, *Synthesis of alumina coating from chelated aluminium alkoxydes.* Journal of non-cristalline solids, 1990. **121**: p. 329-333.

54   Brinker, J. and G.W. Scherer, *Sol-Gel Science.* 1990, Boston: Academic Press. 908.

55   Dupin, T., *Alumina Coating Compositions for Catalyst Supports and Process for their Formulation.* 1984, Rhone Poulenc Specialites Chimiques, Courbevoie, France: US.

56   Jensen, K.F., I.M. Hsing, R. Srinivasan, M.A. Schmidt, M.P. Harold, J.J. Lerou and J.F. Ryley, *Reaction engineering for microreactor systems*, in *Proceedings of the 1st International Conference on Microreaction Technology (IMRET 1)*, W. Ehrfeld, Editor. 1997, Springer: Berlin. p. 2-9.

57   Liauw, M.A., M. Baerns, R. Broucek, V.B. O, J.M. Commenge, J.P. Corriou, K.
      Gebauer, H.J. Hefter, O.U. Langer, M. Matlosz, A. Renken, A. Rouge, R. Schenk, N.
      Steinfeldt and S. Walter. *Periodic Operation in Microchannel Reactors*. in
      Proceedings of the 3rd International Confeence on Microreaction Technology
      (IMRET 3). 2000. Frankfurt am Main: Spinger; 224-234.

58   Franz, A.J., S.K. Ajmera, S.L. Firebaugh, K.F. Jensen and M.A. Schmidt. *Expansion
      of Microreactor Capabilities through Improved Thermal Management and Catalyst
      Deposition*. in Proceedings of the 3rd International Conference on Microreaction
      Technology (IMRET 3). 2000. Frankfurt, D: Springer Verlag; 197-206.

59   Fichtner, M., W. Benzinger, K. Haas-Santo, R. Wunsch and K. Schubert. *Functional
      Coatings for Microstructure Reactors and Heat Exchangers*. in IMRET 3. 2000.
      Frankfort: Springer; 90-101.

60   Pfeifer, P., M. Fichtner, K. Schubert, M.A. Liauw and G. Emig, *Microstructured
      catalysts for methanol steam reforming*, in *Proceedings of the 3rd International
      Conference on Microreaction Technology (IMRET 3)*, W. Ehrfeld, Editor. 2000,
      Springer: Berlin. p. 372-382.

61   Reuse, P., P. Tribolet, L. Kiwi-Minsker and A. Renken, *Catalyst coating in
      microreators for methanol steam reforming: kinetics*, in *Proceedings of the 5th
      International Conference on Microreaction Engineering (IMRET 5)*, W. Ehrfeld,
      Editor. 2001, Springer: Strasbourg. p. 322-331.

62   Armor, J.N., *Overcoming equilibrium limitations in chemical processes*. Applied
      Catalysis a-General, 2001. **222**(1-2): p. 91-99.

63   Schiewe, B., A. Vuin, N. Gunther, K. Gebauer, T. Richter and G. Wegner, *Polymer
      membranes for product enrichment in microreaction technology*. Microreaction
      Technology: Industrial Prospects, Proceedings of the International Conference on
      Microreaction Technology, 3rd, Frankfurt, Apr. 18-21, 1999, 1999: p. 550-555.

64   Schiewe, B., C. Staudt-Bickel, A. Vuin and G. Wegner, *Membrane-based gas
      separation of ethylene/ethylene oxide mixtures for product enrichment in
      microreactor technology*. ChemPhysChem, 2001. **2**(4): p. 211-218.

65   Shu, J., B.P.A. Grandjean, A. Vanneste and S. Kaliaguine, *Catalytic Palladium-
      Based Membrane Reactors - a Review*. Canadian Journal of Chemical Engineering,
      1991. **69**(5): p. 1036-1060.

66   Franz, A.J., K.F. Jensen and M.A. Schmidt. *Palladium membrane microreactors*. in
      Proceedings of the 3rd International Conference on Microreaction Technology
      (IMRET 3). 1999. Frankfurt, D: Springer Verlag; 267-276.

67   Cui, T., J. Fang, A. Zheng, F. Jones and A. Reppond, *Fabrication of microreactors
      for dehydrogenation of cyclohexane to benzene*. Sensors and Actuators, B: Chemical,
      2000. **B71**(3): p. 228-231.

68   Wan, Y.S.S., J.L.H. Chau, A. Gavriilidis and K.L. Yeung, *Design and fabrication of
      zeolite-containing microstructures*, in *Proceedings of the 5th International
      Conference on Microreaction Engineering (IMRET 5)*, W. Ehrfeld, Editor. 2001,
      Springer: Strasbourg. p. 94-102.

69   Wan, Y.S.S., J.L.H. Chau, A. Gavriilidis and K.L. Yeung, *Design and fabrication of
      zeolite-based microreactors and membrane microseparators*. Microporous and
      Mesoporous Materials, 2001. **42**(2-3): p. 157-175.

70   Silveston, P.L., R.R. Hudgins and A. Renken, *Periodic Operation of Catalytic
      Reactors*. Catalysis Today (Special Issue), 1995. **25**: p. 89-195.

71   Silveston, P.L., R.R. Hudgins and A. Renken, *Periodic operation of catalytic reactors
      - Overview;*. Catalysis Today, 1995. **25**: p. 91 - 112.

72   Dettmer, M. and A. Renken, *Kinetic Studies on the Formation of Ethyl Acetate under Steady-state and Non-steady Conditions*. Ger. Chem. Eng., 1983. **6**: p. 356-365.

73   Truffer, M.A. and A. Renken, *Transient Behaviour of Heterogeneous Catalytic Reactions with Educt Inhibition*. AIChE Journal, 1986. **32**: p. 1612 - 1621.

74   Golay, S., O. Wolfrath, R. Doepper and A. Renken, *Model discrimination for reactions with stop-effect*, in *Dynamics of Surfaces and Reaction Kinetics in Heterogeneous Catalysis*, G.F. Froment and K.C. Waugh, Editors. 1997, Elsevier Science B. V.: Amsterdam etc. p. 295 - 304.

75   Golay, S., R. Doepper and A. Renken, *In-situ characterisation of the surface intermediates for the ethanol dehydration reaction over g-alumina under dynamic conditions*. Appl. Catalysis A: General, 1998. **172**: p. 97-106.

76   Thullie, J. and A. Renken, *Forced concentration oscillations for catalytic reactions with stop-effect*. Chem. Eng. Sci., 1991. **46**: p. 1083 - 1088.

77   Renken, A., *Chemical reaction engineering for process optimization: The importance of primary processes on the molecular level*. Chimia, 2002. **56**(4): p. 109-113.

78   Neer, F.J.R.v., A.J. Kodde, H.D. Uil and A. Bliek, *Understanding of Resonance Phenomena on a Catalyst under Forced Concentration and Temperature Oscillations*. The Canadian Journal of Chemical Engineering, 1996. **74**: p. 664-673.

79   Denis, G.H. and R.L. Kabel, *The effect of temperature changes on tubular heterogeneous catalytic reactors*. Chemical Engineering Science, 1970. **25**: p. 1057-1071.

80   Quiram, D.J., K.F. Jensen, M.A. Schmidt, J.F. Ryley, T.M. Delaney, D.J. Kraus and J.S. McCracken. *Development of a turnkey multiple microreactor test station*. in 4th International conference on microreaction technology (IMRET 4). 2000. Atlanta: AIChE; 55-61.

81   Brandner, J., M. Fichtner and K. Schubert. *Electrically heated Microstructure Heat Exchangers and Reactors*. in 3rd International Conference on Microreaction Technology, IMRET 3. 1999. Frankfurt, D: Springer Verlag; 607-616.

82   Rouge, A. and A. Renken. *Forced periodic temperature oscillations in micro-channel reactors*. in Proceedings of the 5th International Conference on Microreaction Engineering (IMRET 5). 2001. Berlin: Springer; 230-239.

Index